

To guarantee the existence of minimizers of the underlying potential in finite elasticity a suitable concept is the polyconvexity condition of the energy function in the sense of Ball, 1977. Until recently, the construction of polyconvex energy functions for the description of anisotropic material behavior was a question yet to be answered. The first transversely isotropic and orthotropic polyconvex energy functions were proposed by Schröder & Neff in the years 2001, 2003.

In the present work a method for the construction of polyconvex, coordinate-invariant energy functions for the description of all existing anisotropic hyperelastic materials is proposed. The key idea is the introduction of so-called crystallographically motivated structural tensors. The applicability of this method is presented within several numerical examples.

Design of Polyconvex Energy Functions for All Anisotropy Classes



Universität Duisburg-Essen
Ingenieurwissenschaften
Abt. Bauwissenschaften
Institut für Mechanik
Prof. Dr.-Ing. J. Schröder

Bericht Nr. 8

Design of Polyconvex Energy Functions for All Anisotropy Classes

Von der Fakultät für Ingenieurwissenschaften,
Abteilung Bauwissenschaften
der Universität Duisburg-Essen
zur Erlangung des akademischen Grades

Doktor-Ingenieurin
genehmigte Dissertation

von

Dipl.-Ing. Vera Ebbing

Hauptberichter: Prof. Dr.-Ing. habil. J. Schröder
Korreferenten: Prof. Dr. rer. nat. habil. P. Neff
Prof. Dr.-Ing. habil. P. Steinmann

Tag der Einreichung: 22. Februar 2010
Tag der mündlichen Prüfung: 31. Mai 2010

Fakultät für Ingenieurwissenschaften,
Abteilung Bauwissenschaften
der Universität Duisburg-Essen
Institut für Mechanik
Prof. Dr.-Ing. habil. J. Schröder

Herausgeber:

Prof. Dr.-Ing. habil. J. Schröder

Organisation und Verwaltung:

Prof. Dr.-Ing. habil. J. Schröder
Institut für Mechanik
Fakultät für Ingenieurwissenschaften
Abteilung Bauwissenschaften
Universität Duisburg-Essen
Universitätsstraße 15
45117 Essen
Tel.: 0201 / 183 - 2682
Fax.: 0201 / 183 - 2680

© Vera Ebbing
Institut für Mechanik
Abteilung Bauwissenschaften
Fakultät für Ingenieurwissenschaften
Universität Duisburg-Essen
Universitätsstraße 15
45117 Essen

Alle Rechte, insbesondere das der Übersetzung in fremde Sprachen, vorbehalten. Ohne Genehmigung des Autors ist es nicht gestattet, dieses Heft ganz oder teilweise auf fotomechanischem Wege (Fotokopie, Mikrokopie) zu vervielfältigen.

ISBN-10 3-9809679-4-8
ISBN-13 978-3-9809679-4-5
EAN 9783980967945

Für meine Eltern und Henning

Preface

The work presented in this thesis was carried out in the years between 2006 and 2010, when I was a co-worker at the Institute of Mechanics at the University of Duisburg-Essen. At the end of this period I thank the Deutsche Forschungsgemeinschaft (DFG) for financial support (Project-No.: NE 902/2-1, SCHR 570/6-1) and I am grateful to a lot of people who accompanied me in these years.

First of all, I thank most sincerely my doctoral advisor Professor Jörg Schröder for providing me the research topic, being one of the areas of interest of him and also of Professor Patrizio Neff. My research activities were based on the foundation stones laid by them. His motivating and animating spirit as well as his intensive support allowed a quick and successful treatment of the research topic. I benefited and learnt a lot from his incredible wealth of knowledge and experience. I am glad that we have been able to develop professional as well as good personal relations.

I am also grateful to my second advisor Professor Patrizio Neff. His mathematical, constructive critical view on my work, especially during the final stage, was very important for me, since the learning level was very high. I owe him maximum support for the mathematically secure elaboration of the thesis.

My special thanks also go to Professor Paul Steinmann for acting as the external examiner of this thesis. Furthermore, I thank him for the cooperation in view of our collective publications in the field of configurational mechanics. He allowed me for my short-term participation in the IUTAM Symposium on Progress in the Theory and Numerics of Configurational Mechanics in Erlangen 2008.

I thank Professor Joachim Bluhm who taught me continuum mechanical foundations and helped me out in many administrative topics.

Next, I would like to thank all co-workers of the institute mentioned below that created a pleasant atmosphere to work with: Juniorprofessor Tim Ricken, Daniel Balzani, Dominik Brands, Sarah Brinkhues, Marc-André Keip, Alexander Schwarz, Wolfgang Moritz Bloßfeld, Robin Wojnowski, Veronika Jorisch, Petra Lindner-Roullé. In particular, I thank Dominik Brands for technical support. My thanks go also to Sarah Brinkhues, Marc-André Keip and Alexander Schwarz for their support in all aspects.

I am grateful to Steffen Specht for his interest in the modeling of woven fiber composites. I supervised him during his bachelor thesis, dealing with the micromechanical FE-analysis of fiber-reinforced membranes. Parts can be found in this thesis.

I would like to express my deepest gratitude to my closest family, including my father and my mother, Christina and Matthias, Marga and Hans-Friedrich, Frederik. They were always there to help and assist me.

Last but not least I thank my boyfriend Henning for his professional technical support and his delightful sense of humor.

Abstract

In order to guarantee the existence of minimizers of the underlying potential in finite elasticity, a suitable concept is the polyconvexity condition of the energy function in the sense of BALL, 1977. Until recently, the construction of polyconvex energy functions for the description of anisotropic material behavior was a question yet to be answered. The first transversely isotropic and orthotropic polyconvex energy functions were presented by SCHRÖDER & NEFF in the years 2001, 2003.

In the present work a method for the construction of polyconvex, coordinate-invariant energy functions for the description of all existing anisotropic hyperelastic materials is proposed. The key idea is the introduction of so-called crystallographically motivated structural tensors. The applicability of this method is shown within several numerical examples.

Zusammenfassung

Ein geeignetes Konzept zur Sicherstellung der Existenz von Minimierern des zugrunde liegenden Potentials im Rahmen der finiten Elastizität ist die Polykonvexitätsbedingung der Energiefunktion nach BALL, 1977. Die Konstruktion von polykonvexen Energiefunktionen für die Beschreibung anisotropen Materialverhaltens stellte bis vor wenigen Jahren ein ungelöstes Problem dar. Die ersten transversal isotropen und orthotropen polykonvexen Energiefunktionen wurden von SCHRÖDER & NEFF in den Jahren 2001, 2003 vorgestellt.

Die vorliegende Arbeit liefert eine Methode zur Konstruktion von polykonvexen, koordinateninvarianten Energiefunktionen für die Beschreibung aller existierenden anisotropen hyperelastischen Materialien. Die wesentliche Idee hierbei ist die Einführung von sogenannten kristallographisch motivierten Strukturtenoren. Die Anwendbarkeit der Methode wird innerhalb verschiedener numerischer Beispiele unter Beweis gestellt.

Contents

| | | |
|----------|---|-----------|
| 1 | Introduction. | 1 |
| 2 | Fundamentals of Continuum Mechanics for Hyperelastic Materials and Variational Principles. | 3 |
| 2.1 | Kinematics. | 3 |
| 2.2 | Orthogonal Transformations. | 7 |
| 2.3 | Objective Physical Quantities. | 7 |
| 2.4 | Material Time Derivatives. | 8 |
| 2.5 | Stresses and Heat Flux. | 9 |
| 2.6 | Balance Principles. | 11 |
| 2.7 | Constitutive Equations for Hyperelastic Materials. | 16 |
| 2.7.1 | Principle of Material Frame Indifference – Objectivity. | 16 |
| 2.7.2 | Principle of Material Symmetry. | 18 |
| 2.8 | Boundary Value Problem and Variational Formulation. | 20 |
| 2.8.1 | Variational Principles. | 20 |
| 2.8.2 | Linearization of the Variational Formulation. | 22 |
| 2.8.3 | Finite-Element-Method: Displacement Formulation. | 23 |
| 3 | Material Symmetry Groups. | 27 |
| 3.1 | Neumann’s Principle. | 27 |
| 3.2 | Space Lattice and its Properties. | 28 |
| 3.3 | Point Symmetry Transformations. | 30 |
| 3.3.1 | Rotations. | 30 |
| 3.3.2 | Rotation-Inversions. | 31 |
| 3.3.3 | Matrix Representations for Point Symmetry Transformations. | 32 |
| 3.4 | Bravais Lattices. | 32 |
| 3.5 | 32 Point Groups of Crystals. | 36 |
| 3.5.1 | Schoenflies/Hermann-Mauguin Symbolism. | 36 |
| 3.5.2 | Matrix Representations of the 32 Point Groups. | 37 |
| 3.5.3 | Orientation of Crystals in Space. | 39 |
| 3.6 | Continuous Point Groups. | 40 |
| 3.7 | Effect of Crystal Symmetry on Tensor Components in Hyperelasticity. | 41 |

| | | |
|----------|---|------------|
| 4 | Isotropic Tensor Functions for Anisotropic Elasticity. | 49 |
| 4.1 | Motivation. | 49 |
| 4.2 | Isotropization of Anisotropic Tensor Functions. | 52 |
| 4.3 | Structural Tensors for All Material Symmetry Groups. | 54 |
| 4.4 | Isotropic Tensor Functions for an Extended Set of Arguments. | 56 |
| 4.4.1 | Extended Set of Second-Order Tensors. | 56 |
| 4.4.2 | Extended Set of Higher-Order Tensors. | 60 |
| 4.5 | "Completeness" of Energy Functions w.r.t. Material Symmetries. | 63 |
| 4.6 | Quadratic Energy Functions of St.Venant-Kirchhoff Type. | 65 |
| 5 | Generalized Convexity Conditions – Hyperelasticity. | 71 |
| 5.1 | Remarks on Growth Conditions, Coercivity. | 72 |
| 5.2 | Remarks on Convexity. | 73 |
| 5.3 | Remarks on Quasiconvexity. | 77 |
| 5.4 | Polyconvexity. | 78 |
| 5.5 | Rank-One Convexity and Ellipticity. | 80 |
| 5.6 | Implications of Convexity Conditions. | 82 |
| 5.7 | Polyconvexity and Ellipticity of Invariant Functions. | 82 |
| 5.7.1 | Invariants in Terms of Second-Order Structural Tensors. | 84 |
| 5.7.2 | Invariants in Terms of Fourth-Order Structural Tensors. | 89 |
| 5.8 | Notes on Polyconvex Isochoric-Volumetric Decoupled Energy Functions. . . | 92 |
| 5.9 | Specific Material Models. | 94 |
| 5.9.1 | Compressible Mooney-Rivlin Material Model. | 94 |
| 5.9.2 | Compressible Neo-Hookean Model. | 97 |
| 5.9.3 | St. Venant-Kirchhoff Material Model. | 97 |
| 5.9.4 | Energy Functions Defined in Terms of the Hencky Tensor | 98 |
| 6 | Invariant Polyconvex Energies on the Basis of Crystallographically Motivated Structural Tensors. | 101 |
| 6.1 | Families of Polyconvex Invariant Functions. | 101 |
| 6.2 | Crystallographically Motivated Structural Tensors. | 104 |
| 6.3 | Consequences of Polyconvex Approach w.r.t. Classical Representations. . . | 112 |
| 6.4 | Polyconvex Material Models. | 115 |
| 6.4.1 | Material Models Based on Second-Order Structural Tensors. | 116 |
| 6.4.2 | Material Models Based on Fourth-Order Structural Tensors. | 124 |

| | |
|--|------------|
| 7 Numerical Examples. | 129 |
| 7.1 Homogeneous Biaxial Tension Test. | 129 |
| 7.2 Cook's Membrane. | 131 |
| 7.3 Anisotropic Moduli – Fitting to Referential Data. | 133 |
| 7.4 Micro- and Macromechanical Modeling of Fiber-Reinforced Composites. . . | 145 |
| 7.4.1 Micromechanical Modeling. | 146 |
| 7.4.2 Macromechanical Modeling: Thin Shells. | 149 |
| 7.4.2.1 The Variational Formulation. | 150 |
| 7.4.2.2 Thin Hexagonal Plate Subjected to Pressure. | 151 |
| 7.4.2.3 Hyperbolic Shell Subjected to Locally Distributed Loads. . | 152 |
| 7.5 Application to Configurational Mechanics. | 156 |
| 7.5.1 Balance of Configurational Forces. | 156 |
| 7.5.2 Cracked SET Specimen. | 161 |
| 8 Summary and Conclusion. | 165 |
| Appendix | 167 |
| A Glossary. | 167 |
| B Matrix Representation of Special Tensors. | 169 |
| C Positive Definiteness of Matrices. | 171 |
| D Classical Sets of Bilinear Invariants. | 172 |
| E Zheng & Spencer's and Xiao's Structural Tensors: Detailed Representations. | 173 |
| F Some Useful Derivatives. | 174 |
| G Additional Sets of Bilinear Invariants and Quadratic Energy Functions. . . . | 175 |
| H Further Proofs of Polyconvexity and Ellipticity | 188 |
| I Table of Crystallographically Motivated Structural Tensors. | 189 |
| List of Figures | 191 |
| List of Tables | 195 |
| References | 197 |

Notation Linear Algebra

| | |
|---|---|
| \mathbb{R} | set of real numbers |
| \mathbb{R}_+ | set of positive real numbers |
| \mathbb{N} | set of natural numbers |
| \mathbb{N}_+ | set of natural numbers without zero |
| \mathbb{R}^3 | three-dimensional Euclidian vector space |
| $\langle \mathbf{a}, \mathbf{b} \rangle$, with $\mathbf{a}, \mathbf{b} \in \mathbb{R}^3$ | standard Euclidian scalar product on \mathbb{R}^3 |
| $\ \mathbf{a}\ = \langle \mathbf{a}, \mathbf{a} \rangle^{1/2}$ | Euclidian vector norm |
| $\mathbb{R}^{3 \times 3}$ | set of real 3×3 matrices |
| $\mathbb{R}_+^{3 \times 3}$ | set of real 3×3 matrices with positive determinant |
| $\text{Sym}(3)$ | set of all real symmetric 3×3 matrices |
| $\text{PSym}(3)$ | set of all real positive definite symmetric 3×3 matrices |
| $\text{Skew}(3)$ | set of all real skew-symmetric 3×3 matrices |
| $\text{GL}(3, \mathbb{R})$ | set of all real invertible 3×3 matrices |
| \otimes | tensor product of vectors in \mathbb{R}^3 |
| $\mathbf{a} \otimes \mathbf{b}$ | matrix of rank one |
| \mathbf{H}^T , with $\mathbf{H} \in \mathbb{R}^{3 \times 3}$ | transpose of 3×3 matrix |
| $\mathbf{1}$ | identity 3×3 matrix (index notation: δ_{ij}) |
| \mathbf{H}^{-1} | inverse of 3×3 matrix |
| $\text{tr}[\mathbf{H}] = \mathbf{H} : \mathbf{1}$ | trace of 3×3 matrix (index notation: $H_{ij}\delta_{ij}$) |
| $\det[\mathbf{H}]$ | determinant of 3×3 matrix |
| $\text{Adj}\mathbf{H} = \det[\mathbf{H}]\mathbf{H}^{-1}$ | adjoint of an invertible 3×3 matrix |
| $\text{Cof}\mathbf{H} = \text{Adj}\mathbf{H}^T$ | cofactor of an invertible 3×3 matrix |
| $\langle \mathbf{H}, \mathbf{B} \rangle = \text{tr}[\mathbf{H}\mathbf{B}^T] = \mathbf{H} : \mathbf{B}$, with $\mathbf{H}, \mathbf{B} \in \mathbb{R}^{3 \times 3}$ | standard Euclidian scalar product on $\mathbb{R}^{3 \times 3}$ (index notation: $H_{ij}B_{ij}$) |
| $\ \mathbf{H}\ = \langle \mathbf{H}, \mathbf{H} \rangle^{1/2}$ | Euclidian matrix norm |
| $\mathbf{H}\mathbf{a}$ | matrix-vector operation index notation: $H_{ij}a_j$ |

1 Introduction.

Anisotropic materials exhibit a wide range of applications in engineering science and appear in a manifold manner. A lot of engineering materials like fiber-reinforced composites or bio-materials like soft-tissues possessing a fibrous structure have to be mentioned in this context. Depending on the structure and orientation of the embedded fibers different anisotropic material behavior of the composites can be observed.

Thus, the modeling of anisotropic material behavior represents a field of research which becomes increasingly important in material science. Especially in finite strain elasticity, the construction of suitable energy functions for the description of anisotropic material behavior was for a long time a question yet to be answered.

The overall question of this thesis is the second open problem in elasticity posed in the article *Some open problems in elasticity* of BALL [10], which reads:

Are there ways of verifying polyconvexity and quasiconvexity for a useful class of anisotropic stored-energy functions?

In **Chapter 2** the fundamentals of continuum mechanics that are used in this thesis are briefly introduced. The *constitutive equations* are provided, which have to be considered for the representation of hyperelastic material behavior within a thermodynamical consistent setting. The *Principle of Material Symmetry* plays a significant role in continuum mechanics for the specification of isotropic and anisotropic material behavior by constitutive equations. Anisotropic material behavior is characterized by invariance properties of the material responses with respect to certain material symmetry transformations, which therefore results in restrictions on the form of the constitutive equations.

For the case of anisotropic elasticity there exist 13 types of anisotropic material symmetry groups. Eleven of them are associated with the 32 crystal point symmetry groups and the remaining two describe the transversely isotropic case. The symmetries of a crystal structure impose certain restrictions on its physical properties. Relations between symmetries of crystals and its physical properties are postulated by Franz Ernst Neumann in 1885: Symmetry elements associated with any physical property of a crystal must include those of the symmetry point group of the crystal. The 32 point symmetry groups for the specification of crystals, the associated eleven material symmetry groups as well as the important symmetry groups for describing non-crystalline materials are presented in **Chapter 3**.

In **Chapter 4** classical representation theorems for isotropic tensor functions are presented. These theorems lead to coordinate-invariant formulations of the constitutive equations in terms of scalar-valued invariants. They are based on vectors and second-order tensors. In case of anisotropy, the concept of structural tensors can be applied, where structural tensors act as additional terms in the constitutive laws. This concept implicates an isotropicization of the anisotropic tensor functions. However, transverse isotropy and orthotropy as well as the triclinic and monoclinic material symmetry groups are the only material symmetry groups, which can be described by second-order structural tensors. Therefore, only in these cases the classical tensor-representation theorems can be

exploited. For the representation of the remaining material symmetry groups structural tensors of order higher than two are required: for the trigonal, tetragonal and cubic systems fourth-order and for the hexagonal systems sixth-order structural tensors are necessary. Representation theorems for isotropic tensor functions with tensors of order higher than two are not yet exhaustively discussed in the literature. However, we took notice of a useful idea, where second-order tensor-valued so called *isotropic extension functions* are introduced.

The mathematical treatment of boundary value problems in our framework is mainly based on the direct methods of the calculus of variations, i.e., to find a minimizing deformation φ of the elastic free energy $\psi(\mathbf{F})$ depending on the deformation gradient $\mathbf{F} = \text{Grad}\varphi$ subject to specific boundary conditions. In finite elasticity, the guarantee of existence of minimizers together with a physically reasonable material modeling was – until the publications of Ball in the 1977's – an outstanding problem. In **Chapter 5** we give an overview of the generalized convexity conditions playing an important role in this regard. The existence of minimizers is based on the notion of sequential weak lower semicontinuity (s.w.l.s.). If the functional to be minimized is s.w.l.s. and the coercivity condition is fulfilled the existence of minimizers is ensured. In order to obtain physically reasonable material models the Legendre-Hadamard Inequality is a suitable condition, because hereby, the existence of real wave speeds inside the material for the corresponding linearization is guaranteed. The most useful condition, however, is the polyconvexity condition introduced by Ball in 1977: It directly implies s.w.l.s. and does not contradict any physical requirement. Moreover, polyconvex functions are also rank-one convex. Considering smooth energy functions the (strict) rank-one convexity implies the (strict) Legendre-Hadamard condition. For the proof of polyconvexity we have to check the convexity of the elastic free energy function $\psi(\mathbf{F})$ with respect to the argument $\{\mathbf{F}, \text{Cof}\mathbf{F}, \det\mathbf{F}\} \in \mathbb{R}^{19}$. There exists a wide range of polyconvex functions for the description of isotropic material behavior, e.g. the Mooney-Rivlin- and Neo-Hooke-type free energy functions. For the description of anisotropic material behavior, polyconvex energies based on well-known structural tensors already exist in the literature for the case of transverse isotropy, orthotropy and cubic symmetry. However, the well-known structural tensors for the construction of polyconvex triclinic, monoclinic, tetragonal and trigonal energy functions were not useful so far.

Therefore, our aim is the representation of polyconvex energy functions for all mechanically relevant anisotropy groups. The key ideas are presented in **Chapter 6**, namely the introduction of

crystallographically motivated symmetric, positive (semi-)definite second- and fourth-order structural tensors for all mechanically relevant anisotropy groups.

On the basis of this approach we are able to construct generic, coordinate-invariant, polyconvex energy functions, which fulfill a priori the stress free reference configuration condition and are suitable for the simulation of real anisotropic material behavior. The latter fact is exemplified by various approximations of the tangent moduli at the reference state to experimentally determined elasticities of real anisotropic materials. The applicability of the proposed energies is furthermore checked in **Chapter 7** within different numerical examples ranging from the simulation of woven fiber composites, thin shell formulations to configurational mechanics.

2 Fundamentals of Continuum Mechanics for Hyperelastic Materials and Variational Principles.

Continuum mechanics deals with the kinematics and mechanical behavior of materials modeled as a continuum, i.e., fluids and solids. We consider solid materials with a hyperelastic material behavior. The aim of this chapter is to give a brief overview of the continuum mechanical background of this work and to introduce the notation that is used. Extensive discussions concerning this topic can be found in TRUESDELL & NOLL [127], MARSDEN & HUGHES [72], OGDEN [89], MALVERN [70]. Recent publications are CHADWICK [37], BAŞAR & WEICHERT [6], HAUPT [58], HOLZAPFEL [62] and DE BOER & SCHRÖDER [42]. We conclude this chapter with the formulation of the boundary value problem, the associated variational formulation and the Finite-Element formulation of finite elastostatics. Exhaustive textbooks dealing with the basic concept of the Finite-Element-Method are ZIENKIEWICZ & TAYLOR [147], BATHE [14] and WRIGGERS [138].

2.1 Kinematics.

We consider a material body \mathcal{B} consisting of a continuous set of material points $P \in \mathcal{B}$ in a three-dimensional *Euclidean space* \mathbb{R}^3 . The surface of \mathcal{B} is denoted by $\partial\mathcal{B}$.

The reference configuration $\mathcal{B}_0 \in \mathbb{R}^3$ –also called material or Lagrangian configuration– is defined by the position \mathbf{X} of the material points P at time $t = t_0$, i.e.,

$$\mathbf{X} = X^J \mathbf{E}_J, \quad J = 1, 2, 3, \quad (2.1)$$

in terms of the right-handed orthonormal (cartesian) basis $\{\mathbf{E}\}_J, J = 1, 2, 3$. A cartesian basis is characterized by

$$\mathbf{E}_I \cdot \mathbf{E}_J = \delta_{IJ} \quad \text{and} \quad \mathbf{E}_I \times \mathbf{E}_J = \epsilon_{IJK} \mathbf{E}_K, \quad (2.2)$$

with the Kronecker symbol δ_{IJ} and the coefficient matrix ϵ_{IJK} of the third-order permutation tensor ϵ :

$$\delta_{IJ} = \begin{cases} 0, & \text{if } I \neq J, \\ 1, & \text{if } I = J, \end{cases} \quad \epsilon_{IJK} = \epsilon^{IJK} = \begin{cases} 0, & \text{if two indices are equal,} \\ 1, & \text{for } \epsilon_{123}, \epsilon_{231}, \epsilon_{312}, \\ -1, & \text{for } \epsilon_{213}, \epsilon_{132}, \epsilon_{321}. \end{cases} \quad (2.3)$$

The actual configuration $\mathcal{B}_t \in \mathbb{R}^3$ –also called spatial or Eulerian configuration– is defined by the position \mathbf{x} of the material points $P \in \mathcal{B}_t$ at time t , i.e.,

$$\mathbf{x} = x^j \mathbf{e}_j, \quad j = 1, 2, 3, \quad (2.4)$$

with the cartesian basis $\{\mathbf{e}\}_j, j = 1, 2, 3$ of the actual configuration.

The motion of the body \mathcal{B} is described by the one-to-one mapping of the material points P of \mathcal{B}_0 into \mathcal{B}_t

$$\varphi : \mathcal{B}_0 \mapsto \mathcal{B}_t. \quad (2.5)$$

The transformation φ maps, at fixed time $t \in \mathbb{R}_+$, points $\mathbf{X} \in \mathcal{B}_0$ of the reference configuration onto points $\mathbf{x} \in \mathcal{B}_t$ of the actual configuration, i.e.,

$$\varphi(\mathbf{X}, t) : \mathbf{X} \mapsto \mathbf{x} = \varphi(\mathbf{X}, t), \quad \text{with} \quad x^j = x^j(X^1, X^2, X^3, t), \quad (2.6)$$

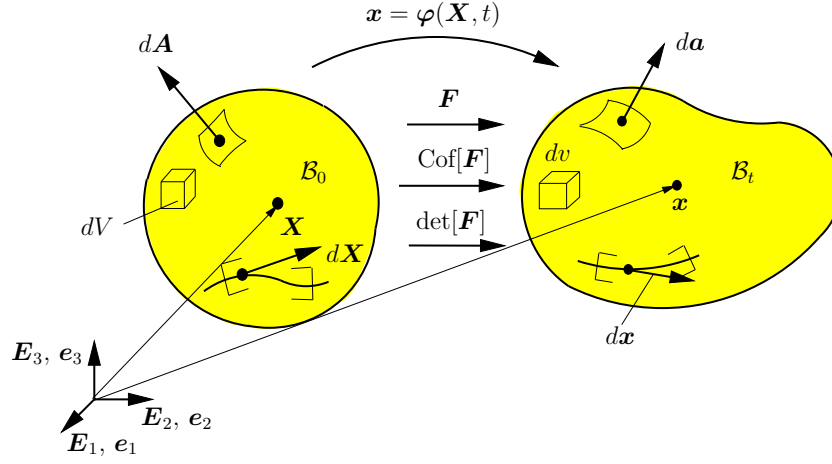


Figure 2.1: Representations of reference and actual configuration and corresponding geometric mappings (transport theorems).

which is assumed to be reversible

$$\boldsymbol{\varphi}^{-1}(\mathbf{x}, t) : \mathbf{x} \mapsto \mathbf{X} = \boldsymbol{\varphi}^{-1}(\mathbf{x}, t), \quad \text{with} \quad X^J = X^J(x^1, x^2, x^3, t), \quad (2.7)$$

If x^i and X^i are single-valued and at least once continuously differentiable with respect to their arguments, the condition (2.7) is satisfied.

As one of the most important kinematic quantities in continuum mechanics we introduce the deformation gradient which is the partial derivative of the deformation mapping $\mathbf{x} = \boldsymbol{\varphi}(\mathbf{X}, t)$ with respect to the material coordinates \mathbf{X} , i.e.,

$$\mathbf{F} = \mathbf{F}(\mathbf{X}, t) := \text{Grad } \mathbf{x} = \nabla_{\mathbf{X}} \mathbf{x} = \frac{\partial \mathbf{x}}{\partial \mathbf{X}}. \quad (2.8)$$

The deformation gradient is a two-point transformation tensor; one base vector is defined with respect to the Eulerian configuration and the other is defined with respect to the Lagrangian configuration:

$$\mathbf{F}(\mathbf{X}, t) = F^i{}_J \mathbf{e}_i \otimes \mathbf{E}^J. \quad (2.9)$$

The arrangement of the deformation gradient components is denoted by

$$F^i{}_J = \frac{\partial x^i}{\partial X^J} = x^i{}_{,J} \quad \Rightarrow \quad [F^i{}_J] = \begin{bmatrix} \frac{\partial x^1}{\partial X^1} & \frac{\partial x^1}{\partial X^2} & \frac{\partial x^1}{\partial X^3} \\ \frac{\partial x^2}{\partial X^1} & \frac{\partial x^2}{\partial X^2} & \frac{\partial x^2}{\partial X^3} \\ \frac{\partial x^3}{\partial X^1} & \frac{\partial x^3}{\partial X^2} & \frac{\partial x^3}{\partial X^3} \end{bmatrix}. \quad (2.10)$$

Since the mapping (2.8) must be one-to-one, the deformation gradient is not allowed to be singular, thus, its inverse

$$\mathbf{F}^{-1}(\mathbf{X}, t) = \text{grad } \mathbf{X} = \nabla_{\mathbf{x}} \mathbf{X} = \frac{\partial \mathbf{X}}{\partial \mathbf{x}} = F^{-1J}{}_i \mathbf{E}_J \otimes \mathbf{e}^i \quad (2.11)$$

must exist. Furthermore the associated components matrix representation appears as

$$F^{-1J}_i = \frac{\partial X^J}{\partial x^i} = X^J_{,i} \Rightarrow [F^{-1J}_i] = \begin{bmatrix} \frac{\partial X^1}{\partial x^1} & \frac{\partial X^1}{\partial x^2} & \frac{\partial X^1}{\partial x^3} \\ \frac{\partial X^2}{\partial x^1} & \frac{\partial X^2}{\partial x^2} & \frac{\partial X^2}{\partial x^3} \\ \frac{\partial X^3}{\partial x^1} & \frac{\partial X^3}{\partial x^2} & \frac{\partial X^3}{\partial x^3} \end{bmatrix}. \quad (2.12)$$

A sufficient condition for the existence of the inverse of $\mathbf{F}(\mathbf{X}, t)$ is that the determinant of $\mathbf{F}(\mathbf{X}, t)$, the *Jacobian* J , is not equal to zero, i.e., $J = \det \mathbf{F}(\mathbf{X}, t) \neq 0$. Together with the continuity of the mapping $\boldsymbol{\varphi}$ we enforce the condition

$$J = \det \mathbf{F}(\mathbf{X}, t) > 0 \quad (2.13)$$

for all motions of the body \mathcal{B} . Otherwise the body could interpenetrate itself, i.e., it could undergo deformations that are unphysical. On the basis of the deformation gradient three fundamental geometric mappings – also called *transport theorems*– are important in continuum mechanics:

(i) Mapping of infinitesimal line elements. The deformation gradient represents a linear mapping of infinitesimal line elements $d\mathbf{X}$ of the reference configuration to infinitesimal line elements

$$d\mathbf{x} = \mathbf{F} d\mathbf{X} \quad (2.14)$$

of the actual configuration.

(ii) Mapping of infinitesimal area elements. The normal to an infinitesimal material area element $d\mathbf{A} = \mathbf{N} dA$, with the material unit outward normal vector \mathbf{N} , are mapped to the normal of an infinitesimal spatial area element $d\mathbf{a} = \mathbf{n} da$, with the spatial unit outward normal vector \mathbf{n} , via *Nanson's Formula* (1878)

$$d\mathbf{a} = J \mathbf{F}^{-T} d\mathbf{A} = \text{Cof}[\mathbf{F}] d\mathbf{A}. \quad (2.15)$$

(iii) Mapping of infinitesimal volume elements. Representing the infinitesimal material and spatial volume elements dV and dv , respectively, as triple product of the corresponding infinitesimal line elements, i.e., $dV = d\mathbf{X}_1 \cdot (d\mathbf{X}_2 \times d\mathbf{X}_3)$ and $dv = d\mathbf{x}_1 \cdot (d\mathbf{x}_2 \times d\mathbf{x}_3)$, and considering the relation (2.14) as well as $J = \det(\frac{\partial \mathbf{x}}{\partial \mathbf{X}}) = \frac{\partial \mathbf{x}}{\partial X_1} \cdot (\frac{\partial \mathbf{x}}{\partial X_2} \times \frac{\partial \mathbf{x}}{\partial X_3})$ yields the mapping of the infinitesimal volume elements

$$dv = J dV. \quad (2.16)$$

A graphical representation of the transport theorems is given in Figure 2.1. Introducing the displacement vector $\mathbf{u}(\mathbf{X}, t)$ as difference between the position vector of the actual and reference configuration

$$\mathbf{u}(\mathbf{X}, t) = \boldsymbol{\varphi}(\mathbf{X}, t) - \mathbf{X} \quad (2.17)$$

leads to the following alternative representation of the deformation gradient (2.8)

$$\mathbf{F} = \text{Grad}[\mathbf{X} + \mathbf{u}(\mathbf{X}, t)] = \mathbf{1} + \text{Grad} \mathbf{u}, \quad (2.18)$$

where $\mathbf{1}$ denotes the second-order identity tensor.

Further strain measures can be defined by using the *polar decomposition* of the local deformation gradient

$$\mathbf{F} = \mathbf{R}\mathbf{U} = \mathbf{V}\mathbf{R}, \quad (2.19)$$

where the rotation tensor \mathbf{R} is a proper orthogonal tensor (with $\mathbf{R}^{-1} = \mathbf{R}^T$), which causes a rotation of the material line elements. The symmetric tensors \mathbf{U} and \mathbf{V} are the so-called *right stretch tensor* and *left stretch tensor of deformation*, respectively. Then, further strain measures can be obtained by multiplicative combinations of (2.19) of the form:

$$\mathbf{C} := \mathbf{F}^T \mathbf{F} = (\mathbf{R}\mathbf{U})^T (\mathbf{R}\mathbf{U}) = \mathbf{U}^2, \quad \text{with } C_{AB} = F^a{}_A \delta_{ab} F^b{}_B, \quad (2.20)$$

$$\mathbf{b} := \mathbf{F}\mathbf{F}^T = (\mathbf{V}\mathbf{R})(\mathbf{V}\mathbf{R})^T = \mathbf{V}^2, \quad \text{with } b^{ab} = F^a{}_A \delta^{AB} F^b{}_B,$$

where \mathbf{C} is the *right Cauchy-Green tensor* and \mathbf{b} the *left Cauchy-Green tensor* (*Finger deformation tensor*). Furthermore, suitable measures can be formed by using half of the difference of the squares of the infinitesimal material and spatial line elements, i.e., $\frac{1}{2}(d\mathbf{x} \cdot d\mathbf{x} - d\mathbf{X} \cdot d\mathbf{X})$. Including the relation (2.14) and $d\mathbf{X} = \mathbf{F}^{-1}d\mathbf{x}$, respectively, leads to the definition of the *Green-Lagrange strain tensor* \mathbf{E} and *Euler-Almansi strain tensor* \mathbf{e} , respectively:

$$\begin{aligned} \mathbf{E} &:= \frac{1}{2}(\mathbf{C} - \mathbf{1}), \quad \text{with } E_{AB} = \frac{1}{2}(C_{AB} - \delta_{AB}), \\ \mathbf{e} &:= \frac{1}{2}(\mathbf{1} - \mathbf{b}^{-1}), \quad \text{with } e_{ab} = \frac{1}{2}(\delta_{ab} - \{b^{-1}\}_{ab}). \end{aligned} \quad (2.21)$$

Inserting the relation (2.18) into (2.21)₁ yields the alternative expression of \mathbf{E} in terms of the displacement \mathbf{u}

$$\mathbf{E} = \frac{1}{2}((\mathbf{1} + \text{Grad}\mathbf{u})^T (\mathbf{1} + \text{Grad}\mathbf{u}) - \mathbf{1}) = \frac{1}{2}(\text{Grad}\mathbf{u} + (\text{Grad}\mathbf{u})^T + (\text{Grad}\mathbf{u})^T (\text{Grad}\mathbf{u})). \quad (2.22)$$

In the geometrically linear theory, both the strains and the displacements are assumed to be infinitesimal small, i.e., (2.17) reduces to $\mathbf{x}^\lambda = \mathbf{X} + \lambda\mathbf{u}$ with an infinitesimally small parameter λ . Inserting this relation into (2.22) gives

$$\mathbf{E}^\lambda = \frac{1}{2}(\lambda \text{Grad}\mathbf{u} + \lambda (\text{Grad}\mathbf{u})^T + \lambda^2 (\text{Grad}\mathbf{u})^T (\text{Grad}\mathbf{u})). \quad (2.23)$$

Since $\lambda \gg \lambda^2$ we may neglect the quadratic term and obtain the strain tensor $\boldsymbol{\varepsilon}$ in the small strain regime

$$\boldsymbol{\varepsilon} = \frac{1}{2}(\text{Grad}\mathbf{u} + (\text{Grad}\mathbf{u})^T). \quad (2.24)$$

Alternatively (2.26) can be derived by applying the linearization procedure on the Green-Lagrange strain tensor, which is governed by the Gâteaux derivative, cf. DE BOER & SCHRÖDER [42], i.e.,

$$\text{Lin}[\mathbf{E}] = \mathbf{E}|_X + \frac{d}{d\lambda}[\mathbf{E}(\mathbf{X} + \lambda\mathbf{u})]|_{\lambda=0}, \quad (2.25)$$

where the second term is the Gâteaux derivative (directional derivative) of \mathbf{E} at \mathbf{X} in the direction of \mathbf{u} . With $\mathbf{E}|_X = \mathbf{0}$ we also obtain (2.24), i.e.,

$$\boldsymbol{\varepsilon} = \text{Lin}[\mathbf{E}]. \quad (2.26)$$

2.2 Orthogonal Transformations.

In this section we consider orthogonal transformations. Such transformations constitute the orthogonal group $O(3)$ and satisfy

$$\mathbf{Q}^{-1} = \mathbf{Q}^T, \det \mathbf{Q} = \pm 1. \quad (2.27)$$

They describe proper and improper rotations. The improper rotations are also known as reflections or rotoinversions. A subgroup of $O(3)$ is the proper orthogonal group $SO(3)$. Elements of $SO(3)$ have the property

$$\mathbf{Q}^{-1} = \mathbf{Q}^T, \det \mathbf{Q} = 1. \quad (2.28)$$

They solely describe proper rotations. For instance \mathbf{R} introduced in (2.19) is an element of $SO(3)$. Details concerning the notion group and matrix representations of special orthogonal transformations are given in the next chapter.

2.3 Objective Physical Quantities.

The following remarks on objective physical quantities are related to the textbooks STEIN & BARTHOLD [121] and HUTTER & JÖHNK [63], see also MALVERN [70], TRUESDELL & NOLL [127]. The description of the motion \mathbf{x} of a body is dependent on the observer, i.e., on the choice of the coordinate system. The different states of motions of the observer lead to a different description of the motion of the body.

Consider two observers. They must secure exactly the same deformation of the body. Both observers relate their measurements to their respective reference system (of which the representation may be different in different reference systems). Let the first observer B_1 be described by the origin O and the cartesian base vectors $\{\mathbf{e}_i, \mathbf{e}_j, \mathbf{e}_k\}$; let the second observer B_2 be described by the origin O^+ and the cartesian base vectors $\{\mathbf{e}_i^+, \mathbf{e}_j^+, \mathbf{e}_k^+\}$.

The difference between the motions of the observers, i.e., the change of the reference systems $\{\mathbf{e}_i\} \rightarrow \{\mathbf{e}_j^+\}$ of the motion of the body, is given by a time dependent rigid body motion, which is defined by

$$\left. \begin{aligned} \mathbf{x}^+ &= \mathbf{Q}(t) \mathbf{x} + \mathbf{c} \\ \text{and } t^+ &= t - \Delta t \end{aligned} \right\} \quad \forall \mathbf{Q}(t) \in SO(3), \text{ with } \mathbf{Q}(t) = \frac{\partial \mathbf{x}^+}{\partial \mathbf{x}}. \quad (2.29)$$

The transformation (2.29) is called *Euclidean transformation*. The time dependent vector $\mathbf{c}(t)$ denotes the mutual translation of the origins O and O^+ . The time dependent orthogonal tensor $\mathbf{Q}(t) \in SO(3)$ represents the mutual rotation of the base systems $\{\mathbf{e}_i, \mathbf{e}_j, \mathbf{e}_k\}$ and $\{\mathbf{e}_i^+, \mathbf{e}_j^+, \mathbf{e}_k^+\}$. Furthermore, a time difference $t^+ = t - \Delta t$, with $\Delta t \in \mathbb{R}$, between the observers may exist. The time independent transformation

$$\mathbf{x}^+ = \mathbf{Q} \mathbf{x} + \mathbf{c} \quad \text{with} \quad \mathbf{Q} = \mathbf{Q}(t) = \text{const. and } \mathbf{c} = \mathbf{c}(t) = \text{const.} \quad \forall \mathbf{Q} \in SO(3) \quad (2.30)$$

is referred to as *rigid transformation*.

Physical quantities are called objective or observer independent, when they follow specific transformation rules under the Euclidean transformation. Eulerian quantities, e.g., a

scalar-valued quantity β , a vector-valued quantity \mathbf{v} and a tensor-valued quantity \mathbf{h} , are objective, if their coordinates transform as

$$\beta^+ = \beta, \quad \mathbf{v}^+ = \mathbf{Q} \mathbf{v}, \quad \mathbf{h}^+ = \mathbf{Q} \mathbf{h} \mathbf{Q}^T, \quad (2.31)$$

with $\mathbf{Q} = \mathbf{Q}(t)$. The deformation gradient \mathbf{F} (two-point tensor) transforms as:

$$\mathbf{F}^+ = \text{Grad} \mathbf{x}^+ = \frac{\partial \mathbf{x}^+}{\partial \mathbf{x}} \frac{\partial \mathbf{x}}{\partial \mathbf{X}} = \mathbf{Q}(t) \mathbf{F}. \quad (2.32)$$

Euclidean transformations have no effect on Lagrangian quantities. For instance, the right Cauchy-Green tensor (2.20) is invariant under an Euclidean transformation:

$$\mathbf{C}^+ = \mathbf{F}^{+T} \mathbf{F}^+ = \mathbf{F}^T \mathbf{Q}(t)^T \mathbf{Q}(t) \mathbf{F} = \mathbf{C}. \quad (2.33)$$

2.4 Material Time Derivatives.

The material time derivative $\frac{d}{dt}[\bullet] = \overline{[\bullet]}$ is the temporal change of the quantity $[\bullet]$ at an arbitrary point of the reference configuration, i.e., $\mathbf{X} = \text{const.}$. For material quantities $P(\mathbf{X}, t)$ the material time derivative is equal to the partial derivative $\frac{\partial P}{\partial t}$; for spatial quantities $p(\mathbf{x}, t) = p(\mathbf{x}(\mathbf{X}, t), t)$ it additively consists of a convective and a local part, i.e.,

$$\dot{p} = \frac{\partial p}{\partial \mathbf{x}} \cdot \frac{\partial \mathbf{x}}{\partial t} + \frac{\partial p}{\partial t} = \text{grad} p \cdot \dot{\mathbf{x}} + \frac{\partial p}{\partial t}. \quad (2.34)$$

The material velocity $\dot{\mathbf{x}}(\mathbf{X}, t)$ is defined as the material time derivative of the motion $\mathbf{x} = \boldsymbol{\varphi}(\mathbf{X}, t)$

$$\mathbf{v} = \dot{\mathbf{x}}(\mathbf{X}, t) = \frac{\partial \boldsymbol{\varphi}}{\partial t}. \quad (2.35)$$

The material acceleration $\ddot{\mathbf{x}}(\mathbf{X}, t)$ is defined as the material time derivative of the material velocity. With (2.35) we get

$$\mathbf{a} = \ddot{\mathbf{x}}(\mathbf{X}, t) = \frac{\partial \dot{\mathbf{x}}}{\partial t} = \frac{\partial^2 \boldsymbol{\varphi}(\mathbf{X}, t)}{\partial t^2}. \quad (2.36)$$

Changing the independent variables in $\dot{\mathbf{x}}(\mathbf{X}, t)$ and $\ddot{\mathbf{x}}(\mathbf{X}, t)$ from material to spatial coordinates leads with (2.7) to the velocity and acceleration

$$\begin{aligned} \mathbf{v} &= \mathbf{v}(\mathbf{x}, t) = \dot{\mathbf{x}}(\boldsymbol{\varphi}^{-1}(\mathbf{x}, t), t), \\ \mathbf{a} &= \mathbf{a}(\mathbf{x}, t) = \ddot{\mathbf{x}}(\boldsymbol{\varphi}^{-1}(\mathbf{x}, t), t) = \frac{\partial \mathbf{v}}{\partial \mathbf{x}} \frac{\partial \mathbf{x}}{\partial t} + \frac{\partial \mathbf{v}}{\partial t} = \mathbf{l} \mathbf{v} + \frac{\partial \mathbf{v}}{\partial t}, \end{aligned} \quad (2.37)$$

where \mathbf{l} is the spatial gradient of the velocity $\mathbf{l} := \text{grad} \mathbf{v}$ which can also be expressed by the material time derivative of \mathbf{F} , i.e., $\dot{\mathbf{F}} = \frac{\partial \dot{\mathbf{x}}}{\partial \mathbf{X}}$, as follows:

$$\mathbf{l} = \frac{\partial \mathbf{v}}{\partial \mathbf{x}} = \frac{\partial \dot{\mathbf{x}}}{\partial \mathbf{X}} \frac{\partial \mathbf{X}}{\partial \mathbf{x}} = \dot{\mathbf{F}} \mathbf{F}^{-1}. \quad (2.38)$$

It can be additively decomposed into a symmetric and a skew-symmetric tensor $\mathbf{l} = \mathbf{d} + \mathbf{w}$, with

$$\mathbf{d} = \frac{1}{2}(\mathbf{l} + \mathbf{l}^T), \quad \mathbf{w} = \frac{1}{2}(\mathbf{l} - \mathbf{l}^T), \quad (2.39)$$

where \mathbf{d} is the *stretching tensor* of the motion and \mathbf{w} is called the *spin tensor*. Moreover, the material time derivative of the Jacobian determinant is calculated by

$$\dot{J} = \frac{\partial}{\partial t}(\det \mathbf{F}) = \frac{\partial \det \mathbf{F}}{\partial \mathbf{F}} : \frac{\partial \mathbf{F}}{\partial t} = \det \mathbf{F} \mathbf{F}^{-T} : \dot{\mathbf{F}} = \det \mathbf{F} \operatorname{tr}[\mathbf{l}] = J \operatorname{div} \mathbf{v}. \quad (2.40)$$

The material time derivatives of the transport theorems (2.14), (2.15) and (2.16) are

$$\begin{aligned} d\dot{\mathbf{x}} &= \dot{\mathbf{F}} d\mathbf{X} = \mathbf{l} \mathbf{F} d\mathbf{X} = \mathbf{l} d\mathbf{x}, \\ d\dot{\mathbf{a}} &= \dot{J} \mathbf{F}^{-T} d\mathbf{A} + J \overline{(\mathbf{F}^{-T})^\cdot} d\mathbf{A} \\ &= J \operatorname{div} \mathbf{v} \mathbf{F}^{-T} d\mathbf{A} - J \mathbf{l}^T \mathbf{F}^{-T} d\mathbf{A} \\ &= (\operatorname{tr}[\mathbf{l}] \mathbf{1} - \mathbf{l}^T) \operatorname{Cof}[\mathbf{F}] d\mathbf{A} = (\operatorname{tr}[\mathbf{l}] \mathbf{1} - \mathbf{l}^T) d\mathbf{a}, \\ d\dot{v} &= \dot{J} dV = J \operatorname{div} \mathbf{v} dV = \operatorname{div} \mathbf{v} dv. \end{aligned} \quad (2.41)$$

2.5 Stresses and Heat Flux.

Let us focus on the mechanical and thermal effects on the surface $\partial \mathcal{B}_t$ of the actual configuration and $\partial \mathcal{B}_0$ of the reference placement, respectively.

Stresses: The mechanical effects on \mathcal{B}_t are given by surface tractions defined as the limit value of the force $\Delta \bar{\mathbf{f}}$ acting on an area element Δa passing through a point $\mathbf{x} \in \partial \mathcal{B}_t$:

$$\mathbf{t}(\mathbf{x}, t) := \lim_{\Delta a \rightarrow 0} \frac{\Delta \bar{\mathbf{f}}}{\Delta a} = \frac{d\bar{\mathbf{f}}}{da}. \quad (2.42)$$

Cauchy's theorem states that the traction vector in a point $\mathbf{x} \in \partial \mathcal{B}_t$ can be expressed as a linear function of the unit outward normal \mathbf{n} of the area element da in \mathbf{x}

$$\mathbf{t}(\mathbf{x}, t, \mathbf{n}) = \boldsymbol{\sigma}(\mathbf{x}, t) \mathbf{n}, \quad (2.43)$$

where $\boldsymbol{\sigma}$ are the *Cauchy stresses* and relates therefore the actual force to the actual area element.

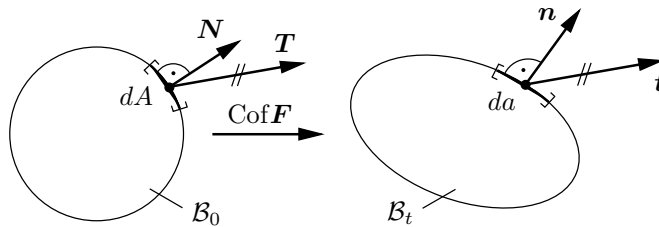


Figure 2.2: Coaxiality of the traction vectors $\mathbf{t} \in \partial \mathcal{B}_t$ and $\mathbf{T} \in \partial \mathcal{B}_0$.

Inserting the actual force depending on the undeformed area element dA , i.e.,

$$d\bar{\mathbf{f}} = \mathbf{t} da = \mathbf{T} dA \quad (2.44)$$

and the relation $d\mathbf{a}\mathbf{n} = \text{Cof}[\mathbf{F}]\mathbf{N}dA$, obtained from (2.15), into (2.43) leads to the definition of the *first Piola-Kirchhoff stress tensor* \mathbf{P} :

$$\boldsymbol{\sigma}\text{Cof}[\mathbf{F}]\mathbf{N}dA = \mathbf{T}dA \quad \Rightarrow \quad \mathbf{P} = \boldsymbol{\sigma}\text{Cof}\mathbf{F} = J\boldsymbol{\sigma}\mathbf{F}^{-T}. \quad (2.45)$$

Consequently the modified version of Cauchy's theorem reads

$$\mathbf{T}dA = \mathbf{P}dA = \mathbf{P}\mathbf{N}dA \quad \Rightarrow \quad \mathbf{T} = \mathbf{P}\mathbf{N}. \quad (2.46)$$

Due to (2.44) and (2.46) \mathbf{P} relates the actual force to the reference area element. The first Piola-Kirchhoff stress tensor can be alternatively expressed as

$$\mathbf{P} = \boldsymbol{\tau}\mathbf{F}^{-T} \quad \Rightarrow \quad \boldsymbol{\tau} = J\boldsymbol{\sigma}, \quad (2.47)$$

where the *Kirchhoff stress tensor* $\boldsymbol{\tau}$ is introduced, which is also denoted as *weighted Cauchy stress tensor*. Finally, we introduce the *second Piola-Kirchhoff stress tensor* \mathbf{S} . It represents the Lagrangian counterpart of the Kirchhoff stress tensor and is calculated by the pull-back operation

$$\mathbf{S} := \mathbf{F}^{-1}\boldsymbol{\tau}\mathbf{F}^{-T} = \mathbf{F}^{-1}\mathbf{P} = J\mathbf{F}^{-1}\boldsymbol{\sigma}\mathbf{F}^{-T}. \quad (2.48)$$

Heat Flux: The thermal effects on \mathcal{B}_t are described by a scalar-valued heat flux q acting on the surface $\partial\mathcal{B}_t$ in outward normal direction. Taking *Stoke's heat flux theorem* into account, the heat flux in a point $\mathbf{x} \in \partial\mathcal{B}_t$ can be expressed as a linear function of the outward normal vector \mathbf{n} passing $\mathbf{x} \in \partial\mathcal{B}_t$ and associated with the area element da :

$$q(\mathbf{x}, t, \mathbf{n}) = \mathbf{q}(\mathbf{x}, t) \mathbf{n}, \quad (2.49)$$

where \mathbf{q} denotes the *Cauchy heat flux vector*. From Nanson's formula (2.15)

$$\mathbf{q}da = \mathbf{q}\text{Cof}[\mathbf{F}]dA$$

we obtain the material counterpart

$$Q_0dA = \mathbf{Q}_0dA = \mathbf{Q}_0\mathbf{N}dA, \quad \text{with} \quad \mathbf{Q}_0 = \mathbf{q}\text{Cof}\mathbf{F}. \quad (2.50)$$

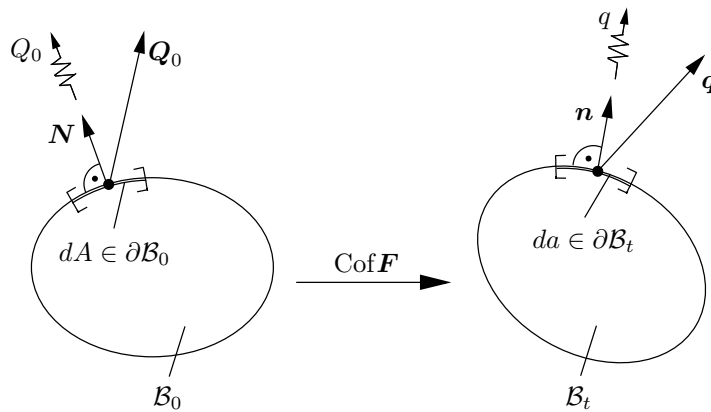


Figure 2.3: Heat flux Q_0 and q with respect to the reference and current placement.

2.6 Balance Principles.

Conservation laws and balance principles for physical quantities constitute the physical basis of continuum mechanics. They are material-independent, i.e., they are valid for every continuum. In detail, four balance equations and one inequality are provided: conservation of mass, balance of linear momentum, balance of angular momentum, balance of energy and the entropy inequality, also referred to as *Clausius-Duhem-Inequality*. In general, these laws balance the material time derivative of a physical quantity A , i.e., $\dot{A} := \frac{d}{dt} A$, with $A := \int_{\mathcal{B}_t} a \, dv$, under consideration of sources z inside the body, sources $\mathbf{s} \cdot \mathbf{n}$ on the surface of the body, where \mathbf{n} is the outward unit normal of the surface, as well as production p inside the body. The general form of the balance principles can be derived as follows: Let the body be represented in the actual configuration \mathcal{B}_t . The material time derivative of the integral equation of Eulerian fields a is

$$\begin{aligned} \dot{A} = \frac{d}{dt} A &= \frac{d}{dt} \int_{\mathcal{B}_t} a \, dv = \frac{d}{dt} \int_{\mathcal{B}_0} a J \, dV = \int_{\mathcal{B}_0} (\dot{a} J + a \dot{J}) \, dV \\ &= \int_{\mathcal{B}_t} (\dot{a} + a \operatorname{div} \mathbf{v}) \, dv = \int_{\mathcal{B}_t} \frac{\partial a}{\partial t} \, dv + \int_{\partial \mathcal{B}_t} a \mathbf{v} \cdot \mathbf{n} \, da, \end{aligned} \quad (2.51)$$

where the relations (2.40), (2.16) and

$$\operatorname{div}[a \mathbf{v}] = \operatorname{grad} a \cdot \mathbf{v} + a \operatorname{div} \mathbf{v} \Leftrightarrow a \operatorname{div} \mathbf{v} = \operatorname{div}[a \mathbf{v}] - \operatorname{grad} a \cdot \mathbf{v} \quad (2.52)$$

as well as the material time derivative $\dot{a} = \frac{\partial a}{\partial t} + \operatorname{grad} a \cdot \mathbf{v}$ and the Gauss divergence theorem

$$\int_{\mathcal{B}_t} \operatorname{div}[a \mathbf{v}] \, dv = \int_{\partial \mathcal{B}_t} a \mathbf{v} \cdot \mathbf{n} \, da, \quad (2.53)$$

are used. Thus, the general global form of the spatial balance law appears as

$$\dot{A} = \frac{d}{dt} A = \int_{\mathcal{B}_t} \frac{\partial a}{\partial t} \, dv + \int_{\partial \mathcal{B}_t} a \mathbf{v} \cdot \mathbf{n} \, da = \int_{\mathcal{B}_t} z \, dv + \int_{\partial \mathcal{B}_t} \mathbf{s} \cdot \mathbf{n} \, da + \int_{\mathcal{B}_t} p \, dv. \quad (2.54)$$

Application of the localization theorem and Gauss divergence theorem (2.53) once again yields the corresponding local or strong form of the spatial balance law (2.54), valid for any $\mathbf{x} \in \mathcal{B}_t$, i.e.,

$$\dot{a} + a \operatorname{div} \mathbf{v} = z + \operatorname{div}[\mathbf{s}] + p. \quad (2.55)$$

For the Clausius-Duhem-Inequality the equations (2.54) and (2.55) carry over obviously with \geq instead $=$.

Conservation of Mass. The law of conservation of mass states that the mass M in a closed system remains constant during the deformation process. The *first global form of conservation of mass* reads

$$M := \int_{\mathcal{B}_0} \rho_0(\mathbf{X}) \, dV = \int_{\mathcal{B}_t} \rho(\mathbf{x}, t) \, dv = m = \text{const.}, \quad (2.56)$$

where ρ_0 and ρ are the referential and actual density, respectively. Exploiting the transformation of volume elements (2.16) yields the *first local form of conservation of mass*

$$\rho_0 = J \rho, \quad \forall \mathbf{X} \in \mathcal{B}_0. \quad (2.57)$$

This equation makes clear that the Jacobian determinant can be interpreted as volume ratio. Thus, for $A = m$, $a = \rho$, $z = 0$, $\mathbf{s} = \mathbf{0}$, $p = 0$ the *second global form of conservation of mass* follows from (2.54), with

$$\dot{m} = \frac{d}{dt} \int_{\mathcal{B}_t} \rho \, dv = \int_{\mathcal{B}_t} \frac{\partial \rho}{\partial t} \, dv + \int_{\partial \mathcal{B}_t} \rho \mathbf{v} \cdot \mathbf{n} \, da = 0, \quad (2.58)$$

and the *second local form of conservation of mass* obtained from (2.55) finally reads:

$$\dot{\rho} + \rho \operatorname{div} \mathbf{v} = 0, \quad \forall \mathbf{x} \in \mathcal{B}_t. \quad (2.59)$$

Balance of Linear Momentum. The balance of linear momentum states that the rate of change of the linear momentum L is equal to the external resultant force \mathbf{f}^{ext} , i.e., $\dot{L} = \mathbf{f}^{ext}$, with $L := \int_{\mathcal{B}_t} \rho \mathbf{v} \, dv$ and $\mathbf{f}^{ext} := \int_{\mathcal{B}_t} \rho \mathbf{f} \, dv + \int_{\partial \mathcal{B}_t} \bar{\mathbf{t}} \, da$; \mathbf{f} is the volume acceleration and $\bar{\mathbf{t}}$ the traction vector acting on the surface $\partial \mathcal{B}_t$. Considering Cauchy's theorem (2.43), Gauss divergence theorem (2.53) yielding

$$\int_{\partial \mathcal{B}_t} \bar{\mathbf{t}} \, da = \int_{\partial \mathcal{B}_t} \boldsymbol{\sigma} \mathbf{n} \, da = \int_{\mathcal{B}_t} \operatorname{div} \boldsymbol{\sigma} \, dv, \quad (2.60)$$

the conservation law of mass (2.59) and setting $a = \rho \mathbf{v}$, $z = \rho \mathbf{f}$, $\mathbf{s} = \boldsymbol{\sigma}$, $p = 0$ in (2.54) and (2.55), respectively, we get the *global form of the spatial balance of linear momentum*

$$\int_{\mathcal{B}_t} \rho \dot{\mathbf{v}} \, dv = \int_{\mathcal{B}_t} (\rho \mathbf{f} + \operatorname{div} \boldsymbol{\sigma}) \, dv, \quad (2.61)$$

and the *local form of the spatial balance of linear momentum*

$$\rho \dot{\mathbf{v}} = \operatorname{div} \boldsymbol{\sigma} + \rho \mathbf{f} \quad \Rightarrow \quad \operatorname{div} \boldsymbol{\sigma} + \rho(\mathbf{f} - \dot{\mathbf{v}}) = 0 \quad \forall \mathbf{x} \in \mathcal{B}_t. \quad (2.62)$$

This fundamental statement is also called *Cauchy's first equation of motion*. Considering (2.16) and (2.57) as well as Gauss divergence theorem (2.53) and (2.44) which yields

$$\int_{\mathcal{B}_t} \operatorname{div} \boldsymbol{\sigma} \, dv = \int_{\partial \mathcal{B}_t} \boldsymbol{\sigma} \mathbf{n} \, da = \int_{\partial \mathcal{B}_t} \boldsymbol{\sigma} \, d\mathbf{a} = \int_{\partial \mathcal{B}_0} \mathbf{P} \mathbf{N} \, dA = \int_{\mathcal{B}_0} \operatorname{Div} \mathbf{P} \, dV, \quad (2.63)$$

the *local form of the material balance of linear momentum* is given by

$$\operatorname{Div} \mathbf{P} + \rho_0(\mathbf{f} - \dot{\mathbf{v}}) = 0 \quad \forall \mathbf{X} \in \mathcal{B}_0. \quad (2.64)$$

Balance of Angular Momentum. The balance of angular momentum is an independent axiom, which postulates that the rate of change of the angular momentum $\mathbf{h}_{(0)}$ that refers to the fixed point \mathbf{x}_0 of the body \mathcal{B}_t is equal to the resultant moment $\mathbf{m}_{(0)}$ of all forces acting on \mathcal{B}_t , i.e., $\dot{\mathbf{h}}_{(0)} = \mathbf{m}_{(0)}$, with $\mathbf{h}_{(0)} := \int_{\mathcal{B}_t} \mathbf{r} \times \rho \mathbf{v} \, dv$ and $\mathbf{m}_{(0)} := \int_{\mathcal{B}_t} \mathbf{r} \times \rho \mathbf{f} \, dv + \int_{\partial \mathcal{B}_t} \mathbf{r} \times \bar{\mathbf{t}} \, da$; \mathbf{r} denotes the moment arm, defined as $\mathbf{r} := \mathbf{x} - \mathbf{x}_0$. Inserting the values $a = \mathbf{r} \times \rho \mathbf{v}$, $z = \mathbf{r} \times \rho \mathbf{f}$, $\mathbf{s} \cdot \mathbf{n} = \mathbf{r} \times \bar{\mathbf{t}}$, $p = 0$ in (2.54) and taking into account the relation

$$\int_{\partial \mathcal{B}_t} \mathbf{r} \times \bar{\mathbf{t}} \, da = \int_{\mathcal{B}_t} (\mathbf{r} \times \operatorname{div} \boldsymbol{\sigma} + \boldsymbol{\epsilon} : \boldsymbol{\sigma}^T) \, dv, \quad (2.65)$$

where ϵ denotes the third order permutation tensor with index notation $(2.3)_2$, as well as (2.62) we finally obtain the *global and local form of the spatial balance of angular momentum*

$$\begin{aligned} \int_{\mathcal{B}_t} \mathbf{r} \times [\operatorname{div} \boldsymbol{\sigma} + \rho(\mathbf{f} - \dot{\mathbf{v}})] dv + \int_{\mathcal{B}_t} \epsilon : \boldsymbol{\sigma}^T dv &= \mathbf{0} \\ \Rightarrow \int_{\mathcal{B}_t} \epsilon : \boldsymbol{\sigma}^T dv = \mathbf{0} &\Rightarrow \epsilon : \boldsymbol{\sigma}^T = \mathbf{0} \quad \forall \mathbf{x} \in \mathcal{B}_t, \end{aligned} \quad (2.66)$$

which is valid if and only if the Cauchy stress tensor is symmetric

$$\boldsymbol{\sigma} = \boldsymbol{\sigma}^T. \quad (2.67)$$

The latter equation (2.67) is also called *Cauchy's second equation of motion*. The relation (2.67) yields the symmetry of the second Piola-Kirchhoff stress tensor (2.48) and Kirchhoff stress tensor (2.47).

The symmetry of the Cauchy stresses is a consequence of the thus postulated balance of angular momentum. Note that in the framework of Cosserat theory or extended continuum mechanics the balance of angular momentum takes a different form and the Cauchy stresses are not necessary symmetric anymore, cf. NEFF [83] and MÜNCH [81].

Note on Stress Power. The rate of the mechanical work of deformations of the body \mathcal{B} due to volume and surface forces in the spatial setting reads

$$\dot{W} = \int_{\mathcal{B}_t} \rho \mathbf{f} \cdot \mathbf{v} dv + \int_{\partial \mathcal{B}_t} \bar{\mathbf{t}} \cdot \mathbf{v} da. \quad (2.68)$$

Exploiting Cauchy's theorem (2.43) and the divergence operation (2.52) under consideration of a vector and a tensor, the balance of linear momentum (2.62) and the balance of angular momentum (2.67) yields

$$\dot{W} = \int_{\mathcal{B}_t} (\rho \mathbf{f} + \operatorname{div} \boldsymbol{\sigma}) \cdot \mathbf{v} dv + \int_{\mathcal{B}_t} \boldsymbol{\sigma} : \mathbf{d} dv \quad \xrightarrow{\text{neglecting acceleration term}} \quad \dot{W} = \int_{\mathcal{B}_t} \boldsymbol{\sigma} : \mathbf{d} dv,$$

which is referred to as *stress power*. With the relation (2.16) and (2.47) we get

$$\dot{W} = \int_{\mathcal{B}_0} \boldsymbol{\tau} : \mathbf{d} dV.$$

Taking the definition of the spatial velocity gradient (2.38) into account we obtain finally the stress power in the material setting

$$\dot{W} = \int_{\mathcal{B}_0} \boldsymbol{\tau} : (\dot{\mathbf{F}} \mathbf{F}^{-1}) dV = \int_{\mathcal{B}_0} \mathbf{P} : \dot{\mathbf{F}} dV = \int_{\mathcal{B}_0} \mathbf{S} : (\mathbf{F}^T \dot{\mathbf{F}})_{sym} dV = \int_{\mathcal{B}_0} \mathbf{S} : \dot{\mathbf{E}} dV.$$

Note that the quantity $\dot{\mathbf{E}}$ is defined by a pull-back operation of \mathbf{d} , i.e., $\dot{\mathbf{E}} = \frac{1}{2} \dot{\mathbf{C}} = \mathbf{F}^T \mathbf{d} \mathbf{F} = (\mathbf{F}^T \dot{\mathbf{F}})_{sym}$. The pairs of quantities

$$(\mathbf{P}, \dot{\mathbf{F}}), \quad (\mathbf{S}, \dot{\mathbf{E}}), \quad (\boldsymbol{\tau}, \mathbf{d}) \quad (2.69)$$

are called *work-conjugated pairs*.

First Principle of Thermodynamics (Balance of Energy). The first principle of thermodynamics postulates that the temporal change of total energy of a physical body is equal to the sum of the rate of work of all forces and all other energies entering and leaving the body per unit time. The total energy can be additively split into the kinetic energy \mathcal{K} and the internal energy \mathcal{E} , with

$$\mathcal{K} := \int_{\mathcal{B}_t} \frac{1}{2} \rho \mathbf{v} \cdot \mathbf{v} \, dv, \quad \mathcal{E} := \int_{\mathcal{B}_t} \rho e \, dv, \quad (2.70)$$

where e denotes the specific energy density per unit mass. A temporal change of the total energy is equal to the power of mechanical tractions and body forces (2.68) denoted here by \mathcal{P} and the thermal power \mathcal{Q} , i.e.,

$$\mathcal{P} := \dot{W}, \quad \mathcal{Q} := \int_{\mathcal{B}_t} \rho r \, dv - \int_{\partial \mathcal{B}_t} q \, da, \quad (2.71)$$

with the heat supply r per unit mass and unit time, and the heat flux q defined in (2.49). Thus, using the heat flux theorem as well as Cauchy's theorem (2.43), setting $A = \mathcal{K} + \mathcal{E}$, $a = \rho(e + \frac{1}{2}\|\mathbf{v}\|^2)$, $z = \rho \mathbf{v} \cdot \mathbf{f}$, $\mathbf{s} = (\mathbf{v} \cdot \boldsymbol{\sigma} - \mathbf{q})$, $p = \rho r$ in (2.54) and (2.55), respectively, as well as (2.59) and (2.62) leads to the *global and local forms of the spatial balance of energy*

$$\frac{d}{dt}(\mathcal{K} + \mathcal{E}) = \mathcal{P} + \mathcal{Q} \quad \Rightarrow \quad \rho \dot{e} = \rho r - \operatorname{div} \mathbf{q} + \boldsymbol{\sigma} : \mathbf{d}, \quad \forall \mathbf{x} \in \mathcal{B}_t. \quad (2.72)$$

Second Principle of Thermodynamics (Clausius-Duhem Inequality). The second law of thermodynamics states that there naturally exists a process direction for thermomechanical processes. The simplest formulation of the second law, according to Rudolf Clausius (1822-1888), reads:

Wärme kann nicht von selbst von einem kälteren in einen wärmeren Körper übergehen.

The axiom can be expressed through the inequality (*global form of spatial entropy inequality*)

$$\frac{d}{dt} \int_{\mathcal{B}_t} \rho \eta \, dv \geq \int_{\mathcal{B}_t} \frac{\rho r}{\Theta} \, dv - \int_{\partial \mathcal{B}_t} \frac{q}{\Theta} \, da, \quad (2.73)$$

which is also referred to as *Clausius-Duhem Inequality*. It means that the temporal change of total entropy $H_e = \int_{\mathcal{B}_t} \rho \eta \, dv$ with the specific entropy per unit mass η is always greater than or equal to the sum of the supply of entropy through surface due to heat flux $-q/\Theta$ and the entropy inside the body $\rho r/\Theta$ due to evolution of temperature. Θ denotes the absolute temperature. Inserting $A = H_e$, $a = \rho \eta$, $z = 0$, $\mathbf{s} = -\mathbf{q}/\Theta$, $p = \rho r/\Theta$ in (2.54) and (2.55), respectively, considering the balance of energy (2.72) and the conservation of mass (2.59) the *local form of spatial entropy inequality* can be represented as

$$\rho \Theta \dot{\eta} - \rho \dot{e} + \boldsymbol{\sigma} : \mathbf{d} - \frac{1}{\Theta} \mathbf{q} \cdot \operatorname{grad} \Theta \geq 0 \quad \forall \mathbf{x} \in \mathcal{B}_t. \quad (2.74)$$

The restriction on the description of isothermal processes characterized by constant temperature, i.e., $\dot{\Theta} = 0$, as well as the introduction of volume-specific values for the internal

energy $\bar{e} = \rho e$, the internal heat production $\bar{r} = \rho r$ and the entropy $\bar{\eta} = \rho \eta$ simplify (2.74) and we obtain

$$\Theta \dot{\bar{\eta}} - \dot{\bar{e}} + \boldsymbol{\sigma} : \mathbf{d} \geq 0 \quad \forall \mathbf{x} \in \mathcal{B}_t. \quad (2.75)$$

As thermodynamical potential we choose the Helmholtz free energy $\bar{\psi}$ per unit actual volume defined by $\bar{\psi} = \rho \tilde{\psi}$ with $\tilde{\psi} = e - \Theta \eta$, so that (2.75) can be reformulated to

$$-\dot{\bar{\psi}} + \boldsymbol{\sigma} : \mathbf{d} \geq 0 \quad \forall \mathbf{x} \in \mathcal{B}_t. \quad (2.76)$$

Taking into account the work-conjugated pairs (2.69) we obtain the material form of (2.76)

$$\mathbf{S} : \dot{\mathbf{E}} - \dot{\bar{\psi}} \geq 0, \quad \forall \mathbf{X} \in \mathcal{B}_0, \quad (2.77)$$

where the Helmholtz free energy function ψ is defined per unit reference volume, i.e., $\psi := \rho_0 \tilde{\psi}$. Neglecting electrical power, the free energy ψ depends only on the strain measure (here \mathbf{E}) and the temperature Θ as process variables. For isothermal processes the material time derivative of ψ results in $\dot{\bar{\psi}} = \partial_{\mathbf{E}} \psi : \dot{\mathbf{E}}$; thus, we get

$$\mathbf{S} : \dot{\mathbf{E}} - \frac{\partial \psi}{\partial \mathbf{E}} : \dot{\mathbf{E}} \geq 0 \quad \forall \mathbf{X} \in \mathcal{B}_0, \quad (2.78)$$

which is postulated to hold for all independent processes. Since we restrict ourselves in the sequel to the description of reversible processes, the inequality sign in (2.76) can be replaced by an equal sign, so that we obtain a tensor-valued function for the second Piola-Kirchhoff stresses formulated in terms of \mathbf{E}

$$\mathbf{S} := \frac{\partial \psi}{\partial \mathbf{E}} = 2 \frac{\partial \psi}{\partial \mathbf{C}}, \quad \text{with} \quad S^{AB} = \frac{\partial \psi}{\partial E_{AB}} = 2 \frac{\partial \psi}{\partial C_{AB}}, \quad (2.79)$$

which represents the so-called *constitutive equation* for the stresses, i.e., a functional dependence between the stress quantity \mathbf{S} and strain quantity $\mathbf{E} = \mathbf{E}(\text{Grad} \mathbf{u})$ or deformation quantity $\mathbf{C} = \mathbf{C}(\text{Grad} \mathbf{u})$, respectively. The resulting symmetric tangent moduli is

$$\mathbb{C} := \frac{\partial \mathbf{S}}{\partial \mathbf{E}} = \frac{\partial^2 \psi}{\partial \mathbf{E} \partial \mathbf{E}} = 4 \frac{\partial^2 \psi}{\partial \mathbf{C} \partial \mathbf{C}}, \quad \text{with} \quad \mathbb{C}^{ABCD} = 2 \frac{\partial S^{AB}}{\partial C_{CD}}. \quad (2.80)$$

In order to determine the constitutive equation for the Cauchy stresses we use the relation

$$\boldsymbol{\sigma} = \frac{2}{J} (\mathbf{F} \frac{\partial \psi}{\partial \mathbf{C}} \mathbf{F}^T),$$

obtained by inserting (2.79) into (2.48). Considering the work-conjugated pair $(\mathbf{P}, \dot{\mathbf{F}})$ (2.69) the material form of (2.76) reads

$$\mathbf{P} : \dot{\mathbf{F}} - \dot{\bar{\psi}} \geq 0, \quad \forall \mathbf{X} \in \mathcal{B}_0. \quad (2.81)$$

Thus, the free energy ψ is here a function of the *primary variables* \mathbf{F} and Θ . With regard to isothermal processes we obtain

$$\mathbf{P} : \dot{\mathbf{F}} - \frac{\partial \psi}{\partial \mathbf{F}} : \dot{\mathbf{F}} \geq 0 \quad \forall \mathbf{X} \in \mathcal{B}_0. \quad (2.82)$$

Hence, the first Piola-Kirchhoff stresses can be derived by the first derivative of ψ with respect to \mathbf{F}

$$\mathbf{P} := \frac{\partial \psi}{\partial \mathbf{F}}, \quad \text{with} \quad P_a^A = \frac{\partial \psi}{\partial F_A^a}, \quad (2.83)$$

which is the constitutive equation for the first Piola-Kirchhoff stress tensor. \mathbf{P} is therefore not symmetric. The corresponding tangent moduli is called *Nominal Tangent* and given by

$$\mathbb{A} := \frac{\partial}{\partial \mathbf{F}} \left(\frac{\partial \psi}{\partial \mathbf{F}} \right), \quad \text{with} \quad \mathbb{A}_a^A{}_b^B = \frac{\partial}{\partial F_B^b} \left(\frac{\partial \psi}{\partial F_A^a} \right). \quad (2.84)$$

2.7 Constitutive Equations for Hyperelastic Materials.

The balance laws are valid for all bodies; a specification of the material behavior can be done by suitable constructions of the constitutive equations. For the formulation of suitable constitutive equations some of the most important principles providing helpful advices for a physically reasonable material modeling may be taken into account: the axioms of i) *causality*, ii) *determinism*, iii) *equipresence*, iv) *objectivity*, v) *material invariance*, vi) *neighborhood*, vii) *memory*, viii) *admissibility* and ix) *dissipation*. We focus in the following on the principles iv) and v). For more details the reader is referred to advanced textbooks, e.g. NOLL [87], MARSDEN & HUGHES [72], HOLZAPFEL [62]. The axiom of admissibility requires that the constitutive equations do not have to contradict the balance equations and the second law of thermodynamics. Material models, which fulfill these conditions, are said to be *thermodynamically consistent*.

Moreover, we consider *homogeneous* elastic materials, i.e., their properties are the same for all material points. Therefore, the constitutive equations do not depend explicitly on the material points \mathbf{X} . Thus, we obtain for instance for the constitutive equations in the reference setting

$$\psi = \psi(\mathbf{X}, \mathbf{F}) = \psi(\mathbf{F}), \quad \mathbf{P} = \mathbf{P}(\mathbf{X}, \mathbf{F}) = \mathbf{P}(\mathbf{F}).$$

2.7.1 Principle of Material Frame Indifference – Objectivity. The principle of material frame indifference requires:

The constitutive equations must be indifferent against a change of reference system.

That means that they have to be observer independent. Observer independence or objectivity of physical quantities is defined in section 2.3.

Let us consider two motionless observers of a deformation of a homogeneous, elastic body. The first observer B_1 describe the deformation of each material point position \mathbf{X} by $\mathbf{x}(\mathbf{X})$, whereas the second observer B_2 describe the deformation of each material point position by $\mathbf{x}^+(\mathbf{X})$.

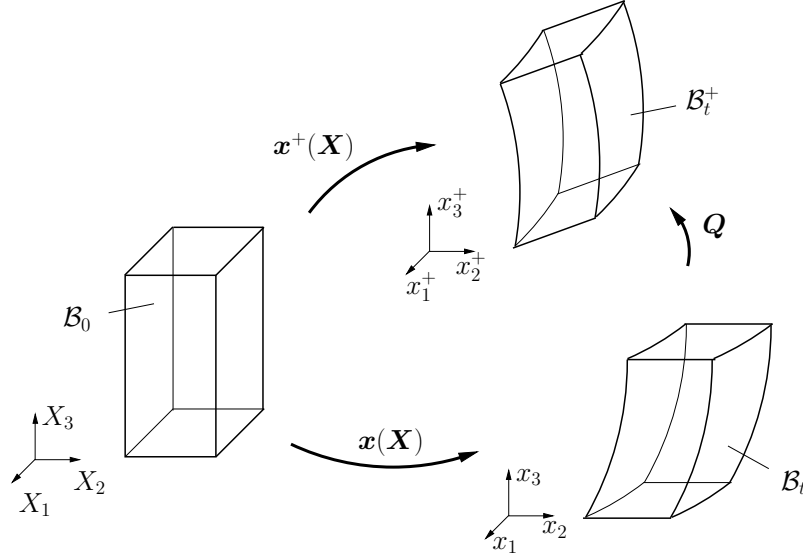


Figure 2.4: Rigid body motion of the actual configuration.

The material point positions $\mathbf{x}(\mathbf{X})$ transform under an Euclidean transformation, also known as rigid body motion (here for the static case: rigid transformation), onto the positions $\mathbf{x}^+(\mathbf{X})$, i.e.,

$$\mathbf{x}^+(\mathbf{X}) = \mathbf{Q} \mathbf{x}(\mathbf{X}) + \mathbf{c} \quad \forall \mathbf{Q} \in \text{SO}(3),$$

where \mathbf{Q} is a rigid body rotation, see Figure 2.4. For the associated deformation gradient $\mathbf{F}^+ = \text{Grad} \mathbf{x}^+$ the relation

$$\mathbf{F}^+ = \frac{\partial \mathbf{x}^+}{\partial \mathbf{x}} \frac{\partial \mathbf{x}}{\partial \mathbf{X}} = \mathbf{Q} \mathbf{F} \quad (2.85)$$

holds.

The principle of material frame indifference requires that the observers secure the same energy and stress state of the deformed body. Therefore, it demands that the constitutive equations also fulfill the rigid transformation rule, i.e., they have to be observer independent (objective):

$$\psi(\mathbf{Q}\mathbf{F}) = \psi(\mathbf{F}), \quad \mathbf{P}(\mathbf{Q}\mathbf{F}) = \mathbf{Q}\mathbf{P}(\mathbf{F}) \quad \forall \mathbf{Q} \in \text{SO}(3). \quad (2.86)$$

The availability of the a priori objective right Cauchy-Green tensor $\mathbf{C}^+ = \mathbf{C} = \mathbf{U}^2$, cf. (2.33), motivates to use reduced constitutive equations that depend only on the right stretch tensor of deformation \mathbf{U} and a priori fulfill the principle of material frame indifference (2.86), i.e.,

$$\psi(\mathbf{C}) = \psi(\mathbf{C}^+), \quad \forall \mathbf{Q} \in \text{SO}(3), \quad (2.87)$$

see e.g. TRUESDELL & NOLL [127]. Thus, in the sequel we use for the formulation of the constitutive equations the functional dependence (2.87). The corresponding stress tensor (2.79), i.e., the second Piola-Kirchhoff stress tensor, and the tangent moduli (2.80) are then calculated by

$$\mathbf{S} = 2 \frac{\partial \psi(\mathbf{C})}{\partial \mathbf{C}}, \quad \mathbb{C} = 4 \frac{\partial^2 \psi(\mathbf{C})}{\partial \mathbf{C} \partial \mathbf{C}}. \quad (2.88)$$

2.7.2 Principle of Material Symmetry. The principle of objectivity requires the indifference of the constitutive equations under a change of reference frame. The constitutive equations must also reflect the symmetry of the physical properties of the underlying material. The principle of material symmetry requires:

The constitutive equations have to be invariant with respect to all transformations of the material coordinates, which belong to the symmetry group \mathcal{G} of the underlying material.

For isotropic materials, the material behavior is identical in all directions, i.e., the constitutive equations are independent against a change of the reference configuration. Thus, an arbitrary reference configuration can be chosen.

For anisotropic materials, there can be special directions in the materials, along which its physical properties are identical. For instance, the material properties of an elastic tetragonal material must be invariant e.g. against the rotation of the reference configuration by 90° , see Figure 2.5. Thus, for anisotropic materials, the constitutive equations have to be independent against a change of the reference configuration under symmetry transformations of the underlying material.

Let us consider the reference configuration \mathcal{B}_0 defined by the material point positions \mathbf{X} (Figure 2.5). The change of this configuration to a second reference configuration \mathcal{B}_0^+ is defined by the one-to-one correspondence of the respective position vectors of the material points, i.e.,

$$\mathbf{X}^+ = \mathbf{Q}\mathbf{X}, \quad \forall \mathbf{Q} \in \mathcal{G} \subset \text{O}(3),$$

where \mathbf{Q} are symmetry transformations belonging to the underlying material symmetry group \mathcal{G} . The material points of the actual configuration \mathcal{B}_t are then given with respect to both reference systems:

$$\mathbf{x} = \mathbf{x}(\mathbf{X}) = \mathbf{x}(\mathbf{X}^+). \quad (2.89)$$

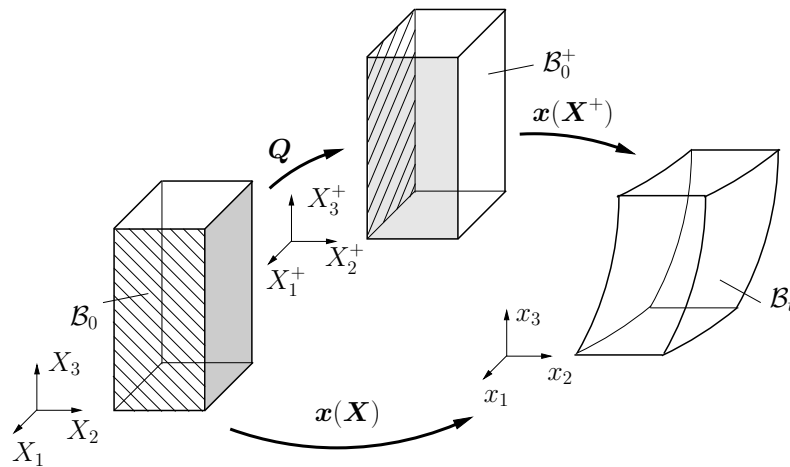


Figure 2.5: Orthogonal Transformations of the reference configuration.

The associated deformation gradient is defined by

$$\mathbf{F}^+ = \frac{\partial \mathbf{x}}{\partial \mathbf{X}} \frac{\partial \mathbf{X}}{\partial \mathbf{X}^+} = \mathbf{F} \mathbf{Q}^T, \quad (2.90)$$

see Figure 2.5. Then, the principle of material symmetry demands that the reduced constitutive equations $\psi(\mathbf{C})$ and $\mathbf{S}(\mathbf{C})$ ^{1.)} have to transform as follows

$$\left. \begin{aligned} \psi(\mathbf{C}) &= \psi(\mathbf{Q} \mathbf{C} \mathbf{Q}^T) \\ \mathbf{Q} \mathbf{S}(\mathbf{C}) \mathbf{Q}^T &= \mathbf{S}(\mathbf{Q} \mathbf{C} \mathbf{Q}^T) \end{aligned} \right\} \quad \forall \mathbf{Q} \in \mathcal{G} \subset \text{O}(3). \quad (2.91)$$

The material symmetry group \mathcal{G} reflects the symmetry of the physical properties of the material. Therefore, it has to be specified for the considered material. Material symmetry groups for crystalline and non-crystalline materials are presented in the next chapter. If \mathcal{G} is equal to the full orthogonal group $\text{O}(3)$, then the material is isotropic. Otherwise, it is anisotropic.

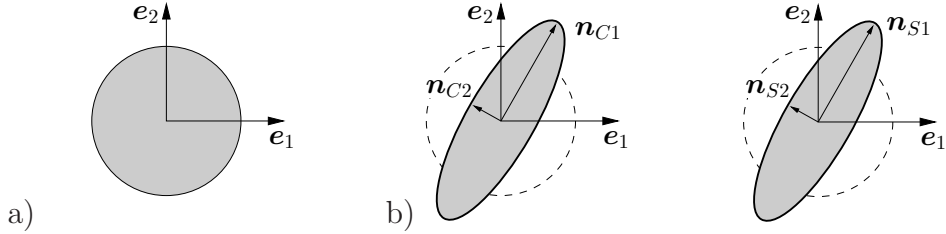


Figure 2.6: Characterization of isotropic elastic material behavior: a) reference configuration, b) deformed configuration: (left) with principal directions $\mathbf{n}_{C1}, \mathbf{n}_{C2}$ of deformation \mathbf{C} , (right) with principal directions $\mathbf{n}_{S1}, \mathbf{n}_{S2}$ of the stresses \mathbf{S} , which are coaxial to $\mathbf{n}_{C1}, \mathbf{n}_{C2}$.

For isotropic material response, one observes a coaxiality of the principal directions of the right Cauchy-Green deformation tensor \mathbf{C} and the second Piola-Kirchhoff stress tensor \mathbf{S} , i.e., $\mathbf{n}_{C1} = \mathbf{n}_{S1}$, $\mathbf{n}_{C2} = \mathbf{n}_{S2}$, see Figure 2.6.

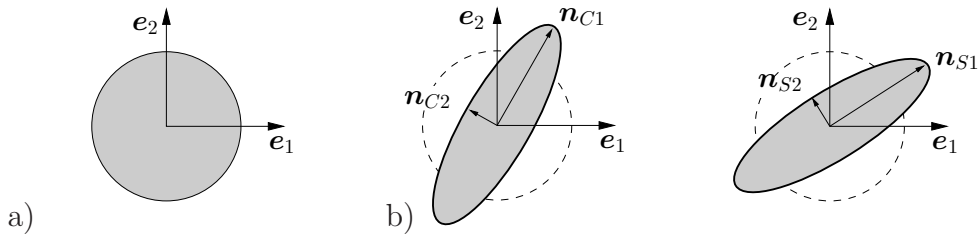


Figure 2.7: Characterization of anisotropic elastic material behavior: a) reference configuration, b) deformed configuration: (left) with principal directions $\mathbf{n}_{C1}, \mathbf{n}_{C2}$ of deformation \mathbf{C} , (right) with principal directions $\mathbf{n}_{S1}, \mathbf{n}_{S2}$ of the stresses \mathbf{S} , which are non-coaxial to $\mathbf{n}_{C1}, \mathbf{n}_{C2}$.

One of the main characteristic of an anisotropic material is the non-coaxiality of the eigenvectors of the stress tensor \mathbf{S} ($\mathbf{n}_{S1}, \mathbf{n}_{S2}$) and the deformation tensor \mathbf{C} ($\mathbf{n}_{C1}, \mathbf{n}_{C2}$), see Fig. 2.7.

^{1.)}We use constitutive equations in terms of the objective right Cauchy-Green tensor, since we fulfill in this way a priori the principle of objectivity.

2.8 Boundary Value Problem and Variational Formulation.

A nonlinear boundary value problem is characterized by a set of nonlinear differential equations (i), i.e., in case of isothermal and quasi-static, hyperelastic problems the balance of linear momentum (2.64) together with the constitutive equation (2.83) (section 2.7), and boundary conditions (ii). A solution of the boundary value problem is a solution of the system of differential equations, which satisfies the imposed boundary conditions.

(i) In case of hyperelasticity, the first Piola-Kirchhoff stresses \mathbf{P} is defined via the constitutive equation (2.83): $\mathbf{P} = \partial_F \psi$. If this is the case and the applied volume forces are conservative, i.e., $\rho_0 \mathbf{f}(\mathbf{u}) = \rho_0 \mathbf{f}$, the balance of linear momentum for the static case in the reference setting gives rise to the following system of three nonlinear partial differential equations with respect to the three unknown components of the displacement field \mathbf{u} :

$$\text{Div} \mathbf{P} + \rho_0 \mathbf{f} = \mathbf{0} \quad \forall \mathbf{X} \in \mathcal{B}_0, \quad (2.92)$$

which is also referred to as *strong form of equilibrium*.

(ii) The reference surface of the body $\partial \mathcal{B}_0$ is divided into two non-overlapping parts: one part for prescribed deformations $\partial \mathcal{B}_{0\varphi}$ and one for prescribed stresses $\partial \mathcal{B}_{0t}$

$$\partial \mathcal{B}_0 = \partial \mathcal{B}_{0t} \cup \partial \mathcal{B}_{0\varphi} \quad \text{and} \quad \partial \mathcal{B}_{0t} \cap \partial \mathcal{B}_{0\varphi} = \emptyset. \quad (2.93)$$

The stresses at the boundaries of \mathcal{B}_0 are prescribed by *Neumann boundary conditions*, which are named after the mathematician Carl Gottfried Neumann (1832-1925), the son of (our) crystal physicist Franz Ernst Neumann (1798-1895), see page 27 (Neumann's Principle),

$$\mathbf{T} = \mathbf{P} \mathbf{N} = \bar{\mathbf{t}} \quad \text{on} \quad \partial \mathcal{B}_{0t} \quad (2.94)$$

and the deformations at the boundary are defined by *Dirichlet boundary conditions*

$$\varphi = \varphi_0 \quad \text{on} \quad \partial \mathcal{B}_{0\varphi}. \quad (2.95)$$

2.8.1 Variational Principles. In general it is impossible to find an analytical solution of the boundary value problem (2.92). Instead, discretization methods based on the direct methods of the calculus of variation can be applied. The direct methods of the calculus of variation lead here to the nonlinear, so-called *weak form of equilibrium*. In view of an iterative solution of the weak form by using the *Newton-Raphson iteration scheme*, the linearization of the weak form is required. The weak form is the basis for the application of the Finite-Element-Method. Here, we focus on the standard displacement formulation.

Multiplying the strong form of equilibrium (2.92) by a suitable vector-valued test function $\delta \varphi$, with $\delta \varphi = \mathbf{0}$ on $\partial \mathcal{B}_{0\varphi}$, and integrating over the volume of the body \mathcal{B}_0 yields

$$\int_{\mathcal{B}_0} (\text{Div} \mathbf{P} + \rho_0 \mathbf{f}) \cdot \delta \varphi \, dV = 0, \quad (2.96)$$

with the boundary conditions (2.94) and (2.95). Exploiting the identity

$$\text{Div} \mathbf{P} \cdot \delta \varphi = \text{Div}(\delta \varphi \cdot \mathbf{P}) - \mathbf{P} : \text{Grad} \delta \varphi \quad (2.97)$$

and the Gauss divergence theorem (2.53) we obtain the weak form of equilibrium

$$G(\boldsymbol{\varphi}, \delta\boldsymbol{\varphi}) := \underbrace{\int_{\mathcal{B}_0} \mathbf{P} : \delta\mathbf{F} dV}_{G^{int}} - \underbrace{\left\{ \int_{\mathcal{B}_0} \rho_0 \mathbf{f} \cdot \delta\boldsymbol{\varphi} dV + \int_{\partial\mathcal{B}_{0t}} \bar{\mathbf{t}} \cdot \delta\boldsymbol{\varphi} dA \right\}}_{G^{ext}} = 0, \quad (2.98)$$

with $\delta\mathbf{F} = \text{Grad}[\delta\boldsymbol{\varphi}]$.

The weak form of equilibrium is formally equivalent to the principle of virtual work. The test function is then the vector of virtual deformations, G^{int} the work of internal forces and G^{ext} the work of external forces acting on the body \mathcal{B}_0 . Solving the boundary value problem is formally equivalent to finding a stationary point $\boldsymbol{\varphi}$ of a functional, called the *total energy* or *potential* Π , with

$$\Pi(\boldsymbol{\varphi}) = \int_{\mathcal{B}_0} \psi(\mathbf{F}) dV - \int_{\mathcal{B}_0} \langle \rho_0 \mathbf{f}, \boldsymbol{\varphi} \rangle dV - \int_{\partial\mathcal{B}_{0t}} \langle \bar{\mathbf{t}}, \boldsymbol{\varphi} \rangle dA \rightarrow \text{stat.} \quad (2.99)$$

The associated Euler-Lagrange equations (the stationarity conditions) are obtained as follows: The classical methods of the calculus of variations are based on a family of variations $\boldsymbol{\varphi}^s$ given in the simple additive form

$$\boldsymbol{\varphi}^s = \boldsymbol{\varphi} + s \delta\boldsymbol{\varphi}, \quad (2.100)$$

and associated deformation gradient

$$\mathbf{F}^s = \text{Grad}\boldsymbol{\varphi} + s \text{Grad}\delta\boldsymbol{\varphi}, \quad \delta\mathbf{F}^s = \text{Grad}\delta\boldsymbol{\varphi} = \delta\mathbf{F}, \quad (2.101)$$

where $\delta\boldsymbol{\varphi}$ is an arbitrary continuous test function that vanishes at the boundary $\partial\mathcal{B}_{0\varphi}$ and $s \in \mathbb{R}$ is a scalar. The potential $\Pi(\boldsymbol{\varphi}^s)$ becomes stationary for $s = 0$, i.e.,

$$\Pi(\boldsymbol{\varphi}) = \Pi(\boldsymbol{\varphi}^s)|_{s=0} \rightarrow \text{stat.}, \quad (2.102)$$

if

$$\delta\Pi(\boldsymbol{\varphi}, \delta\boldsymbol{\varphi}) = \left. \frac{d}{ds} \right|_{s=0} \Pi(\boldsymbol{\varphi}^s) = 0 \quad (2.103)$$

holds. Inserting the family of variations (2.100) into (2.102) yields

$$\Pi(\boldsymbol{\varphi}^s) = \int_{\mathcal{B}_0} \psi(\mathbf{F}^s) dV - \int_{\mathcal{B}_0} \langle \rho_0 \mathbf{f}, \boldsymbol{\varphi}^s \rangle dV - \int_{\partial\mathcal{B}_{0t}} \langle \bar{\mathbf{t}}, \boldsymbol{\varphi}^s \rangle dA. \quad (2.104)$$

The derivative of the last equation with respect to s gives

$$\frac{d}{ds} \Pi(\boldsymbol{\varphi}^s) = \int_{\mathcal{B}_0} \langle \partial_F \psi(\mathbf{F}^s), \delta\mathbf{F}^s \rangle dV - \int_{\mathcal{B}_0} \langle \rho_0 \mathbf{f}, \boldsymbol{\varphi}^s \rangle dV - \int_{\partial\mathcal{B}_{0t}} \langle \bar{\mathbf{t}}, \boldsymbol{\varphi}^s \rangle dA, \quad (2.105)$$

so that (2.103) appears as

$$\delta\Pi(\boldsymbol{\varphi}, \delta\boldsymbol{\varphi}) = \left. \frac{d}{ds} \right|_{s=0} \Pi(\boldsymbol{\varphi}^s) = \int_{\mathcal{B}_0} \langle \mathbf{P}, \delta\mathbf{F} \rangle dV - \int_{\mathcal{B}_0} \langle \rho_0 \mathbf{f}, \delta\boldsymbol{\varphi} \rangle dV - \int_{\partial\mathcal{B}_{0t}} \langle \bar{\mathbf{t}}, \delta\boldsymbol{\varphi} \rangle dA = 0.$$

With the identity $\mathbf{P} : \delta\mathbf{F} = \text{Div}(\mathbf{P}\delta\boldsymbol{\varphi}) - \text{Div}\mathbf{P} \cdot \delta\boldsymbol{\varphi}$ and the Gauss divergence theorem we have

$$\delta\Pi(\boldsymbol{\varphi}, \delta\boldsymbol{\varphi}) = - \int_{\mathcal{B}_0} \langle (\text{Div}\mathbf{P} + \rho_0 \mathbf{f}), \delta\boldsymbol{\varphi} \rangle dV + \int_{\partial\mathcal{B}_{0t}} \langle (\mathbf{P}\mathbf{N} - \bar{\mathbf{t}}), \delta\boldsymbol{\varphi} \rangle dA = 0, \quad (2.106)$$

which must hold for arbitrary test functions $\delta\boldsymbol{\varphi}$ with $\delta\boldsymbol{\varphi} = \mathbf{0}$ on $\partial\mathcal{B}_{0\varphi}$. Using the fundamental lemma of the calculus of variations equation (2.106) is satisfied, if and only if

$$\text{Div}\mathbf{P} + \rho_0\mathbf{f} = \mathbf{0} \quad \forall \mathbf{X} \in \mathcal{B}_0, \quad \mathbf{P}\mathbf{N} = \bar{\mathbf{t}} \quad \text{on} \quad \partial\mathcal{B}_{0t}, \quad (2.107)$$

since $\delta\boldsymbol{\varphi}$ can be varied independently in the interior of \mathcal{B}_0 and on the boundary $\partial\mathcal{B}_{0t}$.

Alternatively, in terms of the symmetric stress tensor \mathbf{S} the weak form is

$$\boxed{\delta\Pi(\boldsymbol{\varphi}, \delta\boldsymbol{\varphi}) = \int_{\mathcal{B}_0} \mathbf{S} : \frac{1}{2}\delta\mathbf{C} dV - \int_{\mathcal{B}_0} \rho_0\mathbf{f} \cdot \delta\boldsymbol{\varphi} dV - \int_{\partial\mathcal{B}_{0t}} \bar{\mathbf{t}} \cdot \delta\boldsymbol{\varphi} dA = 0 =: G(\boldsymbol{\varphi}, \delta\boldsymbol{\varphi}),} \quad (2.108)$$

where the constitutive equation (2.48) and the variation of the Green-Lagrange strain tensor $\delta\mathbf{E} = \frac{1}{2}\delta\mathbf{C}$, with

$$\delta\mathbf{C} = (\delta\mathbf{F})^T \mathbf{F} + \mathbf{F}^T (\delta\mathbf{F}) \quad (2.109)$$

have been taken into account.

2.8.2 Linearization of the Variational Formulation. Since \mathbf{S} and therefore the weak form $G(\boldsymbol{\varphi}, \delta\boldsymbol{\varphi})$ are nonlinear functions in terms of the variable $\boldsymbol{\varphi}$, the weak form is solved iteratively by a Newton-Raphson iteration scheme. The Newton-Raphson iteration method is based on the linearization of $G(\boldsymbol{\varphi}, \delta\boldsymbol{\varphi})$ at $\boldsymbol{\varphi} = \bar{\boldsymbol{\varphi}}$

$$\text{Lin}G(\bar{\boldsymbol{\varphi}}, \delta\boldsymbol{\varphi}, \Delta\boldsymbol{\varphi}) = G(\bar{\boldsymbol{\varphi}}, \delta\boldsymbol{\varphi}) + \Delta G(\bar{\boldsymbol{\varphi}}, \delta\boldsymbol{\varphi}, \Delta\boldsymbol{\varphi}), \quad (2.110)$$

where the linear increment $\Delta G(\bar{\boldsymbol{\varphi}}, \delta\boldsymbol{\varphi}, \Delta\boldsymbol{\varphi})$ is calculated by the directional derivative of G at $\bar{\boldsymbol{\varphi}}$ in the direction of $\Delta\boldsymbol{\varphi}$, i.e.,

$$\Delta G(\bar{\boldsymbol{\varphi}}, \delta\boldsymbol{\varphi}, \Delta\boldsymbol{\varphi}) = \frac{d}{ds}[G(\bar{\boldsymbol{\varphi}} + s\Delta\boldsymbol{\varphi}, \delta\boldsymbol{\varphi})]|_{s=0} = DG(\bar{\boldsymbol{\varphi}}, \delta\boldsymbol{\varphi}) \cdot \Delta\boldsymbol{\varphi}, \quad (2.111)$$

with the incremental deformations $\Delta\boldsymbol{\varphi}$. Considering conservative loads $\rho_0\mathbf{f}$ and $\bar{\mathbf{t}}$, evaluating (2.111) results in

$$\Delta G(\bar{\boldsymbol{\varphi}}, \delta\boldsymbol{\varphi}, \Delta\boldsymbol{\varphi}) = DG^{int}(\bar{\boldsymbol{\varphi}}, \delta\boldsymbol{\varphi}) \cdot \Delta\boldsymbol{\varphi} = \int_{\mathcal{B}_0} \Delta\mathbf{S} : \frac{1}{2}\delta\mathbf{C} dV + \int_{\mathcal{B}_0} \mathbf{S} : \frac{1}{2}\Delta\delta\mathbf{C} dV, \quad (2.112)$$

with the increment of the second Piola-Kirchhoff stresses \mathbf{S} , the increment of the right Cauchy-Green tensor \mathbf{C} and of (2.109)

$$\begin{aligned} \Delta\mathbf{S} &= \mathbb{C} : \frac{1}{2}\Delta\mathbf{C} \quad \text{with} \quad \mathbb{C} = 2\frac{\partial\mathbf{S}}{\partial\mathbf{C}} = 4\frac{\partial^2\psi}{\partial\mathbf{C}\partial\mathbf{C}}, \\ \Delta\mathbf{C} &= \Delta\mathbf{F}^T \mathbf{F} + \mathbf{F}^T \Delta\mathbf{F}, \\ \Delta\delta\mathbf{C} &= \delta\mathbf{F}^T \Delta\mathbf{F} + \Delta\mathbf{F}^T \delta\mathbf{F}. \end{aligned} \quad (2.113)$$

The fourth-order tensor \mathbb{C} denotes the underlying material tangent moduli (2.80). Inserting (2.112) with (2.113)₁ into (2.110) leads to the linearization of the weak form

$$\boxed{\begin{aligned} \text{Lin}G(\bar{\boldsymbol{\varphi}}, \delta\boldsymbol{\varphi}, \Delta\boldsymbol{\varphi}) &= \int_{\mathcal{B}_0} \mathbf{S} : \frac{1}{2}\delta\mathbf{C} dV - \int_{\mathcal{B}_0} \rho_0\mathbf{f} \cdot \delta\boldsymbol{\varphi} dV - \int_{\partial\mathcal{B}_{0t}} \bar{\mathbf{t}} \cdot \delta\boldsymbol{\varphi} dA \\ &\quad + \int_{\mathcal{B}_0} \frac{1}{2}\delta\mathbf{C} : \mathbb{C} : \frac{1}{2}\Delta\mathbf{C} dV + \int_{\mathcal{B}_0} \mathbf{S} : \frac{1}{2}\Delta\delta\mathbf{C} dV. \end{aligned}} \quad (2.114)$$

From the discrete form of the condition $\text{Lin } G = 0$ the discrete incremental deformations $\Delta \varphi$ are computed and the discrete deformations $\bar{\varphi}$ are updated per iteration step until the residuum $G(\bar{\varphi}, \delta \varphi)$ is smaller than a given tolerance. This is done by the Finite-Element-Method, presented in the next section.

2.8.3 Finite-Element-Method: Displacement Formulation. The Finite-Element-Method is a numerical method for finding approximate solutions of partial differential equations. The physical domain \mathcal{B}_0 is approximated by \mathcal{B}_0^h , which denotes the geometrical approximation of the considered body divided into $nele$ -element domains \mathcal{B}_0^e :

$$\mathcal{B}_0 \approx \mathcal{B}_0^h = \bigcup_{e=1}^{nele} \mathcal{B}_0^e. \quad (2.115)$$

The method is here exemplarily applied to the linearized weak form of equilibrium in the three-dimensional reference setting (2.114).

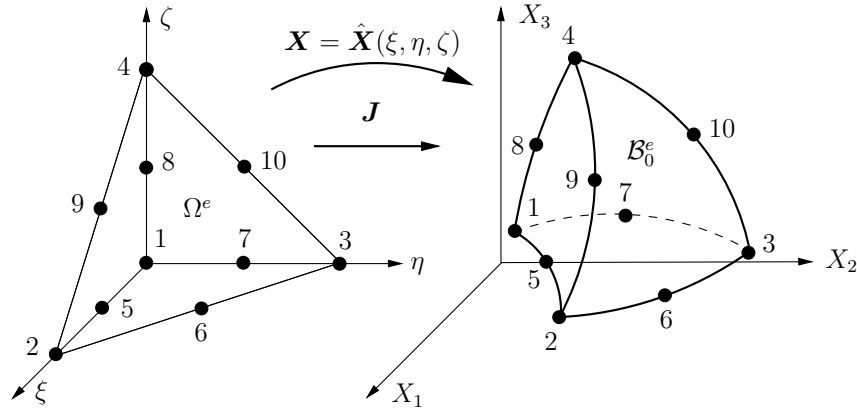


Figure 2.8: Illustration of a ten-noded tetrahedral finite element in the parametrized space Ω^e and reference configuration \mathcal{B}_0^e .

Furthermore, the *isoparametric concept* is taken into account, i.e., the geometry as well as the displacement field φ are approximated by the same *ansatz functions*. Choosing ten-noded tetrahedral finite elements the approximation of the geometry in the reference configuration is given by

$$\mathbf{X} = \mathbf{X}(\xi, \eta, \zeta) = \sum_{I=1}^{nen} N_I(\xi, \eta, \zeta) \mathbf{X}_I, \text{ with } nen = 10. \quad (2.116)$$

The values \mathbf{X}_I represent the nodal coordinates in the reference configuration. The ansatz functions in terms of the natural coordinates of the isoparametric space Ω^e , i.e., $\xi \in [0, 1]$,

$\eta \in [0, 1]$ and $\zeta \in [0, 1]$, are given by

$$\begin{aligned} N_1 &= \lambda(2\lambda - 1), & N_6 &= 4\xi\eta, \\ N_2 &= \xi(2\xi - 1), & N_7 &= 4\eta\lambda, \\ N_3 &= \eta(2\eta - 1), & N_8 &= 4\zeta\lambda, \\ N_4 &= \zeta(2\zeta - 1), & N_9 &= 4\xi\zeta, \\ N_5 &= 4\xi\lambda, & N_{10} &= 4\eta\zeta, \end{aligned} \quad (2.117)$$

with the relation $\lambda = 1 - \xi - \eta - \zeta$. Under consideration of the discrete nodal displacements \mathbf{d}_I we obtain the current geometry by

$$\mathbf{x}_I = \mathbf{X}_I + \mathbf{d}_I. \quad (2.118)$$

The isoparametric space is mapped onto the reference and current space, respectively, by the so-called *Jacobian* of the transformation, i.e.,

$$\mathbf{J} = \frac{\partial \mathbf{X}}{\partial \boldsymbol{\xi}}, \quad \mathbf{j} = \frac{\partial \mathbf{x}}{\partial \boldsymbol{\xi}}, \quad \text{with} \quad \mathbf{j} = \mathbf{F}\mathbf{J}, \quad (2.119)$$

with $\boldsymbol{\xi} := (\xi, \eta, \zeta)^T$. The approximation of the actual, virtual and incremental displacement field \mathbf{u} is given by

$$\mathbf{u} = \sum_{I=1}^{nen} N_I(\xi, \eta, \zeta) \mathbf{d}_I, \quad \delta \mathbf{u} = \sum_{I=1}^{nen} N_I(\xi, \eta, \zeta) \delta \mathbf{d}_I, \quad \Delta \mathbf{u} = \sum_{I=1}^{nen} N_I(\xi, \eta, \zeta) \Delta \mathbf{d}_I. \quad (2.120)$$

Thus, the virtual and incremental deformation gradient is approximated by

$$\begin{aligned} \delta \mathbf{F} &= \text{Grad}[\delta \mathbf{u}] = \sum_{I=1}^{nen} \delta \mathbf{d}_I \otimes \text{Grad} N_I(\xi, \eta, \zeta), \\ \Delta \mathbf{F} &= \text{Grad}[\Delta \mathbf{u}] = \sum_{I=1}^{nen} \Delta \mathbf{d}_I \otimes \text{Grad} N_I(\xi, \eta, \zeta), \end{aligned} \quad (2.121)$$

with the derivatives of the ansatz function with respect to the reference coordinates

$$\text{Grad} N_I(\xi, \eta, \zeta) = \frac{\partial N_I}{\partial \boldsymbol{\xi}} \frac{\partial \boldsymbol{\xi}}{\partial \mathbf{X}} = \mathbf{J}^{-T} \frac{\partial \boldsymbol{\xi}}{\partial \mathbf{X}}. \quad (2.122)$$

In order to obtain in the following more compact formulations, it is appropriate to carry over to matrix notations; for instance the coefficients of second-order tensors are presented in vectors and the components of fourth-order tensors by matrices, see therefore the Appendix B. Hence, the virtual and incremental right Cauchy-Green deformation tensor (2.109) and (2.113)₂ appears as

$$\frac{1}{2} \delta \mathbf{C} = \sum_{I=1}^{nen} \mathbf{B}_I \delta \mathbf{d}_I, \quad \frac{1}{2} \Delta \mathbf{C} = \sum_{I=1}^{nen} \mathbf{B}_I \Delta \mathbf{d}_I, \quad (2.123)$$

where \mathbf{B}_I denotes the so-called three-dimensional *B-Matrix*

$$\mathbf{B}_I = \begin{bmatrix} F_{11}N_{I,X_1} & F_{21}N_{I,X_1} & F_{31}N_{I,X_1} \\ F_{12}N_{I,X_2} & F_{22}N_{I,X_2} & F_{32}N_{I,X_2} \\ F_{13}N_{I,X_3} & F_{23}N_{I,X_3} & F_{33}N_{I,X_3} \\ F_{11}N_{I,X_2} + F_{12}N_{I,X_1} & F_{21}N_{I,X_2} + F_{22}N_{I,X_1} & F_{31}N_{I,X_2} + F_{32}N_{I,X_1} \\ F_{12}N_{I,X_3} + F_{13}N_{I,X_2} & F_{22}N_{I,X_3} + F_{23}N_{I,X_2} & F_{32}N_{I,X_3} + F_{33}N_{I,X_2} \\ F_{11}N_{I,X_3} + F_{13}N_{I,X_1} & F_{21}N_{I,X_3} + F_{23}N_{I,X_1} & F_{31}N_{I,X_3} + F_{33}N_{I,X_1} \end{bmatrix}. \quad (2.124)$$

The discrete weak form of equilibrium (2.98) for a typical finite element \mathcal{B}_0^e in the reference setting has finally the form

$$\boxed{\begin{aligned} G^e(\mathbf{d}, \delta \mathbf{d}) &= \sum_{I=1}^{nen} (\delta \mathbf{d}_I)^T \left(\int_{\mathcal{B}_0^e} \mathbf{B}_I^T \mathbf{S} dV - \int_{\mathcal{B}_0^e} N_I \rho_0 \mathbf{f} dV - \int_{\partial \mathcal{B}_{0t}^e} N_I \bar{\mathbf{t}} dA \right) = 0 \\ &=: \sum_{I=1}^{nen} (\delta \mathbf{d}_I)^T \mathbf{r}_I = (\delta \mathbf{d}^e)^T \mathbf{r}^e, \end{aligned}} \quad (2.125)$$

with the nodal residual vector \mathbf{r}_I , the elemental vector of virtual nodal displacements $(\delta \mathbf{d}^e)^T$ and the elemental residual vector \mathbf{r}^e , i.e.,

$$(\delta \mathbf{d}^e)^T = [\delta \mathbf{d}_1^T | \delta \mathbf{d}_2^T | \dots | \delta \mathbf{d}_{nen}^T], \quad \mathbf{r}^e = [\mathbf{r}_1^T | \mathbf{r}_2^T | \dots | \mathbf{r}_{nen}^T]^T. \quad (2.126)$$

Furthermore, the approximation of the linearized virtual right Cauchy-Green tensor (2.113) in index notation is obtained from

$$\begin{aligned} \frac{1}{2} \Delta \delta C_{AB} &= \frac{1}{2} (\delta F_A^a \delta_{ab} \Delta F_B^b + \Delta F_A^a \delta_{ab} \delta F_B^b) \\ &= \frac{1}{2} \left(\sum_{I=1}^{nen} N_{I,A} \delta d_I^a \delta_{ab} \sum_{J=1}^{nen} N_{J,B} \Delta d_J^b + \sum_{I=1}^{nen} N_{I,A} \Delta d_I^a \delta_{ab} \sum_{J=1}^{nen} N_{J,B} \delta d_J^b \right) \\ &= \sum_{I=1}^{nen} \sum_{J=1}^{nen} N_{I,A} \delta d_I^a \delta_{ab} N_{J,B} \Delta d_J^b. \end{aligned} \quad (2.127)$$

We get the discrete form of the linearized weak form (2.114) by

$$\boxed{LinG = \sum_{I=1}^{nen} (\delta \mathbf{d}_I)^T \mathbf{r}_I + \sum_{I=1}^{nen} \sum_{J=1}^{nen} (\delta \mathbf{d}_I)^T (\mathbf{K}_{IJ}^{e,mat} + \mathbf{K}_{IJ}^{e,geo}) \Delta \mathbf{d}_J = 0,} \quad (2.128)$$

where $\mathbf{K}_{IJ}^{e,mat}$ denotes the material part of the element stiffness matrix \mathbf{K}_{IJ}^e , defined by

$$\mathbf{K}_{IJ}^{e,mat} := \int_{\mathcal{B}_0^e} \mathbf{B}_I^T \mathbb{C}^e \mathbf{B}_J dV. \quad (2.129)$$

Here \mathbb{C}^e is the matrix representation of the material tangent moduli $\mathbb{C} := 2\partial_C \mathbf{S}$, cf. Appendix B. The geometric part $\mathbf{K}_{IJ}^{e,geo}$ of the element stiffness matrix is computed by

$$\mathbf{K}_{IJ}^{e,geo} := \int_{\mathcal{B}_0^e} (N_{I,A} N_{J,B}) S^{AB} dV. \quad (2.130)$$

The complete element stiffness matrix is then calculated by the sum of the material and geometric part

$$\mathbf{K}_{IJ}^e = \mathbf{K}_{IJ}^{e,mat} + \mathbf{K}_{IJ}^{e,geo}. \quad (2.131)$$

After assembling all element stiffness matrices and elemental residual vectors to obtain the global stiffness matrix \mathbf{K} and global residual vector \mathbf{R} , i.e.,

$$\mathbf{K} = \mathbf{A}_{e=1}^{nele} \mathbf{K}^e, \quad \mathbf{R} = \mathbf{A}_{e=1}^{nele} \mathbf{r}^e, \quad (2.132)$$

the overall discrete form of (2.128) for the domain \mathcal{B}_0 results in

$$\boxed{\delta \mathbf{D}^T (\mathbf{K} \Delta \mathbf{D} + \mathbf{R}) = 0 \Rightarrow \Delta \mathbf{D} = -\mathbf{K}^{-1} \mathbf{R}.} \quad (2.133)$$

According to the Newton-Raphson iteration scheme the global nodal displacement field \mathbf{D} is updated $\mathbf{D} \leftarrow \mathbf{D} + \Delta \mathbf{D}$, until the residual vector \mathbf{R} is smaller than a given tolerance.

3 Material Symmetry Groups.

Specific material symmetries impose certain invariance requirements on the material response which result in restrictions on the form of the constitutive equations. Anisotropic materials can be characterized by thirteen *material symmetry groups*. Eleven of them are associated with the 32 *point groups of crystals*. The remaining two are associated with five *continuous point groups*. These two groups are known as transversely isotropic material symmetry groups and used for the characterization of the behavior of engineering materials like fiber-reinforced materials with one family of aligned fibers.

For the definition of the crystal point groups we will give some remarks on the science of crystals, the crystallography. The explanations given in this chapter are mainly based on the textbooks VOIGT [129], BORCHARDT-OTT [34], BERGMANN & SCHÄFER [15], GIACOVAZZO [52] and BORCHARDT & TUROWSKI [33]. The continuous point groups will be described at the end of this chapter.

3.1 Neumann's Principle.

Crystals physically behave anisotropic. The fact, that there are in general some directions in a crystal along which the crystal physical properties are identical, limits the type of crystal anisotropy. The symmetries of the physical properties of a crystal are closely related to the symmetry properties of the crystal structure. Of fundamental relevance to this is a postulate of crystal physics known as *Neumann's Principle*. In GIACOVAZZO [52] this principle is summarized as follows:

Symmetry transformations associated with any physical property of a crystal must include those of the point group of the crystal.

This principle is named after the physicist Franz Ernst Neumann (1798-1895), who is the father of the mathematician Carl Gottfried Neumann, cf. section 2.8. He specified it in 1885 in his work NEUMANN [85]. There on page 164 the author remarks concerning "Elasticität krystalliner Stoffe":

Wir entwickeln desshalb neue allgemeine Formeln, wobei wir als alleinige Grundlagen nur die durch die Krystallform gegebenen Symmetrieverhältnisse der Structur... benutzen.

Woldemar Voigt (1850-1919) was a student and colleague of Franz Neumann. In the book VOIGT [129] on page 20 further notices can be found concerning this fundamental principle:

Die besondere Bedeutung, welche die Kristallform für den Aufbau der Kristallphysik besitzt, liegt darin, dass dieselbe die einfachste und anschaulichste physikalische Wirkung der Konstitution der Substanz darstellt... Die Erfahrung zeigt nämlich, dass in bezug auf alle übrigen physikalischen Eigenschaften die Kristalle eine kleinere Zahl von in sich gleichartigen und voneinander verschiedenen Gruppen bilden, als in bezug auf die Gestalt. Hieraus schließt man, dass in der Kristallform die Eigenarten und die Unterschiede der Konstitution sich vollständiger ausgedrückt finden, als in den übrigen

physikalischen Eigenschaften; ja man beurteilt direkt die Symmetrien dieser Eigenschaften und damit die geometrischen Gesetze der Konstitution nach den Symmetrien der Kristallformen,... . Natürlich ist das herangezogene Resultat der Erfahrung ebenso streng beweisend, als ähnliche Erfahrungssätze in anderen Gebieten der Physik.

Thus, in keeping with this principle, the physical properties may have a higher, but not lower, symmetry than the associated point group of the crystal.

Point Group: The set of all symmetry transformations of a crystal, which leave the crystal structure in a state macroscopically indistinguishable from the origin state, is called point group, since translations are neglected and the symmetry transformations leave one point of the crystal fixed.

Material Symmetry Group: The symmetry transformations associated with any physical property of a crystal constitute the underlying material symmetry group \mathcal{G} of the crystal. The group includes at least the symmetry transformations of the underlying crystal structure (point group).

For the definition of point groups and possible symmetry transformations of crystals we refer the reader to section 3.3. The restriction of \mathcal{G} to be a subgroup of $\text{SO}(3)$ in case of hyperelasticity is explained in section 3.7.

3.2 Space Lattice and its Properties.

The inner structure of ideal crystals is characterized by a regular repeating formation of the atoms, i.e., molecules or ions: the structure is said to be translationally periodic. This periodicity in crystals is conveniently described by the geometry of the repeating formation. The repetition of the formation at intervals a, b, c in three linearly independent directions can be sufficiently represented by the periodic sequence of the center points of gravity of the atoms and ions, respectively, separated by the same intervals a, b, c and directions. Such representation of points is called a *lattice* and shown in Figure 3.1. Note that the position of the lattice with respect to the formation is arbitrary, i.e., if we locate the grid points on any other points of the motif than the center points of gravity, the lattice does not change. We distinguish between grid lines, grid planes and space lattices which depends on the fact that the periodicity is given in one direction, in a plane, or in a three-dimensional space:

(i) Grid line : One grid line \mathbf{a}_1 . Let P_0 be located at the origin of the lattice line, i.e., at \mathbf{x}_0^p . The position vector of an arbitrary grid point P_u is given by

$$\mathbf{x}^p = \mathbf{x}_0^p + u\mathbf{a}_1, \quad \forall u \in \mathbb{N}.$$

(ii) Grid plane: Two linearly independent grid lines $\mathbf{a}_1, \mathbf{a}_2$. We obtain the position vector of an arbitrary grid point P_{uv} from

$$\mathbf{x}^p = \mathbf{x}_0^p + u\mathbf{a}_1 + v\mathbf{a}_2, \quad \forall u, v \in \mathbb{N}. \quad (3.1)$$

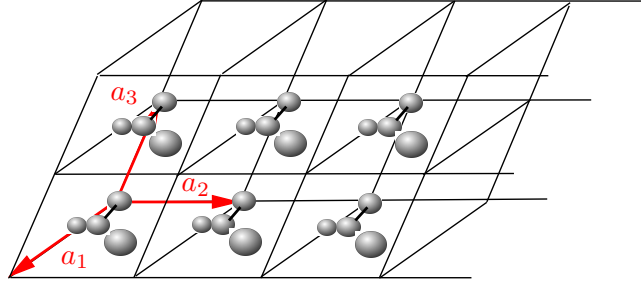


Figure 3.1: Example of crystal structure.

(iii) Space lattice: Three linearly independent grid lines \mathbf{a}_1 , \mathbf{a}_2 , \mathbf{a}_3 . The position vector of each grid point P_{uvw} is uniquely defined by

$$\mathbf{x}^p = \mathbf{x}_0^p + u\mathbf{a}_1 + v\mathbf{a}_2 + w\mathbf{a}_3, \quad \forall u, v, w \in \mathbb{N}. \quad (3.2)$$

Points situated inside the grid line, grid plane or space lattice have the coordinates $u, v, w \in \mathbb{R}$, if the corresponding vectors \mathbf{a}_i of the grid are considered as underlying base vectors.

The three base vectors \mathbf{a}_1 , \mathbf{a}_2 , \mathbf{a}_3 span a parallelepiped, known as *unit cell*. They constitute the underlying crystallographic base system. This base system can be classified by six grid parameters: the lengths of the base vectors $a = \|\mathbf{a}_1\|$, $b = \|\mathbf{a}_2\|$, $c = \|\mathbf{a}_3\|$ and the angles between them, $\alpha = \angle(\mathbf{a}_2, \mathbf{a}_3)$, $\beta = \angle(\mathbf{a}_1, \mathbf{a}_3)$, $\gamma = \angle(\mathbf{a}_1, \mathbf{a}_2)$, see Figure 3.2a). The crystallographic axes along the directions of the base vectors are denoted by a_1, a_2, a_3 .

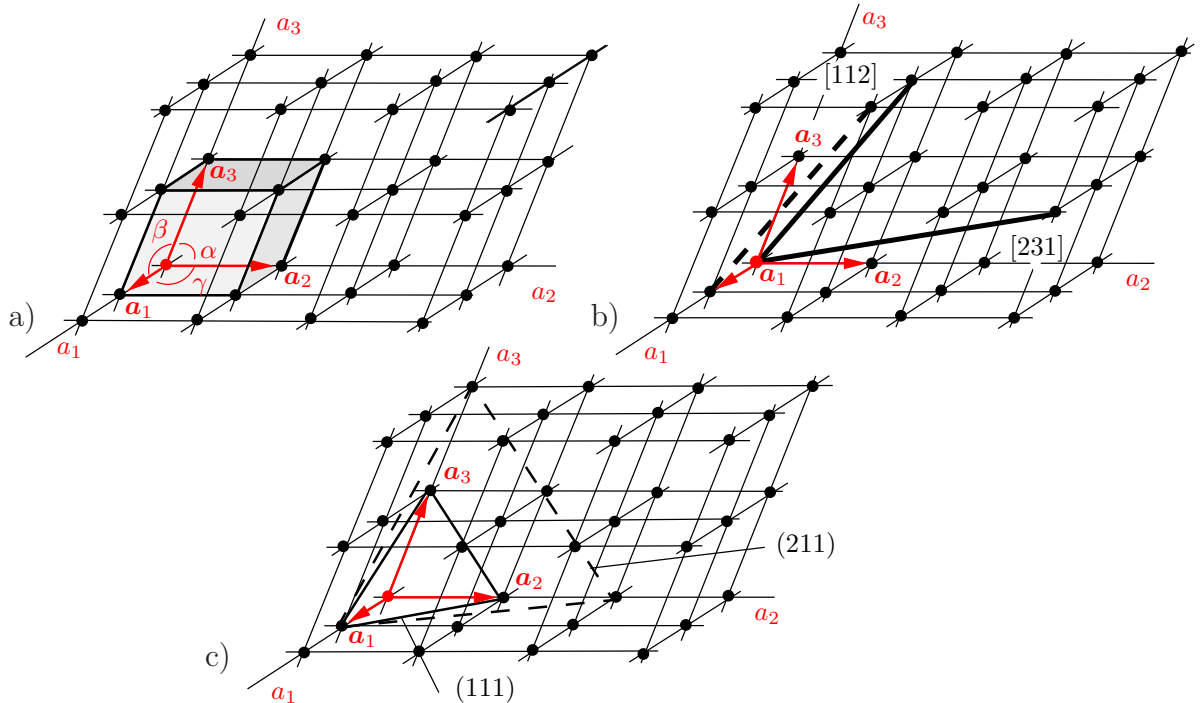


Figure 3.2: Space lattice: a) Unit cell with base vectors \mathbf{a}_1 , \mathbf{a}_2 , \mathbf{a}_3 , axial angles α, β, γ and axes a_1, a_2, a_3 , b) Grid line $[112]$, $[231]$, c) Grid plane (111) , (211) .

Note that for the characterization of a unit cell a grid point at vertex belongs to it for an eighth, a grid point on an edge for a fourth, a grid point on a face for a half and one in

the center of the cell completely refers to it. If the unit cell contains one grid point it is called *primitive*. If it has more than one grid point it is referred to as *non-primitive*.

A space lattice possesses an infinite number of grid planes, grid lines and grid points.

Grid Line of Space Lattice. The position of a grid line passing the origin of the grid and a second grid point is described by the coordinates $[uvw]$ (in squared brackets) of the direction vector (3.2) connecting the origin of the grid \mathbf{x}_0 with $\mathbf{x}_0 = \mathbf{0}$ and the second grid point, see Figure 3.2b). The triple $[uvw]$ does not only describe one grid line but also an infinite number of parallel oriented grid lines with the same translational distance ($[uvw]$:=an infinite group of grid lines). For instance, the broken grid line in Figure 3.2b), which is parallel oriented with respect to the grid line $[112]$, is also denoted by $[112]$.

Grid Plane of Space Lattice. A grid plane passes through points on the axes a_1, a_2, a_3 with coordinates: $\mathbf{x}_1^p = (m, 0, 0)^T$, $\mathbf{x}_2^p = (0, n, 0)^T$, $\mathbf{x}_3^p = (0, 0, p)^T$. With these coordinates the grid plane is uniquely defined. However, for the definition of a grid plane one uses the reciprocal coordinates: $\mathbf{x}_1^p = (h, 0, 0)^T$, $\mathbf{x}_2^p = (0, k, 0)^T$, $\mathbf{x}_3^p = (0, 0, l)^T$, with $h = \frac{1}{m}$, $k = \frac{1}{n}$, $l = \frac{1}{p}$ and the smallest integer values of h, k, l , which are indicated by the triple (hkl) , the so-called *Miller indices*. For instance, the coordinates $m, n, p = 1, 2, 2$ and $h, k, l = 1, \frac{1}{2}, \frac{1}{2}$ lead to the Miller indices (211) , see Figure 3.2c). The triple (hkl) does not only describe one grid plane but also an infinite number of parallel oriented grid planes with equal grid structure and translational distance ((hkl) :=an infinite group of grid planes).

Atomic Structure. The atomic structure of a crystal is determined by the lattice itself and the atomic group assigned to each grid point, also referred to as *basis*. Thus, in an idealize setting,

$$\text{lattice} + \text{group of atoms} = \text{crystal}.$$

The basis is characterized by the same translational periodicity as the lattice. The *motif* is the smallest asymmetric item of matter of a crystal. The basis can include several motifs, which can be brought into coincidence by certain point symmetry transformations, which will be defined later.

Correspondence Between Crystal Structure and Morphology. There exists a correspondence between the crystal structure (inner structure) and the crystal morphology (outer structure): Each surface of a crystal is oriented parallelly to an infinite group of grid planes (hkl) . Each edge of a crystal is oriented parallel to an infinite group of grid lines $[uvw]$.

3.3 Point Symmetry Transformations.

The translational periodicity has no influence on the macroscopic physical properties of a crystal. The crystal appears to be homogeneous and anisotropic. The symmetry of the macroscopic physical properties are therefore determined from the point group.

3.3.1 Rotations. The rotational symmetry operation (rotation around an axis with angle $\alpha = 2\pi/n$, $n \in \mathbb{N}$) is described by the corresponding n -fold rotation axis $\mathbf{f}^{(n)}$. For crystals 1,2,3,4,6-fold rotation axes exist. Four of them and the corresponding stere-

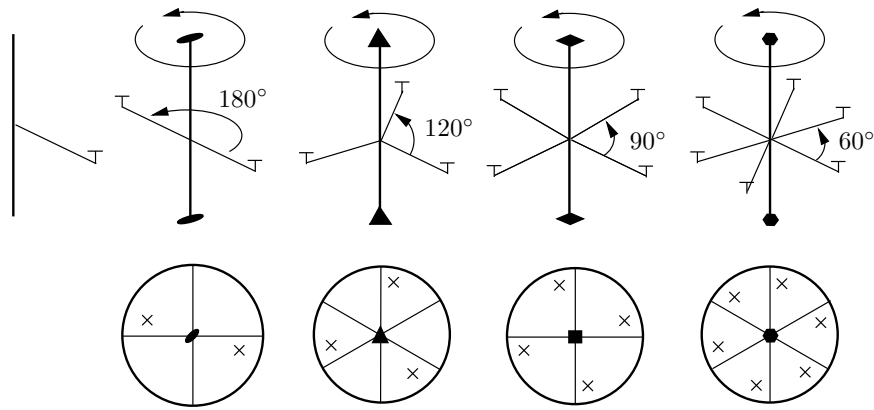


Figure 3.3: 2,3,4,6-fold rotation axes and below the corresponding stereographic projections.

ographic projections ^{2.)} are depicted in Figure 3.3. For crystals 5-fold and n -fold rotation axis with $n \geq 7$, $n \in \mathbb{N}$ are not possible, since such rotational symmetries contradict the postulated translational periodicity of lattices, e.g. regular pentagons cannot fill a planar space.

3.3.2 Rotation-Inversions. The rotation inversion represents a combination of the symmetry operations rotation and reflection with respect to a point (the crystal center=inversion center). It is described by the corresponding \bar{n} -fold rotoinversion axis $f^{(\bar{n})}$. In Figure 3.4 the effect of a $\bar{2}$ -fold rotoinversion axis is illustrated. It is shown that this operation is identical to a mirror plane m (here: grey-coloured plane). The remaining four possible rotoinversion axes of crystals are visualized in Figure 3.4.

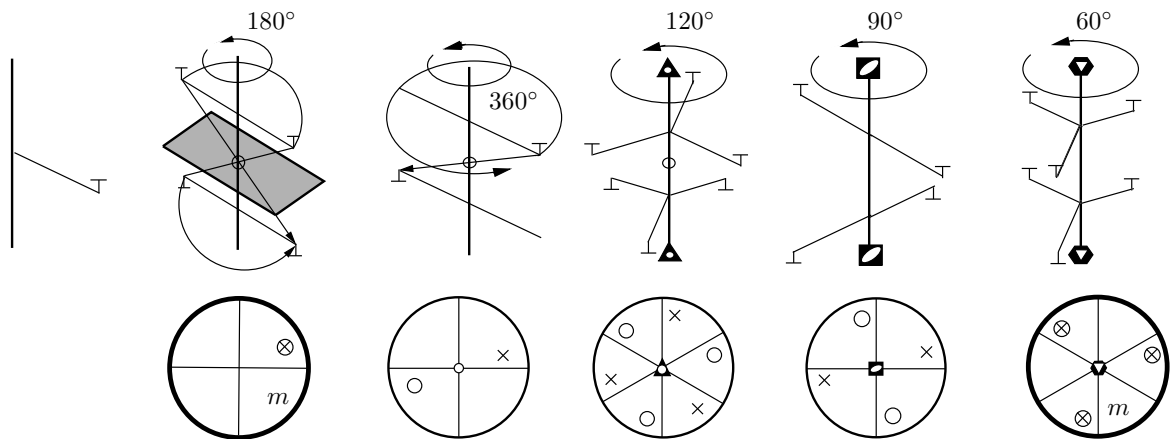


Figure 3.4: $\bar{2}$, $\bar{1}$, $\bar{3}$, $\bar{4}$, $\bar{6}$ -fold rotoinversion axes and below the corresponding stereographic projections.

^{2.)}In crystallography, a sphere is used for the visualization of the point symmetries of a crystal. The inscribed points of this picture reflect the centers of motifs, which can be brought into coincidence by certain point symmetry transformations. Since an axonometric projection of this sphere can give to misunderstanding, a stereographic projection is used, which maps the sphere onto a plane. Today, in practice, this projection is carried out by computer and classically by hand using a special graph paper, called Wulff net (named after the Russian mineralogist George Wulff (1863-1925), WULFF [139]).

3.3.3 Matrix Representations for Point Symmetry Transformations. Point Symmetry Transformations can be described by orthogonal matrices $\mathbf{Q} \in \text{O}(3)$, where $\text{O}(3)$ denotes the full orthogonal group whose elements have the properties

$$\mathbf{Q}^T = \mathbf{Q}^{-1}, \quad \det \mathbf{Q} = \pm 1.$$

The proper orthogonal group $\text{SO}(3)$ as well as the material symmetry group \mathcal{G} are subgroups of $\text{O}(3)$. In a three-dimensional Euclidian space \mathbb{R}^3 rotations through $\alpha = 2\pi/n$, $n \in \mathbb{N}$, around the axis \mathbf{a} with $\|\mathbf{a}\| = 1$ are defined by

$$\mathbf{Q}_a^\alpha = \cos(\alpha)\mathbf{1} + (1 - \cos(\alpha))\mathbf{a} \otimes \mathbf{a} + \sin(\alpha)\boldsymbol{\epsilon}\mathbf{a}, \quad (3.3)$$

with the third order permutation tensor $\boldsymbol{\epsilon}$ defined in (2.3)₂. Rotoinversions have the form

$$-\mathbf{Q}_a^\alpha = (-1)\mathbf{Q}_a^\alpha. \quad (3.4)$$

The identity $\mathbf{1}$ and the central inversion $\bar{\mathbf{1}} = -\mathbf{1}$ are

$$\mathbf{1} = \text{diag}(1, 1, 1) \quad \text{and} \quad -\mathbf{1} = \text{diag}(-1, -1, -1). \quad (3.5)$$

In case of a rotation through the angle $\alpha = 2\pi/n$, $n \in \mathbb{N}$, about the X_1 -, X_2 - and X_3 -axis, respectively, the transformation matrices appear as

$$\begin{aligned} \mathbf{Q}_{X_1}^\alpha &= \begin{bmatrix} 1 & 0 & 0 \\ 0 & \cos(\alpha) & -\sin(\alpha) \\ 0 & \sin(\alpha) & \cos(\alpha) \end{bmatrix}, \\ \mathbf{Q}_{X_2}^\alpha &= \begin{bmatrix} \cos(\alpha) & 0 & -\sin(\alpha) \\ 0 & 1 & 0 \\ \sin(\alpha) & 0 & \cos(\alpha) \end{bmatrix}, \quad \mathbf{Q}_{X_3}^\alpha = \begin{bmatrix} \cos(\alpha) & -\sin(\alpha) & 0 \\ \sin(\alpha) & \cos(\alpha) & 0 \\ 0 & 0 & 1 \end{bmatrix}. \end{aligned} \quad (3.6)$$

Rotations about $2\pi/3$ around the principal diagonal \mathbf{p} of a cube are denoted in the sequel by $\mathbf{Q}_p^{2\pi/3}$.

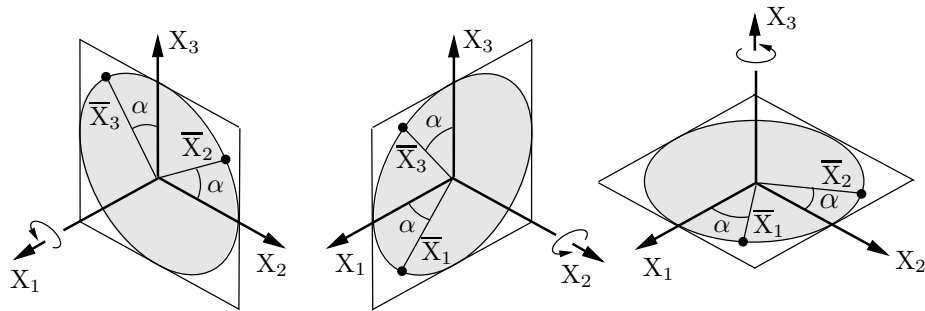


Figure 3.5: Rotations about the X_1 -, X_2 - and X_3 -axis, see DE BOER & SCHRÖDER [42].

3.4 Bravais Lattices.

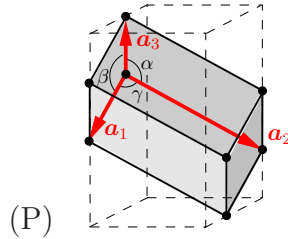
Classifying crystals according to the point symmetry of the lattice, seven crystal systems can be defined. The lattices of all crystals belonging to the same crystal system have the same point symmetry. There exist 14 different space lattices based on both primitive and

Table 3.1: The seven crystal systems.

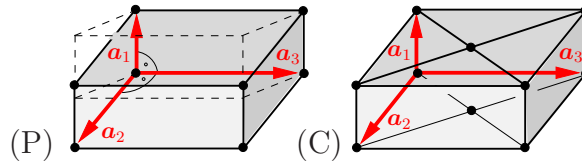
| No. | crystal system | edge lengths | axial angle |
|-----|----------------|-------------------|---|
| 1 | triclinic | $a \neq b \neq c$ | $\alpha \neq \beta \neq \gamma \neq 90^\circ$ |
| 2 | monoclinic | $a \neq b \neq c$ | $\alpha = \beta = 90^\circ; \gamma \neq 90^\circ$ |
| 3 | trigonal | $a = b = c$ | $\alpha = \beta = \gamma \neq 90^\circ$ |
| 4 | hexagonal | $a = b \neq c$ | $\alpha = \beta = 90^\circ; \gamma = 120^\circ$ |
| 5 | rhombic | $a \neq b \neq c$ | $\alpha = \beta = \gamma = 90^\circ$ |
| 6 | tetragonal | $a = b \neq c$ | $\alpha = \beta = \gamma = 90^\circ$ |
| 7 | cubic | $a = b = c$ | $\alpha = \beta = \gamma = 90^\circ$ |

non-primitive cells, the so-called *14 Bravais lattices*, which are named after the physicist Auguste Bravais who first specified them in 1850. The Bravais lattices vary from the most general parallelepiped (triclinic system) to the most restricted one (cubic system). The relations between the corresponding grid parameters are listed in Table 3.1.

Triclinic Lattice. In the triclinic case the unit cell represents the most general form of a unit cell. The only restriction is that the pairs of opposite faces are parallel. The grid parameters are not restricted.

**Figure 3.6:** Triclinic Bravais lattice, (P) Primitive cell: $a \neq b \neq c, \alpha \neq \beta \neq \gamma \neq 90^\circ$.

Monoclinic Lattice. The base vectors \mathbf{a}_1 and \mathbf{a}_2 of the monoclinic unit cell are oriented perpendicularly to \mathbf{a}_3 and the angle γ is unrestricted. There are two distinct monoclinic cells, the primitive cell, P, and the special face-centered cell, C, which can not be transformed one onto the other. Compared to the primitive cell for the classification of the unit cell C two additional nodes centered at two opposite faces are needed.

**Figure 3.7:** Monoclinic Bravais lattice, (P) Primitive and (C) centered cell: $a \neq b \neq c, \gamma \neq \alpha = \beta = 90^\circ$.

Rhombic Lattice. The rhombic cell is described by three mutually orthogonal base vectors of different lengths. Four distinct types of rhombic lattices, P, C, I, and F, exist, see Figure 3.8. The symbol I designates a body-centered lattice, the symbol F stands for a face-centered lattice, where the additional grid points are positioned at the center of each

lattice face. In the sequel the base vectors are chosen to be parallel to the X_1 -, X_2 - and X_3 -axis, respectively.

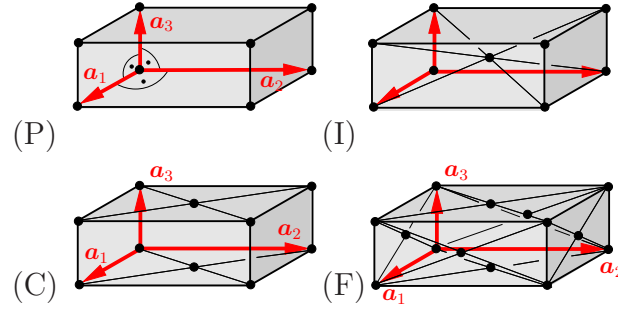


Figure 3.8: Rhombic Bravais lattice, (P) Primitive cell, (C) centered cell, (I) body-centered cell, (F) face-centered cell: $a \neq b \neq c, \gamma = \alpha = \beta = 90^\circ$.

Tetragonal Lattice. The geometry of the tetragonal cell is restricted to $\alpha = \beta = \gamma = 90^\circ$, $a = b \neq c$. Here only two different tetragonal lattices, P and I, are found. The typical four-fold axis is oriented in \mathbf{a}_3 -direction.

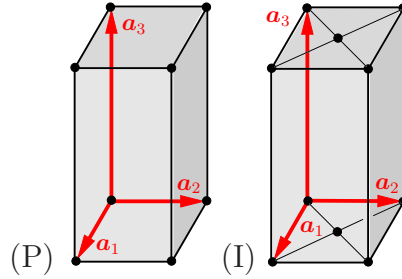


Figure 3.9: Tetragonal Bravais lattice, (P) Primitive cell, (I) body-centered cell: $a = b \neq c, \gamma = \alpha = \beta = 90^\circ$.

Cubic Lattice. Similar to the rhombic and tetragonal lattices the cubic unit cell is described by three mutually orthogonal base vectors, which are in this case of equal lengths. There are three cubic lattices, P, I, F, as depicted in Figure 3.10. In the sequel the directions of the cubic crystallographic base vectors are brought into coincidence with the cartesian base vectors.

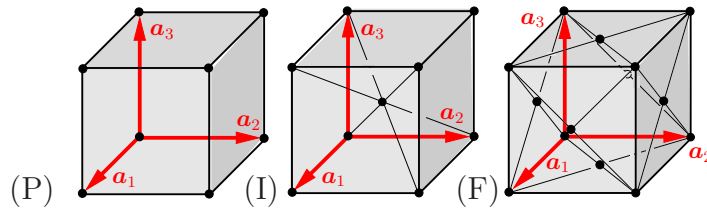


Figure 3.10: Cubic Bravais lattice, (P) Primitive, (I) body-centered, (F) face-centered cell: $a = b = c, \gamma = \alpha = \beta = 90^\circ$.

Hexagonal Lattice. The grid parameters of the hexagonal unit cell satisfy the relations $a = b \neq c, \gamma = 120^\circ, \alpha = \beta = 90^\circ$. P is the only type of hexagonal Bravais lattice. The characteristic six-fold symmetry of the hexagonal system can not be obtained by a parallelepiped as visualized as grey-coloured unit cell in Figure 3.11, but the lattice itself can exhibit that symmetry.

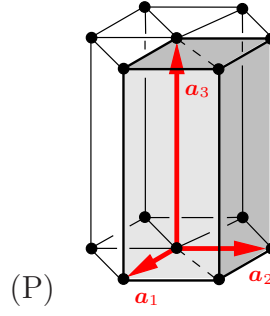


Figure 3.11: Hexagonal Bravais lattice, (P) Primitive cell: $a = b \neq c, \gamma = 120^\circ, \alpha = \beta = 90^\circ$.

In order to capture the inherent symmetries of the hexagonal lattice, Bravais introduced in 1866 in addition to the three base vectors $\mathbf{a}_h = \mathbf{a}_1$, $\mathbf{b}_h = \mathbf{a}_2$, $\mathbf{c}_h = \mathbf{a}_3$ a fourth (redundant) base vector $\mathbf{d}_h = -\mathbf{a}_h - \mathbf{b}_h$ in the $\mathbf{e}_1 - \mathbf{e}_2$ -plane. A lattice of prism shape is obtained, consisting of three primitive hexagonal unit cells. The base vector \mathbf{a}_3 , which is perpendicular to the $\mathbf{e}_1 - \mathbf{e}_2$ -plane, can be then interpreted as six-fold symmetry axis $\mathbf{f}_1^{(6)}$, see Figure 3.12.

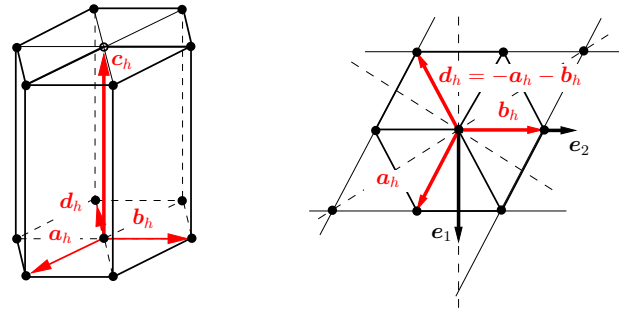


Figure 3.12: Hexagonal lattice with four base vectors: $\mathbf{a}_h, \mathbf{b}_h, \mathbf{c}_h$ and the redundant base vector $\mathbf{d}_h = -\mathbf{a}_h - \mathbf{b}_h$.

Trigonal Lattice. The trigonal lattice is equal to the primitive hexagonal one with restricted grid parameters $a = b \neq c, \gamma = 120^\circ, \alpha = \beta = 90^\circ$. The three-fold symmetry of the trigonal lattice can be captured by a triple hexagonal cell with three centring points or by an associated primitive cell of rhombohedral shape; the hexagonal cell can be in an *obverse* or *reverse* setting, see GIACOVAZZO [52].

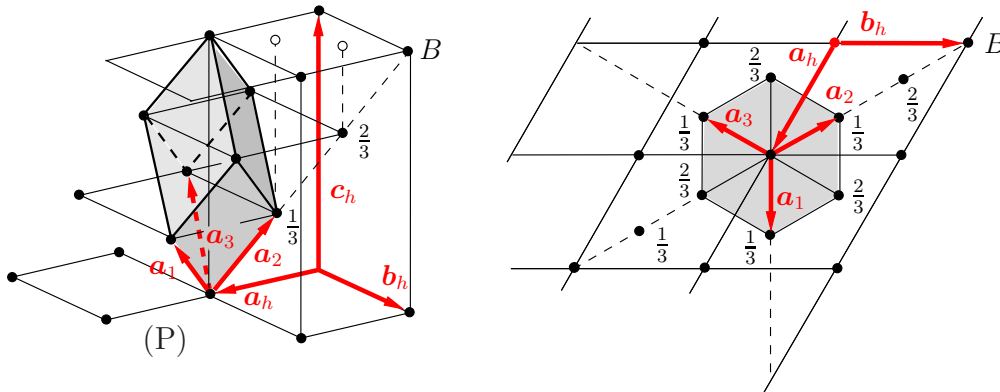


Figure 3.13: Trigonal Bravais lattice, (P) Primitive trigonal cell: $a = b = c, \alpha = \beta = \gamma$.

We focus here on a hexagonal cell in obverse setting with centring points at

$$(0, 0, 0), (2/3, 1/3, 1/3), (1/3, 2/3, 2/3).$$

The hexagonal cell is spanned by the base vectors \mathbf{a}_h , \mathbf{b}_h , \mathbf{c}_h , depicted in Figure 3.12. The basis of the associated rhombohedral cell can be determined by the basis of the hexagonal cell, see Figure 3.13:

$$\mathbf{a}_1 = \frac{1}{3}(2\mathbf{a}_h + \mathbf{b}_h + \mathbf{c}_h), \quad \mathbf{a}_2 = \frac{1}{3}(-\mathbf{a}_h + \mathbf{b}_h + \mathbf{c}_h), \quad \mathbf{a}_3 = \frac{1}{3}(-\mathbf{a}_h - 2\mathbf{b}_h + \mathbf{c}_h),$$

with the three-fold axis along the $(\mathbf{a}_1 + \mathbf{a}_2 + \mathbf{a}_3)$ -direction. The grid parameters are given by the lengths $a = b = c$ and angles $\alpha = \beta = \gamma$.

3.5 32 Point Groups of Crystals.

32 Point Groups of Crystals: Crystals can be classified by 32 point group. A point group consists of the point symmetry transformations of the underlying crystal structure. The point symmetry transformations of a crystal structure are at most equal to those of the lattice and can be limited by those of the group of atoms assigned at each grid point of the lattice.

For instance, in Figure 3.14, the point group symmetry elements and the corresponding crystal structure for the monoclinic point symmetry groups 2 and $2/m$ are visualized. For group $2/m$ – the monoclinic point group of highest symmetry – the symmetry of the crystal structure is that of the lattice, which can be described by two-fold axes perpendicularly oriented to mirror planes m . Here, the group of atoms exhibits the same symmetry properties and does therefore not reduce the symmetry of the crystal, cf. Figure 3.14 a). For group 2, the group of atoms is different. This group leads to a lower symmetry of the crystal structure, given only by two-fold axes as can be seen in Figure 3.14 b). Thus, the typical mirror planes of the underlying monoclinic lattice are not essential any longer and have to be deleted.

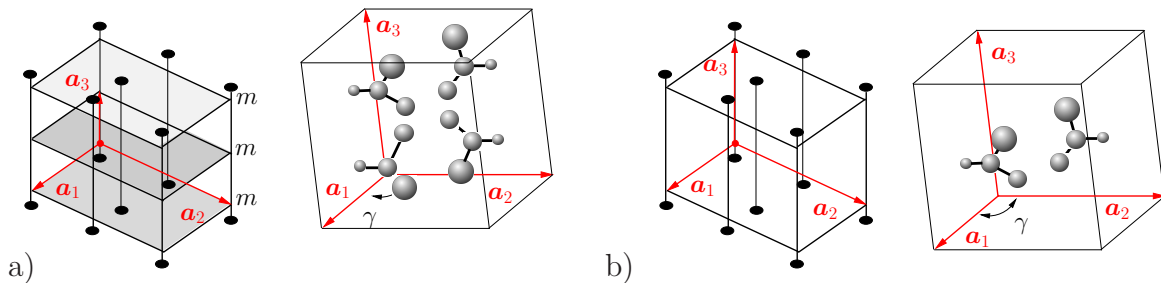


Figure 3.14: Point group symmetry elements (left) and corresponding crystal structure (right) for: a) point group $2/m$, b) point group 2.

3.5.1 Schoenflies/Hermann-Mauguin Symbolism. The point groups presented by the Schoenflies symbolism are divided into four rotation groups:

$$\begin{aligned}
 \mathcal{C}_n | n = 1, 2, 3, 4, 6 & \quad \text{cyclic rotation groups,} \\
 \mathcal{D}_n | n = 1, 2, 3, 4, 6 & \quad \text{dihedral rotation groups,} \\
 \mathcal{T} & \quad \text{tetrahedral rotation groups,} \\
 \mathcal{O} & \quad \text{octahedral rotation groups.}
 \end{aligned} \tag{3.7}$$

With regard to both the Schoenflies and Hermann-Mauguin notations the crystal classes are characterized by the symmetry elements listed in Table 3.2. Here also the relations between the Schoenflies and Hermann-Mauguin symbols are given. Note that each Schoenflies symbol can be expressed by a Hermann-Mauguin symbol, but not vice versa.

Table 3.2: Herrmann-Maugin and Schoenflies Notations

| Schoenflies | H.-M. | n | Symmetry Operation |
|--------------------|--------------|-----------|---|
| \mathcal{C}_n | n | 1,2,3,4,6 | n -fold rotation axis. |
| \mathcal{C}_{ni} | \bar{n} | 1,2,3 | n -fold rotation axis and inversion center (rotoinversion axis). |
| \mathcal{C}_{nh} | n/m | 1,2,3,4,6 | n -fold rotation axis normal to mirror plane. |
| \mathcal{C}_{nv} | $3m$ | 3 | n -fold rotation axis parallel to n mirror planes. |
| | nmm | 2,4,6 | |
| \mathcal{D}_n | $n2$ | 3 | n -fold rotation axis normal to n 2-fold axes. |
| | $n22$ | 2,4,6 | |
| \mathcal{D}_{nh} | $n/m2m$ | 3 | like \mathcal{D}_n plus mirror planes normal to the n -fold axis and bisecting the n 2-fold axes. |
| | n/mmm | 2,4,6 | like \mathcal{D}_n plus mirror planes normal to the n -fold axis and the n 2-fold axes. |
| \mathcal{D}_{2d} | $\bar{4}2m$ | | 4-fold rotoinversion axis normal to two 2-fold axes, two 2-fold axes and two mirror planes bisecting the 2-fold axes |
| \mathcal{D}_{3d} | $\bar{3}2/m$ | | 3-fold rotoinversion axis normal to three 2-fold axes, three 2-fold axes and three mirror planes normal to the 2-fold axes. |

3.5.2 Matrix Representations of the 32 Point Groups. In order to specify the point groups in a three-dimensional Euclidian space \mathbb{R}^3 by the matrix representations of the symmetry elements, we review the mathematical definition of a group consisting of $n \times n$ non-singular matrices. Let $\mathbf{B}_1, \dots, \mathbf{B}_n$ constitute a set of square matrices called \mathcal{S} . The set \mathcal{S} is a group if it satisfies the conditions (i)-(iv)

- (i) Closure: $\mathbf{B}_1, \mathbf{B}_2 \in \mathcal{S}$,
- (ii) Associativity: $(\mathbf{B}_1 \mathbf{B}_2) \mathbf{B}_3 = \mathbf{B}_1 (\mathbf{B}_2 \mathbf{B}_3)$, $\mathbf{B}_1, \mathbf{B}_2, \mathbf{B}_3 \in \mathcal{S}$,
- (iii) Identity Element: $\mathbf{1} \mathbf{B} = \mathbf{B}$, $\mathbf{1}, \mathbf{B} \in \mathcal{S}$,
- (iv) Inverse Element: $\mathbf{B}^{-1} \mathbf{B} = \mathbf{1}$, $\mathbf{1}, \mathbf{B}, \mathbf{B}^{-1} \in \mathcal{S}$.

If furthermore the commutativity condition

$$\mathbf{B}_1 \mathbf{B}_2 = \mathbf{B}_2 \mathbf{B}_1, \quad \mathbf{B}_1, \mathbf{B}_2 \in \mathcal{S}, \quad (3.8)$$

holds for all elements of \mathcal{S} , the group is an *Abelian group*, otherwise it is called a non-Abelian group, which is the case for most of the point groups and also the group of proper rotations $\text{SO}(3)$. The number of different elements of a group is called the order of the group and can be finite or infinite. Point groups of crystals \mathcal{P} consist of a finite number of elements, whereas so-called continuous point groups, like $\text{O}(3)$ and $\text{SO}(3)$, have an infinite number of elements. Any point group can be finally represented as the products of the powers of the so-called *generators* of the group. Note that the definition of generators of groups is not unique. The elements of the point groups are then determined with the help of the generators by applying the product law. For a point group, which has a single generator \mathbf{B} , the n elements are powers of \mathbf{B} , i.e.,

$$\mathcal{P} = \{\mathbf{B}, \mathbf{B}^2, \dots, \mathbf{B}^{n-1}, \mathbf{B}^n = \mathbf{1}\}. \quad (3.9)$$

This group is called *cyclic*. A cyclic group is always Abelian, the converse is not true. An example of a cyclic group of order n is the set of rotations through a certain angle $\alpha = 2\pi/n$, $n \in \mathbb{N}$ around a given axis \mathbf{a} , with $\|\mathbf{a}\| = 1$.

As already pointed out, the point groups denoted by Schoenflies symbolism \mathcal{C}_n , $i = 1, 2, 3, 4, 6$ are cyclic groups. For instance, the trigonal point group \mathcal{C}_3 described by the group generator $\mathbf{Q} := \mathbf{Q}_{X_3}^{2\pi/3}$, constitutes a cyclic group with 3 elements:

$$\mathcal{P} = \{\mathbf{Q}, \mathbf{Q}^2, \mathbf{Q}^3 = \mathbf{1}\}.$$

Table 3.3: Multiplication Table, $\mathbf{Q} = \mathbf{Q}_{X_3}^{2\pi/3}$

| | -1 | \mathbf{Q} | 1 | $-\mathbf{Q}$ | \mathbf{Q}^2 | $-\mathbf{Q}^2$ |
|-----------------|-----------------|-----------------|-----------------|-----------------|-----------------|-----------------|
| -1 | 1 | $-\mathbf{Q}$ | -1 | \mathbf{Q} | $-\mathbf{Q}^2$ | \mathbf{Q}^2 |
| \mathbf{Q} | $-\mathbf{Q}$ | \mathbf{Q}^2 | \mathbf{Q} | $-\mathbf{Q}^2$ | 1 | -1 |
| 1 | -1 | \mathbf{Q} | 1 | $-\mathbf{Q}$ | \mathbf{Q}^2 | $-\mathbf{Q}^2$ |
| $-\mathbf{Q}$ | \mathbf{Q} | $-\mathbf{Q}^2$ | $-\mathbf{Q}$ | \mathbf{Q}^2 | -1 | 1 |
| \mathbf{Q}^2 | $-\mathbf{Q}^2$ | 1 | \mathbf{Q}^2 | -1 | \mathbf{Q} | $-\mathbf{Q}$ |
| $-\mathbf{Q}^2$ | \mathbf{Q}^2 | -1 | $-\mathbf{Q}^2$ | 1 | $-\mathbf{Q}$ | \mathbf{Q} |

In general, a simple method for displaying the products of group generators is based on so-called multiplication tables. Let us exemplarily consider the trigonal point group \mathcal{C}_{3i} , which is governed by the symmetry group generators $-\mathbf{1}, \mathbf{Q}$, with $\mathbf{Q} := \mathbf{Q}_{X_3}^{2\pi/3}$. The multiplication table is then organized in the form presented in Table 3.3. The first multiplication table consists of the multiplications of the generators $\mathbf{1}, \mathbf{Q}$. Since their products yield the new elements $\mathbf{1}, -\mathbf{Q}, \mathbf{Q}^2$ we have to investigate a second multiplication table, consisting of products of the latter and new elements. If the new multiplication table does not include new elements, then the table is closed. If every element has an inverse and the conditions (i)-(iv) of Table 3.5.2 are fulfilled, the constructed matrices form a group. Thus, the trigonal point group \mathcal{C}_{3i} appears as

$$\mathcal{P} := \{\mathbf{1}, -\mathbf{1}, \mathbf{Q}, -\mathbf{Q}, \mathbf{Q}^2, -\mathbf{Q}^2\}. \quad (3.10)$$

3.5.3 Orientation of Crystals in Space. We have seen that the point group of a crystal is defined by the symmetry of the underlying crystal structure. For our further analyses it is important to point out that each point group is of course also determinable by the general position of the crystal in space, see BORCHARDT & TUROWSKI [33]. Of high relevance here is the orientation of the crystallographical axes (inner structure) with respect to the morphology (outer structure) of the crystal. The names of the crystals are also associated with that position. Exemplarily, in Figures 3.15 and 3.16 the following characteristics of eleven point groups \mathcal{P} are depicted: the general position of the crystal in space, the name of the crystal, the cross-section perpendicular to the crystallographical a_3 -axis as well as the corresponding stereographic projection.

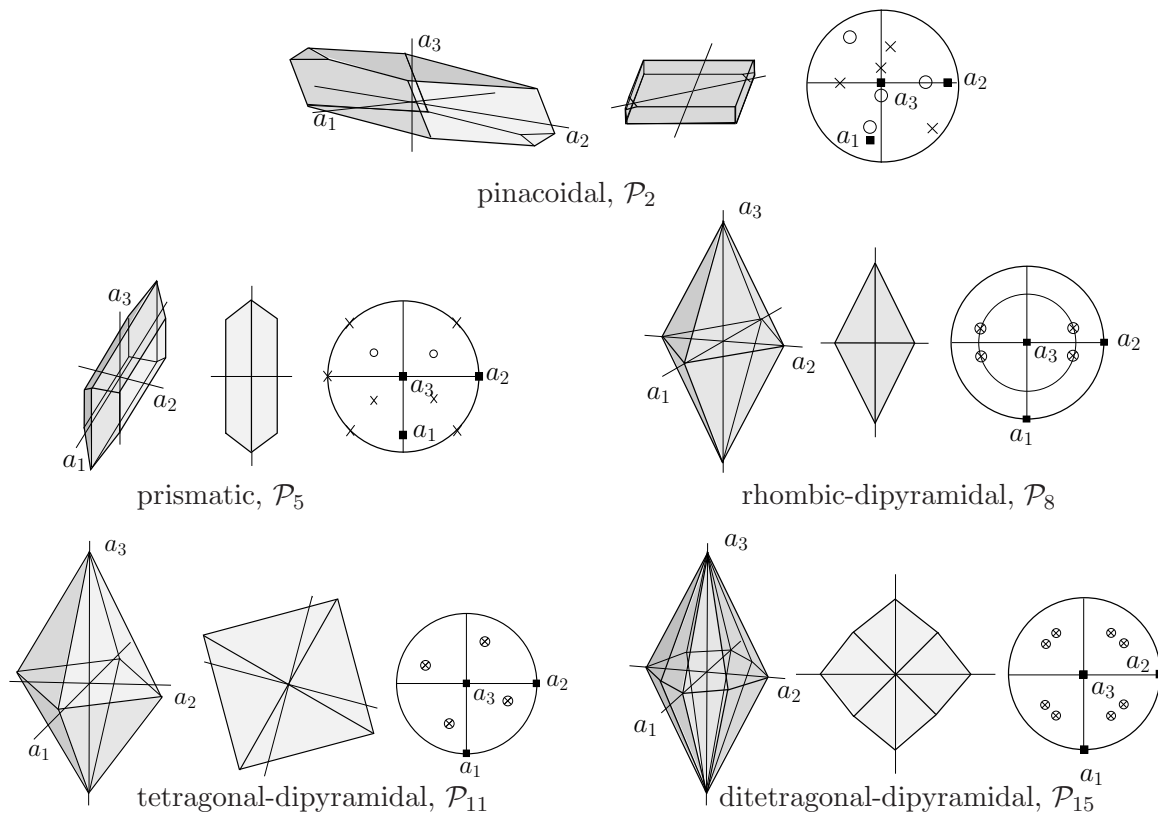


Figure 3.15: Orientation of crystals in space I, left: general form with crystallographical axes, center: cross-section perpendicular to a_3 -axis, right: stereographic projection.

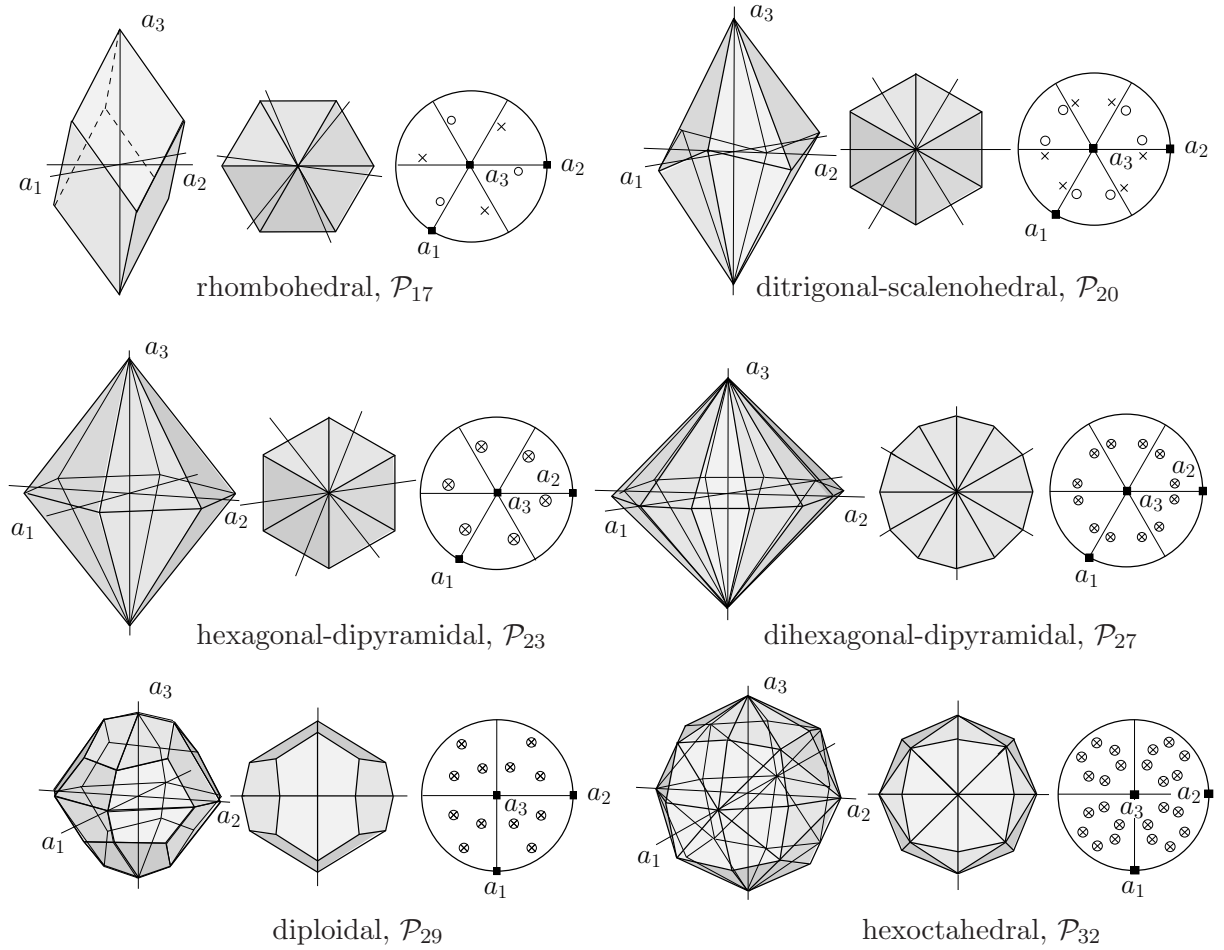


Figure 3.16: Orientation of crystals in space II, left: general form with crystallographical axes, center: cross-section perpendicular to a_3 -axis, right: stereographic projection.

3.6 Continuous Point Groups.

We have already introduced the continuous point groups $O(3)$ and $SO(3)$, where $O(3)$ reflect the symmetry properties of isotropic materials. They are spherical point groups and depicted in Figure 3.17. Here an infinite number of rotations ($SO(3)$, $O(3)$) and rotoinversions ($O(3)$) through $\alpha = 2\pi/n$, $n \in \mathbb{N}$ around the axis \mathbf{a} and through $\beta = 2\pi/n$, $n \in \mathbb{N}$ around the orthogonal axis \mathbf{b} are possible. Thus, the spherical point group $SO(3)$, called hemitropic, is characterized by two infinite rotation axes $\mathbf{a} = \mathbf{f}_1^{(\infty)}$, $\mathbf{b} = \mathbf{f}_2^{(\infty)}$. The spherical point group $O(3)$, called isotropic, is described by both, infinite rotation and rotoinversion axes $\mathbf{a} = \mathbf{f}_1^{(\infty)}$, $\mathbf{f}_1^{(\infty)}$, $\mathbf{b} = \mathbf{f}_2^{(\infty)}$, $\mathbf{f}_2^{(\infty)}$, see Figure 3.18.

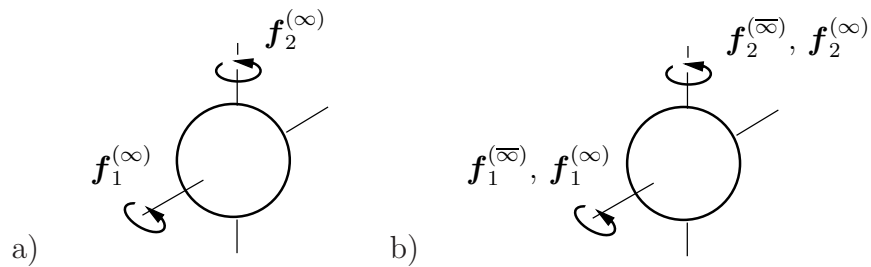


Figure 3.17: Visualization of the spherical point groups. a) $SO(3)$, b) $O(3)$.

The description of transversely isotropic materials, which exhibit a preferred material behavior in one direction \mathbf{a} of the material, is based on further continuous point groups, the so-called cylindrical point groups. Here an infinite number of rotations through $\alpha = 2\pi/n$, $n \in \mathbb{N}$ around one axis \mathbf{a} are possible. Thus, we have $\mathbf{a} = \mathbf{f}^{(\infty)}$. The corresponding matrix representation is introduced in (3.3).

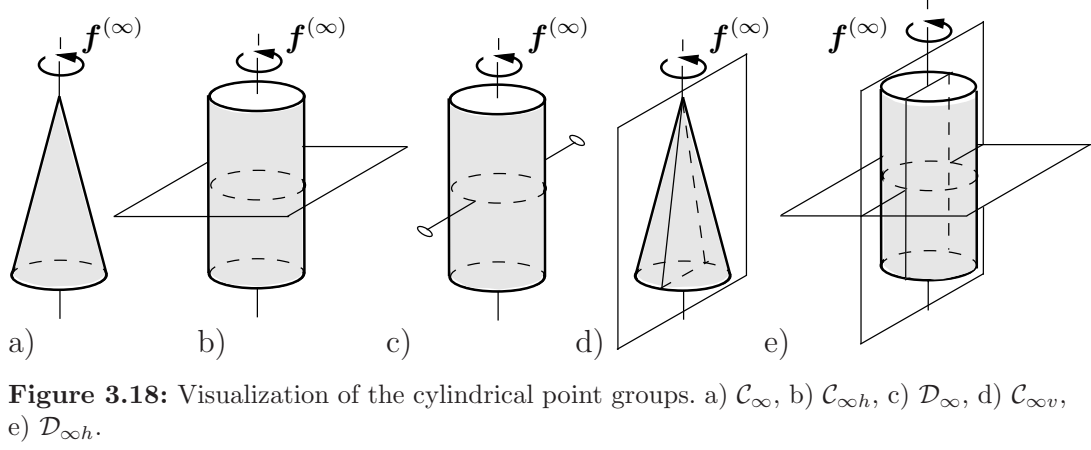


Figure 3.18: Visualization of the cylindrical point groups. a) \mathcal{C}_∞ , b) $\mathcal{C}_{\infty h}$, c) \mathcal{D}_∞ , d) $\mathcal{C}_{\infty v}$, e) $\mathcal{D}_{\infty h}$.

Combinations with a two-fold axis perpendicular to the infinite rotation axis and with the central inversion yield five different cylindrical point groups, see Figure 3.18.

Detailed representations of the generators of the groups are given in Tables 3.4 -3.6, where \mathbf{a} is chosen to be the X_3 -axis, the axis \mathbf{b} of the spherical groups is given by the X_1 -axis and the two-fold axis of the cylindrical groups is also considered by the X_1 -axis.

3.7 Effect of Crystal Symmetry on Tensor Components in Hyperelasticity.

For the modeling of the physical properties of anisotropic hyperelastic materials the energy has to satisfy the principle of material symmetry

$$\psi(\mathbf{C}) = \psi(\overline{\mathbf{C}}) \quad \text{with} \quad \overline{\mathbf{C}}_{IJ} = Q_{IK} C_{KL} Q_{JL} \quad \forall \mathbf{Q} \in \mathcal{G}, \quad (3.11)$$

where once again \mathcal{G} denotes the material symmetry group of the underlying crystal. Taking for the energy function the simple quadratic form

$$\psi(\mathbf{C}) = \frac{1}{4} \left[\left(\frac{1}{2}(\mathbf{C} - \mathbf{1}) \right) : \mathbb{C} : \left(\frac{1}{2}(\mathbf{C} - \mathbf{1}) \right) \right] \quad \text{with} \quad \mathbb{C} = 4 \frac{\partial \psi(\mathbf{C})}{\partial \mathbf{C} \partial \mathbf{C}} = \text{const.}, \quad (3.12)$$

the invariance requirement (3.11) reads

$$\psi(\mathbf{C}) = \psi(\overline{\mathbf{C}}) \quad \Rightarrow \quad (\mathbf{C} - \mathbf{1}) : \mathbb{C} : (\mathbf{C} - \mathbf{1}) = (\overline{\mathbf{C}} - \mathbf{1}) : \mathbb{C} : (\overline{\mathbf{C}} - \mathbf{1}). \quad (3.13)$$

In index notation we obtain

$$(C_{IJ} - \delta_{IJ})(C_{KL} - \delta_{KL})Q_{AI}Q_{MJ}Q_{RK}Q_{SL}\mathbb{C}_{AMRS} = (C_{IJ} - \delta_{IJ})(C_{KL} - \delta_{KL})\mathbb{C}_{IJKL}, \quad (3.14)$$

which reduces to the following invariance requirement of the tangent moduli for quadratic energy functions

$$\mathbb{C}_{IJKL} = Q_{AI}Q_{MJ}Q_{RK}Q_{SL}\mathbb{C}_{AMRS} \quad \forall \mathbf{Q} \in \mathcal{G}. \quad (3.15)$$

The latter invariance requirement is of course the same as that which we obtain for the anisotropic elasticity tensors in linear elasticity. Thus, in general, the material symmetry group has an effect on the form of the corresponding energy; for quadratic energies, it reduces the number of independent components of the corresponding tangent moduli. We have already introduced the point groups of the crystals, but how do the material symmetry groups of crystals look like in case of anisotropic hyperelasticity?

Effect on Material Symmetry Groups^{3.)}: For instance, the hyperelastic anisotropic material properties of the monoclinic crystals $\mathcal{C}_2, \mathcal{C}_{1h}, \mathcal{C}_{2h}$ obey the same symmetries. Thus, they can be described by the same material symmetry group. According to the principle of material symmetry (3.11) the energy function of a monoclinic crystal has to fulfill (3.11); the tangent moduli \mathbb{C} obtained for a quadratic energy has to satisfy (3.15). The underlying monoclinic point groups $\mathcal{P}_3, \mathcal{P}_4, \mathcal{P}_5$ have the forms

$$\mathcal{P}_3 = \{Q_{X_3}^\pi, \mathbf{1}\}, \quad \mathcal{P}_4 = \{-Q_{X_3}^\pi, \mathbf{1}\}, \quad \mathcal{P}_5 = \{Q_{X_3}^\pi, -Q_{X_3}^\pi, \mathbf{1}, -\mathbf{1}\}.$$

It is obvious that a rotation Q and the corresponding rotoinversion $-Q$ have the same effect on the transformation of C and the invariance requirement of \mathbb{C} ^{4.)}, i.e.,

$$\begin{aligned} \bar{C} &= Q C Q^T = (-Q) C (-Q)^T = (-1)^2 Q C Q^T, \\ \mathbb{C} &= Q \boxtimes Q : \mathbb{C} : Q^T \boxtimes Q^T = (-Q) \boxtimes (-Q) : \mathbb{C} : (-Q)^T \boxtimes (-Q)^T \\ &= (-1)^4 Q \boxtimes Q : \mathbb{C} : Q^T \boxtimes Q^T. \end{aligned}$$

Hence, the point groups of the monoclinic crystals have the same effects on the form of the energy function and – for quadratic energies – on the type of tangent moduli. Therefore, the anisotropic hyperelastic material behavior of the crystals can be described by one material symmetry group (chosen here to be \mathcal{P}_5 , cf. [146]):

$$\mathcal{G}_2 = \{Q_{X_3}^\pi, -Q_{X_3}^\pi, \mathbf{1}, -\mathbf{1}\}. \quad (3.16)$$

Performing this analysis for all crystal classes, we come to the conclusion that – for the description of the hyperelastic material properties of crystals – the 32 point groups $\mathcal{P}_i, i = 1, \dots, 32$ can be summarized into 11 material symmetry groups $\mathcal{G}_i, i = 1, \dots, 11$ and the 5 transversely isotropic groups can be summarized into the 2 material symmetry groups $\mathcal{G}_{12}, \mathcal{G}_{13}$. The results are presented in Tables 3.4 -3.6, where we use the notation of ZHENG & SPENCER [146], see column (ZS). Thus, all in all there exist 13 different material symmetry groups for the modeling of anisotropic hyperelastic material behavior.

Effect on Quadratic Energy: Once again, in linear elasticity as well as for quadratic energies in finite elasticity, the fulfillment of the principle of material symmetry results in the invariance condition (3.15) of \mathbb{C} . This requirement reduces the independent components of the elasticity tensor \mathbb{C} according to the underlying material symmetry group: in

^{3.)}see the definition on page 28.

^{4.)} $(A \boxtimes B)(a \otimes b) := Aa \otimes Bb \forall A, B \in \mathbb{R}^{3 \times 3}, a, b \in \mathbb{R}^3$, cf. [56], [42].

anisotropic hyperelasticity, from 21 in the most general ^{5.)} triclinic case to 3 coefficients in the most restricted cubic case. The coefficient matrices of the classical elasticity tensors can be found in many publications, such as e.g. in VOIGT [128]. For instance, for the monoclinic material symmetry \mathcal{G}_2 , the only symmetry transformation, which has an effect on the form of the tangent moduli, is

$$\pm \mathbf{Q}_{X_3}^\pi = \pm \text{diag}[-1, -1, 1].$$

Equation (3.15) appears as

$$\mathbb{C}_{IJKL} = Q_{II}Q_{JJ}Q_{KK}Q_{LL}\mathbb{C}_{IJKL},$$

which implies cancellations of components in which the index 3 appears an odd number of times, so that $Q_{II}Q_{JJ}Q_{KK}Q_{LL} = -1$. Thus, 13 constants remain and the coefficient matrix in Voigt notation is

Monoclinic Elasticity Tensor (MSG^{6.)} \mathcal{G}_2):

$$\mathbb{C}^{(V)m} = \begin{bmatrix} \mathbb{C}_{1111} & \mathbb{C}_{1122} & \mathbb{C}_{1133} & \mathbb{C}_{1112} & 0 & 0 \\ & \mathbb{C}_{2222} & \mathbb{C}_{2233} & \mathbb{C}_{2212} & 0 & 0 \\ & & \mathbb{C}_{3333} & \mathbb{C}_{3312} & 0 & 0 \\ & & & \mathbb{C}_{1212} & 0 & 0 \\ & sym. & & & \mathbb{C}_{2323} & \mathbb{C}_{2313} \\ & & & & & \mathbb{C}_{1313} \end{bmatrix}.$$

The effect of material symmetry groups on the components and relations between the components of all anisotropic elasticity tensors is e.g. presented in VOIGT [129]. The remaining elasticity tensors have the forms:

Triclinic Elasticity Tensor (MSG \mathcal{G}_1):

$$\mathbb{C}^{(V)a} = \begin{bmatrix} \mathbb{C}_{1111} & \mathbb{C}_{1122} & \mathbb{C}_{1133} & \mathbb{C}_{1112} & \mathbb{C}_{1123} & \mathbb{C}_{1113} \\ & \mathbb{C}_{2222} & \mathbb{C}_{2233} & \mathbb{C}_{2212} & \mathbb{C}_{2223} & \mathbb{C}_{2213} \\ & & \mathbb{C}_{3333} & \mathbb{C}_{3312} & \mathbb{C}_{3323} & \mathbb{C}_{3313} \\ & & & \mathbb{C}_{1212} & \mathbb{C}_{1223} & \mathbb{C}_{1213} \\ & sym. & & & \mathbb{C}_{2323} & \mathbb{C}_{2313} \\ & & & & & \mathbb{C}_{1313} \end{bmatrix}$$

Rhombic Elasticity Tensor (MSG \mathcal{G}_3):

$$\mathbb{C}^{(V)o} = \begin{bmatrix} \mathbb{C}_{1111} & \mathbb{C}_{1122} & \mathbb{C}_{1133} & 0 & 0 & 0 \\ & \mathbb{C}_{2222} & \mathbb{C}_{2233} & 0 & 0 & 0 \\ & & \mathbb{C}_{3333} & 0 & 0 & 0 \\ & & & \mathbb{C}_{1212} & 0 & 0 \\ & sym. & & & \mathbb{C}_{2323} & 0 \\ & & & & & \mathbb{C}_{1313} \end{bmatrix}$$

^{5.)}The coefficient matrix of the fourth-order tangent moduli \mathbb{C} has 81 components. In case of elasticity, where the relation $\mathbb{C} = 2\partial_C \mathbf{S}$ holds, the symmetries of the second Piola-Kirchhoff stress tensor \mathbf{S} and of the right Cauchy-Green tensor \mathbf{C} reduce the number of independent components of \mathbb{C} from 81 to 36. In hyperelasticity, \mathbb{C} can be also determined by the second derivative of the energy ψ w.r.t. the symmetric right Cauchy-Green tensor, i.e., $\mathbb{C} = 4\partial_{CC}\psi$, which reduces finally the independent components of \mathbb{C} from 36 to 21. For more details see Appendix B.

^{6.)}MSG is here the abbreviation for Material Symmetry Group.

Tetragonal Elasticity Tensor (MSG \mathcal{G}_4):

$$\mathbb{C}^{(V) t1} = \begin{bmatrix} \mathbb{C}_{1111} & \mathbb{C}_{1122} & \mathbb{C}_{1133} & \mathbb{C}_{1112} & 0 & 0 \\ & \mathbb{C}_{1111} & \mathbb{C}_{1133} & -\mathbb{C}_{1112} & 0 & 0 \\ & & \mathbb{C}_{3333} & 0 & 0 & 0 \\ & & & \mathbb{C}_{1212} & 0 & 0 \\ & sym. & & & \mathbb{C}_{2323} & 0 \\ & & & & & \mathbb{C}_{2323} \end{bmatrix}$$

Tetragonal Elasticity Tensor (MSG \mathcal{G}_5):

$$\mathbb{C}^{(V) t2} = \begin{bmatrix} \mathbb{C}_{1111} & \mathbb{C}_{1122} & \mathbb{C}_{1133} & 0 & 0 & 0 \\ & \mathbb{C}_{1111} & \mathbb{C}_{1133} & 0 & 0 & 0 \\ & & \mathbb{C}_{3333} & 0 & 0 & 0 \\ & & & \mathbb{C}_{1212} & 0 & 0 \\ & sym. & & & \mathbb{C}_{2323} & 0 \\ & & & & & \mathbb{C}_{2323} \end{bmatrix}$$

Trigonal Elasticity Tensor (MSG \mathcal{G}_8):

$$\mathbb{C}^{(V) ht1} = \begin{bmatrix} \mathbb{C}_{1111} & \mathbb{C}_{1122} & \mathbb{C}_{1133} & 0 & \mathbb{C}_{1123} & \mathbb{C}_{1113} \\ & \mathbb{C}_{1111} & \mathbb{C}_{1133} & 0 & -\mathbb{C}_{1123} & -\mathbb{C}_{1113} \\ & & \mathbb{C}_{3333} & 0 & 0 & 0 \\ & & & \frac{1}{2}(\mathbb{C}_{1111} - \mathbb{C}_{1122}) & -\mathbb{C}_{1113} & \mathbb{C}_{1123} \\ & sym. & & & \mathbb{C}_{2323} & 0 \\ & & & & & \mathbb{C}_{2323} \end{bmatrix}$$

Trigonal Elasticity Tensor (MSG \mathcal{G}_9):

$$\mathbb{C}^{(V) ht2} = \begin{bmatrix} \mathbb{C}_{1111} & \mathbb{C}_{1122} & \mathbb{C}_{1133} & 0 & \mathbb{C}_{1123} & 0 \\ & \mathbb{C}_{1111} & \mathbb{C}_{1133} & 0 & -\mathbb{C}_{1123} & 0 \\ & & \mathbb{C}_{3333} & 0 & 0 & 0 \\ & & & \frac{1}{2}(\mathbb{C}_{1111} - \mathbb{C}_{1122}) & 0 & \mathbb{C}_{1123} \\ & sym. & & & \mathbb{C}_{2323} & 0 \\ & & & & & \mathbb{C}_{2323} \end{bmatrix}$$

Cubic Elasticity Tensor (MSG $\mathcal{G}_6, \mathcal{G}_7$):

$$\mathbb{C}^{(V) c1} = \begin{bmatrix} \mathbb{C}_{1111} & \mathbb{C}_{1122} & \mathbb{C}_{1122} & 0 & 0 & 0 \\ & \mathbb{C}_{1111} & \mathbb{C}_{1122} & 0 & 0 & 0 \\ & & \mathbb{C}_{1111} & 0 & 0 & 0 \\ & & & \mathbb{C}_{1212} & 0 & 0 \\ & sym. & & & \mathbb{C}_{1212} & 0 \\ & & & & & \mathbb{C}_{1212} \end{bmatrix}$$

Hexagonal Elasticity Tensor (MSG $\mathcal{G}_{10}, \mathcal{G}_{11}$), Transversely Isotropic Elasticity Tensor (MSG $\mathcal{G}_{12}, \mathcal{G}_{13}$):

$$\mathbb{C}^{(V)ti} = \begin{bmatrix} \mathbb{C}_{1111} & \mathbb{C}_{1122} & \mathbb{C}_{1122} & 0 & 0 & 0 \\ & \mathbb{C}_{1111} & \mathbb{C}_{1122} & 0 & 0 & 0 \\ & & \mathbb{C}_{1111} & 0 & 0 & 0 \\ & & & \mathbb{C}_{1212} & 0 & 0 \\ & sym. & & & \mathbb{C}_{1212} & 0 \\ & & & & & \mathbb{C}_{1212} \end{bmatrix}$$

Effect on General Energy: In order to generalize the above-mentioned observations for quadratic energies we introduce a more general energy function $\psi(\mathbf{C})$ formulated in the six independent components of the symmetric right Cauchy-Green tensor

$$\psi(\mathbf{C}) = \psi(C_{11}, C_{22}, C_{33}, C_{12}, C_{23}, C_{13}) \quad (3.17)$$

and enforce the principle of material symmetry (3.11). The evaluation of (3.11) leads to restrictions of the functional dependency of $\psi(\mathbf{C})$ in terms of the components of \mathbf{C} . It is obvious, that the energy function is allowed to depend only on those coefficients of \mathbf{C} , which remain unaltered by the underlying symmetry transformation, i.e., on the corresponding scalar-valued invariants of the coefficient matrix of \mathbf{C} .

For instance, in case of transverse isotropy characterized by the material symmetry group \mathcal{G}_{13} , performing the transformation $\mathbf{Q}_{X_3}^\alpha$ of C_{IJ} yields

$$\begin{aligned} \overline{C}_{11} &= C_{11} \cos^2 \alpha + C_{22} \sin^2 \alpha + 2 C_{12} \sin \alpha \cos \alpha \\ \overline{C}_{22} &= C_{11} \sin^2 \alpha + C_{22} \cos^2 \alpha - 2 C_{12} \sin \alpha \cos \alpha \\ \overline{C}_{23} &= C_{23} \cos \alpha - C_{13} \sin \alpha \\ \overline{C}_{13} &= C_{23} \sin \alpha + C_{13} \cos \alpha \\ \overline{C}_{12} &= (C_{22} - C_{11}) \sin \alpha \cos \alpha + C_{12} (\cos^2 \alpha - \sin^2 \alpha) \\ \overline{C}_{33} &= C_{33} . \end{aligned} \quad (3.18)$$

Adding (3.18)₁ and (3.18)₂ leads to

$$\begin{aligned} \overline{C}_{11} &= C_{11} \cos^2 \alpha + C_{22} \sin^2 \alpha + 2 C_{12} \sin \alpha \cos \alpha \\ + \overline{C}_{22} &= C_{11} \sin^2 \alpha + C_{22} \cos^2 \alpha - 2 C_{12} \sin \alpha \cos \alpha \\ \hline \overline{C}_{11} + \overline{C}_{22} &= C_{11} + C_{22} . \end{aligned} \quad (3.19)$$

Summing the squares of (3.18)₃ and (3.18)₄ gives

$$\begin{aligned} \overline{C}_{23}^2 &= (C_{23} \cos \alpha - C_{13} \sin \alpha)^2 \\ + \overline{C}_{13}^2 &= (C_{23} \sin \alpha + C_{13} \cos \alpha)^2 \\ \hline \overline{C}_{23}^2 + \overline{C}_{13}^2 &= C_{23}^2 + C_{13}^2 . \end{aligned} \quad (3.20)$$

Furthermore we have

$$\overline{C}_{11}\overline{C}_{22} - \overline{C}_{12}^2 = C_{11}C_{22} - C_{12}^2 \quad (3.21)$$

and

$$\det \overline{\mathbf{C}} = \det \mathbf{C}. \quad (3.22)$$

Finally we obtain the set

$$C_{11} + C_{22}, C_{33}, C_{11}C_{22} - C_{12}^2, C_{13}^2 + C_{23}^2, \det \mathbf{C}, \quad (3.23)$$

see e.g. DE BOER & SCHRÖDER [42]. Thus, if we assume the anisotropic scalar-valued energy function ψ is given in terms of the arguments listed in (3.23), ψ is invariant under the associated material symmetry group.

Table 3.4: Point Group Symbols I: 32 Crystal Classes.

| Symmetry | No. \mathcal{P} | Material Symmetry Group (ZS) | Notation (Schoen.) | Group Generators |
|------------|----------------------|------------------------------------|-----------------------|--|
| triclinic | 1 | \mathcal{G}_1 | \mathcal{C}_1 | $\mathbf{1}$ |
| | 2 | | \mathcal{C}_i | $-\mathbf{1}$ |
| monoclinic | 3 | \mathcal{G}_2 | \mathcal{C}_2 | $Q_{X_3}^\pi$ |
| | 4 | | \mathcal{C}_{1h} | $-Q_{X_3}^\pi$ |
| | 5 | | \mathcal{C}_{2h} | $Q_{X_3}^\pi, -\mathbf{1}$ |
| rhombic | 6 | \mathcal{G}_3 | \mathcal{D}_2 | $Q_{X_1}^\pi, Q_{X_3}^\pi$ |
| | 7 | | \mathcal{C}_{2v} | $-Q_{X_1}^\pi, Q_{X_3}^\pi$ |
| | 8 | | \mathcal{D}_{2h} | $Q_{X_3}^\pi, Q_{X_1}^\pi, -\mathbf{1}$ |
| tetragonal | 9 | \mathcal{G}_4 | \mathcal{C}_4 | $Q_{X_3}^{\pi/2}$ |
| | 10 | | \mathcal{C}_{2i} | $-Q_{X_3}^{\pi/2}$ |
| | 11 | | \mathcal{C}_{4h} | $Q_{X_3}^{\pi/2}, -\mathbf{1}$ |
| | 12 | \mathcal{G}_5 | \mathcal{D}_4 | $Q_{X_3}^{\pi/2}, Q_{X_1}^\pi$ |
| | 13 | | \mathcal{C}_{4v} | $Q_{X_3}^{\pi/2}, -Q_{X_1}^\pi$ |
| | 14 | | \mathcal{D}_{2d} | $-Q_{X_3}^{\pi/2}, -Q_{X_1}^\pi$ |
| | 15 | | \mathcal{D}_{4h} | $Q_{X_3}^{\pi/2}, Q_{X_1}^\pi, -\mathbf{1}$ |
| trigonal | 16 | \mathcal{G}_8 | \mathcal{C}_3 | $Q_{X_3}^{2\pi/3}$ |
| | 17 | | \mathcal{C}_{3i} | $Q_{X_3}^{2\pi/3}, -\mathbf{1}$ |
| | 18 | \mathcal{G}_9 | \mathcal{D}_3 | $Q_{X_3}^{2\pi/3}, Q_{X_1}^\pi$ |
| | 19 | | \mathcal{C}_{3v} | $Q_{X_3}^{2\pi/3}, -Q_{X_1}^\pi$ |
| | 20 | | \mathcal{D}_{3d} | $Q_{X_3}^{2\pi/3}, Q_{X_1}^\pi, -\mathbf{1}$ |

Table 3.5: Point Group Symbols II: 32 Crystal Classes.

| Symmetry | No. \mathcal{P} | Material Symmetry Group (ZS) | Notation (Schoen.) | Group Generators |
|-----------|----------------------|------------------------------------|-----------------------|--|
| hexagonal | 21 | \mathcal{G}_{10} | \mathcal{C}_6 | $Q_{X_3}^{\pi/3}$ |
| | 22 | | \mathcal{C}_{3h} | $-Q_{X_3}^{\pi/3}$ |
| | 23 | | \mathcal{C}_{6h} | $Q_{X_3}^{\pi/3}, -1$ |
| | 24 | \mathcal{G}_{11} | \mathcal{D}_6 | $Q_{X_3}^{\pi/3}, Q_{X_1}^{\pi}$ |
| | 25 | | \mathcal{C}_{6v} | $Q_{X_3}^{\pi/3}, -Q_{X_1}^{\pi}$ |
| | 26 | | \mathcal{D}_{3h} | $-Q_{X_3}^{\pi/3}, -Q_{X_1}^{\pi}$ |
| | 27 | | \mathcal{D}_{6h} | $Q_{X_3}^{\pi/3}, Q_{X_1}^{\pi}, -1$ |
| cubic | 28 | \mathcal{G}_6 | \mathcal{T} | $Q_p^{2\pi/3}, Q_{X_1}^{\pi}, Q_{X_2}^{\pi}$ |
| | 29 | | \mathcal{T}_h | $Q_p^{2\pi/3}, Q_{X_1}^{\pi}, Q_{X_2}^{\pi}, -1$ |
| | 30 | \mathcal{G}_7 | \mathcal{O} | $Q_p^{2\pi/3}, Q_{X_1}^{\pi/2}, Q_{X_2}^{\pi}$ |
| | 31 | | \mathcal{T}_d | $Q_p^{2\pi/3}, -Q_{X_1}^{\pi/2}, Q_{X_2}^{\pi}$ |
| | 32 | | \mathcal{O}_h | $Q_p^{2\pi/3}, Q_{X_1}^{\pi/2}, Q_{X_2}^{\pi}, -1$ |

Table 3.6: Point Group Symbols III: Non-Crystal Classes.

| Symmetry | No. \mathcal{P} | Material Symmetry Group (ZS) | Notation (Schoen.) | Group Generators |
|------------------------|----------------------|------------------------------------|--|---|
| transversely isotropic | 33 | \mathcal{G}_{13} | $\mathcal{C}_{\infty} = \mathcal{T}_1$ | $Q_{X_3}^{\alpha}$ |
| | 34 | | $\mathcal{C}_{\infty h} = \mathcal{T}_3$ | $Q_{X_3}^{\alpha}, -1$ |
| | 35 | \mathcal{G}_{12} | $\mathcal{C}_{\infty v} = \mathcal{T}_2$ | $Q_{X_3}^{\alpha}, -Q_{X_1}^{\pi}$ |
| | 36 | | $\mathcal{D}_{\infty} = \mathcal{T}_5$ | $Q_{X_3}^{\alpha}, Q_{X_1}^{\pi}$ |
| | 37 | | $\mathcal{D}_{\infty h} = \mathcal{T}_4$ | $Q_{X_3}^{\alpha}, -Q_{X_1}^{\pi}, -1$ |
| isotropic | 38 | | $\mathcal{K} = \text{O}(3)$ | $Q_{X_3}^{\alpha}, Q_{X_1}^{\beta}$ |
| | 39 | | $\mathcal{K}_h = \text{SO}(3)$ | $Q_{X_3}^{\alpha}, Q_{X_1}^{\beta}, -1$ |

4 Isotropic Tensor Functions for Anisotropic Elasticity.

In this chapter we present the continuum mechanical modeling of anisotropic elasticity within the framework of isotropic tensor functions.

Isotropic Tensor Functions: Let $\delta \in \mathbb{R}$ and $\mathbf{D} \in \mathbb{R}^{3 \times 3}$ then y and \mathbf{Y} are scalar- and second-order tensor-valued isotropic functions, respectively, if for any argument the following conditions are satisfied

$$\left. \begin{aligned} y(\delta, \mathbf{D}) &= y(\delta, \mathbf{QDQ}^T) \\ \mathbf{QY}(\delta, \mathbf{D})\mathbf{Q}^T &= \mathbf{Y}(\delta, \mathbf{QDQ}^T) \end{aligned} \right\} \forall \mathbf{Q} \in \text{O}(3). \quad (4.1)$$

The isotropic functions y and \mathbf{Y} are also denoted as coordinate-invariant functions. Note that, otherwise, if equation (4.1) is only valid for $\mathbf{Q} \in \mathcal{G} \subset \text{O}(3)$, the \mathcal{G} -invariant functions are called anisotropic with respect to the whole argument list.

Of fundamental relevance to this is that for isotropic tensor functions there exist representation theorems in the literature, which are mainly proposed by WANG [131, 132, 133] and SMITH [115], using different approaches. As an answer to Smith's criticism, SMITH [114], on the papers [132, 133], Wang published new representations [134, 135] and a corrigendum [136]. In his work on irreducible representations of isotropic scalar functions BOEHLER [27] compared and corrected both approaches and finally derived a unified representation. In this context we also refer to BOEHLER [30] and SPENCER [118] and the references therein^{7.)}.

Representation theorems based on the theory of matrix polynomials are proposed e.g. in RIVLIN [96]. In the context of isotropic tensor polynomials we refer also to the classical textbooks of SCHUR [108], WEYL [137], GRACE & YOUNG [53] and GUREWICH [55] among many others. Formulation of constitutive polynomials in continuum mechanics and applications can be found in BOEHLER [30], SPENCER [118, 117] and BETTEN [20]. See also SCHRÖDER [99].

4.1 Motivation.

We have already seen that the constitutive equations $\psi(\mathbf{C})$ and $\mathbf{S}(\mathbf{C})$ in terms of the right Cauchy-Green tensor \mathbf{C} are isotropic, if

$$\left. \begin{aligned} \psi(\mathbf{C}) &= \psi(\mathbf{QCQ}^T) \\ \mathbf{QS}(\mathbf{C})\mathbf{Q}^T &= \mathbf{S}(\mathbf{QCQ}^T) \end{aligned} \right\} \forall \mathbf{Q} \in \text{O}(3) \quad (4.2)$$

is fulfilled. Thus, we notice that the usage of isotropic tensor functions for the constitutive equations $\psi(\mathbf{C})$ and $\mathbf{S}(\mathbf{C})$ for the description of isotropic material behavior leads to an automatical fulfillment of the principle of material symmetry.

^{7.)}The representation theorems of isotropic tensor functions are based on scalar-, vector- and second-order tensor-valued arguments. We neglect here vector-valued arguments, since we do not need them in our applications. For the corresponding representations the reader is referred e.g. to [30].

A very useful representation theorem for isotropic tensor functions is the Cayley-Hamilton theorem. This theorem states that an arbitrary quadratic tensor satisfies his own characteristic equation. Taking the tensor $\mathbf{D} \in \mathbb{R}^{3 \times 3}$ that means

$$\mathbf{p}(\mathbf{D}) = -\mathbf{D}^3 + I_1 \mathbf{D}^2 - I_2 \mathbf{D} + I_3 \mathbf{1} = \mathbf{0} \quad \Rightarrow \quad \mathbf{D}^3 = I_1 \mathbf{D}^2 - I_2 \mathbf{D} + I_3 \mathbf{1}, \quad (4.3)$$

where I_1, I_2, I_3 are the principal invariants of \mathbf{D}

$$I_1 = \text{tr} \mathbf{D}, \quad I_2 = \text{tr}[\text{Cof} \mathbf{D}], \quad I_3 = \det \mathbf{D}. \quad (4.4)$$

The latter scalar-valued functions are isotropic, because they are invariant with respect to orthogonal transformations $\mathbf{Q} \in \text{O}(3)$ in the sense

$$\text{tr} \mathbf{D} = \text{tr}[\mathbf{Q} \mathbf{D} \mathbf{Q}^T], \quad \text{tr}[\text{Cof} \mathbf{D}] = \text{tr}[\text{Cof}[\mathbf{Q} \mathbf{D} \mathbf{Q}^T]], \quad \det \mathbf{D} = \det[\mathbf{Q} \mathbf{D} \mathbf{Q}^T]. \quad (4.5)$$

An important consequence of the Cayley-Hamilton theorem is that any power $\mathbf{D}^n, n \geq 3$, can be expressed in terms of the first two powers \mathbf{D}, \mathbf{D}^2 and $\mathbf{1}$, e.g.,

$$\begin{aligned} \mathbf{D}^4 &= \mathbf{D}^3 \mathbf{D} = I_1 \mathbf{D}^3 - I_2 \mathbf{D}^2 + I_3 \mathbf{D} \\ &= I_1(I_1 \mathbf{D}^2 - I_2 \mathbf{D} + I_3 \mathbf{1}) - I_2 \mathbf{D}^2 + I_3 \mathbf{D} \\ &= (I_1^2 - I_2) \mathbf{D}^2 - (I_1 I_2 - I_3) \mathbf{D} + I_1 I_3 \mathbf{1}. \end{aligned} \quad (4.6)$$

For invertible tensors negative powers can be also given as tensor polynomials of order two. Multiplying (4.3) with \mathbf{D}^{-1} yields

$$\mathbf{D}^2 = I_1 \mathbf{D} - I_2 \mathbf{1} + I_3 \mathbf{D}^{-1} \quad \Rightarrow \quad \mathbf{D}^{-1} = \frac{1}{I_3}(\mathbf{D}^2 - I_1 \mathbf{D} + I_2 \mathbf{1}). \quad (4.7)$$

Thus, a polynomial tensor function $\mathbf{Y}(\mathbf{D})$ of arbitrary order greater than two can be expressed as a polynomial function of order two of its tensorial argument \mathbf{D} :

$$\mathbf{Y}(\mathbf{D}) = f_1 \mathbf{1} + f_2 \mathbf{D} + f_3 \mathbf{D}^2,$$

where the coefficients f_1, f_2, f_3 are scalar-valued polynomial functions in terms of the principal invariants of \mathbf{D} , i.e.,

$$f_a = \hat{f}_a[I_1(\mathbf{D}), I_2(\mathbf{D}), I_3(\mathbf{D})] \quad a = 1, 2, 3. \quad (4.8)$$

Hence, for the description of isotropic material behavior this theorem can be easily applied on the second Piola-Kirchhoff stress tensor \mathbf{S} in terms of the right Cauchy-Green tensor \mathbf{C} . This leads to the isotropic polynomial tensor function

$$\mathbf{S}(\mathbf{C}) = 2 \frac{\partial \psi}{\partial \mathbf{C}} = f_1 \mathbf{1} + f_2 \mathbf{C} + f_3 \mathbf{C}^2, \quad (4.9)$$

with $f_a = \hat{f}_a[I_1(\mathbf{C}), I_2(\mathbf{C}), I_3(\mathbf{C})]$, $a = 1, 2, 3$. In the sequel we always use

$$I_1 = \text{tr} \mathbf{C}, \quad I_2 = \text{tr}[\text{Cof} \mathbf{C}], \quad I_3 = \det \mathbf{C}. \quad (4.10)$$

The relation (4.9) is true if we express now the free energy function $\psi(\mathbf{C})$ as isotropic scalar-valued function in terms of the whole set of principal invariants of \mathbf{C}

$$\psi(\mathbf{C}) = \psi(I_1, I_2, I_3), \quad (4.11)$$

so that we can directly identify the scalar-valued isotropic coefficients:

$$f_1 = 2 \left(\frac{\partial \psi}{\partial I_1} + \frac{\partial \psi}{\partial I_2} I_1 + \frac{\partial \psi}{\partial I_3} I_2 \right), \quad f_2 = 2 \left(\frac{\partial \psi}{\partial I_2} + \frac{\partial \psi}{\partial I_3} I_1 \right), \quad f_3 = 2 \left(\frac{\partial \psi}{\partial I_3} \right). \quad (4.12)$$

If the reader is interested in the derivatives of the principal invariants of \mathbf{C} with respect to \mathbf{C} we refer to the Appendix F. Inserting the relation (4.7)₁ into \mathbf{S} , where we exploit that $\text{Cof} \mathbf{C} = I_3 \mathbf{C}^{-T} = I_3 \mathbf{C}^{-1}$, we obtain the alternative expression

$$\mathbf{S} = 2 \left[\left(\frac{\partial \psi}{\partial I_1} + \frac{\partial \psi}{\partial I_2} I_1 \right) \mathbf{1} - \frac{\partial \psi}{\partial I_2} \mathbf{C} + \frac{\partial \psi}{\partial I_3} \text{Cof} \mathbf{C} \right]. \quad (4.13)$$

The Lagrangian elastic moduli are obtained by exploiting $\frac{\partial^2 \psi}{\partial I_i \partial I_j} = \frac{\partial^2 \psi}{\partial I_j \partial I_i}$ as ^{8.)}

$$\begin{aligned} \mathbb{C} = & 4 \left[\frac{\partial^2 \psi}{\partial I_1 \partial I_1} \mathbf{1} \otimes \mathbf{1} + \frac{\partial^2 \psi}{\partial I_2 \partial I_2} \{I_1 \mathbf{1} - \mathbf{C}\} \otimes \{I_1 \mathbf{1} - \mathbf{C}\} \right. \\ & + \frac{\partial^2 \psi}{\partial I_3 \partial I_3} \text{Cof} \mathbf{C} \otimes \text{Cof} \mathbf{C} \\ & + \frac{\partial^2 \psi}{\partial I_2 \partial I_1} [\mathbf{1} \otimes \{I_1 \mathbf{1} - \mathbf{C}\} + \{I_1 \mathbf{1} - \mathbf{C}\} \otimes \mathbf{1}] \\ & + \frac{\partial^2 \psi}{\partial I_3 \partial I_1} [\mathbf{1} \otimes \text{Cof} \mathbf{C} + \text{Cof} \mathbf{C} \otimes \mathbf{1}] \\ & + \frac{\partial^2 \psi}{\partial I_3 \partial I_2} [\{I_1 \mathbf{1} - \mathbf{C}\} \otimes \text{Cof} \mathbf{C} + \text{Cof} \mathbf{C} \otimes \{I_1 \mathbf{1} - \mathbf{C}\}] \\ & \left. + \frac{\partial \psi}{\partial I_2} [\mathbf{1} \otimes \mathbf{1} - \mathbf{1} \boxtimes \mathbf{1}] + \frac{\partial \psi}{\partial I_3} I_3 [\mathbf{C}^{-1} \otimes \mathbf{C}^{-1} - \mathbf{C}^{-1} \boxtimes \mathbf{C}^{-1}] \right]. \end{aligned} \quad (4.14)$$

Remarks. For subsequent applications of the isotropic constitutive equations (4.9) and (4.11) in terms of the symmetric right Cauchy-Green tensor it may be convenient to express the principal invariants I_1, I_2, I_3 (4.10) in terms of the so-called *main invariants* (J_1, J_2, J_3) and vice versa. The main invariants are defined as the traces of the powers of \mathbf{C} by

$$J_1 = \text{tr} \mathbf{C} = I_1, \quad J_2 = \text{tr} [\mathbf{C}^2], \quad J_3 = \text{tr} [\mathbf{C}^3]. \quad (4.15)$$

Analyzing the trace of (4.7)₁ with $\mathbf{D} = \mathbf{C}$ under consideration of the relation $\text{tr} [I_3 \mathbf{C}^{-1}] = \text{tr} [I_3 \mathbf{C}^{-T}] = \text{tr} [\text{Cof} \mathbf{C}]$ yields

$$J_2 = \text{tr} [\mathbf{C}^2] = I_1 \text{tr} \mathbf{C} - 3I_2 + \text{tr} [\text{Cof} \mathbf{C}] = I_1^2 - 2I_2 \Rightarrow I_2 = \frac{1}{2}(J_1^2 - J_2). \quad (4.16)$$

In order to derive the relationship between J_3 and the principal invariants as well as between I_3 and the main invariants we evaluate the trace of (4.3)₂ with $\mathbf{D} = \mathbf{C}$, it follows

$$\begin{aligned} J_3 = \text{tr} [\mathbf{C}^3] &= I_1 \text{tr} \mathbf{C}^2 - I_2 \text{tr} \mathbf{C} + 3I_3 = I_1 J_2 - I_2 J_1 + 3I_3 \\ &= I_1 (I_1^2 - 2I_2) - I_2 I_1 + 3I_3 = I_1^3 - 3I_1 I_2 + 3I_3 \\ \Rightarrow I_3 &= \frac{1}{3} (J_3 - J_1 J_2 + \frac{1}{2} (J_1^2 - J_2) J_1) = \frac{1}{3} (J_3 - \frac{3}{2} J_1 J_2 + \frac{1}{2} J_1^3). \end{aligned} \quad (4.17)$$

Table 4.1: Invariants Depending on One Tensor-Valued Variable.

| Variable | Invariants |
|--------------|---|
| \mathbf{A} | $\text{tr } \mathbf{A}, \text{tr } \mathbf{A}^2, \text{tr } \mathbf{A}^3$ |
| \mathbf{W} | $\text{tr } \mathbf{W}^2$ |

For the representation of an isotropic tensor function $\mathbf{Y}(\mathbf{W})$ depending on a skew-symmetric tensor $\mathbf{W} \in \text{Skew}(3)$ with $\mathbf{W} = -\mathbf{W}^T$, i.e.,

$$\mathbf{W} = \begin{bmatrix} 0 & W_{12} & W_{13} \\ -W_{12} & 0 & W_{23} \\ -W_{13} & -W_{23} & 0 \end{bmatrix} \quad (4.18)$$

the only non-vanishing invariant is

$$J_2 = \text{tr}[\mathbf{W}^2], \quad (4.19)$$

which is always negative, since

$$\mathbf{W}^2 = \begin{bmatrix} -(W_{12}^2 + W_{13}^2) & -W_{13}W_{23} & W_{12}W_{23} \\ -W_{13}W_{23} & -(W_{12}^2 + W_{23}^2) & -W_{12}W_{13} \\ W_{12}W_{23} & -W_{12}W_{13} & -(W_{13}^2 + W_{23}^2) \end{bmatrix}. \quad (4.20)$$

In Table 4.1 the invariants with a single tensor-valued argument, i.e., a symmetric second-order tensor $\mathbf{A} \in \text{Sym}(3)$ with $\mathbf{A} = \mathbf{A}^T$ and skew-symmetric tensor $\mathbf{W} \in \text{Skew}(3)$ with $\mathbf{W} = -\mathbf{W}^T$, respectively, are listed.

4.2 Isotropization of Anisotropic Tensor Functions.

The constitutive equations $\psi(\mathbf{C})$ and $\mathbf{S}(\mathbf{C})$ in terms of the right Cauchy-Green tensor \mathbf{C} are anisotropic, if

$$\left. \begin{aligned} \psi(\mathbf{C}) &= \psi(\mathbf{Q}\mathbf{C}\mathbf{Q}^T) \\ \mathbf{Q}\mathbf{S}(\mathbf{C})\mathbf{Q}^T &= \mathbf{S}(\mathbf{Q}\mathbf{C}\mathbf{Q}^T) \end{aligned} \right\} \forall \mathbf{Q} \in \mathcal{G} \subset \text{O}(3) \quad (4.21)$$

is fulfilled. This definition is identical to the requirement of the principle of material symmetry for the description of anisotropic material behavior.

Anisotropic material behavior can be characterized by structural tensors $\mathbf{\Xi}$, with

$$\mathbf{\Xi} = \{\mathbf{\Xi}_1, \mathbf{\Xi}_2\}, \quad \text{with} \quad \mathbf{\Xi}_1 = \{\mathbf{K}_1, \mathbf{K}_2, \dots\}, \quad \mathbf{\Xi}_2 = \{\mathbb{P}_1, \mathbb{P}_2, \dots\}, \quad (4.22)$$

^{8.)} $(\mathbf{A} \boxtimes \mathbf{B})(\mathbf{a} \otimes \mathbf{b}) := \mathbf{A}\mathbf{a} \otimes \mathbf{B}\mathbf{b} \forall \mathbf{A}, \mathbf{B} \in \mathbb{R}^{3 \times 3}, \mathbf{a}, \mathbf{b} \in \mathbb{R}^3$, cf. [56], [42].

collecting the set Ξ_1 of second-order structural tensors $\mathbf{K}_1, \mathbf{K}_2, \dots$, the set Ξ_2 of all structural tensors of order higher than two, e.g. fourth-order structural tensors $\mathbb{P}_1, \mathbb{P}_2, \dots$ and so on. They reflect the symmetry properties of the underlying anisotropic material, i.e.,

$$\Xi = \mathbf{Q} * \Xi, \quad \forall \quad \mathbf{Q} \in \mathcal{G}, \quad (4.23)$$

where \mathcal{G} is the underlying material symmetry group and we use the abbreviation

$$\begin{aligned} \mathbf{Q} * \Xi = \{ & \mathbf{Q}\mathbf{K}_1\mathbf{Q}^T, \mathbf{Q}\mathbf{K}_2\mathbf{Q}^T, \dots, \\ & \mathbf{Q} \boxtimes \mathbf{Q} : \mathbb{P}_1 : \mathbf{Q}^T \boxtimes \mathbf{Q}^T, \mathbf{Q} \boxtimes \mathbf{Q} : \mathbb{P}_2 : \mathbf{Q}^T \boxtimes \mathbf{Q}^T, \dots \}. \end{aligned}$$

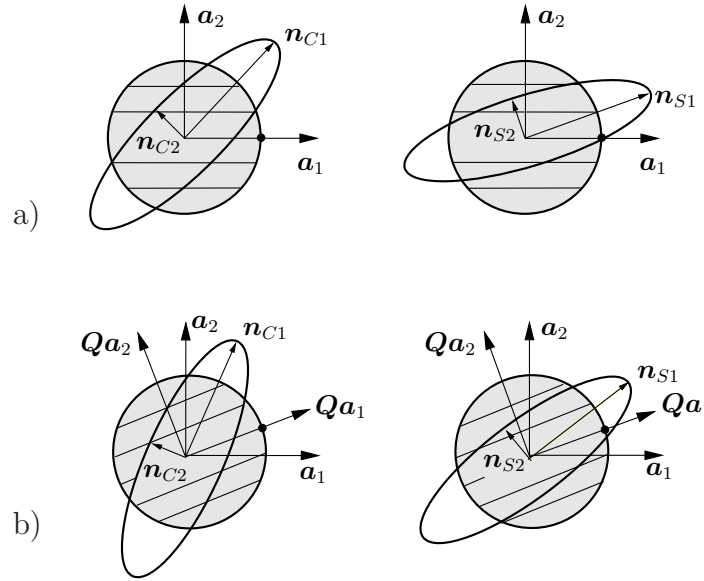


Figure 4.1: Principle of Isotropy of Space: a) the eigenvectors $\mathbf{n}_{C1}, \mathbf{n}_{C2}$ of the deformation \mathbf{C} and the eigenvectors $\mathbf{n}_{S1}, \mathbf{n}_{S2}$ of the stresses \mathbf{S} , respectively, w.r.t. the initial basis $\mathbf{a}_1, \mathbf{a}_2$, b) the same eigenvectors of \mathbf{C} and \mathbf{S} , respectively, w.r.t. the transformed basis $\mathbf{Q}\mathbf{a}_1, \mathbf{Q}\mathbf{a}_2$.

For more details on the structural tensors of the individual material symmetry groups the reader is referred to the next section. Inserting this extended list of argument tensors Ξ into (4.21) yields

$$\left. \begin{aligned} \psi(\mathbf{C}, \Xi) &= \psi(\mathbf{Q}\mathbf{C}\mathbf{Q}^T, \mathbf{Q} * \Xi), \\ \mathbf{Q}\mathbf{S}(\mathbf{C}, \Xi)\mathbf{Q}^T &= \mathbf{S}(\mathbf{Q}\mathbf{C}\mathbf{Q}^T, \mathbf{Q} * \Xi) \end{aligned} \right\} \quad \forall \quad \mathbf{Q} \in \text{O}(3), \quad (4.24)$$

which is the definition of isotropic tensor functions in the complete list of arguments (\mathbf{C}, Ξ) . This isotropicization of anisotropic tensor functions is also known as concept of structural tensors, first introduced with important applications in BOEHLER [27]. It is a consequence of the *Principle of Isotropy of Space*, which is visualized in Figure 4.1. There it is shown that applying a rotation \mathbf{Q} to the anisotropic material (represented by a circle with preferred directions $\mathbf{a}_1, \mathbf{a}_2$), whose material behavior can be characterized by a structural tensor of the set Ξ , and also to the deformation \mathbf{C} results in the same transformation \mathbf{Q} of the material response \mathbf{S} , i.e.,

$$\mathbf{C} \Rightarrow \mathbf{Q}\mathbf{C}\mathbf{Q}^T, \quad \Xi \Rightarrow \mathbf{Q} * \Xi, \quad \mathbf{S} \Rightarrow \mathbf{Q}\mathbf{S}\mathbf{Q}^T.$$

A unified approach summarizing the developments in this field can be found in ZHENG [144]. It should be noted that the functions (4.24) are anisotropic with respect to \mathbf{C} alone:

$$\left. \begin{aligned} \psi(\mathbf{C}, \Xi) &= \psi(\mathbf{Q}\mathbf{C}\mathbf{Q}^T, \Xi) \\ \mathbf{Q}\mathbf{S}(\mathbf{C}, \Xi)\mathbf{Q}^T &= \mathbf{S}(\mathbf{Q}\mathbf{C}\mathbf{Q}^T, \Xi) \end{aligned} \right\} \forall \mathbf{Q} \in \mathcal{G}. \quad (4.25)$$

Thus, with (4.24) we ensure a priori the principle of material symmetry (4.21). For the fulfillment of equation (4.24) extensions of the already introduced representation theorem for isotropic tensor functions with respect to a larger argument list (\mathbf{C}, Ξ) have to be applied.

4.3 Structural Tensors for All Material Symmetry Groups.

In case of transverse isotropy and orthotropy the structural tensors are in general of the type

$$\mathbf{M}_i = \mathbf{a}_i \otimes \mathbf{a}_i, \quad (4.26)$$

cf. BOEHLER [30], where \mathbf{a}_i , with $\|\mathbf{a}_i\| = 1$, represents the i -th preferred direction of the underlying material. A transversely isotropic material is characterized by one preferred direction \mathbf{a} . Choosing the X_3 -axis as preferred direction the transversely isotropic structural tensor \mathbf{M} , whose invariance group preserves the material symmetry group \mathcal{G}_{12} , is then given by the symmetric, rank-one tensor

$$\mathbf{M} = \mathbf{e}_3 \otimes \mathbf{e}_3. \quad (4.27)$$

Orthotropic materials can be described by symmetry relations with respect to three orthogonal planes. The corresponding preferred directions are chosen as the intersections of these planes and are denoted by the vectors $\mathbf{a}_1, \mathbf{a}_2$ and \mathbf{a}_3 with unit length. Thus $(\mathbf{a}_1, \mathbf{a}_2, \mathbf{a}_3)$ represents an orthonormal privileged frame. Based on this, Boehler [30] presented the structural tensors

$$\mathbf{M}_1 = \mathbf{a}_1 \otimes \mathbf{a}_1, \quad \mathbf{M}_2 = \mathbf{a}_2 \otimes \mathbf{a}_2 \quad \text{and} \quad \mathbf{M}_3 = \mathbf{a}_3 \otimes \mathbf{a}_3, \quad (4.28)$$

which are \mathcal{G}_3 -invariant. The structural tensors satisfy:

$$\begin{aligned} (\mathbf{M}_i)^p &= \mathbf{M}_i, \quad \text{tr} \mathbf{M}_i = 1 \quad \text{for } i = 1, 2, 3, \\ \mathbf{M}_i \mathbf{M}_j &= 0 \quad \text{for } i \neq j, \quad i, j = 1, 2, 3, \\ (\mathbf{M}_1 \mathbf{C} + \mathbf{C} \mathbf{M}_1) &+ (\mathbf{M}_2 \mathbf{C} + \mathbf{C} \mathbf{M}_2) + (\mathbf{M}_3 \mathbf{C} + \mathbf{C} \mathbf{M}_3) = 2\mathbf{C}, \\ \text{tr}[\mathbf{M}_1 \mathbf{C}] &+ \text{tr}[\mathbf{M}_2 \mathbf{C}] + \text{tr}[\mathbf{M}_3 \mathbf{C}] = \text{tr} \mathbf{C}. \end{aligned} \quad (4.29)$$

Furthermore, the sum of the three structural tensors yields

$$\sum_{i=1}^3 \mathbf{M}_i = \mathbf{1} \quad \text{hence} \quad \mathbf{M}_3 = \mathbf{1} - \mathbf{M}_1 - \mathbf{M}_2, \quad (4.30)$$

therefore, \mathbf{M}_3 can be cancelled from the set of structural tensors. With regard to e.g. ZHENG & SPENCER [146], ZHENG [144], XIAO [140], ZHANG & RYCHLEWSKI [142] we notice that

Table 4.2: Structural Tensors which Characterize Material Symmetry Groups.

| Crystal System | Mechanics Symmetry Group | Zheng & Spencer, [146] | | Xiao, [140] |
|-------------------------|--------------------------|----------------------------------|---|--|
| | | Structural Tensors | Single Structural Tensor | Structural Tensors |
| Triclinic | \mathcal{G}_1 | $P'_2, \epsilon e_1$ | $P'_2 + \epsilon e_1$ | $\epsilon e_1, \epsilon e_2$ |
| Monoclinic | \mathcal{G}_2 | $P_2, \epsilon e_3$ | $P_2 + \epsilon e_3$ | $e_1 \otimes e_1 - e_2 \otimes e_2, \epsilon e_3$ |
| Rhombic | \mathcal{G}_3 | P_2 | P_2 | $e_1 \otimes e_1 - e_2 \otimes e_2$ |
| Tetragonal | \mathcal{G}_4 | $\mathbb{P}_4, \epsilon e_3$ | $\mathbb{P}_4 + \epsilon e_3^{(3)}$ | $e_1^{(4)} + e_2^{(4)}, \epsilon e_3$ |
| | \mathcal{G}_5 | \mathbb{P}_4 | \mathbb{P}_4 | $e_1^{(4)} + e_2^{(4)}, e_3 \otimes e_3$ |
| Trigonal ^{9.)} | \mathcal{G}_8 | $e_3 \otimes P'_3, \epsilon e_3$ | $e_3 \otimes P'_3 + \epsilon e_3^{(3)}$ | $\sum_{i=1}^3 \epsilon n_i^{(3)}, \epsilon e_3$ |
| | \mathcal{G}_9 | $e_3 \otimes P'_3$ | $e_3 \otimes P'_3$ | $\sum_{i=1}^3 \epsilon n_i^{(3)}, e_3 \otimes e_3$ |
| Hexagonal | \mathcal{G}_{10} | $P_6, \epsilon e_3$ | $P_6 + \epsilon e_3^{(5)}$ | $\sum_{i=1}^3 n_i^{(6)}, \epsilon e_3$ |
| | \mathcal{G}_{11} | P_6 | P_6 | $\sum_{i=1}^3 n_i^{(6)}, e_3 \otimes e_3$ |
| Cubic | \mathcal{G}_6 | Λ | Λ | $\mathbb{T}_h := \mathbb{T}_h^a + \mathbb{T}_h^s$ |
| | \mathcal{G}_7 | Θ | Θ | $e_1^{(4)} + e_2^{(4)} + e_3^{(4)}$ |
| Transverse | \mathcal{G}_{12} | $e_3 \otimes e_3$ | $e_3 \otimes e_3$ | $e_3 \otimes e_3$ |
| Isotropy | \mathcal{G}_{13} | ϵe_3 | ϵe_3 | ϵe_3 |

transverse isotropy, orthotropy as well as the triclinic and monoclinic symmetry groups are the only symmetry groups, which can be completely characterized by second-order structural tensors.

In ZHENG & SPENCER [146] it is shown that each anisotropic symmetry group can be characterized by one single structural tensor (of order up to six): for the representations of triclinic, monoclinic, rhombic as well as transversely isotropic symmetry second-order structural tensors are necessary, whereas, unfortunately,

for the trigonal, tetragonal and cubic systems fourth-order tensors are needed and for the hexagonal systems sixth-order structural tensors are required.

These single structural tensors are presented in Table 4.2. Since the rhombic, tetragonal \mathcal{G}_5 -, trigonal \mathcal{G}_9 - and hexagonal \mathcal{G}_{11} - symmetry groups are finite subgroups of the transversely isotropic symmetry group \mathcal{G}_{12} , the transversely isotropic structural tensor is an additional structural tensor of these mechanically relevant symmetry groups, ZHENG & SPENCER [146]. For a comparison we also listed the structural tensors presented in XIAO [140]. in Table 4.2. Furthermore, the abbreviation $e_i^{(n)}$ of the cartesian base vectors used in Table 4.2 is defined by

$$e_i^{(n)} = \underbrace{e_i \otimes \cdots \otimes e_i}_n, \quad i = 1, 2, 3, n = 1, \dots, 6.$$

Detailed representations of the tensors up to order six appearing in Table 4.2 are given in the Appendix E.

^{9.)} According to [140], [3] the underlying vectors for material symmetry groups $\mathcal{G}_8 - \mathcal{G}_{11}$ are: $n_1 = e_1$, $n_2 = -1/2e_1 + \sqrt{3}/2e_2$, $n_3 = -1/2e_1 - \sqrt{3}/2e_2$.

4.4 Isotropic Tensor Functions for an Extended Set of Arguments.

4.4.1 Extended Set of Second-Order Tensors. A representation of an isotropic polynomial tensor function $\mathbf{Y}(\mathbf{A}_1, \mathbf{A}_2)$ in terms of two symmetric second-order tensors \mathbf{A}_1 and \mathbf{A}_2 as well as scalar-valued polynomial coefficients was first shown in RIVLIN [96]. The explicit representation is

$$\begin{aligned} \mathbf{Y}(\mathbf{A}_1, \mathbf{A}_2) = & f_1 \mathbf{1} + f_2 \mathbf{A}_1 + f_3 \mathbf{A}_1^2 + f_4 \mathbf{A}_2 + f_5 \mathbf{A}_2^2 + f_6 (\mathbf{A}_1 \mathbf{A}_2 + \mathbf{A}_2 \mathbf{A}_1) \\ & + f_7 (\mathbf{A}_1^2 \mathbf{A}_2 + \mathbf{A}_2 \mathbf{A}_1^2) + f_8 (\mathbf{A}_1 \mathbf{A}_2^2 + \mathbf{A}_2^2 \mathbf{A}_1) + f_9 (\mathbf{A}_1^2 \mathbf{A}_2^2 + \mathbf{A}_2^2 \mathbf{A}_1^2). \end{aligned} \quad (4.31)$$

The coefficients $f_a, a = 1, \dots, 9$ are scalar-valued polynomial functions in terms of the principal and *mixed* invariants of \mathbf{A}_1 and \mathbf{A}_2 :

$$f_a = \hat{f}_a[I_1, \dots, I_{10}], \quad I_i \in \mathcal{I}, \quad a = 1, \dots, 9,$$

with the whole set of invariants of the arguments \mathbf{A}_1 and \mathbf{A}_2

$$\mathcal{I} = \{\text{tr} \mathbf{A}_1, \text{tr} \mathbf{A}_1^2, \text{tr} \mathbf{A}_1^3, \text{tr} \mathbf{A}_2, \text{tr} \mathbf{A}_2^2, \text{tr} \mathbf{A}_2^3, \text{tr}[\mathbf{A}_1 \mathbf{A}_2], \text{tr}[\mathbf{A}_1^2 \mathbf{A}_2], \text{tr}[\mathbf{A}_1 \mathbf{A}_2^2], \text{tr}[\mathbf{A}_1^2 \mathbf{A}_2^2]\}.$$

Applying this representation for isotropic tensor functions in terms of the symmetric right Cauchy Green tensor, i.e., $\mathbf{A}_1 = \mathbf{C}$, and a symmetric second-order structural tensor, i.e., $\mathbf{A}_2 = \mathbf{M}$, on the second Piola-Kirchhoff stress tensor we obtain

$$\begin{aligned} \mathbf{S}(\mathbf{C}, \mathbf{M}) = 2 \frac{\partial \psi}{\partial \mathbf{C}} = & f_1 \mathbf{1} + f_2 \mathbf{C} + f_3 \mathbf{C}^2 + f_4 \mathbf{M} + f_5 \mathbf{M}^2 + f_6 (\mathbf{C} \mathbf{M} + \mathbf{M} \mathbf{C}) \\ & + f_7 (\mathbf{C}^2 \mathbf{M} + \mathbf{M} \mathbf{C}^2) + f_8 (\mathbf{C} \mathbf{M}^2 + \mathbf{M}^2 \mathbf{C}) + f_9 (\mathbf{C}^2 \mathbf{M}^2 + \mathbf{M}^2 \mathbf{C}^2), \end{aligned} \quad (4.32)$$

with the energy function as isotropic function in terms of the whole set of principal and mixed invariants of \mathbf{C} and \mathbf{M} :

$$\psi(\mathbf{C}, \mathbf{M}) = \psi(I_1, \dots, I_{10}), \quad I_i \in \mathcal{I}. \quad (4.33)$$

The representation for the more general case of our interest, when the isotropic tensor function $\mathbf{Y}(\mathbf{C}, \mathbf{x})$ should depend on an arbitrary number of second-order tensor arguments \mathbf{x} , with

$$\mathbf{x} = \{\mathbf{A}_1, \mathbf{A}_2, \dots, \mathbf{W}_1, \mathbf{W}_2, \dots\} \quad (4.34)$$

i.e., symmetric tensors $\mathbf{A} \in \text{Sym}(3)$ and skew-symmetric tensors $\mathbf{W} \in \text{Skew}(3)$ can be found in SPENCER & RIVLIN [119].

Sets of Invariants. We have noticed that for the representation of the energy function ψ and hence, the stresses $\mathbf{S} = 2\partial_{\mathbf{C}}\psi$, depending on \mathbf{C} and structural tensors, as isotropic tensor functions we need the whole set of scalar-valued invariants in terms of all arguments. One of the main goal in invariant theory is therefore to find a set of basic invariants for a given set of tensor arguments from which all other invariants can be generated. This is possible, due to *Hilbert's Theorem*. At age 26 David Hilbert (1862-1943) proved the existence of this Finiteness Theorem in his work HILBERT [59]. There the original Theorem reads:

*Ist ein System von Grundformen mit beliebig vielen Veränderlichenreihen gegeben, welche in vorgeschriebener Weise den nämlichen oder verschiedenen linearen Transformationen unterliegen, so giebt es für dasselbe stets eine **endliche Zahl** von ganzen und rationalen Invarianten, durch welche sich jede andere ganze und rationale Invariante in ganzer und rationaler Weise ausdrücken lässt.*

In HILBERT [60] he published a second proof.

Integrity Basis: The set of invariants for a given set of tensor arguments relative to a fixed symmetry group \mathcal{G} is called an *integrity basis* \mathcal{I} , if an arbitrary polynomial invariant of the same arguments can be expressed as a polynomial in the basic invariants. If no element of the considered set can be expressed as a polynomial in the remaining invariants of \mathcal{I} , it is called *irreducible*.

Functional Basis: The set of invariants is called a *functional basis* \mathcal{F} , if an arbitrary invariant in terms of the underlying arguments can be expressed as a function (not necessarily polynomial) in terms of the elements of \mathcal{F} . It is said to be *irreducible*, if none of the elements of the basic set \mathcal{F} can be expressed as a function of the other invariants of \mathcal{F} , i.e., if all elements of \mathcal{F} are *functionally independent*.

In DIMITRIENKO [43] a system of scalar invariants I_1, \dots, I_p is called *functionally independent*, if for every nontrivial function $f(I_1, \dots, I_p)$ of the invariants of the set the relation $f(I_1, \dots, I_p) \neq 0$ is valid.

According to BOEHLER [27, 30] we present the functional bases for two, three and four tensor arguments in Table 4.3.^{10.)}

Table 4.3: Invariants Depending on Two, Three or Four Tensor-Valued Variables ($\mathbf{A} \in \text{Sym}(3)$, $\mathbf{W} \in \text{Skew}(3)$), cf. BOEHLER [30].

| Variable | Invariants |
|--|---|
| $\mathbf{A}_1, \mathbf{A}_2$ | $\text{tr}(\mathbf{A}_1 \mathbf{A}_2), \text{tr}(\mathbf{A}_1^2 \mathbf{A}_2), \text{tr}(\mathbf{A}_1 \mathbf{A}_2^2), \text{tr}(\mathbf{A}_1^2 \mathbf{A}_2^2)$ |
| \mathbf{A}, \mathbf{W} | $\text{tr}(\mathbf{A} \mathbf{W}^2), \text{tr}(\mathbf{A}^2 \mathbf{W}^2), \text{tr}(\mathbf{A}^2 \mathbf{W}^2 \mathbf{A} \mathbf{W})$ |
| $\mathbf{W}_1, \mathbf{W}_2$ | $\text{tr}(\mathbf{W}_1 \mathbf{W}_2)$ |
| $\mathbf{A}_1, \mathbf{A}_2, \mathbf{A}_3$ | $\text{tr}(\mathbf{A}_1 \mathbf{A}_2 \mathbf{A}_3)$ |
| $\mathbf{A}, \mathbf{W}_1, \mathbf{W}_2$ | $\text{tr}(\mathbf{A} \mathbf{W}_1 \mathbf{W}_2), \text{tr}(\mathbf{A} \mathbf{W}_1^2 \mathbf{W}_2), \text{tr}(\mathbf{A} \mathbf{W}_1 \mathbf{W}_2^2)$ |
| $\mathbf{A}_1, \mathbf{A}_2, \mathbf{W}$ | $\text{tr}(\mathbf{A}_1 \mathbf{A}_2 \mathbf{W}), \text{tr}(\mathbf{A}_1^2 \mathbf{A}_2 \mathbf{W}), \text{tr}(\mathbf{A}_1 \mathbf{W}^2 \mathbf{A}_2 \mathbf{W}), \text{tr}(\mathbf{A}_1 \mathbf{A}_2^2 \mathbf{W})$ |
| $\mathbf{W}_1, \mathbf{W}_2, \mathbf{W}_3$ | $\text{tr}(\mathbf{W}_1 \mathbf{W}_2 \mathbf{W}_3)$ |

Note that although the basis presented in Table 4.3, is irreducible for arbitrary tensor arguments, cf. PENNISI & TROVATO [91], a special choice of these tensors could lead to

^{10.)}Once again, we are not interested in invariants depending on vector-valued arguments. For their representations see e.g. [30].

redundant elements.

Set of Invariants: For the formulations of isotropic tensor functions in terms of the right Cauchy-Green tensor \mathbf{C} and structural tensors we construct our *sets of invariants* using Table 4.1 and 4.3. Obvious functionally dependent invariants are neglected. However, the irreducibility of our *sets of invariants* will not be explicitly checked as for example done in DIMITRIENKO [43]. Furthermore, due to our definition of *completeness* of an energy function (section 4.5) our *set of invariants* must include at least the corresponding *set of bilinear invariants*.

Set of Bilinear Invariants: For our *complete* energy functions it is sufficient to use *sets of bilinear invariants*, i.e., sets consisting of all obviously functionally independent invariants that are linear and quadratic in \mathbf{C} .

Classical Set of Bilinear Invariants: We denote the sets of all invariants in terms of the right Cauchy-Green tensor \mathbf{C} and structural tensors, that are linear and quadratic in \mathbf{C} and that appear in classical functional bases e.g. given in DIMITRIENKO [43], as *classical sets of bilinear invariants*. They are presented in Appendix D.

However, the classical representation theorems for isotropic tensor functions offers us only useful representations for isotropic tensor functions depending on second-order tensorial arguments \mathbf{x} given in (4.34). That means, that we are able to exploit these theorems only for those material symmetry groups, which can be completely described by second-order structural tensors, i.e., Ξ_1 and not for the whole set of interest Ξ , see (4.22).

In the following, let us consider an anisotropic material whose material symmetry properties can be characterized by a second-order structural tensor

$$\mathbf{K} = \mathbf{Q}\mathbf{K}\mathbf{Q}^T \quad \forall \mathbf{Q} \in \mathcal{G}. \quad (4.35)$$

In view of the construction of isotropic tensor functions for the underlying constitutive equations ψ and \mathbf{S} in terms of the arguments \mathbf{C} and \mathbf{K} we require the *set of invariants*. According to Table 4.1 and 4.3 a set, which serves for the special cases $\mathbf{K} = -\mathbf{K}^T$ and $\mathbf{K} = \mathbf{K}^T = \mathbf{K}^2$, respectively, consists of the principal invariants (4.10) and mixed invariants in terms of \mathbf{C} and \mathbf{K} :

$$\mathcal{F}(\mathbf{C}, \mathbf{K}) := \{\text{tr}[\mathbf{C}], \text{tr}[\text{Cof} \mathbf{C}], \det[\mathbf{C}], \text{tr}[\mathbf{C}\tilde{\mathbf{K}}], \text{tr}[\mathbf{C}^2\tilde{\mathbf{K}}]\}. \quad (4.36)$$

In case of $\mathbf{K} = -\mathbf{K}^T$ we have $\tilde{\mathbf{K}} = \mathbf{K}^2$ and for $\mathbf{K} = \mathbf{K}^T = \mathbf{K}^2$ we insert $\tilde{\mathbf{K}} = \mathbf{K}$ in the latter basis. Furthermore, we will neglect obvious functionally dependent invariants. Denoting the mixed invariants by

$$I_4 = \text{tr}[\mathbf{C}\tilde{\mathbf{K}}], \quad I_5 = \text{tr}[\mathbf{C}^2\tilde{\mathbf{K}}], \quad (4.37)$$

yields the functional basis

$$\mathcal{F}(\mathbf{C}, \mathbf{K}) := \{I_1, I_2, I_3, I_4, I_5\}. \quad (4.38)$$

This set is the basis for the formulation of the free energy function

$$\psi = \sum_k \psi_k(I_j | I_j \in \mathcal{F}(\mathbf{C}, \mathbf{K})) + c. \quad (4.39)$$

In order to fulfill the non-essential normalization condition $\psi(\mathbf{1}) = 0$ we introduce the constant $c \in \mathbb{R}$. Hence, the second Piola-Kirchhoff stresses are computed by

$$\mathbf{S}^{aniso,1} = 2 \sum_j \left(\frac{\partial \psi}{\partial I_j} \frac{\partial I_j}{\partial \mathbf{C}} \right) \quad \text{with} \quad I_j \in \mathcal{F}(\mathbf{C}, \mathbf{K}). \quad (4.40)$$

For the first and second derivatives of the mixed invariants with respect to the right Cauchy-Green tensor we refer to the Appendix F. Applying the chain rule we obtain the second Piola-Kirchhoff stresses

$$\mathbf{S}^{aniso,1} = 2 \left\{ \left(\frac{\partial \psi}{\partial I_1} + \frac{\partial \psi}{\partial I_2} I_1 \right) \mathbf{1} - \frac{\partial \psi}{\partial I_2} \mathbf{C} + \frac{\partial \psi}{\partial I_3} \text{Cof} \mathbf{C} + \left(\frac{\partial \psi}{\partial I_4} \tilde{\mathbf{K}} + \frac{\partial \psi}{\partial I_5} (\mathbf{C} \tilde{\mathbf{K}}^T + \tilde{\mathbf{K}}^T \mathbf{C}) \right) \right\}. \quad (4.41)$$

The material tangent moduli are computed via $\mathbb{C}^{aniso,1} := 4 \partial_{\mathbf{C}} \mathbf{S}^{aniso,1}$, with

$$\begin{aligned} \mathbb{C}^{aniso,1} = & 4 \left[\frac{\partial^2 \psi}{\partial I_1 \partial I_1} \mathbf{1} \otimes \mathbf{1} + \frac{\partial^2 \psi}{\partial I_2 \partial I_2} \{I_1 \mathbf{1} - \mathbf{C}\} \otimes \{I_1 \mathbf{1} - \mathbf{C}\} \right. \\ & + \frac{\partial^2 \psi}{\partial I_3 \partial I_3} \text{Cof} \mathbf{C} \otimes \text{Cof} \mathbf{C} + \frac{\partial^2 \psi}{\partial I_2 \partial I_1} [\mathbf{1} \otimes \{I_1 \mathbf{1} - \mathbf{C}\} + \{I_1 \mathbf{1} - \mathbf{C}\} \otimes \mathbf{1}] \\ & + \frac{\partial^2 \psi}{\partial I_3 \partial I_1} [\mathbf{1} \otimes \text{Cof} \mathbf{C} + \text{Cof} \mathbf{C} \otimes \mathbf{1}] \\ & + \frac{\partial^2 \psi}{\partial I_3 \partial I_2} [\{I_1 \mathbf{1} - \mathbf{C}\} \otimes \text{Cof} \mathbf{C} + \text{Cof} \mathbf{C} \otimes \{I_1 \mathbf{1} - \mathbf{C}\}] \\ & + \frac{\partial \psi}{\partial I_2} [\mathbf{1} \otimes \mathbf{1} - \mathbf{1} \boxtimes \mathbf{1}] + \frac{\partial \psi}{\partial I_3} I_3 [\mathbf{C}^{-1} \otimes \mathbf{C}^{-1} - \mathbf{C}^{-1} \boxtimes \mathbf{C}^{-1}] \\ & + \left(\frac{\partial^2 \psi}{\partial I_4 \partial I_4} \tilde{\mathbf{K}} \otimes \tilde{\mathbf{K}} + \frac{\partial^2 \psi}{\partial I_5 \partial I_5} \{\mathbf{C} \tilde{\mathbf{K}}^T + \tilde{\mathbf{K}}^T \mathbf{C}\} \otimes \{\mathbf{C} \tilde{\mathbf{K}}^T + \tilde{\mathbf{K}}^T \mathbf{C}\} \right. \\ & + \frac{\partial^2 \psi}{\partial I_1 \partial I_4} [\mathbf{1} \otimes \tilde{\mathbf{K}} + \tilde{\mathbf{K}} \otimes \mathbf{1}] \\ & + \frac{\partial^2 \psi}{\partial I_1 \partial I_5} [\mathbf{1} \otimes \{\mathbf{C} \tilde{\mathbf{K}}^T + \tilde{\mathbf{K}}^T \mathbf{C}\} + \{\mathbf{C} \tilde{\mathbf{K}}^T + \tilde{\mathbf{K}}^T \mathbf{C}\} \otimes \mathbf{1}] \\ & \left. + \frac{\partial^2 \psi}{\partial I_2 \partial I_4} [\{I_1 \mathbf{1} - \mathbf{C}\} \otimes \tilde{\mathbf{K}} + \tilde{\mathbf{K}} \otimes \{I_1 \mathbf{1} - \mathbf{C}\}] \right] \end{aligned} \quad (4.42)$$

$$\begin{aligned}
& + \frac{\partial^2 \psi}{\partial I_2 \partial I_5} [\{I_1 \mathbf{1} - \mathbf{C}\} \otimes \{\mathbf{C} \tilde{\mathbf{K}}^T + \tilde{\mathbf{K}}^T \mathbf{C}\} + \{\mathbf{C} \tilde{\mathbf{K}}^T + \tilde{\mathbf{K}}^T \mathbf{C}\} \otimes \{I_1 \mathbf{1} - \mathbf{C}\}] \\
& + \frac{\partial^2 \psi}{\partial I_3 \partial I_4} [\text{Cof} \mathbf{C} \otimes \tilde{\mathbf{K}} + \tilde{\mathbf{K}} \otimes \text{Cof} \mathbf{C}] \\
& + \frac{\partial^2 \psi}{\partial I_3 \partial I_5} [\text{Cof} \mathbf{C} \otimes \{\mathbf{C} \tilde{\mathbf{K}}^T + \tilde{\mathbf{K}}^T \mathbf{C}\} + \{\mathbf{C} \tilde{\mathbf{K}}^T + \tilde{\mathbf{K}}^T \mathbf{C}\} \otimes \text{Cof} \mathbf{C}] \\
& + \frac{\partial^2 \psi}{\partial I_4 \partial I_5} [\{\mathbf{C} \tilde{\mathbf{K}}^T + \tilde{\mathbf{K}}^T \mathbf{C}\} \otimes \tilde{\mathbf{K}} + \tilde{\mathbf{K}} \otimes \{\mathbf{C} \tilde{\mathbf{K}}^T + \tilde{\mathbf{K}}^T \mathbf{C}\}] \\
& + \frac{\partial \psi}{\partial I_5} [(\mathbf{1} \boxtimes \tilde{\mathbf{K}})^{34}_T + (\tilde{\mathbf{K}}^T \boxtimes \mathbf{1})^{34}_T] \Big],
\end{aligned}$$

where the symmetry $\frac{\partial^2 \psi}{\partial I_k \partial I_j} = \frac{\partial^2 \psi}{\partial I_j \partial I_k}$ is considered and the operation $(\bullet)^{34}_T$ appears in index notation as $(\{(\bullet)\}_{ijkl})^{34}_T = \{(\bullet)\}_{ijlk}$.

4.4.2 Extended Set of Higher-Order Tensors. Unfortunately, a direct generalization of the representation theorems for isotropic tensor functions with respect to tensorial arguments of order higher than two is not yet exhaustively discussed in the literature. There are only a few particular cases treating this topic, e.g. BETTEN [18, 19, 21, 22], BETTEN & HELISCH [23, 24, 25], ZHENG & BETTEN [145] and ZHENG [144, 143]. In the papers [22, 23] combinatorial approaches are used which allow the construction of tensor functions in terms of irreducible invariants based on symmetric second- and fourth-order tensors; but for the formulation of specific energy functions these representations are unmanageable and hence, not useful. For instance in our case of a symmetric second-order and a symmetric fourth-order tensor there exist more than 156 irreducible invariants.

A useful idea is to modify Boehler's extension of anisotropic tensor functions to isotropic tensor functions in such a way, that the classical representation theorems can be still applied. In this context XIAO [140, 141] proposed an extension method based on the introduction of so-called *second-order isotropic extension functions* besides the constant second-order structural tensors for all 32 crystal and non-crystal classes. In APEL [3] the application of this isotropic extension method leads to possible formulations of quadratic energy functions for all material symmetry groups. Therefore, let us go more into detail here.

With regard to the introduced isotropicization method (4.24) the idea of XIAO [140] is the following: The author proposes the introduction of a set $\Xi_2(\mathbf{C})$ of second-order symmetric and skew-symmetric tensor-valued anisotropic tensor functions depending on the constant structural tensors of order higher than two of the set Ξ_2 , defined in (4.22) and satisfying (4.23). These anisotropic tensor functions are denoted as *isotropic extension functions* and fulfill the invariance requirement

$$\mathbf{Q}(\Xi_2(\mathbf{C}))\mathbf{Q}^T = \Xi_2(\mathbf{Q}\mathbf{C}\mathbf{Q}^T) \quad \forall \mathbf{Q} \in \mathcal{G}. \quad (4.43)$$

Inserting into (4.24) instead of the whole set of structural tensors Ξ given in (4.22) its subset of second-order structural tensors Ξ_1 and the extension functions $\Xi_2(\mathbf{C})$ in terms

of the structural tensors of the set Ξ_2 the invariance condition results in

$$\left. \begin{aligned} \psi(\mathbf{C}, \Xi_1, \Xi_2(\mathbf{C})) &= \psi(\mathbf{Q}\mathbf{C}\mathbf{Q}^T, \mathbf{Q}\Xi_1\mathbf{Q}^T, \mathbf{Q}\Xi_2(\mathbf{C})\mathbf{Q}^T) \\ \mathbf{Q}\mathbf{S}(\mathbf{C}, \Xi_1, \Xi_2(\mathbf{C}))\mathbf{Q}^T &= \mathbf{S}(\mathbf{Q}\mathbf{C}\mathbf{Q}^T, \mathbf{Q}\Xi_1\mathbf{Q}^T, \mathbf{Q}\Xi_2(\mathbf{C})\mathbf{Q}^T) \end{aligned} \right\} \forall \mathbf{Q} \in \mathcal{O}(3). \quad (4.44)$$

The constitutive equations are anisotropic with respect to \mathbf{C} alone:

$$\left. \begin{aligned} \psi(\mathbf{C}, \Xi_1, \Xi_2(\mathbf{C})) &= \psi(\mathbf{Q}\mathbf{C}\mathbf{Q}^T, \Xi_1, \Xi_2(\mathbf{Q}\mathbf{C}\mathbf{Q}^T)) \\ \mathbf{Q}\mathbf{S}(\mathbf{C}, \Xi_1, \Xi_2(\mathbf{C}))\mathbf{Q}^T &= \mathbf{S}(\mathbf{Q}\mathbf{C}\mathbf{Q}^T, \Xi_1, \Xi_2(\mathbf{Q}\mathbf{C}\mathbf{Q}^T)) \end{aligned} \right\} \forall \mathbf{Q} \in \mathcal{G}. \quad (4.45)$$

These extension makes the application of the classical representation theorems for isotropic tensor functions for those material symmetry groups possible, which are characterized by structural tensors of order higher than two. We denote the symmetric extension functions by $\mathbf{A}(\mathbf{C})$ with $\mathbf{A}(\mathbf{C}) = \mathbf{A}(\mathbf{C})^T$ and the skew-symmetric ones by $\mathbf{W}(\mathbf{C})$ with $\mathbf{W}(\mathbf{C}) = -\mathbf{W}(\mathbf{C})^T$.

Let us exemplarily evaluate Xiao's isotropic extension concept for the description of those anisotropies, which can be characterized by a fourth-order and a second-order structural tensor, respectively:

$$\mathbb{P} = \mathbf{Q} \boxtimes \mathbf{Q} : \mathbb{P} : \mathbf{Q}^T \boxtimes \mathbf{Q}^T, \quad \mathbf{K} = \mathbf{Q}\mathbf{K}\mathbf{Q}^T, \quad \forall \mathbf{Q} \in \mathcal{G}, \quad (4.46)$$

with the material symmetry group \mathcal{G} . For the representation of *complete*^{11.)} energy functions in terms of the right Cauchy-Green tensor and the structural tensors as coordinate-invariant functions we need the corresponding *set of invariants*. The *set of invariants* is here based on the arguments \mathbf{C} , \mathbf{K} and $\mathbf{A}_i(\mathbf{C})$, $i = 1, 2, 3, 4$, with

$$\mathbf{A}_1(\mathbf{C}) = \mathbb{P} : \mathbf{C}, \quad \mathbf{A}_2(\mathbf{C}) = \mathbf{C} : \mathbb{P}, \quad \mathbf{A}_3(\mathbf{C}) = \mathbb{P} : \mathbf{C}^2, \quad \mathbf{A}_4(\mathbf{C}) = \mathbf{C}^2 : \mathbb{P}. \quad (4.47)$$

For all four functions the invariance relation (4.43) hold: we have the relations

$$\left. \begin{aligned} \mathbf{Q}(\mathbf{A}_1(\mathbf{C}))\mathbf{Q}^T &= \mathbf{Q}(\mathbb{P} : \mathbf{C})\mathbf{Q}^T = \mathbf{Q} \boxtimes \mathbf{Q} : \mathbb{P} : \mathbf{Q}^T \boxtimes \mathbf{Q}^T : \mathbf{Q}\mathbf{C}\mathbf{Q}^T \\ &= \mathbb{P} : \mathbf{Q}\mathbf{C}\mathbf{Q}^T = \mathbf{A}_1(\mathbf{Q}\mathbf{C}\mathbf{Q}^T), \\ \mathbf{Q}(\mathbf{A}_2(\mathbf{C}))\mathbf{Q}^T &= \mathbf{Q}(\mathbf{C} : \mathbb{P})\mathbf{Q}^T = \mathbf{Q}\mathbf{C}\mathbf{Q}^T : \mathbf{Q} \boxtimes \mathbf{Q} : \mathbb{P} : \mathbf{Q}^T \boxtimes \mathbf{Q}^T \\ &= \mathbf{Q}\mathbf{C}\mathbf{Q}^T : \mathbb{P} = \mathbf{A}_2(\mathbf{Q}\mathbf{C}\mathbf{Q}^T) \end{aligned} \right\} \forall \mathbf{Q} \in \mathcal{G} \quad (4.48)$$

and analogous invariance properties of $\mathbf{A}_3(\mathbf{C})$ and $\mathbf{A}_4(\mathbf{C})$. With \mathbf{K} and the isotropic extension functions (4.47) in hand we construct –with regard to Table 4.3 and the set (4.36)– the *set of invariants*

$$\mathcal{F}(\mathbf{C}, \mathbf{K}, \mathbf{A}_i(\mathbf{C})) := \{\mathcal{F}(\mathbf{C}, \mathbf{K}), \mathcal{F}^1, \mathcal{F}^2, \mathcal{F}^3, \mathcal{F}^4\}, \quad (4.49)$$

with

$$\begin{aligned} \mathcal{F}^1 &= \{\text{tr}[\mathbf{A}_1], \text{tr}[\mathbf{A}_1^2], \text{tr}[\mathbf{A}_2], \text{tr}[\mathbf{A}_2^2], \text{tr}[\mathbf{A}_3], \text{tr}[\mathbf{A}_4]\}, \\ \mathcal{F}^2 &= \{\text{tr}[\mathbf{A}_1\mathbf{C}], \text{tr}[\mathbf{A}_2\mathbf{C}]\}, \\ \mathcal{F}^3 &= \{\text{tr}[\mathbf{A}_1\tilde{\mathbf{K}}], \text{tr}[\mathbf{A}_1^2\tilde{\mathbf{K}}], \text{tr}[\mathbf{A}_2\tilde{\mathbf{K}}], \text{tr}[\mathbf{A}_2^2\tilde{\mathbf{K}}], \text{tr}[\mathbf{A}_3\tilde{\mathbf{K}}], \text{tr}[\mathbf{A}_4\tilde{\mathbf{K}}]\}, \\ \mathcal{F}^4 &= \{\text{tr}[\mathbf{C}\mathbf{A}_1\mathbf{K}], \text{tr}[\mathbf{C}\mathbf{A}_2\mathbf{K}]\}. \end{aligned} \quad (4.50)$$

^{11.)}Completeness of the energy function means that the corresponding linearized tangent moduli at the reference state obeys the same symmetry properties as the corresponding classical anisotropic elasticity tensor. See the remarks in section 4.5.

Note, for the sake of conciseness mixed invariants of the following type have been neglected here, since they will be dropped in subsequent specifications: mixed invariants only in terms of the isotropic extension functions $\mathbf{A}_i, i = 1, 2, 3, 4$, mixed invariants only in terms of skew-symmetric arguments as well as the additional invariants

$$\text{tr}[\mathbf{A}_1 \mathbf{K}^2 \mathbf{C} \mathbf{K}] \quad \text{and} \quad \text{tr}[\mathbf{A}_2 \mathbf{K}^2 \mathbf{C} \mathbf{K}]. \quad (4.51)$$

For a symmetric constant structural tensor $\mathbf{K} = \mathbf{K}^T = \mathbf{A}$ we presume $\mathbf{A} = \mathbf{A}^2$, such that $\tilde{\mathbf{K}} = \mathbf{A}$. For a skew-symmetric structural tensor \mathbf{W} the relation $\mathbf{K} = \mathbf{W}$ and $\tilde{\mathbf{K}} = \mathbf{W}^2$ are valid. Denoting the invariants by

$$\begin{aligned} I_6 &= \text{tr}[\mathbf{A}_1], \quad I_7 = \text{tr}[\mathbf{A}_1^2], \quad I_8 = \text{tr}[\mathbf{A}_3], \\ I_9 &= \text{tr}[\mathbf{A}_1 \mathbf{C}], \quad I_{10} = \text{tr}[\mathbf{A}_1 \tilde{\mathbf{K}}], \quad I_{11} = \text{tr}[\mathbf{A}_1^2 \tilde{\mathbf{K}}], \quad I_{12} = \text{tr}[\mathbf{A}_3 \tilde{\mathbf{K}}], \\ I_{13} &= \text{tr}[\mathbf{C} \mathbf{A}_1 \mathbf{K}], \\ I_{14} &= \text{tr}[\mathbf{A}_2], \quad I_{15} = \text{tr}[\mathbf{A}_2^2], \quad I_{16} = \text{tr}[\mathbf{A}_4], \\ I_{17} &= \text{tr}[\mathbf{A}_2 \mathbf{C}], \quad I_{18} = \text{tr}[\mathbf{A}_2 \tilde{\mathbf{K}}], \quad I_{19} = \text{tr}[\mathbf{A}_2^2 \tilde{\mathbf{K}}], \quad I_{20} = \text{tr}[\mathbf{A}_4 \tilde{\mathbf{K}}], \\ I_{21} &= \text{tr}[\mathbf{C} \mathbf{A}_2 \mathbf{K}], \end{aligned} \quad (4.52)$$

leads to the *set of invariants*

$$\mathcal{F}(\mathbf{C}, \mathbf{K}, \mathbf{A}_i(\mathbf{C}) | i = 1, \dots, 4) := \{I_1, \dots, I_{21}\}. \quad (4.53)$$

Based on this set of scalar-valued arguments we formulate the energy function as isotropic function in analogy to (4.39)

$$\psi = \sum_k \psi_k(I_j | I_j \in \mathcal{F}(\mathbf{C}, \mathbf{K}, \mathbf{A}_i(\mathbf{C}) | i = 1, \dots, 4)) + c \quad (4.54)$$

and compute the second Piola-Kirchhoff stresses

$$\begin{aligned} \mathbf{S}^{aniso,2} &= 2 \sum_j \left(\frac{\partial \psi}{\partial I_j} \frac{\partial I_j}{\partial \mathbf{C}} \right) = \mathbf{S}^{aniso,1} + 2 \sum_{j+5} \left(\frac{\partial \psi}{\partial I_{j+5}} \frac{\partial I_{j+5}}{\partial \mathbf{C}} \right), \\ \text{with } I_j &\in \mathcal{F}(\mathbf{C}, \mathbf{K}, \mathbf{A}_i(\mathbf{C}) | i = 1, \dots, 4), \end{aligned} \quad (4.55)$$

where the stresses $\mathbf{S}^{aniso,1}$ can be found in (4.41). The index notation of the first and second-order derivatives of the invariants I_6, \dots, I_{14} with respect to the right Cauchy-Green tensor are presented in the Appendix F. Analogously to (4.42) the material tangent moduli is calculated by

$$\mathbb{C}^{aniso,2} := 4 \frac{\partial^2 \psi}{\partial \mathbf{C} \partial \mathbf{C}} \quad (4.56)$$

and results in

$$\begin{aligned} \mathbb{C}^{aniso,2} &:= \mathbb{C}^{aniso,1} + 4 \sum_r \sum_s \left[\frac{\partial^2 \psi}{\partial I_r \partial I_s} \frac{\partial I_r}{\partial \mathbf{C}} \otimes \frac{\partial I_s}{\partial \mathbf{C}} \right] + 4 \sum_s \sum_{r=1}^5 \left[\frac{\partial^2 \psi}{\partial I_s \partial I_r} \frac{\partial I_s}{\partial \mathbf{C}} \otimes \frac{\partial I_r}{\partial \mathbf{C}} \right] \\ &\quad + 4 \sum_s \left[\frac{\partial \psi}{\partial I_s} \frac{\partial^2 I_s}{\partial \mathbf{C} \partial \mathbf{C}} \right], \end{aligned} \quad (4.57)$$

with $r = 1, \dots, 21, s = 6, \dots, 21, r \neq s$.

4.5 "Completeness" of Energy Functions w.r.t. Material Symmetries.

The linearization of the second Piola-Kirchhoff stress tensor \mathbf{S} at origin state $\mathbf{E}|_{C=1} = \mathbf{0}$ reads

$$\text{Lin}[\mathbf{S}] = \mathbf{S}|_{E=0} + \left. \frac{\partial \mathbf{S}}{\partial \mathbf{E}} \right|_{E=0} : \frac{d}{d\lambda} [\mathbf{E}(\mathbf{X} + \lambda \mathbf{u})] |_{\lambda=0}. \quad (4.58)$$

In the undeformed, stress-free reference placement $\mathbf{S}|_{E=0} = \mathbf{0}$ and with the relation $\mathbb{C}|_{E=0} := \partial_E \mathbf{S}|_{E=0}$ we arrive at

$$\text{Lin}[\mathbf{S}] = \mathbb{C}|_{E=0} : \frac{d}{d\lambda} [\mathbf{E}(\mathbf{X} + \lambda \mathbf{u})] |_{\lambda=0} = \mathbb{C}|_{E=0} : \text{Lin}[\mathbf{E}]. \quad (4.59)$$

With (2.26) we get

$$\text{Lin}[\mathbf{S}] = \mathbb{C}^{lin} : \boldsymbol{\varepsilon}, \quad \text{with} \quad \mathbb{C}^{lin} := \mathbb{C}|_{E=0} = \mathbb{C}|_{C=1}. \quad (4.60)$$

The linearized second Piola-Kirchhoff stress tensor at a stress-free reference state represents therefore the stress tensor $\bar{\boldsymbol{\sigma}}(\boldsymbol{\varepsilon})$ in the small strain regime. The tangent moduli $\mathbb{C}|_{C=1}$ is denoted as linear moduli \mathbb{C}^{lin} .

Complete Energy Functions: We say that our energy functions for the description of anisotropic finite elasticity are *complete*, if the coefficient matrix of the linear moduli \mathbb{C}^{lin} exhibits the same zero, non-zero, equal and opposite components and relations between the components as the corresponding classical anisotropic elasticity tensor of linear elasticity. This means that \mathbb{C}^{lin} has to obey the same symmetry properties as the corresponding classical anisotropic elasticity tensor. This does not mean that the exact values of the components of the corresponding anisotropic elasticity tensor can always be generated.

The classical anisotropic elasticity tensor in hyperelasticity can be completely obtained as second derivative of a quadratic energy $\psi(\mathbf{C})$. Therefore, in our case it is sufficient to use *sets of bilinear invariants*.

The possible types of components appearing in the elasticity tensors are specified in section 3.7. There the effect of material symmetry groups on the components and relations between the components of all anisotropic elasticity tensors of linear elasticity are visualized, cf. VOIGT [129].

Anisotropy Group: Material symmetry intervenes to reduce the number of components and the relations between the components of the anisotropic elasticity tensor. In section 3.7 it is shown that the representations of the classical elasticity tensors for the symmetry groups $\mathcal{G}_{10} - \mathcal{G}_{13}$ as well as \mathcal{G}_6 and \mathcal{G}_7 in Voigt notation are identical. Consequently, these elasticity tensors obey the same symmetry properties. A consequence of our *completeness* of energy functions is therefore, that we finally distinguish between nine instead of thirteen different material symmetries for the description of anisotropic material behavior. We call the corresponding nine material symmetry groups *anisotropy groups*. They are given together with the isotropy group by: $\mathcal{G}_1, \mathcal{G}_2, \mathcal{G}_3, \mathcal{G}_4, \mathcal{G}_5, \mathcal{G}_8, \mathcal{G}_9, \mathcal{G}_7, \mathcal{G}_{12}, \text{O}(3)$.

Quadratic Energies of Simple Form. For instance, in the linear theory for the case of isotropic material symmetry described by the orthogonal group $\text{O}(3)$, a quadratic strain energy is usually of the simple form

$$\psi^{iso}(\boldsymbol{\varepsilon}) = \frac{1}{2}\lambda \text{tr}[\boldsymbol{\varepsilon}]^2 + \mu \text{tr}[\boldsymbol{\varepsilon}^2], \quad (4.61)$$

with the Lamé constants λ and μ and the small strain tensor $\boldsymbol{\varepsilon} = \frac{1}{2}(\text{Grad}\mathbf{u}^T + \text{Grad}\mathbf{u})$. Here, it is possible to uniquely express the components of the tangent moduli in Voigt notation

$$\mathbb{C}^{iso(V)} = \begin{bmatrix} \mathbb{C}_{1111} & \mathbb{C}_{1122} & \mathbb{C}_{1122} & 0 & 0 & 0 \\ \mathbb{C}_{1122} & \mathbb{C}_{1111} & \mathbb{C}_{1122} & 0 & 0 & 0 \\ \mathbb{C}_{1122} & \mathbb{C}_{1122} & \mathbb{C}_{1111} & 0 & 0 & 0 \\ 0 & 0 & 0 & \frac{1}{2}(\mathbb{C}_{1111} - \mathbb{C}_{1122}) & 0 & 0 \\ 0 & 0 & 0 & 0 & \frac{1}{2}(\mathbb{C}_{1111} - \mathbb{C}_{1122}) & 0 \\ 0 & 0 & 0 & 0 & 0 & \frac{1}{2}(\mathbb{C}_{1111} - \mathbb{C}_{1122}) \end{bmatrix}$$

by the material parameters

$$\mathbb{C}_{1111} = \lambda + 2\mu, \quad \mathbb{C}_{1122} = \lambda$$

and therefore it is here possible to exactly generate all values of the components of the elasticity tensor $\mathbb{C}^{iso(V)}$. If we replace in (4.61) $\boldsymbol{\varepsilon}$ by the Green-Lagrange strain tensor \mathbf{E} , we obtain the classical St. Venant-Kirchhoff material model $\psi^{iso}(\mathbf{E})$ — a well-known extension of the linearized theory into the nonlinear case:

$$\psi^{iso}(\mathbf{E}) := \frac{1}{2}\lambda \text{tr}[\mathbf{E}]^2 + \mu \text{tr}[\mathbf{E}^2]. \quad (4.62)$$

This material model can be extended for the description of all anisotropy types. This will be shown in subsequent sections. They have then the form

$$\psi^{aniso}(\mathbf{E}) = \sum_{i=1}^n \alpha_i L_i, \quad L_i \in \mathcal{B}(\mathbf{E}), \quad (4.63)$$

where the sum of the first two terms represents the classical isotropic St. Venant-Kirchhoff material model (4.62), i.e., $\psi^{aniso}(\mathbf{E}) = \alpha_1 L_1 + \alpha_2 L_2 := \psi^{iso}(\mathbf{E})$. The term $\mathcal{B}(\mathbf{E})$ denotes the set of all corresponding a priori quadratic invariants and all multiplicative combinations of linear invariants. For those energy functions a direct identification of the material parameters by the components of the associated elasticity tensors is always possible. However, the drawback of these material models is that they can be only used within boundary value problems with large rotations but small strains. This statement will be precised in the next section by the results of a biaxial tension test.

Polyconvex Energies. For the modeling of finite elasticity, we will be interested in the satisfaction of further restrictions of the free energy function like the polyconvexity condition. This condition often imposes restrictions on the material parameters. Furthermore, the polyconvex approach, which will be later introduced, as well as the separate fulfillment of the condition of a stress-free reference state at $\mathbf{E} = \mathbf{0}$ leads to dependencies between the material parameters. Thus, in the polyconvex framework a direct identification of the material parameters with the components of the elasticity tensor may be non-trivial. Here, we are therefore not interested in exactly capturing all values appearing in the elasticity tensor as pointed out in the previous box. More details are given in chapter 6.

4.6 Quadratic Energy Functions of St.Venant-Kirchhoff Type.

We construct now *complete* quadratic energies of St. Venant-Kirchhoff type. Thereby, the *sets of bilinear invariants* are presented. We exemplarily show the construction for the case of hexagonal/ transversely isotropic material behavior given by the anisotropy group \mathcal{G}_{12} and tetragonal anisotropy properties characterized by the group \mathcal{G}_4 . The results for the remaining anisotropy groups can be found in the Appendix G.

The *complete* quadratic energies have the form

$$\psi^{aniso}(\mathbf{E}) = \sum_{i=1}^n \alpha_i L_i, \quad L_i \in \mathcal{B}(\mathbf{E}),$$

see (4.63). Due to the general representations of the stresses and tangent moduli we prefer the dependency of ψ on the right Cauchy-Green tensor, i.e., we finally set $\mathbf{E} = \frac{1}{2}(\mathbf{C} - \mathbf{1})$ in the material model.

Hexagonal and Transversely Isotropic Anisotropy Group \mathcal{G}_{12} :

Set of Bilinear Invariants: We describe the properties of the anisotropy group \mathcal{G}_{12} by a coordinate-invariant quadratic energy function on the basis of the transversely isotropic structural tensor (4.27). There, the preferred direction of the material is set to $\mathbf{a} = \mathbf{e}_3$. The invariants up to the power of two, which are constructed with the help of Table 4.3, are listed in Table 4.4 and constitutes the underlying *set of bilinear invariants*

$$\mathcal{F}^{ti}(\mathbf{E}, \mathbf{M}) := \{\text{tr}[\mathbf{E}], \text{tr}[\mathbf{E}^2], \text{tr}[\mathbf{E}\mathbf{M}], \text{tr}[\mathbf{E}^2\mathbf{M}]\}. \quad (4.64)$$

With respect to the coordinates of \mathbf{E} this set is given by:

$$\boxed{\mathcal{F}^{ti}(\mathbf{E}, \mathbf{M}) = \{E_{11} + E_{22} + E_{33}, E_{11}^2 + E_{22}^2 + E_{33}^2 + 2E_{12}^2 + 2E_{13}^2 + 2E_{23}^2, E_{33}, E_{33}^2 + E_{13}^2 + E_{23}^2\}} \quad (4.65)$$

The *classical set of bilinear invariants* reads in terms of the components of \mathbf{E}

$$\bar{\mathcal{F}}^{ti} = \{E_{11} + E_{22}, E_{33}, E_{13}^2 + E_{23}^2, E_{11}^2 + E_{22}^2 + 2E_{12}^2\}, \quad (4.66)$$

cf. DIMITRIENKO [43]. All elements of (4.65) can be uniquely obtained by the combination of the linear and quadratic components of the *classical set of bilinear invariants* $\bar{\mathcal{F}}^{ti1}$.

Table 4.4: Set of Bilinear Invariants, \mathcal{G}_{12} .

| | |
|---------------------------------------|--|
| Structural Tensors: | $\mathbf{M} = \mathbf{e}_3 \otimes \mathbf{e}_3$ |
| Invariants depending on one variable: | $\text{tr}[\mathbf{E}], \text{tr}[\mathbf{E}^2]$ |
| Invariants for two arguments: | $\text{tr}[\mathbf{E}\mathbf{M}], \text{tr}[\mathbf{E}^2\mathbf{M}]$ |

Quadratic Energy Function: For the construction of the quadratic coordinate-invariant energy function (4.63) the set containing all quadratic invariants and quadratic combinations of linear invariants of the set (4.65) appears then as

$$\mathcal{B}^{ti} := \{\text{tr}[\mathbf{E}]^2, \text{tr}[\mathbf{E}^2], \text{tr}[\mathbf{E}]\text{tr}[\mathbf{E}\mathbf{M}], \text{tr}[\mathbf{E}^2\mathbf{M}], \text{tr}[\mathbf{E}\mathbf{M}]^2\}. \quad (4.67)$$

Thus we obtain the quadratic free energy function

$$\psi^{ti} = \frac{1}{2}\lambda \text{tr}[\mathbf{E}]^2 + \mu \text{tr}[\mathbf{E}^2] + \alpha_3 \text{tr}[\mathbf{E}] \text{tr}[\mathbf{E}\mathbf{M}] + \alpha_4 \text{tr}[\mathbf{E}^2\mathbf{M}] + \alpha_5 \text{tr}[\mathbf{E}\mathbf{M}]^2. \quad (4.68)$$

We consider the dependency of ψ on the right Cauchy-Green tensor \mathbf{C} , i.e., we reformulate the free energy function (4.68) as follows

$$\begin{aligned} \psi^{ti} = & \frac{1}{8}\lambda (I_1 - 3)^2 + \frac{1}{4}\mu (I_1^2 - 2(I_1 + I_2) + 3) + \frac{1}{4}\alpha_3 (I_1 - 3)(I_4 - 1) \\ & + \frac{1}{4}\alpha_4 (I_5 - 2I_4 + 1) + \frac{1}{4}\alpha_5 (I_4 - 1)^2. \end{aligned} \quad (4.69)$$

The second Piola-Kirchhoff stresses are obtained from the general representation (4.41):

$$\begin{aligned} \mathbf{S} = & \frac{1}{2}\lambda (I_1 - 3)\mathbf{1} + \mu (\mathbf{C} - \mathbf{1}) + \frac{1}{2}\alpha_3 [(I_1 - 3)\mathbf{M} + (I_4 - 1)\mathbf{1}] \\ & + \frac{1}{2}\alpha_4 (\mathbf{C}\mathbf{M} + \mathbf{M}\mathbf{C} - 2\mathbf{M}) + \alpha_5 (I_4 - 1)\mathbf{M}. \end{aligned} \quad (4.70)$$

In consideration of the general representation of anisotropic tangent moduli given in (4.42), \mathbb{C} can be written as

$$\begin{aligned} \mathbb{C} = & \lambda \mathbf{1} \otimes \mathbf{1} + 2\mu \mathbf{1} \boxtimes \mathbf{1} + \alpha_3 [\mathbf{1} \otimes \mathbf{M} + \mathbf{M} \otimes \mathbf{1}] \\ & + \alpha_4 (\mathbf{1} \boxtimes \mathbf{M} + \mathbf{M} \boxtimes \mathbf{1}) + 2\alpha_5 \mathbf{M} \otimes \mathbf{M}. \end{aligned} \quad (4.71)$$

The classical matrix notation of the hexagonal as well as transversely isotropic elasticity tensor is given with the X_3 -axis as axis of symmetry by

$$\mathbb{C}^{(V)ti} = \begin{bmatrix} \mathbb{C}_{1111} & \mathbb{C}_{1122} & \mathbb{C}_{1133} & 0 & 0 & 0 \\ \mathbb{C}_{1122} & \mathbb{C}_{1111} & \mathbb{C}_{1133} & 0 & 0 & 0 \\ \mathbb{C}_{1133} & \mathbb{C}_{1133} & \mathbb{C}_{3333} & 0 & 0 & 0 \\ 0 & 0 & 0 & \frac{1}{2}(\mathbb{C}_{1111} - \mathbb{C}_{1122}) & 0 & 0 \\ 0 & 0 & 0 & 0 & \mathbb{C}_{2323} & 0 \\ 0 & 0 & 0 & 0 & 0 & \mathbb{C}_{2323} \end{bmatrix}. \quad (4.72)$$

Evaluating the Voigt notation of (4.71) with $\mathbf{M} = \text{diag}(0, 0, 1)$, we obtain the same arrangement of components as in (4.72) and can identify

$$\begin{aligned} \mathbb{C}_{1111} &= \lambda + 2\mu, \quad \mathbb{C}_{1122} = \lambda, \\ \mathbb{C}_{1133} &= \lambda + \alpha_3, \quad \mathbb{C}_{3333} = \lambda + 2\mu + 2\alpha_3 + 2\alpha_4 + 2\alpha_5, \quad \mathbb{C}_{2323} = \mu + 1/2\alpha_4. \end{aligned} \quad (4.73)$$

Biaxial Tension Test. In order to show the main characteristics of a St. Venant-Kirchhoff type material model we perform a biaxial compression/tension test of the described anisotropic material with homogeneous Dirichlet boundary conditions. The reference configuration, a cube with length l_0 , is shown in Figure 4.2 a). The applied displacement u in X_2 - and X_3 -direction is varied in the range from $-0.8 l_0$ to $1.3 l_0$. To visualize in this case the anisotropy ratios the characteristic surface of Young's moduli is plotted, see Figure 4.2 b). Here, we refer to SHUVALOV [110], where characteristic surfaces of elasticities for several anisotropic materials can be found.

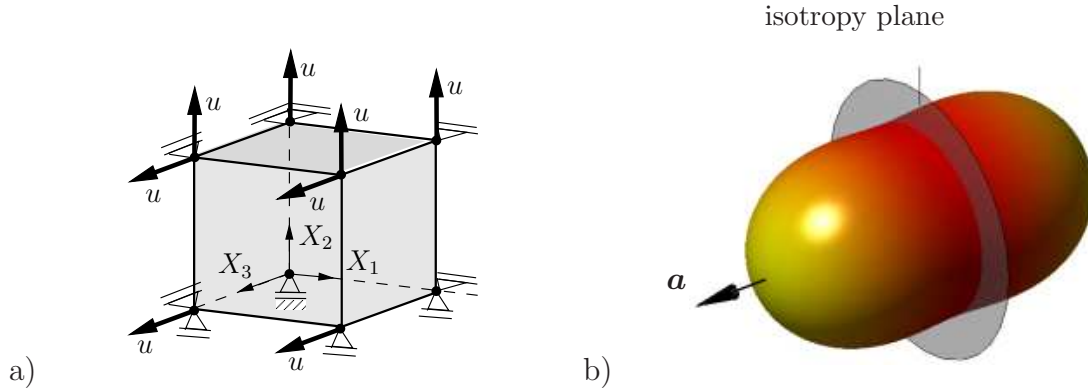


Figure 4.2: a) Homogeneous biaxial compression/tension test, b) Characteristic surface of transversely isotropic elasticities.

We have homogeneous deformations $\mathbf{x} = \mathbf{F}\mathbf{X}$ with

$$\mathbf{F} = \text{diag}(\sqrt{C_{11}}, \tilde{\lambda}, \tilde{\lambda}), \quad \text{with} \quad \tilde{\lambda} = (l_0 + u)/l_0 \rightarrow C_{22} = C_{33} = \tilde{\lambda}^2. \quad (4.74)$$

The stresses in X_1 -direction are equal to zero. Inserting (4.74) into the constitutive equation (4.69) for the stresses yields the component C_{11}

$$\begin{aligned} S_{11} &= \left(\frac{1}{2}\lambda + \mu\right)(C_{11} - 1) + (\lambda + \alpha_3/2)(\tilde{\lambda}^2 - 1) = 0 \\ &\rightarrow C_{11} = \frac{2}{\lambda + 2\mu}[-(\lambda + \alpha_3/2)(\tilde{\lambda}^2 - 1)] + 1. \end{aligned} \quad (4.75)$$

Setting the material parameters to

$$\lambda = 2, \mu = 2, \alpha_3 = 3, \alpha_4 = 4, \alpha_5 = 5 \quad [\text{N/mm}^2] \quad (4.76)$$

and inserting (4.75) into S_{22} and S_{33} leads to the first Piola-Kirchhoff stresses in X_2 - and X_3 -direction:

$$\begin{aligned} P_{22} &= \frac{\mu}{\lambda + 2\mu} [3\lambda + 2\mu + \alpha_3] \tilde{\lambda}(\tilde{\lambda}^2 - 1) = 4\frac{1}{3} \tilde{\lambda}(\tilde{\lambda}^2 - 1), \\ P_{33} &= [6\lambda\mu + 4\mu^2 + 6\mu\alpha_3 - \alpha_3^2 + 2\lambda\alpha_4 + 4\mu\alpha_4 + 2\lambda\alpha_5 + 4\mu\alpha_5] \frac{\tilde{\lambda}(\tilde{\lambda}^2 - 1)}{2\lambda + 4\mu} \\ &= 14\frac{7}{12} \tilde{\lambda}(\tilde{\lambda}^2 - 1). \end{aligned} \quad (4.77)$$

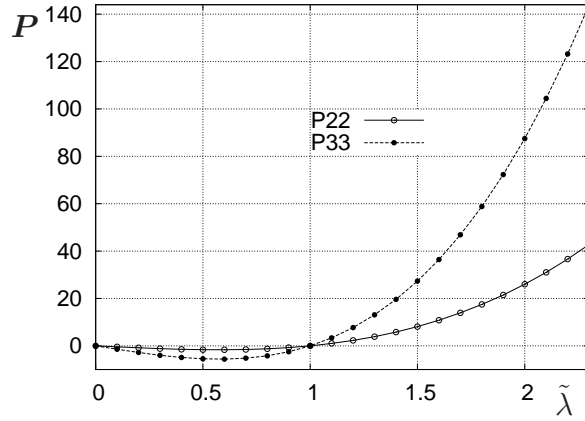


Figure 4.3: Values of first Piola-Kirchhoff stresses in X_2 - and X_3 -directions in $[\text{N/mm}^2]$.

A graphical representation of the first Piola-Kirchhoff stresses in the X_2 - and X_3 -directions versus the stretch in the X_2 - and X_3 -direction $\tilde{\lambda}$ is depicted in Figure 4.3.

Remark. Thus, for $\tilde{\lambda} \rightarrow 0$, i.e., $u \rightarrow -l_0$, we obtain the unphysical result $P_{22}, P_{33} \rightarrow 0$, as can be seen in Figure 4.3. This effect is well-known for the St.-Venant-Kirchhoff type materials, because these models do not fulfill the growth conditions specified in chapter 5. These growth conditions are of great importance in finite strain elasticity also from a mathematical point of view. Furthermore, they do not fulfill the important Legendre-Hadamard ellipticity condition, which will be defined in chapter 5. Therefore, St. Venant-Kirchhoff material models can be only used within boundary value problems with large rotations but small strains.

Tetragonal Anisotropy Group \mathcal{G}_4 :

Set of Bilinear Invariants: The isotropic extension functions that allow for modeling of tetragonal \mathcal{G}_4 -invariant tensor functions with representation theorems for isotropic functions are presented in Table 4.5 together with the invariants obtained from Table 4.3.

Table 4.5: Set of Bilinear Invariants, \mathcal{G}_4 .

| | |
|---------------------------------------|---|
| Structural Tensors: | $\mathbf{A} = \mathbb{P}_4 : \mathbf{E}$, $\mathbf{B} = \mathbb{P}_4 : \mathbf{E}^2$, $\mathbf{W} = \epsilon \epsilon_3$ |
| Invariants depending on one variable: | $\text{tr}[\mathbf{E}]$, $\text{tr}[\mathbf{E}^2]$, $\text{tr}[\mathbf{A}]$, $\text{tr}[\mathbf{A}^2]$, $\text{tr}[\mathbf{B}]$ |
| Invariants for two arguments: | $\text{tr}[\mathbf{EA}]$, $\text{tr}[\mathbf{EW}^2]$, $\text{tr}[\mathbf{E}^2 \mathbf{W}^2]$, |
| | $\text{tr}[\mathbf{BW}^2]$, $\text{tr}[\mathbf{AW}^2]$, $\text{tr}[\mathbf{A}^2 \mathbf{W}^2]$ |
| Invariants for three arguments: | $\text{tr}[\mathbf{EAW}]$, $\text{tr}[\mathbf{EW}^2 \mathbf{AW}]$ |

Taking into account the functional dependencies between the invariants

$$\begin{aligned} \text{tr}[\mathbf{A}] &= 0, \text{tr}[\mathbf{B}] = 0, \text{tr}[\mathbf{AW}^2] = 0, \text{tr}[\mathbf{BW}^2] = 0, \\ \text{tr}[\mathbf{A}^2 \mathbf{W}^2] &= -\text{tr}[\mathbf{A}^2], \text{tr}[\mathbf{EW}^2 \mathbf{AW}] = -\text{tr}[\mathbf{EAW}], \\ \text{tr}[\mathbf{A}^2] &= 4 \text{tr}[\mathbf{E}]^2 + 8 \text{tr}[\mathbf{E}] \text{tr}[\mathbf{EW}^2] + 2 \text{tr}[\mathbf{EW}^2]^2 - 8 \text{tr}[\mathbf{E}^2 \mathbf{W}^2] - 4 \text{tr}[\mathbf{E}^2], \end{aligned}$$

we get the *set of bilinear invariants*

$$\mathcal{F}^{t1}(\mathbf{E}, \mathbf{A}, \mathbf{W}) = \{\text{tr}[\mathbf{E}], \text{tr}[\mathbf{E}^2], \text{tr}[\mathbf{EA}], \text{tr}[\mathbf{EW}^2], \text{tr}[\mathbf{E}^2 \mathbf{W}^2], \text{tr}[\mathbf{EAW}]\} \quad (4.78)$$

and in detail:

$$\begin{aligned} \mathcal{F}^{t1}(\mathbf{E}, \mathbf{A}, \mathbf{W}) &= \{E_{11} + E_{22} + E_{33}, E_{11}^2 + E_{22}^2 + E_{33}^2 + 2 E_{12}^2 + 2 E_{13}^2 \\ &\quad + 2 E_{23}^2, (E_{11} - E_{22})^2 - 4 E_{12}^2, -E_{11} - E_{22}, -E_{11}^2 - E_{22}^2 \\ &\quad - 2 E_{12}^2 - E_{13}^2 - E_{23}^2, 4 E_{12}(E_{11} - E_{22})\}. \end{aligned} \quad (4.79)$$

The invariants in the proposed approach (4.78) can also be expressed by nontrivial combinations of the invariants of the corresponding *classical set of bilinear invariants*, cf. DIMITRIENKO [43]:

$$\bar{\mathcal{F}}^{t1} = \{E_{11} + E_{22}, E_{33}, E_{13}^2 + E_{23}^2, E_{11}^2 + E_{22}^2, E_{12}(E_{11} - E_{22})\}. \quad (4.80)$$

Quadratic Energy Function: Collecting arbitrary quadratic combinations of the invariants of the set $\mathcal{F}^{t1}(\mathbf{E} = \mathbf{E}, \mathbf{A}, \mathbf{W})$ and all a priori quadratic invariants of $\mathcal{F}^{t1}(\mathbf{E} = \mathbf{E}, \mathbf{A}, \mathbf{W})$ yields the set \mathcal{B}^{t1} :

$$\begin{aligned} \mathcal{B}^{t1} &:= \{\text{tr}[\mathbf{E}]^2, \text{tr}[\mathbf{E}^2], \text{tr}[\mathbf{EA}], \text{tr}[\mathbf{EW}^2]^2, \text{tr}[\mathbf{EAW}], \\ &\quad \text{tr}[\mathbf{E}] \text{tr}[\mathbf{EW}^2], \text{tr}[\mathbf{E}^2 \mathbf{W}^2]\}. \end{aligned} \quad (4.81)$$

Hence, coordinate-invariant tetragonal functions $\psi^{t1}(\mathbf{C}, \mathbf{A}, \mathbf{W})$ are constructed by the 7 quadratic, linearly independent elements of the set \mathcal{B}^{t1} while inserting $\mathbf{E} = \frac{1}{2}(\mathbf{C} - \mathbf{1})$:

$$\psi^{t1}(\mathbf{C}, \mathbf{A}, \mathbf{W}) = \sum_{i=1}^7 \alpha_i L_i, \quad L_i \in \mathcal{B}^{t1}.$$

The second derivative with respect to \mathbf{C} , i.e., $\mathbb{C}^{t1} = 4 \partial_{\mathbf{CC}} \psi^{t1}(\mathbf{C}, \mathbf{A}, \mathbf{W})$, with

$$\begin{aligned} \mathbb{C}^{t1} &= \lambda \mathbf{1} \otimes \mathbf{1} + 2\mu \mathbf{1} \boxtimes \mathbf{1} + 2\alpha_3 \mathbb{P}_4 + 2\alpha_4(\mathbf{W}^2 \otimes \mathbf{W}^2) + \alpha_5 \mathbb{D} \\ &\quad + \alpha_6(\mathbf{1} \otimes \mathbf{W}^2 + \mathbf{W}^2 \otimes \mathbf{1}) + \alpha_7[\mathbf{1} \boxtimes \mathbf{W}^2 + \mathbf{W}^2 \boxtimes \mathbf{1}], \end{aligned} \quad (4.82)$$

where we have the index notation of $\mathbb{D}_{abmn} = \mathbb{P}_{4,nkab}W_{km} + \mathbb{P}_{4,bkmn}W_{ka}$, appears in Voigt notation identically to the classical fourth-order tetragonal elasticity tensor of \mathcal{G}_4 -type:

$$\mathbb{C}^{(V)t1} = \begin{bmatrix} \mathbb{C}_{1111} & \mathbb{C}_{1122} & \mathbb{C}_{1133} & \mathbb{C}_{1112} & 0 & 0 \\ & \mathbb{C}_{1111} & \mathbb{C}_{1133} & -\mathbb{C}_{1112} & 0 & 0 \\ & & \mathbb{C}_{3333} & 0 & 0 & 0 \\ & & & \mathbb{C}_{1212} & 0 & 0 \\ & sym. & & & \mathbb{C}_{2323} & 0 \\ & & & & & \mathbb{C}_{2323} \end{bmatrix}.$$

The coefficients are given in terms of the material parameters as follows

$$\begin{aligned} \mathbb{C}_{1111} &= \lambda + 2\mu + 2\alpha_3 + 2\alpha_4 - 2\alpha_6 - 2\alpha_7, \\ \mathbb{C}_{1122} &= \lambda - 2\alpha_3 + 2\alpha_4 - 2\alpha_6, & \mathbb{C}_{1133} &= \lambda - \alpha_6, \\ \mathbb{C}_{1112} &= 2\alpha_5, & \mathbb{C}_{3333} &= \lambda + 2\mu, \\ \mathbb{C}_{1212} &= \mu - 2\alpha_3 - \alpha_7, & \mathbb{C}_{2323} &= \mu - \frac{1}{2}\alpha_7. \end{aligned}$$

5 Generalized Convexity Conditions – Hyperelasticity.

For the description of anisotropic and isotropic hyperelastic material behavior, the principle of material symmetry imposes certain restrictions on the constitutive equations. These important requirements can be fulfilled by exploiting representation theorems for isotropic tensor functions in both, the isotropic as well as the anisotropic cases. In cases of anisotropy the concept of structural tensors and in a few of these cases extensions of this concept makes this application possible. These representations theorems lead to coordinate-invariant formulations of the constitutive equations based on a set of scalar-valued invariants. During these investigations we pointed out that direct extensions of quadratic energy functions of the linear theory into the nonlinear case, represented by St. Venant-Kirchhoff type material models, are not very useful in finite elasticity, since certain growth conditions and the important Legendre-Hadamard ellipticity condition are not satisfied.

During the last decades further restrictions on the form of the energy function than the ones given in the previous sections were proposed for the specification of the general representation of finite elasticity. Amongst many others further conditions for a physically reasonable material modeling were required, e.g the *Baker-Ericksen Inequality*. The Baker-Ericksen inequality, BAKER & ERICKSEN [7], requires that the larger principal Cauchy stresses σ_i occur in direction of the larger principal stretches λ_i . It states that

$$\frac{\sigma_i - \sigma_j}{\lambda_i - \lambda_j} > 0 \quad \text{if } \lambda_i \neq \lambda_j. \quad (5.1)$$

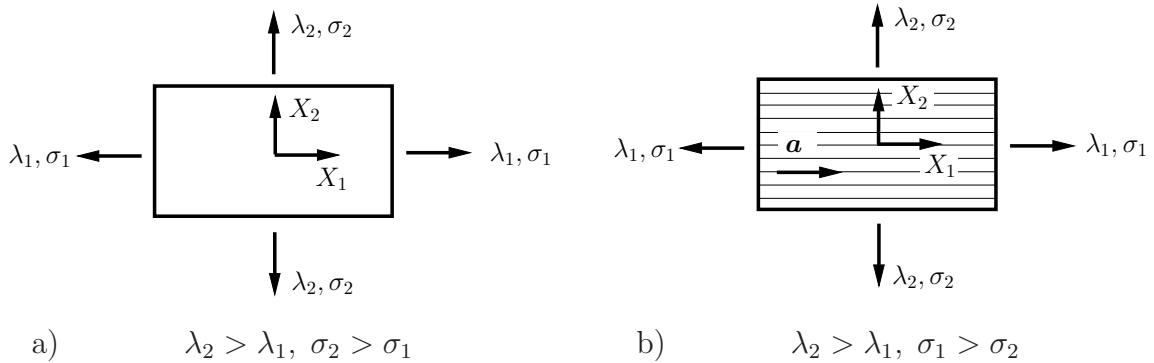


Figure 5.1: Relations between principal stresses and stretches, a) of an isotropic material, b) of an transversely isotropic material with preferred direction \mathbf{a} .

This inequality can be illustrated by the following physical situation: two rectangular planes of a material with energy function ψ are deformed by $x_i = \lambda_i X_i$, see Figure 5.1a and b. Thus, for the two-dimensional case we have $\mathbf{F} = \text{diag}(\lambda_1, \lambda_2)$. Since the first Piola-Kirchhoff stresses are defined by $\mathbf{P}(\mathbf{F}) = \partial_{\mathbf{F}}\psi$, we get here $\mathbf{P}(\mathbf{F}) = \text{diag}(T_1, T_2)$, where T_i are the forces per unit reference area. Consequently, we obtain the Cauchy stresses in diagonal form

$$\boldsymbol{\sigma} = \frac{1}{J} \mathbf{P} \mathbf{F}^T = \frac{1}{J} \text{diag}(\lambda_1 T_1, \lambda_2 T_2) = \text{diag}(\sigma_1, \sigma_2).$$

Consider the first plane of isotropic material (Figure 5.1a), it is obvious that if $\lambda_2 > \lambda_1$ then $\sigma_2 > \sigma_1$ holds, which is correctly described by the Baker-Ericksen inequality (5.1).

Consider the second plane of transversely isotropic material (Figure 5.1b) with a preferred material behavior in \mathbf{a} - (here X_1)-direction, i.e., with a much larger stiffness in X_1 -direction than in the other directions. One expects that although $\lambda_2 > \lambda_1$ still $\sigma_1 > \sigma_2$ could hold due to the increased stiffness in X_1 -direction. Thus, already for the most simple case of anisotropy, the Baker-Ericksen inequality (5.1) is not valid anymore.

Therefore, in general, it has to be ruled out for the construction of anisotropic constitutive equations. The most suitable condition in this context for modeling of both, isotropic and anisotropic hyperelastic material behavior, is the so-called *Legendre-Hadamard Inequality*. This condition ensures the existence of real wave speeds at each material point of the body and in each direction. It is investigated by the analysis of the ellipticity of the corresponding acoustic tensor. The acoustic tensor is deduced from the linearization of the balance of momentum at an equilibrium state at each material point. It is strongly related to the notion of *rank-one convexity*. If it is satisfied the material is said to be *stable*.

In finite elasticity, the existence of minimizers of (2.99) is inextricably linked with further properties of the free energy function ψ . The general aim is the construction of energy functions ensuring both the success of solving the underlying boundary value problem and a physically reasonable material modeling. Unfortunately, the requirement of the Legendre-Hadamard inequality on the constitutive equations are not enough to guarantee the existence of solutions of the considered boundary value problem. More details are discussed in section 5.5. In BALL [8] existence theorems for equilibrium boundary value problems of nonlinear elasticity under realistic hypotheses on the material response are presented. A sufficient condition for the existence of minimizers is sequential weak lower semicontinuity (s.w.l.s.) of $\int_B \psi(\mathbf{F})dV$ and the coercivity of ψ . Details concerning the notion of s.w.l.s. can be found in advanced textbooks on variational methods.

Hence, the question is: *Are there ways of satisfying the coercivity condition and s.w.l.s. together with a physically reasonable material modeling?*

5.1 Remarks on Growth Conditions, Coercivity.

According to ANTMAN [2] the behavior of hyperelastic energies for large strains should reflect that *infinite stress is accompanied by extreme strains*; possible measures are therefore

$$\psi(\mathbf{F}) \rightarrow +\infty \quad \text{as} \quad \lambda_i(\mathbf{C}) \rightarrow 0^+ \text{ or } \lambda_i(\mathbf{C}) \rightarrow +\infty, \quad (5.2)$$

where $\lambda_i(\mathbf{C})$ denotes anyone of the eigenvalues of \mathbf{C} in an interval of $]0, +\infty[$. However, we make the following assumptions capturing the behavior of ψ at large strains

$$\begin{aligned} \psi(\mathbf{F}) &\rightarrow +\infty & \text{as} & \det \mathbf{F} \rightarrow 0^+, \quad \forall \mathbf{F} \in \mathbb{R}_+^{3 \times 3}, \text{ or} \\ \psi(\mathbf{F}) &\rightarrow +\infty & \text{as} & \{\|\mathbf{F}\| + \|\text{Cof} \mathbf{F}\| + (\det \mathbf{F})\} \rightarrow +\infty, \quad \forall \mathbf{F} \in \mathbb{R}_+^{3 \times 3}. \end{aligned} \quad (5.3)$$

The first assumption reflects the idea that *an infinite energy should be required to annihilate volume*. The second physically reasonable assumption can be replaced by the sharper *coercivity inequality*:

$$\psi(\mathbf{F}) \geq \alpha \{\|\mathbf{F}\|^p + \|\text{Cof} \mathbf{F}\|^q + (\det \mathbf{F})^r\} + \beta, \quad \forall \mathbf{F} \in \mathbb{R}_+^{3 \times 3}, \quad (5.4)$$

with $\alpha > 0, \beta, p \geq 2, q \geq \frac{p}{p-1}, r > 1$ to obtain useful existence results. See also the coerciveness conditions documented in PEDREGAL [90] and DACOROGNA [41].

5.2 Remarks on Convexity.

Strictly convex functions have a unique (global) minimum. Convex functions are automatically s.w.l.s., but are they useful also from a physical point of view? In order to prepare the answer we observe a two-dimensional set K . This set is convex, whenever

$$\lambda \mathbf{x}_1 + (1 - \lambda) \mathbf{x}_2 \in K \quad \forall \mathbf{x}_1, \mathbf{x}_2 \in K \text{ and } \lambda \in [0, 1], \quad (5.5)$$

see Figure 5.2. In geometric terms this definition states that the line joining \mathbf{x}_1 and \mathbf{x}_2 is included in K . For the definition of a one-dimensional and a nine-dimensional convex set the points in (5.5) have to be replaced by scalars and second-order tensors, respectively.

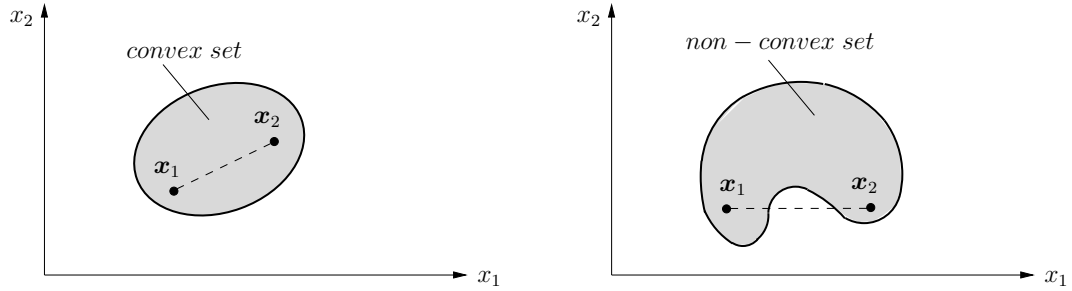


Figure 5.2: Two-dimensional convex and non-convex set.

A scalar-valued function $f : K \rightarrow \mathbb{R}$ defined on a convex set K is (strictly) convex if

$$f(\lambda x_1 + (1 - \lambda) x_2) \leq \lambda f(x_1) + (1 - \lambda) f(x_2) \quad \forall x_1, x_2 \in K, \lambda \in [0, 1]. \quad (5.6)$$

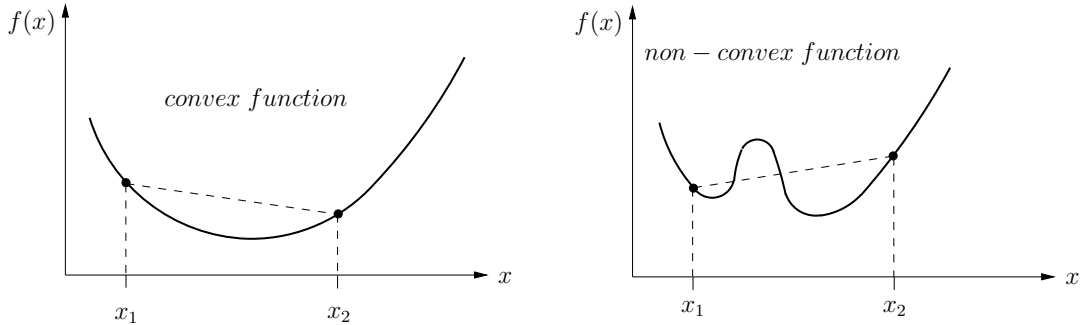


Figure 5.3: One-dimensional convex and non-convex function.

and strictly convex on K if

$$f(\lambda x_1 + (1 - \lambda) x_2) < \lambda f(x_1) + (1 - \lambda) f(x_2) \quad \forall x_1, x_2 \in K, x_1 \neq x_2, \lambda \in]0, 1[. \quad (5.7)$$

In Figure 5.3 an example of a strictly convex and non-convex one-dimensional function is illustrated. Relations between convexity and differentiability are the following: The function $f : K \rightarrow \mathbb{R}$ defined on a convex set K and which is differentiable over K is convex on K if and only if

$$f(x_1) + Df(x_1)(x_2 - x_1) \leq f(x_2) \quad \forall x_1, x_2 \in K \quad (5.8)$$

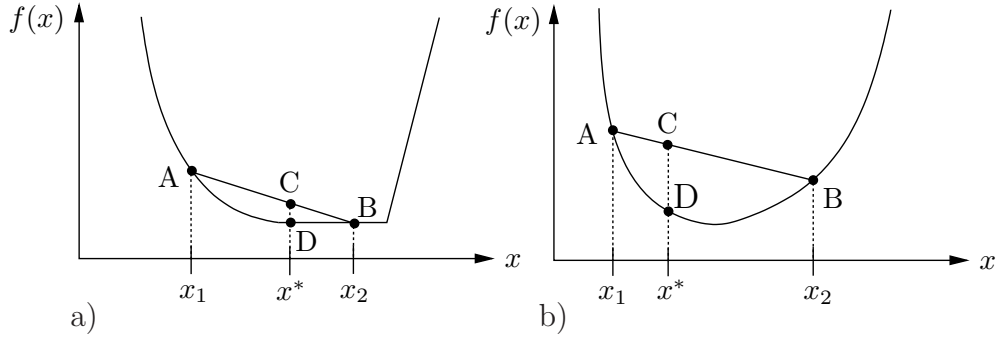


Figure 5.4: a) Convex and b) strictly convex function.

and strictly convex on K if and only if

$$f(x_1) + Df(x_1)(x_2 - x_1) < f(x_2) \quad \forall x_1, x_2 \in K, x_1 \neq x_2. \quad (5.9)$$

The twice differentiable function $f : K \rightarrow \mathbb{R}$ defined on a convex set K is (strictly) convex on K if and only if

$$f''(x)(\cdot) \geq 0 \quad \forall x \in K. \quad (5.10)$$

A corresponding geometrical interpretation is that the linear combination C of two function values $A = f(x_1)$ and $B = f(x_2)$, i.e., $C = \lambda A + (1 - \lambda)B$, is always above (Fig. 5.4 a), b)) or equal (Fig. 5.4 b)) the corresponding function value $D = f(C)$. In case of scalar-valued tensor functions a (strictly) convex function, e.g. the free energy function ψ in terms of the deformation gradient \mathbf{F} , is defined on the nine-dimensional convex set $\mathbb{R}^{3 \times 3}$ as

$$\psi(\lambda \mathbf{F}_1 + (1 - \lambda) \mathbf{F}_2) \leq \lambda \psi(\mathbf{F}_1) + (1 - \lambda) \psi(\mathbf{F}_2) \quad \forall \mathbf{F}_1, \mathbf{F}_2 \in \mathbb{R}^{3 \times 3}, \lambda \in [0, 1], \quad (5.11)$$

cf. e.g. SCHRÖDER [100]. If $\psi(\mathbf{F})$ is once differentiable, the convexity condition reads analogously to (5.8)

$$\psi(\mathbf{F}) + \mathbf{P}(\mathbf{F}) : \Delta \mathbf{F} \leq \psi(\mathbf{F} + \Delta \mathbf{F}) \quad \forall \mathbf{F}, \Delta \mathbf{F} \in \mathbb{R}^{3 \times 3}, \lambda \in [0, 1], \quad (5.12)$$

where $\mathbf{P} = \partial_{\mathbf{F}} \psi$, $\mathbf{F} = \mathbf{F}_1$ and $\Delta \mathbf{F} = \mathbf{F}_2 - \mathbf{F}_1$. For strictly convex functions $\psi(\mathbf{F})$ the statement (5.12) carries over with $<$ instead \leq , $\mathbf{F}_1 \neq \mathbf{F}_2$ and $\lambda \in]0, 1[$.

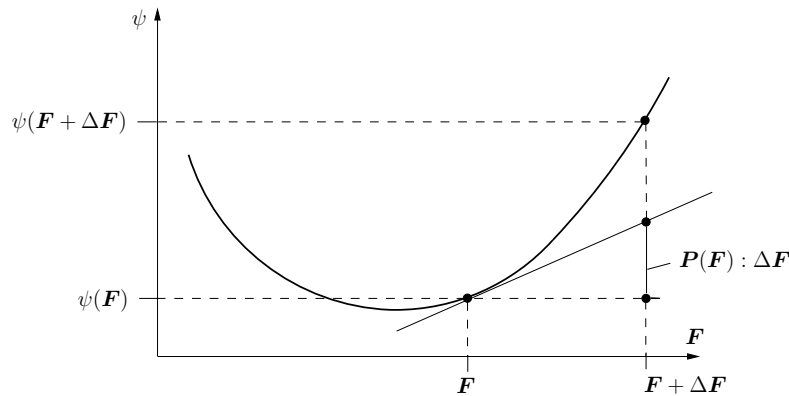


Figure 5.5: Illustration of strict convexity of $\psi(\mathbf{F})$.

As depicted in Figure 5.5 strict convexity means that the function value $\psi(\mathbf{F} + \Delta\mathbf{F})$ for all $(\mathbf{F} + \Delta\mathbf{F})$ must be higher than the value given by $\psi(\mathbf{F}) + \mathbf{P}(\mathbf{F}) : \Delta\mathbf{F}$. The alternative representation of the (strict) convexity condition is

$$[\mathbf{P}(\mathbf{F}_2) - \mathbf{P}(\mathbf{F}_1)] : (\mathbf{F}_2 - \mathbf{F}_1)(>) \geq 0 \quad \forall \mathbf{F}_1, \mathbf{F}_2 \in \mathbb{R}^{3 \times 3} \quad (5.13)$$

which represents the monotonicity of \mathbf{P} . If ψ is twice differentiable, the equivalent (strict) convexity condition to (5.10) reads

$$\Delta\mathbf{F} : \mathbb{A} : \Delta\mathbf{F}(>) \geq 0 \quad \forall \mathbf{F}, \Delta\mathbf{F} \in \mathbb{R}^{3 \times 3}, \quad \text{with } \mathbb{A} := \frac{\partial^2 \psi(\mathbf{F})}{\partial \mathbf{F} \partial \mathbf{F}}, \quad (5.14)$$

which represents the requirement of a positive (semi-)definite nominal tangent \mathbb{A} . Nevertheless, the convexity condition cannot be used, since this property contradicts the most immediate physical requirements (cf. e.g. CIARLET [38]):

(i) The set $\{\mathbf{F} \mid \det \mathbf{F} > 0\}$, i.e., $\{\mathbf{F} \in \mathbb{R}_+^{3 \times 3}\}$, is not convex: In case of a convex set $\{\mathbf{F} \mid \det \mathbf{F} > 0\}$ an arbitrary linear convex combination $\mathbf{F} = \lambda \mathbf{F}_1 + (1 - \lambda) \mathbf{F}_2$ has to be also an element of $\mathbb{R}_+^{3 \times 3}$. As a simple counterexample we consider the deformation gradients

$$\mathbf{F}_1 = \text{diag}(1, 1, 1), \quad \mathbf{F}_2 = \text{diag}(-1, -1, 1), \quad \text{with } \det \mathbf{F}_1 = \det \mathbf{F}_2 = 1 > 0. \quad (5.15)$$

The determinant of their linear convex combination ($\lambda = \frac{1}{2}$) is finally given by

$$\det \mathbf{F} = 0, \quad \text{with } \mathbf{F} = \frac{1}{2} \mathbf{F}_1 + \frac{1}{2} \mathbf{F}_2 = \text{diag}(0, 0, 1). \quad (5.16)$$

Therefore, convexity precludes the reasonable requirement that $\psi(\mathbf{F}) \rightarrow +\infty$ as $\det \mathbf{F} \rightarrow 0^+$, $\mathbf{F} \in \mathbb{R}_+^{3 \times 3}$, see (5.3)₁. Furthermore, the behavior of a homogeneous, isotropic, (quasi-) incompressible rubber sheet can not be modeled by a convex energy function, see BALL [9]: Perform homogeneous deformations of such a rubber sheet

$$\mathbf{F} = \text{diag}(\lambda_1, \lambda_2, 1), \quad \text{with } \det \mathbf{F} = \lambda_1 \lambda_2. \quad (5.17)$$

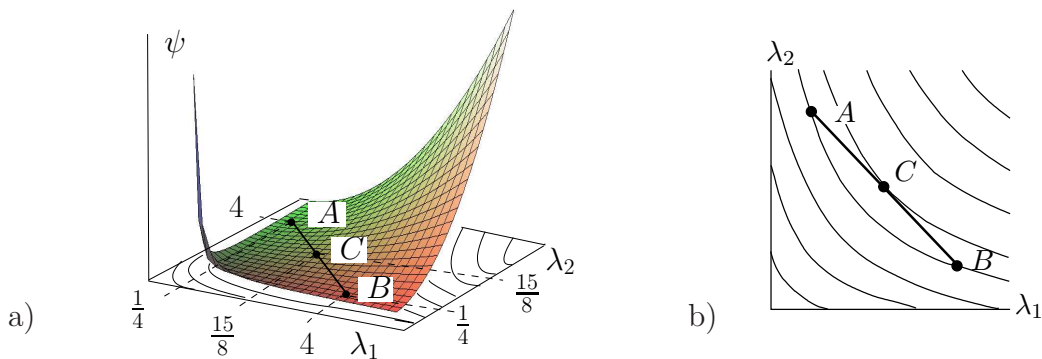


Figure 5.6: a) Non-convex function ψ ((5.18) with $\alpha = 1$) describing quasi-incompressibility of a typical rubber sheet in a homogeneous deformation, b) projection of ψ to the $\lambda_1 - \lambda_2$ -plane.

Take into account for the description of the quasi-incompressibility e.g. the energy function

$$\psi(\mathbf{F}) = \psi(\lambda_1, \lambda_2) = ((\det \mathbf{F})^2 + \frac{1}{(\det \mathbf{F})^2} - 2)^\alpha = (\lambda_1^2 \lambda_2^2 + \frac{1}{\lambda_1^2 \lambda_2^2} - 2)^\alpha, \quad \alpha \geq 1, \quad (5.18)$$

with $\psi(\mathbf{F}) = 0$ for $\det \mathbf{F} = 1$ and $\psi(\mathbf{F}) \rightarrow \infty$ for $\det \mathbf{F} \neq 1$, i.e., $\det \mathbf{F} \rightarrow 0^+$ and $\det \mathbf{F} \rightarrow \infty$. Then, however, the contours of equal energy are "banana-shaped" as depicted in Figure 5.6. There, one can see that, considering the energy (5.18) with $\alpha = 1$, e.g. the relation

$$\psi(\mathbf{F}_C) = \psi\left(\frac{15}{8}, \frac{15}{8}\right) \approx 10.44 > \frac{1}{2}(\psi(\mathbf{F}_A) + \psi(\mathbf{F}_B)) = \frac{1}{2}\left(\psi\left(\frac{1}{4}, 4\right) + \psi\left(4, \frac{1}{4}\right)\right) = 0,$$

holds; thus, the energy (5.18) is not convex.

(ii) For the fulfillment of the principle of material frame indifference (see section 2.7.1) using convex energy functions physically unreasonable inequalities would be implied, cf. COLEMAN & NOLL [40], TRUESDELL & NOLL [127], CIARLET [38]: For hyperelastic materials the principle of material frame indifference (section 2.7.1) requires

$$\psi(\mathbf{F}) = \psi(\mathbf{QF}) \quad \forall \mathbf{Q} \in \text{SO}(3), \forall \mathbf{F}. \quad (5.19)$$

According to (5.12) convexity of ψ leads to

$$\psi(\mathbf{F}) + \mathbf{P}(\mathbf{F}) : (\mathbf{QF} - \mathbf{F}) \leq \psi(\mathbf{QF}) \quad \forall \mathbf{Q} \in \text{SO}(3), \forall \mathbf{F}. \quad (5.20)$$

Inserting (5.19) in (5.20) gives

$$\mathbf{P}(\mathbf{F}) : (\mathbf{Q} - \mathbf{1})\mathbf{F} \leq 0 \quad \forall \mathbf{Q} \in \text{SO}(3), \forall \mathbf{F}. \quad (5.21)$$

With the tensor operation $\mathbf{A} : \mathbf{BC} = \mathbf{AC}^T : \mathbf{B}$ we obtain

$$\boldsymbol{\tau} : (\mathbf{Q} - \mathbf{1}) \leq 0 \quad \forall \mathbf{Q} \in \text{SO}(3), \forall \mathbf{F}. \quad (5.22)$$

We may choose the expression of the Kirchhoff stresses $\boldsymbol{\tau} = \text{diag}(\lambda_{\tau,1}, \lambda_{\tau,2}, \lambda_{\tau,3})$ in terms of three distinct eigenvalues $\lambda_{\tau,i}$, $i = 1, 2, 3$ and the orthogonal transformations

$$\mathbf{Q} = \mathbf{Q}_{X_1}^\pi, \mathbf{Q}_{X_2}^\pi, \mathbf{Q}_{X_3}^\pi, \quad (5.23)$$

in these three cases the evaluation of (5.22) implies

$$\lambda_{\tau,2} + \lambda_{\tau,3} \geq 0, \lambda_{\tau,1} + \lambda_{\tau,3} \geq 0, \lambda_{\tau,1} + \lambda_{\tau,2} \geq 0. \quad (5.24)$$

From the physical point of view the eigenvalues of $\boldsymbol{\tau}$ cannot be expected to ensure the inequalities (5.24) for all deformations, e.g. in case of physically reasonable compressive stresses in two different principal directions $\lambda_{\tau,i}$, $\lambda_{\tau,i+1}$ the inequalities are not satisfied.

(iii) Strictly convex energy functions have at most one minimum, in contradiction with the counterexamples to uniqueness, cf. HILL [61], RIVLIN [94, 95]. Thus, it precludes stability problems such as buckling.

Remark 1: Regarding items (i)-(iii) we conclude that the convexity condition is too restrictive from a physical point of view. Therefore, we focus on the quasiconvexity condition, which ensures, together with the fulfillment of the growth condition,

$$\psi(\mathbf{F}) \leq c_1 \|\mathbf{F}\|^p + c_2 \quad \text{with} \quad c_1 > 0, c_2, p > 1, \quad (5.25)$$

s.w.l.s.. Furthermore, quasiconvexity is a sufficient condition for rank-one convexity, which is strongly related to the Legendre-Hadamard-Inequality condition (section 5.5). The important concept of *quasiconvexity* was introduced by MORREY [77]. This integral inequality condition implies that the state of minimum energy for a homogeneous body under homogeneous Dirichlet boundary conditions is itself homogeneous.

5.3 Remarks on Quasiconvexity.

Following KRAWIETZ [68] the mechanical criterion of material stability states that *it is impossible to release energy from a body made of a stable and homogeneous material through an isothermal process if the body is fixed at the boundaries*. For hyperelastic materials this condition reads

$$\int_{t_0}^t \int_{\mathcal{B}_0} \mathbf{P} : \dot{\mathbf{F}} dV dt = \int_{\mathcal{B}_0} \psi(\mathbf{F}, t) dV - \int_{\mathcal{B}_0} \psi(\bar{\mathbf{F}}, t_0) dV \geq 0 \quad (5.26)$$

with a constant $\mathbf{F} = \bar{\mathbf{F}}$ over \mathcal{B}_0 at an initial time t_0 , such that $\psi(\mathbf{F}, t_0) = \psi(\bar{\mathbf{F}})$, and homogeneous Dirichlet boundary conditions $\mathbf{x} = \bar{\mathbf{F}}\mathbf{X}$ on $\partial\mathcal{B}_0$.

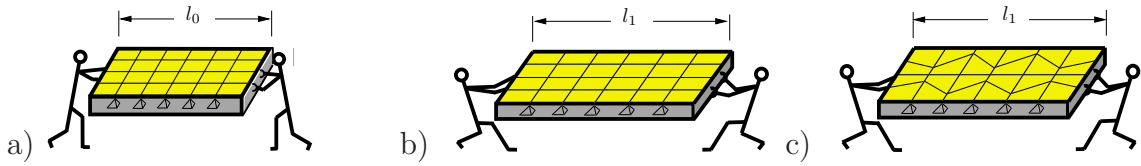


Figure 5.7: ^{12.)}Physical interpretation of quasiconvexity condition: a) reference configuration: homogeneous body subjected to homogeneous boundary conditions, actual configuration with b) homogeneous deformations $\mathbf{F} = \bar{\mathbf{F}}$, c) inhomogeneous deformations $\mathbf{F} = \bar{\mathbf{F}} + \text{Grad}\mathbf{w}$.

Only the positions of material points inside the body are varied, so that the deformation gradient of inner material points has the form

$$\mathbf{F} = \bar{\mathbf{F}} + \text{Grad}\mathbf{w} \quad (5.27)$$

with the fluctuation field \mathbf{w} in \mathcal{B}_0 satisfying $\mathbf{w} = \mathbf{0}$ on $\partial\mathcal{B}_0$. Inserting (5.27) into (5.26) yields the definition of quasiconvexity:

Definition of Quasiconvexity: The elastic stored energy is quasiconvex whenever for all $\mathcal{B}_0 \subset \mathbb{R}^3$, all constant $\bar{\mathbf{F}} \in \mathbb{R}^{3 \times 3}$ and all $\mathbf{w} \in C_0^\infty(\mathcal{B}_0)$, satisfying $\mathbf{w} = \mathbf{0}$ on $\partial\mathcal{B}_0$, the integral inequality

$$\int_{\mathcal{B}_0} \psi(\bar{\mathbf{F}} + \text{Grad}\mathbf{w}) dV \geq \int_{\mathcal{B}_0} \psi(\bar{\mathbf{F}}) dV = \psi(\bar{\mathbf{F}}) \times \text{Vol}(\mathcal{B}_0) \quad (5.28)$$

is valid, MORREY [77].

A physical interpretation of this condition is as follows: Consider a block composed of a homogeneous material with energy function ψ . The block is subjected to homogeneous Dirichlet boundary conditions $\mathbf{x} = \bar{\mathbf{F}}\mathbf{X}$ on $\partial\mathcal{B}_0$. The reference configuration is illustrated in Figure 5.7a. In the actual configuration \mathcal{B}_t two situations are presented: a homogeneous deformation $\mathbf{w} = \mathbf{0}$ in \mathcal{B}_t (Figure 5.7b) and an inhomogeneous deformation $\mathbf{w} \neq \mathbf{0}$ in \mathcal{B}_t (Figure 5.7c). If the energy is quasiconvex, the homogeneous deformations are always a solution of the underlying boundary value problem. This does not mean, that there are no further solutions (inhomogeneous deformations) of the underlying boundary value problem, but these deformations lead to a higher energy value than the homogeneous deformations. Thus, the constant solution $\text{Grad}\boldsymbol{\varphi} = \bar{\mathbf{F}}$ of the boundary value problem

$$\text{Div}\mathbf{P} = \text{Div}[\partial_{\mathbf{F}}\psi(\text{Grad}\boldsymbol{\varphi})] = \mathbf{0} \quad \text{with} \quad \mathbf{x} = \bar{\mathbf{F}}\mathbf{X} \quad \text{on} \quad \partial\mathcal{B}_0$$

^{12.)}The figures are taken from [42].

is a global minimizer for a quasiconvex functional.

Remark 2: The integral inequality of the quasiconvexity condition must be satisfied for arbitrary fluctuations \mathbf{w} ; hence, this condition is rather complicated to verify. A drawback of the quasiconvexity condition is that the growth condition (5.25) to be additionally satisfied precludes the physically reasonable requirement (5.3)₁, cf. *Problem 1* in [10]. Therefore, we search for a convexity condition which ensures quasiconvexity and s.w.l.s., in order to overcome the problem of verifying (5.25).

The most suitable condition for practical use is the notion of polyconvexity in the sense of BALL [8, 9], which is a sufficient (but not necessary) condition for quasiconvexity and implies s.w.l.s., see also MARSDEN & HUGHES [72] and CIARLET [38].

5.4 Polyconvexity.

The polyconvexity condition represents a pointwise requirement on the free energy function. The notion of polyconvexity underlies the first existence result in finite elasticity, given by BALL [9, 8].

Definition of Polyconvexity: $\mathbf{F} \mapsto \psi(\mathbf{F})$ is polyconvex if and only if there exists a function $P : \mathbb{R}^{3 \times 3} \times \mathbb{R}^{3 \times 3} \times \mathbb{R} \mapsto \mathbb{R}$ (in general non-unique) such that

$$\psi(\mathbf{F}) = \mathcal{P}(\mathbf{F}, \text{Cof} \mathbf{F}, \det \mathbf{F}), \quad (5.29)$$

and the function $\mathbb{R}^{19} \mapsto \mathbb{R}$, $(\mathbf{F}, \text{Cof} \mathbf{F}, \det \mathbf{F}) \mapsto \mathcal{P}(\mathbf{F}, \text{Cof} \mathbf{F}, \det \mathbf{F})$ is convex for all points $\mathbf{X} \in \mathbb{R}^3$.

In order to arrive at a more compact notation, we may omit the \mathbf{X} -dependence of the individual functions in the definition below if there is no danger of confusion. Note that the argument $(\mathbf{F}, \text{Cof} \mathbf{F}, \det \mathbf{F})$ plays an important role with regard to the transport theorems, see section 2.1. According to the definition of convexity the polyconvexity of ψ is satisfied if

$$\begin{aligned} \psi(\lambda [\mathbf{F}_1, \text{Cof} \mathbf{F}_1, \det \mathbf{F}_1] + (1 - \lambda) [\mathbf{F}_2, \text{Cof} \mathbf{F}_2, \det \mathbf{F}_2]) &\leq \\ \lambda \psi(\mathbf{F}_1, \text{Cof} \mathbf{F}_1, \det \mathbf{F}_1) + (1 - \lambda) \psi(\mathbf{F}_2, \text{Cof} \mathbf{F}_2, \det \mathbf{F}_2) \end{aligned} \quad (5.30)$$

$\forall \mathbf{F}_1, \mathbf{F}_2 \in \mathbb{R}^{3 \times 3}$, $\lambda \in [0, 1]$. In the sequel we focus on energy functions $\psi(\mathbf{F}) = \mathcal{P}(\mathbf{F}, \text{Cof} \mathbf{F}, \det \mathbf{F})$ which are twice continuous differentiable, i.e., $\psi \in C^2(\mathbb{R}^{3 \times 3}, \mathbb{R})$. The polyconvexity of ψ is proved by a positive second Fréchet derivative of

$$\psi(\mathbf{F}) = \mathcal{P}(\boldsymbol{\xi}) \quad \text{with respect to} \quad \boldsymbol{\xi} := (\mathbf{F}, \text{Cof} \mathbf{F}, \det \mathbf{F}), \quad \boldsymbol{\xi} \in \mathbb{R}^{19}.$$

The first Fréchet derivative of P is given by

$$\left(\frac{\partial \mathcal{P}(\boldsymbol{\xi})}{\partial \boldsymbol{\xi}} \right)^T \delta \boldsymbol{\xi} = \frac{\partial \mathcal{P}(\boldsymbol{\xi})}{\partial \mathbf{F}} : \delta \mathbf{F} + \frac{\partial \mathcal{P}(\boldsymbol{\xi})}{\partial \text{Cof} \mathbf{F}} : \delta \text{Cof} \mathbf{F} + \frac{\partial \mathcal{P}(\boldsymbol{\xi})}{\partial \det \mathbf{F}} \delta \det \mathbf{F}.$$

The second Fréchet derivative is represented in a suitable matrix scheme as

$$\delta \boldsymbol{\xi}^T \frac{\partial^2 \mathcal{P}(\boldsymbol{\xi})}{\partial \boldsymbol{\xi} \partial \boldsymbol{\xi}} \delta \boldsymbol{\xi} = \underbrace{\begin{pmatrix} \delta \mathbf{F} \\ \delta \text{Cof} \mathbf{F} \\ \delta \det \mathbf{F} \end{pmatrix}^T}_{\delta \boldsymbol{\xi}^T} \underbrace{\begin{bmatrix} \frac{\partial^2 \mathcal{P}}{\partial \mathbf{F} \partial \mathbf{F}} & \frac{\partial}{\partial \text{Cof} \mathbf{F}} \left(\frac{\partial \mathcal{P}}{\partial \mathbf{F}} \right) & \frac{\partial}{\partial \det \mathbf{F}} \left(\frac{\partial \mathcal{P}}{\partial \mathbf{F}} \right) \\ \frac{\partial}{\partial \mathbf{F}} \left(\frac{\partial \mathcal{P}}{\partial \text{Cof} \mathbf{F}} \right) & \frac{\partial^2 \mathcal{P}}{\partial \text{Cof} \mathbf{F} \partial \text{Cof} \mathbf{F}} & \frac{\partial}{\partial \det \mathbf{F}} \left(\frac{\partial \mathcal{P}}{\partial \text{Cof} \mathbf{F}} \right) \\ \frac{\partial}{\partial \mathbf{F}} \left(\frac{\partial \mathcal{P}}{\partial \det \mathbf{F}} \right) & \frac{\partial}{\partial \text{Cof} \mathbf{F}} \left(\frac{\partial \mathcal{P}}{\partial \det \mathbf{F}} \right) & \frac{\partial^2 \mathcal{P}}{\partial \det \mathbf{F} \partial \det \mathbf{F}} \end{bmatrix}}_{\frac{\partial^2 \mathcal{P}(\boldsymbol{\xi})}{\partial \boldsymbol{\xi} \partial \boldsymbol{\xi}}} \underbrace{\begin{pmatrix} \delta \mathbf{F} \\ \delta \text{Cof} \mathbf{F} \\ \delta \det \mathbf{F} \end{pmatrix}}_{\delta \boldsymbol{\xi}},$$

with $\delta \boldsymbol{\xi} \in \mathbb{R}^{19}$ and $\partial_{\boldsymbol{\xi}\boldsymbol{\xi}}^2 \mathcal{P}(\boldsymbol{\xi}) \in \mathbb{R}^{19 \times 19}$. The polyconvexity condition finally reads

$$\delta \boldsymbol{\xi}^T \frac{\partial^2 \mathcal{P}(\boldsymbol{\xi})}{\partial \boldsymbol{\xi} \partial \boldsymbol{\xi}} \delta \boldsymbol{\xi} \geq 0 \quad \forall \boldsymbol{\xi}, \delta \boldsymbol{\xi}, \quad (5.31)$$

which is equal to the proof of positive (semi-)definiteness of the 19×19 matrix $\partial_{\boldsymbol{\xi}\boldsymbol{\xi}}^2 \mathcal{P}(\boldsymbol{\xi})$, see Appendix C.

The advantage of the polyconvexity condition is that –contrary to convexity– such an assumption does not conflict with any physical requirement. As a simple example for a polyconvex function we consider the third principal invariant in terms of \mathbf{F} , i.e., $\psi(\mathbf{F}) = \det \mathbf{F} \quad \forall \mathbf{F} \in \mathbb{R}^{3 \times 3}$. The function is non-convex with respect to \mathbf{F} , but polyconvex, since the function $\psi(\mathbf{F}) = \mathcal{P}(\det \mathbf{F}) = \det \mathbf{F}$ is convex with respect to its argument $(\det \mathbf{F})$. In this example the non-uniqueness of the polyconvex function is given by $\psi(\mathbf{F}) = \mathcal{P}_1(\det \mathbf{F}) = \det \mathbf{F} = \mathcal{P}_2(\mathbf{F}, \text{Cof} \mathbf{F}) = \mathbf{F} : \text{Cof} \mathbf{F}$, i.e., the function can be expressed in terms of the argument $(\det \mathbf{F})$ and $(\mathbf{F}, \text{Cof} \mathbf{F})$, respectively.

Analogously, the powers of $\det \mathbf{F}$, i.e.,

$$\psi(\mathbf{F}) = (\det \mathbf{F})^k = (\det \mathbf{F})^{2k} = J^{2k} = \mathcal{P}(J) \quad \forall k \geq 1 \quad (5.32)$$

are convex with respect to $\det \mathbf{F}$ and hence polyconvex. The polyconvexity of the principal and main invariants in terms of the right Cauchy-Green tensor is well-known and documented in many publications.

Proof. We evaluate (5.10), i.e., here the second derivative of (5.32) w.r.t. the scalar-valued argument J and obtain

$$\partial_{JJ} \mathcal{P}(J) = 2k(2k-1) J^{2k-2}, \quad (5.33)$$

which is always positive for $k \geq 1$, $J > 0$.

Additive Polyconvex Functions. Let

$$\psi(\mathbf{F}) = \mathcal{P}_1(\mathbf{F}) + \mathcal{P}_2(\text{Cof} \mathbf{F}) + \mathcal{P}_3(\det \mathbf{F}).$$

If $\mathcal{P}_i, i = 1, 2, 3$ are convex in the associated variable, then $\psi(\mathbf{F})$ is altogether polyconvex, cf. Corollary 3.2 in HARTMANN & NEFF [57] and SCHRÖDER & NEFF [104].

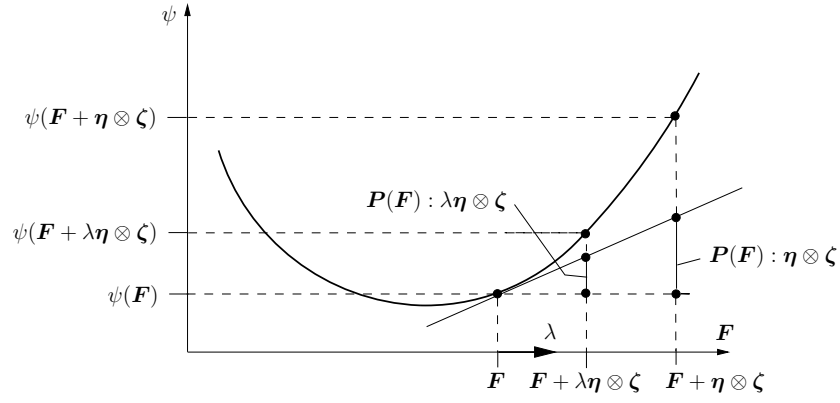


Figure 5.8: Rank-one convex function $\psi(\mathbf{F})$.

5.5 Rank-One Convexity and Ellipticity.

Rank-one convexity describes the convexity of a function along a straight line of the considered set, where the difference between the initial and end point is given by a second-order rank-one tensor. Formulating the free energy function in terms of the deformation gradient, the definition of (strict) rank-one convexity has the same form as the convexity definition (5.12), but here $\Delta \mathbf{F} = \mathbf{F}_2 - \mathbf{F}_1 = \boldsymbol{\eta} \otimes \boldsymbol{\zeta}$ has to be inserted, i.e.,

$$\psi(\mathbf{F} + \lambda \boldsymbol{\eta} \otimes \boldsymbol{\zeta}) \leq \psi(\mathbf{F}) + \lambda [\psi(\mathbf{F} + \boldsymbol{\eta} \otimes \boldsymbol{\zeta}) - \psi(\mathbf{F})] \quad (5.34)$$

$\forall \mathbf{F} \in \mathbb{R}^{3 \times 3}$, $\forall \boldsymbol{\eta}, \boldsymbol{\zeta} \in \mathbb{R}^3 \setminus \{\mathbf{0}\}$, $\lambda \in [0, 1]$ ($\lambda \in]0, 1[$), see e.g. BALL [8] and Figure 5.8. Analogously to (5.12) we obtain the definition for once differentiable $\psi(\mathbf{F})$

$$\psi(\mathbf{F}) + \mathbf{P}(\mathbf{F}) : (\boldsymbol{\eta} \otimes \boldsymbol{\zeta}) \leq \psi(\mathbf{F} + \boldsymbol{\eta} \otimes \boldsymbol{\zeta}) \quad (5.35)$$

$$\forall \mathbf{F} \in \mathbb{R}^{3 \times 3}, \forall \boldsymbol{\eta}, \boldsymbol{\zeta} \in \mathbb{R}^3 \setminus \{\mathbf{0}\}, \lambda \in [0, 1] (\lambda \in]0, 1[).$$

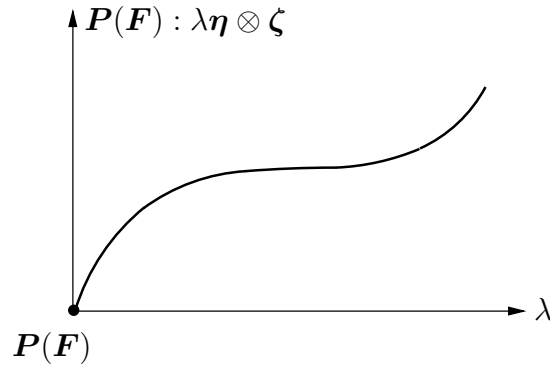


Figure 5.9: Monotonicity of \mathbf{P} with respect to all rank-one deformation tensors $\boldsymbol{\eta} \otimes \boldsymbol{\zeta}$.

A reformulation of this rank-one convexity condition according to (5.13) yields the expression

$$[\mathbf{P}(\mathbf{F} + \lambda \boldsymbol{\eta} \otimes \boldsymbol{\zeta}) - \mathbf{P}(\mathbf{F})] : (\lambda \boldsymbol{\eta} \otimes \boldsymbol{\zeta}) \geq 0, \lambda \in [0, 1] (\lambda \in]0, 1[). \quad (5.36)$$

Thus, \mathbf{P} has to be a monotone increasing function with respect to all rank-one deformation tensors, see Figure 5.9. Finally, analogously to (5.14), the definition for twice differentiable

$\psi(\mathbf{F})$ is

$$(\boldsymbol{\eta} \otimes \boldsymbol{\zeta}) : \mathbb{A} : (\boldsymbol{\eta} \otimes \boldsymbol{\zeta})(\cdot) \geq 0 \quad \text{with} \quad \mathbb{A} := \partial_{\mathbf{F}\mathbf{F}}^2 \psi(\mathbf{F}), \quad (5.37)$$

$\forall \mathbf{F} \in \mathbb{R}^{3 \times 3}, \forall \boldsymbol{\eta}, \boldsymbol{\zeta} \in \mathbb{R}^3 \setminus \{\mathbf{0}\}$, which is referred to as (strict) Legendre-Hadamard-Ellipticity.

Remark 3: Note that rank-one convexity and ellipticity of twice differentiable (smooth) energy functions are equivalent. Polyconvexity of smooth energy functions implies ellipticity. The converse is not true. The proof of this statement is based on standard results in the calculus of variations, see e.g. DACOROGNA [41].

Definition of Ellipticity: The energy function $\psi(\mathbf{F})$ leads to a (strictly) uniformly elliptic equilibrium system whenever the so-called uniform Legendre-Hadamard condition

$$\begin{aligned} \exists \epsilon > 0, \forall \mathbf{F} \in \mathbb{M}^{3 \times 3} : \forall \boldsymbol{\eta}, \boldsymbol{\zeta} \in \mathbb{R}^3 \setminus \{\mathbf{0}\} : \\ (\boldsymbol{\eta} \otimes \boldsymbol{\zeta}) : \mathbb{A} : (\boldsymbol{\eta} \otimes \boldsymbol{\zeta})(\cdot) \geq \epsilon \|\boldsymbol{\eta}\|^2 \|\boldsymbol{\zeta}\|^2 \end{aligned} \quad (5.38)$$

holds.

Omitting body forces, the equation of motion reads

$$\rho_0 \ddot{\mathbf{x}} = \text{Div} \mathbf{P}. \quad (5.39)$$

The linearization of (5.39) at the equilibrium state $\mathbf{x} := \mathbf{X} + \mathbf{u}_0$ with the associated deformation gradient $\mathbf{F}_0 := \mathbf{1} + \text{Grad} \mathbf{u}_0$ and $\text{Lin} \mathbf{P} = \mathbf{P}(\mathbf{F}_0) + \mathbb{A}(\mathbf{F}_0) : \Delta \mathbf{F}$, leads to the linearized equation

$$\text{Div}[\mathbf{P}(\mathbf{F}_0) + \mathbb{A}(\mathbf{F}_0) : \Delta \mathbf{F}] - \rho_0(\ddot{\mathbf{u}} + \Delta \ddot{\mathbf{u}}) = \mathbf{0} \Rightarrow \text{Div}[\mathbb{A}(\mathbf{F}_0) : \Delta \mathbf{F}] - \rho_0 \Delta \ddot{\mathbf{u}} = \mathbf{0}. \quad (5.40)$$

Seeking solutions in the form of traveling waves, i.e.,

$$\Delta \mathbf{u} = f(\mathbf{X} \cdot \boldsymbol{\zeta} - ct) \boldsymbol{\eta}, \quad (5.41)$$

where $\boldsymbol{\zeta} \in \mathbb{R}^3 \setminus \{\mathbf{0}\}, \|\boldsymbol{\zeta}\| = 1$, denotes the referential direction of wave propagation, $\boldsymbol{\eta} \in \mathbb{R}^3 \setminus \{\mathbf{0}\}$ is the polarization vector describing the orientation of the oscillations and c the referential phase speed of propagation, (5.40) appears as

$$f''(\mathbf{X} \cdot \boldsymbol{\zeta} - ct) \boldsymbol{\eta} [\bar{\mathbf{Q}}(\boldsymbol{\zeta}) - \rho_0 c^2 \mathbf{1}] = \mathbf{0} \Rightarrow [\bar{\mathbf{Q}}(\boldsymbol{\zeta}) - \rho_0 c^2 \mathbf{1}] \boldsymbol{\eta} = \mathbf{0}, \quad (5.42)$$

with the so-called acoustic tensor

$$\bar{Q}^a_b = \mathbb{A}^{aA}_b \zeta_A \zeta_B. \quad (5.43)$$

Non-trivial solutions of (5.42) are obtained by solving the characteristic polynomial

$$p(\lambda) = \det[\bar{\mathbf{Q}}(\boldsymbol{\zeta}) - \lambda \mathbf{1}] = 0 \quad (5.44)$$

with respect to the eigenvalue $\lambda = \rho_0 c^2$. For this special eigenvalue problem $\boldsymbol{\eta}$ is the corresponding eigenvector. Since $\rho_0, c^2 > 0$ and therefore $\lambda > 0$, the acoustic tensor has to be positive definite for all possible orientations $\boldsymbol{\zeta}$ to ensure traveling waves with positive wave speeds, i.e., all main minors of $\bar{\mathbf{Q}}$ must be positive:

$$q_1 = \bar{Q}_{11} > 0, \quad q_2 = \bar{Q}_{11} \bar{Q}_{22} - \bar{Q}_{12} \bar{Q}_{21} > 0, \quad q_3 = \det \bar{\mathbf{Q}} > 0. \quad (5.45)$$

A positive definite acoustic tensor leads to an automatic fulfillment of (5.38). Thus, *the existence of traveling waves with real wave speeds implies Legendre-Hadamard-Ellipticity* (5.38), cf. MARSDEN & HUGHES [72]. See also TRUESDELL & NOLL [127].

A suitable localization measure for the numerical analysis of ellipticity is

$$q := \text{sign}[\min[q_1, q_2, q_3]] |q_3| > 0, \quad (5.46)$$

cf. SCHRÖDER, NEFF & BALZANI [105]. If the latter condition is satisfied for all possible orientations ζ , the corresponding acoustic tensor is positive definite and the considered energy function is elliptic. We denote such material states as *materially stable*. If the Legendre-Hadamard inequality is pointwise violated, i.e., if the latter equation yields $q \leq 0$ for at least one direction ζ , then the acoustic tensor is not positive definite and we say that the system loses its ellipticity. We describe such material states as *materially unstable*. Instabilities in fiber-reinforced elastic materials induced by loss of ellipticity are discussed in MERODIO & OGDEN [75] and MERODIO & NEFF [74].

5.6 Implications of Convexity Conditions.

For finite-valued, continuous functions the important implications of the generalized convexity conditions are

$$\text{convexity} \Rightarrow \text{polyconvexity} \Rightarrow \text{quasiconvexity} \Rightarrow \text{rank-one convexity},$$

see also Figure 5.10. Note that the inverse implications are not true. Further discussions concerning the implications of the generalized convexity conditions can be found in the books DACOROGNA [41], SILHAVÝ [130], CIARLET [38] and MARSDEN & HUGHES [72].

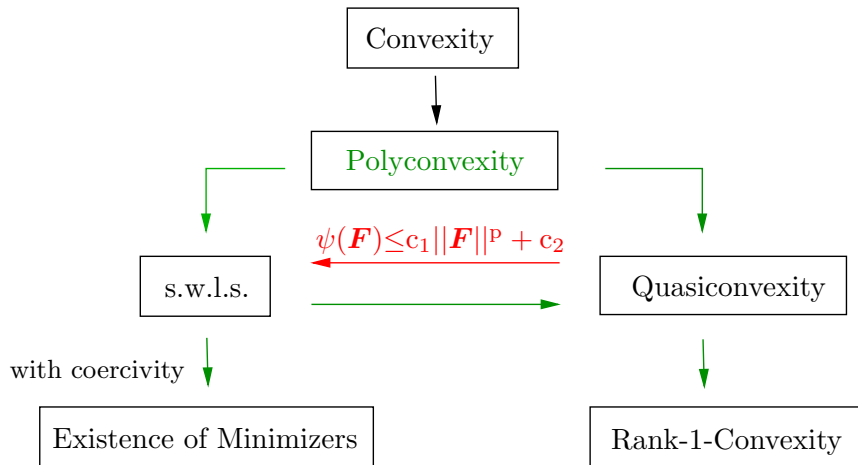


Figure 5.10: Implications of generalized convexity conditions, s.w.l.s. and existence of minimizers.

5.7 Polyconvexity and Ellipticity of Invariant Functions.

In the literature, we find a variety of polyconvex energies for the description of isotropic material behavior, e.g. STEIGMANN [120], HARTMANN & NEFF [57] and MIELKE [76]. In 2002 Ball formulated some open problems in elasticity, BALL [10]; *Problem 2* –which is the overall question of this thesis–reads:

Are there ways of verifying polyconvexity and quasiconvexity for a useful class of anisotropic stored-energy functions?

Almost at the same time SCHRÖDER & NEFF [103, 104] developed the first polyconvex energies for the case of transverse isotropy and orthotropy in a coordinate-invariant setting. The energies are formulated in terms of a transversely isotropic structural tensor and orthotropic structural tensors, respectively. Modifications and case studies in the framework of this approach are given in SCHRÖDER, NEFF & BALZANI [105], BALZANI [11], ITSKOV & AKSEL [64], MARKERT, EHLERS & KARAJAN [71]. A direct extension of SCHRÖDER & NEFF [104], by introducing a single fourth-order structural tensor, has been used by KAMBOUCHEV, FERNANDEZ & RADOVITZKY [66] for the set up of a polyconvex cubic free energy. Interesting is that the fourth-order structural tensor used there is equal to the cubic \mathcal{G}_7 -invariant structural tensor Θ given in Table 4.2.

However, suitable polyconvex energy functions for the representation of triclinic, monoclinic, tetragonal and trigonal symmetry properties had not yet been discussed in the literature.

For a coordinate-invariant formulation of energy functions for all anisotropy groups the construction of our *sets of invariants* is explained and the corresponding *sets of bilinear invariants* are given in the previous chapter. In this chapter we analyze the usefulness of the bilinear invariants of the introduced sets for the material modeling in finite elasticity. That means we investigate them in view of their polyconvexity and ellipticity properties and construct then our *sets of polyconvex invariants*. Remember, the polyconvexity of the principal and main invariants of the right Cauchy-Green tensor is well-known. Thus, we always consider these isotropic invariants as elements of the underlying *set of polyconvex invariants*.

In order to prove the polyconvexity of specific functions we have to show the convexity of P in the representation

$$\psi(\mathbf{F}) = \mathcal{P}(\boldsymbol{\xi}) \quad \text{w.r.t.} \quad \boldsymbol{\xi} := \{\mathbf{F}, \text{Cof}\mathbf{F}, \det\mathbf{F}\}.$$

For the assumed twice-continuous-differentiable scalar-valued energy densities $\psi \in C^2(\mathbb{R}^{3 \times 3}, \mathbb{R})$ we have therefore to check if

$$\delta \boldsymbol{\xi}^T \frac{\partial \mathcal{P}(\boldsymbol{\xi})}{\partial \boldsymbol{\xi} \partial \boldsymbol{\xi}} \delta \boldsymbol{\xi} \geq 0, \quad \forall \boldsymbol{\xi}, \delta \boldsymbol{\xi}$$

holds, where $\delta \boldsymbol{\xi}$ are arbitrary increments. Polyconvexity implies Legendre-Hadamard ellipticity. However, if a function is not polyconvex, it can be still Legendre-Hadamard elliptic. To prove ellipticity, we have to check if

$$\delta \mathbf{F} : \partial_{\mathbf{F}\mathbf{F}}^2 \mathcal{P}(\mathbf{F}) : \delta \mathbf{F} \geq 0$$

holds for reasonable rank-one tensors $\delta \mathbf{F} = \boldsymbol{\eta} \otimes \boldsymbol{\zeta}$, with $\boldsymbol{\eta}, \boldsymbol{\zeta} \in \mathbb{R}^3 \setminus \{\mathbf{0}\}$.

Set of Polyconvex Invariants: Our *sets of polyconvex invariants* consist of the polyconvex isotropic principal invariants of the right Cauchy-Green tensor \mathbf{C} and additional polyconvex invariants of the corresponding *set of bilinear invariants*.

5.7.1 Invariants in Terms of Second-Order Structural Tensors. We consider the often used mixed invariants

$$\text{i)} I_4^k = \text{tr}[\mathbf{C}\tilde{\mathbf{K}}] = \text{tr}[\mathbf{F}^T \mathbf{F} \tilde{\mathbf{K}}]$$

and

$$\text{ii)} I_5 = \text{tr}[\mathbf{C}^2 \tilde{\mathbf{K}}] = \text{tr}[\mathbf{F}^T \mathbf{F} \mathbf{F}^T \mathbf{F} \tilde{\mathbf{K}}],$$

where $\tilde{\mathbf{K}}$ denotes a symmetric structural tensor or the square of a skew-symmetric structural tensor. Furthermore, we give in the present section some remarks on multiplicative combinations of linear invariants which are useful for representations of *complete* energy functions, i.e.,

$$\text{iii)} I_1 I_4 \quad \text{and} \quad \text{iv)} I_{4_1} I_{4_2} = \text{tr}[\mathbf{C}\tilde{\mathbf{K}}_1] \text{tr}[\mathbf{C}\tilde{\mathbf{K}}_2].$$

We analyze the invariants under consideration of Zheng and Spencer's structural tensors, ZHENG & SPENCER [146], listed in Table 4.2^{13.)}, i.e., for the three special cases

$$\tilde{\mathbf{K}} = \mathbf{P}'_2 = \mathbf{e}_1 \otimes \mathbf{e}_2 + \mathbf{e}_2 \otimes \mathbf{e}_1, \quad \tilde{\mathbf{K}} = \mathbf{P}_2 = \mathbf{e}_1 \otimes \mathbf{e}_1 - \mathbf{e}_2 \otimes \mathbf{e}_2, \quad \tilde{\mathbf{K}} = \mathbf{W}^2, \quad (5.47)$$

with

$$\mathbf{W} = \epsilon \mathbf{e}_1 = \mathbf{e}_2 \otimes \mathbf{e}_3 - \mathbf{e}_3 \otimes \mathbf{e}_2, \quad (5.48)$$

and show also the proofs for

$$\tilde{\mathbf{K}} = \mathbf{M} = \mathbf{a} \otimes \mathbf{a}.$$

i) Let us analyze the polyconvexity of expressions in powers of the mixed invariant I_4 :

$$I_4^k = (\text{tr}[\mathbf{C}\tilde{\mathbf{K}}])^k = (\text{tr}[\mathbf{F}^T \mathbf{F} \tilde{\mathbf{K}}])^k = \langle \mathbf{F}, \mathbf{F} \tilde{\mathbf{K}} \rangle^k \quad \text{with} \quad k \geq 1. \quad (5.49)$$

Proof We get

$$\begin{aligned} \mathcal{P}(\mathbf{F}) &= \langle \mathbf{F}, \mathbf{F} \tilde{\mathbf{K}} \rangle^k \\ \partial_{\mathbf{F}} \mathcal{P}(\mathbf{F}) : \delta \mathbf{F} &= k \langle \mathbf{F}, \mathbf{F} \tilde{\mathbf{K}} \rangle^{k-1} (\langle \delta \mathbf{F}, \mathbf{F} \tilde{\mathbf{K}} \rangle + \langle \mathbf{F}, \delta \mathbf{F} \tilde{\mathbf{K}} \rangle) \\ \delta \mathbf{F} : \partial_{\mathbf{F}\mathbf{F}}^2 \mathcal{P}(\mathbf{F}) : \delta \mathbf{F} &= k(k-1) \langle \mathbf{F}, \mathbf{F} \tilde{\mathbf{K}} \rangle^{k-2} (\langle \delta \mathbf{F}, \mathbf{F} \tilde{\mathbf{K}} \rangle + \langle \mathbf{F}, \delta \mathbf{F} \tilde{\mathbf{K}} \rangle)^2 + \\ &\quad 2k \langle \mathbf{F}, \mathbf{F} \tilde{\mathbf{K}} \rangle^{k-1} \langle \delta \mathbf{F}, \delta \mathbf{F} \tilde{\mathbf{K}} \rangle. \end{aligned} \quad (5.50)$$

i.a) Evaluating (5.50) with $\tilde{\mathbf{K}} = \mathbf{a} \otimes \mathbf{a}$ we get positive second derivatives

$$\delta \mathbf{F} : \partial_{\mathbf{F}\mathbf{F}}^2 \mathcal{P}(\mathbf{F}) : \delta \mathbf{F} = 4k(k-1) \|\mathbf{F}\mathbf{a}\|^{2(k-2)} \langle \mathbf{F}\mathbf{a}, \delta \mathbf{F}\mathbf{a} \rangle^2 + 2k \|\delta \mathbf{F}\mathbf{a}\|^2 \|\mathbf{F}\mathbf{a}\|^{2(k-1)} \geq 0. \quad (5.51)$$

^{13.)} Since the structure of the second-order structural tensors proposed in [142] and [140] is similar to the structure of Zheng and Spencer's structural tensors [146], we neglect them in our analysis.

Thus, the term (5.49) with $\tilde{\mathbf{K}} = \mathbf{a} \otimes \mathbf{a}$ is convex w.r.t. \mathbf{F} . This proof is first given in SCHRÖDER & NEFF [103, 104].

i.b) For $\tilde{\mathbf{K}} = \mathbf{P}'_2 = \mathbf{e}_1 \otimes \mathbf{e}_2 + \mathbf{e}_2 \otimes \mathbf{e}_1$ the invariant I_4^k appears due to the symmetry $\mathbf{C} = \mathbf{C}^T$ as

$$I_4^k = (2 \operatorname{tr}[\mathbf{C}\mathbf{e}_1 \otimes \mathbf{e}_2])^k = 2^k (\operatorname{tr}[\mathbf{C}\mathbf{e}_1 \otimes \mathbf{e}_2])^k.$$

This term does not fulfill the polyconvexity condition, since it is not elliptic. Inserting

$$\mathbf{F} = \begin{bmatrix} 1 & 1 & 0 \\ 0 & 1/n & 0 \\ 0 & 0 & 2 \end{bmatrix}, \quad \delta\mathbf{F} = \boldsymbol{\eta} \otimes \boldsymbol{\zeta}, \quad \boldsymbol{\eta} = \begin{pmatrix} 0 \\ 1 \\ 0 \end{pmatrix}, \quad \boldsymbol{\zeta} = \begin{pmatrix} -1/\sqrt{5} \\ 2/\sqrt{5} \\ 0 \end{pmatrix}, \quad (5.52)$$

with $n = 2\sqrt{r-1}$ and $\tilde{\mathbf{K}} = \mathbf{e}_1 \otimes \mathbf{e}_2$ into (5.50) and multiplying this result by 2^k yields the second derivative

$$\delta\mathbf{F} : \partial_{\mathbf{F}\mathbf{F}}^2 \mathcal{P}(\mathbf{F}) : \delta\mathbf{F} = -\frac{3}{4} 2^k k < 0. \quad (5.53)$$

This proves the non-ellipticity of $\operatorname{tr}[\mathbf{C}\mathbf{P}'_2]^k$ for $k \geq 1$.

i.c) For $\tilde{\mathbf{K}} = \mathbf{P}_2 = \mathbf{e}_1 \otimes \mathbf{e}_1 - \mathbf{e}_2 \otimes \mathbf{e}_2$ the invariant I_4^k has the form

$$I_4^k = (\operatorname{tr}[\mathbf{C}\mathbf{e}_1 \otimes \mathbf{e}_1] - \operatorname{tr}[\mathbf{C}\mathbf{e}_2 \otimes \mathbf{e}_2])^k.$$

With (5.52), where $n \in \mathbb{R}$, and $\tilde{\mathbf{K}} = \mathbf{e}_1 \otimes \mathbf{e}_1 - \mathbf{e}_2 \otimes \mathbf{e}_2$ the second derivative (5.50) results in

$$\delta\mathbf{F} : \partial_{\mathbf{F}\mathbf{F}}^2 \mathcal{P}(\mathbf{F}) : \delta\mathbf{F} = \left(-\frac{1}{n^2}\right)^k k n^2 (-2 + 3.2k),$$

which is negative for odd numbers $k \geq 1$. Inserting

$$\mathbf{F} = \operatorname{diag}(1, 2k, 1), \quad \delta\mathbf{F} = \boldsymbol{\eta} \otimes \boldsymbol{\zeta}, \quad \boldsymbol{\eta} = \boldsymbol{\zeta} = \mathbf{e}_1 \quad (5.54)$$

and $\tilde{\mathbf{K}} = \mathbf{e}_1 \otimes \mathbf{e}_1 - \mathbf{e}_2 \otimes \mathbf{e}_2$ into (5.50) we arrive at the second derivative

$$\delta\mathbf{F} : \partial_{\mathbf{F}\mathbf{F}}^2 \mathcal{P}(\mathbf{F}) : \delta\mathbf{F} = \frac{2(1-4k^2)^k}{(1-4k^2)} k \left(\frac{2(k-1)}{(1-4k^2)} + 1 \right),$$

which is negative for even numbers $k \geq 1$. Thus, the term (5.49) with $\tilde{\mathbf{K}} = \mathbf{P}_2$ is not elliptic and hence not polyconvex for $k \geq 1$.

i.d) For $\tilde{\mathbf{K}} = \mathbf{W}^2$, with $\mathbf{W} = \epsilon\mathbf{e}_1 = \mathbf{e}_2 \otimes \mathbf{e}_3 - \mathbf{e}_3 \otimes \mathbf{e}_2$, the invariant I_4^k has the form

$$I_4^k = (\operatorname{tr}[\mathbf{C}(\mathbf{e}_2 \otimes \mathbf{e}_3 - \mathbf{e}_3 \otimes \mathbf{e}_2)^2])^k = (\operatorname{tr}[\mathbf{C}(-\mathbf{e}_2 \otimes \mathbf{e}_2 - \mathbf{e}_3 \otimes \mathbf{e}_3)])^k.$$

Using $\tilde{\mathbf{K}} = \mathbf{W}^2$ and (5.52), where $n \in \mathbb{R}$, in (5.50) the second derivative of I_4^k reads

$$\delta\mathbf{F} : \partial_{\mathbf{F}\mathbf{F}}^2 \mathcal{P}(\mathbf{F}) : \delta\mathbf{F} = \frac{8kn^2}{5(5n^2+1)^2} (2k+5n^2-1) \left(-\frac{5n^2+1}{n^2} \right)^k,$$

which is negative for odd numbers $k \geq 1$. This proves the non-ellipticity of I_4^k with $\tilde{\mathbf{K}} = \mathbf{W}^2$ for odd numbers $k \geq 1$. Note that for even numbers $k \geq 1$ one can write

$$I_4^k = (\text{tr}[\mathbf{C}(-\mathbf{e}_2 \otimes \mathbf{e}_2 - \mathbf{e}_3 \otimes \mathbf{e}_3)])^k = (\text{tr}[\mathbf{C}(\mathbf{e}_2 \otimes \mathbf{e}_2 + \mathbf{e}_3 \otimes \mathbf{e}_3)])^k.$$

This term has the typical form of a linear convex combination of positive polyconvex terms, which is always polyconvex. More details are explained in part **iv)** of this section.

ii) The mixed invariant

$$I_5 = \text{tr}[\mathbf{C}^2 \tilde{\mathbf{K}}] = \text{tr}[\mathbf{F}^T \mathbf{F} \mathbf{F}^T \mathbf{F} \tilde{\mathbf{K}}] = \langle \mathbf{F}^T \mathbf{F}, \mathbf{F}^T \mathbf{F} \tilde{\mathbf{K}} \rangle \quad (5.55)$$

is in general not elliptic and hence non-quasiconvex.

Proof We obtain

$$\begin{aligned} \mathcal{P}(\mathbf{F}) &= \langle \mathbf{F}^T \mathbf{F}, \mathbf{F}^T \mathbf{F} \tilde{\mathbf{K}} \rangle \\ \partial_{\mathbf{F}} \mathcal{P}(\mathbf{F}) : \delta \mathbf{F} &= (\langle \delta \mathbf{F}^T \mathbf{F}, \mathbf{F}^T \mathbf{F} \tilde{\mathbf{K}} \rangle + \langle \mathbf{F}^T \delta \mathbf{F}, \mathbf{F}^T \mathbf{F} \tilde{\mathbf{K}} \rangle \\ &\quad + \langle \mathbf{F}^T \mathbf{F}, \delta \mathbf{F}^T \mathbf{F} \tilde{\mathbf{K}} \rangle + \langle \mathbf{F}^T \mathbf{F}, \mathbf{F}^T \delta \mathbf{F} \tilde{\mathbf{K}} \rangle) \\ \delta \mathbf{F} : \partial_{\mathbf{F} \mathbf{F}}^2 \mathcal{P}(\mathbf{F}) : \delta \mathbf{F} &= 2(\langle \delta \mathbf{F}^T \delta \mathbf{F}, \mathbf{F}^T \mathbf{F} \tilde{\mathbf{K}} \rangle + \langle \delta \mathbf{F}^T \mathbf{F}, \delta \mathbf{F}^T \mathbf{F} \tilde{\mathbf{K}} \rangle \\ &\quad + \langle \delta \mathbf{F}^T \mathbf{F}, \mathbf{F}^T \delta \mathbf{F} \tilde{\mathbf{K}} \rangle + \langle \mathbf{F}^T \delta \mathbf{F}, \delta \mathbf{F}^T \mathbf{F} \tilde{\mathbf{K}} \rangle \\ &\quad + \langle \mathbf{F}^T \delta \mathbf{F}, \mathbf{F}^T \delta \mathbf{F} \tilde{\mathbf{K}} \rangle + \langle \mathbf{F}^T \mathbf{F}, \delta \mathbf{F}^T \delta \mathbf{F} \tilde{\mathbf{K}} \rangle). \end{aligned} \quad (5.56)$$

ii.a) Considering $\tilde{\mathbf{K}} = \mathbf{a} \otimes \mathbf{a}$ the proof of non-ellipticity of I_5 is given in SCHRÖDER & NEFF [104].

ii.b) We take now $\tilde{\mathbf{K}} = \mathbf{P}_2', \mathbf{P}_2, \mathbf{W}^2$, introduced in (5.47), into account. Evaluating for these cases the second derivative (5.56)₃ with the following deformation gradient \mathbf{F} and incremental rank-one deformation gradient $\delta \mathbf{F}$

$$\mathbf{F} = \begin{bmatrix} 1 & 0 & 0 \\ 0 & 2 & 0 \\ 0 & 0 & 1/n \end{bmatrix}, \quad \delta \mathbf{F} = \boldsymbol{\eta} \otimes \boldsymbol{\zeta}, \quad \boldsymbol{\eta} = \begin{pmatrix} 0 \\ 0 \\ 1 \end{pmatrix}, \quad \boldsymbol{\zeta} = \frac{1}{\sqrt{3}} \begin{pmatrix} 1 \\ -1 \\ 1 \end{pmatrix}, \quad (5.57)$$

we notice that the Legendre-Hadamard condition is not satisfied:

$$\begin{aligned} \text{for } \tilde{\mathbf{K}} = \mathbf{P}_2' : \quad \delta \mathbf{F} : \partial_{\mathbf{F} \mathbf{F}}^2 \mathcal{P}(\mathbf{F}) : \delta \mathbf{F} &= -\frac{4(5n^2 + 1)}{3n^2} < 0, \\ \text{for } \tilde{\mathbf{K}} = \mathbf{P}_2 : \quad \delta \mathbf{F} : \partial_{\mathbf{F} \mathbf{F}}^2 \mathcal{P}(\mathbf{F}) : \delta \mathbf{F} &= -4 < 0, \\ \text{for } \tilde{\mathbf{K}} = \mathbf{W}^2 : \quad \delta \mathbf{F} : \partial_{\mathbf{F} \mathbf{F}}^2 \mathcal{P}(\mathbf{F}) : \delta \mathbf{F} &= -\frac{2(9 + 8n^2)}{3n^2} < 0. \end{aligned} \quad (5.58)$$

ii(alternative)) In the previous section we showed the convexity of $I_4^k = \text{tr}[\mathbf{C} \tilde{\mathbf{K}}]^k$ with $\tilde{\mathbf{K}} = \mathbf{a} \otimes \mathbf{a}$ w.r.t. \mathbf{F} . SCHRÖDER & NEFF [104] proposed, that in analogy to this the powers of

$$K_1 = \text{tr}[\text{Cof}[\mathbf{C}] \tilde{\mathbf{K}}] \quad (5.59)$$

with $\tilde{\mathbf{K}} = \mathbf{a} \otimes \mathbf{a}$ are also polyconvex. The Cayley-Hamilton theorem (4.3) for the argument tensor \mathbf{C} reads:

$$\mathbf{C}^3 - I_1 \mathbf{C}^2 + I_2 \mathbf{C} - I_3 \mathbf{1} = \mathbf{0} . \quad (5.60)$$

Multiplying (5.60) with $\mathbf{C}^{-1} \tilde{\mathbf{K}}$ from the left yields

$$\mathbf{C}^2 \tilde{\mathbf{K}} - I_1 \mathbf{C} \tilde{\mathbf{K}} + I_2 \tilde{\mathbf{K}} - I_3 \mathbf{C}^{-1} \tilde{\mathbf{K}} = \mathbf{0} . \quad (5.61)$$

Exploiting the symmetry of the right Cauchy-Green tensor,

$$I_3 \mathbf{C}^{-1} = I_3 \mathbf{C}^{-T} = \text{Cof} \mathbf{C} , \quad (5.62)$$

yields

$$\text{Cof}[\mathbf{C}] \tilde{\mathbf{K}} = \mathbf{C}^2 \tilde{\mathbf{K}} - I_1 \mathbf{C} \tilde{\mathbf{K}} + I_2 \tilde{\mathbf{K}} . \quad (5.63)$$

Taking the trace of the previous equation leads to

$$K_1 = I_5 - I_1 I_4 + I_2 \text{tr} \tilde{\mathbf{K}} . \quad (5.64)$$

To show the polyconvexity of this term we have to prove the convexity of

$$K_1^k = (\text{tr}[\text{Cof}[\mathbf{C}] \tilde{\mathbf{K}}])^k$$

for $k \geq 1$, w.r.t. $\text{Cof} \mathbf{F}$. The proof is given by (5.50) by replacing \mathbf{F} with $\text{Cof} \mathbf{F}$.

ii(alternative).a) The proof of convexity of K_1^k with $\tilde{\mathbf{K}} = \mathbf{M} = \mathbf{a} \otimes \mathbf{a}$ is analogous to **i.a)** by replacing \mathbf{F} with $\text{Cof} \mathbf{F}$, see SCHRÖDER & NEFF [104].

ii(alternative).b) The proof of non-ellipticity of K_1^k with $\tilde{\mathbf{K}} = \mathbf{P}'_2, \mathbf{P}_2, \mathbf{W}^2$ is analogous to **i.b), i.c), i.d)** by replacing \mathbf{F} with $\text{Cof} \mathbf{F}$.

iii) Furthermore, the product

$$I_1 I_4 = \text{tr}[\mathbf{C}] \text{tr}[\mathbf{C} \tilde{\mathbf{K}}] = \text{tr}[\mathbf{F}^T \mathbf{F}] \text{tr}[\mathbf{F}^T \mathbf{F} \tilde{\mathbf{K}}] = \|\mathbf{F}\|^2 \langle \mathbf{F}, \mathbf{F} \tilde{\mathbf{K}} \rangle$$

(5.65)

is often necessary for the representations of *complete* energy functions. However, the term $I_1 I_4$ does in general not fulfill the polyconvexity condition, because it is not elliptic and hence not quasiconvex.

Proof We obtain

$$\begin{aligned} \mathcal{P}(\mathbf{F}) &= \|\mathbf{F}\|^2 \langle \mathbf{F}, \mathbf{F} \tilde{\mathbf{K}} \rangle \\ \partial_{\mathbf{F}} \mathcal{P}(\mathbf{F}) : \delta \mathbf{F} &= 2 \langle \mathbf{F}, \delta \mathbf{F} \rangle \langle \mathbf{F}, \mathbf{F} \tilde{\mathbf{K}} \rangle + \|\mathbf{F}\|^2 (\langle \delta \mathbf{F}, \mathbf{F} \tilde{\mathbf{K}} \rangle + \langle \delta \mathbf{F} \tilde{\mathbf{K}}, \mathbf{F} \rangle) \\ \delta \mathbf{F} : \partial_{\mathbf{F} \mathbf{F}}^2 \mathcal{P}(\mathbf{F}) : \delta \mathbf{F} &= 2 (\|\delta \mathbf{F}\|^2 \langle \mathbf{F}, \mathbf{F} \tilde{\mathbf{K}} \rangle + 2 \langle \delta \mathbf{F}, \mathbf{F} \rangle (\langle \delta \mathbf{F}, \mathbf{F} \tilde{\mathbf{K}} \rangle + \langle \delta \mathbf{F} \tilde{\mathbf{K}}, \mathbf{F} \rangle) \\ &\quad + \|\mathbf{F}\|^2 \langle \delta \mathbf{F}, \delta \mathbf{F} \tilde{\mathbf{K}} \rangle) . \end{aligned} \quad (5.66)$$

This expression is in general non-positive, which excludes convexity. However, it is possible to show the non-ellipticity as well.

iii.a) The proof of non-ellipticity of $I_1 I_4$ with $\tilde{\mathbf{K}} = \mathbf{a} \otimes \mathbf{a}$ is first given in SCHRÖDER & NEFF [104].

iii.b) For the proof of non-ellipticity of $I_1 I_4$ with $\tilde{\mathbf{K}} = \mathbf{P}'_2, \mathbf{P}_2, \mathbf{W}^2$, given in (5.47), we choose (5.52) and insert these relations into (5.66)₃. Then we observe that the Legendre-Hadamard condition is violated:

$$\begin{aligned} \text{for } \tilde{\mathbf{K}} = \mathbf{P}'_2 : \quad \delta \mathbf{F} : \partial_{\mathbf{F}\mathbf{F}}^2 \mathcal{P}(\mathbf{F}) : \delta \mathbf{F} &= -\frac{4(7n^2 + 6)}{5n^2} < 0, \\ \text{for } \tilde{\mathbf{K}} = \mathbf{P}_2 : \quad \delta \mathbf{F} : \partial_{\mathbf{F}\mathbf{F}}^2 \mathcal{P}(\mathbf{F}) : \delta \mathbf{F} &= -\frac{12(3n^2 + 4)}{5n^2} < 0, \\ \text{for } \tilde{\mathbf{K}} = \mathbf{W}^2 : \quad \delta \mathbf{F} : \partial_{\mathbf{F}\mathbf{F}}^2 \mathcal{P}(\mathbf{F}) : \delta \mathbf{F} &= -\frac{2(49n^2 + 25)}{5n^2} < 0. \end{aligned} \quad (5.67)$$

iv) For representations of *complete* anisotropic energy functions we also need functions which include multiplicative terms in the mixed invariants with respect to different structural tensors. However, functions of the type

$$I_{4_1}^{poly} I_{4_2}^{poly} = \text{tr}[\mathbf{C} \tilde{\mathbf{K}}_1] \text{tr}[\mathbf{C} \tilde{\mathbf{K}}_2], \quad (5.68)$$

where even $I_{4_1}^{poly} = \text{tr}[\mathbf{C} \tilde{\mathbf{K}}_1]$ and $I_{4_2}^{poly} = \text{tr}[\mathbf{C} \tilde{\mathbf{K}}_2]$ are individual polyconvex functions, are in general not polyconvex, cf. Remark B.8 in SCHRÖDER & NEFF [104]. To overcome this problem SCHRÖDER & NEFF [104] proposed to use powers of linear convex combinations of positive polyconvex functions

$$P_1(X, Y) \geq 0 \quad \text{and} \quad P_2(X, Y) \geq 0.$$

In this case functions of the form

$$P := [\lambda P_1(X, Y) + (1 - \lambda) P_2(X, Y)]^q, \quad \lambda \in [0, 1] \quad \text{and} \quad q \in \mathbb{N}_+ \quad (5.69)$$

are polyconvex. With this construction we are able to design a variety of free energy terms, which involve multiplicative coupled terms in the mixed invariants associated to different structural tensors. For instance

$$[\lambda I_{4_1}^{poly} + (1 - \lambda) I_{4_2}^{poly}]^2 \quad \text{with } \lambda \in [0, 1] \quad (5.70)$$

leads to the invariant representation

$$\lambda^2 (I_{4_1}^{poly})^2 + 2\lambda(1 - \lambda) I_{4_1}^{poly} I_{4_2}^{poly} + (1 - \lambda)^2 (I_{4_2}^{poly})^2 \quad \text{with } \lambda \in [0, 1], \quad (5.71)$$

which has a multiplicative term in the mixed invariants of the traces of the product of $(\mathbf{C}, \tilde{\mathbf{K}}_1)$ and $(\mathbf{C}, \tilde{\mathbf{K}}_2)$. A possible set of such kind of functions can be computed by

$$\begin{aligned} &\{ \lambda I_{4_1}^{poly} + (1 - \lambda) I_{4_2}^{poly} \}^q, \\ &\{ \lambda I_{5_1}^{poly} + (1 - \lambda) I_{5_2}^{poly} \}^q, \\ &\{ \lambda I_{4_i}^{poly} + (1 - \lambda) I_{5_i}^{poly} \}^q, \quad i = 1, 2 \end{aligned} \quad (5.72)$$

with $\lambda \in [0, 1]$, $q \in \mathbb{N}_+$, and the individual polyconvex functions $I_{5_1}^{poly} = \text{tr}[\text{Cof}[\mathbf{C}]\tilde{\mathbf{K}}_1]$ and $I_{5_2}^{poly} = \text{tr}[\text{Cof}[\mathbf{C}]\tilde{\mathbf{K}}_2]$.

Remark 4. For the description of transversely isotropic as well as orthotropic materials SCHRÖDER & NEFF [104] were able to construct polyconvex invariant functions in terms of the classical structural tensor (4.26). The *set of polyconvex invariants* for transverse isotropy is given by

$$\mathcal{G}_{12} : \quad \mathcal{F}_{poly}^{ti} := \{I_1, I_2, I_3, I_4, K_1\}, \quad (5.73)$$

with $\mathbf{K} = \mathbf{a} \otimes \mathbf{a}$. In the orthotropic case our *set of polyconvex invariants* reads

$$\mathcal{G}_3 : \quad \mathcal{F}_{poly}^o := \{I_1, I_2, I_3, I_{4_1}, K_{1_1}, I_{4_2}, K_{1_2}\}, \quad (5.74)$$

with the mixed invariants

$$I_{4_1} = \text{tr}[\mathbf{C}\mathbf{M}_1], \quad K_{1_1} = \text{tr}[\text{Cof}[\mathbf{C}]\mathbf{M}_1], \quad I_{4_2} = \text{tr}[\mathbf{C}\mathbf{M}_2], \quad K_{1_2} = \text{tr}[\text{Cof}[\mathbf{C}]\mathbf{M}_2]. \quad (5.75)$$

The problem of generating polyconvex multiplicative terms for *complete* orthotropic energy functions can be overcome, see **iv**).

However, in section 5.7.1 we noticed that the formulation of polyconvex invariants based on Zheng and Spencer's structural tensors, respectively, especially for the triclinic and monoclinic case, failed.

5.7.2 Invariants in Terms of Fourth-Order Structural Tensors. The sets of invariants in terms of fourth-order structural tensors are mainly based on the mixed invariants

$$\text{i) } I_8 = \mathbf{C} : \mathbb{P} : \mathbf{C}, \quad \text{ii) } I_9 = (\mathbb{P} : \mathbf{C})^2 : \mathbf{1}, \quad (5.76)$$

where \mathbb{P} denotes the underlying fourth-order structural tensor, see (4.46). We analyze the invariants in terms of Zheng and Spencer's and Xiao's fourth-order structural tensors of Table 4.2.^{14.)} The sets of invariants with Xiao's structural tensors are specified in APEL [3]. The invariant I_8 appears in the tetragonal and trigonal sets of bilinear invariants depending on Zheng and Spencer's structural tensors as well as in the tetragonal sets in terms of Xiao's structural tensor, i.e., we consider I_8 with

$$\begin{aligned} \mathbb{P} = \mathbb{P}_4 &= \mathbf{e}_1^{(4)} - \mathbf{e}_1^{(2)} \otimes \mathbf{e}_2^{(2)} - \mathbf{e}_2^{(2)} \otimes \mathbf{e}_1^{(2)} + \mathbf{e}_2^{(4)} - 4\mathbf{e}_1 \otimes \mathbf{e}_2 \otimes \mathbf{e}_1 \otimes \mathbf{e}_2, \\ \mathbb{P} = \mathbf{e}_3 \otimes \mathbf{P}'_3 &= \mathbf{e}_3 \otimes \mathbf{e}_1 \otimes (\mathbf{e}_1 \otimes \mathbf{e}_2 + \mathbf{e}_2 \otimes \mathbf{e}_1) + \mathbf{e}_3 \otimes \mathbf{e}_2 \otimes (\mathbf{e}_1 \otimes \mathbf{e}_1 - \mathbf{e}_2 \otimes \mathbf{e}_2), \\ \mathbb{P} &= \mathbf{e}_1^{(4)} + \mathbf{e}_2^{(4)}. \end{aligned} \quad (5.77)$$

The invariant I_9 is part of the cubic *set of bilinear invariants* with Zheng and Spencer's structural tensor and of the trigonal set governed by Xiao's structural tensor, i.e., we

^{14.)}Since the structure of the fourth-order structural tensors proposed in [142] is similar to the structure of the structural tensors given in [140] and [146], we neglect them in our analysis.

check I_9 with

$$\begin{aligned}\mathbb{P}=\Theta &= \mathbf{e}_1^{(4)} + \mathbf{e}_2^{(4)} + \mathbf{e}_3^{(4)}, \\ \mathbb{P} &= \sum_{i=1}^3 \epsilon \mathbf{n}_i \otimes \mathbf{n}_i \otimes \mathbf{n}_i,\end{aligned}\tag{5.78}$$

where the vectors are defined as

$$\mathbf{n}_1 = \mathbf{e}_1, \mathbf{n}_2 = -\frac{1}{2}\mathbf{e}_1 + \frac{\sqrt{3}}{2}\mathbf{e}_2, \mathbf{n}_3 = -\frac{1}{2}\mathbf{e}_1 - \frac{\sqrt{3}}{2}\mathbf{e}_2.$$

i) The invariant I_8 depends on the deformation gradient as follows

$$I_8 = \mathbf{C} : \mathbb{P} : \mathbf{C} = \mathbf{F}^T \mathbf{F} : \mathbb{P} : \mathbf{F}^T \mathbf{F}.\tag{5.79}$$

Proof We get

$$\begin{aligned}\mathcal{P}(\mathbf{F}) &= \mathbf{F}^T \mathbf{F} : \mathbb{P} : \mathbf{F}^T \mathbf{F} \\ \partial_{\mathbf{F}} \mathcal{P}(\mathbf{F}) : \delta \mathbf{F} &= \delta \mathbf{F}^T \mathbf{F} : \mathbb{P} : \mathbf{F}^T \mathbf{F} + \mathbf{F}^T \delta \mathbf{F} : \mathbb{P} : \mathbf{F}^T \mathbf{F} \\ &\quad + \mathbf{F}^T \mathbf{F} : \mathbb{P} : \delta \mathbf{F}^T \mathbf{F} + \mathbf{F}^T \mathbf{F} : \mathbb{P} : \mathbf{F}^T \delta \mathbf{F} \\ \delta \mathbf{F} : \partial_{\mathbf{F}}^2 \mathcal{P}(\mathbf{F}) : \delta \mathbf{F} &= 2(\delta \mathbf{F}^T \delta \mathbf{F} : \mathbb{P} : \mathbf{F}^T \mathbf{F} + \delta \mathbf{F}^T \mathbf{F} : \mathbb{P} : \delta \mathbf{F}^T \mathbf{F} \\ &\quad + \delta \mathbf{F}^T \mathbf{F} : \mathbb{P} : \mathbf{F}^T \delta \mathbf{F} + \mathbf{F}^T \delta \mathbf{F} : \mathbb{P} : \delta \mathbf{F}^T \mathbf{F} \\ &\quad + \mathbf{F}^T \delta \mathbf{F} : \mathbb{P} : \mathbf{F}^T \delta \mathbf{F} + \mathbf{F}^T \mathbf{F} : \mathbb{P} : \delta \mathbf{F}^T \delta \mathbf{F})\end{aligned}\tag{5.80}$$

i.a) For $\mathbb{P} = \mathbb{P}_4$ the term (5.79) is not elliptic. To show the non-ellipticity we calculate the second derivative (5.80)₃ with

$$\mathbf{F} = \begin{bmatrix} \frac{1}{\sqrt{2}} & \frac{1}{\sqrt{2}} & 0 \\ \frac{1}{\sqrt{2}} & \frac{1}{\sqrt{2}} & 0 \\ 0 & 0 & \frac{1}{n} \end{bmatrix}, \delta \mathbf{F} = \boldsymbol{\eta} \otimes \boldsymbol{\zeta}, \boldsymbol{\eta} = \begin{pmatrix} 1 \\ 1 \\ 0 \end{pmatrix}, \boldsymbol{\zeta} = \begin{pmatrix} \frac{1}{\sqrt{2}} \\ \frac{1}{\sqrt{2}} \\ 0 \end{pmatrix}.\tag{5.81}$$

This choice yields the relations

$$\delta \mathbf{F}^T \mathbf{F} = \delta \mathbf{F}^T \delta \mathbf{F} = \mathbf{F}^T \delta \mathbf{F}\tag{5.82}$$

and therewith a negative second derivative

$$\begin{aligned}\delta \mathbf{F} : \partial_{\mathbf{F}}^2 \mathcal{P}(\mathbf{F}) : \delta \mathbf{F} &= 2 \delta \mathbf{F}^T \delta \mathbf{F} : \mathbb{P}_4 : \mathbf{F}^T \mathbf{F} + 2 \mathbf{F}^T \mathbf{F} : \mathbb{P}_4 : \delta \mathbf{F}^T \delta \mathbf{F} \\ &\quad + 8 \delta \mathbf{F}^T \mathbf{F} : \mathbb{P}_4 : \delta \mathbf{F}^T \mathbf{F} = 2(-4) + 2(-4) + 8(-4) < 0.\end{aligned}$$

i.b) For $\mathbb{P} = \mathbf{e}_3 \otimes \mathbf{P}'_3$ the function (5.79) is not elliptic, hence not polyconvex. We analyze the second derivative (5.80)₃ while setting

$$\mathbf{F} = \begin{bmatrix} 1/n & 0 & 0 \\ 0 & 2 & 1 \\ 0 & 1 & 2 \end{bmatrix}, \delta \mathbf{F} = \boldsymbol{\eta} \otimes \boldsymbol{\zeta}, \boldsymbol{\eta} = \begin{pmatrix} 0 \\ 1 \\ 1 \end{pmatrix}, \boldsymbol{\zeta} = \begin{pmatrix} 0 \\ \frac{1}{\sqrt{2}} \\ \frac{1}{\sqrt{2}} \end{pmatrix},\tag{5.83}$$

yielding the relation

$$\mathbf{F}^T \delta \mathbf{F} = \delta \mathbf{F}^T \mathbf{F}. \quad (5.84)$$

The result of the analysis is

$$\begin{aligned} \mathcal{P}(\mathbf{F}) = 2 \delta \mathbf{F}^T \delta \mathbf{F} : (\mathbf{e}_3 \otimes \mathbf{P}'_3) : \mathbf{F}^T \mathbf{F} + 2 \mathbf{F}^T \mathbf{F} : (\mathbf{e}_3 \otimes \mathbf{P}'_3) : \delta \mathbf{F}^T \delta \mathbf{F} \\ + 8 \delta \mathbf{F}^T \mathbf{F} : (\mathbf{e}_3 \otimes \mathbf{P}'_3) : \delta \mathbf{F}^T \mathbf{F} = -\frac{2(27n^2 - 1)}{n^2}, \end{aligned} \quad (5.85)$$

which is negative for $n^2 > 1/27$.

i.c) For $\mathbb{P} = \mathbf{e}_1^{(4)} + \mathbf{e}_2^{(4)}$ we obtain a positive second derivative of I_8 , i.e., (5.80)₃:

$$\begin{aligned} \delta \mathbf{F} : \partial_{\mathbf{F}\mathbf{F}}^2 \mathcal{P}(\mathbf{F}) : \delta \mathbf{F} = 4 \|\delta \mathbf{F} \mathbf{e}_1\|^2 \|\mathbf{F} \mathbf{e}_1\|^2 \|\delta \mathbf{F} \mathbf{e}_2\|^2 \|\mathbf{F} \mathbf{e}_2\|^2 \\ + 8 \langle \delta \mathbf{F} \mathbf{e}_1, \mathbf{F} \mathbf{e}_1 \rangle^2 \langle \delta \mathbf{F} \mathbf{e}_2, \mathbf{F} \mathbf{e}_2 \rangle^2 > 0. \end{aligned} \quad (5.86)$$

This shows the convexity of I_8 in terms of $\mathbb{P} = \mathbf{e}_1^{(4)} + \mathbf{e}_2^{(4)}$ w.r.t. \mathbf{F} .

ii) The second invariant under consideration has in terms of the deformation gradient the form

$$I_9 = (\mathbb{P} : \mathbf{C})^2 : \mathbf{1} = (\mathbb{P} : \mathbf{F}^T \mathbf{F})^2 : \mathbf{1}. \quad (5.87)$$

ii.a) Considering $\mathbb{P} = \Theta$ we can reformulate the invariant:

$$(\mathbb{P} : \mathbf{C})^2 : \mathbf{1} = (\text{tr}[\mathbf{C}\mathbf{M}_1])^2 + (\text{tr}[\mathbf{C}\mathbf{M}_2])^2 + (\text{tr}[\mathbf{C}\mathbf{M}_3])^2, \quad (5.88)$$

with \mathbf{M}_i , $i = 1, 2, 3$ introduced in (4.28). The individual functions appearing in (5.88) are convex w.r.t. \mathbf{F} , see (5.51). Hence, the function (5.79) is convex.

ii.b) Evaluating I_9 with $\mathbb{P} = \sum_{i=1}^3 \epsilon \mathbf{n}_i \otimes \mathbf{n}_i \otimes \mathbf{n}_i$ ^{15.)} the invariant can be reformulated to

$$\begin{aligned} (\mathbb{P} : \mathbf{C})^2 : \mathbf{1} &= \sum_{i=1}^3 \sum_{j=1}^3 [\text{tr}[\mathbf{C}\mathbf{n}_i \otimes \mathbf{n}_i] \text{tr}[\mathbf{C}\mathbf{n}_j \otimes \mathbf{n}_j] \text{tr}[\mathbf{W}_i \mathbf{W}_j]] \\ &= \sum_{i=1}^3 \sum_{j=1}^3 [\|\mathbf{F}\mathbf{n}_i\|^2 \|\mathbf{F}\mathbf{n}_j\|^2 \text{tr}[\mathbf{W}_i \mathbf{W}_j]]. \end{aligned} \quad (5.89)$$

With $\mathbf{W}_i = \epsilon \mathbf{n}_i$ we have $\text{tr}[\mathbf{W}_i^2] = -2$, $\text{tr}[\mathbf{W}_i \mathbf{W}_j] = 1$, $i \neq j$ and obtain

$$\mathcal{P}(\mathbf{F}) := (\mathbb{P} : \mathbf{C})^2 : \mathbf{1} = -2 \sum_{i=1}^3 \|\mathbf{F}\mathbf{n}_i\|^4 + \sum_{i=1}^3 \sum_{j=1}^3 \|\mathbf{F}\mathbf{n}_i\|^2 \|\mathbf{F}\mathbf{n}_j\|^2, \quad i \neq j. \quad (5.90)$$

The second derivative of this term is given by

$$\begin{aligned} \delta \mathbf{F} : \partial_{\mathbf{F}\mathbf{F}}^2 \mathcal{P}(\mathbf{F}) : \delta \mathbf{F} &= -8 \sum_{i=1}^3 \|\delta \mathbf{F} \mathbf{n}_i\|^2 \|\mathbf{F} \mathbf{n}_i\|^2 + 2 \sum_{i=1}^3 \sum_{j=1}^3 [\|\delta \mathbf{F} \mathbf{n}_i\|^2 \|\mathbf{F} \mathbf{n}_j\|^2 \\ &\quad + 8 \langle \mathbf{F} \mathbf{n}_i, \delta \mathbf{F} \mathbf{n}_i \rangle \langle \mathbf{F} \mathbf{n}_j, \delta \mathbf{F} \mathbf{n}_j \rangle], \quad i \neq j. \end{aligned} \quad (5.91)$$

^{15.)} $\mathbf{n}_1 = \mathbf{e}_1$, $\mathbf{n}_2 = -1/2\mathbf{e}_1 + \sqrt{3}/2\mathbf{e}_2$, $\mathbf{n}_3 = -1/2\mathbf{e}_1 - \sqrt{3}/2\mathbf{e}_2$, cf. [140], [3].

which reduces to

$$\delta \mathbf{F} : \partial_{\mathbf{F}\mathbf{F}}^2 \mathcal{P}(\mathbf{F}) : \delta \mathbf{F} = -9 < 0 ,$$

if we consider $\delta \mathbf{F} = \boldsymbol{\eta} \otimes \boldsymbol{\zeta}$ with $\boldsymbol{\eta} = (0, 1, 0)^T$, $\boldsymbol{\zeta} = (-1, 0, 0)^T$ and $\mathbf{F} = \mathbf{1}$. This proves the non-ellipticity and hence, the non-polyconvexity of the invariant I_9 in terms of Zheng and Spencer's trigonal structural tensor $\mathbb{P} = \sum_{i=1}^3 \boldsymbol{\epsilon} \mathbf{n}_i \otimes \mathbf{n}_i \otimes \mathbf{n}_i$.

Remark 5. In KAMBOUCHEV, FERNANDEZ & RADOVITZKY [66] polyconvex coordinate-invariant function depending on the cubic fourth-order structural tensor $\boldsymbol{\Theta}$ (Table 4.2) are provided. The set of polyconvex invariants for cubic symmetry has the elements in terms of \mathbf{C}

$$\mathcal{G}_7 : \quad \mathcal{F}_{poly}^c := \{I_1, I_2, I_3, I_9\} , \quad (5.92)$$

with $\mathbb{P} = \boldsymbol{\Theta}$, see **ii.a.** Moreover, the convexity of the tetragonal mixed invariants I_8 in terms of Xiao's tetragonal structural tensor $\mathbb{P} = \mathbf{e}_1^{(4)} + \mathbf{e}_2^{(4)}$ with respect to the deformation gradient could be shown in **i.c.** We have investigated therefore further mixed invariants in terms of Xiao's tetragonal structural tensor. If the reader is interested in detailed results we refer to the Appendix H. The invariants I_8 and I_9 in terms of the remaining structural tensors are all non-elliptic and can not be represented by useful alternative expressions. Thus, since we are interested in a unified approach for the representation of anisotropic finite elasticity, neither the introduced tetragonal sets nor the trigonal sets of bilinear invariants in the previous section seem to be useful for us.

Hence, the fundamental idea proposed in the next chapter is the introduction of a crystallographically motivated approach for the construction of polyconvex invariant functions.

5.8 Notes on Polyconvex Isochoric-Volumetric Decoupled Energy Functions.

For the description of quasi-incompressible anisotropic material behavior the energy function is classically assumed to be additively decomposed into a volumetric part and an isochoric part, i.e.,

$$\psi(\mathbf{C}) = \psi^{vol}(J) + \psi^{isoch}(\tilde{\mathbf{C}}) , \quad (5.93)$$

where $\tilde{\mathbf{C}} := J^{-2/3} \mathbf{C}$ with $\det \tilde{\mathbf{C}} = 1$ denotes the isochoric part of the right Cauchy-Green tensor, cf. e.g. SIMO [112], WRIGGERS [138].

i) Volumetric polyconvex free energy functions $\psi^{vol}(J)$ in terms of $\det \mathbf{C}$ and $J = \det \mathbf{F}$, respectively, are e.g.

$$\begin{aligned} \mathbf{F} &\mapsto \det \mathbf{C} \\ \mathbf{F} &\mapsto -\ln(\sqrt{\det \mathbf{C}}) = -\ln(\det \mathbf{F}) \\ \mathbf{F} &\mapsto (\det \mathbf{C} + 1/\det \mathbf{C}) \\ \mathbf{F} &\mapsto (\det \mathbf{C} - 1)^2 \\ \mathbf{F} &\mapsto 1/\det \mathbf{C} . \end{aligned} \quad (5.94)$$

For instance, the second term is polyconvex, because $\mathcal{P}(J) = -\ln(\det \mathbf{F}) = -\ln(J)$ is convex w.r.t. to its argument J , i.e., we have the second derivative of $\mathcal{P}(J)$ with respect

to J

$$\partial_{JJ}^2 \mathcal{P}(J) = \frac{1}{J^2} > 0. \quad (5.95)$$

Further examples for volumetric polyconvex free energy terms, which are convex in $\det \mathbf{F}$ on the natural domain of definition $\det \mathbf{F} > 0$, are (cf. HARTMANN & NEFF [57])

$$\begin{aligned} \mathbf{F} &\mapsto \left(\det \mathbf{C} + \frac{1}{\det \mathbf{C}} - 2 \right)^k && \text{with } k \geq 1 \\ \mathbf{F} &\mapsto \left((\det \mathbf{C})^p + \frac{1}{(\det \mathbf{C})^p} - 2 \right)^k && \text{with } p \geq k \geq 1, p \geq \frac{1}{2} \\ \mathbf{F} &\mapsto (\sqrt{\det \mathbf{C}} - 1)^k && \text{with } k \geq 1 \\ \mathbf{F} &\mapsto (\det \mathbf{C} - \ln[\det \mathbf{C}]) \\ \mathbf{F} &\mapsto (\det \mathbf{C} - \ln[\det \mathbf{C}] + (\ln[\det \mathbf{C}])^2). \end{aligned} \quad (5.96)$$

Note, that the latter terms are each polyconvex and have a stress-free reference configuration.

ii) For the derivation of isochoric polyconvex functions $\psi^{isoch}(\tilde{\mathbf{C}})$ we first observe the polyconvex general term

$$\boxed{\frac{I_1^{p/2}}{I_3^{\bar{\alpha}/2}} = \frac{\|\mathbf{F}\|^p}{(\det \mathbf{F})^{\bar{\alpha}}} = J^{-\bar{\alpha}} \|\mathbf{F}\|^p \quad \text{for } p, \bar{\alpha}, J > 0 \quad \text{and} \quad (p-1) \geq \bar{\alpha}.} \quad (5.97)$$

For the proof see Lemma C.1 in SCHRÖDER & NEFF [104]. Analogously, we notice that the terms

$$\boxed{\frac{I_2^{p/2}}{I_3^{\bar{\alpha}/2}} = \frac{\|\text{Cof} \mathbf{F}\|^p}{(\det \mathbf{F})^{\bar{\alpha}}} = J^{-\bar{\alpha}} \|\text{Cof} \mathbf{F}\|^p \quad \text{for } p, \bar{\alpha}, J > 0 \quad \text{and} \quad (p-1) \geq \bar{\alpha}} \quad (5.98)$$

are also polyconvex. Finally, polyconvex isochoric terms which can be derived by (5.97) and (5.98) are

$$\text{tr}[\tilde{\mathbf{C}}]^k = \frac{I_1^k}{J^{2/3k}}, \quad \text{tr}[\text{Cof} \tilde{\mathbf{C}}]^{2k} = \frac{I_2^{2k}}{J^{8/3k}}, \quad k \geq 1. \quad (5.99)$$

Unfortunately, the purely isochoric term

$$\text{tr}[\text{Cof} \tilde{\mathbf{C}}] = I_3^{1/3} \text{tr}[\mathbf{C}^{-1}] \quad (5.100)$$

is not polyconvex, cf. SCHRÖDER & NEFF [104]. The following polyconvex isochoric terms

lead to a stress-free natural state, see HARTMANN & NEFF [57]

$$\begin{aligned}
\mathbf{F} &\mapsto \left(\frac{\|\mathbf{F}\|^{2k}}{(\det \mathbf{F})^{\frac{2k}{3}}} - 3^k \right)^i && \text{with } i \geq 1, k \geq 1 \\
\mathbf{F} &\mapsto \left(\frac{\|\text{Cof} \mathbf{F}\|^{3k}}{(\det \mathbf{F})^{2k}} - (3\sqrt{3})^k \right)^j && \text{with } j \geq 1, k \geq 1 \\
\mathbf{F} &\mapsto \exp \left[\left(\frac{\|\mathbf{F}\|^{2k}}{(\det \mathbf{F})^{\frac{2k}{3}}} - 3^k \right)^i \right] - 1 && \text{with } i \geq 1, k \geq 1 \\
\mathbf{F} &\mapsto \exp \left[\left(\frac{\|\text{Cof} \mathbf{F}\|^{3k}}{(\det \mathbf{F})^{2k}} - (3\sqrt{3})^k \right)^j \right] - 1 && \text{with } j \geq 1, k \geq 1 .
\end{aligned} \tag{5.101}$$

We refer to further remarks on isochoric-volumetric decouplings in DACOROGNA [41].

5.9 Specific Material Models.

Let us report some important classes of material models and point out if they satisfy the polyconvexity condition. An important class for the description of isotropic material behavior in finite elasticity are the Ogden-type materials, OGDEN [88], given by

$$\psi = \sum_{i=1}^m \alpha_i \|\mathbf{F}\|^{\gamma_i} + \sum_{i=1}^n \beta_i \|\text{Cof} \mathbf{F}\|^{\delta_i} + \Gamma(\det \mathbf{F}), \tag{5.102}$$

with the material parameter restrictions

$$\alpha_i > 0, \beta_i > 0, \quad \gamma_i \geq 2, \delta_i \geq 2, \tag{5.103}$$

and the property

$$\Gamma(\det \mathbf{F}) \rightarrow +\infty \quad \text{as} \quad \det \mathbf{F} \rightarrow 0^+, \tag{5.104}$$

cf. CIARLET [38]. Furthermore, the equation (5.102) satisfies the coercivity condition (5.4) with $\alpha > 0$, $p = \max \gamma_i$, $q = \max \delta_i$. Ensuring the convexity of the third function $\Gamma(\det \mathbf{F})$ with respect to its argument $(\det \mathbf{F})$ the polyconvexity of (5.102) is given. As special cases of Ogden-type models we enumerate the polyconvex compressible Mooney-Rivlin model, CIARLET & GEYMONAT [39], and the polyconvex compressible Neo-Hookean material according to BLATZ [26], which are both specified in the sequel.

5.9.1 Compressible Mooney-Rivlin Material Model. The compressible Mooney-Rivlin model has the form

$$\psi^{iso} = \alpha_1 \text{tr} [\mathbf{C}] + \alpha_2 \text{tr} [\text{Cof} [\mathbf{C}]] + \Gamma(J) = \alpha_1 I_1 + \alpha_2 I_2 + \Gamma(J), \tag{5.105}$$

with $J = \det \mathbf{F}$, $\alpha_1 > 0, \alpha_2 > 0$ and

$$\Gamma(\det \mathbf{F}) = \delta_1 J^2 - \delta_2 \ln(J) = \delta_1 I_3 - \delta_2 \ln(\sqrt{I_3}), \quad \delta_1 > 0, \delta_2 > 0. \tag{5.106}$$

The first and second derivatives of the polyconvex base functions (4.10) with respect to the right Cauchy-Green tensor can be found in the Appendix F. The second Piola-Kirchhoff stresses are

$$\begin{aligned}\mathbf{S}^{iso} &= 2 \left[(\alpha_1 + \alpha_2 I_1) \mathbf{1} - \alpha_2 \mathbf{C} + \left(\delta_1 I_3 - \frac{\delta_2}{2} \right) \mathbf{C}^{-1} \right] \\ &= (2 \alpha_1 + 2 \alpha_2 I_1) \mathbf{1} - 2 \alpha_2 \mathbf{C} + (2 \delta_1 - \delta_2 / I_3) \text{Cof} \mathbf{C} .\end{aligned}\quad (5.107)$$

Evaluating the condition of a stress-free reference configuration at $\mathbf{C} = \mathbf{1}$, i.e.,

$$\mathbf{S}(\mathbf{C} = \mathbf{1}) = \mathbf{0} ,$$

with

$$I_1(\mathbf{C} = \mathbf{1}) = I_2(\mathbf{C} = \mathbf{1}) = 3, \quad I_3(\mathbf{C} = \mathbf{1}) = 1 , \quad (5.108)$$

gives a dependent material parameter $\delta_2 \in \mathbb{R}_+$, i.e.,

$$\begin{aligned}\mathbf{S}^{iso}(\mathbf{C} = \mathbf{1}) = \mathbf{0} &\Rightarrow 2 \left(\alpha_1 + 3\alpha_2 - \alpha_2 + \delta_1 - \frac{\delta_2}{2} \right) \mathbf{1} = \mathbf{0} \\ &\Rightarrow \delta_2 = 2\alpha_1 + 4\alpha_2 + 2\delta_1 .\end{aligned}\quad (5.109)$$

The associated Lagrangian moduli are computed with (4.14) to

$$\begin{aligned}\mathbb{C}^{iso} &= 4 \left[\frac{\delta_2}{2 I_3^2} \text{Cof} \mathbf{C} \otimes \text{Cof} \mathbf{C} + \alpha_2 [\mathbf{1} \otimes \mathbf{1} - \mathbf{1} \boxtimes \mathbf{1}] \right. \\ &\quad \left. + \left(\delta_1 - \frac{\delta_2}{2 I_3} \right) I_3 [\mathbf{C}^{-1} \otimes \mathbf{C}^{-1} - \mathbf{C}^{-1} \boxtimes \mathbf{C}^{-1}] \right] \\ &= 4 \delta_1 I_3 \mathbf{C}^{-1} \otimes \mathbf{C}^{-1} + 4 \alpha_2 [\mathbf{1} \otimes \mathbf{1} - \mathbf{1} \boxtimes \mathbf{1}] \\ &\quad + (2 \delta_2 - 4 \delta_1 I_3) \mathbf{C}^{-1} \boxtimes \mathbf{C}^{-1} .\end{aligned}\quad (5.110)$$

In the unloaded reference placement the moduli (5.110) appears as

$$\mathbb{C}^{iso}(\mathbf{C} = \mathbf{1}) = (4 \delta_1 + 4 \alpha_2) \mathbf{1} \otimes \mathbf{1} + (2 \delta_2 - 4 \delta_1 - 4 \alpha_2) \mathbf{1} \boxtimes \mathbf{1}, \quad (5.111)$$

whose index arrangement in Voigt notation is identical to the classical isotropic elasticity tensor given by

$$\mathbb{C}^{iso(V)} = \begin{bmatrix} \mathbb{C}_{1111} & \mathbb{C}_{1122} & \mathbb{C}_{1122} & 0 & 0 & 0 \\ \mathbb{C}_{1122} & \mathbb{C}_{1111} & \mathbb{C}_{1122} & 0 & 0 & 0 \\ \mathbb{C}_{1122} & \mathbb{C}_{1122} & \mathbb{C}_{1111} & 0 & 0 & 0 \\ 0 & 0 & 0 & \frac{1}{2}(\mathbb{C}_{1111} - \mathbb{C}_{1122}) & 0 & 0 \\ 0 & 0 & 0 & 0 & \frac{1}{2}(\mathbb{C}_{1111} - \mathbb{C}_{1122}) & 0 \\ 0 & 0 & 0 & 0 & 0 & \frac{1}{2}(\mathbb{C}_{1111} - \mathbb{C}_{1122}) \end{bmatrix} .$$

The relations between the Ogden-parameters and the isotropic moduli in the natural state are

$$4\delta_1 + 4\alpha_2 = \mathbb{C}_{1122} \quad \text{and} \quad 2\delta_2 = \mathbb{C}_{1111} . \quad (5.112)$$

The solution of the three equations (5.109) and (5.112) for the four material parameters $(\delta_1, \delta_2, \alpha_1, \alpha_2)$ is

$$\left. \begin{aligned} \alpha_1 &:= [\mathbb{C}_{1111} + (\xi - 2)\mathbb{C}_{1122}]/4 \\ \alpha_2 &:= (1 - \xi) \mathbb{C}_{1122}/4 \\ \delta_1 &:= \xi \mathbb{C}_{1122}/4 \\ \delta_2 &:= \mathbb{C}_{1111}/2 \end{aligned} \right\} \quad \text{with } \xi \in [0, 1]. \quad (5.113)$$

We introduce the expressions of the isotropic moduli in terms of the Lamé-constants λ and μ , so we get $\mathbb{C}_{1111} = \lambda + 2\mu$ and $\mathbb{C}_{1122} = \lambda$. We observe that it is always possible to choose a set of positive parameters for $\lambda > 0$ and $\mu > 0$ that satisfy (5.113) with $(\delta_1, \delta_2, \alpha_1, \alpha_2) \in \mathbb{R}^+$, see CIARLET [38], pages 185-190.

Uniaxial Tension Test of a Compressible Mooney-Rivlin Material. Let us specify the Mooney-Rivlin model for the case of a compression/tension test of a cube, whose transverse contraction is equal zero. The characteristic surface of isotropic Young's moduli is a sphere, see Figure 5.11a. In this trivial case, the deformation gradient and hence the right Cauchy-Green tensor have the forms

$$\mathbf{F} = \text{diag}(\tilde{\lambda}, 1, 1) \Rightarrow \mathbf{C} = \text{diag}(\tilde{\lambda}^2, 1, 1) \quad (5.114)$$

with $\det \mathbf{F} = \tilde{\lambda}$ and $\tilde{\lambda} = (l_0 + u)/l_0$.

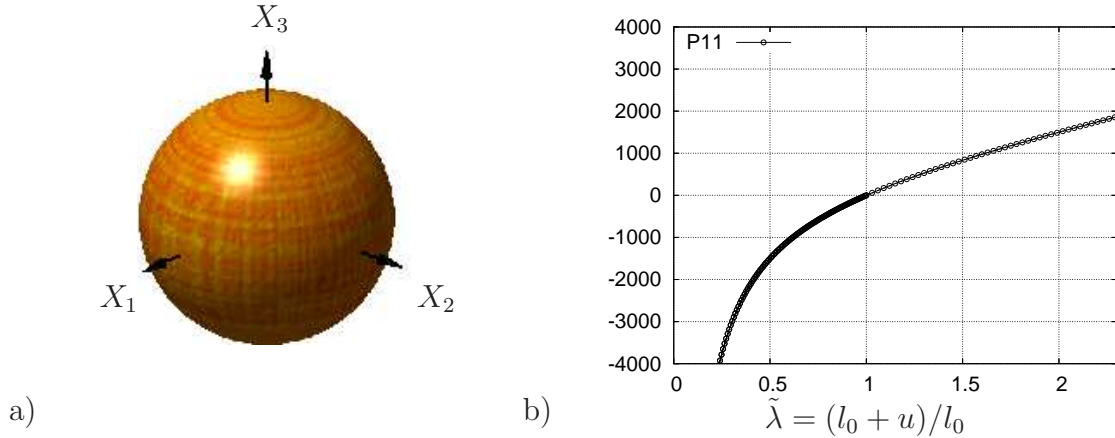


Figure 5.11: a) Characteristic surface of isotropic elasticities, b) Values of first Piola-Kirchhoff stresses in x_1 -direction.

Inserting (5.114) into (5.107) yields the second Piola-Kirchhoff stress in x_1 -direction

$$S_{11} = \delta_2 \frac{(\tilde{\lambda}^2 - 1)}{\tilde{\lambda}^2} = \delta_2 \left(1 - \frac{1}{\tilde{\lambda}^2}\right), \quad (5.115)$$

where the condition (5.109) is taken into account. Finally the first Piola-Kirchhoff stress in x_1 -direction reads

$$P_{11} = F_{11} S_{11} = \delta_2 \left(\tilde{\lambda} - \frac{1}{\tilde{\lambda}}\right). \quad (5.116)$$

Setting the material parameters of (5.105) to

$$\alpha_1 = 200, \alpha_2 = 100, \delta_1 = 100 \Rightarrow \delta_2 = 1000 \quad (5.117)$$

in N/mm^2 leads to a distribution of P_{11} which is shown in Figure 5.11. From (5.116) and Figure 5.11b we notice that for $\tilde{\lambda} \rightarrow 0$, we obtain $P_{11} \rightarrow -\infty$, and for $\tilde{\lambda} \rightarrow +\infty$ the behavior $P_{11} \rightarrow +\infty$ is given. In this case, the material model (5.105) satisfies the coercivity condition (5.4) with $\alpha > 0$, $p = 2$, $q = 2$ as well as the important growth condition (5.3)₁

5.9.2 Compressible Neo-Hookean Model. As a second example of an Ogden-type polyconvex material model we consider a compressible Neo-Hookean model characterized by (5.105) with $\alpha_2 = 0$, $\alpha_1 > 0$, cf. BLATZ [26]. In this case we obtain the identification from (5.113) for $\xi = 1$, meaning that we need a minimum of three material parameters to fulfill the conditions (5.113).

5.9.3 St. Venant-Kirchhoff Material Model. However, some simple energy functions, e.g. the St. Venant-Kirchhoff material model, are not polyconvex, see CIARLET [38], RAOULT [92] and NEFF [82]. Furthermore, this material model is not even elliptic, cf. NEFF [82]. From equation (4.63) we know that this model has the form

$$\psi = \frac{1}{2}\lambda (\text{tr } \mathbf{E})^2 + \mu \text{tr } [\mathbf{E}^2] \quad (5.118)$$

A reformulation in terms of \mathbf{C} yields

$$\psi = \frac{1}{8}\lambda (I_1^2 - 6 I_1 + 9) + \frac{1}{4}\mu (J_2 - 2 I_1 + 3), \quad (5.119)$$

which can be alternatively represented as

$$\psi = \mathcal{P}(\mathbf{F}) = \frac{1}{8}\lambda (\|\mathbf{F}\|^4 - 6 \|\mathbf{F}\|^2 + 9) + \frac{1}{4}\mu (\|\mathbf{F}^T \mathbf{F}\|^2 - 2 \|\mathbf{F}\|^2 + 3). \quad (5.120)$$

The second Fréchet derivative of $\mathcal{P}(\mathbf{F})$ results in the following equation

$$\begin{aligned} \delta \mathbf{F} : \partial_{\mathbf{F}\mathbf{F}} \mathcal{P}(\mathbf{F}) : \delta \mathbf{F} &= \frac{1}{8}\lambda (4 \|\mathbf{F}\|^2 \|\delta \mathbf{F}\|^2 + 8 \langle \mathbf{F}, \delta \mathbf{F} \rangle^2 - 12 \|\delta \mathbf{F}\|^2) + \frac{1}{4}\mu (4 \|\delta \mathbf{F} \mathbf{F}^T\|^2 \\ &\quad + 2(\|\delta \mathbf{F} \mathbf{F}^T\|^2 + \|\mathbf{F}^T \delta \mathbf{F}\|^2 + 2 \langle \delta \mathbf{F}^T \mathbf{F}, \mathbf{F}^T \delta \mathbf{F} \rangle) - 4 \|\delta \mathbf{F}\|^2). \end{aligned}$$

For the proof of ellipticity we have to set $\delta \mathbf{F} = \boldsymbol{\eta} \otimes \boldsymbol{\zeta}$. With $\langle \boldsymbol{\eta}, \boldsymbol{\zeta} \rangle = 0$ the second derivative reduces to

$$\begin{aligned} \delta \mathbf{F} : \partial_{\mathbf{F}\mathbf{F}} \mathcal{P}(\mathbf{F}) : \delta \mathbf{F} &= \frac{1}{2}\lambda \|\mathbf{F}\|^2 \|\boldsymbol{\eta}\|^2 \|\boldsymbol{\zeta}\|^2 + \frac{3}{2}\mu \|\boldsymbol{\eta}\|^2 \|\mathbf{F} \boldsymbol{\zeta}\|^2 \\ &\quad + \mu \|\boldsymbol{\zeta}\|^2 \|\mathbf{F}^T \boldsymbol{\eta}\|^2 - \left(\frac{3}{2}\lambda + \mu\right) \|\boldsymbol{\eta}\|^2 \|\boldsymbol{\zeta}\|^2. \end{aligned}$$

Furthermore, we choose $\mathbf{F} = \frac{1}{n}\mathbf{1}$, $\boldsymbol{\eta} = (-1, 0, 0)^T$ and $\boldsymbol{\zeta} = (0, 1, 0)^T$, so that we finally obtain

$$\delta \mathbf{F} : \partial_{\mathbf{F}\mathbf{F}} \mathcal{P}(\mathbf{F}) : \delta \mathbf{F} = \frac{1}{n^2} \left(\frac{3}{2}\lambda + 2\mu \right) - \left(\frac{3}{2}\lambda + \mu \right).$$

For a sufficient high parameter n , i.e., $n^2 \geq (3/2\lambda + 2\mu)/(3/2\lambda + \mu)$,

$$\delta \mathbf{F} : \partial_{\mathbf{F}\mathbf{F}} \mathcal{P}(\mathbf{F}) : \delta \mathbf{F} < 0$$

is valid, which proves the non-ellipticity of the classical St. Venant-Kirchhoff model.

5.9.4 Energy Functions Defined in Terms of the Hencky Tensor The matrix-logarithm $\ln \mathbf{C}$ is called Hencky tensor. Energies defined in terms of the Hencky tensor are in general not elliptic, which was first shown in NEFF [82], see also BERTRAM, BÖHLKE & SILHAVÝ [16]. Let us reproduce the proof given in NEFF [82]. Energies of the type

$$\psi(\mathbf{F}) = \text{tr}[\ln \mathbf{C}]^p = [\ln(J^2)]^p = [2 \ln J]^p = 2^p (\ln J)^p, \quad J = \det \mathbf{F} > 0, \quad p \geq 2 \quad (5.121)$$

are not elliptic.

Proof We obtain

$$\begin{aligned} \mathcal{P}(\mathbf{F}) &= 2^p (\ln J)^p \\ \partial_{\mathbf{F}} \mathcal{P}(\mathbf{F}) : \delta \mathbf{F} &= p 2^p (\ln J)^{p-1} \langle \mathbf{F}^{-T}, \delta \mathbf{F} \rangle \\ \delta \mathbf{F} : \partial_{\mathbf{F} \mathbf{F}} \mathcal{P}(\mathbf{F}) : \delta \mathbf{F} &= p(p-1) 2^p (\ln J)^{p-2} \langle \mathbf{F}^{-T}, \delta \mathbf{F} \rangle^2 \\ &\quad - p 2^p (\ln J)^{p-1} \langle \delta \mathbf{F} \mathbf{F}^{-1}, (\delta \mathbf{F} \mathbf{F}^{-1})^T \rangle. \end{aligned} \quad (5.122)$$

With $\delta \mathbf{F} = \boldsymbol{\eta} \otimes \boldsymbol{\zeta}$ and $\mathbf{F} = n \mathbf{1}$ we obtain the second derivative (5.122) in the form

$$\begin{aligned} \delta \mathbf{F} : \partial_{\mathbf{F} \mathbf{F}} \mathcal{P}(\mathbf{F}) : \delta \mathbf{F} &= p(p-1) 2^p (\ln(n^3))^{p-2} \frac{1}{n^2} \langle \boldsymbol{\eta}, \boldsymbol{\zeta} \rangle^2 - p 2^p (\ln(n^3))^{p-1} \frac{1}{n^2} \langle \boldsymbol{\eta}, \boldsymbol{\zeta} \rangle^2 \\ &= p 2^p (\ln(n^3))^{p-2} \frac{1}{n^2} \langle \boldsymbol{\eta}, \boldsymbol{\zeta} \rangle^2 ((p-1) - \ln(n^3)). \end{aligned} \quad (5.123)$$

The last term in (5.123) becomes negative for

$$\frac{(p-1)}{3} < \ln n,$$

which excludes ellipticity and hence polyconvexity of (5.121). Furthermore, Neff has proven that the quadratic energy function in terms of the Hencky tensor

$$\psi(\mathbf{F}) = \frac{\kappa}{3} \langle \ln \mathbf{C}, \mathbf{1} \rangle^2 + \mu \|\text{dev}(\ln \mathbf{C})\|^2$$

with the bulk modulus κ and shear modulus μ is not rank-one convex and hence not elliptic.

Proof Consider the function

$$\psi(\mathbf{F}) = \psi(\mathbf{F}_1 + \Delta \mathbf{F}) := f(n), \quad \text{with} \quad \mathbf{F}_1 = \mathbf{1}, \quad \Delta \mathbf{F} = \boldsymbol{\eta} \otimes \boldsymbol{\zeta},$$

where we set

$$\boldsymbol{\eta} = \begin{pmatrix} 0 \\ n \\ 0 \end{pmatrix} \quad \text{and} \quad \boldsymbol{\zeta} = \begin{pmatrix} 1 \\ 0 \\ 0 \end{pmatrix}.$$

The right Cauchy-Green tensor has then the form

$$\mathbf{C} = \mathbf{F}^T \mathbf{F} = (\mathbf{F}_1 + \Delta \mathbf{F})^T (\mathbf{F}_1 + \Delta \mathbf{F}) = \begin{bmatrix} 1 & n & 0 \\ n & 1+n^2 & 0 \\ 0 & 0 & 1 \end{bmatrix}.$$

To obtain a more simple representation of $f(n)$ we are interested in an expression of $f(n)$ in terms of the eigenvalues of \mathbf{C} . The eigenvalues are the solutions of the characteristic polynomial

$$p(\lambda) = \det(\mathbf{C} - \lambda \mathbf{1}) = (1 - \lambda)(\lambda^2 - \lambda(2 + n^2) + 1)$$

and obtained by

$$\lambda_1 = 1, \quad \lambda_2 = \frac{1}{2}(2 + n^2 + n\sqrt{4 + n^2}), \quad \lambda_3 = \frac{1}{2}(2 + n^2 - n\sqrt{4 + n^2}).$$

They have the properties

$$\begin{aligned} \lambda_1 \lambda_2 \lambda_3 = 1 & \Rightarrow \ln(\text{tr}[\ln \mathbf{C}]) = \ln \lambda_1 \lambda_2 \lambda_3 = \ln \lambda_2 \lambda_3 = 0, \\ & \Leftrightarrow \ln \lambda_2 = -\ln \lambda_3. \end{aligned}$$

Thus, the function $f(n)$ can be recast to

$$\begin{aligned} f(n) &= \lambda (\ln \lambda_1 \lambda_2 \lambda_3)^2 + \mu \left((\ln \lambda_1)^2 + (\ln \lambda_1)^2 + (\ln \lambda_1)^2 - \frac{1}{3} (\ln \lambda_1 + \ln \lambda_2 + \ln \lambda_3)^2 \right) \\ &= 2\mu (\ln \lambda_2)^2 \\ &= 2\mu (\ln(2 + n^2 + n\sqrt{4 + n^2}) - \ln 2)^2, \end{aligned}$$

which is not convex w.r.t. n . The non-convex function $f(n)$ is depicted in Figure 5.12. Consequently, ψ is not rank-one convex and therefore not elliptic.

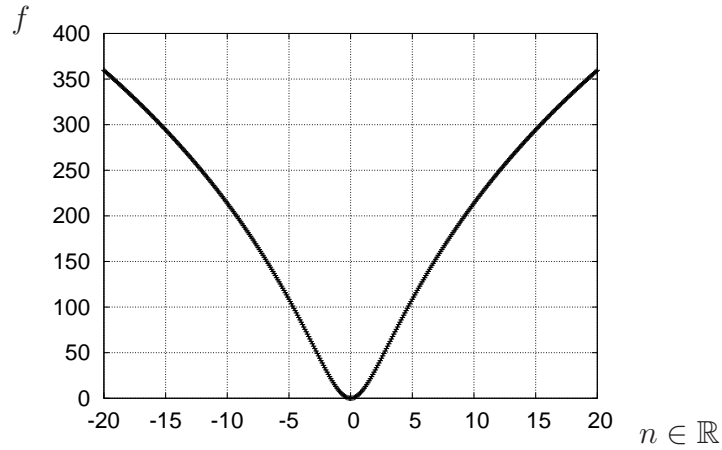


Figure 5.12: Non-convex function $f(n)$.

6 Invariant Polyconvex Energies on the Basis of Crystallographically Motivated Structural Tensors.

In finite elasticity, the existence of minimizers of the underlying boundary value problem is guaranteed if the variational functional to be minimized is sequentially weakly lower semicontinuous (s.w.l.s.) and coercive. Polyconvex functions are always s.w.l.s. and can therefore be preferably used. A large variety of isotropic polyconvex material models already exists; but in case of anisotropy, only for a few anisotropic material symmetries the construction of polyconvex energy functions was successful so far. In this regard transverse isotropy and orthotropy have to be mentioned, which were first described in a polyconvex, coordinate-invariant setting by SCHRÖDER & NEFF [103, 104]. There, the anisotropy types can be described by second-order rank-one structural tensors. A direct extension of this polyconvex approach to cubic symmetry has been used by KAMBOUCHEV, FERNANDEZ & RADOVITZKY [66]. A full characterization of cubic symmetry properties requires a fourth-order structural tensor. Kambouchev et. al show that for this type of anisotropy this tensor can be constructed in a simple way.

For the representation of the remaining six anisotropy groups (one triclinic, one monoclinic, two tetragonal and two trigonal groups) by coordinate-invariant energy functions, the second- and fourth-order structural tensors, introduced up to now in the literature, have a more complicated and complex structure. Moreover, we have shown that their forms are not useful for the construction of suitable polyconvex energies, see sections 5.7.1 and 5.7.2. The question which will be answered in the present chapter is therefore

Are there ways of verifying polyconvexity (and quasiconvexity) for triclinic, monoclinic, tetragonal as well as trigonal energy functions?

The first key idea was published in SCHRÖDER, NEFF & EBBING [106]. The proposed concept is based on second-order, *crystallographically motivated* structural tensors and makes the approximation of such material symmetries by polyconvex energies possible, which can be *completely* described by second-order structural tensors. These are the triclinic, monoclinic, orthotropic, hexagonal/ transversely isotropic symmetries. Some corresponding analyses are presented in EBBING, SCHRÖDER & NEFF [45, 46, 47].

The second key idea was published in SCHRÖDER, NEFF & EBBING [107]. In analogy to the first idea, specific fourth-order, *crystallographically motivated* structural tensors are introduced. They realize the approximation of such material symmetries by polyconvex energies, that can be *completely* described by fourth-order structural tensors, namely the tetragonal, trigonal and cubic symmetries.

6.1 Families of Polyconvex Invariant Functions.

Remember: On the basis of well-known representation theorems of isotropic tensor functions we first construct the *sets of invariants* for a given set of tensor arguments and formulate then coordinate-invariant, *complete* ^{16.)} energy functions in terms of these in-

^{16.)}Completeness of energy functions means that the corresponding tangent moduli at reference state obeys the same symmetries as the corresponding anisotropic elasticity tensor of linearized elasticity, cf. section 4.5. For this *completeness*, *sets of bilinear invariants* are sufficient.

variants. Hence, for the construction of coordinate-invariant, *complete* polyconvex energy functions, we have hitherto first checked the polyconvexity of these individual invariants, before we have considered them in the *sets of polyconvex invariants*. Since this way was in general not successful (see previous chapter) we choose now the other way round: We construct first coordinate-invariant polyconvex functions and check then, if they depend at least on all (often non-polyconvex) elements of the *classical set of bilinear invariants*.

The first fundamental idea is the introduction of a single symmetric and positive (semi-) definite second-order structural tensor \mathbf{G} for triclinic, monoclinic, rhombic as well as hexagonal/ transversely isotropic material symmetry groups. Each symmetric and positive (semi-)definite tensor \mathbf{G} can be multiplicatively decomposed into

$$\mathbf{G} = \mathbf{H}\mathbf{H}^T, \quad (6.1)$$

where detailed suitable expressions for the second-order tensor \mathbf{H} will be given in section 6.2. The structural tensor \mathbf{G} is solely invariant with respect to symmetry transformations of the underlying material symmetry group, i.e.,

$$\mathbf{G} = \mathbf{Q}\mathbf{G}\mathbf{Q}^T \quad \forall \mathbf{Q} \in \mathcal{G}. \quad (6.2)$$

The family of polyconvex invariant functions appears as

$$\mathcal{F}_p^{a,m,o,ti1} := \{I_1, I_2, I_3, J_4, J_5\}. \quad (6.3)$$

where the mixed invariant terms

$$J_4 := \text{tr}[\mathbf{C}\mathbf{G}], \quad J_5 := \text{tr}[\text{Cof}[\mathbf{C}]\mathbf{G}] \quad (6.4)$$

are used.

Family of Polyconvex Invariant Functions: Our *families of polyconvex invariant functions* consist of the polyconvex isotropic principal invariants of \mathbf{C} and additional polyconvex functions that are invariant with respect to the underlying anisotropy group \mathcal{G} . The polyconvex functions must be at least functions of the invariants of the corresponding *classical set of bilinear invariants*. For detailed representations we refer to section 6.3.

Generic mixed coordinate-invariant functions of the type

$$I_4^k =: (\text{tr}[\mathbf{C}\mathbf{G}])^k = (\text{tr}[\mathbf{F}^T \mathbf{F} \mathbf{G}])^k = (\mathbf{F}^T \mathbf{F} : \mathbf{G})^k = \|\mathbf{F}\mathbf{H}\|^{2k} = \langle \mathbf{F}\mathbf{H}, \mathbf{F}\mathbf{H} \rangle^k \quad (6.5)$$

and

$$K_5^k = (\text{tr}[\text{Cof}[\mathbf{C}]\mathbf{G}])^k = (\text{tr}[\text{Cof}[\mathbf{F}^T]\text{Cof}[\mathbf{F}]\mathbf{G}])^k = (\text{Cof}[\mathbf{F}^T \mathbf{F}] : \mathbf{G})^k, \quad (6.6)$$

with $k \geq 1$ and $\mathbf{G} \in \text{PSym}(3)$ are convex with respect to the assigned arguments \mathbf{F} and $\text{Cof}\mathbf{F}$, respectively, and therefore polyconvex.

The proof is documented in SCHRÖDER, NEFF & EBBING [106] as follows: The convexity of $(\text{tr}[\mathbf{F}^T \mathbf{F} \mathbf{G}])^k$, $k \geq 1$ w.r.t. \mathbf{F} can be proved by the positivity of the second derivative.

Proof The reader is referred to the proof instructions on page 83. We obtain

$$\begin{aligned}
 \mathcal{P}(\mathbf{F}) &= (\text{tr}[\mathbf{C}\mathbf{G}])^k = (\text{tr}[\mathbf{F}^T \mathbf{F} \mathbf{G}])^k = (\mathbf{F}^T \mathbf{F} : \mathbf{G})^k \\
 &= \|\mathbf{F}\mathbf{H}\|^{2k} = \langle \mathbf{F}\mathbf{H}, \mathbf{F}\mathbf{H} \rangle^k \\
 \partial_{\mathbf{F}} \mathcal{P}(\mathbf{F}) : \delta \mathbf{F} &= 2k \langle \mathbf{F}\mathbf{H}, \mathbf{F}\mathbf{H} \rangle^{k-1} \langle \mathbf{F}\mathbf{H}, \delta \mathbf{F}\mathbf{H} \rangle \\
 \delta \mathbf{F} : \partial_{\mathbf{F}\mathbf{F}}^2 \mathcal{P}(\mathbf{F}) : \delta \mathbf{F} &= 2k \langle \mathbf{F}\mathbf{H}, \mathbf{F}\mathbf{H} \rangle^{k-1} \langle \delta \mathbf{F}\mathbf{H}, \delta \mathbf{F}\mathbf{H} \rangle \\
 &\quad + 4k(k-1) \langle \mathbf{F}\mathbf{H}, \mathbf{F}\mathbf{H} \rangle^{k-2} \langle \mathbf{F}\mathbf{H}, \delta \mathbf{F}\mathbf{H} \rangle^2 \\
 &= 2k \|\mathbf{F}\mathbf{H}\|^{2k-2} \|\delta \mathbf{F}\mathbf{H}\|^2 \\
 &\quad + 4k(k-1) \|\mathbf{F}\mathbf{H}\|^{2k-4} \langle \mathbf{F}\mathbf{H}, \delta \mathbf{F}\mathbf{H} \rangle^2 \geq 0.
 \end{aligned} \tag{6.7}$$

The proof of the convexity of $(\text{tr}[\text{Cof}[\mathbf{F}^T] \text{Cof}[\mathbf{F}]\mathbf{G}])^k$, $k \geq 1$ is analogous when replacing \mathbf{F} by $\text{Cof} \mathbf{F}$.

The second-order tensors \mathbf{G} can be interpreted as structural tensors introduced by BOEHLER [28, 29, 31] and LIU [69] in some sense. The main difference here is the required positive (semi-)definiteness of \mathbf{G} , necessary for satisfying the polyconvexity condition.

The second fundamental idea is the introduction of a symmetric and positive (semi-)definite fourth-order structural tensor \mathbb{G} for each tetragonal, trigonal and the cubic anisotropy group. Based on our experiences with respect to the polyconvexity of functions governed by fourth-order structural tensors, it is advantageous to construct structural tensors as "fourth-order tensor products", i.e.,

$$\mathbb{G} = \sum_{i=1}^3 \mathbf{a}_i \otimes \mathbf{a}_i \otimes \mathbf{a}_i \otimes \mathbf{a}_i. \tag{6.8}$$

With regard to the vectors \mathbf{a}_i , $i = 1, 2, 3, \in \mathbb{R}^3$ we go more into detail in section 6.2. The families of polyconvex invariant functions for trigonal, tetragonal and cubic symmetry consist of the elements

$$\mathcal{F}_p^{t1,t2,ht1,ht2,c} := \{I_1, I_2, I_3, J_6, J_7, J_8\}. \tag{6.9}$$

The individual mixed invariants are given by

$$J_6 = \mathbf{1} : \mathbb{G} : \mathbf{C}, \quad J_7 = \mathbf{1} : \mathbb{G} : \text{Cof} \mathbf{C}, \quad J_8 = \mathbf{C} : \mathbb{G} : \mathbf{C}. \tag{6.10}$$

The proof of polyconvexity of the mixed invariants J_6 , J_7 and J_8 can be found in SCHRÖDER, NEFF & EBBING [107]. Let us recapitulate:

Proof. Each function J_6 , J_7 and J_8 can be additively decomposed into the polconvex functions $(\text{tr}[\mathbf{C}(\mathbf{a}_i \otimes \mathbf{a}_i)])^k$, $k = 1, 2, i = 1, 2, 3$ and $(\text{tr}[\text{Cof}[\mathbf{C}](\mathbf{a}_i \otimes \mathbf{a}_i)])^k$, $k = 1, 2, i = 1, 2, 3$, respectively. In detail, we obtain the expressions

$$\begin{aligned}
 J_6 &= \sum_{i=1}^3 \text{tr}(\mathbf{a}_i \otimes \mathbf{a}_i) \text{tr}[\mathbf{C}(\mathbf{a}_i \otimes \mathbf{a}_i)], \quad J_7 = \sum_{i=1}^3 \text{tr}(\mathbf{a}_i \otimes \mathbf{a}_i) \text{tr}[\text{Cof}[\mathbf{C}](\mathbf{a}_i \otimes \mathbf{a}_i)], \\
 J_8 &= \sum_{i=1}^3 \text{tr}[\mathbf{C}(\mathbf{a}_i \otimes \mathbf{a}_i)]^2.
 \end{aligned} \tag{6.11}$$

The proof of polyconvexity of the individual terms appearing in J_6 , J_7 and J_8 is documented in SCHRÖDER & NEFF [103, 104]. Furthermore, we use the fact that the sum of polyconvex functions is also polyconvex, cf. Corollary 3.2 in [104].

6.2 Crystallographically Motivated Structural Tensors.

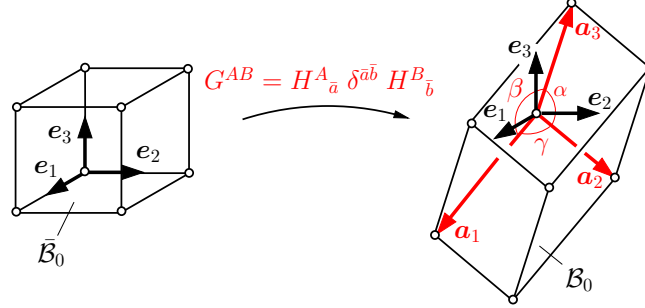


Figure 6.1: Push-forward operation \mathbf{G} .

In analogy to MENZEL & STEINMANN [73] we introduce a fictitious reference configuration $\bar{\mathcal{B}}_0$. Let \mathbf{H} represent a linear tangent map, which maps cartesian base vectors $\mathbf{e}_i \in \bar{\mathcal{B}}_0$ onto crystallographically motivated base vectors $\mathbf{a}_i \in \mathcal{B}_0$, related to the base vectors of the underlying Bravais lattice, i.e.,

$$\mathbf{H} : \mathbf{e}^{\bar{a}} \mapsto \mathbf{a}_{\bar{a}} \quad \rightarrow \quad \mathbf{H} = \mathbf{a}_{\bar{a}} \otimes \mathbf{e}^{\bar{a}} = H^A_{\bar{a}} \mathbf{e}_A \otimes \mathbf{e}^{\bar{a}}, \quad (6.12)$$

with

$$H^A_{\bar{a}} = [\mathbf{a}_1, \mathbf{a}_2, \mathbf{a}_3] \quad \text{and} \quad \mathbf{a}_{\bar{a}} = H^A_{\bar{a}} \mathbf{e}_A = \mathbf{H} \mathbf{e}_{\bar{a}}. \quad (6.13)$$

Then a second-order symmetric and positive (semi-)definite structural tensor \mathbf{G} can be interpreted as a push-forward of the cartesian metric of the fictitious configuration $\bar{\mathcal{B}}_0$ onto the real reference configuration \mathcal{B}_0 , defined by

$$\mathbf{G} = \mathbf{H} \mathbf{H}^T = H^A_{\bar{a}} \mathbf{e}_A \otimes \mathbf{e}^{\bar{a}} (\delta^{\bar{c}\bar{d}} \mathbf{e}_{\bar{c}} \otimes \mathbf{e}_{\bar{d}}) H^B_{\bar{b}} \mathbf{e}^{\bar{b}} \otimes \mathbf{e}_B = H^A_{\bar{a}} \delta^{\bar{a}\bar{b}} H^B_{\bar{b}} \mathbf{e}_A \otimes \mathbf{e}_B = G^{AB} \mathbf{e}_A \otimes \mathbf{e}_B,$$

which is depicted in Figure 6.1. Thus, the structural tensor \mathbf{G} is also referred to as *anisotropic metric tensor*. The crystallographic base vectors $\mathbf{a}_1, \mathbf{a}_2, \mathbf{a}_3$ depend on the six geometrical values necessary for the classification of the crystal lattice and the angle φ . This angle describes the relative orientation of the crystallographic base system with respect to the base system $\mathbf{c}_1, \mathbf{c}_2, \mathbf{c}_3$ of the morphology, which represents the symmetry of the geometry of the outer structure of the crystal.

In Figure 6.2 a) the base systems coincide. That means that the symmetry of the lattice is equal to the symmetry of the outer structure of the crystal. In Figure 6.2 b) the base systems do not coincide. That means that the symmetry of the crystal is limited by the relative orientation of the base systems. We make special choices for the orientations of the base vectors $\mathbf{c}_1, \mathbf{c}_2, \mathbf{c}_3$: $\mathbf{c}_1 \parallel \mathbf{e}_1$ and $\mathbf{c}_2 \perp \mathbf{e}_3$. If the crystallographic base vectors are given by $\mathbf{a}_1 \parallel \mathbf{c}_1, \mathbf{a}_2 \parallel \mathbf{c}_2$, where $\varphi = 0$, the representation of the tensor \mathbf{H} is

$$\mathbf{H} = \begin{bmatrix} a_{11} & a_{12} & a_{13} \\ 0 & a_{22} & a_{23} \\ 0 & 0 & a_{33} \end{bmatrix}. \quad (6.14)$$

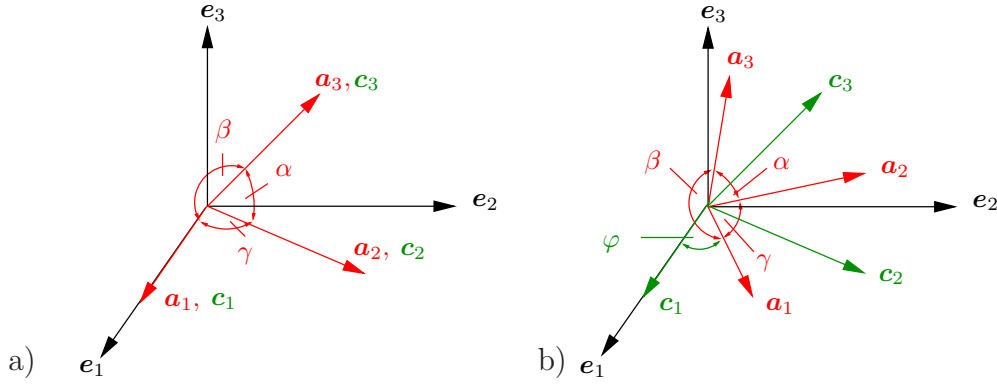


Figure 6.2: Possible orientations of the crystallographical base system $\mathbf{a}_1, \mathbf{a}_2, \mathbf{a}_3$ of the lattice and the base system $\mathbf{c}_1, \mathbf{c}_2, \mathbf{c}_3$ of the morphology (geometry of the outer structure) of the crystal: a) coincidence, b) relative orientation described by the angle φ .

The geometric interpretation of the components of the upper triangular matrix \mathbf{H} is depicted in Figure 6.2 a). The angles are given by the relations

$$\cos \alpha = \frac{\mathbf{a}_2 \cdot \mathbf{a}_3}{\|\mathbf{a}_2\| \|\mathbf{a}_3\|}, \quad \cos \beta = \frac{\mathbf{a}_3 \cdot \mathbf{a}_1}{\|\mathbf{a}_3\| \|\mathbf{a}_1\|}, \quad \cos \gamma = \frac{\mathbf{a}_1 \cdot \mathbf{a}_2}{\|\mathbf{a}_1\| \|\mathbf{a}_2\|}. \quad (6.15)$$

Substituting the lengths a, b, c of the individual crystallographic base vectors $\mathbf{a}_1, \mathbf{a}_2$ and \mathbf{a}_3 , respectively, and (6.15) into (6.14) yields

$$\mathbf{H} = \begin{bmatrix} a & b \cos \gamma & c \cos \beta \\ 0 & b \sin \gamma & c (\cos \alpha - \cos \beta \cos \gamma) / \sin \gamma \\ 0 & 0 & c [1 + 2 \cos \alpha \cos \beta \cos \gamma - (\cos^2 \alpha + \cos^2 \beta + \cos^2 \gamma)]^{1/2} / \sin \gamma \end{bmatrix}. \quad (6.16)$$

The triclinic, monoclinic, rhombic system as well as the hexagonal/transversely isotropic symmetry can be described by such a specific second-order metric tensor.

For the remaining anisotropy groups we propose a fourth-order structural tensor \mathbb{G} . The construction of this tensor is also crystallographically motivated. It is built up as the sum of dyadic products of the crystallographic base vectors $\mathbf{a}_1, \mathbf{a}_2, \mathbf{a}_3$:

$$\mathbb{G} = \sum_{i=1}^3 \mathbf{a}_i \otimes \mathbf{a}_i \otimes \mathbf{a}_i \otimes \mathbf{a}_i, \quad (6.17)$$

cf. SCHRÖDER, NEFF & EBBING [107]. The advantage of this definition is that it leads to anisotropic elasticity tensor-type representations of the fourth-order structural tensors.

For each anisotropy group we now show the general position of associated crystals in space together with the relative orientations of the base vectors of the underlying lattice. Furthermore, in some cases the plane perpendicular to the \mathbf{a}_3 -axis of the lattice is visualized. If the reader needs more informations concerning material symmetry properties of crystals, we refer again to chapter 3. The parameters $a, b, c, \alpha, \beta, \gamma, \varphi$ and $\tilde{a}, \tilde{b}, \tilde{c}, \tilde{d}, \tilde{e}, \tilde{f}$, which will be used, can be interpreted in the sequel as additional material parameters.

Triclinic Structural Tensor. In Figure 6.3 the triclinic crystal of the point group \mathcal{C}_i is shown, which represents the symmetry properties of the anisotropy group \mathcal{G}_1 . In the triclinic case no restrictions on the orientation or lengths of the base vectors of the lattice have to be taken into account, i.e., the base vectors have the most general form. Choosing $\mathbf{a}_1 \parallel \mathbf{e}_1$ we get

$$\mathbf{a}_1 = (a, 0, 0)^T, \quad \mathbf{a}_2 = (b \cos \gamma, b \sin \gamma, 0)^T, \quad \mathbf{a}_3 = (c \cos \beta, X, Y)^T, \quad (6.18)$$

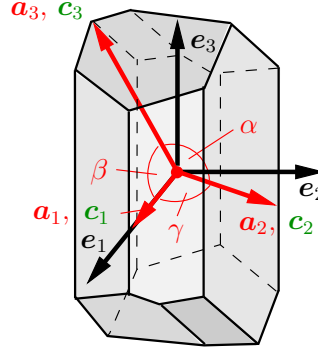


Figure 6.3: Triclinic Crystal \mathcal{C}_i .

with the abbreviations

$$\begin{aligned} X &= c (\cos \alpha - \cos \beta \cos \gamma) / \sin \gamma, \\ Y &= c [1 + 2 \cos \alpha \cos \beta \cos \gamma - (\cos^2 \alpha + \cos^2 \beta + \cos^2 \gamma)]^{1/2} / \sin \gamma. \end{aligned} \quad (6.19)$$

Thus, inserting (6.18) into (6.14) leads to the most general representation of the transformation tensor $\mathbf{H}^a = \mathbf{H}$. The triclinic structural tensor appears as

$$\mathbf{G}^a = \mathbf{H}^a \mathbf{H}^{aT} = \begin{bmatrix} \tilde{a} & \tilde{d} & \tilde{e} \\ \tilde{d} & \tilde{b} & \tilde{f} \\ \tilde{e} & \tilde{f} & \tilde{c} \end{bmatrix}, \quad (6.20)$$

where the parameters satisfy the relations

$$\begin{aligned} \tilde{a} &= a^2 + b^2 \cos^2 \gamma + c^2 \cos^2 \beta, \quad \tilde{b} = b^2 \sin^2 \gamma + \frac{c^2 (\cos \alpha - \cos \beta \cos \gamma)^2}{\sin^2 \gamma}, \\ \tilde{c} &= \frac{c^2 (1 + 2 \cos \alpha \cos \beta \cos \gamma - \cos^2 \alpha - \cos^2 \beta - \cos^2 \gamma)}{\sin^2 \gamma}, \\ \tilde{d} &= b^2 \cos \gamma \sin \gamma + \frac{c^2 \cos \beta (\cos \alpha - \cos \beta \cos \gamma)}{\sin \gamma}, \\ \tilde{e} &= \frac{c^2 \cos \beta (1 + 2 \cos \alpha \cos \beta \cos \gamma - \cos^2 \alpha - \cos^2 \beta - \cos^2 \gamma)^{1/2}}{\sin \gamma}, \\ \tilde{f} &= \frac{c^2 (\cos \alpha - \cos \beta \cos \gamma)}{\sin \gamma} \cdot \frac{(1 + 2 \cos \alpha \cos \beta \cos \gamma - \cos^2 \alpha - \cos^2 \beta - \cos^2 \gamma)^{1/2}}{\sin \gamma}. \end{aligned} \quad (6.21)$$

We prefer the representation (6.20) of \mathbf{G}^a in terms of \tilde{a} , \tilde{b} , \tilde{c} , \tilde{d} , \tilde{e} , \tilde{f} and satisfy the conditions for the positive (semi-)definiteness of the structural tensor by

$$\tilde{a} \geq 0, \quad \tilde{a}\tilde{b} - \tilde{d}^2 \geq 0, \quad \tilde{a}\tilde{b}\tilde{c} - \tilde{a}\tilde{f}^2 - \tilde{c}\tilde{d}^2 + 2\tilde{d}\tilde{e}\tilde{f} - \tilde{b}\tilde{e}^2 \geq 0. \quad (6.22)$$

Monoclinic Structural Tensor. The monoclinic crystal with point group \mathcal{C}_{2h} , presented in Figure (6.4), reflects the properties of the anisotropy group \mathcal{G}_2 . In the monoclinic case the base vector \mathbf{a}_1 as well as \mathbf{a}_2 are oriented perpendicularly to \mathbf{a}_3 ; therefore the relation $\gamma \neq \alpha = \beta = 90^\circ$ must hold. In detail, the monoclinic base vectors appear as

$$\mathbf{a}_1 = (a, 0, 0)^T, \quad \mathbf{a}_2 = (b \cos \gamma, b \sin \gamma, 0)^T, \quad \mathbf{a}_3 = (0, 0, c)^T. \quad (6.23)$$

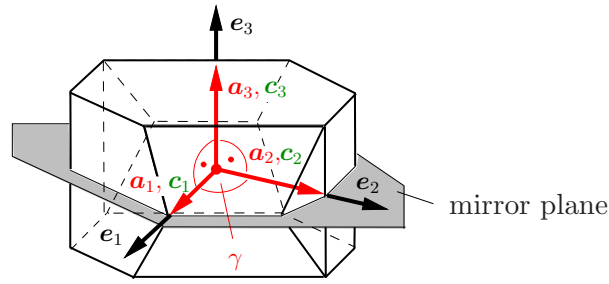


Figure 6.4: Monoclinic Crystal \mathcal{C}_{2h} .

Considering (6.23) and (6.14) gives the monoclinic structural tensor $\mathbf{G}^m = \mathbf{H}^m \mathbf{H}^{mT}$, with

$$\mathbf{G}^m = \begin{bmatrix} a^2 + b^2 \cos^2 \gamma & b^2 \cos \gamma \sin \gamma & 0 \\ b^2 \cos \gamma \sin \gamma & b^2 \sin^2 \gamma & 0 \\ 0 & 0 & c^2 \end{bmatrix} \Rightarrow \mathbf{G}^m = \begin{bmatrix} \tilde{a} & \tilde{d} & 0 \\ \tilde{d} & \tilde{b} & 0 \\ 0 & 0 & \tilde{c} \end{bmatrix}, \quad (6.24)$$

where \tilde{a} , \tilde{b} , \tilde{c} , \tilde{d} act as material parameters and have to fulfill the conditions

$$\tilde{a}, \tilde{c} \geq 0, \quad \tilde{a}\tilde{b} - \tilde{d}^2 \geq 0. \quad (6.25)$$

Rhombic Structural Tensor. The rhombic crystal of the point group \mathcal{D}_{2h} in Figure 6.5 visualizes all symmetry elements of the rhombic anisotropy group \mathcal{G}_3 . The base vectors of the rhombic Bravais lattices are aligned in the directions of the three mutually orthogonal two-fold axes:

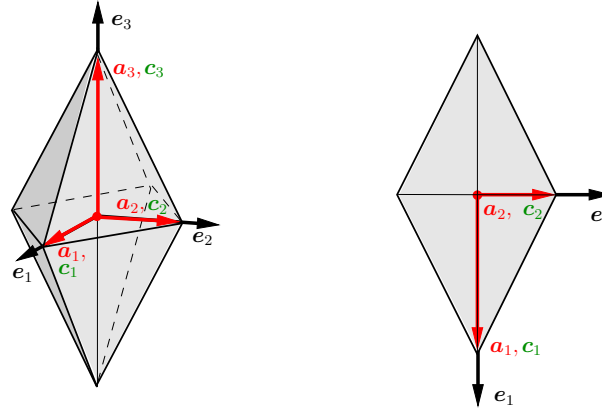
$$\mathbf{a}_1 = (a, 0, 0)^T, \quad \mathbf{a}_2 = (0, b, 0)^T, \quad \mathbf{a}_3 = (0, 0, c)^T. \quad (6.26)$$

Equation (6.14) with (6.26) yields the rhombic structural tensor of the type

$$\mathbf{G}^o = \mathbf{H}^o \mathbf{H}^{oT} = \begin{bmatrix} a^2 & 0 & 0 \\ 0 & b^2 & 0 \\ 0 & 0 & c^2 \end{bmatrix} \Rightarrow \mathbf{G}^o = \begin{bmatrix} \tilde{a} & 0 & 0 \\ 0 & \tilde{b} & 0 \\ 0 & 0 & \tilde{c} \end{bmatrix}, \quad (6.27)$$

with the material parameters \tilde{a} , \tilde{b} , \tilde{c} and the conditions

$$\tilde{a}, \tilde{b}, \tilde{c} \geq 0. \quad (6.28)$$

Figure 6.5: Rhombic Crystal \mathcal{D}_{2h} .

Transversely Isotropic/ Hexagonal Structural Tensor. Hexagonal as well as transversely isotropic material behaviour can be sufficiently described by transversely isotropic, \mathcal{G}_{12} -invariant tensor functions. Hence, these types of anisotropy can be represented by the same structural tensor.

Transversely isotropic material behavior is characterized by one preferred direction oriented perpendicularly to an isotropy plane. For the description of that anisotropy we assume a base system, which is defined by three mutually orthogonal base vectors $\mathbf{a}_i, i = 1, 2, 3$, where the lengths satisfy the relation $a = b \neq c$. The orientation of the base vector \mathbf{a}_3 coincides with the preferred direction of the material. We choose the cartesian base system as underlying base system of the crystal, i.e.,

$$\mathbf{a}_1 = a \mathbf{e}_1, \mathbf{a}_2 = a \mathbf{e}_2, \mathbf{a}_3 = c \mathbf{e}_3. \quad (6.29)$$

Therefore, we obtain the transversely isotropic/hexagonal structural tensor by

$$\mathbf{G}^{ti} = \begin{bmatrix} a^2 & 0 & 0 \\ 0 & a^2 & 0 \\ 0 & 0 & c^2 \end{bmatrix} \Rightarrow \mathbf{G}^{ti} = \begin{bmatrix} \tilde{a} & 0 & 0 \\ 0 & \tilde{a} & 0 \\ 0 & 0 & \tilde{c} \end{bmatrix}. \quad (6.30)$$

If we use the second representation of \mathbf{G}^{ti} we have to ensure the positive definiteness of \mathbf{G}^{ti} by

$$\tilde{a}, \tilde{c} \geq 0. \quad (6.31)$$

Tetragonal Structural Tensors. In Figure 6.6 a) we see a \mathcal{C}_{4h} -type crystal illustrating the symmetry properties of the anisotropy group \mathcal{G}_4 . The base system of the lattice is characterized by two orthogonal base vectors \mathbf{a}_1 and \mathbf{a}_2 of equal lengths, which are perpendicular to the four-fold axis in \mathbf{a}_3 -direction. Describing the outer structure of the crystal by the base vectors

$$\mathbf{c}_1 = a \mathbf{e}_1, \mathbf{c}_2 = a \mathbf{e}_2, \mathbf{c}_3 = c \mathbf{e}_3, \quad (6.32)$$

the base vectors $\mathbf{a}_i, i = 1, 2, 3$ of the lattice have to be taken as

$$\mathbf{a}_i = \mathbf{Q} \mathbf{c}_i, \quad i = 1, 2, 3, \quad \text{with} \quad \mathbf{Q} = \begin{bmatrix} \cos(\varphi) & -\sin(\varphi) & 0 \\ \sin(\varphi) & \cos(\varphi) & 0 \\ 0 & 0 & 1 \end{bmatrix}, \quad (6.33)$$

which results in

$$\begin{aligned} \mathbf{a}_1 &= (a \cos(\varphi), a \sin(\varphi), 0)^T, & \mathbf{a}_2 &= (-a \sin(\varphi), a \cos(\varphi), 0)^T, & \mathbf{a}_3 &= (0, 0, c)^T, \\ \Rightarrow \mathbf{a}_1 &= (\tilde{a}, \tilde{b}, 0)^T, & \mathbf{a}_2 &= (-\tilde{b}, \tilde{a}, 0)^T, & \mathbf{a}_3 &= (0, 0, \tilde{c})^T. \end{aligned} \quad (6.34)$$

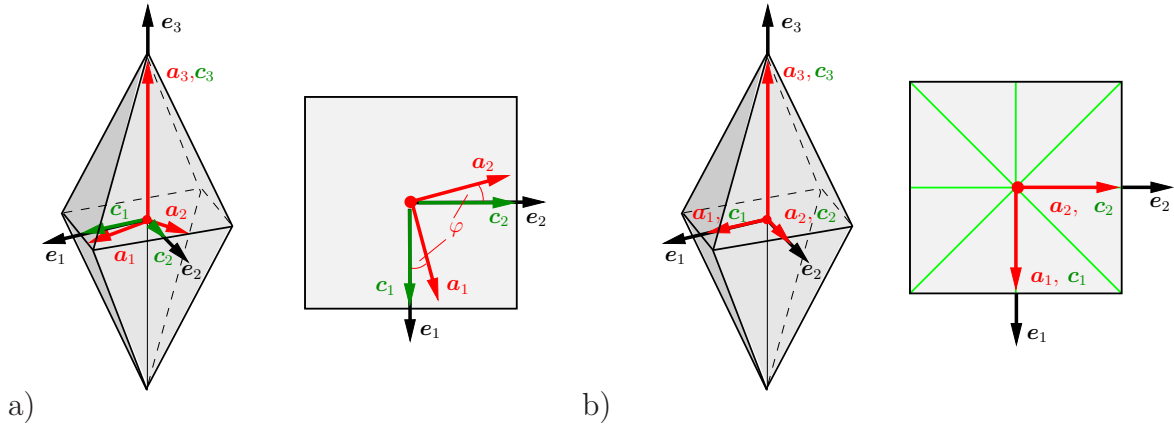


Figure 6.6: Tetragonal Crystals, a) C_{4h} , b) D_{4h} .

Evaluating (6.17) with (6.34)₂ the fourth-order structural tensor of C_{4h} -type appears as

$$\mathbb{G}^{t1} = \begin{bmatrix} \tilde{a}^4 + \tilde{b}^4 & 2\tilde{a}^2\tilde{b}^2 & 0 & \tilde{a}^3\tilde{b} - \tilde{b}^3\tilde{a} & 0 & 0 \\ & \tilde{a}^4 + \tilde{b}^4 & 0 & \tilde{b}^3\tilde{a} - \tilde{a}^3\tilde{b} & 0 & 0 \\ & & \tilde{c}^4 & 0 & 0 & 0 \\ & sym. & & 2\tilde{a}^2\tilde{b}^2 & 0 & 0 \\ & & & & 0 & 0 \\ & & & & & 0 \end{bmatrix}. \quad (6.35)$$

Figure 6.6 b) depicts a crystal of point group D_{4h} with the associated orientation of the lattice. The symmetry of this crystal, which is here given by that of the underlying lattice, presents the symmetry properties of the anisotropy group \mathcal{G}_5 . The base vectors \mathbf{a}_1 and \mathbf{a}_2 are aligned in directions of two mutually orthogonal two-fold axes, visualized in Figure 6.6 b) as green-coloured lines. Thus, we have to set in (6.34) $\varphi = 0^\circ$ or $\varphi = 45^\circ$. For instance, for $\varphi = 0^\circ$ we obtain

$$\mathbf{a}_1 = a \mathbf{e}_1, \quad \mathbf{a}_2 = a \mathbf{e}_2, \quad \mathbf{a}_3 = c \mathbf{e}_3, \quad (6.36)$$

so that the fourth-order structural tensor for \mathcal{G}_5 -anisotropy is given by

$$\mathbb{G}^{t2} = \text{diag}[a^4, a^4, c^4, 0, 0, 0]. \quad (6.37)$$

Trigonal Structural Tensors. Trigonal symmetry of crystal structures can be represented by a Bravais lattice of rhombohedral type situated inside a hexagonal centered cell. This lattice is given by $\mathbf{a}_1, \mathbf{a}_2, \mathbf{a}_3$ of equal lengths and including the same angle $\alpha = \beta = \gamma$

with one another. The typical trigonal three-fold axis is oriented in $(\mathbf{a}_1 + \mathbf{a}_2 + \mathbf{a}_3)$ -direction. Figure 6.7 shows a crystal belonging to the \mathcal{C}_{3i} -point group, whose symmetry properties are representative for the trigonal anisotropy group \mathcal{G}_8 . The symmetry of the crystal is limited by the orientation of the crystallographic axes.

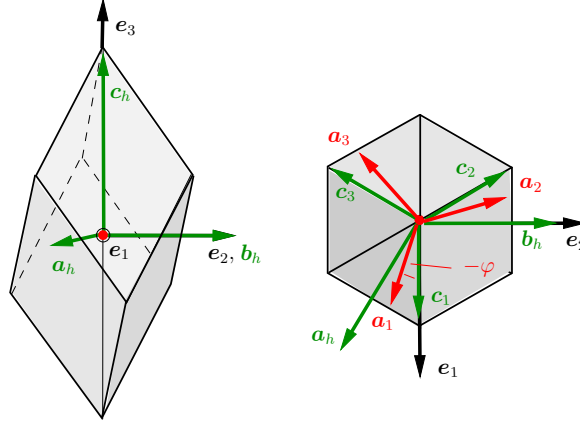


Figure 6.7: Trigonal Crystal \mathcal{C}_{3i} .

The symmetry of the outer structure of the crystal can be captured by the base system

$$\mathbf{c}_1 = \frac{1}{3}(2\mathbf{a}_h + \mathbf{b}_h + \mathbf{c}_h), \quad \mathbf{c}_2 = \frac{1}{3}(-\mathbf{a}_h + \mathbf{b}_h + \mathbf{c}_h), \quad \mathbf{c}_3 = \frac{1}{3}(-\mathbf{a}_h - 2\mathbf{b}_h + \mathbf{c}_h), \quad (6.38)$$

where the hexagonal base vectors are chosen to be

$$\mathbf{a}_h = (a \cos(30^\circ), -a \sin(30^\circ), 0)^T, \quad \mathbf{b}_h = a \mathbf{e}_2, \quad \mathbf{c}_h = c \mathbf{e}_3. \quad (6.39)$$

Applying an arbitrary rotation \mathbf{Q} defined in (6.33) through $-\varphi$ around the \mathbf{e}_3 -axis on the vectors $\mathbf{c}_i, i = 1, 2, 3$, we obtain the base vectors $\mathbf{a}_i, i = 1, 2, 3$ of the underlying lattice by:

$$\mathbf{a}_1 = \begin{pmatrix} \frac{\tilde{a}}{\sqrt{3}} \\ -\frac{\tilde{b}}{\sqrt{3}} \\ \frac{\tilde{c}}{3} \end{pmatrix}, \quad \mathbf{a}_2 = \begin{pmatrix} -\frac{\tilde{a}}{2\sqrt{3}} + \frac{\tilde{b}}{2} \\ \frac{\tilde{b}}{2\sqrt{3}} + \frac{\tilde{a}}{2} \\ \frac{\tilde{c}}{3} \end{pmatrix}, \quad \mathbf{a}_3 = \begin{pmatrix} -\frac{\tilde{a}}{2\sqrt{3}} - \frac{\tilde{b}}{2} \\ \frac{\tilde{b}}{2\sqrt{3}} - \frac{\tilde{a}}{2} \\ \frac{\tilde{c}}{3} \end{pmatrix}, \quad (6.40)$$

where the material parameters $\tilde{a}, \tilde{b}, \tilde{c}$ depend on the geometrical values a, c, φ , i.e.,

$$\tilde{a} = a \cos \varphi, \quad \tilde{b} = a \sin \varphi, \quad \tilde{c} = c. \quad (6.41)$$

The \mathcal{G}_8 -invariant fourth-order structural tensor finally results in

$$\mathbb{G}^{ht1} = \begin{bmatrix} \frac{1}{8} C^2 & \frac{1}{24} C^2 & \frac{1}{18} C \tilde{c}^2 & 0 & A & B \\ & \frac{1}{8} C^2 & \frac{1}{18} C \tilde{c}^2 & 0 & -A & -B \\ & & \frac{1}{27} \tilde{c}^4 & 0 & 0 & 0 \\ & sym. & & \frac{1}{24} C^2 & -B & A \\ & & & & \frac{1}{18} C \tilde{c}^2 & 0 \\ & & & & & \frac{1}{18} C \tilde{c}^2 \end{bmatrix}, \quad (6.42)$$

with the abbreviations

$$A = -\frac{1}{4\sqrt{3}}\tilde{a}^2\tilde{b}\tilde{c} + \frac{1}{12\sqrt{3}}\tilde{b}^3\tilde{c}, \quad B = -\frac{1}{4\sqrt{3}}\tilde{a}\tilde{b}^2\tilde{c} + \frac{1}{12\sqrt{3}}\tilde{a}^3\tilde{c}, \quad C = \tilde{a}^2 + \tilde{b}^2. \quad (6.43)$$

Having a look at the crystal in Figure 6.8, which possesses the symmetry properties of the anisotropy group \mathcal{G}_9 , one notices a higher symmetry. Here, the symmetry of the crystal is equal to that of the lattice.

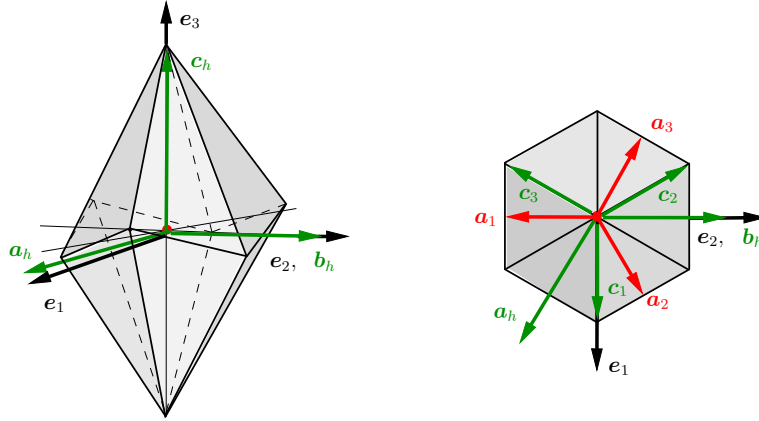


Figure 6.8: Trigonal Crystal \mathcal{D}_{3d} .

The base vectors \mathbf{a}_i are aligned perpendicularly to the three two-fold axes of the trigonal crystal defined by

$$\mathbf{f}_1 = \mathbf{e}_1, \quad \mathbf{f}_2 = -\frac{1}{2}\mathbf{e}_1 + \frac{\sqrt{3}}{2}\mathbf{e}_2, \quad \mathbf{f}_3 = -\frac{1}{2}\mathbf{e}_1 - \frac{\sqrt{3}}{2}\mathbf{e}_2. \quad (6.44)$$

They satisfy $\mathbf{a}_1 \perp \mathbf{f}_1$, $\mathbf{a}_2 \perp \mathbf{f}_2$, $\mathbf{a}_3 \perp \mathbf{f}_3$ and have the forms

$$\begin{aligned} \mathbf{a}_1 &= \frac{1}{3}(2\mathbf{a}_h + \mathbf{b}_h + \mathbf{c}_h) = \frac{1}{3} \left(-\sqrt{3}\tilde{b}\mathbf{e}_2 + \tilde{c}\mathbf{e}_3 \right), \\ \mathbf{a}_2 &= \frac{1}{3}(-\mathbf{a}_h + \mathbf{b}_h + \mathbf{c}_h) = \frac{1}{3} \left(\frac{3}{2}\tilde{b}\mathbf{e}_1 + \frac{\sqrt{3}}{2}\tilde{b}\mathbf{e}_2 + \tilde{c}\mathbf{e}_3 \right), \\ \mathbf{a}_3 &= \frac{1}{3}(-\mathbf{a}_h - 2\mathbf{b}_h + \mathbf{c}_h) = \frac{1}{3} \left(-\frac{3}{2}\tilde{b}\mathbf{e}_1 + \frac{\sqrt{3}}{2}\tilde{b}\mathbf{e}_2 + \tilde{c}\mathbf{e}_3 \right). \end{aligned} \quad (6.45)$$

They can be directly determined by (6.40) while setting $\varphi = 90^\circ$ in (6.41), which leads to the following \mathcal{G}_9 -invariant fourth-order structural tensor

$$\mathbb{G}^{ht2} = \begin{bmatrix} \frac{1}{8}\tilde{b}^4 & \frac{1}{24}\tilde{b}^4 & \frac{1}{18}\tilde{b}^2\tilde{c}^2 & 0 & \frac{1}{12\sqrt{3}}\tilde{b}^3\tilde{c} & 0 \\ & \frac{1}{8}\tilde{b}^4 & \frac{1}{18}\tilde{b}^2\tilde{c}^2 & 0 & -\frac{1}{12\sqrt{3}}\tilde{b}^3\tilde{c} & 0 \\ & & \frac{1}{27}\tilde{c}^4 & 0 & 0 & 0 \\ & sym. & & \frac{1}{24}\tilde{b}^4 & 0 & \frac{1}{12\sqrt{3}}\tilde{b}^3\tilde{c} \\ & & & & \frac{1}{18}\tilde{b}^2\tilde{c}^2 & 0 \\ & & & & & \frac{1}{18}\tilde{b}^2\tilde{c}^2 \end{bmatrix}. \quad (6.46)$$

Cubic Structural Tensor. The anisotropic material behaviour of cubic materials can be sufficiently represented by \mathcal{G}_7 -invariant tensor functions. The associated crystal of hexoctahedral type visualizing the symmetry properties of the anisotropy group \mathcal{G}_7 can be found in Figure 6.9.

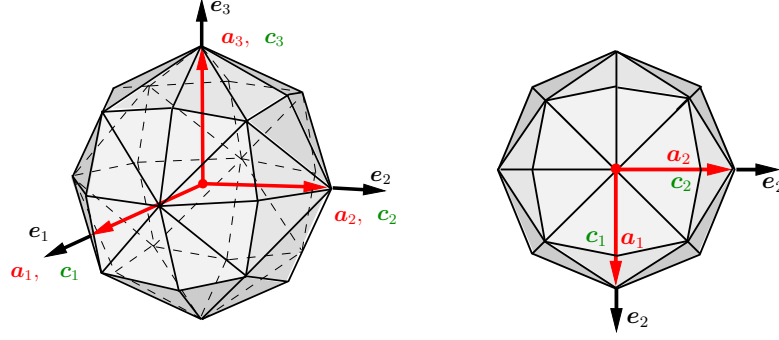


Figure 6.9: Cubic Crystal \mathcal{O}_h .

The three mutually orthogonal base vectors \mathbf{a}_i , $i = 1, 2, 3$ of equal lengths coincide with the three symmetry axes, chosen here to be the cartesian base vectors, i.e.,

$$\mathbf{a}_i = a \mathbf{e}_i, \quad i = 1, 2, 3. \quad (6.47)$$

The cubic fourth-order structural tensor results in

$$\mathbb{G}^c = \text{diag}[a^4, a^4, a^4, 0, 0, 0]. \quad (6.48)$$

In order to get an overview all structural tensors are listed again in Appendix I.

6.3 Consequences of Polyconvex Approach w.r.t. Classical Representations.

Now we check the consequences of the polyconvex approach on the basis of crystallographically motivated structural tensors with respect to the well-known representations of anisotropic tensor functions (described in chapter 4). It is obvious that the proposed polyconvex invariant functions appearing in the families (6.3) and (6.9) depend on invariants of the corresponding *classical sets of bilinear invariants*. Nevertheless, for interested readers we give now detailed representations of the introduced individual polyconvex functions. We recommend the reader to have simultaneously a look at the *classical sets of bilinear invariants* presented in the Appendix D.

Triclinic Family of Polyconvex Invariant Functions. In the triclinic case the elements of the *family of polyconvex invariant functions* \mathcal{F}_p^a have the forms

$$J_4 = \mathbf{C} : \mathbf{G}^a = \tilde{a} C_{11} + \tilde{b} C_{22} + \tilde{c} C_{33} + 2\tilde{d} C_{12} + 2\tilde{e} C_{13} + 2\tilde{f} C_{23}$$

$$J_5 = \mathbf{C} : \mathbf{G}^a = \tilde{a} \text{Cof} C_{11} + \tilde{b} \text{Cof} C_{22} + \tilde{c} \text{Cof} C_{33} + 2\tilde{d} \text{Cof} C_{12} + 2\tilde{e} \text{Cof} C_{13} + 2\tilde{f} \text{Cof} C_{23}.$$

Monoclinic Family of Polyconvex Invariant Functions. The polyconvex functions of the monoclinic *family of polyconvex invariant functions* \mathcal{F}_p^m appear in detail as

$$\begin{aligned} J_4 &= \mathbf{C} : \mathbf{G}^m &= \tilde{a} C_{11} + 2\tilde{d} C_{12} + \tilde{b} C_{22} + \tilde{c} C_{33}, \\ J_5 &= \text{Cof} \mathbf{C} : \mathbf{G}^m &= \tilde{a} (C_{22} C_{33} - C_{23}^2) + 2\tilde{d} (C_{23} C_{13} - C_{12} C_{33}) \\ &&+ \tilde{b} (C_{11} C_{33} - C_{13}^2) + \tilde{c} (C_{11} C_{22} - C_{12}^2). \end{aligned}$$

Rhombic Family of Polyconvex Invariant Functions. The rhombic polyconvex functions of the associated *family of polyconvex invariant functions* \mathcal{F}_p^o are:

$$\begin{aligned} J_4 &= \mathbf{C} : \mathbf{G}^o &= \tilde{a} C_{11} + \tilde{b} C_{22} + \tilde{c} C_{33}, \\ J_5 &= \text{Cof} \mathbf{C} : \mathbf{G}^o &= \tilde{a} (C_{22} C_{33} - C_{23}^2) + \tilde{b} (C_{11} C_{33} - C_{13}^2) + \tilde{c} (C_{11} C_{22} - C_{12}^2). \end{aligned}$$

In section 5.7.2 we pointed out that SCHRÖDER & NEFF [104] showed the proof of non-polyconvexity of multiplicative couplings between the rhombic invariants formulated in terms of the three "classical" structural tensors, i.e., the invariant terms $C_{11}C_{22}$, $C_{11}C_{33}$, $C_{22}C_{33}$, which are needed for a *complete* energy function in case of rhombic symmetry. Therefore, SCHRÖDER & NEFF [104] proposed linear convex combinations of the individual polyconvex rhombic invariant functions to overcome such a problem. The great benefit of the proposed approach is here that such terms are a priori included in the above-mentioned polyconvex invariant functions.

Hexagonal/Transversely Isotropic Family of Polyconvex Bilinear Invariant Functions. The polyconvex functions of the transversely isotropic/hexagonal *family of polyconvex invariant functions* \mathcal{F}_p^{ti} have the form

$$\begin{aligned} J_4 &= \mathbf{C} : \mathbf{G}^{ti} &= \tilde{a} (C_{11} + C_{22}) + \tilde{c} C_{33}, \\ J_5 &= \text{Cof} \mathbf{C} : \mathbf{G}^{ti} &= \tilde{a} (C_{22} C_{33} - C_{23}^2 + C_{11} C_{33} - C_{13}^2) + \tilde{c} (C_{11} C_{22} - C_{12}^2). \end{aligned}$$

The last term given in J_5 is an alternative element of the hexagonal/ transversely isotropic *classical set of bilinear invariants* instead of the element $C_{11}^2 + C_{22}^2 + 2C_{12}^2$, since the following relation holds:

$$C_{11} C_{22} - C_{12}^2 = \frac{1}{2} ((C_{11} + C_{22})^2 - (C_{11}^2 + C_{22}^2 + 2C_{12}^2)). \quad (6.49)$$

Tetragonal Families of Polyconvex Invariant Functions. In case of tetragonal symmetry described by the material symmetry group \mathcal{G}_4 the *set of polyconvex invariant functions* \mathcal{F}_p^{t1} includes the polyconvex functions

$$\begin{aligned} J_6 &= \mathbf{C} : \mathbb{G}^{t1} : \mathbf{1} &= (\tilde{a}^2 + \tilde{b}^2)^2 (C_{11} + C_{22}) + \tilde{c}^4 C_{33}, \\ J_7 &= \text{Cof} \mathbf{C} : \mathbb{G}^{t1} : \mathbf{1} &= (\tilde{a}^2 + \tilde{b}^2)^2 (C_{22} C_{33} - C_{23}^2 + C_{11} C_{33} - C_{13}^2) + \tilde{c}^4 (C_{11} C_{22} - C_{12}^2), \\ J_8 &= \mathbf{C} : \mathbb{G}^{t1} : \mathbf{C} &= (\tilde{a}^4 + \tilde{b}^4) (C_{11}^2 + C_{22}^2) + 4 (\tilde{a}^3 \tilde{b} - \tilde{b}^3 \tilde{a}) (C_{12} (C_{11} - C_{22})) \\ &&+ 4 \tilde{a}^2 \tilde{b}^2 (C_{11} C_{22} + 2 C_{12}^2) + \tilde{c}^4 C_{33}^2. \end{aligned}$$

The terms $C_{11}C_{22} - C_{12}^2$ and $C_{11}C_{22} + 2C_{12}^2$, can be generated in terms of the elements of the *classical set of bilinear invariants* as follows

$$\begin{aligned} C_{11}C_{22} - C_{12}^2 &= \frac{1}{2} [((C_{11} + C_{22})^2) - (C_{11}^2 + C_{22}^2)] - \left[\frac{C_{12}(C_{11} - C_{22})(C_{11} + C_{22})}{(C_{11}^2 + C_{22}^2)} \right]^2, \\ C_{11}C_{22} + 2C_{12}^2 &= \frac{1}{2} [((C_{11} + C_{22})^2) - (C_{11}^2 + C_{22}^2)] + 2 \left[\frac{C_{12}(C_{11} - C_{22})(C_{11} + C_{22})}{(C_{11}^2 + C_{22}^2)} \right]^2. \end{aligned}$$

For tetragonal symmetry described by the material symmetry group \mathcal{G}_5 the evaluation of the polyconvex functions of the associated *family of polyconvex invariant functions* \mathcal{F}_p^{t2} yields

$$\begin{aligned} J_6 = \mathbf{C} : \mathbb{G}^{t2} : \mathbf{1} &= a^4 (C_{11} + C_{22}) + c^4 C_{33} \\ J_7 = \text{Cof} \mathbf{C} : \mathbb{G}^{t2} : \mathbf{1} &= a^4 (C_{22}C_{33} - C_{23}^2 + C_{11}C_{33} - C_{13}^2) + c^4 (C_{11}C_{22} - C_{12}^2) \\ J_8 = \mathbf{C} : \mathbb{G}^{t2} : \mathbf{C} &= a^4 (C_{11}^2 + C_{22}^2) + c^4 C_{33}^2, \end{aligned}$$

The term $C_{11}C_{22} - C_{12}^2$ can be derived by three elements of the *classical set of bilinear invariants* as follows

$$C_{11}C_{22} - C_{12}^2 = \frac{1}{2} [(C_{11} + C_{22})^2 - (C_{11}^2 + C_{22}^2)] - C_{12}^2.$$

Trigonal Families of Polyconvex Invariant Functions. The trigonal \mathcal{G}_8 -invariant functions depending on the structural tensor (6.42) and appearing in the corresponding trigonal *family of polyconvex invariant functions* \mathcal{F}_p^{ht1} read

$$\begin{aligned} J_6 = \mathbf{C} : \mathbb{G}^{ht1} : \mathbf{1} &= \left(\frac{1}{6} \tilde{a}^4 + \frac{1}{6} \tilde{b}^4 + \frac{1}{3} \tilde{a}^2 \tilde{b}^2 + \frac{1}{18} \tilde{a}^2 \tilde{c}^2 + \frac{1}{18} \tilde{b}^2 \tilde{c}^2 \right) (C_{11} + C_{22}) \\ &\quad + \left(\frac{1}{9} \tilde{a}^2 \tilde{c}^2 + \frac{1}{27} \tilde{a}^4 + \frac{1}{9} \tilde{b}^2 \tilde{c}^2 \right) C_{33}, \\ J_7 = \text{Cof} \mathbf{C} : \mathbb{G}^{ht1} : \mathbf{1} &= \left(\frac{1}{6} \tilde{a}^4 + \frac{1}{6} \tilde{b}^4 + \frac{1}{3} \tilde{a}^2 \tilde{b}^2 + \frac{1}{18} \tilde{a}^2 \tilde{c}^2 + \frac{1}{18} \tilde{b}^2 \tilde{c}^2 \right) (C_{11}C_{33} - C_{13}^2 \\ &\quad + C_{22}C_{33} - C_{23}^2) + \left(\frac{1}{9} \tilde{a}^2 \tilde{c}^2 + \frac{1}{27} \tilde{a}^4 + \frac{1}{9} \tilde{b}^2 \tilde{c}^2 \right) (C_{11}C_{22} - C_{12}^2), \\ J_8 = \mathbf{C} : \mathbb{G}^{ht1} : \mathbf{C} &= \left(\frac{1}{9} \tilde{a}^3 \sqrt{3} \tilde{c} - \frac{1}{3} \tilde{a} \sqrt{3} \tilde{b}^2 \tilde{c} \right) (C_{13}(C_{11} - C_{22}) - 2C_{12}C_{23}) \\ &\quad + \left(\frac{1}{9} \tilde{b}^3 \sqrt{3} \tilde{c} - \frac{1}{3} \tilde{b} \sqrt{3} \tilde{a}^2 \tilde{c} \right) (C_{23}(C_{11} - C_{22}) + 2C_{12}C_{13}) \\ &\quad + \frac{1}{8} (\tilde{a}^4 + \tilde{b}^4) (C_{11}^2 + C_{22}^2 + 2C_{12}^2) \\ &\quad + \frac{1}{12} (\tilde{a}^4 + \tilde{b}^4) (C_{11}C_{22} - C_{12}^2) \\ &\quad + \left(\frac{1}{9} \tilde{a}^2 \tilde{c}^2 + \frac{1}{9} \tilde{b}^2 \tilde{c}^2 \right) (C_{22}C_{33} + C_{11}C_{33} + 2C_{13}^2 + 2C_{23}^2) \\ &\quad + \frac{1}{27} \tilde{c}^4 C_{33}^2. \end{aligned}$$

Evaluating the polyconvex trigonal \mathcal{G}_9 -invariant functions of the corresponding trigonal

family of polyconvex invariant functions \mathcal{F}_p^{ht2} we get

$$\begin{aligned} J_6 = \mathbf{C} : \mathbb{G}^{ht2} : \mathbf{1} &= \left(\frac{1}{6}\tilde{b}^4 + \frac{1}{18}\tilde{b}^2\tilde{c}^2\right) (C_{11} + C_{22}) + \frac{1}{9}\tilde{b}^2\tilde{c}^2 C_{33}, \\ J_7 = \text{Cof} \mathbf{C} : \mathbb{G}^{ht2} : \mathbf{1} &= \left(\frac{1}{6}\tilde{b}^4 + \frac{1}{18}\tilde{b}^2\tilde{c}^2\right) (C_{11}C_{33} - C_{13}^2 + C_{22}C_{33} - C_{23}^2) \\ &\quad + \frac{1}{9}\tilde{b}^2\tilde{c}^2 (C_{11}C_{22} - C_{12}^2), \\ J_8 = \mathbf{C} : \mathbb{G}^{ht2} : \mathbf{C} &= \frac{1}{9}\tilde{b}^3\sqrt{3}\tilde{c} (C_{23}(C_{11} - C_{22}) + 2C_{12}C_{13}) \\ &\quad + \frac{1}{8}\tilde{b}^4 (C_{11}^2 + C_{22}^2 + 2C_{12}^2) \\ &\quad + \frac{1}{12}\tilde{b}^4 (C_{11}C_{22} - C_{12}^2) \\ &\quad + \frac{1}{9}\tilde{b}^2\tilde{c}^2 (C_{22}C_{33} + C_{11}C_{33} + 2C_{13}^2 + 2C_{23}^2) \\ &\quad + \frac{1}{27}\tilde{c}^4 C_{33}^2. \end{aligned}$$

With regard to the element $C_{11}C_{22} - C_{12}^2$ we also refer to (6.49).

Cubic Family of Polyconvex Invariant Functions. The polyconvex invariant functions with cubic structural tensor (6.48) of the cubic *family of polyconvex invariant functions* \mathcal{F}_p^c are in detail given by

$$\begin{aligned} J_6 = \mathbf{C} : \mathbb{G}^{t2} : \mathbf{1} &= a^4 (C_{11} + C_{22} + C_{33}) \\ J_7 = \text{Cof} \mathbf{C} : \mathbb{G}^{t2} : \mathbf{1} &= a^4 (C_{22}C_{33} - C_{23}^2 + C_{11}C_{33} - C_{13}^2 + C_{11}C_{22} - C_{12}^2) \\ J_8 = \mathbf{C} : \mathbb{G}^{t2} : \mathbf{C} &= a^4 (C_{11}^2 + C_{22}^2 + C_{33}^2). \end{aligned}$$

The second function can be formulated in terms of the elements of the *classical set of bilinear invariants* as follows:

$$\begin{aligned} (C_{22}C_{33} - C_{23}^2 + C_{11}C_{33} - C_{13}^2 + C_{11}C_{22} - C_{12}^2) = \\ \frac{1}{2}((C_{11} + C_{22} + C_{33})^2 - (C_{11}^2 + C_{22}^2 + C_{33}^2)) - (C_{12}^2 + C_{23}^2 + C_{13}^2). \end{aligned}$$

6.4 Polyconvex Material Models.

In general, we consider an additive decomposition of the free energy into an isotropic and an anisotropic part, i.e.,

$$\psi = \psi^{iso}(I_1, I_2, I_3) + \psi^{aniso}(\bar{J}_i), \quad \bar{J}_i \in \mathcal{F}_p = \{I_1, \dots, J_m\}. \quad (6.50)$$

The isotropic part ψ^{iso} depends on the three principal invariants I_1, I_2 and I_3 (4.10), whereas for the construction of the anisotropic part ψ^{aniso} both, principal and mixed invariants, can be considered. The values $\bar{J}_i \in \mathcal{F}_p = \{I_1, \dots, J_m\}$ represent the invariants of the corresponding *family of polyconvex invariant functions* \mathcal{F}_p (6.3) and (6.9), respectively. The second Piola-Kirchhoff stress tensor consists then of two parts

$$\begin{aligned} \mathbf{S} := \mathbf{S}^{iso} + \mathbf{S}^{aniso}, \text{ with } \mathbf{S}^{iso} &:= 2 \frac{\partial \psi^{iso}}{\partial \mathbf{C}} = 2 \sum_{i=1}^3 \frac{\partial \psi^{iso}}{\partial I_i} \frac{\partial I_i}{\partial \mathbf{C}} \\ \text{and } \mathbf{S}^{aniso} &:= 2 \frac{\partial \psi^{aniso}}{\partial \mathbf{C}} = 2 \sum_{i=1}^m \frac{\partial \psi^{aniso}}{\partial \bar{J}_i} \frac{\partial \bar{J}_i}{\partial \mathbf{C}}. \end{aligned} \quad (6.51)$$

The isotropic part of the stress tensor is computed by

$$\mathbf{S}^{iso} = 2 \left[\left(\frac{\partial \psi^{iso}}{\partial I_1} + \frac{\partial \psi^{iso}}{\partial I_2} I_1 \right) \mathbf{1} - \frac{\partial \psi^{iso}}{\partial I_2} \mathbf{C} + \frac{\partial \psi^{iso}}{\partial I_3} I_3 \mathbf{C}^{-1} \right]. \quad (6.52)$$

For the derivation of the material tangent tensor we write the tangent moduli as sum of an isotropic and anisotropic part as follows

$$\begin{aligned} \mathbb{C} &:= \mathbb{C}^{iso} + \mathbb{C}^{aniso}, \text{ with } \mathbb{C}^{iso} := 4 \frac{\partial^2 \psi^{iso}}{\partial \mathbf{C} \partial \mathbf{C}} = 2 \frac{\partial \mathbf{S}^{iso}}{\partial \mathbf{C}} \\ \text{and } \mathbb{C}^{aniso} &:= 4 \frac{\partial^2 \psi^{aniso}}{\partial \mathbf{C} \partial \mathbf{C}} = 2 \frac{\partial \mathbf{S}^{aniso}}{\partial \mathbf{C}}. \end{aligned} \quad (6.53)$$

The isotropic part of the tangent moduli is obtained from

$$\begin{aligned} \mathbb{C}^{iso} = 4 \left[\frac{\partial^2 \psi^{iso}}{\partial I_1 \partial I_1} \mathbf{1} \otimes \mathbf{1} + \frac{\partial \psi^{iso}}{\partial I_2} [\mathbf{1} \otimes \mathbf{1} - \mathbf{1} \boxtimes \mathbf{1}] + \frac{\partial^2 \psi^{iso}}{\partial I_2 \partial I_2} \{I_1 \mathbf{1} - \mathbf{C}\} \otimes \{I_1 \mathbf{1} - \mathbf{C}\} \right. \\ \left. + \frac{\partial \psi^{iso}}{\partial I_3} I_3 [\mathbf{C}^{-1} \otimes \mathbf{C}^{-1} - \mathbf{C}^{-1} \boxtimes \mathbf{C}^{-1}] + \frac{\partial^2 \psi^{iso}}{\partial I_3 \partial I_3} \text{Cof} \mathbf{C} \otimes \text{Cof} \mathbf{C} \right]. \end{aligned} \quad (6.54)$$

In the sequel, we choose for the isotropic part ψ^{iso} a compressible Mooney-Rivlin model of the form (5.102), i.e.,

$$\psi^{iso} = \alpha_1 I_1 + \alpha_2 I_2 + \delta_1 I_3 - \delta_2 \ln(\sqrt{I_3}), \quad \forall \alpha_1, \alpha_2, \delta_1, \delta_2 \geq 0, \quad (6.55)$$

which is polyconvex and coercive. For details, especially concerning the second Piola-Kirchhoff stress tensor \mathbf{S}^{iso} and the tangent moduli \mathbb{C}^{iso} , we refer to section 5.9.1. Suitable anisotropic parts ψ^{aniso} are introduced in the following sections.

Remark: In order to ensure the existence of minimizers, the energy function has to be sequentially weakly lower semicontinuous (s.w.l.s.) and coercive, cf. chapter 5. Polyconvexity directly implies s.w.l.s., but the coercivity condition has to be separately proven. Using only additively decomposed energy functions with positive additive terms and satisfying the coercivity condition of at least one additive term, then the whole energy is a priori coercive.

6.4.1 Material Models Based on Second-Order Structural Tensors. For the triclinic, monoclinic, rhombic as well as hexagonal/transversely isotropic symmetry groups the anisotropic part of the free energy function (6.50) appears as, cf. SCHRÖDER, NEFF & EBBING [106],

$$\psi^{aniso} = \sum_r^n \sum_j^m \psi_{rj}^{aniso}(I_3, J_{4j}, J_{5j}). \quad (6.56)$$

The mixed invariants in the anisotropic part (6.56) are defined by

$$J_{4j} = \text{tr}[\mathbf{C} \mathbf{G}_j], \quad J_{5j} = \text{tr}[\text{Cof}[\mathbf{C}] \mathbf{G}_j], \quad (6.57)$$

governed by the j -th metric tensor \mathbf{G}_j , which is in the triclinic case of the type

$$\mathbf{G}_j = \begin{bmatrix} a_j & d_j & e_j \\ d_j & b_j & f_j \\ e_j & f_j & c_j \end{bmatrix}, \quad \text{with} \quad a_j \geq 0, \quad a_j b_j - d_j^2 \geq 0, \quad \det[\mathbf{G}_j] \geq 0. \quad (6.58)$$

Furthermore, the trace of \mathbf{G}_j is denoted by

$$g_j := \text{tr}[\mathbf{G}_j], \quad \text{with} \quad g_j \geq 0. \quad (6.59)$$

The first and the second derivatives of the generic anisotropic invariants (6.57)₁ with respect to the right Cauchy-Green tensor are

$$\partial_C(\mathbf{G}_j : \mathbf{C}) = \mathbf{G}_j, \quad \partial_C^2(\mathbf{G}_j : \mathbf{C}) = \mathbf{0}. \quad (6.60)$$

The derivatives of (6.57)₂ are given by the expressions

$$\begin{aligned} \partial_C(\mathbf{G}_j : \text{Cof} \mathbf{C}) &= J_{5j} \mathbf{C}^{-1} - I_3 \mathbf{C}^{-1} \mathbf{G}_j \mathbf{C}^{-1}, \\ \partial_C^2(\mathbf{G}_j : \text{Cof} \mathbf{C}) &= J_{5j} \{ \mathbf{C}^{-1} \otimes \mathbf{C}^{-1} - \mathbf{C}^{-1} \boxtimes \mathbf{C}^{-1} \} \\ &\quad - \{ \text{Cof} \mathbf{C} \otimes \mathbf{C}^{-1} \mathbf{G}_j \mathbf{C}^{-1} + \mathbf{C}^{-1} \mathbf{G}_j \mathbf{C}^{-1} \otimes \text{Cof} \mathbf{C} \} \\ &\quad + \{ \text{Cof} \mathbf{C} \boxtimes \mathbf{C}^{-1} \mathbf{G}_j \mathbf{C}^{-1} + \mathbf{C}^{-1} \mathbf{G}_j \mathbf{C}^{-1} \boxtimes \text{Cof} \mathbf{C} \}. \end{aligned} \quad (6.61)$$

Hence the anisotropic stress tensor \mathbf{S}^{aniso} (6.51) is

$$\begin{aligned} \mathbf{S}^{aniso} &= 2 \sum_{r=1}^n \sum_{j=1}^m \left[\left(\frac{\partial \psi_{rj}^{aniso}}{\partial I_3} I_3 + \frac{\partial \psi_{rj}^{aniso}}{\partial J_{5j}} J_{5j} \right) \mathbf{C}^{-1} + \frac{\partial \psi_{rj}^{aniso}}{\partial J_{4j}} \mathbf{G}_j \right. \\ &\quad \left. - \frac{\partial \psi_{rj}^{aniso}}{\partial J_{5j}} I_3 \mathbf{C}^{-1} \mathbf{G}_j \mathbf{C}^{-1} \right]. \end{aligned} \quad (6.62)$$

The anisotropic part of the material tangent tensor (6.53) appears as

$$\mathbb{C}^{aniso} := \sum_r^n \sum_j^m \mathbb{C}_{rj}^{aniso} = \sum_r^n \sum_j^m 4 \frac{\partial \psi_{rj}^{aniso}}{\partial \mathbf{C} \partial \mathbf{C}}, \quad (6.63)$$

with

$$\begin{aligned}
\mathbb{C}_{rj}^{aniso} = 4 \bigg[& \frac{\partial \psi_{rj}^{aniso}}{\partial I_3} I_3 [\mathbf{C}^{-1} \otimes \mathbf{C}^{-1} - \mathbf{C}^{-1} \boxtimes \mathbf{C}^{-1}] + \frac{\partial^2 \psi_{rj}^{aniso}}{\partial I_3 \partial I_3} \text{Cof} \mathbf{C} \otimes \text{Cof} \mathbf{C} \\
& + \frac{\partial^2 \psi_{rj}^{aniso}}{\partial J_{4j} \partial J_{4j}} \mathbf{G}_j \otimes \mathbf{G}_j + \frac{\partial \psi_{rj}^{aniso}}{\partial J_{5j}} [J_{5j} \{\mathbf{C}^{-1} \otimes \mathbf{C}^{-1} - \mathbf{C}^{-1} \boxtimes \mathbf{C}^{-1}\} \\
& \quad - \{\text{Cof} \mathbf{C} \otimes \mathbf{C}^{-1} \mathbf{G}_j \mathbf{C}^{-1} + \mathbf{C}^{-1} \mathbf{G}_j \mathbf{C}^{-1} \otimes \text{Cof} \mathbf{C}\} \\
& \quad + \{\text{Cof} \mathbf{C} \boxtimes \mathbf{C}^{-1} \mathbf{G}_j \mathbf{C}^{-1} + \mathbf{C}^{-1} \mathbf{G}_j \mathbf{C}^{-1} \boxtimes \text{Cof} \mathbf{C}\}] \\
& + \frac{\partial^2 \psi_{rj}^{aniso}}{\partial J_{5j} \partial J_{5j}} \{J_{5j} \mathbf{C}^{-1} - I_3 \mathbf{C}^{-1} \mathbf{G}_j \mathbf{C}^{-1}\} \otimes \{J_{5j} \mathbf{C}^{-1} - I_3 \mathbf{C}^{-1} \mathbf{G}_j \mathbf{C}^{-1}\} \\
& + \frac{\partial^2 \psi_{rj}^{aniso}}{\partial I_3 \partial J_{4j}} [\text{Cof} \mathbf{C} \otimes \mathbf{G}_j + \mathbf{G}_j \otimes \text{Cof} \mathbf{C}] \\
& + \frac{\partial^2 \psi_{rj}^{aniso}}{\partial I_3 \partial J_{5j}} [\text{Cof} \mathbf{C} \otimes \{J_{5j} \mathbf{C}^{-1} - I_3 \mathbf{C}^{-1} \mathbf{G}_j \mathbf{C}^{-1}\} \\
& \quad + \{J_{5j} \mathbf{C}^{-1} - I_3 \mathbf{C}^{-1} \mathbf{G}_j \mathbf{C}^{-1}\} \otimes \text{Cof} \mathbf{C}] \bigg] , \tag{6.64}
\end{aligned}$$

where we take into account the symmetry of mixed derivatives, i.e., $\frac{\partial^2 \psi}{\partial I_i \partial I_j} = \frac{\partial^2 \psi}{\partial I_j \partial I_i}$, and neglect $\frac{\partial^2 \psi}{\partial J_i \partial J_j}$, with $i \neq j$.

Model Problem I. Suitable anisotropic energies in terms of individual polyconvex anisotropic functions $f_{4rj}(J_{4j})$, $f_{5rj}(J_{5j})$ are, e.g.,

$$\psi_I^{aniso} = \sum_{r=1}^n \sum_{j=1}^m [f_{4rj}(J_{4j}) + f_{5rj}(J_{5j})] , \tag{6.65}$$

cf. SCHRÖDER, NEFF & EBBING [106]. For this choice we obtain

$$\mathbf{S}_I^{aniso} = 2 \sum_{r=1}^n \sum_{j=1}^m \left[\frac{\partial f_{5rj}}{\partial J_{5j}} J_{5j} \mathbf{C}^{-1} + \frac{\partial f_{4rj}}{\partial J_{4j}} \mathbf{G}_j - \frac{\partial f_{5rj}}{\partial J_{5j}} I_3 \mathbf{C}^{-1} \mathbf{G}_j \mathbf{C}^{-1} \right] . \tag{6.66}$$

In order to satisfy the natural state condition of a stress-free reference configuration in the unloaded system we have to enforce that the second Piola-Kirchhoff stress tensor (6.51) at $\mathbf{C} = \mathbf{1}$ is equal to zero, i.e., $\mathbf{S}(\mathbf{C} = \mathbf{1}) = \mathbf{0}$. Hence, we get the two additional conditions

$$\begin{aligned}
& \left(\frac{\partial \psi^{iso}}{\partial I_1} + 2 \frac{\partial \psi^{iso}}{\partial I_2} + \frac{\partial \psi^{iso}}{\partial I_3} + \sum_{r=1}^n \sum_{j=1}^m \frac{\partial f_{5rj}}{\partial J_{5j}} g_j \right) \mathbf{1} = \mathbf{0} , \\
& \sum_{r=1}^n \sum_{j=1}^m \left[\frac{\partial f_{4rj}}{\partial J_{4j}} - \frac{\partial f_{5rj}}{\partial J_{5j}} \right] \mathbf{G}_j = \mathbf{0} ,
\end{aligned} \tag{6.67}$$

under consideration of the values (5.108) of the principal invariants and mixed invariants

$$J_{4j}(\mathbf{C} = \mathbf{1}) = J_{5j}(\mathbf{C} = \mathbf{1}) = g_j \tag{6.68}$$

at natural state. Evaluating (6.67)₁ with the special isotropic energy (6.55) at $\mathbf{C} = \mathbf{1}$ yields

$$\delta_2 = 2 \left(\alpha_1 + 2\alpha_2 + \delta_1 + \sum_{r=1}^n \sum_{j=1}^m \frac{\partial f_{5rj}}{\partial J_{5j}} g_j \right) \geq 0. \quad (6.69)$$

Equation (6.67)₂ has to be fulfilled for each metric tensor \mathbf{G}_j independently, thus we impose

$$\sum_{r=1}^n \left[\frac{\partial f_{4rj}}{\partial J_{4j}} - \frac{\partial f_{5rj}}{\partial J_{5j}} \right] = 0 \quad \forall \mathbf{G}_j. \quad (6.70)$$

A further more restrictive assumption is based on the enforcement of the latter for each constant r independently, i.e.,

$$\forall r : f'_{4rj} = f'_{5rj}. \quad (6.71)$$

Example 1: As first specific model problem we consider for the anisotropic part of (6.50) the anisotropic energy (6.65) with $r = j = 1$, denoted by $\psi_{I,1}^{aniso}$. We set $f_{41}(J_{41}) = f_4(J_4)$ and $f_{51}(J_{51}) = f_5(J_5)$ and choose

$$f_4(J_4) = \frac{1}{\alpha_4 g^{\alpha_4}} \eta_1 J_4^{\alpha_4}, \quad f_5(J_5) = \frac{1}{\alpha_4 g^{\alpha_4}} \eta_1 J_5^{\alpha_4}. \quad (6.72)$$

Therefore we obtain

$$\psi_{I,1}^{aniso} = \frac{1}{\alpha_4 g^{\alpha_4}} \eta_1 (J_4^{\alpha_4} + J_5^{\alpha_4}), \quad \forall \eta_1 \geq 0, \alpha_4 \geq 1. \quad (6.73)$$

Evaluating (6.51) with (6.52) and (6.55), (6.62) and (6.73) yields the second Piola-Kirchhoff stresses in the form

$$\begin{aligned} \mathbf{S}_{I,1} = 2 \left[(\alpha_1 + \alpha_2 I_1) \mathbf{1} - \alpha_2 \mathbf{C} + \left(\delta_1 I_3 - \frac{\delta_2}{2} + \frac{\partial \psi_{I,1}^{aniso}}{\partial J_5} J_5 \right) \mathbf{C}^{-1} \right. \\ \left. + \frac{\partial \psi_{I,1}^{aniso}}{\partial J_4} \mathbf{G} - \frac{\partial \psi_{I,1}^{aniso}}{\partial J_5} I_3 \mathbf{C}^{-1} \mathbf{G} \mathbf{C}^{-1} \right], \end{aligned} \quad (6.74)$$

with the first derivatives of (6.73) with respect to the mixed invariants J_4 and J_5

$$\frac{\partial \psi_{I,1}^{aniso}}{\partial J_4} = \frac{1}{g^{\alpha_4}} \eta_1 J_4^{\alpha_4-1}, \quad \frac{\partial \psi_{I,1}^{aniso}}{\partial J_5} = \frac{1}{g^{\alpha_4}} \eta_1 J_5^{\alpha_4-1}. \quad (6.75)$$

Let us first enforce the condition of a stress-free reference configuration, $\mathbf{S}_{I,1}(\mathbf{C} = \mathbf{1}) = \mathbf{0}$. At the natural state the values of the invariants are

$$J_4(\mathbf{C} = \mathbf{1}) = \text{tr} \mathbf{G} =: g, \quad J_5(\mathbf{C} = \mathbf{1}) = \text{tr} \mathbf{G} =: g, \quad (6.76)$$

together with (5.108) and hence, the stress tensor appears in the form

$$\begin{aligned} \mathbf{S}_{I,1}|_{\mathbf{C}=\mathbf{1}} = 2 \left[\underbrace{\left(\frac{\partial \psi^{iso}}{\partial I_1} + 2 \frac{\partial \psi^{iso}}{\partial I_2} + \frac{\partial \psi^{iso}}{\partial I_3} + \frac{\partial \psi_{I,1}^{aniso}}{\partial J_5} g \right)}_{:= x_1^* = 0} \mathbf{1} + \underbrace{\left(\frac{\partial \psi_{I,1}^{aniso}}{\partial J_4} - \frac{\partial \psi_{I,1}^{aniso}}{\partial J_5} \right)}_{:= x_2^* = 0} \mathbf{G} \right]. \end{aligned} \quad (6.77)$$

In this case the second condition, $x_2^* = 0$, is automatically fulfilled. Thus, only the first condition, $x_1^* = 0$, must be enforced, which leads to the dependent material parameter $\delta_2 \in \mathbb{R}_+$

$$\delta_2 = 2\alpha_1 + 4\alpha_2 + 2\delta_1 + 2\eta_1. \quad (6.78)$$

Example 2: As a second possible anisotropic function for the anisotropic part (6.65) of the material model problem (6.50) we consider

$$\psi_{I,2}^{aniso} = \eta_1 (J_4^{\alpha_4} + \beta_1 J_5^{\alpha_5}), \quad \forall \eta_1, \beta_1 \geq 0, \alpha_4, \alpha_5 \geq 1, \quad (6.79)$$

with the first derivatives with respect to J_4 and J_5

$$\frac{\partial \psi_{I,2}^{aniso}}{\partial J_4} = \alpha_4 \eta_1 J_4^{\alpha_4-1}, \quad \frac{\partial \psi_{I,2}^{aniso}}{\partial J_5} = \alpha_5 \eta_1 \beta_1 J_5^{\alpha_5-1}. \quad (6.80)$$

In order to satisfy the condition of a stress-free reference configuration $\mathbf{S}_{I,2}(\mathbf{C} = \mathbf{1}) = \mathbf{0}$, we have to meet both requirements, $x_1^* = 0$ and $x_2^* = 0$, given in (6.77) with $\psi_{I,2}^{aniso}$. Here we obtain the following dependencies between the isotropic and anisotropic material parameters

$$\begin{aligned} x_1^* = 0 : \quad & \left. \frac{\partial \psi_{I,2}^{aniso}}{\partial J_4} \right|_{C=1} = \left. \frac{\partial \psi_{I,2}^{aniso}}{\partial J_5} \right|_{C=1} \Rightarrow \beta_1 = \frac{\alpha_4}{\alpha_5} g^{\alpha_4 - \alpha_5}, \\ x_2^* = 0 : \quad & \delta_2 = 2\alpha_1 + 4\alpha_2 + 2\delta_1 + 2 \left. \frac{\partial \psi_{I,2}^{aniso}}{\partial J_5} J_5 \right|_{C=1} \\ & \Rightarrow \delta_2 = 2\alpha_1 + 4\alpha_2 + 2\delta_1 + 2\alpha_4 \eta_1 g^{\alpha_4}. \end{aligned} \quad (6.81)$$

Model Problem II. In order to obtain a free energy representation with a decoupling between the isotropic and anisotropic material parameters we consider a set of generic polyconvex functions in terms of I_3, J_{4j} and J_{5j} . We are interested in enforcing the stress-free reference configuration condition for the anisotropic energy term $\sum_{r,j} f'_{5rj} g_j \mathbf{1}$, appearing in (6.67)₁, independently for each r, j . In this situation (6.67)₁ and (6.69) appear in the form (5.109), i.e.,

$$\left(\frac{\partial \psi^{iso}}{\partial I_1} + 2 \frac{\partial \psi^{iso}}{\partial I_2} + \frac{\partial \psi^{iso}}{\partial I_3} \right) \mathbf{1} = \mathbf{0} \Rightarrow \delta_2 = 2(\alpha_1 + 2\alpha_2 + \delta_1). \quad (6.82)$$

The modification (6.82) for the condition of a stress-free reference configuration associated to the isotropic energy contributions (6.55) is possible, if we choose anisotropic energies like

$$\psi_{II}^{aniso} = \sum_{r=1}^n \sum_{j=1}^m [f_{3rj}(I_3) + f_{4rj}(J_{4j}) + f_{5rj}(J_{5j})]. \quad (6.83)$$

The second Piola-Kirchhoff stresses for the anisotropic energy contribution (6.83) denoted with $\mathbf{S}_{II}^{aniso} := 2\partial_C \psi_{II}^{aniso}$ are

$$\mathbf{S}_{II}^{aniso} = 2 \sum_{r=1}^n \sum_{j=1}^m \left[\left(\frac{\partial f_{3rj}}{\partial I_3} I_3 + \frac{\partial f_{5rj}}{\partial J_{5j}} J_{5j} \right) \mathbf{C}^{-1} + \frac{\partial f_{4rj}}{\partial J_{4j}} \mathbf{G}_j - \frac{\partial f_{5rj}}{\partial J_{5j}} I_3 \mathbf{C}^{-1} \mathbf{G}_j \mathbf{C}^{-1} \right]. \quad (6.84)$$

Let us enforce the natural state condition independently for (6.52) and (6.84). For the latter we get

$$\sum_{r=1}^n \sum_{j=1}^m \left[\left(\frac{\partial f_{3rj}}{\partial I_3} + \frac{\partial f_{5rj}}{\partial J_{5j}} g_j \right) \mathbf{1} + \left(\frac{\partial f_{4rj}}{\partial J_{4j}} - \frac{\partial f_{5rj}}{\partial J_{5j}} \right) \mathbf{G}_j \right] = \mathbf{0}, \quad (6.85)$$

with g_j defined in (6.59). In general we impose

$$\sum_{r=1}^n \sum_{j=1}^m \left(\frac{\partial f_{3rj}}{\partial I_3} + \frac{\partial f_{5rj}}{\partial J_{5j}} g_j \right) = 0 \quad \text{and} \quad \sum_{r=1}^n \left(\frac{\partial f_{4rj}}{\partial J_{4j}} - \frac{\partial f_{5rj}}{\partial J_{5j}} \right) = 0 \quad \forall \mathbf{G}_j, \quad (6.86)$$

or more restrictive for all r and j independently

$$\frac{\partial f_{5rj}}{\partial J_{5j}} g_j = -\frac{\partial f_{3rj}}{\partial I_3} \quad \text{and} \quad \frac{\partial f_{4rj}}{\partial J_{4j}} = \frac{\partial f_{5rj}}{\partial J_{5j}}. \quad (6.87)$$

Some specific functions which automatically satisfy (6.87) are, e.g.,

$$\begin{aligned} f_{4rj} &= \xi_{rj} \frac{1}{\alpha_{rj} + 1} \frac{1}{(g_j)^{\alpha_{rj}}} (J_{4j})^{\alpha_{rj}+1} & \text{with} & \quad f'_{4rj} = \xi_{rj} \frac{1}{(g_j)^{\alpha_{rj}}} (J_{4j})^{\alpha_{rj}}, \\ f_{5rj} &= \xi_{rj} \frac{1}{\beta_{rj} + 1} \frac{1}{(g_j)^{\beta_{rj}}} (J_{5j})^{\beta_{rj}+1} & \text{with} & \quad f'_{5rj} = \xi_{rj} \frac{1}{(g_j)^{\beta_{rj}}} (J_{5j})^{\beta_{rj}}, \\ f_{3rj} &= \xi_{rj} \frac{g_j}{\gamma_{rj}} (I_3)^{-\gamma_{rj}} & \text{with} & \quad f'_{3rj} = -\xi_{rj} g_j (I_3)^{-\gamma_{rj}-1}, \end{aligned} \quad (6.88)$$

with the second derivatives

$$\begin{aligned} f''_{4rj} &= \xi_{rj} \frac{1}{\alpha_{rj} (g_j)^{\alpha_{rj}}} (J_{4j})^{\alpha_{rj}-1}, & f''_{5rj} &= \xi_{rj} \frac{1}{\beta_{rj} (g_j)^{\beta_{rj}}} (J_{5j})^{\beta_{rj}-1}, \\ f''_{3rj} &= \xi_{rj} (\gamma_{rj} + 1) g_j (I_3)^{-\gamma_{rj}-2}, \end{aligned} \quad (6.89)$$

and the polyconvexity conditions

$$\xi_{rj} \geq 0, \quad \alpha_{rj} \geq 0, \quad \beta_{rj} \geq 0, \quad \gamma_{rj} \geq -1/2. \quad (6.90)$$

Considering (6.88) the final anisotropic energy in terms of I_3 , J_{4j} and J_{5j} reads

$$\begin{aligned} \psi_{II}^{aniso} &= \sum_{r=1}^n \sum_{j=1}^m \xi_{rj} \left[\frac{1}{\alpha_{rj} + 1} \frac{1}{(g_j)^{\alpha_{rj}}} (J_{4j})^{\alpha_{rj}+1} \right. \\ &\quad \left. + \frac{1}{\beta_{rj} + 1} \frac{1}{(g_j)^{\beta_{rj}}} (J_{5j})^{\beta_{rj}+1} + \frac{g_j}{\gamma_{rj}} (I_3)^{-\gamma_{rj}} \right], \end{aligned} \quad (6.91)$$

and the associated anisotropic stresses are given by the expression

$$\begin{aligned} \mathbf{S}_{II}^{aniso} &= \sum_{r=1}^n \sum_{j=1}^m 2\xi_{rj} \left[(-g_j I_3^{-\gamma_{rj}} + \frac{1}{(g_j)^{\beta_{rj}}} J_{5j}^{\beta_{rj}+1}) \mathbf{C}^{-1} + \frac{1}{(g_j)^{\alpha_{rj}}} J_{4j}^{\alpha_{rj}} \mathbf{G}_j \right. \\ &\quad \left. - \frac{1}{(g_j)^{\beta_{rj}}} J_{5j}^{\beta_{rj}} I_3 \mathbf{C}^{-1} \mathbf{G}_j \mathbf{C}^{-1} \right]. \end{aligned} \quad (6.92)$$

Furthermore, the term f_{3rj} in (6.88) can be replaced by the polyconvex term

$$f_{3rj} = -\xi_{rj} \ln(I_3^{g_j}), \quad \forall \xi \geq 0, \quad \text{with} \quad f'_{3rj} = -\xi_{rj} \frac{g_j}{I_3}. \quad (6.93)$$

Remark: The anisotropic free energy function (6.91) can be used stand-alone, i.e. the free energy function given in (6.50) can be considered without the isotropic term ψ^{iso} (6.55). The reason for this lies in the fact, that (6.91) is already sufficient for satisfying the coercivity condition (5.4). The proof of coercivity of the anisotropic energy function (6.91) is taken from SCHRÖDER, NEFF & EBBING [106]: Let us recall for symmetric, positive definite \mathbf{G}_j

$$\begin{aligned} g_j &= \text{tr} \mathbf{G}_j = \text{tr}[\mathbf{H}_j \mathbf{H}_j^T] = \|\mathbf{H}_j\|^2 > 0 \\ J_{4j} &= \text{tr}[\mathbf{C} \mathbf{G}_j] = \langle \mathbf{F}^T \mathbf{F}, \mathbf{H}_j \mathbf{H}_j^T \rangle = \langle \mathbf{F} \mathbf{H}_j, \mathbf{F} \mathbf{H}_j \rangle \\ &= \|\mathbf{F} \mathbf{H}_j\|^2 = \|\mathbf{H}_j^T \mathbf{F}^T\|^2 \geq \lambda_{\min}(\mathbf{H}_j \mathbf{H}_j^T) \|\mathbf{F}^T\|^2 = \lambda_{\min}(\mathbf{G}_j) \|\mathbf{F}\|^2, \\ J_{5j} &= \text{tr}[\text{Cof}[\mathbf{C}] \mathbf{G}_j] = \langle \text{Cof} \mathbf{F}^T \text{Cof} \mathbf{F} \mathbf{H}_j \mathbf{H}_j^T \rangle = \langle \text{Cof}[\mathbf{F}] \mathbf{H}_j, \text{Cof}[\mathbf{F}] \mathbf{H}_j \rangle \\ &= \|\text{Cof}[\mathbf{F}] \mathbf{H}_j\|^2 = \|\mathbf{H}_j^T \text{Cof} \mathbf{F}^T\|^2 \geq \lambda_{\min}(\mathbf{H}_j \mathbf{H}_j^T) \|\text{Cof} \mathbf{F}^T\|^2 \\ &= \lambda_{\min}(\mathbf{G}_j) \|\text{Cof} \mathbf{F}\|^2, \\ I_3 &= \det \mathbf{C} = (\det \mathbf{F})^2 \leq \frac{1}{3\sqrt{3}} \|\text{Cof} \mathbf{F}\|^3; \end{aligned} \quad (6.94)$$

for the last inequality see HARTMANN & NEFF [57]. Since \mathbf{G}_j is here assumed to be strictly positive definite we know that the smallest eigenvalue $\lambda_{\min}(\mathbf{G}_j) > 0$ is strictly positive. With these preliminaries let us proceed to show that the anisotropic energy ψ_{II}^{aniso} satisfies a local coercivity condition, which is needed, together with polyconvexity of ψ_{II}^{aniso} to ensure the existence of global energy. More precisely, by local coercivity we mean an estimate of the type, see BALL [10],

$$\forall \mathbf{F} \in \mathbb{R}^{3 \times 3} : \quad \psi_{II}^{aniso}(\mathbf{F}) \geq C_1 (\|\mathbf{F}\|^p + \|\text{Cof} \mathbf{F}\|^q) - C_2, \quad p \geq 2, \quad q \geq \frac{3}{2}, \quad (6.95)$$

with constants $C_1 > 0$ and $C_2 \geq 0$. The function ψ_{II}^{aniso} has the generic form (taking only the relevant structure into account, i.e. setting $\alpha_{rj} = \alpha$, $\beta_{rj} = \beta$, $\gamma_{rj} = \gamma$, $g_j = g$, $J_{4j} = J_4$, $J_{5j} = J_5$)

$$\psi_{II}^{aniso}(\mathbf{F}) = \frac{1}{1+\alpha} \frac{1}{g^\alpha} J_4^{1+\alpha} + \frac{1}{1+\beta} \frac{1}{g^\beta} J_5^{1+\beta} + \frac{g}{\gamma} I_3^{-\gamma}. \quad (6.96)$$

Thus it follows easily, taking the relations (6.94) into account, that for $\alpha, \beta \geq 0$

$$\begin{aligned} \psi_{II}^{aniso}(\mathbf{F}) &\geq \frac{1}{1+\alpha} \frac{1}{g^\alpha} J_4 + \frac{1}{1+\beta} \frac{1}{g^\beta} J_5 + \frac{g}{\gamma} I_3^{-\gamma} \\ &\geq \frac{1}{1+\alpha} \frac{1}{g^\alpha} \lambda_{\min}(\mathbf{G}_j) \|\mathbf{F}\|^2 + \frac{1}{1+\beta} \frac{1}{g^\beta} \lambda_{\min}(\mathbf{G}_j) \|\text{Cof} \mathbf{F}\|^2 + \frac{g}{\gamma} I_3^{-\gamma} \\ &= c_1^+ \|\mathbf{F}\|^2 + c_2^+ \|\text{Cof} \mathbf{F}\|^2 + \frac{g}{\gamma} (\det \mathbf{F})^{-2\gamma}, \end{aligned} \quad (6.97)$$

for some given constants $c_1^+, c_2^+ > 0$. In case that γ is positive we have shown (6.95) with $C_1 = \min(c_1^+, c_2^+)$, $C_2 = 0$ and $p = q = 2$. In the case where γ is negative with $0 \geq \gamma \geq -\frac{1}{2}$ we may continue estimating

$$\begin{aligned} \psi_{II}^{aniso}(\mathbf{F}) &\geq c_1^+ \|\mathbf{F}\|^2 + c_2^+ \|\text{Cof} \mathbf{F}\|^2 + \frac{g}{\gamma} (\det \mathbf{F})^{-2\gamma}, \\ &\geq c_1^+ \|\mathbf{F}\|^2 + c_2^+ \|\text{Cof} \mathbf{F}\|^2 - c_3^+ (\det \mathbf{F})^{-2\gamma}, \\ &= c_1^+ \|\mathbf{F}\|^2 + c_2^+ \|\text{Cof} \mathbf{F}\|^2 - c_3^+ ((\det \mathbf{F})^2)^{|\gamma|}, \\ &\geq c_1^+ \|\mathbf{F}\|^2 + c_2^+ \|\text{Cof} \mathbf{F}\|^2 - c_3^+ [\det \mathbf{F} + 1], \quad 0 \leq |\gamma| \leq \frac{1}{2} \\ &\geq c_1^+ \|\mathbf{F}\|^2 + c_2^+ \|\text{Cof} \mathbf{F}\|^2 - c_3^+ \left[\frac{1}{\sqrt{3\sqrt{3}}} \|\text{Cof} \mathbf{F}\|^{\frac{3}{2}} + 1 \right]. \end{aligned} \quad (6.98)$$

It is obvious that for all $k_1, k_2 > 0$ there exist numbers $\tilde{k}_1, \tilde{k}_2 > 0$ such that

$$\forall x \in \mathbb{R}_+ : \quad k_1 x^2 - k_2 x^{3/2} \geq \tilde{k}_1 x^{3/2} - \tilde{k}_2. \quad (6.99)$$

Applying this reasoning on $x = \|\text{Cof} \mathbf{F}\|$ yields the existence of numbers $C_2^+, C_3^+ > 0$ such that

$$\begin{aligned} \psi_{II}^{aniso}(\mathbf{F}) &\geq c_1^+ \|\mathbf{F}\|^2 + c_2^+ \|\text{Cof} \mathbf{F}\|^2 - c_3^+ \left[\frac{1}{\sqrt{3\sqrt{3}}} \|\text{Cof} \mathbf{F}\|^{\frac{3}{2}} + 1 \right] \\ &\geq c_1^+ \|\mathbf{F}\|^2 + C_2^+ \|\text{Cof} \mathbf{F}\|^{3/2} - C_3^+. \end{aligned} \quad (6.100)$$

This shows local coercivity with $C_1 = \min(c_1^+, C_2^+)$ and $p = 2$ and $q = \frac{3}{2}$ also for $0 \geq \gamma \geq -\frac{1}{2}$.^{17.)}

Model Problem III. Further anisotropic polyconvex functions for (6.50), automatically satisfying the condition of a stress-free reference configuration, are

$$\psi_{III}^{aniso} = \sum_{r=1}^n \sum_{j=1}^m [f_{3rj}(I_3) + f_{6rj}(I_3, J_{4j}) + f_{7rj}(I_3, J_{5j})]. \quad (6.101)$$

The second Piola-Kirchhoff stresses $\mathbf{S}_{III}^{aniso} := 2\partial_C \psi_{III}^{aniso}$ are then given by

$$\begin{aligned} \mathbf{S}_{III}^{aniso} &= 2 \sum_{r=1}^n \sum_{j=1}^m \left[\left(\frac{\partial f_{3rj}}{\partial I_3} I_3 + \frac{\partial f_{6rj}}{\partial I_3} I_3 + \frac{\partial f_{7rj}}{\partial I_3} I_3 + \frac{\partial f_{7rj}}{\partial J_{5j}} J_{5j} \right) \mathbf{C}^{-1} \right. \\ &\quad \left. + \frac{\partial f_{6rj}}{\partial J_{4j}} \mathbf{G}_j - \frac{\partial f_{7rj}}{\partial J_{5j}} I_3 \mathbf{C}^{-1} \mathbf{G}_j \mathbf{C}^{-1} \right]. \end{aligned} \quad (6.102)$$

^{17.)} An attractive way to account a priori for a stress-free reference configuration without dependencies between isotropic and anisotropic material parameters was proposed in ITSKOV & AKSEL [64]. There, the energy function depends on the classical structural tensor (4.26). The polyconvexity of the individual terms appearing in the energy are first documented in [103, 104]. However, there the energy function is only introduced for the description of the most simple anisotropies, namely transverse isotropy and orthotropy.

Again enforcing $\mathbf{S}(\mathbf{C} = \mathbf{1}) = \mathbf{S}^{iso}(\mathbf{C} = \mathbf{1}) + \mathbf{S}^{aniso}(\mathbf{C} = \mathbf{1}) = \mathbf{0}$ with the more restrictive assumptions $\mathbf{S}^{iso}(\mathbf{C} = \mathbf{1}) = \mathbf{0}$, given by (6.82), and $\mathbf{S}^{aniso}(\mathbf{C} = \mathbf{1}) = \mathbf{S}_{III}^{aniso}(\mathbf{C} = \mathbf{1}) = \mathbf{0}$ yields for the anisotropic part

$$2 \sum_{r=1}^n \sum_{j=1}^m \left[\left(\frac{\partial f_{3rj}}{\partial I_3} + \frac{\partial f_{6rj}}{\partial I_3} + \frac{\partial f_{7rj}}{\partial I_3} + \frac{\partial f_{7rj}}{\partial J_{5j}} g_j \right) \mathbf{1} + \left(\frac{\partial f_{6rj}}{\partial J_{4j}} - \frac{\partial f_{7rj}}{\partial J_{5j}} \right) \mathbf{G}_j \right] = \mathbf{0}. \quad (6.103)$$

For the independent tensor generators $\mathbf{1}$ and \mathbf{G}_j for $j = 1, \dots, m$ the following identities have to be satisfied

$$\frac{\partial f_{3rj}}{\partial I_3} + \frac{\partial f_{6rj}}{\partial I_3} + \frac{\partial f_{7rj}}{\partial I_3} = -\frac{\partial f_{7rj}}{\partial J_{5j}} g_j, \quad \text{and} \quad \frac{\partial f_{6rj}}{\partial J_{4j}} = \frac{\partial f_{7rj}}{\partial J_{5j}} \quad \forall r, j. \quad (6.104)$$

Some specific functions and their derivatives which automatically satisfy (6.104)₂ are

$$\begin{aligned} f_{6rj} &= \frac{J_{4j}^{\alpha_{rj}}}{I_3^{1/3}}, & \frac{\partial f_{6rj}}{\partial I_3} &= -\frac{1}{3} I_3^{-4/3} J_{4j}^{\alpha_{rj}}, & \frac{\partial f_{6rj}}{\partial J_{4j}} &= \alpha_{rj} J_{4j}^{\alpha_{rj}-1} I_3^{-1/3}, \\ f_{7rj} &= \frac{J_{5j}^{\alpha_{rj}}}{I_3^{1/3}}, & \frac{\partial f_{7rj}}{\partial I_3} &= -\frac{1}{3} I_3^{-4/3} J_{5j}^{\alpha_{rj}}, & \frac{\partial f_{7rj}}{\partial J_{5j}} &= \alpha_{rj} J_{5j}^{\alpha_{rj}-1} I_3^{-1/3}, \end{aligned} \quad (6.105)$$

with $\alpha_{rj} \geq 1$. For the function $f_{3rj}(I_3)$ we may use

$$f_{3rj} = \frac{g_j^{\alpha_{rj}}}{\beta_{rj}} I_3^{-\beta_{rj}}, \quad \frac{\partial f_{3rj}}{\partial I_3} = -g_j^{\alpha_{rj}} I_3^{-\beta_{rj}-1}, \quad \text{with} \quad \beta_{rj} \geq -1/2; \quad (6.106)$$

inserting (6.105) and (6.106) into (6.104)₁ leads directly to the material parameter α_{rj} , i.e., $\alpha_{rj} = \frac{5}{3}$. Alternatively we can consider the function

$$f_{3rj} = -g_j^{\alpha_{rj}} \beta_{rj} \ln(I_3), \quad \frac{\partial f_{3rj}}{\partial I_3} = -\beta_{rj} \frac{g_j^{\alpha_{rj}}}{I_3} \quad \text{with} \quad \alpha_{rj} \geq 1; \quad (6.107)$$

using (6.105) and (6.107) in (6.104)₁ we obtain the restriction $\beta_{rj} = \alpha_{rj} - \frac{2}{3}$. Based on the aforementioned analysis of different anisotropic polyconvex energies we summarize 4 suitable explicit functions in Table 6.1, which a priori satisfy the stress-free reference configuration condition.

6.4.2 Material Models Based on Fourth-Order Structural Tensors. For the description of the tetragonal, trigonal and cubic symmetry groups anisotropic functions based on fourth-order structural tensors are needed. The anisotropic energy function (6.50) is taken in the form

$$\psi^{aniso} = \sum_{r=1}^n \sum_{j=1}^m \psi_{rj}^{aniso}(I_3, J_{6j}, J_{7j}, J_{8j}). \quad (6.108)$$

The generic mixed invariants are given by

$$J_{6j} = \mathbf{1} : \mathbb{G}_j : \mathbf{C}, \quad J_{7j} = \mathbf{1} : \mathbb{G}_j : \text{Cof} \mathbf{C}, \quad J_{8j} = \mathbf{C} : \mathbb{G}_j : \mathbf{C}, \quad (6.109)$$

Table 6.1: Polyconvex Anisotropic Energy Functions Satisfying the Stress-Free Reference Configuration Condition.

| |
|---|
| $\psi_1^{aniso} = \sum_{r=1}^n \sum_{j=1}^m \xi_{rj} \left[\frac{1}{\alpha_{rj} + 1} \frac{1}{(g_j)^{\alpha_{rj}}} (J_{4j})^{\alpha_{rj}+1} \right. \\ \left. + \frac{1}{\beta_{rj} + 1} \frac{1}{(g_j)^{\beta_{rj}}} (J_{5j})^{\beta_{rj}+1} + \frac{g_j}{\gamma_{rj}} (I_3)^{-\gamma_{rj}} \right]$ <p>with $\xi_{rj} \geq 0, \quad \alpha_{rj} \geq 0, \quad \beta_{rj} \geq 0, \quad \gamma_{rj} \geq -1/2$</p> |
| $\psi_2^{aniso} = \sum_{r=1}^n \sum_{j=1}^m \xi_{rj} \left[\frac{1}{\alpha_{rj} + 1} \frac{1}{(g_j)^{\alpha_{rj}}} (J_{4j})^{\alpha_{rj}+1} \right. \\ \left. + \frac{1}{\beta_{rj} + 1} \frac{1}{(g_j)^{\beta_{rj}}} (J_{5j})^{\beta_{rj}+1} - \ln(I_3^{g_j}) \right]$ <p>with $\xi_{rj} \geq 0, \quad \alpha_{rj} \geq 0, \quad \beta_{rj} \geq 0$</p> |
| $\psi_3^{aniso} = \sum_{r=1}^n \sum_{j=1}^m \left[\frac{J_{4j}^{\alpha_{rj}}}{I_3^{1/3}} + \frac{J_{5j}^{\alpha_{rj}}}{I_3^{1/3}} + \frac{g_j^{\alpha_{rj}}}{\beta_{rj}} I_3^{-\beta_{rj}} \right]$ <p>with $\alpha_{rj} = 5/3, \quad \beta_{rj} \geq -1/2$</p> |
| $\psi_4^{aniso} = \sum_{r=1}^n \sum_{j=1}^m \left[\frac{J_{4j}^{\alpha_{rj}}}{I_3^{1/3}} + \frac{J_{5j}^{\alpha_{rj}}}{I_3^{1/3}} - g_j^{\alpha_{rj}} \beta_{rj} \ln(I_3) \right]$ <p>with $\alpha_{rj} \geq 1, \quad \beta_{rj} = \alpha_{rj} - 2/3$</p> |

with the j -th structural tensor \mathbb{G}_j . For example in the tetragonal \mathcal{G}_5 case we have

$$\mathbb{G}_j = \text{diag}[a_j^4, a_j^4, c_j^4, 0, 0, 0]. \quad (6.110)$$

Furthermore, the invariants at the natural state, i.e., at $\mathbf{C} = \mathbf{1}$, appear as

$$J_{6j}(\mathbf{C} = \mathbf{1}) = J_{7j}(\mathbf{C} = \mathbf{1}) = J_{8j}(\mathbf{C} = \mathbf{1}) = \mathbf{1} : \mathbb{G}_j : \mathbf{1} =: m_j. \quad (6.111)$$

The anisotropic second Piola-Kirchhoff stresses of (6.51) are $\mathbf{S}^{aniso} = 2\partial_{\mathbf{C}}\psi^{aniso}$, with

$$\mathbf{S}^{aniso} = 2 \sum_{r=1}^n \sum_{j=1}^m \left[\left(\frac{\partial \psi_{rj}^{aniso}}{\partial I_3} I_3 + \frac{\partial \psi_{rj}^{aniso}}{\partial J_{7j}} J_{7j} \right) \mathbf{C}^{-1} + \frac{\partial \psi_{rj}^{aniso}}{\partial J_{6j}} (\mathbb{G}_j : \mathbf{1}) \right. \\ \left. - \frac{\partial \psi_{rj}^{aniso}}{\partial J_{7j}} I_3 \mathbf{C}^{-1} (\mathbb{G}_j : \mathbf{1}) \mathbf{C}^{-1} + 2 \frac{\partial \psi_{rj}^{aniso}}{\partial J_{8j}} (\mathbb{G}_j : \mathbf{C}) \right]. \quad (6.112)$$

The anisotropic part of the material tangent tensor is

$$\begin{aligned}
\mathbb{C}_{rj}^{aniso} = & 4 \left[\frac{\partial \psi_{rj}^{aniso}}{\partial I_3} I_3 [\mathbf{C}^{-1} \otimes \mathbf{C}^{-1} - \mathbf{C}^{-1} \boxtimes \mathbf{C}^{-1}] + \frac{\partial^2 \psi_{rj}^{aniso}}{\partial I_3 \partial I_3} \text{Cof} \mathbf{C} \otimes \text{Cof} \mathbf{C} \right. \\
& + \frac{\partial^2 \psi_{rj}^{aniso}}{\partial J_{6j} \partial J_{6j}} (\mathbb{G}_j : \mathbf{1}) \otimes (\mathbb{G}_j : \mathbf{1}) + \frac{\partial \psi_{rj}^{aniso}}{\partial J_{7j}} [J_{7j} \{\mathbf{C}^{-1} \otimes \mathbf{C}^{-1} - \mathbf{C}^{-1} \boxtimes \mathbf{C}^{-1}\} \\
& - \{\text{Cof} \mathbf{C} \otimes \mathbf{C}^{-1} (\mathbb{G}_j : \mathbf{1}) \mathbf{C}^{-1} + \mathbf{C}^{-1} (\mathbb{G}_j : \mathbf{1}) \mathbf{C}^{-1} \otimes \text{Cof} \mathbf{C}\} \\
& + \{\text{Cof} \mathbf{C} \boxtimes \mathbf{C}^{-1} (\mathbb{G}_j : \mathbf{1}) \mathbf{C}^{-1} + \mathbf{C}^{-1} (\mathbb{G}_j : \mathbf{1}) \mathbf{C}^{-1} \boxtimes \text{Cof} \mathbf{C}\}] \\
& + \frac{\partial^2 \psi_{rj}^{aniso}}{\partial J_{7j} \partial J_{7j}} \{J_{7j} \mathbf{C}^{-1} - I_3 \mathbf{C}^{-1} (\mathbb{G}_j : \mathbf{1}) \mathbf{C}^{-1}\} \otimes \{J_{7j} \mathbf{C}^{-1} - I_3 \mathbf{C}^{-1} (\mathbb{G}_j : \mathbf{1}) \mathbf{C}^{-1}\} \\
& \left. + \frac{\partial \psi_{rj}^{aniso}}{\partial J_{8j}} 2 \mathbb{G}_j + \frac{\partial^2 \psi_{rj}^{aniso}}{\partial J_{8j} \partial J_{8j}} 2 (\mathbb{G}_j : \mathbf{C}) \otimes 2 (\mathbb{G}_j : \mathbf{C}) \right], \tag{6.113}
\end{aligned}$$

where no derivatives of the type $\frac{\partial^2 \psi}{\partial I_3 \partial J_j}$, $j = 6, 7, 8$, $\frac{\partial^2 \psi}{\partial J_i \partial J_j}$, $i \neq j$ are taken into account.

Model Problem Based on Additive Decomposition of ψ . As specific function for the description of the anisotropy groups \mathcal{G}_4 , \mathcal{G}_5 and \mathcal{G}_7 , \mathcal{G}_8 , \mathcal{G}_9 we choose the anisotropic part (6.108) of (6.50) as

$$\psi^{aniso} = \sum_{r=1}^n \sum_{j=1}^m [f_{6rj}(J_{6j}) + f_{7rj}(J_{7j}) + f_{8rj}(J_{8j}) + f_{3rj}(I_3)], \tag{6.114}$$

with the polyconvex functions

$$\begin{aligned}
f_{6rj}(J_{6j}) &= \frac{\xi_{rj}}{(\alpha_{rj} + 1) m_j^{\alpha_{rj}}} J_{6j}^{(\alpha_{rj} + 1)}, \quad f_{7rj}(J_{7j}) = \frac{3 \xi_{rj}}{(\beta_{rj} + 1) m_j^{\beta_{rj}}} J_{7j}^{(\beta_{rj} + 1)}, \\
f_{8rj}(J_{8j}) &= \frac{\xi_{rj}}{(\eta_{rj} + 1) m_j^{\eta_{rj}}} J_{8j}^{(\eta_{rj} + 1)}, \quad f_{3rj}(I_3) = \xi_{rj} \frac{3 m_j}{\gamma_{rj}} I_3^{-\gamma_{rj}}, \tag{6.115}
\end{aligned}$$

where the polyconvexity restrictions

$$\alpha_{rj}, \beta_{rj}, \eta_{rj}, \xi_{rj} \geq 0, \gamma_{rj} \geq -\frac{1}{2} \tag{6.116}$$

are taken into account. The first and second derivatives of the individual functions are

$$\begin{aligned}
f'_{6rj} &= \frac{\xi_{rj}}{m_j^{\alpha_{rj}}} J_{6j}^{\alpha_{rj}}, & f''_{6rj} &= \frac{\xi_{rj}}{\alpha_{rj} m_j^{\alpha_{rj}}} J_{6j}^{\alpha_{rj}-1}, \\
f'_{7rj} &= \frac{3 \xi_{rj}}{m_j^{\beta_{rj}}} J_{7j}^{\beta_{rj}}, & f''_{7rj} &= \frac{3 \xi_{rj}}{\beta_{rj} m_j^{\beta_{rj}}} J_{7j}^{\beta_{rj}-1}, \\
f'_{8rj} &= \frac{\xi_{rj}}{m_j^{\eta_{rj}}} J_{8j}^{\eta_{rj}}, & f''_{8rj} &= \frac{\xi_{rj}}{\eta_{rj} m_j^{\eta_{rj}}} J_{8j}^{\eta_{rj}-1}, \\
f'_{3rj} &= -3 \xi_{rj} m_j (I_3)^{-\gamma_{rj}-1}, & f''_{3rj} &= 3 \xi_{rj} (\gamma_{rj} + 1) m_j (I_3)^{-\gamma_{rj}-2}. \tag{6.117}
\end{aligned}$$

The second Piola-Kirchhoff stresses at the natural state, which are here automatically equal to zero, i.e., $\mathbf{S} = 2\partial_C\psi|_{C=1} = \mathbf{S}^{iso}|_{C=1} + \mathbf{S}^{aniso}|_{C=1} = \mathbf{0}$, are obtained by (5.109) or (6.82) and

$$\begin{aligned} \mathbf{S}^{aniso}|_{C=1} = & 2 \sum_{r=1}^n \sum_{j=1}^m \left[\left(\frac{\partial \psi_{rj}^{aniso}}{\partial I_3} + \frac{\partial \psi_{rj}^{aniso}}{\partial J_{7j}} m_j \right) \mathbf{1} \right. \\ & \left. + \left(\frac{\partial \psi_{rj}^{aniso}}{\partial J_{6j}} - \frac{\partial \psi_{rj}^{aniso}}{\partial J_{7j}} + 2 \frac{\partial \psi_{rj}^{aniso}}{\partial J_{8j}} \right) (\mathbb{G}_j : \mathbf{1}) \right]. \end{aligned} \quad (6.118)$$

Inserting the partial derivatives of the individual functions (6.115) with respect to the invariants yields

$$\begin{aligned} \mathbf{S}^{aniso}|_{C=1} = 2\partial_C\psi^{aniso}|_{C=1} = & \sum_{r=1}^n \sum_{j=1}^m 2\xi_{rj} \left[(-3m_j + \frac{3}{(m_j)^{\beta_{rj}}} m_j^{\beta_{rj}+1}) \mathbf{1} \right. \\ & \left. + (\frac{1}{(m_j)^{\alpha_{rj}}} m_j^{\alpha_{rj}} - \frac{3}{(m_j)^{\beta_{rj}}} m_j^{\beta_{rj}} + \frac{2}{(m_j)^{\eta_{rj}}} m_j^{\eta_{rj}}) (\mathbb{G}_j : \mathbf{1}) \right] = \mathbf{0}. \end{aligned} \quad (6.119)$$

7 Numerical Examples.

With regard to the modeling of anisotropic material behavior at finite strains using polyconvex energy functions there exist many publications in the literature: applications in the field of biomechanics are e.g. documented in BALZANI [11], BALZANI, NEFF, SCHRÖDER & HOLZAPFEL [105], EHRET, ITSKOV & MAVRILLAS [65], EHRET & ITSKOV [51]; the modeling of thin shells can be found e.g. in BALZANI, GRUTTMANN & SCHRÖDER [12] and in BALZANI, SCHRÖDER & NEFF [13].

In this chapter we present the capability of the proposed polyconvex energy functions to simulate anisotropy effects within several numerical examples ranging from biaxial tension tests of anisotropic materials to applications in configurational mechanics. First, we illustrate the usefulness of the introduced polyconvex material models within homogeneous biaxial tension tests of a transversely isotropic material. Thereby, we illustrate that the model fulfill the important physically reasonable growth conditions (5.3), cf. SCHRÖDER, NEFF & EBBING [106]. Furthermore, the results of the well-known Cook's membrane problem, obtained by using the introduced polyconvex functions, are documented. In SCHRÖDER [101] the same analysis is done, but based on the classical structural tensor $\mathbf{M} = \mathbf{a} \otimes \mathbf{a}$. Here, we show the same results by replacing \mathbf{M} with the corresponding metric tensor. We present moreover in this chapter the *completeness* (in the sense of the definition given in section 4.5) of the proposed polyconvex energy functions.

Second, we focus on the simulation of fiber-reinforced composites, where the anisotropic hyperelastic behavior of such composites is micro- as well as macromechanically modeled by polyconvex energies. Corresponding publications are EBBING, SCHRÖDER, NEFF & GRUTTMANN [49] and EBBING ET AL. [44]. Furthermore, we apply a polyconvex energy in the field of configurational mechanics; details are given in EBBING, SCHRÖDER, STEINMANN & NEFF [50].

7.1 Homogeneous Biaxial Tension Test.

(The following analysis is first published in SCHRÖDER, NEFF & EBBING [106].)

We perform a deformation driven homogeneous biaxial compression/tension test of a transversely isotropic material. The unit cube is discretized with one eight-noded standard displacement element. The deformed configuration and the boundary conditions are depicted in Figure 7.1. The specimen is equally stretched in x_1 - and x_2 -direction, where the biaxial stretches are driven in the range of $\lambda = 0.2$ up to $\lambda = 2.3$; the stretches are defined by $\lambda = (l_1 + u_1)/l_1 = (l_2 + u_2)/l_2$.

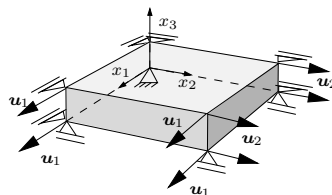


Figure 7.1: Boundary conditions of the homogeneous biaxial compression/tension test.

The preferred direction of the material is oriented parallel to the x_1 -direction. We take two transversely isotropic energy functions into account, first the energy function (6.50) with the anisotropic part (6.73), i.e.,

$$\psi_I^{ti} = \psi^{iso} + \psi_{I,1}^{aniso} \quad (7.1)$$

and second the energy function (6.50) with the anisotropic part (6.79), i.e.,

$$\psi_{II}^{ti} = \psi^{iso} + \psi_{I,2}^{aniso}. \quad (7.2)$$

Furthermore, we choose a unimodular transversely isotropic metric tensor \mathbf{G}^{ti} of the type

$$\mathbf{G}^{ti} = \text{diag} \left[\gamma_1^2, \frac{1}{\gamma_1}, \frac{1}{\gamma_1} \right]. \quad (7.3)$$

For the simulation we use the material parameters listed in Table 7.1. The documented Young's moduli are calculated from the coefficients of the inverse fourth-order elasticity tensor at the reference configuration:

$$E_1 = 1/\mathbb{C}_{1111}^{-1} \quad \text{and} \quad E_2 = 1/\mathbb{C}_{2222}^{-1}.$$

Table 7.1: Table of material parameters (MP) and Young's moduli (YM).

| | ψ_I^{ti} | | ψ_{II}^{ti} | |
|--------------|---------------|--------|------------------|----------|
| γ_1 | 2.0 | 20.0 | 2.0 | 5.0 |
| α_1 | 8.0 | 8.0 | 8.0 | 8.0 |
| α_2 | 0.0 | 0.0 | 0.0 | 0.0 |
| δ_1 | 10.0 | 10.0 | 10.0 | 10.0 |
| (δ_2) | 56.0 | 56.0 | 786.0 | 9868.24 |
| η_1 | 10.0 | 10.0 | 1.0 | 0.1 |
| (β_1) | - | - | 7.50 | 38.10 |
| α_4 | 2.0 | 2.0 | 3.0 | 3.0 |
| α_5 | - | - | 2.0 | 2.0 |
| YM | | | | |
| E_1 | 115.49 | 140.20 | 3367.12 | 57824.63 |
| $E_2 = E_3$ | 67.05 | 56.78 | 622.86 | 680.37 |
| E_1/E_2 | 1.72 | 2.47 | 5.41 | 84.99 |

$(\cdot) := \text{dependent}$

The first Piola-Kirchhoff stresses in x_1 -direction and x_2 -direction with respect to the stretch λ can be seen in Figure 7.2. We notice a physically reasonable distribution of the stresses for a transversely isotropic material with higher stiffness in x_1 -direction.

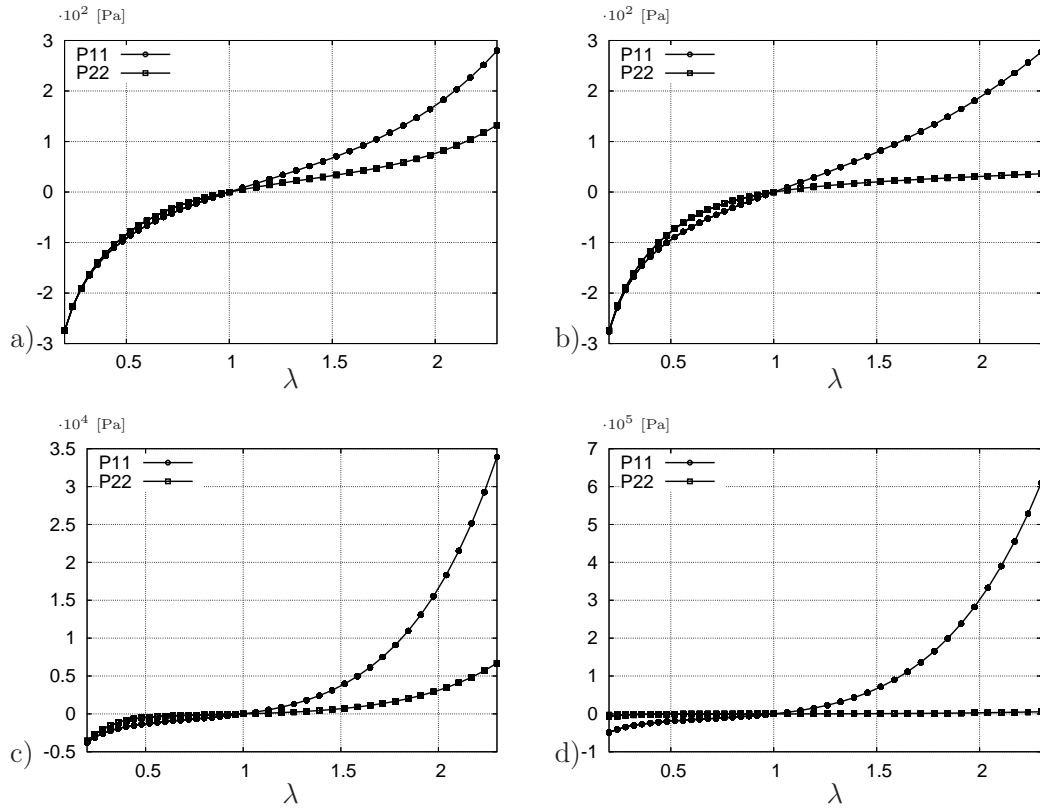


Figure 7.2: First Piola-Kirchhoff stresses in x_1 -direction and x_2 -direction versus stretch λ :
a) $\psi_{I,1}^{ti}$, b) $\psi_{I,2}^{ti}$, c) $\psi_{II,1}^{ti}$, d) $\psi_{II,2}^{ti}$.

7.2 Cook's Membrane.

(The following results are first published in SCHRÖDER [101].)

Let us consider a tapered cantilever, associated to the Cook's membrane problem, clamped on the left hand side and subjected to a constant traction $\lambda \mathbf{t}$ in vertical direction on the right hand side with $\mathbf{t} = (5.0, 0.0, 0.0)$. Here λ denotes the load parameter. The system and the boundary conditions are depicted in Figure 7.3.

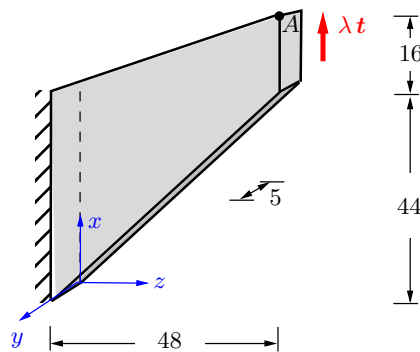


Figure 7.3: Tapered cantilever. System and boundary conditions.

The cantilever is discretized with 10512 ten-noded tetrahedral finite elements; here we use a mixed method with an element-wise constant ansatz for the volume dilatation.

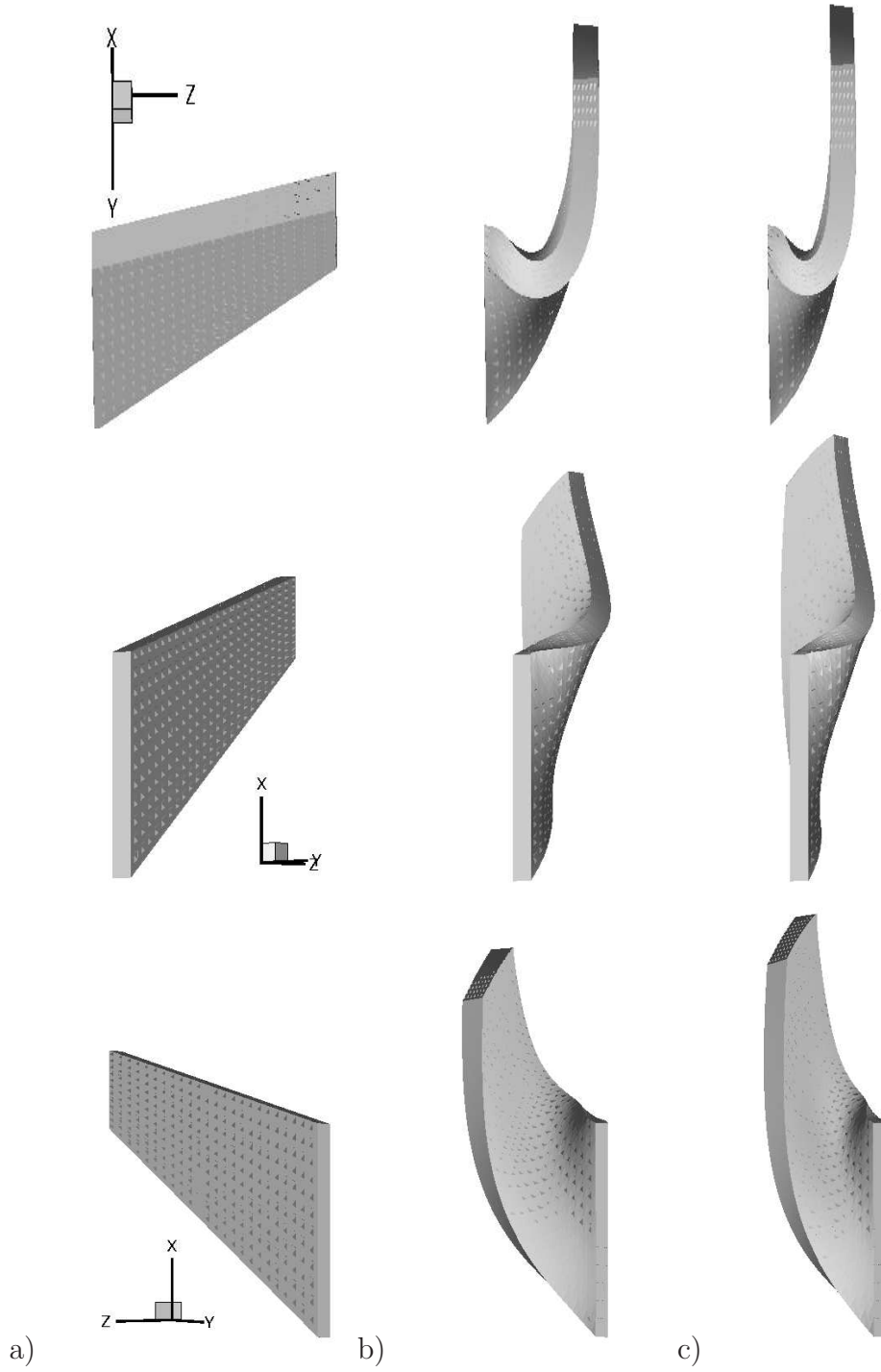


Figure 7.4: Tapered cantilever. Different views on a) the undeformed system, deformed system at b) $\lambda = 0.50$ and c) $\lambda = 1.00$, cf. SCHRÖDER [101].

The transversely isotropic free energy function (6.50) with the anisotropic part (6.91) is taken into account, where we set $n = 1, m = 2$. The transversely isotropic metric tensors with respect to the local base system are given by

$$\mathbf{G}_1^{ti,l} = \text{diag}[1, 0, 0], \quad \mathbf{G}_2^{ti,l} = \text{diag}[0, 1, 1]. \quad (7.4)$$

Since the local base vectors are set to be

$$\tilde{\mathbf{e}}_1 = (1/\sqrt{3}, 1/\sqrt{3}, 1/\sqrt{3})^T, \quad \tilde{\mathbf{e}}_2 = (1/\sqrt{2}, -1/\sqrt{2}, 0)^T, \quad \tilde{\mathbf{e}}_3 = (-1/\sqrt{6}, -1/\sqrt{6}, \sqrt{2}/\sqrt{3})^T,$$

the metric tensors with respect to the global cartesian base system are then calculated by

$$\mathbf{G}_1^{ti} = \mathbf{R}\mathbf{G}_1^{ti,l}\mathbf{R}^T, \quad \mathbf{G}_2^{ti} = \mathbf{R}\mathbf{G}_2^{ti,l}\mathbf{R}^T, \quad (7.5)$$

with the orthogonal rotation tensor $\mathbf{R} = [\tilde{\mathbf{e}}_1, \tilde{\mathbf{e}}_2, \tilde{\mathbf{e}}_3]$. The set of non-vanishing material parameters

$$\alpha_1 = 1, \alpha_2 = 1, \delta_1 = 1, \xi_{11} = 1, \alpha_{11} = 10, \beta_{11} = 1, \gamma_{11} = 1, \xi_{12} = 1, \gamma_{12} = 1 \quad (7.6)$$

is chosen for the simulation. The load parameter is increased by increments $\Delta\lambda = 0.01$ until a final value of $\lambda = 1.00$ is reached. Figure 7.4 depicts different views on the undeformed and deformed system at $\lambda = 1.00$, respectively. Due to the orientation of the preferred direction a salient out-of-plane bending deformation can be observed. The displacements \mathbf{u}_A at node A with $(x_A, y_A, z_A)^T = (60, 5, 48)^T$, see Figure 7.3, are finally given by

$$\mathbf{u}_A = (26.77, -5.57, -30.51)^T. \quad (7.7)$$

7.3 Anisotropic Moduli – Fitting to Referential Data.

(A part of the following results is already published in SCHRÖDER, NEFF & EBBING [106] and SCHRÖDER, NEFF & EBBING [107].)

Since our introduced polyconvex energy functions depend on the elements of the underlying *family of polyconvex invariant functions*, it is obvious that the polyconvex energy functions are *complete* according to our definition of *completeness* given in section 4.5. That means once again, that the linearized tangent moduli at reference state

$$\mathbb{C}^{lin} = \mathbb{C}|_{C=1} = 4 \partial_{CC} \psi|_{C=1}$$

have the same non-zero coefficients and relations between these coefficients like the corresponding classical anisotropic elasticity tensor. For interested readers we show this correspondence for all cases of anisotropy. Due to the dependencies between the individual terms appearing in the polyconvex functions, a direct identification of the material parameters with the components of the associated elasticity tensor is almost impossible.

Let us show the *completeness* of the above introduced polyconvex triclinic, monoclinic, rhombic, transversely isotropic and hexagonal energy function

$$\psi = \sum_{r=1}^n \sum_{j=1}^m \xi_{rj} \left[\frac{1}{\alpha_{rj} + 1} \frac{1}{(g_j)^{\alpha_{rj}}} (J_{4j})^{\alpha_{rj}+1} + \frac{1}{\beta_{rj} + 1} \frac{1}{(g_j)^{\beta_{rj}}} (J_{5j})^{\beta_{rj}+1} + \frac{g_j}{\gamma_{rj}} (I_3)^{-\gamma_{rj}} \right], \quad (7.8)$$

with the invariant functions (6.57) and the trace of the underlying metric tensor (6.59), as well as of the polyconvex tetragonal, trigonal and cubic energy function

$$\begin{aligned} \psi = \sum_{r=1}^n \sum_{j=1}^m \xi_{rj} \left[\frac{1}{\alpha_{rj} + 1} \frac{1}{(m_j)^{\alpha_{rj}}} (J_{6j})^{\alpha_{rj}+1} + \frac{3}{\beta_{rj} + 1} \frac{1}{(m_j)^{\beta_{rj}}} (J_{7j})^{\beta_{rj}+1} \right. \\ \left. + \frac{1}{\eta_{rj} + 1} \frac{1}{(m_j)^{\eta_{rj}}} (J_{8j})^{\eta_{rj}+1} + \frac{3m_j}{\gamma_{rj}} (I_3)^{-\gamma_{rj}} \right], \end{aligned} \quad (7.9)$$

with the invariants (6.109) and $m_j = \mathbf{1} : \mathbb{G}_j : \mathbf{1}$.

Furthermore, due to the polyconvexity restrictions of the material parameters not all values of elasticities may be exactly captured. This statement is checked by several fittings of the linear moduli to some available data on elasticities of real anisotropic materials. A huge variety of data are available in SIMMONS & WANG [111] as well as in SHUVALOV [110] and ROYER & DIEULESAINT [97], from which we obtained experimental values on monoclinic, rhombic, hexagonal, tetragonal, trigonal (type \mathcal{G}_9) and cubic elasticities. In detail, the fitting of moduli is done by minimizing the error function

$$e = \frac{\| \mathbb{C}^{(V)c} - \mathbb{C}^{(V)e} \|}{\| \mathbb{C}^{(V)e} \|}. \quad (7.10)$$

Here $\mathbb{C}^{(V)c} \in \mathbb{R}^{6 \times 6}$ denotes the computed linear moduli \mathbb{C}^{lin} in Voigt notation. Furthermore, $\mathbb{C}^{(V)e} \in \mathbb{R}^{6 \times 6}$ is the associated coefficient scheme of experimental values. The used norm of the matrix schemes are defined by

$$\| \mathbb{C}^{(V)} \| = \sqrt{\sum_{i=1}^6 \sum_{j=1}^6 (\mathbb{C}_{ij}^{(V)})^2}. \quad (7.11)$$

The performed parameter adjustments have been done with the evolution strategy proposed by SCHWEFEL [109] and RECHENBERG [93]. Furthermore, we plot the characteristic surfaces of Young's modulus for the adjusted elasticities to visualize the anisotropy ratios, see SHUVALOV [110] and BÖHLKE & BRÜGGEMANN [32].

In SCHRÖDER, NEFF & EBBING [106] and EBBING, SCHRÖDER & NEFF [47] approximations of rhombic and monoclinic elasticity tensors using the polyconvex function (6.50) with the anisotropic part (6.91) can be found. For the adjustments of several anisotropic elasticity tensors in EBBING, SCHRÖDER & NEFF [48] the same polyconvex energy (6.50) with (6.91), but also with the anisotropic part (6.114), is taken into account. In SCHRÖDER, NEFF & EBBING [107] trigonal elasticities are fitted only by considering the anisotropic energy (6.114).

Triclinic Polyconvex Material Model. Considering in the triclinic case the energy function (7.8) with $n = 1$, $m = 3$ and the structural tensors $\mathbf{G}_1 = \mathbf{G}^a$, $\mathbf{G}_2 = \mathbf{G}^m$, $\mathbf{G}_3 = \mathbf{G}^o$, i.e.,

$$\mathbf{G}_1 = \begin{bmatrix} a_1 & d_1 & e_1 \\ d_1 & b_1 & f_1 \\ e_1 & f_1 & c_1 \end{bmatrix}, \quad \mathbf{G}_2 = \begin{bmatrix} a_2 & d_2 & 0 \\ d_2 & b_2 & 0 \\ 0 & 0 & c_2 \end{bmatrix}, \quad \mathbf{G}_3 = \text{diag}[a_3, b_3, c_3]. \quad (7.12)$$

and taking the relations $\gamma_{11} = \gamma_{12} = \gamma_{13} = \gamma$ and $\xi_{12} = \xi_{13} = 1$ into account, we have 21 material parameters: ξ_{11} , α_{11} , α_{12} , α_{13} , β_{11} , β_{12} , β_{13} , γ , a_1 , b_1 , c_1 , d_1 , e_1 , f_1 , a_2 , b_2 , c_2 , d_2 , a_3 , b_3 , c_3 . The triclinic material tangent $\mathbb{C}^a|_{C=1} = 4\partial_{CC}\psi|_{C=1}$ appears in Voigt notation with 21 different components, i.e., in the classical form of the triclinic elasticity tensor. A detailed representation is given by

$$\mathbb{C}^{(V)a}|_{C=1} = \begin{bmatrix} \mathbb{C}_{1111} & \mathbb{C}_{1122} & \mathbb{C}_{1133} & \mathbb{C}_{1112} & \mathbb{C}_{1123} & \mathbb{C}_{1113} \\ & \mathbb{C}_{2222} & \mathbb{C}_{2233} & \mathbb{C}_{2212} & \mathbb{C}_{2223} & \mathbb{C}_{2213} \\ & & \mathbb{C}_{3333} & \mathbb{C}_{3312} & \mathbb{C}_{3323} & \mathbb{C}_{3313} \\ & & & \mathbb{C}_{1212} & \mathbb{C}_{1223} & \mathbb{C}_{1213} \\ & sym. & & & \mathbb{C}_{2323} & \mathbb{C}_{2313} \\ & & & & & \mathbb{C}_{1313} \end{bmatrix}.$$

Monoclinic Polyconvex Material Model. To obtain a *complete* energy function ψ for monoclinic symmetry in the polyconvex framework, the function (7.8) with $n = 1$, $m = 2$ can be considered, where the metric tensors have different structures, i.e., a monoclinic and a rhombic and/or a transversely isotropic structure. Here, we take the tensors

$$\mathbf{G}_1 = \mathbf{G}^m = \begin{bmatrix} a_1 & d_1 & 0 \\ d_1 & b_1 & 0 \\ 0 & 0 & c_1 \end{bmatrix}, \quad \mathbf{G}_2 = \mathbf{G}^o = \begin{bmatrix} a_2 & 0 & 0 \\ 0 & b_2 & 0 \\ 0 & 0 & c_2 \end{bmatrix}. \quad (7.13)$$

We set $\gamma_{11} = \gamma_{12} = \gamma$, $\xi_{12} = 1$ and get 13 material parameters: ξ_{11} , α_{11} , α_{12} , β_{11} , β_{12} , γ , a_1 , b_1 , c_1 , d_1 , a_2 , b_2 , c_2 . The monoclinic material tangent $\mathbb{C}^m = 4\partial_{CC}\psi$ at $\mathbf{C} = \mathbf{1}$ in Voigt notation results in the classical monoclinic elasticity tensor, i.e.,

$$\mathbb{C}^{(V)m}|_{C=1} = \begin{bmatrix} \mathbb{C}_{1111} & \mathbb{C}_{1122} & \mathbb{C}_{1133} & \mathbb{C}_{1112} & 0 & 0 \\ & \mathbb{C}_{2222} & \mathbb{C}_{2233} & \mathbb{C}_{2212} & 0 & 0 \\ & & \mathbb{C}_{3333} & \mathbb{C}_{3312} & 0 & 0 \\ & & & \mathbb{C}_{1212} & 0 & 0 \\ sym. & & & & \mathbb{C}_{2323} & \mathbb{C}_{2313} \\ & & & & & \mathbb{C}_{1313} \end{bmatrix}. \quad (7.14)$$

Let us fit the monoclinic tangent moduli (7.14) to the elasticity tensor of the monoclinic material Aegirite.

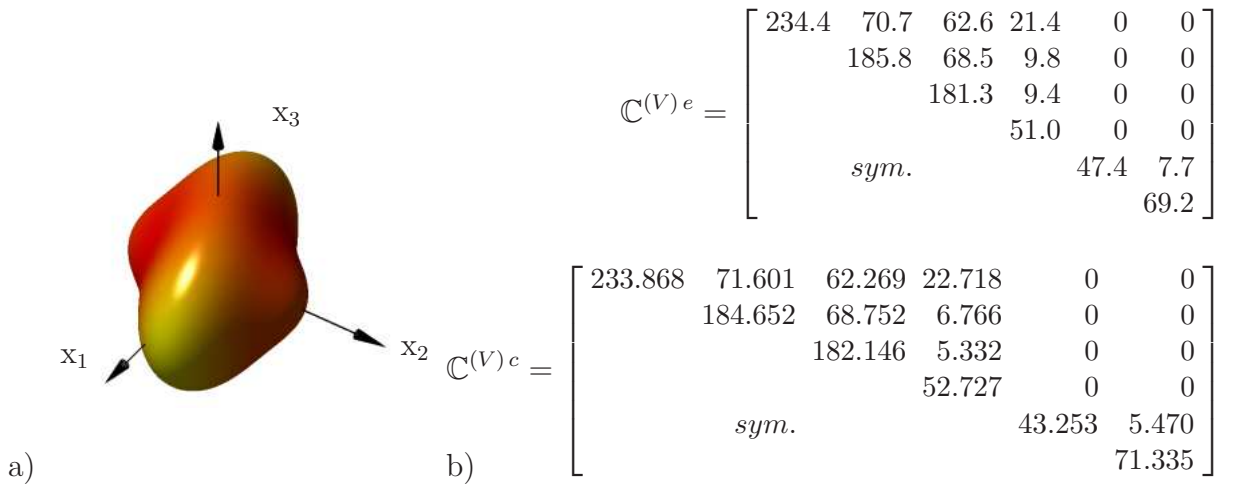


Figure 7.5: Aegirite: a) Characteristic surface of Young's moduli, b) $\mathbb{C}^{(V)e}$ and $\mathbb{C}^{(V)c}$ in [GPa].

Table 7.2: Material parameter set of Aegirite

| energy (7.8): $n = 1$, $m = 2$ | | | | | | metric tensors: | | | |
|----------------------------------|-----|---------------|-------------------|---------------|------------|---------------------|--|--|--|
| anisotropic material parameters: | | | | | | | | | |
| r | j | α_{rj} | β_{rj} | γ_{rj} | ξ_{rj} | | | | |
| 1 | 1 | 4.000 | $6 \cdot 10^{-7}$ | -0.5 | 4.096 | | | | |
| 1 | 2 | 0.670 | 3.261 | -0.5 | 1.000 | | | | |
| | | | | | | error: $e = 1.81\%$ | | | |

The characteristic surface and representations of the experimentally determined and computed elasticity tensor can be found in Fig. 7.5. The optimization of the error function (7.10) yields a relative error e of approximately 1.81 %. The optimized set of material parameters and resulting monoclinic and rhombic structural tensors are shown in Table 7.2.

Rhombic Polyconvex Material Model. For the rhombic energy function ψ we put $n = 1$, $m = 2$ in (7.8) and use the two different metric tensors

$$\mathbf{G}_1 = \mathbf{G}^o = \begin{bmatrix} a_1 & 0 & 0 \\ 0 & b_1 & 0 \\ 0 & 0 & c_1 \end{bmatrix}, \quad \mathbf{G}_2 = \mathbf{G}^{ti} = \begin{bmatrix} a_2 & 0 & 0 \\ 0 & a_2 & 0 \\ 0 & 0 & c_2 \end{bmatrix}. \quad (7.15)$$

Here, considering e.g. the dependencies $\gamma_{11} = \gamma_{12} = \gamma$ and fixed parameters $\xi_{11} = 3$, $\xi_{12} = 1$ all in all 10 material parameters remain: α_{11} , α_{12} , β_{11} , β_{12} , a_1 , b_1 , c_1 , a_2 , b_2 , γ . The Voigt notation of the rhombic tangent moduli at natural state $\mathbb{C}^o|_{C=1} = 4\partial_{CC}\psi|_{C=1}$ exhibits the classical arrangement of rhombic elasticities, i.e.,

$$\mathbb{C}^{(V)o}|_{C=1} = \begin{bmatrix} \mathbb{C}_{1111} & \mathbb{C}_{1122} & \mathbb{C}_{1133} & 0 & 0 & 0 \\ & \mathbb{C}_{2222} & \mathbb{C}_{2233} & 0 & 0 & 0 \\ & & \mathbb{C}_{3333} & 0 & 0 & 0 \\ & & & \mathbb{C}_{1212} & 0 & 0 \\ sym. & & & & \mathbb{C}_{2323} & 0 \\ & & & & & \mathbb{C}_{1313} \end{bmatrix}. \quad (7.16)$$

The values of the rhombic tangent moduli (7.16) at reference state are fitted to the experimentally determined elasticities of Aragonite.

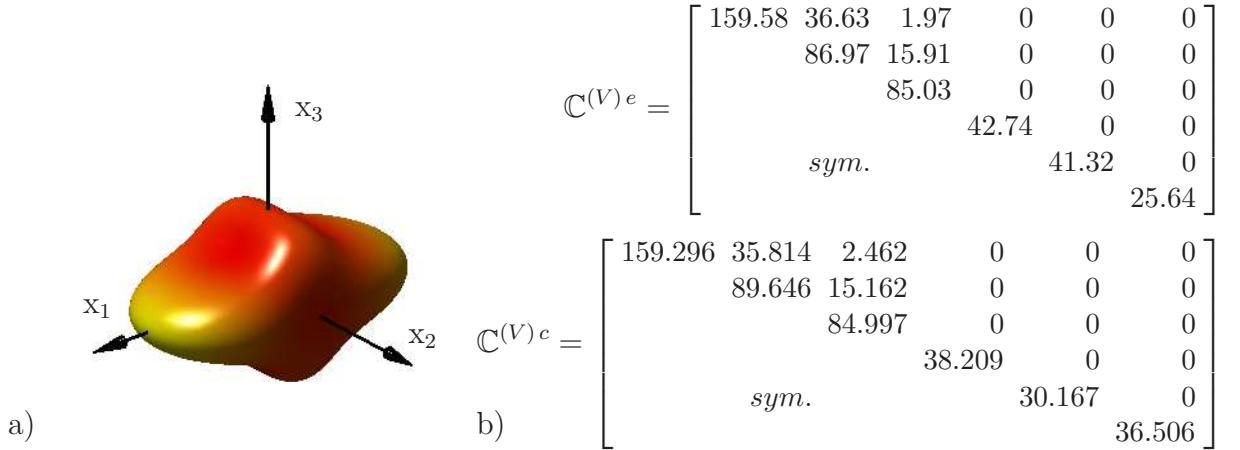


Figure 7.6: Aragonite: a) Characteristic surface of Young's moduli, b) $\mathbb{C}^{(V)e}$ and $\mathbb{C}^{(V)c}$ in [GPa].

Table 7.3: Material parameter set of Aragonite

| energy (7.8): $n = 1$, $m = 2$ | | | | | | metric tensors: | |
|----------------------------------|-----|---------------|---------------------|---------------|------------|---|--|
| anisotropic material parameters: | | | | | | $\mathbf{G}_1 = \text{diag}(3.032, 0.976, 10^{-7})$ | |
| r | j | α_{rj} | β_{rj} | γ_{rj} | ξ_{rj} | $\mathbf{G}_2 = \text{diag}(5.040, 5.040, 7.116)$ | |
| 1 | 1 | 5.495 | 0.002 | -0.500 | 3.000 | error: $e = 6.57\%$ | |
| 1 | 2 | 2.758 | $2.3 \cdot 10^{-6}$ | -0.500 | 1.000 | | |

The characteristic surface of Young's moduli reflects the typical rhombic symmetry properties, see Fig. 7.6. Optimizing (7.10) leads here to an error of $e = 6.57\%$. Detailed results on the computed elasticities and the material parameters can be found in Figure 7.6 and in Table 7.3.

Polyconvex Material Model for Transverse Isotropy and Hexagonal Symmetry.

For a *complete* description of transversely isotropic and hexagonal material behavior it is sufficient to consider (7.8) with $n = 1$, $m = 1$ as underlying energy function ψ and the transversely isotropic/hexagonal structural tensor

$$\mathbf{G}_1 = \mathbf{G}^{ti} \text{diag}[a_1, a_1, c_1]. \quad (7.17)$$

Setting $\xi_{11} = 1$ we get 5 material parameters α_{11} , β_{11} , a_1 , c_1 , γ . The evaluation of the tangent moduli $\mathbb{C}^{ti} = 4\partial_{CC}\psi$ at reference state $\mathbf{C} = \mathbf{1}$ with $n = m = 1$ and the metric tensor (7.17) in Voigt notation yields the well-known transversely isotropic and hexagonal elasticity tensor, i.e.,

$$\mathbb{C}^{(V)ti}|_{C=1} = \begin{bmatrix} \mathbb{C}_{1111} & \mathbb{C}_{1122} & \mathbb{C}_{1133} & 0 & 0 & 0 \\ \mathbb{C}_{1122} & \mathbb{C}_{1111} & \mathbb{C}_{1133} & 0 & 0 & 0 \\ \mathbb{C}_{1133} & \mathbb{C}_{1133} & \mathbb{C}_{3333} & 0 & 0 & 0 \\ 0 & 0 & 0 & \frac{1}{2}(\mathbb{C}_{1111} - \mathbb{C}_{1122}) & 0 & 0 \\ 0 & 0 & 0 & 0 & \mathbb{C}_{2323} & 0 \\ 0 & 0 & 0 & 0 & 0 & \mathbb{C}_{2323} \end{bmatrix}. \quad (7.18)$$

In [110] we found data on experimental values of hexagonal Young's moduli. We choose the referential values of Rhenium, to which we adjust the transversely isotropic/ hexagonal tangent moduli (7.18) at reference state. The characteristic surface of Young's moduli is illustrated in Figure 7.7, where the typical isotropy plane is immediately observable. It lies here in the $x_1 - x_2$ -plane. The error (7.10) takes finally the value $e = 4.94\%$. The resulting computed elasticities and the material parameters are given in Figure 7.7 and in Table 7.4.

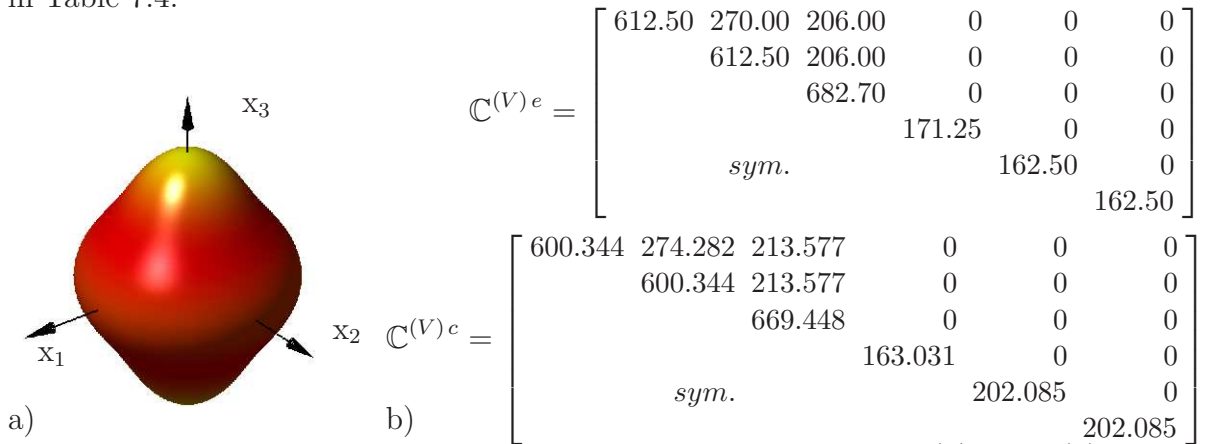


Figure 7.7: Rhenium: a) Characteristic surface of Young's moduli, b) $\mathbb{C}^{(V)e}$ and $\mathbb{C}^{(V)c}$ in [GPa].

Table 7.4: Material parameter set of Rhenium

| energy (7.8): $n = m = 1$ | | | | | | hexagonal metric tensor: | |
|----------------------------------|-----|---------------|--------------|---------------|------------|---|--|
| anisotropic material parameters: | | | | | | $\mathbf{G}_1 = \text{diag}(5.357, 5.357, 7.923)$ | |
| r | j | α_{rj} | β_{rj} | γ_{rj} | ξ_{rj} | | |
| 1 | 1 | 2.495 | 0.694 | -0.5 | 7.609 | error: 4.94% | |

Tetragonal Polyconvex Material Model, \mathcal{G}_4 . In the case of tetragonal \mathcal{G}_4 -anisotropy the energy function ψ given in (7.9) with $n = 1$, $m = 1$ and $\xi_{11} = 1$ is considered. The tetragonal structural tensor consisting of three material parameters is then

$$\mathbb{G}_1 = \mathbb{G}_1^{t1} = \begin{bmatrix} \tilde{a}_1^4 + \tilde{b}_1^4 & 2\tilde{a}_1^2\tilde{b}_1^2 & 0 & \tilde{a}_1^3\tilde{b}_1 - \tilde{b}_1^3\tilde{a}_1 & 0 & 0 \\ & \tilde{a}_1^4 + \tilde{b}_1^4 & 0 & \tilde{b}_1^3\tilde{a}_1 - \tilde{a}_1^3\tilde{b}_1 & 0 & 0 \\ & & \tilde{c}_1^4 & 0 & 0 & 0 \\ & sym. & & 2\tilde{a}_1^2\tilde{b}_1^2 & 0 & 0 \\ & & & & 0 & 0 \\ & & & & & 0 \end{bmatrix}. \quad (7.19)$$

The second-order tensor $\tilde{\mathbf{G}}_1 = \mathbb{G}_1^{t1} : \mathbf{1}$ which appears in the energy function (7.9) is of “transversely isotropic” type, i.e., of diagonal type and two entries are identical: $\tilde{\mathbf{G}}_1 = \mathbb{G}_1^{t1} : \mathbf{1} = \text{diag}[(\tilde{a}_1^2 + \tilde{b}_1^2)^2, (\tilde{a}_1^2 + \tilde{b}_1^2)^2, \tilde{c}_1^4]$. The 7 material parameters under consideration are: γ_{11} , α_{11} , β_{11} , η_{11} , \tilde{a}_1 , \tilde{b}_1 , \tilde{c}_1 . The tetragonal \mathcal{G}_4 -invariant tangent moduli is obtained by $\mathbb{C}^{t1}|_{C=1} = 4\partial_{CC}\psi|_{C=1}$, with

$$\mathbb{C}^{(V)t1}|_{C=1} = \begin{bmatrix} \mathbb{C}_{1111} & \mathbb{C}_{1122} & \mathbb{C}_{1133} & \mathbb{C}_{1112} & 0 & 0 \\ & \mathbb{C}_{1111} & \mathbb{C}_{1133} & -\mathbb{C}_{1112} & 0 & 0 \\ & & \mathbb{C}_{3333} & 0 & 0 & 0 \\ & & & \mathbb{C}_{1212} & 0 & 0 \\ sym. & & & & \mathbb{C}_{2323} & 0 \\ & & & & & \mathbb{C}_{2323} \end{bmatrix}. \quad (7.20)$$

We adjust the tetragonal moduli to experimental elasticities of Calcium molybdate, given in Figure 7.8.

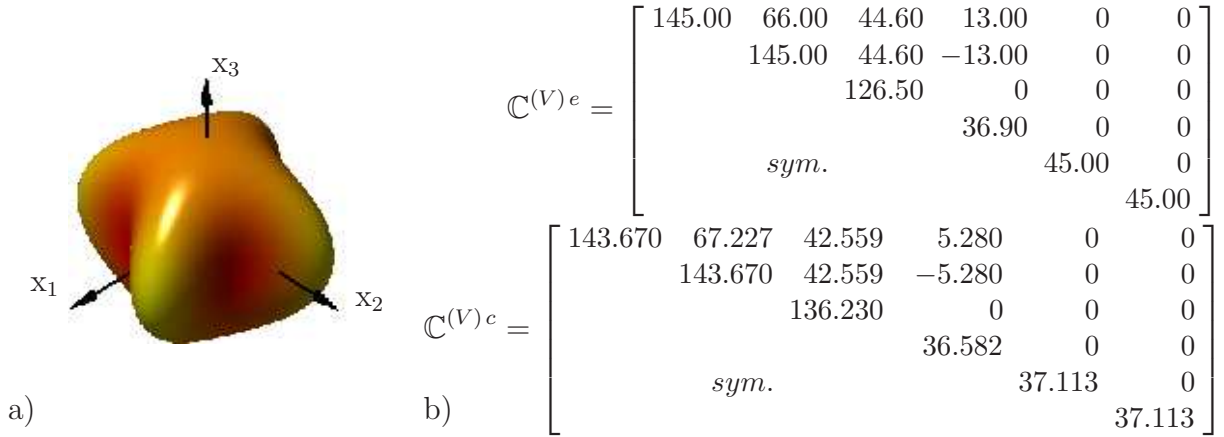


Figure 7.8: Calcium molybdate: a) Characteristic surface of Young's moduli, b) $\mathbb{C}^{(V)e}$ and $\mathbb{C}^{(V)c}$ in [GPa].

Table 7.5: Material parameter set of Calcium molybdate

| | | | | | | | | | | | | | |
|----------------------------------|-----|---------------------|--------------|---------------|-------------------|------------|---|--|--|--|--|--|--|
| energy (7.9): $n = m = 1$ | | | | | | | tetragonal structural tensor: | | | | | | |
| anisotropic material parameters: | | | | | | | $\mathbb{G}_1 = \begin{bmatrix} 2.106 & 0.565 & 0 & 0.660 & 0 & 0 \\ & 2.106 & 0 & -0.660 & 0 & 0 \\ & & 3.514 & 0 & 0 & 0 \\ & & & 0.565 & 0 & 0 \\ & & & & sym. & 0 \\ & & & & & 0 \end{bmatrix}$ | | | | | | |
| r | j | α_{rj} | β_{rj} | γ_{rj} | η_{rj} | ξ_{rj} | | | | | | | |
| 1 | 1 | $2.2 \cdot 10^{-6}$ | 1.421 | -0.500 | $2 \cdot 10^{-7}$ | 1.000 | | | | | | | |
| error: $e = 7.71\%$ | | | | | | | | | | | | | |

From the visualization of the characteristic surface of Young's moduli the material behavior of this tetragonal material can be determined. We obtain the optimized results on elasticities and non-vanishing material parameters shown in Figure 7.8 and Table 7.3, respectively. The optimization (7.10) yields an error of 7.71%.

Tetragonal Polyconvex Material Model, \mathcal{G}_5 . We formulate the energy function (7.9) with $n = 1$, $m = 1$, $\xi_{11} = 1$. The structural tensor contains two material parameters, i.e.,

$$\mathbb{G}_1 = \mathbb{G}_1^{t2} = \text{diag}[\tilde{a}_1^4, \tilde{a}_1^4, \tilde{c}_1^4, 0, 0, 0], \quad (7.21)$$

so that the tensor $\tilde{\mathbf{G}}_1 = \mathbb{G}_1^{t2} : \mathbf{1}$ gets the form $\tilde{\mathbf{G}}_1 = \text{diag}[\tilde{a}_1^4, \tilde{a}_1^4, \tilde{c}_1^4]$. The 6 material parameters γ_{11} , α_{11} , β_{11} , η_{11} , \tilde{a}_1 , \tilde{c}_1 are finally considered. The tetragonal \mathcal{G}_5 -invariant tangent moduli $\mathbb{C}^{t2}|_{C=1} = 4\partial_{CC}\psi|_{C=1}$ results in Voigt notation in the well-known structure:

$$\mathbb{C}^{(V)t2}|_{C=1} = \begin{bmatrix} \mathbb{C}_{1111} & \mathbb{C}_{1122} & \mathbb{C}_{1133} & 0 & 0 & 0 \\ & \mathbb{C}_{1111} & \mathbb{C}_{1133} & 0 & 0 & 0 \\ & & \mathbb{C}_{3333} & 0 & 0 & 0 \\ & & & \mathbb{C}_{1212} & 0 & 0 \\ & sym. & & & \mathbb{C}_{2323} & 0 \\ & & & & & \mathbb{C}_{2323} \end{bmatrix}.$$

We fit the tangent moduli (7.3) to the elasticities of Indium, see $\mathbb{C}^{(V)e}$ in Fig. 7.9. The characteristic surface of Young's moduli depicted in Fig. 7.9 shows here the typical symmetry properties of a tetragonal material of \mathcal{G}_5 -type.

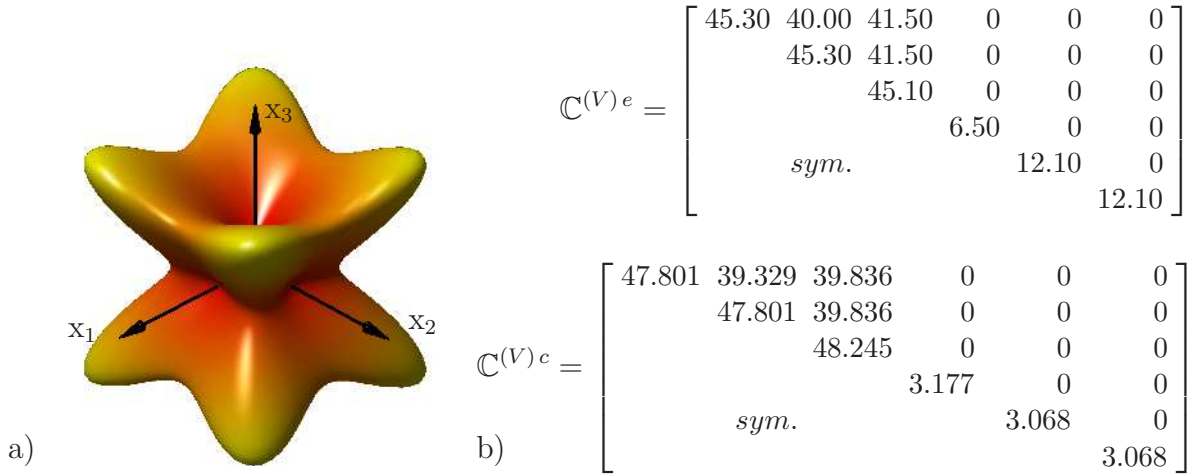


Figure 7.9: Indium: a) Characteristic surface of Young's moduli, b) $\mathbb{C}^{(V)e}$, $\mathbb{C}^{(V)c}$ in [GPa].

Table 7.6: Material parameter set of Indium

| energy (7.9): $n = m = 1$ | | | | | | | tetragonal structural tensor: |
|----------------------------------|-----|---------------|--------------|---------------|-------------|------------|--|
| anisotropic material parameters: | | | | | | | $\mathbb{G}_1 = \text{diag}(0.265, 0.265, 0.247, 0, 0, 0)$ |
| r | j | α_{rj} | β_{rj} | γ_{rj} | η_{rj} | ξ_{rj} | |
| 1 | 1 | 0.095 | 2.038 | 3.014 | 0.020 | 1.000 | |
| error: $e = 11.22\%$ | | | | | | | |

The optimization procedure yields the 6 material parameters and the tetragonal structural tensor as listed in Table 7.3; the obtained error is $e = 11.22\%$. The computed tangent moduli (7.3), which is here denoted by $\mathbb{C}^{(V)c}$ is presented in Figure 7.9.

Trigonal Polyconvex Material Model, \mathcal{G}_8 . We use the energy function (7.9) with $n = 1$, $m = 1$, $\xi_{11} = 1$ and the structural tensor

$$\mathbb{G}_1 = \mathbb{G}_1^{ht1} = \begin{bmatrix} \frac{1}{8} \tilde{c}_1^2 & \frac{1}{24} \tilde{c}_1^2 & \frac{1}{18} C \tilde{c}_1^2 & 0 & A & B \\ & \frac{1}{8} \tilde{c}_1^2 & \frac{1}{18} C \tilde{c}_1^2 & 0 & -A & -B \\ & & \frac{1}{27} \tilde{c}_1^4 & 0 & 0 & 0 \\ & sym. & & \frac{1}{24} \tilde{c}_1^2 & -B & A \\ & & & & \frac{1}{18} C \tilde{c}_1^2 & 0 \\ & & & & & \frac{1}{18} C \tilde{c}_1^2 \end{bmatrix},$$

where we have introduced the abbreviations

$$A = -\frac{1}{4\sqrt{3}} \tilde{a}_1^2 \tilde{b}_1 \tilde{c}_1 + \frac{1}{12\sqrt{3}} \tilde{b}_1^3 \tilde{c}_1, \quad B = -\frac{1}{4\sqrt{3}} \tilde{a}_1 \tilde{b}_1^2 \tilde{c}_1 + \frac{1}{12\sqrt{3}} \tilde{a}_1^3 \tilde{c}_1, \quad C = \tilde{a}_1^2 + \tilde{b}_1^2.$$

The tensor $\tilde{\mathbf{G}}_1 = \mathbb{G}_1^{ht} : \mathbf{1}$ also reduces to a “transversely isotropic” structure, i.e., $\tilde{\mathbf{G}}_1 = \text{diag}[1/6 C^2 + 1/18 C \tilde{c}_1^2, 1/6 C^2 + 1/18 C \tilde{c}_1^2, 1/9 C \tilde{c}_1^2 + 1/27 \tilde{c}_1^4]$. Finally, we establish the energy (7.9) with 7 independent parameters γ_{11} , α_{11} , β_{11} , η_{11} , \tilde{a}_1 , \tilde{b}_1 , c_1 . Then, the tetragonal \mathcal{G}_8 -invariant tangent moduli $\mathbb{C}^{ht1}|_{C=1} = 4\partial_{CC}\psi|_{C=1}$ at reference state exhibits in Voigt notation the classical form, i.e.,

$$\mathbb{C}^{(V)ht1}|_{C=1} = \begin{bmatrix} \mathbb{C}_{1111} & \mathbb{C}_{1122} & \mathbb{C}_{1133} & 0 & \mathbb{C}_{1123} & \mathbb{C}_{1113} \\ & \mathbb{C}_{1111} & \mathbb{C}_{1133} & 0 & -\mathbb{C}_{1123} & -\mathbb{C}_{1113} \\ & & \mathbb{C}_{3333} & 0 & 0 & 0 \\ & & & \frac{1}{2}(\mathbb{C}_{1111} - \mathbb{C}_{1122}) & -\mathbb{C}_{1113} & \mathbb{C}_{1123} \\ & sym. & & & \mathbb{C}_{2323} & 0 \\ & & & & & \mathbb{C}_{2323} \end{bmatrix}.$$

Trigonal Polyconvex Material Model, \mathcal{G}_9 . We consider the energy (7.9) with $n = 1$, $m = 1$, $\xi_{11} = 1$ and the corresponding structural tensor including two independent material parameters:

$$\mathbb{G}_1 = \mathbb{G}_1^{ht2} = \begin{bmatrix} \frac{1}{8} \tilde{b}_1^4 & \frac{1}{24} \tilde{b}_1^4 & \frac{1}{18} \tilde{b}_1^2 \tilde{c}_1^2 & 0 & \frac{1}{12\sqrt{3}} \tilde{b}_1^3 \tilde{c}_1 & 0 \\ & \frac{1}{8} \tilde{b}_1^4 & \frac{1}{18} \tilde{b}_1^2 \tilde{c}_1^2 & 0 & -\frac{1}{12\sqrt{3}} \tilde{b}_1^3 \tilde{c}_1 & 0 \\ & & \frac{1}{27} \tilde{c}_1^4 & 0 & 0 & 0 \\ & sym. & & \frac{1}{24} \tilde{b}_1^4 & 0 & \frac{1}{12\sqrt{3}} \tilde{b}_1^3 \tilde{c}_1 \\ & & & & \frac{1}{18} \tilde{b}_1^2 \tilde{c}_1^2 & 0 \\ & & & & & \frac{1}{18} \tilde{b}_1^2 \tilde{c}_1^2 \end{bmatrix}. \quad (7.22)$$

We have consequently $\tilde{\mathbf{G}}_1 = \mathbb{G}_1 : \mathbf{1} = \text{diag}[1/6 \tilde{b}_1^4 + 1/18 \tilde{b}_1^2 \tilde{c}_1^2, 1/6 \tilde{b}_1^4 + 1/18 \tilde{b}_1^2 \tilde{c}_1^2, 1/9 \tilde{b}_1^2 \tilde{c}_1^2 + 1/27 \tilde{c}_1^4]$ and the 6 material parameters γ_{11} , α_{11} , β_{11} , η_{11} , \tilde{b}_1 , \tilde{c}_1 . The trigonal \mathcal{G}_9 -invariant tangent moduli $\mathbb{C}^{ht2}|_{C=1} = 4\partial_{CC}\psi|_{C=1}$ appears in Voigt notation in classical form:

$$\mathbb{C}^{(V)ht2}|_{C=1} = \begin{bmatrix} \mathbb{C}_{1111} & \mathbb{C}_{1122} & \mathbb{C}_{1133} & 0 & \mathbb{C}_{1123} & 0 \\ & \mathbb{C}_{1111} & \mathbb{C}_{1133} & 0 & -\mathbb{C}_{1123} & 0 \\ & & \mathbb{C}_{3333} & 0 & 0 & 0 \\ & & & \frac{1}{2}(\mathbb{C}_{1111} - \mathbb{C}_{1122}) & 0 & \mathbb{C}_{1123} \\ & sym. & & & \mathbb{C}_{2323} & 0 \\ & & & & & \mathbb{C}_{2323} \end{bmatrix}. \quad (7.23)$$

A comparison of the fitted tangent moduli (7.23) denoted by $\mathbb{C}^{(V)c}$ and the experimentally determined elasticity tensor $\mathbb{C}^{(V)e}$ of Lithium niobate, see Figure 7.10, shows that the energy function (7.9) with $m = 1$ can be used for an adequate description of such trigonal material behavior; the error is 9.12%. For more details on the material parameters see Table 7.3. In [107] it is pointed out that a higher number of invariant terms and therewith of the material parameters, i.e., the energy function (7.9) with $n = 1, m = 2$, leads to an error of only 0.1%. The corresponding material parameters are presented in Table 7.3. Thus, in this case, an increasing number of n and m in (6.114) leads to significant better fitting results.

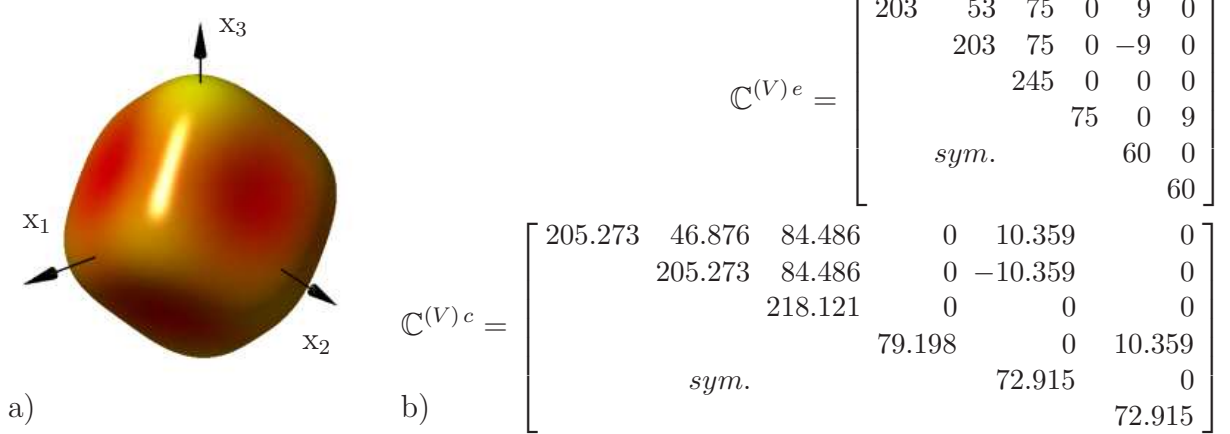


Figure 7.10: Lithium niobate: a) Characteristic surface of Young's moduli, b) $\mathbb{C}^{(V)e}$ and $\mathbb{C}^{(V)c}$ in [GPa].

Table 7.7: Material parameter set 1 of Lithium niobate

| | | | | | | | |
|----------------------------------|-----|-------------------|--------------|---------------|-------------------|------------|---|
| energy (7.9): $n = m = 1$ | | | | | | | trigonal structural tensor: |
| anisotropic material parameters: | | | | | | | $\mathbb{G}_1 = \begin{bmatrix} 3.247 & 1.082 & 1.549 & 0 & 1.295 & 0 \\ & 3.247 & 1.549 & 0 & -1.295 & 0 \\ & & 1.109 & 0 & 0 & 0 \\ & & & 1.082 & 0 & 1.295 \\ & sym. & & & 1.549 & 0 \\ & & & & & 1.549 \end{bmatrix}$ |
| r | j | α_{rj} | β_{rj} | γ_{rj} | η_{rj} | ξ_{rj} | |
| 1 | 1 | $4 \cdot 10^{-7}$ | 1.092 | -0.500 | $3 \cdot 10^{-7}$ | 1.000 | |
| error: $e = 9.12\%$ | | | | | | | |

Table 7.8: Material parameter set 2 of Lithium niobate

| | | | | | | | | | | | | |
|----------------------------------|-----|---------------|--------------|---------------|-------------|------------|---|--|--|--|--|--|
| energy (7.9): $n = 1, m = 2$ | | | | | | | trigonal structural tensors: | | | | | |
| anisotropic material parameters: | | | | | | | $\mathbb{G}_1 = \begin{bmatrix} 3.30 & 1.10 & 1.11 & 0 & 1.11 & 0 \\ & 3.30 & 1.11 & 0 & -1.11 & 0 \\ & & 0.56 & 0 & 0 & 0 \\ & & & 1.10 & 0 & 1.11 \\ sym. & & & & 1.11 & 0 \\ & & & & & 1.11 \end{bmatrix}$ $\mathbb{G}_2 = \text{diag}(0.0, 0.0, 0.25, 0.0, 0.0, 0.0)$ | | | | | |
| r | j | α_{rj} | β_{rj} | γ_{rj} | η_{rj} | ξ_{rj} | | | | | | |
| 1 | 1 | 0.84 | 0.79 | -0.47 | 0.67 | 1.00 | | | | | | |
| 1 | 2 | 2.28 | 2.75 | -0.17 | 13.97 | 1.00 | | | | | | |
| error: $e = 0.1\%$ | | | | | | | | | | | | |

Cubic Polyconvex Material Model. In the cubic case we consider the energy (7.9) with $n = 1$, $m = 1$, $\xi_{11} = 1$ and the cubic fourth-order structural tensor

$$\mathbb{G}_1 = \mathbb{G}_1^{c1} = \text{diag}[a_1^4, a_1^4, a_1^4, 0, 0, 0]. \quad (7.24)$$

Furthermore, we take for the cubic energy function (7.9) with (7.24) at least 5 material parameters α_{11} , β_{11} , γ_{11} , η_{11} , a_1 into account. The classical cubic elasticity tensor is then obtained by the cubic tangent moduli $\mathbb{C}^c|_{C=1} = 4\partial_{CC}\psi|_{C=1}$ in Voigt notation at reference state, i.e.,

$$\mathbb{C}^{(V)c1}|_{C=1} = \begin{bmatrix} \mathbb{C}_{1111} & \mathbb{C}_{1122} & \mathbb{C}_{1122} & 0 & 0 & 0 \\ & \mathbb{C}_{1111} & \mathbb{C}_{1122} & 0 & 0 & 0 \\ & & \mathbb{C}_{1111} & 0 & 0 & 0 \\ & & & \mathbb{C}_{1212} & 0 & 0 \\ & sym. & & & \mathbb{C}_{1212} & 0 \\ & & & & & \mathbb{C}_{1212} \end{bmatrix}. \quad (7.25)$$

Figure 7.11 depicts the experimental values on elasticities of Aluminium and the optimized moduli (7.25) as well as the characteristic surface of Young's moduli reflecting the cubic symmetry properties of Aluminium. The corresponding cubic material parameters and the resulting cubic structural tensor can be found in Table 7.3. From the optimization of (7.10) we obtain a relative error of approximately 15.64%. Note that in [48] we use the energy function (6.50) with the anisotropic part (6.91) and $m = 3$, i.e., a higher number of invariant functions and material parameters, which has a significant effect on the minimization of the error function (7.10). There we could achieve an error of 3.07%. The associated material parameters are also given here, see Table 7.10.

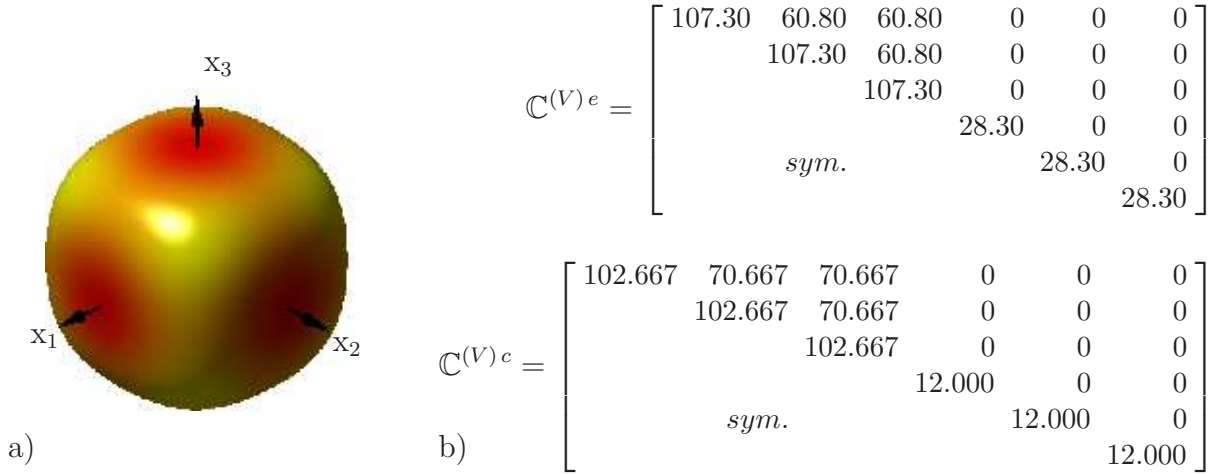


Figure 7.11: Aluminium: a) Characteristic surface of Young's moduli, b) $\mathbb{C}^{(V)e}$ and $\mathbb{C}^{(V)c}$ in [GPa].

Table 7.9: Material parameter set 1 of Aluminium

| energy (7.9): $n = m = 1$ | | | | | | | cubic structural tensor: | |
|----------------------------------|-----|---------------|--------------|---------------|-------------|------------|--|--|
| anisotropic material parameters: | | | | | | | $\mathbb{G}_1 = \text{diag}(1.000, 1.000, 1.000, 0, 0, 0)$ | |
| r | j | α_{rj} | β_{rj} | γ_{rj} | η_{rj} | ξ_{rj} | | |
| 1 | 1 | 1.000 | 1.000 | 1.000 | 1.000 | 1.000 | | |
| error: $e = 15.64\%$ | | | | | | | | |

Table 7.10: Material parameter set 2 of Aluminium

| | | | | | | | |
|---|----------------------------------|-----|---------------|--------------|---------------|-------------|------------|
| energy (6.50) with (6.91): $m = 3$ | anisotropic material parameters: | | | | | | |
| isotropic material parameters: | r | j | α_{rj} | β_{rj} | γ_{rj} | η_{rj} | ξ_{rj} |
| $\delta_1 = 4.76, \quad \delta_2 = 7.56, \quad \delta_3 = 7.41$ | 1 | 1 | 0.07 | 2.17 | 2.54 | 1.46 | 1.14 |
| cubic structural tensors: | 2 | 1 | 1.26 | 1.55 | 0.50 | 1.52 | 1.00 |
| $\mathbb{G}_1 = \text{diag}(0.0065^4, 0.0065^4, 0.0065^4, 0, 0, 0)$ | 3 | 1 | 1.02 | 2.32 | 2.58 | 0.25 | 0.37 |
| $\mathbb{G}_2 = \text{diag}(0.0024^4, 0.0024^4, 0.0024^4, 0, 0, 0)$ | 1 | 2 | 2.29 | 2.58 | 3.34 | 2.59 | 1.31 |
| $\mathbb{G}_3 = \text{diag}(0.0012^4, 0.0012^4, 0.0012^4, 0, 0, 0)$ | 2 | 2 | 1.78 | 3.51 | 1.17 | 0.91 | 0.16 |
| | 3 | 2 | 0.97 | 4.15 | 2.46 | 1.51 | 2.14 |
| | 1 | 3 | 1.94 | 2.20 | 1.81 | 0.88 | 0.29 |
| | 2 | 3 | 2.43 | 1.65 | 2.59 | 1.94 | 0.59 |
| | 3 | 3 | 1.61 | 3.10 | 2.96 | 2.68 | 0.46 |
| | error: 3.07% | | | | | | |

Cuticle of the American Lobster. Due to the outstanding mechanical properties and multi-functionality of biological materials their investigation is particularly interesting from a bionic point of view. The "Max-Planck-Institut für Eisenforschung" situated in Düsseldorf, Germany, focussed on the cuticle or shell of the lobster *Homarus americanus* as a novel model material, cp. NIKOLOV, PETROV, LYMPERAKIS, FRIÁK, SACHS, FABRITIUS, RAABE, NEUGEBAUER [86] and the references therein. This material possesses high toughness, stiffness, and strength related to its low density. The identification of essential structural features which are responsible for its efficiency may contribute to the design of engineering materials with similar properties.



www.neaq.com

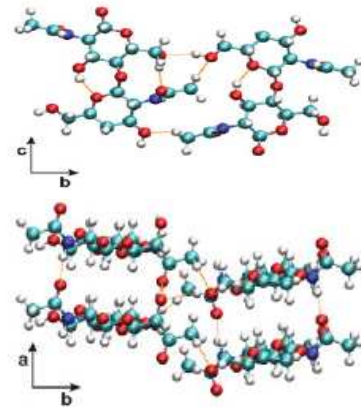


Figure 7.12: a) Cuticle of *Homarus americanus*, b) Structure of single crystalline α -chitin with crystallographic base vectors $\mathbf{a}_1, \mathbf{a}_2, \mathbf{a}_3$ taken from [86].

The cuticle of the lobster *Homarus americanus* is a nano-composite material. It consists of a matrix of chitin-protein fibers associated with various amounts of crystalline and amorphous calcium carbonate in the rigid parts of the body. It is hierarchically organized on all length scales. Its structural properties at all length scales down to the molecular level should be taken into account to understand the macroscopic mechanical properties of the material.

Table 7.11: Material parameter set of American Lobster

| energy (7.8): $n = 1, m = 2$ | | | | | | metric tensors: | |
|----------------------------------|-----|---------------|---------------------|---------------|------------|---|--|
| anisotropic material parameters: | | | | | | $\mathbf{G}_1 = \text{diag}(1.741, 10^{-7}, 0.295)$ | |
| r | j | α_{rj} | β_{rj} | γ_{rj} | ξ_{rj} | $\mathbf{G}_2 = \text{diag}(5 \cdot 10^{-7}, 1.617, 0.000)$ | |
| 1 | 1 | 5.302 | $1.6 \cdot 10^{-6}$ | 0.000 | 3.000 | error: $e = 9.88\%$ | |
| 1 | 2 | 0.789 | 1.225 | -0.500 | 1.000 | | |

At length scale 0.1 nm-10 nm, where the hierarchical structure unit is α -chitin (H-bonded anti-parallel N-acetyl-glucosamine molecular chains), the material exhibits a rhombic elastic behavior, see [86]. The corresponding elasticity tensor $\mathbb{C}^{(V)e}$ and the associated characteristic surface of Young's moduli are visualized in Fig. 7.13. The tensor is defined with respect to a local cartesian coordinate frame, where the base vectors of the rhombic unit cell of α -chitin \mathbf{a}_1 , \mathbf{a}_2 and \mathbf{a}_3 (chain direction) are oriented in x_2 -, x_3 - and x_1 -direction, respectively.

We were interested in the description of this elastic behavior by the crystallographically motivated polyconvex energies. Therefore, we consider the rhombic energy function (7.8) with $n = 1, m = 2$ and fixed parameters $\xi_{11} = 3$, $\xi_{12} = 1$. Thus, we have 12 material parameters α_{11} , α_{12} , β_{11} , β_{12} , a_1 , b_1 , c_1 , a_2 , b_2 , c_2 , γ_{11} , γ_{12} and obtain the same arrangement of coefficients of the underlying rhombic tangent moduli $\mathbb{C}^{(V)c}$ as introduced in (7.16). The adjustment of $\mathbb{C}^{(V)c}$ to the referential data $\mathbb{C}^{(V)e}$, i.e., the minimization of the error function (7.10), leads here to an error of $e = 9.88\%$ and to the final tangent moduli $\mathbb{C}^{(V)c}$ at reference state presented in Fig. 7.13.

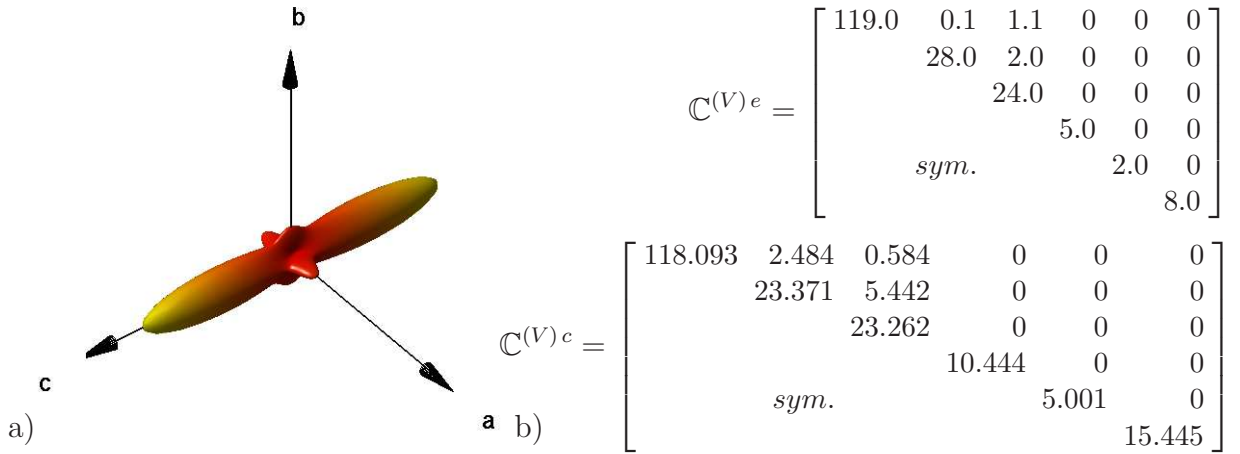


Figure 7.13: Cuticle of American Lobster: a) Characteristic surface of Young's moduli, b) $\mathbb{C}^{(V)e}$ and $\mathbb{C}^{(V)c}$ in [GPa].

Remark. Due to the generic character of the introduced polyconvex energy functions an extension of the fitted models by increasing the number of material parameters is straightforward, which often leads to better optimization results. In particular in the trigonal (symmetry type \mathcal{G}_9) and cubic case we have observed this positive effect, cf. [48] and [107].

7.4 Micro- and Macromechanical Modeling of Fiber-Reinforced Composites.

Due to their light weight, high stiffness, strength and toughness, fiber reinforced composites are becoming increasingly important in many engineering applications ranging from roof constructions (Figure 7.14) to weather-proof awnings. In numerous cases special materials come to operation, which consist of a fiber network made of e.g., glass-, textile- or synthetic fibers, embedded in a silicone-, polymer- or rubber-like matrix. For this reason a highly nonlinear material behavior and, due to the fiber-reinforcement of the material, strong anisotropy effects have to be taken into account. For an optimal design of such constructions a prediction of their stress-strain behavior is required.



a) www.stahl-online.de

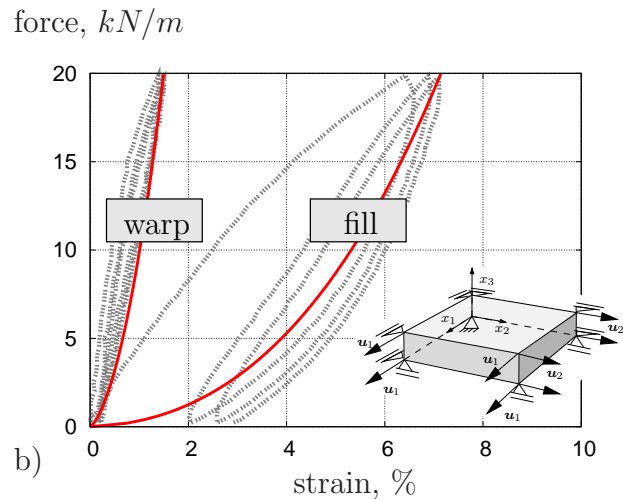


b) de.fifa.com

Figure 7.14: Lightweight constructions: a) Olympia Stadium, Berlin, b) Nelson Mandela Bay Stadium, Port Elizabeth, South Africa.



a)



b)

Figure 7.15: a) Machine for biaxial tension tests. b) Load-strain behavior of a PVC-Polyester composite.

In Figure 7.15a) the machine for the performance of biaxial tension tests of fiber reinforced materials of the laboratory for light surface structures of the University Duisburg-Essen^{18.)} is depicted. The anisotropic and nonlinear load-strain behavior of a typical composite, which was obtained from such a test, is visualized in Figure 7.15b). Here also visco-elastic and irreversible effects can be noticed. However, in the following we restrict ourselves to anisotropic finite elasticity of fiber reinforced materials.

^{18.)}The correspondence with Dipl.-Ing. Klaus Saxe, chief of the laboratory of light surface structures (University Duisburg-Essen, Germany), is gratefully acknowledged.

First, we are interested in the micromechanical modeling of woven fiber composites from which effective anisotropic polyconvex energies can be constructed, see section 7.4.1. In detail, a virtual experiment of the microstructure of the considered composite is performed and the results are used for the specification of an effective macroscopic anisotropic polyconvex model. The virtual experiments are of great importance for woven fiber composite designer, since they are interested in evaluations of the macroscopic material behavior from the material properties of the individual phases of the composite. Second, in sections 7.4.2 and 7.4.2.3 we focus on the macromechanical modeling of fiber reinforced composites. Since the mentioned lightweight structures have a very small thickness compared to the dimension in other directions, we consider shell elements and investigate the influence of anisotropy modeled by the proposed polyconvex energy functions on the deformation of two different shell geometries, a hexagonal plate and a hyperbolic shell. The nonlinear shell theory is based on the Reissner–Mindlin kinematic along with inextensible director vectors.

7.4.1 Micromechanical Modeling. (First results are published in EBBING, SCHRÖDER, NEFF & GRUTTMANN [49].)

We concentrate on a phenomenological description of a class of textile composites in which two fiber families are aligned in mutually orthogonal directions, the warp and fill direction, (Figure 7.16a)). To derive a homogenized macroscopic model we concentrate -as a first step- on the performance and the results of a biaxial tension test of a microstructure. In detail, the structure of a glass fiber reinforced material is chosen. The geometrical data are taken from pictures of a representative microstructure, obtained from the laboratory of light surface structures of the University of Duisburg-Essen, see Figure 7.16b). Each component, the two fiber families and the matrix, are assumed to be individually isotropic, hyperelastic materials and therefore described by isotropic polyconvex energies. Finally, we adjust the overall stress-strain curves obtained for the heterogeneous microstructure to a rhombic polyconvex model for an assumed homogeneous macrostructure.

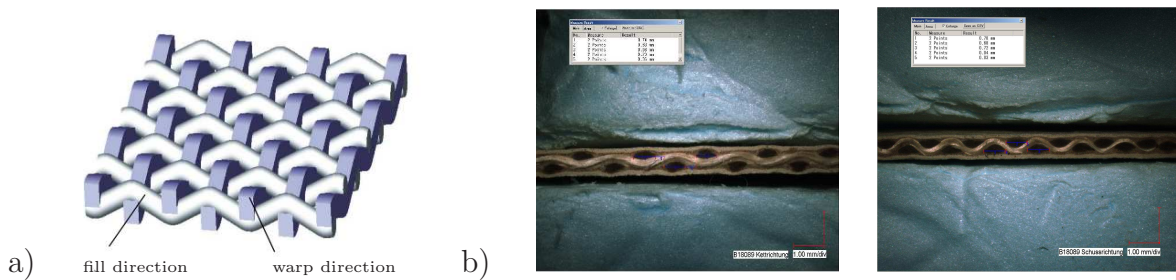


Figure 7.16: Microstructure of a woven fiber composite: a) fibers in fill and warp direction, b) cross-sections perpendicular to the warp direction (left) and to the fill direction right.

We simulate a force-driven biaxial tension test of the microstructure depicted in Figure 7.17a). The length and height of the structure are set to $L = 6\text{mm}$, $H = 3.1\text{mm}$. For the Finite-Element formulation the microstructure is discretized by 11992 ten-noded tetrahedral finite elements, cf. Figure 7.17b). The geometry is taken from SPECHT [116]. In general, we choose an additive decomposed polyconvex energy, which is easy to handle:

$$\psi = \psi^{iso} + \tilde{\psi}. \quad (7.26)$$

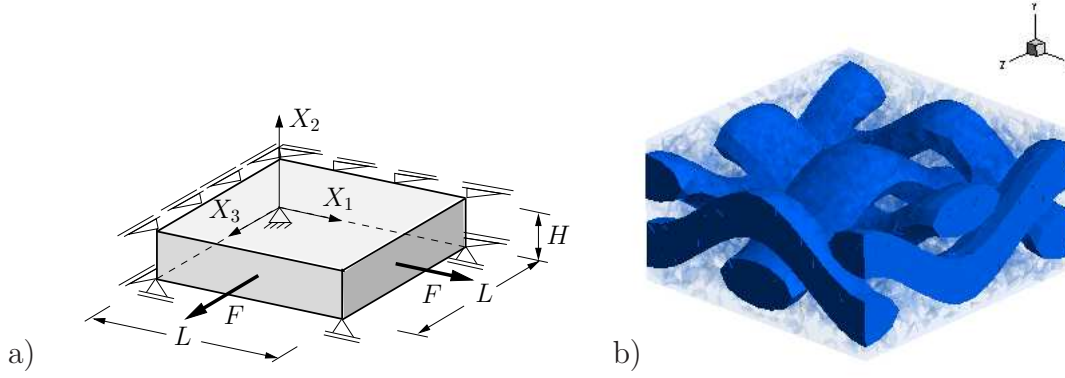


Figure 7.17: Biaxial tension test of microstructure: a) Boundary conditions, b) FE-Discretization.

Table 7.12: Material Parameter Sets.

| | α_1 | α_2 | δ_1 | ξ_{11} | ξ_{12} | α_{11} | β_{11} | γ_{11} | α_{12} | β_{12} | γ_{12} |
|----------|----------------------|------------|------------|------------|------------|---------------|--------------|---------------|---------------|--------------|---------------|
| ψ^w | 3133.60 | 13.90 | 19.90 | 50.00 | — | 0.002 | 38.59 | −0.50 | — | — | — |
| ψ^f | — | — | — | 5.00 | 5.00 | 62.66 | 0.0008 | −0.50 | 0.00 | 0.00 | 0.00 |
| ψ^m | — | — | — | 4.90 | 4.90 | 62.00 | 0.0007 | −0.50 | 4.90 | 0.00 | 0.00 |
| ψ^o | 0.49 | 0.78 | 1.13 | 83.98 | 1.85 | 0.13 | 1.10 | 2.25 | 1.90 | 3.59 | 0.47 |
| | [N/mm ²] | | | | [—] | | | | | | |

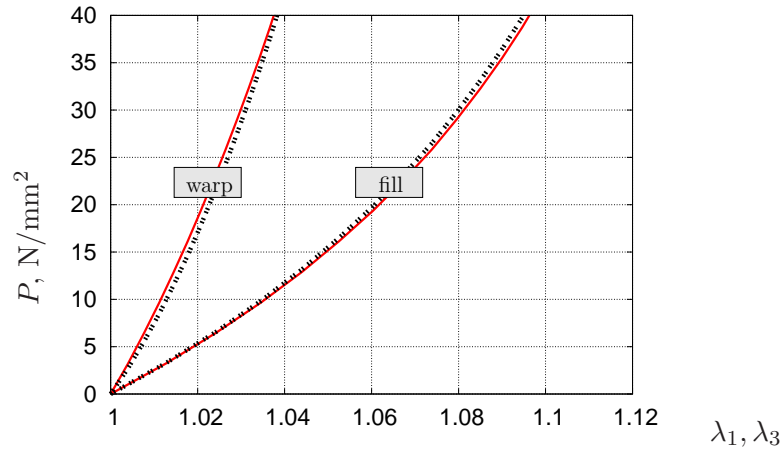


Figure 7.18: Fitting of macroscopic model: First Piola-Kirchhoff-stresses P_{33} (left curve) and P_{11} (right curve) vs. stretches $\lambda_3 = 1 + u_3/L$ and $\lambda_1 = 1 + u_1/L$, respectively.

The part ψ^{iso} is defined in (6.55) and the function (6.91) with $n = 1$, $m = 2$ is used for $\tilde{\psi}$.

If the metric tensors $\mathbf{G}_1, \mathbf{G}_2$ are equal to the second-order identity tensor $\mathbf{1}$, the function (7.26) is isotropic and can be considered for the components of the microstructure; otherwise if $\mathbf{G}_1, \mathbf{G}_2$ are equal to specific structural tensors, we obtain an anisotropic function (7.26) suitable for the description of the behavior of the macrostructure. Each component of the microstructure, i.e., the fibers in warp direction (w) and the fibers in fill direction (f) as well as the matrix (m), is described by isotropic polyconvex energies (7.26) with $\mathbf{G}_1 = \mathbf{G}_2 = \mathbf{1}$ given by

$$\psi^{w,f,m} = \psi(\mathbf{C}, \mathbf{G}_1 = \mathbf{1}, \mathbf{G}_2 = \mathbf{1}), \quad (7.27)$$

with the material parameters presented in Table 7.12. The normal displacements u_1 and u_3 of the load-contact surfaces (Figure 7.17a) of the microstructure are linked. The biaxial

tension leads to a distribution of the Cauchy stresses $\boldsymbol{\sigma} = J^{-1}\mathbf{F}\mathbf{S}\mathbf{F}^T$ in x_3 -direction, which is shown in Figure 7.19, and to an assumed overall stress-strain-behavior of the microstructure, presented as red-coloured curves in Figure 7.18.

Here the strong anisotropy effect of the fiber-reinforcement of the material can be immediately noticed, since the first Piola-Kirchhoff stresses in the considered directions enormously differ from each other. As an effective macroscopic model also the energy given by (7.26) is chosen; the anisotropy is incorporated by inserting the rhombic metric tensor (6.27) and the transversely isotropic metric tensor (6.30) into (7.26), i.e.,

$$\psi^o = \psi(\mathbf{C}, \mathbf{G}_1^o, \mathbf{G}_2^{ti}), \quad \text{with} \quad \mathbf{G}_1^o = \text{diag}(a_1, b_1, c_1), \quad \mathbf{G}_2^{ti} = \text{diag}(a_2, b_2, a_2), \quad (7.28)$$

$$a_1, a_2, b_1, b_2, c_1 > 0.$$

The isotropic part ψ^{iso} can be then interpreted as energy of the weak matrix and the part $\tilde{\psi}$ as energy of the embedded fibers. This rhombic model, depicted as black-coloured curves in Figure 7.18, is finally adjusted to the "experimental" red-coloured curves; the material parameters of the macroscopic anisotropic model are identified as $\mathbf{G}_1^o = \text{diag}[0.038, 0.154, 1.037]$, $\mathbf{G}_2^{ti} = \text{diag}[0.017, 1.106, 0.017]$ and as shown in Table 7.12.

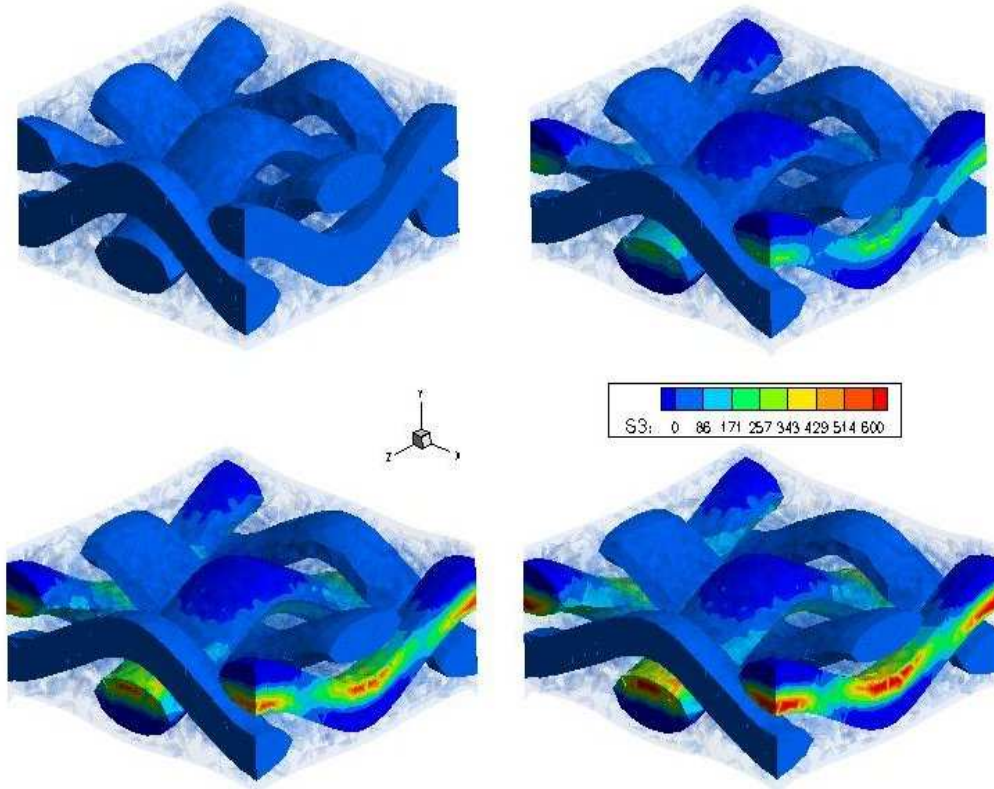


Figure 7.19: Distribution of Cauchy stresses in x_3 -direction (σ_{33}) at different stretch states.

7.4.2 Macromechanical Modeling: Thin Shells. (A part of the subsequent results is first published in EBBING ET AL. [44].)

For the macromechanically modeling of fiber composites we consider shell elements within the Finite-Element formulation. Their anisotropic, hyperelastic material behavior is described by an anisotropic polyconvex energy function of the form (6.50). Due to the fact that low order elements like quadrilaterals based on a standard displacement interpolation are usually characterized by locking phenomena, we use a mixed finite shell element with an improved convergence behavior. The first existence results for geometrically exact true two-dimensional shell models based on the Reissner-Mindlin kinematics have been given in NEFF [84, 83] for isotropy. Here, we consider a general three-dimensional anisotropic model, where the dimensional reduction appears implicitly in the numerical algorithm. An analysis of thin shells using anisotropic polyconvex energy densities is given in BALZANI, GRUTTMANN & SCHRÖDER [12] and in BALZANI, SCHRÖDER & NEFF [13]. Since the mixed finite element formulation on which the following results are based is completely taken from BETSCH ET AL. [17] we give only some remarks on the variational formulation without going into detail. For this, we refer to BETSCH ET AL. [17] and BALZANI ET AL. [12].

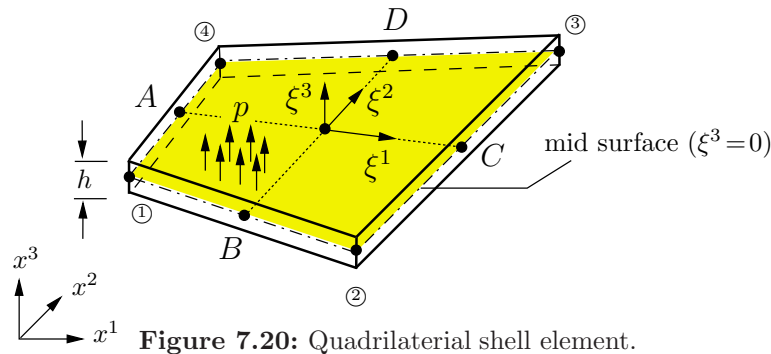


Figure 7.20: Quadrilateral shell element.

Let us first introduce the basic Reissner-Mindlin kinematics. The shell body in the reference configuration $\mathcal{B}_0 \subset \mathbb{R}^3$ is parametrized in Φ and the current configuration $\mathcal{B}_t \subset \mathbb{R}^3$ is parametrized in ϕ . The position vector Φ of any point $P \in \mathcal{B}_0$ is defined by

$$\Phi(\xi^1, \xi^2, \xi^3) = \mathbf{X}(\xi^1, \xi^2) + \xi^3 \mathbf{D}(\xi^1, \xi^2), \quad \text{with } \|\mathbf{D}(\xi^1, \xi^2)\| = 1, \quad (7.29)$$

$\xi^i, i = 1, 2, 3$ are the convected coordinates of the underlying convected coordinate system of the shell, ξ^3 with $-h/2 \leq \xi^3 \leq h/2$ is the thickness coordinate, h denotes the thickness and the midsurface Ω is defined by $\xi^3 = 0$. $\mathbf{D}(\xi^1, \xi^2)$ is a vector oriented perpendicularly to Ω . The geometry of the deformed shell is given by

$$\phi(\xi^1, \xi^2, \xi^3) = \mathbf{x}(\xi^1, \xi^2) + \xi^3 \mathbf{d}(\xi^1, \xi^2), \quad \text{with } \|\mathbf{d}(\xi^1, \xi^2)\| = 1.$$

Note that \mathbf{d} is not normal to the current configuration, hence, the assumed kinematic (7.4.2) allows for transverse shear strains. The Green-Lagrange strain tensor (2.21)₁ is here determined by

$$\mathbf{E} = \frac{1}{2}(\mathbf{F}^T \mathbf{F} - \mathbf{1}) = E_{AB} \bar{\mathbf{G}}^A \otimes \bar{\mathbf{G}}^B,$$

with $\bar{\mathbf{G}}^A = \frac{\partial \xi^A}{\partial X^J} \mathbf{E}^J$ and the index notation

$$\begin{aligned} E_{AB} &= \frac{1}{2} \left[\left(\frac{\partial \phi}{\partial \xi^A} \right)^T \frac{\partial \phi}{\partial \xi^B} - \left(\frac{\partial \Phi}{\partial \xi^A} \right)^T \frac{\partial \Phi}{\partial \xi^B} \right] \\ \Rightarrow E_{\alpha\beta} &= \varepsilon_{\alpha\beta} + \xi^3 \kappa_{\alpha\beta} + (\xi^3)^2 \rho_{\alpha\beta}, \quad 2 E_{\alpha 3} = \gamma_\alpha, \quad \alpha, \beta = 1, 2, \end{aligned}$$

with the membrane strains $\varepsilon_{\alpha\beta}$, curvatures $\kappa_{\alpha\beta}$ and shear strains γ_α

$$\begin{aligned} \varepsilon_{\alpha\beta} &= \frac{1}{2} (\mathbf{x}_{,\alpha}^T \mathbf{x}_{,\beta} - \mathbf{X}_{,\alpha}^T \mathbf{X}_{,\beta}), \quad \kappa_{\alpha\beta} = \frac{1}{2} (\mathbf{x}_{,\alpha}^T \mathbf{d}_{,\beta} + \mathbf{x}_{,\beta}^T \mathbf{d}_{,\alpha} - \mathbf{X}_{,\alpha}^T \mathbf{D}_{,\beta} - \mathbf{X}_{,\beta}^T \mathbf{D}_{,\alpha}), \\ \gamma_\alpha &= \mathbf{x}_{,\alpha}^T \mathbf{d} - \mathbf{X}_{,\alpha}^T \mathbf{D}. \end{aligned}$$

For thin structures the second-order curvatures $\rho_{\alpha\beta}$ are neglected and the shell strains are summarized in the vector

$$\boldsymbol{\varepsilon} = [\varepsilon_{11}, \varepsilon_{22}, 2\varepsilon_{13}, \kappa_{11}, \kappa_{22}, 2\kappa_{12}, \gamma_1, \gamma_2]^T. \quad (7.30)$$

The strains in thickness direction E_{33} are computed iteratively in such a way that the stresses in thickness-direction vanish, cf. BETSCH ET AL. [17] and BALZANI ET AL. [12].

7.4.2.1 The Variational Formulation.

The present finite element formulation is based on a three field variational functional as introduced by SIMO & AMERO [113] for large strains using enhanced displacement gradients. In BETSCH ET AL. [17] the Green-Lagrangian membrane strains $\boldsymbol{\varepsilon}$ are enhanced as follows

$$\hat{\boldsymbol{\varepsilon}} = \boldsymbol{\varepsilon}(\mathbf{v}) + \tilde{\boldsymbol{\varepsilon}}. \quad (7.31)$$

$\tilde{\boldsymbol{\varepsilon}}$, and $\tilde{\boldsymbol{\sigma}}$ denote the enhanced strain and stress part and \mathbf{v} is the vector of independent displacements \mathbf{u} and rotational parameters of the shell middle surface $\boldsymbol{\omega}$, i.e., $\mathbf{v} = [\mathbf{u}^T, \boldsymbol{\omega}^T]^T$. The shell is loaded statically by surface loads \mathbf{p} on Ω and by boundary forces \mathbf{t} on the boundary Γ_t . The variational framework for the enhanced assumed strain method is the following three field variational functional in a Lagrangian representation

$$\Pi(\mathbf{v}, \tilde{\boldsymbol{\varepsilon}}, \tilde{\boldsymbol{\sigma}}) = \int_{\Omega} [\psi(\hat{\boldsymbol{\varepsilon}}) - \tilde{\boldsymbol{\sigma}}^T \tilde{\boldsymbol{\varepsilon}}] dA - \int_{\Omega} \mathbf{u}^T \mathbf{p} dA - \int_{\Gamma_t} \mathbf{u}^T \mathbf{t} ds. \quad (7.32)$$

Considering the orthogonality condition for $\tilde{\boldsymbol{\sigma}}$ and $\tilde{\boldsymbol{\varepsilon}}$ as constraint in order to eliminate the independent stresses from the set of equations, variation of Π with respect to all arguments leads to a two-field weak form of equilibrium

$$\delta \Pi(\mathbf{v}, \tilde{\boldsymbol{\varepsilon}}) = \int_{\Omega} \delta \hat{\boldsymbol{\varepsilon}}^T \partial_{\hat{\boldsymbol{\varepsilon}}} \psi dA - \int_{\Omega} \delta \mathbf{u}^T \mathbf{p} dA - \int_{\Gamma_t} \delta \mathbf{u}^T \mathbf{t} ds = 0, \quad (7.33)$$

with $\delta \hat{\boldsymbol{\varepsilon}} = \delta \boldsymbol{\varepsilon} + \delta \tilde{\boldsymbol{\varepsilon}}$. The associated Euler-Lagrange equations of (7.32) are given by the following equations in Ω :

$$\begin{aligned} \frac{1}{j} (j \mathbf{n}^\alpha)_{,\alpha} + \mathbf{p} &= \mathbf{0}, & \tilde{\boldsymbol{\varepsilon}} &= \mathbf{0}, \\ \frac{1}{j} (j \mathbf{m}^\alpha)_{,\alpha} + \mathbf{x}_{,\alpha} \times \mathbf{n}_\alpha &= \mathbf{0}, & \partial_{\boldsymbol{\varepsilon}} \psi - \tilde{\boldsymbol{\sigma}} &= \mathbf{0}, \end{aligned} \quad (7.34)$$

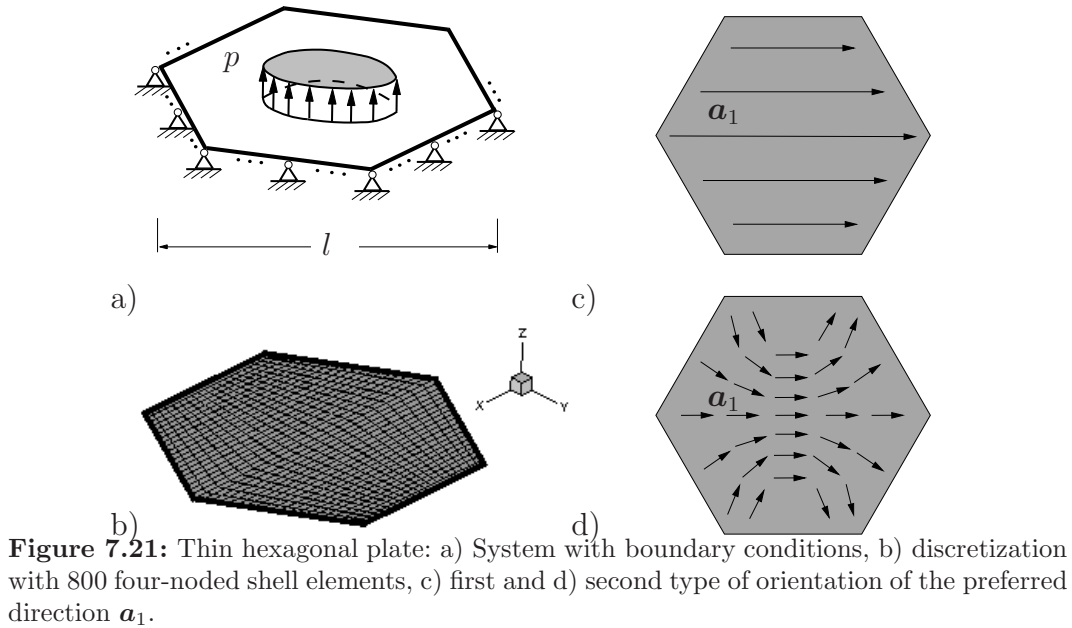
with the stress boundary conditions $j(\mathbf{n}^\alpha \nu_\alpha) - \mathbf{t} = \mathbf{0}$, $j(\mathbf{m}^\alpha \nu_\alpha) = \mathbf{0}$ on Γ_t and the geometric boundary conditions $\mathbf{u} = \mathbf{u}_0$ on Γ_u . Furthermore, the vector \mathbf{n}^α and \mathbf{m}^α are defined by $\mathbf{n}^\alpha := \mathbf{x}_{,\beta} + q^\alpha \mathbf{d} := \tilde{n}^{\alpha\beta} \mathbf{x}_{,\beta} + \tilde{q}^\alpha \mathbf{d} + \tilde{m}^{\alpha\beta} \mathbf{d}_{,\beta}$, $\mathbf{m}^\alpha := \mathbf{d} \times m^{\alpha\beta} \mathbf{x}_{,\beta}$ with the membrane forces $\tilde{n}^{\alpha\beta} = \tilde{n}^{\beta\alpha}$, bending moments $\tilde{m}^{\alpha\beta} = \tilde{m}^{\beta\alpha}$ with $m^{\alpha\beta} = \tilde{m}^{\alpha\beta}$, shear forces \tilde{q}^α and the components ν_α of the normal vector to the boundary. The stress resultants $\boldsymbol{\sigma} := \partial_{\hat{\boldsymbol{\varepsilon}}} \psi$ are organized according to (7.30) in the vector

$$\boldsymbol{\sigma} = [\tilde{n}^{11}, \tilde{n}^{22}, \tilde{n}^{12}, \tilde{m}^{11}, \tilde{m}^{22}, \tilde{m}^{12}, \tilde{q}^1, \tilde{q}^2]^T. \quad (7.35)$$

Then we approximate the field variables by using the isoparametric concept and bi-linear ansatz functions for the position and director vectors and linearize the weak form; for further details we refer to BALZANI ET AL. [12].

7.4.2.2 Thin Hexagonal Plate Subjected to Pressure.

In this numerical example, a thin hexagonal plate made of an i) isotropic and ii+iii) two types of transversely isotropic hyperelastic materials is subjected to a follower load p



(pressure at the undersurface), see Figure 7.21 a). The length of the plate depicted in Figure 7.21 a) is set to $l = 600.0$ cm and the thickness to 0.2 cm. We consider the Finite-Element discretization with 800 four-noded shell elements as shown in Figure 7.21 b). The free energy function (6.50) with the anisotropic part (6.73) is chosen, i.e.,

$$\psi = \psi^{iso} + \psi_{I,1}^{aniso}, \quad (7.36)$$

with the non-zero material parameters

$$\begin{aligned} \alpha_1 &= 8 \text{ kN/cm}^2, \quad \delta_1 = 10 \text{ kN/cm}^2, \quad \alpha_4 = 50, \\ \eta_1 &= 10 \text{ kN/cm}^2. \end{aligned} \quad (7.37)$$

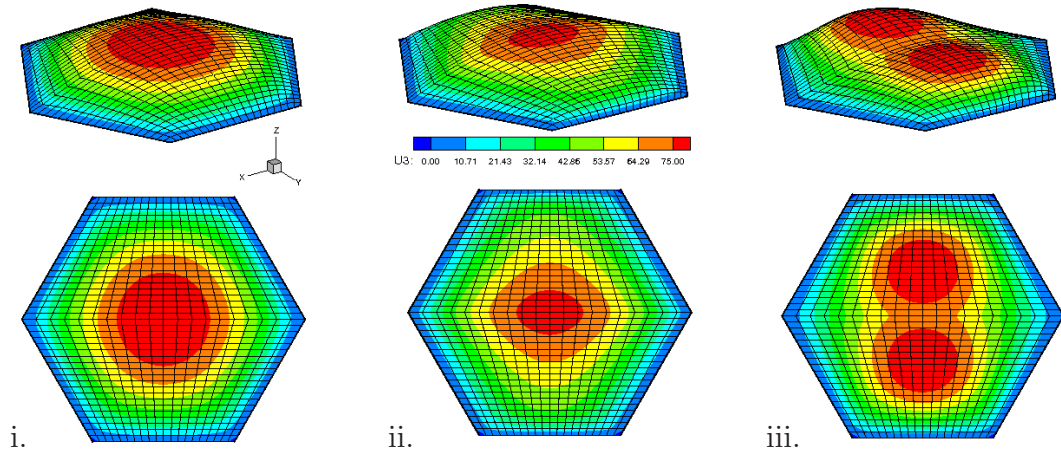


Figure 7.22: Contour plot of the vertical displacements for the isotropic i) and anisotropic ii+iii) plates.

In the following analysis we compare the results for i) an isotropic plate, described by (7.36) with

$$\mathbf{G}^{ti,i} = \mathbf{1}, \quad (7.38)$$

with the solutions ii+iii) of the anisotropic plates, using (7.36) with

$$\mathbf{G}^{ti,ii} = \text{diag}(1, 0.1, 0.1) \quad \text{and} \quad \mathbf{G}^{ti,iii} = \mathbf{R}\mathbf{G}^{ti,ii}\mathbf{R}^T, \quad (7.39)$$

respectively. \mathbf{R} is the transformation matrix from the local base system to the global coordinate system, i.e., $\mathbf{R} = [\tilde{\mathbf{e}}_1, \tilde{\mathbf{e}}_2, \tilde{\mathbf{e}}_3]$, where $\tilde{\mathbf{e}}_1, \tilde{\mathbf{e}}_2$ and $\tilde{\mathbf{e}}_3$ are the base vectors of the underlying local base system. The orientation of the base vector \mathbf{a}_1 is depicted in Figure 7.21d). The load parameter p is increased until a maximum vertical displacement of approximately 75 cm is obtained in all cases, see Figure 7.22. Figure 7.22 depicts two different views on the contour plot of the out of plane displacements for the deformed isotropic and anisotropic plate.

A comparison of these plots shows the significant differences between these cases. In the isotropic case we observe a four-fold symmetric distribution of the vertical displacements. In the first anisotropic case there is a rhombic distribution in the center of the plate, whereas in the second anisotropic case a pair of identical circles occurs. For both anisotropic plates we obtain a two-fold symmetry. The anisotropy effect can be also pointed out by comparing the deformations of the considered plates, see Figure 7.22. While the deformation of the isotropic plate is symmetric with view to all coordinate axes, a kink of the first anisotropic plate at its widest part can be noticed. The last anisotropic plate deforms to a pair of identical hills.

7.4.2.3 Hyperbolic Shell Subjected to Locally Distributed Loads.

In this numerical example we investigate the deformation of a hyperbolic shell subjected to four pairs of locally distributed vertical loads, cf. [4] or [5]. They are applied at the top and bottom of the hyperboloid and extend the structure in z -direction. In Figure 7.23a,b

the boundary value problem and the discretization with 4608 four-noded shell elements are depicted.

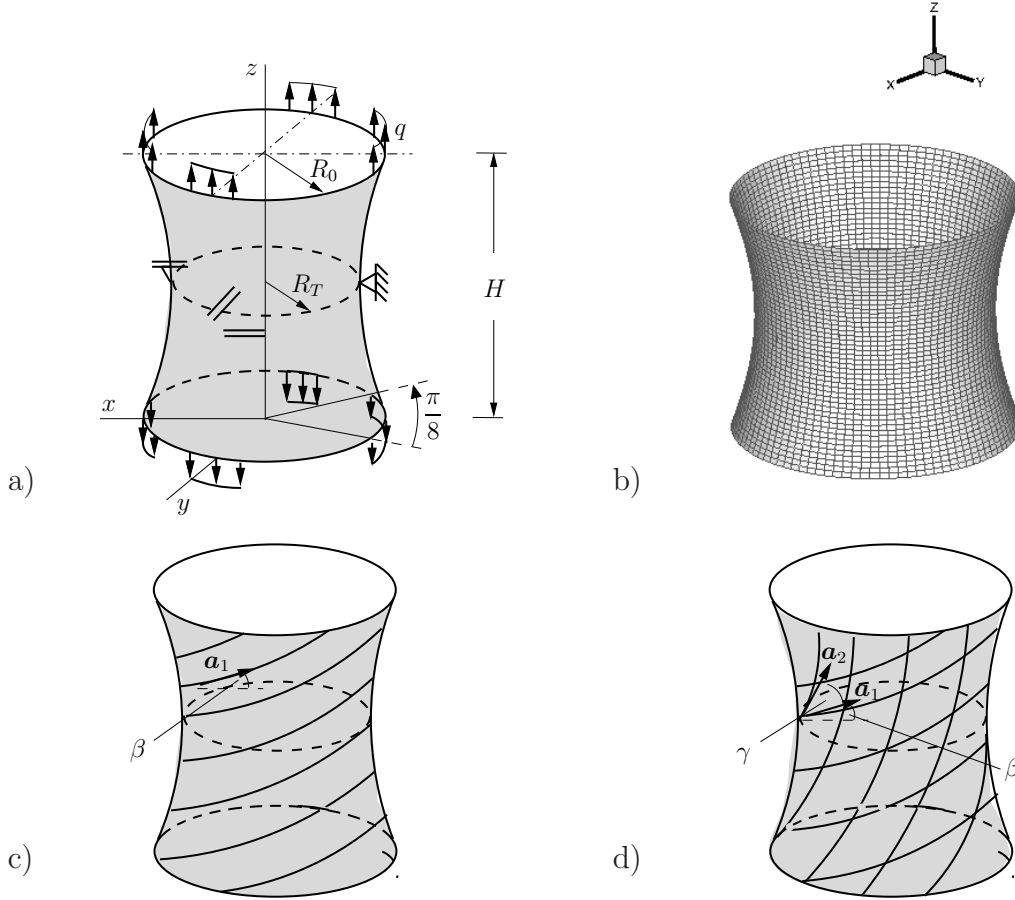


Figure 7.23: Hyperbolic shell: a) schematic sketch of the system with boundary conditions, b) discretization with 4608 four-node shell elements, c) orientation of fiber direction \mathbf{a}_1 of the transversely isotropic shell and d) orientation of fiber directions \mathbf{a}_1 and \mathbf{a}_2 of the monoclinic shell.

The height is defined to be $H = 6.0$ m and for the thickness of the shell we consider 0.05 m. The radius of the hyperbolic shell depends on the z -coordinate:

$$R(z) = R_T \sqrt{1 + \left(\frac{z - \frac{H}{2}}{2.0} \right)^2}, \quad (7.40)$$

where the minimum radius is set to $R_T = 3.0$ m and the maximum radius at the top and at the bottom of the shell is $R_0 = 4.0$ m. For an illustration of the anisotropy we compare the simulation of an i) isotropic, a ii) transversely isotropic and a iii) monoclinic shell. In all cases we consider the energy (6.50) with the anisotropic part (6.91) and $n = m = 1$. For the transversely isotropic shell one fiber direction is taken into account, which is aligned as a helix around the hyperbolic shell with $\beta = 45^\circ$, see Figure 7.23c. The local coordinate system at each Gauss point is characterized by three mutually orthogonal base vectors,

where one base vector is oriented in fiber direction, so that the base vectors are given by

$$\begin{aligned}\tilde{\mathbf{e}}_1 &= (-x_{2,GP}/r \cos\beta, x_{1,GP}/r \cos\beta, \sin\beta)^T, \\ \tilde{\mathbf{e}}_2 &= (x_{2,GP}/r \sin\beta, -x_{1,GP}/r \sin\beta, \cos\beta)^T, \\ \tilde{\mathbf{e}}_3 &= (x_{1,GP}/r, x_{2,GP}/r, 0)^T.\end{aligned}\tag{7.41}$$

The values $x_{1,GP}, x_{2,GP}$ are the coordinates of the Gauss points in \mathbf{x}_1 - and \mathbf{x}_2 -direction. The transversely isotropic metric tensors at each Gauss point with respect to a local coordinate system is chosen to be

$$\mathbf{G}_1^{l,ti} = \text{diag}[100, 0.001, 0.001].\tag{7.42}$$

Furthermore, we study the deformation of the shell, where two fibers are aligned helically around the shell with the angles $\beta = \gamma = 45^\circ$, see Figure 7.23d. This anisotropy is here described by a monoclinic metric tensor, which appears with respect to the local coordinate system as

$$\mathbf{G}_1^{l,m} = \begin{bmatrix} 100 & 10 & 0 \\ 10 & 10 & 0 \\ 0 & 0 & 0.001 \end{bmatrix}.\tag{7.43}$$

Considering here the crystallographic motivation of the structural tensors, cf. Section 6.2, we notice that the representation of this anisotropy is based on a local monoclinic crystallographic base system with the following lengths of the base vectors and characteristic angle:

$$a = \sqrt{90}, b = \sqrt{20}, c = \sqrt{0.001}, \gamma = 45^\circ.\tag{7.44}$$

The significant different lengths a and b of the crystallographic base vectors \mathbf{a}_1 and \mathbf{a}_2 , respectively, indicate that the fibers oriented in local $\tilde{\mathbf{e}}_1$ -direction are the stiffest fibers. The metric tensors with respect to the global coordinate system are calculated by

$$\mathbf{G}_1^{ti} = \mathbf{R}\mathbf{G}_1^{l,ti}\mathbf{R}^T, \quad \mathbf{G}_1^m = \mathbf{R}\mathbf{G}_1^{l,m}\mathbf{R}^T,\tag{7.45}$$

with the orthogonal transformation tensor $\mathbf{R} = [\tilde{\mathbf{e}}_1, \tilde{\mathbf{e}}_2, \tilde{\mathbf{e}}_3]$. The material parameters are

$$\begin{aligned}\alpha_1 &= 1000.0 \text{ kN/m}^2, \alpha_2 = 1.23 \text{ kN/m}^2, \delta_1 = 8.7 \text{ kN/m}^2, \\ \xi_{11} &= 10.63 \text{ kN/m}^2, \alpha_{11} = 10.63, \beta_{11} = 0.01, \gamma_{11} = 1.0.\end{aligned}\tag{7.46}$$

The hyperboloid is stretched until a final vertical displacement u_3 of approximately 1.0 m is reached. Thus, we are able to qualitatively compare the deformations of the anisotropic shells and the isotropic shell. The deformations at different stretch states are visualized in Figure 7.24, where the differences become obvious. While the isotropic shell deforms symmetrically with respect to the global coordinate axes, both anisotropic shells are twisted around the z -axis, although only loads are applied which are symmetrically oriented in z -direction. This is due to the stiffer fibers in $\tilde{\mathbf{e}}_1$ -direction in the transversely as well as monoclinic case, that provide a strong reinforcement in diagonal direction around the hyperbolic shell. Since the monoclinic shell is twice fiber-reinforced, the rotation of the shell around the z -axis is less distinct than the one of the transversely isotropic shell.

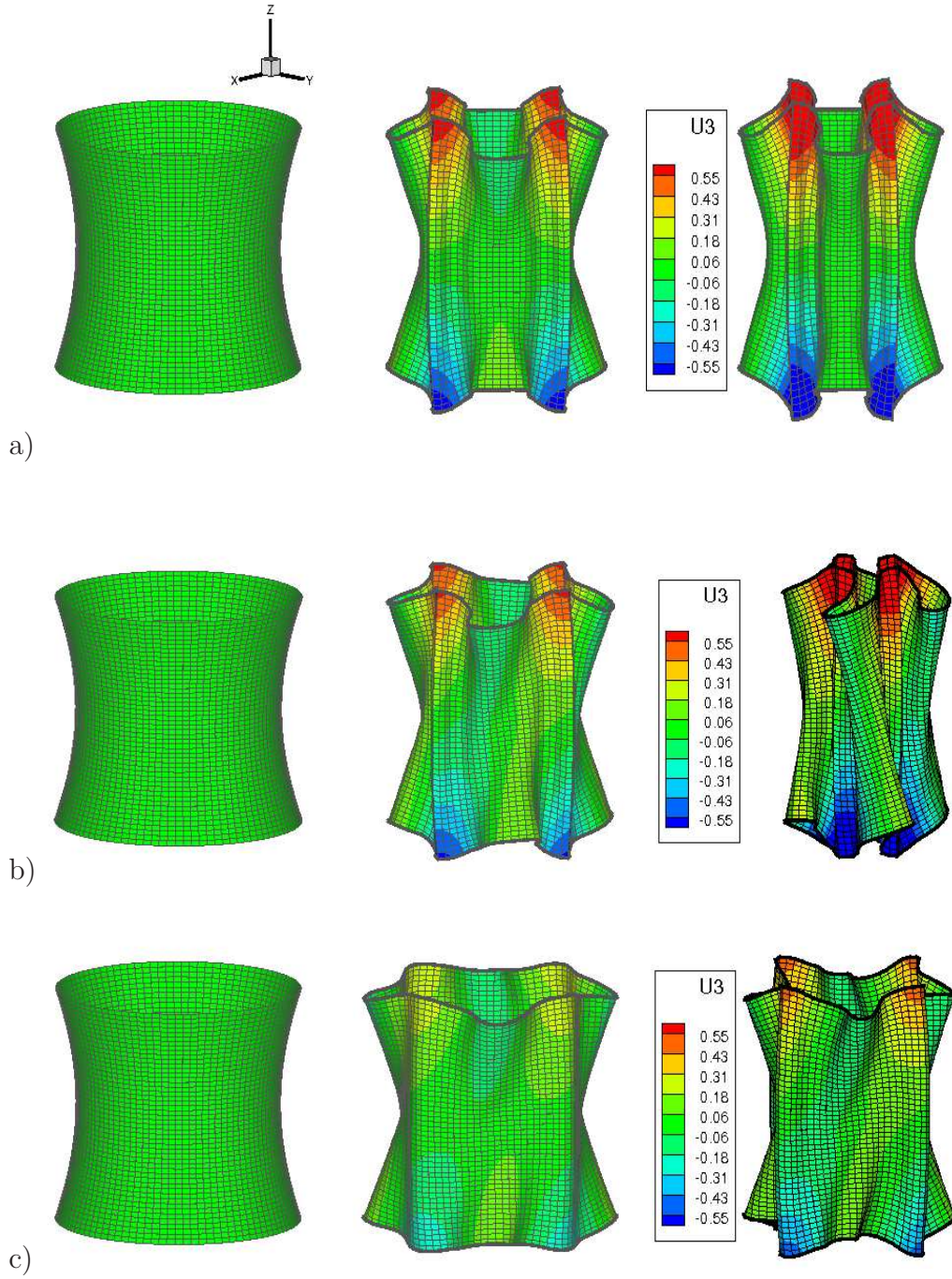


Figure 7.24: Different deformation states (from the left to the right: from the undeformed to the completely deformed state) for the a) isotropic, b) transversely isotropic and c) monoclinic shell.

7.5 Application to Configurational Mechanics.

(Parts of the following analysis are first published in EBBING, SCHRÖDER, STEINMANN & NEFF [50] and SCHRÖDER, EBBING, STEINMANN [102].)

In the field of configurational mechanics energetic changes associated to variations of material configurations are studied. The central part there is played by the energy momentum tensor, also known as the Eshelby stress tensor, which enters the configurational force balance. The mechanics of material forces has been successfully applied to a variety of fields in applied mechanics such as e.g. the evolution of interfaces, growth in biomechanical systems, the kinetics of dislocations, fracture mechanics and morphology/structure optimization in heterogeneous microstructures. A scheme of configurational forces entering computational mechanics was first mentioned in BRAUN [35]. A prominent application in the field of fracture mechanics is STEINMANN [122] and STEINMANN, ACKERMANN & BARTH [123]. Here the material forces are directly related to the classical J -integral, see e.g. KIENZLER & HERRMANN [67] and GROSS & SEELIG [54]. Besides the application of this concept in physical problems it can also be used as an error indicator in the adaptive Finite-Element-Method, see e.g. MÜLLER, KOLLING & GROSS [79], MÜLLER & MAUGIN [80], MÜLLER, GROSS & MAUGIN [78], THOUTIREDDY & ORTIZ [126] and SCHERER, DENZER & STEINMANN [98]. For an overview of recent developments in this expanding branch of continuum mechanics we refer to STEINMANN & MAUGIN [124] and STEINMANN, SCHERER & DENZER [125]. However, in most contributions configurational forces are computed for isotropic bodies; in BRÜNIG [36] a framework for anisotropically damaged elastic-plastic solids and a definition of the Eshelby stress tensor in large strain anisotropic damage mechanics is given. In this section we will compute configurational forces for anisotropic, hyperelastic solids.

As a specific model problem we consider a single-edged-tension specimen, where we analyze the sensitivity of the configurational forces in amplitude and orientation with respect to changing main axes of anisotropy of a hyperelastic material. These configurational forces can then be used as driving forces on the crack tips of the considered boundary value problem, which are directly related to the classical J -integral in fracture mechanics. For the description of the anisotropic, hyperelastic material behavior we use one of the proposed polyconvex energy functions or more specifically the energy (6.50). As a starting point we derive the balance of configurational forces in detail based on a variational argument.

7.5.1 Balance of Configurational Forces. The configurational force balance reads

$$-\text{Div}\Sigma - \tilde{\mathbf{f}} = \mathbf{0}, \quad (7.47)$$

where Σ and $\tilde{\mathbf{f}}$ denote the Eshelby stress tensor and the configurational body forces, respectively. These quantities can be derived from the energy density $\psi(\mathbf{F}, \mathbf{X})$ as follows

$$\Sigma = \psi \mathbf{1} - \mathbf{F}^T \mathbf{P}, \quad \tilde{\mathbf{f}} = -\partial_{\mathbf{X}} \psi - \mathbf{F}^T \rho_0 \mathbf{f}. \quad (7.48)$$

But how can we derive the balance of configurational forces (7.47), considering the calculus of variations ?

Let us introduce two parametrizations of the reference configuration $\mathcal{B}_0 \subset \mathbb{R}^3$, i.e., a parametrization of \mathcal{B}_0 in \mathbf{X} and a re-parametrization of \mathcal{B}_0 in $\boldsymbol{\xi}$. The map $\varphi_p^s(\mathbf{X}, t_0) : \mathcal{B}_0 \rightarrow \mathcal{B}_0$ will introduce a "material re-arrangement" of the material points in \mathcal{B}_0 :

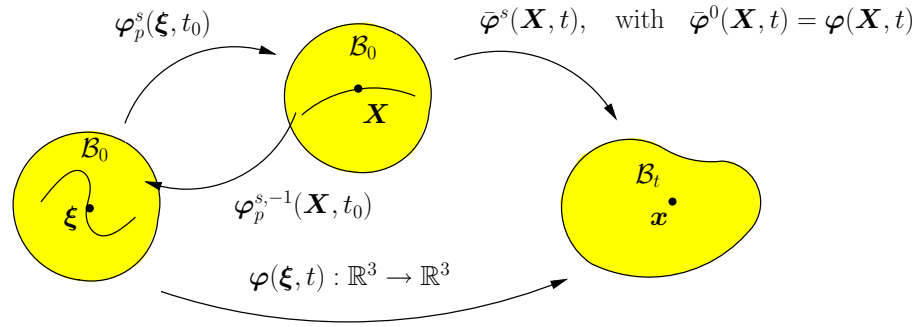


Figure 7.25: Configurational Mechanics: two parametrizations of the same reference configuration \mathcal{B}_0 .

Consider any family of smooth maps

$$\vartheta(\xi, s) : \mathcal{B}_0 \times \mathbb{R} \rightarrow \mathcal{B}_0 \quad (7.49)$$

such that $\vartheta(\cdot, s) : \mathcal{B}_0 \rightarrow \mathcal{B}_0$ is a smooth diffeomorphism for all $s \in \mathbb{R}$, with the property that

$$\vartheta(\xi, 0) = \xi. \quad (7.50)$$

Expanding with respect to $s \in \mathbb{R}$ in the neighbourhood of zero yields

$$\vartheta(\xi, s) = \vartheta(\xi, 0) + s \partial_s \vartheta(\xi, 0) + \frac{1}{2} s^2 \partial_s^2 \vartheta(\xi, 0) + \dots = \xi + s \partial_s \vartheta(\xi, 0) + \dots \quad (7.51)$$

We write in the following the family of "material variations" ("referential variations")

$$\varphi_p^s(\xi) := \vartheta(\xi, s) = \xi + s \delta \varphi_p(\xi) + \frac{1}{2} s^2 \partial_s^2 \vartheta(\xi, 0) + \dots \quad (7.52)$$

The corresponding gradient is

$$\mathbf{F}_p^s(\xi) = \nabla_\xi \varphi_p^s(\xi) = \mathbf{1} + s \nabla_\xi \delta \varphi_p^s(\xi) + \dots \quad (7.53)$$

Due to the assumption on ϑ , $\varphi_p^s : \mathcal{B}_0 \rightarrow \mathcal{B}_0$ is bijective.

With regard to Fig. 7.25 the deformation map φ can be expressed by

$$\varphi(\mathbf{X}) = \varphi(\varphi_p^{0,-1}(\mathbf{X})) \quad (7.54)$$

and

$$\varphi(\xi) = \varphi(\varphi_p^0(\xi)). \quad (7.55)$$

The deformation mapping can naturally be embedded in a family of variations $\bar{\varphi}^s$; in terms of \mathbf{X} it reads

$$\bar{\varphi}^s(\mathbf{X}) = \varphi(\varphi_p^{s,-1}(\mathbf{X})), \quad \text{with} \quad \bar{\varphi}^0(\mathbf{X}) = \varphi(\mathbf{X}) = \varphi(\xi). \quad (7.56)$$

The associated gradient is

$$\begin{aligned} \bar{\mathbf{F}}^s(\mathbf{X}) &= \nabla_{\mathbf{X}} \bar{\varphi}^s(\mathbf{X}) = \nabla_\xi \varphi(\varphi_p^{s,-1}(\mathbf{X})) \nabla_{\mathbf{X}} \varphi_p^{s,-1}(\mathbf{X}) \\ &= \nabla_\xi \varphi(\xi) [\nabla_\xi \varphi_p^s(\xi)]^{-1} \\ &= \mathbf{F}(\xi) \quad \mathbf{F}_p^{s,-1}(\xi). \end{aligned} \quad (7.57)$$

In terms of $\boldsymbol{\xi}$ we have

$$\bar{\boldsymbol{\varphi}}^s(\boldsymbol{\varphi}_p^s(\boldsymbol{\xi})) = \boldsymbol{\varphi}(\boldsymbol{\xi}). \quad (7.58)$$

The associated gradient is

$$\begin{aligned} \mathbf{F}(\boldsymbol{\xi}) &= \nabla_{\boldsymbol{\xi}} \boldsymbol{\varphi}(\boldsymbol{\xi}) = \nabla_X \bar{\boldsymbol{\varphi}}^s(\boldsymbol{\varphi}_p^s(\boldsymbol{\xi})) \nabla_{\boldsymbol{\xi}} \boldsymbol{\varphi}_p^s(\boldsymbol{\xi}) \\ &= \nabla_X \bar{\boldsymbol{\varphi}}^s(\mathbf{X}) \nabla_{\boldsymbol{\xi}} \boldsymbol{\varphi}_p^s(\boldsymbol{\xi}) \\ &= \bar{\mathbf{F}}^s(\mathbf{X}) \mathbf{F}_p^s(\boldsymbol{\xi}). \end{aligned} \quad (7.59)$$

In hyperelasticity, $\boldsymbol{\varphi}$ is a critical point of the associated free energy, therefore the potential $\Pi(\bar{\boldsymbol{\varphi}}^s(\mathbf{X}))$ becomes stationary for $s = 0$, i.e.,

$$\Pi(\bar{\boldsymbol{\varphi}}^s(\mathbf{X}))|_{s=0} = \Pi(\boldsymbol{\varphi}(\mathbf{X})) \rightarrow \text{stat.}, \quad (7.60)$$

if

$$\delta \Pi = \left. \frac{d}{ds} \right|_{s=0} \Pi(\bar{\boldsymbol{\varphi}}^s(\mathbf{X})) = 0 \quad (7.61)$$

holds. Without Neumann boundary conditions the potential reads

$$\Pi(\bar{\boldsymbol{\varphi}}^s(\mathbf{X})) = \int_{X \in \mathcal{B}_0} \psi(\bar{\mathbf{F}}^s(\mathbf{X})) dV - \int_{X \in \mathcal{B}_0} \langle \rho_0 \mathbf{f}, \bar{\boldsymbol{\varphi}}^s(\mathbf{X}) \rangle dV. \quad (7.62)$$

The internal material change of variable leads to

$$\begin{aligned} \Pi &= \int_{X \in \mathcal{B}_0} \psi(\bar{\mathbf{F}}^s(\mathbf{X})) dV - \int_{X \in \mathcal{B}_0} \langle \rho_0 \mathbf{f}, \bar{\boldsymbol{\varphi}}^s(\mathbf{X}) \rangle dV \\ &= \underbrace{\int_{\boldsymbol{\xi} \in \boldsymbol{\varphi}_p^{s,-1}(\mathcal{B}_0) = \mathcal{B}_0} \psi(\mathbf{F}(\boldsymbol{\xi}) \mathbf{F}_p^{s,-1}(\boldsymbol{\xi})) \det \mathbf{F}_p^s(\boldsymbol{\xi}) dV}_{\Pi^{int}} - \underbrace{\int_{\boldsymbol{\xi} \in \boldsymbol{\varphi}_p^{s,-1}(\mathcal{B}_0) = \mathcal{B}_0} \langle \rho_0 \mathbf{f}, \boldsymbol{\varphi}(\boldsymbol{\xi}) \rangle \det \mathbf{F}_p^s(\boldsymbol{\xi}) dV}_{\Pi^{ext}} \\ &= \Pi^{int} + \Pi^{ext}. \end{aligned}$$

The first derivative of the first part with respect to s yields

$$\begin{aligned} \frac{d}{ds} \Pi^{int} &= \frac{d}{ds} \int_{\boldsymbol{\xi} \in \mathcal{B}_0} \psi(\mathbf{F} \mathbf{F}_p^{s,-1}) \det \mathbf{F}_p^s dV \\ &= \int_{\boldsymbol{\xi} \in \mathcal{B}_0} \left[\frac{d}{ds} \psi(\mathbf{F} \mathbf{F}_p^{s,-1}) \right] \det \mathbf{F}_p^s dV + \int_{\boldsymbol{\xi} \in \mathcal{B}_0} \psi(\mathbf{F} \mathbf{F}_p^{s,-1}) \left[\frac{d}{ds} \det \mathbf{F}_p^s \right] dV \\ &= \int_{\boldsymbol{\xi} \in \mathcal{B}_0} \left[\langle \partial_F \psi(\mathbf{F} \mathbf{F}_p^{s,-1}), \mathbf{F} \frac{d}{ds} [\mathbf{F}_p^{s,-1}] \rangle \det \mathbf{F}_p^s + \psi(\mathbf{F} \mathbf{F}_p^{s,-1}) \langle \text{Cof} \mathbf{F}_p^s, \frac{d}{ds} \mathbf{F}_p^s \rangle \right] dV \\ &= \int_{\boldsymbol{\xi} \in \mathcal{B}_0} \left[\langle \mathbf{F}^T \partial_F \psi(\mathbf{F} \mathbf{F}_p^{s,-1}), \frac{d}{ds} [\mathbf{F}_p^{s,-1}] \rangle \det \mathbf{F}_p^s + \psi(\mathbf{F} \mathbf{F}_p^{s,-1}) \langle \text{Cof} \mathbf{F}_p^s, \frac{d}{ds} \mathbf{F}_p^s \rangle \right] dV, \end{aligned}$$

where we have applied the chain rule

$$\frac{d}{ds} \psi = \partial_F \psi : \partial_{\mathbf{F}_p^{s,-1}} \mathbf{F} : \frac{d}{ds} \mathbf{F}_p^{s,-1}.$$

With the relation

$$\frac{d}{ds} \mathbf{F}_p^{s,-1} = \partial_{\mathbf{F}_p^s} \mathbf{F}_p^{s,-1} : \frac{d}{ds} \mathbf{F}_p^s = -\mathbf{F}_p^{s,-1} \frac{d}{ds} [\mathbf{F}_p^s] \mathbf{F}_p^{s,-T}$$

we get

$$\begin{aligned}
\frac{d}{ds} \Pi^{int} &= \int_{\xi \in \mathcal{B}_0} \left[\langle \mathbf{F}^T \partial_F \psi(\mathbf{F}^s \mathbf{F}_p^{s,-1}), -\mathbf{F}_p^{s,-1} \frac{d}{ds} [\mathbf{F}_p^s] \mathbf{F}_p^{s,-T} \rangle \det \mathbf{F}_p^s + \psi(\mathbf{F} \mathbf{F}_p^{s,-1}) \langle \text{Cof} \mathbf{F}_p^s, \frac{d}{ds} \mathbf{F}_p^s \rangle \right] dV \\
&= \int_{\xi \in \mathcal{B}_0} \left[\langle -(\mathbf{F} \mathbf{F}_p^{s,-1})^T \partial_F \psi(\mathbf{F} \mathbf{F}_p^{s,-1}), \frac{d}{ds} [\mathbf{F}_p^s] \mathbf{F}_p^{s,-T} \rangle \det \mathbf{F}_p^s + \psi(\mathbf{F} \mathbf{F}_p^{s,-1}) \langle \text{Cof} \mathbf{F}_p^s, \frac{d}{ds} \mathbf{F}_p^s \rangle \right] dV \\
&= \int_{\xi \in \mathcal{B}_0} \left[\langle -(\bar{\mathbf{F}}^s)^T \partial_F \psi(\bar{\mathbf{F}}^s), \frac{d}{ds} [\mathbf{F}_p^s] \mathbf{F}_p^{s,-T} \rangle \det \mathbf{F}_p^s + \psi(\bar{\mathbf{F}}^s) \langle \text{Cof} \mathbf{F}_p^s, \frac{d}{ds} \mathbf{F}_p^s \rangle \right] dV.
\end{aligned}$$

At $s = 0$ the following relations hold:

$$\boldsymbol{\xi} = \mathbf{X}, \quad \bar{\mathbf{F}}^0 = \mathbf{F}, \quad \frac{d}{ds} \Big|_{s=0} \mathbf{F}_p^s = \nabla_X \delta \boldsymbol{\varphi}_p, \quad \mathbf{F}_p^0 = \mathbf{1}, \quad \text{Cof} \mathbf{F}_p^0 = \mathbf{1}.$$

Thus, the evaluation of $\frac{d}{ds} \Pi^{int}$ at $s = 0$ gives

$$\begin{aligned}
\frac{d}{ds} \Big|_{s=0} \Pi^{int} &= \frac{d}{ds} \Big|_{s=0} \int_{X \in \mathcal{B}_0} \underbrace{\langle -\mathbf{F}^T \partial_F \psi(\mathbf{F}) + \psi(\mathbf{F}) \mathbf{1}, \nabla_X \delta \boldsymbol{\varphi}_p \rangle}_{\boldsymbol{\Sigma}} dV = \int_{X \in \mathcal{B}_0} \langle \boldsymbol{\Sigma}, \nabla_X \delta \boldsymbol{\varphi}_p \rangle dV \\
&= \int_{X \in \mathcal{B}_0} [-\langle \text{Div} \boldsymbol{\Sigma}, \delta \boldsymbol{\varphi}_p \rangle + \text{Div}(\boldsymbol{\Sigma} \delta \boldsymbol{\varphi}_p)] dV \\
&= \int_{X \in \mathcal{B}_0} \langle -\text{Div} \boldsymbol{\Sigma}, \delta \boldsymbol{\varphi}_p \rangle dV + \int_{X \in \partial \mathcal{B}_{0t}} \langle \boldsymbol{\Sigma} \mathbf{N}, \delta \boldsymbol{\varphi}_p \rangle dA,
\end{aligned}$$

where the Eshelby stress tensor $\boldsymbol{\Sigma}$ is defined in (7.48). The first derivative of the second part Π^{ext} with respect to s yields

$$\frac{d}{ds} \Pi^{ext} = \frac{d}{ds} \int_{\xi \in \mathcal{B}_0} -\langle \rho_0 \mathbf{f}, \boldsymbol{\varphi} \rangle \det \mathbf{F}_p^s dV = \int_{\xi \in \mathcal{B}_0} -\langle \rho_0 \mathbf{f}, \boldsymbol{\varphi} \rangle \langle \text{Cof} \mathbf{F}_p^s, \frac{d}{ds} \mathbf{F}_p^s \rangle dV.$$

Evaluation at $s = 0$ gives

$$\begin{aligned}
\frac{d}{ds} \Big|_{s=0} \Pi^{ext} &= \int_{X \in \mathcal{B}_0} -\langle \rho_0 \mathbf{f}, \boldsymbol{\varphi} \rangle \langle \mathbf{1}, \nabla_X \delta \boldsymbol{\varphi}_p \rangle dV = \int_{X \in \mathcal{B}_0} -\langle \rho_0 \mathbf{f}, \boldsymbol{\varphi} \rangle \text{Div} \delta \boldsymbol{\varphi}_p dV \\
&= \int_{X \in \mathcal{B}_0} -\text{Div}(\langle \rho_0 \mathbf{f}, \boldsymbol{\varphi} \rangle \delta \boldsymbol{\varphi}_p) dV + \int_{X \in \mathcal{B}_0} \langle \nabla_X \langle \rho_0 \mathbf{f}, \boldsymbol{\varphi} \rangle, \delta \boldsymbol{\varphi}_p \rangle dV \\
&= \underbrace{\int_{X \in \partial \mathcal{B}_{0\varphi_p}} -\langle \langle \rho_0 \mathbf{f}, \boldsymbol{\varphi} \rangle \mathbf{N}, \delta \boldsymbol{\varphi}_p \rangle dA}_{= 0, \text{ since } \delta \boldsymbol{\varphi}_p = \mathbf{0} \text{ on } \partial \mathcal{B}_{0\varphi_p}} + \int_{X \in \mathcal{B}_0} \langle \nabla_X \langle \rho_0 \mathbf{f}, \boldsymbol{\varphi} \rangle, \delta \boldsymbol{\varphi}_p \rangle dV \\
&= \int_{X \in \mathcal{B}_0} \langle (\nabla_X \boldsymbol{\varphi})^T \rho_0 \mathbf{f}, \delta \boldsymbol{\varphi}_p \rangle dV = \int_{X \in \mathcal{B}_0} \langle \mathbf{F}^T \rho_0 \mathbf{f}, \delta \boldsymbol{\varphi}_p \rangle dV.
\end{aligned}$$

The first variation of the whole potential Π (7.62) results therefore in

$$\delta \Pi = \int_{X \in \mathcal{B}_0} -\langle (\text{Div} \boldsymbol{\Sigma} + \tilde{\mathbf{f}}), \delta \boldsymbol{\varphi}_p \rangle dV + \int_{X \in \partial \mathcal{B}_{0t}} \langle \boldsymbol{\Sigma} \mathbf{N}, \delta \boldsymbol{\varphi}_p \rangle dA = 0, \quad \forall \delta \boldsymbol{\varphi}_p(\mathcal{B}_0) \quad (7.63)$$

$$\text{with } \tilde{\mathbf{f}} = -\mathbf{F}^T \rho_0 \mathbf{f}.$$

Applying the fundamental lemma of the calculus of variation yields the corresponding (so-called second form of) Euler-Lagrange equations

$$\text{Div}\Sigma + \tilde{\mathbf{f}} = \mathbf{0} \quad \forall \mathbf{X} \in \mathcal{B}_0, \quad \Sigma \mathbf{N} = \mathbf{0} \quad \text{on} \quad \partial\mathcal{B}_{0t}, \quad (7.64)$$

since $\delta\varphi_p$ can be varied independently in the interior of \mathcal{B}_0 and on the boundary $\partial\mathcal{B}_{0t}$. $\tilde{\mathbf{f}}$ denotes the transformed body forces in the configurational framework.

In the literature, there are several approaches leading formally to the balance of configurational forces (7.47). Let us briefly introduce a further derivation. For homogeneous, hyperelastic materials the free energy function depends only on \mathbf{F} , i.e., $\psi = \psi(\mathbf{F})$. The gradient of ψ then yields

$$\text{Grad}\psi = \partial_{\mathbf{F}}\psi : \text{Grad}\mathbf{F} = \mathbf{P} : \text{Grad}\mathbf{F} \Rightarrow \text{Grad}\psi - \partial_{\mathbf{F}}\psi : \text{Grad}\mathbf{F} = \mathbf{0}. \quad (7.65)$$

In index notation, with respect to a cartesian coordinate system, the term $\mathbf{P} : \text{Grad}\mathbf{F}$ appears as $P_{ij} : F_{ij,k}$. We apply the relation

$$\text{Div}(\mathbf{F}^T \mathbf{P}) = \mathbf{P} : \text{Grad}\mathbf{F} + \mathbf{F}^T \text{Div}\mathbf{P} \Leftrightarrow \mathbf{P} : \text{Grad}\mathbf{F} = \text{Div}(\mathbf{F}^T \mathbf{P}) - \mathbf{F}^T \text{Div}\mathbf{P}.$$

That the first equation is true can be easily seen in index notation, since

$$(F_{ij} P_{ik})_{,k} = F_{ij,k} P_{ik} + F_{ij} P_{ik,k} = F_{ik,j} P_{ik} + F_{ij} P_{ik,k}, \quad (7.66)$$

where we use the Theorem of Schwarz on the interchangeability of second derivatives, here of $\text{Grad}\mathbf{F} = \text{Grad}(\text{Grad}\varphi)$, i.e., in index notation

$$F_{ij,k} = (\varphi_{i,j})_{,k} = \varphi_{i,j,k} = \varphi_{i,k,j} = F_{ik,j}.$$

We obtain then the universal identity

$$\text{Grad}\psi - \text{Div}(\mathbf{F}^T \mathbf{P}) - \mathbf{F}^T \text{Div}\mathbf{P} = \mathbf{0}. \quad (7.67)$$

Inserting the classical balance of linear momentum $\text{Div}\mathbf{P} = \rho_0 \mathbf{f}$ (see (2.107)₁), and taking into account that

$$\text{Div}(\psi \mathbf{1}) = \text{Div} \begin{bmatrix} \psi & 0 & 0 \\ 0 & \psi & 0 \\ 0 & 0 & \psi \end{bmatrix} = \begin{bmatrix} \frac{\partial \psi}{\partial X_1} \\ \frac{\partial \psi}{\partial X_2} \\ \frac{\partial \psi}{\partial X_3} \end{bmatrix} = \text{Grad}\psi, \quad (7.68)$$

so that the divergence of the Eshelby stress tensor (7.48) can be written as

$$\text{Div}\Sigma = \text{Div}(\psi \mathbf{1} - \mathbf{F}^T \mathbf{P}) = \text{Grad}\psi - \text{Div}(\mathbf{F}^T \mathbf{P}),$$

leads finally to the following reformulation of (7.67)

$$\text{Div}\Sigma - \mathbf{F}^T \rho_0 \mathbf{f} = \mathbf{0}.$$

Provided that the solution φ is smooth enough, this equation is valid if and only if the classical balance of linear momentum holds. It can therefore be used as an independent check of any approximate solution to (2.107)₁. Indeed, it may act as an error indicator.

In the example which we will consider we neglect configurational body forces for the sake of simplicity since our numerical example will exclusively concentrate on homogeneous material properties and vanishing (spatial) body forces. Note that this case corresponds to divergence free (solenoidal) Eshelby stresses and thus to path-independent J -integrals, an attractive property in fracture mechanics.

Next, the test function is selected from a proper finite dimensional test space \mathcal{V}_0^h that is typically spanned by polynomial basis functions N_I as already used in the Finite-Element-discretization of the spatial deformation problem. Finally, the discrete configurational (nodal) material force \mathbf{f}_I^{config} at node point I are computed by

$$\delta \Pi = \underbrace{\int_{\mathcal{B}_0} [\text{Grad} \delta \boldsymbol{\varphi}_p : \boldsymbol{\Sigma}] dV}_{\sum_I^{nen} \delta \mathbf{d}_I^T \cdot \mathbf{f}_I^{config}} - \int_{\partial \mathcal{B}_{0t}} \delta \boldsymbol{\varphi}_p \cdot \boldsymbol{\Sigma} \mathbf{N} dA = 0, \quad (7.69)$$

$$\sum_I^{nen} \delta \mathbf{d}_I^T \cdot \mathbf{f}_I^{config} = \sum_I^{nen} \delta \mathbf{d}_I^T \cdot \int_{\mathcal{B}_0} [\text{Grad} N_I]^T \boldsymbol{\Sigma} dV.$$

These vectorial quantities are power conjugated to configurational changes of the material node point positions, they are easily calculated in a *post processing* step, the so-called *Material Force Method*, once the solution to the spatial deformation problem has been computed, see ACKERMANN, BARTH & STEINMANN [1]. Here the sign convention associates a configurational change of the material node point position in the direction of the discrete material node point force with an energy increase of the system. Thus in order to release energy, that can then potentially be used for other physical processes like, e.g., the creation of new surfaces or the motion of defects, material node point positions have to move opposite to the material node point forces.

7.5.2 Cracked SET Specimen. As a numerical example we consider a single-edged-tension specimen (SET) consisting of a hyperelastic, transversely isotropic material as shown in Figure 7.26. We study the influence of the orientation of the main axes of anisotropy on the amplitude and orientation of the configurational forces at the crack tips. The main axis of anisotropy corresponds to the preferred direction \mathbf{a}_1 of the transversely isotropic material.

The orientation of the preferred direction is described by the angle $\varphi = \angle(\mathbf{a}_1, \mathbf{e}_1)$, whereas the direction of the configurational force at the crack tip A is characterized by the angle $\eta = \angle(\mathbf{f}_A^{config}, \mathbf{e}_1)$. The material behavior is described by the polyconvex energy function (6.50) with the anisotropic part (6.91) and $n = m = 1$, i.e.,

$$\psi^{ti} = \psi^{iso} + \psi_{II}^{aniso}, \quad (7.70)$$

where the transversely isotropic metric tensor with respect to the local coordinate system appears as

$$\mathbf{G}_1^{ti,l} = \text{diag}[1, 0, 0]. \quad (7.71)$$

The local base vectors are given by $\tilde{\mathbf{e}}_1 = (\cos \varphi, \sin \varphi, 0)^T$, $\tilde{\mathbf{e}}_2 = (-\sin \varphi, \cos \varphi, 0)^T$, $\tilde{\mathbf{e}}_3 = (0, 0, 1)^T$. The metric tensor is transformed to the global coordinate system by $\mathbf{G}_1^{ti} = \mathbf{R} \mathbf{G}_1^{ti,l} \mathbf{R}^T$, with the rotation tensor $\mathbf{R} = [\tilde{\mathbf{e}}_1, \tilde{\mathbf{e}}_2, \tilde{\mathbf{e}}_3]$. The Eshelby stress tensor, defined in (7.48), is finally calculated by

$$\boldsymbol{\Sigma} = \psi_0^{ti} \mathbf{1} - \mathbf{C} \mathbf{S}, \quad (7.72)$$

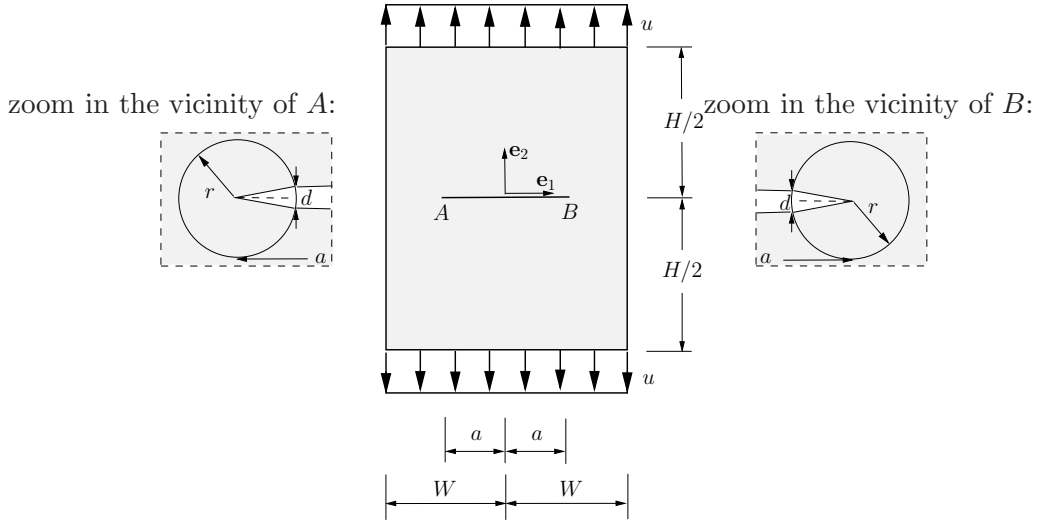


Figure 7.26: Undeformed SET specimen, boundary conditions.

where we have introduced the abbreviation

$$\psi_0^{ti} = \psi^{ti} - \psi^{ti}(\mathbf{C} = \mathbf{1}), \quad (7.73)$$

in order to satisfy the condition $\Sigma = \mathbf{0}$ in the unloaded reference configuration. The material parameters are set to

$$\begin{aligned} \alpha_1 &= 1 \text{ N/mm}^2, \quad \alpha_2 = 1 \text{ N/mm}^2, \quad \delta_1 = 1 \text{ N/mm}^2, \\ \xi_{11} &= 1 \text{ N/mm}^2, \quad \alpha_{11} = 10, \quad \beta_{11} = 1, \quad \gamma_{11} = 1. \end{aligned} \quad (7.74)$$

The height to width ratio of the SET specimen is chosen to be $H/W = 120 \text{ mm}/40 \text{ mm}$, the crack length to width ratio is set to $a/W = 0.5$ and the thickness of the crack is $d = 0.2 \text{ mm}$, see Figure 7.26. The specimen is discretized by 7886 six-noded triangle elements and the mesh is strongly refined in the vicinity of the crack tips as shown in Figure 7.27. In detail, we discretized a circular area around each crack tip with the radius $r = r_{10} = 0.52 \text{ mm}$. The radii of the inner circles of finite elements of these domains are calculated by geometric series

$$r_i = \omega^{i-1} r_1, \quad i = 1, \dots, 10, \quad \text{with} \quad r_1 = 0.1 \text{ mm}, \quad \omega = 1.2. \quad (7.75)$$

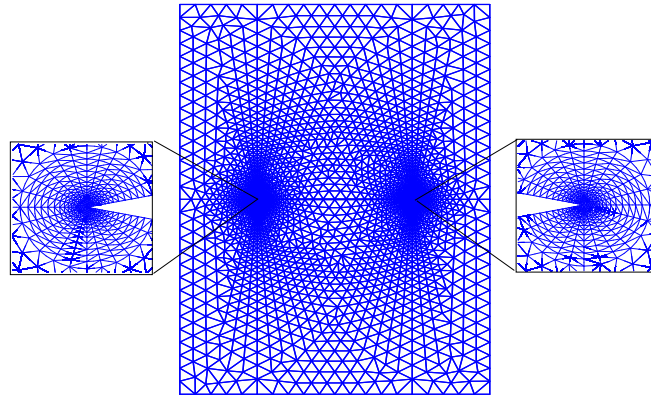


Figure 7.27: Undeformed SET specimen, discretization with 7886 6-noded triangle elements.

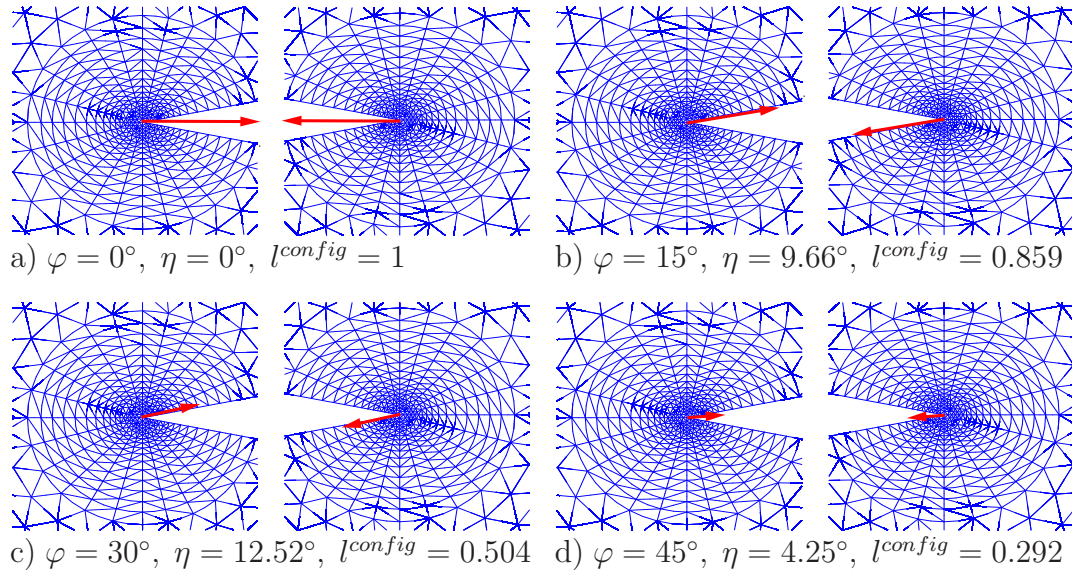


Figure 7.28: Angle η versus angle φ . Ratios of norms of material forces.

For a good approximation of the material force \mathbf{f}^{config} acting at crack tips A and B with the Material Force Method, we choose the whole circular area around the crack tip as the integration domain. Figure 7.28 depicts the results of the orientation and amplitudes of the configurational forces at both crack tips for four different orientations of the preferred direction. The amplitudes of the material forces are normalized with respect to the amplitude to the material force in case of $\varphi = 0^\circ$, i.e.,

$$l^{config}(\varphi) = \|\mathbf{f}^{config}(\varphi)\| / \|\mathbf{f}^{config}(\varphi = 0^\circ)\|. \quad (7.76)$$

Comparing these ratios we notice that the amplitude of the forces becomes significantly smaller by increasing the angle of anisotropy up to 45° . Regarding the changes of the angles φ and η Figure 7.28 shows the following: for $\varphi = 0^\circ, 15^\circ, 30^\circ$ the angle of orientation of \mathbf{f}^{config} rises from 0° to about 12° , whereas for $\varphi = 45^\circ$ we obtain the angle $\eta \approx 4.25^\circ$. This fact can be also noticed by observing Figure 7.29, where the relation between the angles η and φ is depicted, see also SCHRÖDER, EBBING, STEINMANN [102]. Figure 7.29 especially shows the 180° -periodicity of the $\varphi - \eta$ -curve. Therefore, a high sensitivity of the configurational forces in amplitude as well as in orientation appears in the considered boundary value problem.

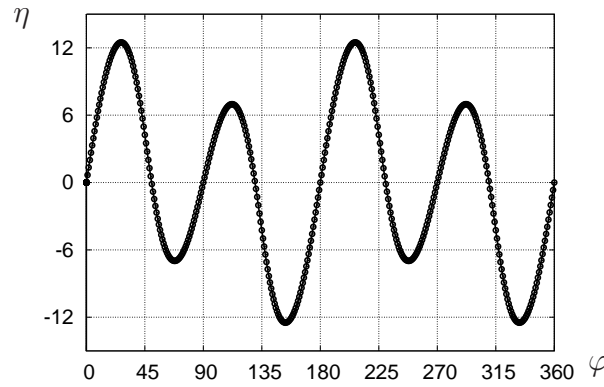


Figure 7.29: Angle of configurational force η versus angle of preferred direction φ , $[\circ]$.

8 Summary and Conclusion.

The overall question of this thesis is the second open problem in elasticity posed in the article *Some open problems in elasticity* of BALL [10], which reads:

Are there ways of verifying polyconvexity and quasiconvexity for a useful class of anisotropic stored-energy functions?

We have started with the definition of constitutive equations for the representation of hyperelasticity and important restrictions of these equations like the principle of material symmetry for the specification of isotropic and anisotropic material behaviour. Anisotropic material behaviour can be classified by thirteen mechanically important symmetry groups. Eleven of them are associated with 32 crystal symmetry classes and the remaining two are the transversely isotropic cases. Tensor representation theorems for isotropic tensor functions have been applied, which lead to coordinate-invariant formulations of the constitutive equations in terms of scalar-valued invariants of an underlying set of invariants. For the exploitation of these theorems also in the anisotropic case, the concept of structural tensors has been considered. However, these classical theorems are based on tensors up to the second order and could therefore only be established for those anisotropies, which can be described by structural tensors of such an order. Triclinic, monoclinic, rhombic as well as transversely isotropic symmetries can be characterized by second-order structural tensors; the description of tetragonal, trigonal, hexagonal and cubic symmetries requires higher-order structural tensors up to the sixth order. Unfortunately, we could not find exhaustive discussions of tensor representation theorems for isotropic tensor functions on the basis of tensor-valued arguments of order higher than two in the literature. The most useful approach, which could be found in the literature, is the introduction of second-order isotropic extension functions as additional arguments of the tensor function. In view of a physically reasonable material modeling and in order to guarantee the existence of solutions of the underlying boundary value problem in finite strain elasticity, a further restriction of the energy function has been satisfied, namely the polyconvexity condition. It guarantees the existence of minimizers of the corresponding variational functional – if in addition the coercivity condition is fulfilled – and ensures the strict Legendre-Hadamard ellipticity – if the underlying energy function is smooth enough. This ellipticity condition is related to material stability, because it leads to a positive definite acoustic tensor and therefore to real wave speeds inside the material.

We have shown that the sets of invariants derived on the basis of the isotropic extension concept and the well-known structural tensors are in general not polyconvex and even not elliptic. We were therefore interested in the construction of different structural tensors, which automatically fulfill the polyconvexity condition. A fundamental new idea is the introduction of

symmetric and positive (semi-)definite, crystallographically motivated second- and fourth-order structural tensors for all mechanically important anisotropy groups.

Based on these tensors and the right Cauchy-Green tensor constructions of polyconvex mixed invariants were possible. Furthermore, polyconvex energy functions satisfying a

priori the stress-free reference configuration condition have been formulated. Due to the generic character of the proposed energies the simulation of real anisotropic material behaviour was successful. Their applicability within a few numerical examples has been presented. For instance, they were used for an in-silico micromechanical analysis of a woven fiber composite, from which the material parameters of an effective polyconvex anisotropic energy have been obtained.

The present thesis deals with a theoretical, continuum mechanical description of all mechanically important anisotropy classes and less with specific application areas in engineering science. This may be a topic for further research activities. In the author's opinion micromechanical analyses of more complicated fiber-reinforced textures would be interesting.

A Glossary.

Point Group: The set of all symmetry transformations of a crystal, which leave the crystal structure in a state macroscopically indistinguishable from the origin state, is called point group, since translations are neglected and the symmetry transformations leave one point of the crystal fixed.

Material Symmetry Group: The symmetry transformations associated with any physical property of a crystal constitute the underlying material symmetry group \mathcal{G} of the crystal. The group includes at least the symmetry transformations of the underlying crystal structure (point group).

32 Point Groups of Crystals: Crystals can be classified by 32 point group. A point group consists of the point symmetry transformations of the underlying crystal structure. The point symmetry transformations of a crystal structure are at most equal to those of the lattice and can be limited by those of the group of atoms assigned at each grid point of the lattice.

Integrity Basis: The set of invariants for a given set of tensor arguments relative to a fixed symmetry group \mathcal{G} is called an *integrity basis* \mathcal{I} , if an arbitrary polynomial invariant of the same arguments can be expressed as a polynomial in the basic invariants. If no element of the considered set can be expressed as a polynomial in the remaining invariants of \mathcal{I} , it is called *irreducible*.

Functional Basis: The set of invariants is called a *functional basis* \mathcal{F} , if an arbitrary invariant in terms of the underlying arguments can be expressed as a function (not necessarily polynomial) in terms of the elements of \mathcal{F} . It is said to be *irreducible*, if none of the elements of the basic set \mathcal{F} can be expressed as a function of the other invariants of \mathcal{F} , i.e., if all elements of \mathcal{F} are *functionally independent*. In DIMITRIENKO [43] a system of scalar invariants I_1, \dots, I_p is called *functionally independent*, if for every nontrivial function $f(I_1, \dots, I_p)$ of the invariants of the set the relation $f(I_1, \dots, I_p) \neq 0$ is valid.

Set of Invariants: For the formulations of isotropic tensor functions in terms of the right Cauchy-Green tensor \mathbf{C} and structural tensors we construct our *sets of invariants* using Table 4.1 and 4.3. Obvious functionally dependent invariants are neglected. However, the irreducibility of our *sets of invariants* will not be explicitly checked as for example done in DIMITRIENKO [43]. Furthermore, due to our definition of *completeness* of an energy function (section 4.5) our *set of invariants* must include at least the corresponding *set of bilinear invariants*.

Set of Bilinear Invariants: For our *complete* energy functions it is sufficient to use *sets of bilinear invariants*, i.e., sets consisting of all obviously functionally independent invariants that are linear and quadratic in \mathbf{C} .

Classical Set of Bilinear Invariants: We denote the sets of all invariants in terms of the right Cauchy-Green tensor \mathbf{C} and structural tensors, that are linear and quadratic in \mathbf{C} and that appear in classical functional bases e.g. given in DIMITRIENKO [43], as *classical sets of bilinear invariants*. They are presented in Appendix D.

Complete Energy Functions: We say that our energy functions for the description of anisotropic finite elasticity are *complete*, if the coefficient matrix of the linear moduli \mathbb{C}^{lin} exhibits the same zero, non-zero, equal and opposite components and relations between the components as the corresponding classical anisotropic elasticity tensor of linear elasticity. This means that \mathbb{C}^{lin} has to obey the same symmetry properties as the corresponding classical anisotropic elasticity tensor. This does not mean that the exact values of the components of the corresponding anisotropic elasticity tensor can always be generated.

The classical anisotropic elasticity tensor in hyperelasticity can be completely obtained as second derivative of a quadratic energy $\psi(\mathbf{C})$. Therefore, in our case it is sufficient to use *sets of bilinear invariants*.

Set of Polyconvex Invariants: Our *sets of polyconvex invariants* consist of the polyconvex isotropic principal invariants of the right Cauchy-Green tensor \mathbf{C} and additional polyconvex invariants of the corresponding *set of bilinear invariants*.

Family of Polyconvex Invariant Functions: Our *families of polyconvex invariant functions* consist of the polyconvex isotropic principal invariants of \mathbf{C} and additional polyconvex functions that are invariant with respect to the underlying anisotropy group \mathcal{G} . The polyconvex functions must be at least functions of the invariants of the corresponding *classical set of bilinear invariants*. For detailed representations we refer to section 6.3.

B Matrix Representation of Special Tensors.

The symmetry of the right Cauchy-Green tensor \mathbf{C} , i.e., in index notation $C^{AB} = C^{BA}$, and the constitutive equation for the second Piola-Kirchhoff stresses

$$\mathbf{S} = 2 \partial_{\mathbf{C}} \psi \quad (\text{B.1})$$

yields the symmetry of \mathbf{S} , i.e., $S^{AB} = S^{BA}$. In general, the associated tangent moduli $\mathbb{C} = 4 \partial_{\mathbf{C}}^2 \psi$ is represented by 81 independent components:

| | 11 | 22 | 33 | 12 | 23 | 13 | 21 | 32 | 31 |
|----|---------------------|---------------------|---------------------|---------------------|---------------------|---------------------|---------------------|---------------------|---------------------|
| 11 | \mathbb{C}_{1111} | \mathbb{C}_{1122} | \mathbb{C}_{1133} | \mathbb{C}_{1112} | \mathbb{C}_{1123} | \mathbb{C}_{1113} | \mathbb{C}_{1121} | \mathbb{C}_{1132} | \mathbb{C}_{1131} |
| 22 | \mathbb{C}_{2211} | \mathbb{C}_{2222} | \mathbb{C}_{2233} | \mathbb{C}_{2212} | \mathbb{C}_{2223} | \mathbb{C}_{2213} | \mathbb{C}_{2221} | \mathbb{C}_{2232} | \mathbb{C}_{2231} |
| 33 | \mathbb{C}_{3311} | \mathbb{C}_{3322} | \mathbb{C}_{3333} | \mathbb{C}_{3312} | \mathbb{C}_{3323} | \mathbb{C}_{3313} | \mathbb{C}_{3321} | \mathbb{C}_{3332} | \mathbb{C}_{3331} |
| 12 | \mathbb{C}_{1211} | \mathbb{C}_{1222} | \mathbb{C}_{1233} | \mathbb{C}_{1212} | \mathbb{C}_{1223} | \mathbb{C}_{1213} | \mathbb{C}_{1221} | \mathbb{C}_{1232} | \mathbb{C}_{1231} |
| 23 | \mathbb{C}_{2311} | \mathbb{C}_{2322} | \mathbb{C}_{2333} | \mathbb{C}_{2312} | \mathbb{C}_{2323} | \mathbb{C}_{2313} | \mathbb{C}_{2321} | \mathbb{C}_{2332} | \mathbb{C}_{2331} |
| 13 | \mathbb{C}_{1311} | \mathbb{C}_{1322} | \mathbb{C}_{1333} | \mathbb{C}_{1312} | \mathbb{C}_{1323} | \mathbb{C}_{1313} | \mathbb{C}_{1321} | \mathbb{C}_{1332} | \mathbb{C}_{1331} |
| 21 | \mathbb{C}_{2111} | \mathbb{C}_{2122} | \mathbb{C}_{2133} | \mathbb{C}_{2112} | \mathbb{C}_{2123} | \mathbb{C}_{2113} | \mathbb{C}_{2121} | \mathbb{C}_{2132} | \mathbb{C}_{2131} |
| 32 | \mathbb{C}_{3211} | \mathbb{C}_{3222} | \mathbb{C}_{3233} | \mathbb{C}_{3212} | \mathbb{C}_{3223} | \mathbb{C}_{3213} | \mathbb{C}_{3221} | \mathbb{C}_{3232} | \mathbb{C}_{3231} |
| 31 | \mathbb{C}_{3111} | \mathbb{C}_{3122} | \mathbb{C}_{3133} | \mathbb{C}_{3112} | \mathbb{C}_{3123} | \mathbb{C}_{3113} | \mathbb{C}_{3121} | \mathbb{C}_{3132} | \mathbb{C}_{3131} |

(B.2)

Due to the symmetry of \mathbf{C} the following symmetry properties of \mathbb{C} are valid

$$\mathbb{C}_{ABCD} = \mathbb{C}_{BACD} = \mathbb{C}_{ABDC} = \mathbb{C}_{BADC},$$

so that we can reduce \mathbb{C} first to the form depending on 36 components:

| | 11 | 22 | 33 | 12 | 23 | 13 |
|----|--|--|--|--|--|--|
| 11 | \mathbb{C}_{1111} | \mathbb{C}_{1122} | \mathbb{C}_{1133} | $\frac{1}{2}(\mathbb{C}_{1112} + \mathbb{C}_{1121})$ | $\frac{1}{2}(\mathbb{C}_{1123} + \mathbb{C}_{1132})$ | $\frac{1}{2}(\mathbb{C}_{1113} + \mathbb{C}_{1131})$ |
| 22 | \mathbb{C}_{2211} | \mathbb{C}_{2222} | \mathbb{C}_{2233} | $\frac{1}{2}(\mathbb{C}_{2212} + \mathbb{C}_{2221})$ | $\frac{1}{2}(\mathbb{C}_{2223} + \mathbb{C}_{2232})$ | $\frac{1}{2}(\mathbb{C}_{2213} + \mathbb{C}_{2231})$ |
| 33 | \mathbb{C}_{3311} | \mathbb{C}_{3322} | \mathbb{C}_{3333} | $\frac{1}{2}(\mathbb{C}_{3312} + \mathbb{C}_{3321})$ | $\frac{1}{2}(\mathbb{C}_{3323} + \mathbb{C}_{3332})$ | $\frac{1}{2}(\mathbb{C}_{3313} + \mathbb{C}_{3331})$ |
| 12 | $\frac{1}{2}(\mathbb{C}_{1211} + \mathbb{C}_{2111})$ | $\frac{1}{2}(\mathbb{C}_{1222} + \mathbb{C}_{2122})$ | $\frac{1}{2}(\mathbb{C}_{1233} + \mathbb{C}_{2133})$ | $\frac{1}{4}(\mathbb{C}_{1212} + \mathbb{C}_{1221} + \mathbb{C}_{2112} + \mathbb{C}_{2121})$ | $\frac{1}{4}(\mathbb{C}_{1223} + \mathbb{C}_{1232} + \mathbb{C}_{2123} + \mathbb{C}_{2132})$ | $\frac{1}{4}(\mathbb{C}_{1213} + \mathbb{C}_{1231} + \mathbb{C}_{2113} + \mathbb{C}_{2131})$ |
| 23 | $\frac{1}{2}(\mathbb{C}_{2311} + \mathbb{C}_{3211})$ | $\frac{1}{2}(\mathbb{C}_{2322} + \mathbb{C}_{3222})$ | $\frac{1}{2}(\mathbb{C}_{2333} + \mathbb{C}_{3233})$ | $\frac{1}{4}(\mathbb{C}_{2312} + \mathbb{C}_{2321} + \mathbb{C}_{3212} + \mathbb{C}_{3221})$ | $\frac{1}{4}(\mathbb{C}_{2323} + \mathbb{C}_{2332} + \mathbb{C}_{3223} + \mathbb{C}_{3232})$ | $\frac{1}{4}(\mathbb{C}_{2313} + \mathbb{C}_{2331} + \mathbb{C}_{3213} + \mathbb{C}_{3231})$ |
| 13 | $\frac{1}{2}(\mathbb{C}_{1311} + \mathbb{C}_{3111})$ | $\frac{1}{2}(\mathbb{C}_{1322} + \mathbb{C}_{3122})$ | $\frac{1}{2}(\mathbb{C}_{1333} + \mathbb{C}_{3133})$ | $\frac{1}{4}(\mathbb{C}_{1312} + \mathbb{C}_{1321} + \mathbb{C}_{3112} + \mathbb{C}_{3121})$ | $\frac{1}{4}(\mathbb{C}_{1323} + \mathbb{C}_{1332} + \mathbb{C}_{3123} + \mathbb{C}_{3132})$ | $\frac{1}{4}(\mathbb{C}_{1313} + \mathbb{C}_{1331} + \mathbb{C}_{3113} + \mathbb{C}_{3131})$ |

(B.3)

which appears in a more compact form as

| | 11 | 22 | 33 | 12 | 23 | 13 |
|----|---------------------|---------------------|---------------------|---------------------|---------------------|---------------------|
| 11 | \mathbb{C}_{1111} | \mathbb{C}_{1122} | \mathbb{C}_{1133} | \mathbb{C}_{1112} | \mathbb{C}_{1123} | \mathbb{C}_{1113} |
| 22 | \mathbb{C}_{2211} | \mathbb{C}_{2222} | \mathbb{C}_{2233} | \mathbb{C}_{2212} | \mathbb{C}_{2223} | \mathbb{C}_{2213} |
| 33 | \mathbb{C}_{3311} | \mathbb{C}_{3322} | \mathbb{C}_{3333} | \mathbb{C}_{3312} | \mathbb{C}_{3323} | \mathbb{C}_{3313} |
| 12 | \mathbb{C}_{1211} | \mathbb{C}_{1222} | \mathbb{C}_{1233} | \mathbb{C}_{1212} | \mathbb{C}_{1223} | \mathbb{C}_{1213} |
| 23 | \mathbb{C}_{2311} | \mathbb{C}_{2322} | \mathbb{C}_{2333} | \mathbb{C}_{2312} | \mathbb{C}_{2323} | \mathbb{C}_{2313} |
| 13 | \mathbb{C}_{1311} | \mathbb{C}_{1322} | \mathbb{C}_{1333} | \mathbb{C}_{1312} | \mathbb{C}_{1323} | \mathbb{C}_{1313} |

(B.4)

Since the additional relation

$$\frac{\partial^2 \psi}{\partial C_{AB} \partial C_{CD}} = \frac{\partial^2 \psi}{\partial C_{CD} \partial C_{AB}}$$

holds, it follows the well-known matrix representation of \mathbb{C} with 21 independent components:

| | 11 | 22 | 33 | 12 | 23 | 13 |
|----|---------------------|---------------------|---------------------|---------------------|---------------------|---------------------|
| 11 | \mathbb{C}_{1111} | \mathbb{C}_{1122} | \mathbb{C}_{1133} | \mathbb{C}_{1112} | \mathbb{C}_{1123} | \mathbb{C}_{1113} |
| 22 | | \mathbb{C}_{2222} | \mathbb{C}_{2233} | \mathbb{C}_{2212} | \mathbb{C}_{2223} | \mathbb{C}_{2213} |
| 33 | | | \mathbb{C}_{3333} | \mathbb{C}_{3312} | \mathbb{C}_{3323} | \mathbb{C}_{3313} |
| 12 | | | | \mathbb{C}_{1212} | \mathbb{C}_{1223} | \mathbb{C}_{1213} |
| 23 | | <i>sym</i> | | | \mathbb{C}_{2323} | \mathbb{C}_{2313} |
| 13 | | | | | | \mathbb{C}_{1313} |

(B.5)

This is the representation of \mathbb{C} in the most general case of anisotropic elasticity, namely the triclinic case. The vector representations of \mathbf{S} and \mathbf{C} are then given by

$$\begin{aligned} \mathbf{S} &= [S_{11} \quad S_{22} \quad S_{33} \quad | S_{12} \quad S_{23} \quad S_{13}]^T, \\ \mathbf{C} &= [C_{11} \quad C_{22} \quad C_{33} \quad | 2C_{12} \quad 2C_{23} \quad 2C_{13}]^T. \end{aligned}$$

C Positive Definiteness of Matrices.

An $n \times n$ symmetric real matrix $\mathbf{A} \in \mathbb{R}^{n \times n}$ is positive (semi-) definite if

$$\mathbf{v}^T \mathbf{A} \mathbf{v} > (\geq) 0 \quad (\text{C.1})$$

is valid for all real non-zero vectors $\mathbf{v} \in \mathbb{R}^n$. The positive definiteness of \mathbf{A} can be also proved by the check of positive main minors. For a 4×4 matrix

$$\mathbf{A} = \begin{bmatrix} A_{11} & A_{12} & A_{13} & A_{14} \\ A_{12} & A_{22} & A_{23} & A_{24} \\ A_{13} & A_{23} & A_{33} & A_{34} \\ A_{14} & A_{24} & A_{34} & A_{44} \end{bmatrix} \quad (\text{C.2})$$

the main minors are positive if

$$A_{11} > 0, \det \begin{bmatrix} A_{11} & A_{12} \\ A_{12} & A_{22} \end{bmatrix} > 0, \det \begin{bmatrix} A_{11} & A_{12} & A_{13} \\ A_{12} & A_{22} & A_{23} \\ A_{13} & A_{23} & A_{33} \end{bmatrix} > 0, \det[\mathbf{A}] > 0. \quad (\text{C.3})$$

For the computation of the determinant of a block partitioned matrix with the regular quadratic matrix \mathbf{A} and the quadratic matrix \mathbf{D} we obtain

$$\det \begin{bmatrix} \mathbf{A} & \mathbf{B} \\ \mathbf{C} & \mathbf{D} \end{bmatrix} = \det \mathbf{A} \det \mathbf{S} \quad (\text{C.4})$$

with the Schur complement

$$\mathbf{S} = \mathbf{D} - \mathbf{C} \mathbf{A}^{-1} \mathbf{B}. \quad (\text{C.5})$$

This condition is valid, because the "block diagonalization" procedure

$$\begin{bmatrix} \mathbf{A} & \mathbf{B} \\ \mathbf{C} & \mathbf{D} \end{bmatrix} = \begin{bmatrix} \mathbf{1} & \mathbf{0} \\ \mathbf{C} \mathbf{A}^{-1} & \mathbf{1} \end{bmatrix} \begin{bmatrix} \mathbf{A} & \mathbf{0} \\ \mathbf{0} & \mathbf{S} \end{bmatrix} \begin{bmatrix} \mathbf{1} & \mathbf{A}^{-1} \mathbf{B} \\ \mathbf{0} & \mathbf{1} \end{bmatrix} \quad (\text{C.6})$$

yields

$$\begin{aligned} \det \begin{bmatrix} \mathbf{A} & \mathbf{B} \\ \mathbf{C} & \mathbf{D} \end{bmatrix} &= \det \begin{bmatrix} \mathbf{1} & \mathbf{0} \\ \mathbf{C} \mathbf{A}^{-1} & \mathbf{1} \end{bmatrix} \det \begin{bmatrix} \mathbf{A} & \mathbf{0} \\ \mathbf{0} & \mathbf{S} \end{bmatrix} \det \begin{bmatrix} \mathbf{1} & \mathbf{A}^{-1} \mathbf{B} \\ \mathbf{0} & \mathbf{1} \end{bmatrix} \\ &= \det \mathbf{A} \det \mathbf{S}. \end{aligned} \quad (\text{C.7})$$

D Classical Sets of Bilinear Invariants.

| Anisotropy Group | Classical Sets of Bilinear Invariants in Terms of the Components of the Symmetric Second-Order Tensor \mathbf{C} , cf. DIMITRIENKO [43] |
|----------------------------|--|
| Triclinic \mathcal{G}_1 | $\{C_{11}, C_{22}, C_{33}, C_{12}, C_{23}, C_{13}\}$ |
| Monoclinic \mathcal{G}_2 | $\{C_{11}, C_{22}, C_{33}, C_{12}, C_{13}^2, C_{13}C_{23}\}$ |
| Rhombic \mathcal{G}_3 | $\{C_{11}, C_{22}, C_{33}, C_{23}^2, C_{13}^2\}$ |
| Tetragonal \mathcal{G}_4 | $\{C_{11} + C_{22}, C_{33}, C_{13}^2 + C_{23}^2, C_{11}^2 + C_{22}^2, C_{12}(C_{11} - C_{22})\}$ |
| Tetragonal \mathcal{G}_5 | $\{C_{11} + C_{22}, C_{33}, C_{13}^2 + C_{23}^2, C_{11}^2 + C_{22}^2, C_{12}^2\}$ |
| Trigonal \mathcal{G}_8 | $\{C_{11} + C_{22}, C_{33}, C_{13}^2 + C_{23}^2, C_{13}(C_{11} - C_{22}) - 2C_{12}C_{23},$ $C_{11}^2 + C_{22}^2 + 2C_{12}^2, C_{23}(C_{11} - C_{22}) + 2C_{12}C_{13}\}$ |
| Trigonal \mathcal{G}_9 | $\{C_{11} + C_{22}, C_{33}, C_{13}^2 + C_{23}^2,$ $C_{23}(C_{11} - C_{22}) + 2C_{12}C_{13}^{19.)}, C_{11}^2 + C_{22}^2 + 2C_{12}^2\}$ |
| Cubic \mathcal{G}_7 | $\{C_{11} + C_{22} + C_{33}, C_{11}^2 + C_{22}^2 + C_{33}^2, C_{12}^2 + C_{13}^2 + C_{23}^2\}$ |

^{19.)}In [43], in the trigonal \mathcal{G}_9 -invariant set of invariants, originally instead of $C_{23}(C_{11} - C_{22}) + 2C_{12}C_{13}$ the term $C_{13}(C_{11} - C_{22}) - 2C_{12}C_{23}$ is given. This depends on the fact that for the trigonal crystal \mathcal{D}_{3h} two types exist. That means with regard to Figure 6.8 that the angle φ can be chosen to be $\varphi = 0^\circ$ or $\varphi = 90^\circ$. For the description of the material behavior of the crystal with $\varphi = 0^\circ$ (case of [43]) we have to consider the invariant $C_{13}(C_{11} - C_{22}) - 2C_{12}C_{23}$. For the description of the material behavior of the crystal with $\varphi = 90^\circ$ (our case) we have to consider the invariant $C_{23}(C_{11} - C_{22}) + 2C_{12}C_{13}$.

E Zheng & Spencer's and Xiao's Structural Tensors: Detailed Representations.

In ZHENG & SPENCER [146] the following second-order structural tensors are proposed:

$$\mathbf{P}'_2 = \begin{bmatrix} 0 & 1 & 0 \\ 1 & 0 & 0 \\ 0 & 0 & 0 \end{bmatrix}, \quad \mathbf{P}_2 = \begin{bmatrix} 1 & 0 & 0 \\ 0 & -1 & 0 \\ 0 & 0 & 0 \end{bmatrix},$$

$$\boldsymbol{\epsilon}\mathbf{e}_1 = \begin{bmatrix} 0 & 0 & 0 \\ 0 & 0 & 1 \\ 0 & -1 & 0 \end{bmatrix}, \quad \boldsymbol{\epsilon}\mathbf{e}_3 = \begin{bmatrix} 0 & 1 & 0 \\ -1 & 0 & 0 \\ 0 & 0 & 0 \end{bmatrix}.$$

In ZHENG & SPENCER [146] the following fourth-order structural tensors are proposed:

$$\mathbb{P}_4 = \mathbf{P}_2 \otimes \mathbf{P}_2 - \mathbf{P}'_2 \otimes \mathbf{P}'_2, \quad \mathbb{P}_4^{(V)} = \begin{bmatrix} 1 & -1 & 0 & 0 & 0 & 0 \\ & 1 & 0 & 0 & 0 & 0 \\ & & 0 & 0 & 0 & 0 \\ & & & sym. & -1 & 0 & 0 \\ & & & & 0 & 0 \\ & & & & & 0 \end{bmatrix},$$

$$\mathbb{P}'_4 = \mathbf{P}_2 \otimes \mathbf{P}'_2 + \mathbf{P}'_2 \otimes \mathbf{P}_2,$$

$$\begin{aligned} \mathbb{P}_3 &= \mathbf{e}_3 \otimes \mathbf{P}'_3 = \mathbf{e}_3 \otimes \mathbf{e}_1 \otimes \mathbf{P}'_2 + \mathbf{e}_3 \otimes \mathbf{e}_2 \otimes \mathbf{P}_2 \\ &= \mathbf{e}_3 \otimes \mathbf{e}_1 \otimes (\mathbf{e}_1 \otimes \mathbf{e}_2 + \mathbf{e}_2 \otimes \mathbf{e}_1) + \mathbf{e}_3 \otimes \mathbf{e}_2 \otimes (\mathbf{e}_1 \otimes \mathbf{e}_1 - \mathbf{e}_2 \otimes \mathbf{e}_2), \end{aligned}$$

$$\mathbf{P}_6 = \mathbf{P}_2 \otimes \mathbb{P}_4 - \mathbf{P}'_2 \otimes \mathbb{P}'_4,$$

$$\boldsymbol{\Lambda} = (\mathbf{e}_2^{(2)} \otimes \mathbf{e}_3^{(2)} + \mathbf{e}_3^{(2)} \otimes \mathbf{e}_1^{(2)} + \mathbf{e}_1^{(2)} \otimes \mathbf{e}_2^{(2)}) - (\mathbf{e}_3^{(2)} \otimes \mathbf{e}_2^{(2)} + \mathbf{e}_1^{(2)} \otimes \mathbf{e}_3^{(2)} + \mathbf{e}_2^{(2)} \otimes \mathbf{e}_1^{(2)}),$$

$$\boldsymbol{\Theta} = \mathbf{e}_1^{(4)} + \mathbf{e}_2^{(4)} + \mathbf{e}_3^{(4)},$$

with the abbreviation

$$\mathbf{e}_i^{(n)} = \underbrace{\mathbf{e}_i \otimes \cdots \otimes \mathbf{e}_i}_n, \quad i = 1, 2, 3, \quad n = 1, \dots, 6.$$

In XIAO [140] the following cubic \mathcal{G}_6 -invariant structural tensors are proposed:

$$\mathbb{T}_h = \mathbb{T}_h^a + \mathbb{T}_h^s,$$

$$\mathbb{T}_h^s = \boldsymbol{\Lambda}$$

$$\begin{aligned} \mathbb{T}_h^a &= \boldsymbol{\epsilon}\mathbf{e}_1 \otimes (\mathbf{e}_2 \otimes \mathbf{e}_3 + \mathbf{e}_3 \otimes \mathbf{e}_2) + \boldsymbol{\epsilon}\mathbf{e}_2 \otimes (\mathbf{e}_3 \otimes \mathbf{e}_1 + \mathbf{e}_1 \otimes \mathbf{e}_3) \\ &\quad + \boldsymbol{\epsilon}\mathbf{e}_3 \otimes (\mathbf{e}_1 \otimes \mathbf{e}_2 + \mathbf{e}_2 \otimes \mathbf{e}_1), \end{aligned}$$

where $\boldsymbol{\epsilon}$ is the third-order permutation tensor.

F Some Useful Derivatives.

The first and second derivatives of invariants in terms of second-order tensors $\mathbf{C} = \mathbf{C}^T$ and \mathbf{L} with respect to \mathbf{C} are ^{20.) 21.)} :

| invariants[•] | first derivative $\frac{\partial[\bullet]}{\partial \mathbf{C}}$ | second derivative $\frac{\partial^2[\bullet]}{\partial \mathbf{C} \partial \mathbf{C}}$ |
|---|--|--|
| $\mathbf{C} : \mathbf{1}$ | $\mathbf{1}$ | |
| $\mathbf{C}^2 : \mathbf{1}$ | $2\mathbf{C}$ | $2\mathbf{1} \boxtimes \mathbf{1}$ |
| $\det \mathbf{C}$ | $\det(\mathbf{C})\mathbf{C}^{-1}$ | $\det \mathbf{C} \mathbf{C}^{-1} \otimes \mathbf{C}^{-1} - \det \mathbf{C} \mathbf{C}^{-1} \boxtimes \mathbf{C}^{-1}$ |
| $\text{Cof} \mathbf{C} : \mathbf{1}$ | $\text{tr}(\mathbf{C})\mathbf{1} - \mathbf{C}$ | $\mathbf{1} \otimes \mathbf{1} - \mathbf{1} \boxtimes \mathbf{1}$ |
| $\mathbf{C}\mathbf{L} : \mathbf{1}$ | \mathbf{L} | |
| $\mathbf{C}^2\mathbf{L} : \mathbf{1}$ | $\mathbf{C}\mathbf{L}^T + \mathbf{L}^T\mathbf{C}$ | $(\mathbf{1} \boxtimes \mathbf{L})^{\text{34}} + (\mathbf{L}^T \boxtimes \mathbf{1})^{\text{34}}$ |
| $\text{Cof}[\mathbf{C}]\mathbf{L} : \mathbf{1}$ | $\text{tr}[\text{Cof}[\mathbf{C}]\mathbf{L}]\mathbf{C}^{-1}$ $-\text{Cof}[\mathbf{C}]\mathbf{L}^T\mathbf{C}^{-1}$ | $\text{tr}[\text{Cof}[\mathbf{C}]\mathbf{L}][\mathbf{C}^{-1} \otimes \mathbf{C}^{-1} - \mathbf{C}^{-1} \boxtimes \mathbf{C}^{-1}]$ $-\text{Cof} \mathbf{C} \otimes \mathbf{C}^{-1} \mathbf{L}^T \mathbf{C}^{-1} + \mathbf{C}^{-1} \mathbf{L}^T \mathbf{C}^{-1} \otimes \text{Cof} \mathbf{C}$ $+[\text{Cof} \mathbf{C} \boxtimes \mathbf{C}^{-1} \mathbf{L} \mathbf{C}^{-1} + \mathbf{C}^{-1} \mathbf{L}^T \mathbf{C}^{-1} \boxtimes \text{Cof} \mathbf{C}]$ |

For the representation of the first and second derivatives of invariants in terms of the second-order tensors $\mathbf{C} = \mathbf{C}^T$, \mathbf{L} and the fourth-order tensor \mathbb{P} with respect to \mathbf{C} we prefer the index notation:

| invariants [•] | first derivative $\frac{\partial[\bullet]}{\partial C_{op}}$ | second derivative $\frac{\partial^2[\bullet]}{\partial C_{op} \partial C_{ab}}$ |
|--|---|---|
| $(\mathbb{P} : \mathbf{C}) : \mathbf{L}$ | $L_{ij} \mathbb{P}_{ijop}$ | |
| $(\mathbb{P} : \mathbf{C}^2) : \mathbf{L}$ | $L_{ij} \mathbb{P}_{ijol} C_{lp} + L_{ij} \mathbb{P}_{ijkp} C_{ko}$ | $L_{ij} \mathbb{P}_{ijoa} \delta_{pb} + L_{ij} \mathbb{P}_{ijap} \delta_{ob}$ |
| $(\mathbb{P} : \mathbf{C})^2 : \mathbf{L}$ | $\mathbb{P}_{ijop} \mathbb{P}_{jrst} C_{st} L_{ir} + \mathbb{P}_{ijkl} C_{kl} \mathbb{P}_{jrop} L_{ir}$ | $\mathbb{P}_{ijop} \mathbb{P}_{jrab} L_{ir} + \mathbb{P}_{ijab} \mathbb{P}_{jrop} L_{ir}$ |
| $(\mathbb{P} : \mathbf{C}) : \mathbf{C}$ | $\mathbb{P}_{opkl} C_{kl} + C_{ij} \mathbb{P}_{ijop}$ | $\mathbb{P}_{opab} + \mathbb{P}_{abop}$ |
| $(\mathbb{P} : \mathbf{C}) : (\mathbf{C}\mathbf{L})$ | $L_{pj} \mathbb{P}_{ojkl} C_{kl} + C_{im} L_{mj} \mathbb{P}_{ijop}$ | $\mathbb{P}_{ojab} L_{pj} + L_{bj} \mathbb{P}_{ajop}$ |
| $\mathbf{C}(\mathbb{P} : \mathbf{C}) : \mathbf{L}$ | $\mathbb{P}_{pklm} C_{lm} L_{ok} + C_{ij} \mathbb{P}_{jkop} L_{ik}$ | $\mathbb{P}_{pkab} L_{ok} + \mathbb{P}_{bkop} L_{ak}$ |

^{20.)} $(\mathbf{A} \boxtimes \mathbf{B})(\mathbf{a} \otimes \mathbf{b}) = \mathbf{A}\mathbf{a} \otimes \mathbf{B}\mathbf{b} \forall \mathbf{A}, \mathbf{B} \in \mathbb{R}^{3 \times 3}, \mathbf{a}, \mathbf{b} \in \mathbb{R}^3$, [56], [42].

^{21.)} $(\bullet)^{\text{34}}$ in index notation is $(\{\bullet\}_{ijkl})^{\text{34}} = \{\bullet\}_{ijlk}$

G Additional Sets of Bilinear Invariants and Quadratic Energy Functions.

Triclinic Anisotropy Group \mathcal{G}_1 :

Set of Bilinear Invariants: We use the triclinic structural tensors $\mathbf{P}'_2 + \epsilon\mathbf{e}_1$. Since the classical tensor representation theory deals with symmetric and skew-symmetric second-order tensors, we have to divide the triclinic tensor into a symmetric and a skew-symmetric part. Thus, we evaluate Table 4.3 under consideration of the two second-order structural tensors $\mathbf{A} = \mathbf{P}'_2$ and $\mathbf{W} = \epsilon\mathbf{e}_1$ characterizing the triclinic symmetry group \mathcal{G}_1 . For the construction of the triclinic *set of bilinear invariants* the linear and quadratic invariants in \mathbf{E} obtained from Table 4.3 are relevant and presented in Table G.1.

Table G.1: Set of Triclinic Bilinear Invariants.

| | |
|---------------------------------|--|
| Structural Tensors: | $\mathbf{A} = \mathbf{P}'_2, \mathbf{W} = \epsilon\mathbf{e}_1$ |
| Invariants for one argument: | $\text{tr}[\mathbf{E}], \text{tr}[\mathbf{E}^2]$ |
| Invariants for two arguments: | $\text{tr}[\mathbf{EA}], \text{tr}[\mathbf{E}^2\mathbf{A}], \text{tr}[\mathbf{EA}^2], \text{tr}[\mathbf{E}^2\mathbf{A}^2], \text{tr}[\mathbf{E}\mathbf{W}^2], \text{tr}[\mathbf{E}^2\mathbf{W}^2]$ |
| Invariants for three arguments: | $\text{tr}[\mathbf{EAW}], \text{tr}[\mathbf{E}^2\mathbf{AW}], \text{tr}[\mathbf{E}\mathbf{W}^2\mathbf{AW}], \text{tr}[\mathbf{EA}^2\mathbf{W}]$ |

Since the identities

$$\begin{aligned}
\text{tr}[\mathbf{E}^2] &= (\text{tr}[\mathbf{E}] + \text{tr}[\mathbf{E}\mathbf{W}^2])^2 + \frac{1}{2}\text{tr}[\mathbf{EA}]^2 + 2\text{tr}[\mathbf{EAW}]^2 + 2\text{tr}[\mathbf{EA}^2\mathbf{W}]^2 \\
&\quad + (\text{tr}[\mathbf{EA}^2] - \text{tr}[\mathbf{E}\mathbf{W}^2] - \text{tr}[\mathbf{E}])^2 + (\text{tr}[\mathbf{E}] - \text{tr}[\mathbf{EA}^2])^2, \\
\text{tr}[\mathbf{E}^2\mathbf{A}] &= \text{tr}[\mathbf{EA}]\text{tr}[\mathbf{EA}^2] + 2\text{tr}[\mathbf{EAW}]\text{tr}[\mathbf{EA}^2\mathbf{W}], \\
\text{tr}[\mathbf{E}^2\mathbf{A}^2] &= (\text{tr}[\mathbf{EA}^2] - (\text{tr}[\mathbf{E}] + \text{tr}[\mathbf{E}\mathbf{W}^2]))^2 + (\text{tr}[\mathbf{E}] + \text{tr}[\mathbf{E}\mathbf{W}^2])^2 \\
&\quad + \frac{1}{2}\text{tr}[\mathbf{EA}]^2 + \text{tr}[\mathbf{EAW}]^2 + \text{tr}[\mathbf{EA}^2\mathbf{W}]^2, \\
\text{tr}[\mathbf{E}^2\mathbf{W}^2] &= -\frac{1}{4}\text{tr}[\mathbf{EA}]^2 - (\text{tr}[\mathbf{EA}^2] - \text{tr}[\mathbf{E}\mathbf{W}^2] - \text{tr}[\mathbf{E}])^2 \\
&\quad - 2\text{tr}[\mathbf{EA}^2\mathbf{W}]^2 - \text{tr}[\mathbf{EAW}]^2 - (\text{tr}[\mathbf{E}] - \text{tr}[\mathbf{EA}^2])^2, \\
\text{tr}[\mathbf{E}^2\mathbf{AW}] &= \text{tr}[\mathbf{EAW}](2\text{tr}[\mathbf{E}] + \text{tr}[\mathbf{E}\mathbf{W}^2] - \text{tr}[\mathbf{EA}^2]) + \frac{1}{2}\text{tr}[\mathbf{EA}]\text{tr}[\mathbf{EA}^2\mathbf{W}], \\
\text{tr}[\mathbf{E}\mathbf{W}^2\mathbf{AW}] &= 0
\end{aligned}$$

are valid, we obtain the *set of bilinear invariants*

$$\mathcal{F}^a(\mathbf{E}, \mathbf{A}, \mathbf{W}) := \{\text{tr}[\mathbf{E}], \text{tr}[\mathbf{EA}], \text{tr}[\mathbf{EA}^2], \text{tr}[\mathbf{E}\mathbf{W}^2], \text{tr}[\mathbf{EAW}], \text{tr}[\mathbf{EA}^2\mathbf{W}]\}, \quad (\text{G.1})$$

which reads in terms of the six components of \mathbf{E}

$$\boxed{\mathcal{F}^a(\mathbf{E}, \mathbf{A}, \mathbf{W}) = \{E_{11} + E_{22} + E_{33}, 2E_{12}, E_{11} + E_{22}, \\ -(E_{22} + E_{33}), E_{13}, E_{23}\}.} \quad (\text{G.2})$$

Comparing it with the triclinic *classical set of bilinear invariants* given in [43] (here in terms of the components of \mathbf{E}), i.e.,

$$\bar{\mathcal{F}}^a = \{E_{11}, E_{22}, E_{33}, E_{12}, E_{23}, E_{13}\}, \quad (\text{G.3})$$

we notice that all elements appearing in (G.1) can be uniquely expressed by the terms of the set given in (G.3).

Quadratic Energy Function: For the construction of the triclinic coordinate-free energy function (4.63) the set (G.1), with \mathcal{F}^a is used. Under consideration of all possible multiplicative combinations of linear invariants of \mathcal{F}^a that are quadratic in \mathbf{E} and hence in \mathbf{C} and all quadratic invariants of \mathcal{F}^a we get the final triclinic set

$$\begin{aligned} \mathcal{B}^a := & \{ \text{tr}[\mathbf{E}]^2, \text{tr}[\mathbf{E}]^2, \text{tr}[\mathbf{E}\mathbf{A}^2]^2, \text{tr}[\mathbf{E}\mathbf{W}^2]^2, \text{tr}[\mathbf{E}\mathbf{A}\mathbf{W}]^2, \\ & \text{tr}[\mathbf{E}\mathbf{A}^2\mathbf{W}]^2, \text{tr}[\mathbf{E}]\text{tr}[\mathbf{E}\mathbf{A}], \text{tr}[\mathbf{E}]\text{tr}[\mathbf{E}\mathbf{A}^2], \\ & \text{tr}[\mathbf{E}]\text{tr}[\mathbf{E}\mathbf{W}^2], \text{tr}[\mathbf{E}]\text{tr}[\mathbf{E}\mathbf{A}\mathbf{W}], \text{tr}[\mathbf{E}]\text{tr}[\mathbf{E}\mathbf{A}^2\mathbf{W}], \\ & \text{tr}[\mathbf{E}\mathbf{A}]\text{tr}[\mathbf{E}\mathbf{A}^2], \text{tr}[\mathbf{E}\mathbf{A}]\text{tr}[\mathbf{E}\mathbf{W}^2], \text{tr}[\mathbf{E}\mathbf{A}]\text{tr}[\mathbf{E}\mathbf{A}\mathbf{W}], \\ & \text{tr}[\mathbf{E}\mathbf{A}]\text{tr}[\mathbf{E}\mathbf{A}^2\mathbf{W}], \text{tr}[\mathbf{E}\mathbf{A}^2]\text{tr}[\mathbf{E}\mathbf{W}^2], \text{tr}[\mathbf{E}\mathbf{A}^2]\text{tr}[\mathbf{E}\mathbf{A}\mathbf{W}], \\ & \text{tr}[\mathbf{E}\mathbf{A}^2]\text{tr}[\mathbf{E}\mathbf{A}^2\mathbf{W}], \text{tr}[\mathbf{E}\mathbf{W}^2]\text{tr}[\mathbf{E}\mathbf{A}\mathbf{W}], \text{tr}[\mathbf{E}\mathbf{W}^2]\text{tr}[\mathbf{E}\mathbf{A}^2\mathbf{W}], \\ & \text{tr}[\mathbf{E}\mathbf{A}\mathbf{W}]\text{tr}[\mathbf{E}\mathbf{A}^2\mathbf{W}] \}. \end{aligned} \quad (\text{G.4})$$

Thus, 21 invariant terms L_i , $i = 1, \dots, 21$ and therefore 21 independent material parameters α_i , $i = 1, \dots, 21$ have to be considered for the formulation of the triclinic quadratic function (4.63). Inserting $\mathbf{E} = \frac{1}{2}(\mathbf{C} - \mathbf{1})$ into the invariants of \mathcal{B}^a leads to the dependency of the energy function on \mathbf{C} :

$$\psi^a(\mathbf{C}, \mathbf{A}, \mathbf{W}) = \sum_{i=1}^{21} \alpha_i L_i, \quad L_i \in \mathcal{B}^a.$$

The second derivative with respect to \mathbf{C} , i.e., $\mathbb{C}^a = 4\partial_{\mathbf{C}\mathbf{C}}\psi^a(\mathbf{C}, \mathbf{A}, \mathbf{W})$, results in

$$\begin{aligned} \mathbb{C}^a = & \lambda \mathbf{1} \otimes \mathbf{1} + 2\mu \mathbf{1} \boxtimes \mathbf{1} + 2\alpha_3 \mathbf{A}^2 \otimes \mathbf{A}^2 + 2\alpha_4 \mathbf{W}^2 \otimes \mathbf{W}^2 \\ & + 2\alpha_5 \mathbf{A}\mathbf{W} \otimes \mathbf{A}\mathbf{W} + 2\alpha_6 \mathbf{A}^2\mathbf{W} \otimes \mathbf{A}^2\mathbf{W} + \alpha_7(\mathbf{1} \otimes \mathbf{A} + \mathbf{A} \otimes \mathbf{1}) \\ & + \alpha_8(\mathbf{1} \otimes \mathbf{A}^2 + \mathbf{A}^2 \otimes \mathbf{1}) + \alpha_9(\mathbf{1} \otimes \mathbf{W}^2 + \mathbf{W}^2 \otimes \mathbf{1}) + \alpha_{10}(\mathbf{1} \otimes \mathbf{A}\mathbf{W} + \mathbf{A}\mathbf{W} \otimes \mathbf{1}) \\ & + \alpha_{11}(\mathbf{1} \otimes \mathbf{A}^2\mathbf{W} + \mathbf{A}^2\mathbf{W} \otimes \mathbf{1}) + \alpha_{12}(\mathbf{A}^2 \otimes \mathbf{A} + \mathbf{A} \otimes \mathbf{A}^2) \\ & + \alpha_{13}(\mathbf{A} \otimes \mathbf{W}^2 + \mathbf{W}^2 \otimes \mathbf{A}) + \alpha_{14}(\mathbf{A} \otimes \mathbf{A}\mathbf{W} + \mathbf{A}\mathbf{W} \otimes \mathbf{A}) \\ & + \alpha_{15}(\mathbf{A} \otimes \mathbf{A}^2\mathbf{W} + \mathbf{A}^2\mathbf{W} \otimes \mathbf{A}) + \alpha_{16}(\mathbf{A}^2 \otimes \mathbf{W}^2 + \mathbf{W}^2 \otimes \mathbf{A}^2) \\ & + \alpha_{17}(\mathbf{A}^2 \otimes \mathbf{A}\mathbf{W} + \mathbf{A}\mathbf{W} \otimes \mathbf{A}^2) + \alpha_{18}(\mathbf{A}^2 \otimes \mathbf{A}^2\mathbf{W} + \mathbf{A}^2\mathbf{W} \otimes \mathbf{A}^2) \\ & + \alpha_{19}(\mathbf{W}^2 \otimes \mathbf{A}\mathbf{W} + \mathbf{A}\mathbf{W} \otimes \mathbf{W}^2) + \alpha_{20}(\mathbf{W}^2 \otimes \mathbf{A}^2\mathbf{W} + \mathbf{A}^2\mathbf{W} \otimes \mathbf{W}^2) \\ & + \alpha_{21}(\mathbf{A}\mathbf{W} \otimes \mathbf{A}^2\mathbf{W} + \mathbf{A}^2\mathbf{W} \otimes \mathbf{A}\mathbf{W}), \end{aligned}$$

which has in Voigt notation the form of the classical constant triclinic fourth-order elasticity tensor, i.e.,

$$\mathbb{C}^{(V)a} = \begin{bmatrix} \mathbb{C}_{1111} & \mathbb{C}_{1122} & \mathbb{C}_{1133} & \mathbb{C}_{1112} & \mathbb{C}_{1123} & \mathbb{C}_{1113} \\ & \mathbb{C}_{2222} & \mathbb{C}_{2233} & \mathbb{C}_{2212} & \mathbb{C}_{2223} & \mathbb{C}_{2213} \\ & & \mathbb{C}_{3333} & \mathbb{C}_{3312} & \mathbb{C}_{3323} & \mathbb{C}_{3313} \\ & & & \mathbb{C}_{1212} & \mathbb{C}_{1223} & \mathbb{C}_{1213} \\ & \text{sym.} & & & \mathbb{C}_{2323} & \mathbb{C}_{2313} \\ & & & & & \mathbb{C}_{1313} \end{bmatrix},$$

with the coefficients in terms of the 21 independent material parameters

$$\begin{aligned}
\mathbb{C}_{1111} &= \lambda + 2\mu + 2\alpha_3 + 2\alpha_8, & \mathbb{C}_{1122} &= \lambda + 2\alpha_3 + 2\alpha_8 - \alpha_9 - \alpha_{16}, \\
\mathbb{C}_{1133} &= \lambda + \alpha_8 - \alpha_9 - \alpha_{16}, & \mathbb{C}_{1112} &= \alpha_7 + \alpha_{12}, \\
\mathbb{C}_{1123} &= \frac{1}{2}\alpha_{11} + \frac{1}{2}\alpha_{18}, & \mathbb{C}_{1113} &= \frac{1}{2}\alpha_{10} + \frac{1}{2}\alpha_{17}, \\
\mathbb{C}_{2222} &= \lambda + 2\mu + 2\alpha_3 + 2\alpha_4 + 2\alpha_8 - 2\alpha_9 - 2\alpha_{16}, \\
\mathbb{C}_{2233} &= \lambda + 2\alpha_4 + \alpha_8 - 2\alpha_9 - \alpha_{16}, \\
\mathbb{C}_{2212} &= \alpha_7 + \alpha_{12} - \alpha_{13}, & \mathbb{C}_{2223} &= \frac{1}{2}\alpha_{11} + \frac{1}{2}\alpha_{18} - \frac{1}{2}\alpha_{20}, \\
\mathbb{C}_{2213} &= \frac{1}{2}\alpha_{10} + \frac{1}{2}\alpha_{17} - \frac{1}{2}\alpha_{19}, & \mathbb{C}_{3333} &= \lambda + 2\mu + 2\alpha_4 - 2\alpha_9, \\
\mathbb{C}_{3312} &= \alpha_7 - \alpha_{13}, & \mathbb{C}_{3323} &= \frac{1}{2}\alpha_{11} - \frac{1}{2}\alpha_{20}, \\
\mathbb{C}_{3313} &= \frac{1}{2}\alpha_{10} - \frac{1}{2}\alpha_{19}, & \mathbb{C}_{1212} &= \mu, \\
\mathbb{C}_{1223} &= \frac{1}{2}\alpha_{15}, & \mathbb{C}_{1213} &= \frac{1}{2}\alpha_{14}, \\
\mathbb{C}_{2323} &= \mu + \frac{1}{2}\alpha_6, & \mathbb{C}_{2313} &= \frac{1}{4}\alpha_{21}, \\
\mathbb{C}_{1313} &= \mu + \frac{1}{2}\alpha_5.
\end{aligned}$$

Monoclinic Anisotropy Group \mathcal{G}_2 :

Set of Bilinear Invariants: Having a look at Table 4.2 we notice that for the characterization of the monoclinic symmetry group \mathcal{G}_2 a symmetric and a skew-symmetric second order structural tensor are sufficient, i.e., $\mathbf{A} = \mathbf{P}_2$, $\mathbf{W} = \epsilon\mathbf{e}_3$. In Table G.2 the invariants taken from Table 4.3 are listed. Dropping out the obvious functionally dependent elements

$$\begin{aligned}
\text{tr}[\mathbf{E}^2] &= 2\text{tr}[\mathbf{E}^2\mathbf{A}^2] + (\text{tr}[\mathbf{E}] - \text{tr}[\mathbf{E}\mathbf{A}^2])^2 - \frac{1}{4}(\text{tr}[\mathbf{E}\mathbf{A}] + \text{tr}[\mathbf{E}\mathbf{A}^2])^2 \\
&\quad - \frac{1}{4}(\text{tr}[\mathbf{E}\mathbf{A}] - \text{tr}[\mathbf{E}\mathbf{A}^2])^2 - \frac{1}{2}\text{tr}[\mathbf{E}\mathbf{A}\mathbf{W}]^2, \\
\text{tr}[\mathbf{E}\mathbf{W}^2] &= -\text{tr}[\mathbf{E}\mathbf{A}^2], \quad \text{tr}[\mathbf{E}^2\mathbf{W}^2] = -\text{tr}[\mathbf{E}^2\mathbf{A}^2], \\
\text{tr}[\mathbf{E}^2\mathbf{A}\mathbf{W}] &= \text{tr}[\mathbf{E}\mathbf{A}\mathbf{W}]\text{tr}[\mathbf{E}\mathbf{A}^2] + 2E_{13}E_{23}, \\
\text{tr}[\mathbf{E}\mathbf{W}^2\mathbf{A}\mathbf{W}] &= -\text{tr}[\mathbf{E}\mathbf{A}\mathbf{W}], \quad \text{tr}[\mathbf{E}\mathbf{A}^2\mathbf{W}] = 0,
\end{aligned} \tag{G.5}$$

with

$$\begin{aligned}
E_{13} &= \left(\frac{1}{2}(\text{tr}[\mathbf{E}^2\mathbf{A}^2] + \text{tr}[\mathbf{E}^2\mathbf{A}]) - \frac{1}{4}(\text{tr}[\mathbf{E}\mathbf{A}] + \text{tr}[\mathbf{E}\mathbf{A}^2])^2 - \frac{1}{4}(\text{tr}[\mathbf{E}\mathbf{A}\mathbf{W}])^2\right)^{\frac{1}{2}}, \\
E_{23} &= \left(\frac{1}{2}\text{tr}[\mathbf{E}^2\mathbf{A}^2] - \frac{1}{4}(\text{tr}[\mathbf{E}\mathbf{A}\mathbf{W}])^2 - \frac{1}{4}(\text{tr}[\mathbf{E}\mathbf{A}] - \text{tr}[\mathbf{E}\mathbf{A}^2])^2 - \frac{1}{2}\text{tr}[\mathbf{E}^2\mathbf{A}]\right)^{\frac{1}{2}}.
\end{aligned} \tag{G.6}$$

leads to the *set of bilinear invariants* in terms of \mathbf{E}

$$\mathcal{F}^m(\mathbf{E}, \mathbf{A}, \mathbf{W}) = \{\text{tr}[\mathbf{E}], \text{tr}[\mathbf{E}\mathbf{A}], \text{tr}[\mathbf{E}^2\mathbf{A}], \text{tr}[\mathbf{E}\mathbf{A}^2], \text{tr}[\mathbf{E}^2\mathbf{A}^2], \text{tr}[\mathbf{E}\mathbf{A}\mathbf{W}]\}. \tag{G.7}$$

In detail, the set (G.7) has the form

$$\boxed{\mathcal{F}^m(\mathbf{E}, \mathbf{A}, \mathbf{W}) = \{E_{11} + E_{22} + E_{33}, E_{11} - E_{22}, E_{11}^2 + E_{13}^2 - E_{22}^2 - E_{23}^2, E_{11} + E_{22}, E_{11}^2 + 2E_{12}^2 + E_{13}^2 + E_{22}^2 + E_{23}^2, 2E_{12}\}}. \tag{G.8}$$

Table G.2: Set of Monoclinic Bilinear Invariants.

| | |
|---------------------------------|--|
| Structural Tensors: | $\mathbf{A} = \mathbf{P}_2, \mathbf{W} = \epsilon \mathbf{e}_3$ |
| Invariants for one argument: | $\text{tr}[\mathbf{E}], \text{tr}[\mathbf{E}^2]$ |
| Invariants for two arguments: | $\text{tr}[\mathbf{EA}], \text{tr}[\mathbf{E}^2 \mathbf{A}], \text{tr}[\mathbf{EA}^2], \text{tr}[\mathbf{E}^2 \mathbf{A}^2], \text{tr}[\mathbf{EW}^2], \text{tr}[\mathbf{E}^2 \mathbf{W}^2]$ |
| Invariants for three arguments: | $\text{tr}[\mathbf{EAW}], \text{tr}[\mathbf{E}^2 \mathbf{AW}], \text{tr}[\mathbf{EW}^2 \mathbf{AW}], \text{tr}[\mathbf{EA}^2 \mathbf{W}]$ |

In DIMITRIENKO [43] we find the *classical set of bilinear invariants* depending on the coefficients of \mathbf{E}

$$\bar{\mathcal{F}}^m = \{E_{11}, E_{22}, E_{33}, E_{12}, E_{13}^2, E_{13}E_{23}\}. \quad (\text{G.9})$$

A comparison of (G.7) with (G.9) shows that all elements of the reference set (G.9) appear in (G.7), but in a nontrivial sense.

Quadratic Energy Function: The monoclinic final set \mathcal{B}^m consists of the following 13 independent elements in terms of the quadratic and multiplicative combinations of all linear invariants of $\mathcal{F}^m(\mathbf{E}, \mathbf{A}, \mathbf{W})$:

$$\begin{aligned} \mathcal{B}^m := & \{ \text{tr}[\mathbf{E}]^2, \text{tr}[\mathbf{E}^2], \text{tr}[\mathbf{EA}]^2, \text{tr}[\mathbf{E}^2 \mathbf{A}], \text{tr}[\mathbf{EA}^2]^2, \text{tr}[\mathbf{E}^2 \mathbf{AW}], \\ & \text{tr}[\mathbf{EAW}]^2, \text{tr}[\mathbf{E}]\text{tr}[\mathbf{EA}], \text{tr}[\mathbf{E}]\text{tr}[\mathbf{EA}^2], \\ & \text{tr}[\mathbf{E}]\text{tr}[\mathbf{EAW}], \text{tr}[\mathbf{EA}]\text{tr}[\mathbf{EA}^2], \text{tr}[\mathbf{EA}]\text{tr}[\mathbf{EAW}], \\ & \text{tr}[\mathbf{EA}^2]\text{tr}[\mathbf{EAW}] \}. \end{aligned} \quad (\text{G.10})$$

The coordinate-invariant monoclinic quadratic function $\psi^m(\mathbf{C}, \mathbf{A}, \mathbf{W})$ can be now formulated in terms of the elements of the final set \mathcal{B}^m while setting $\mathbf{E} = \frac{1}{2}(\mathbf{C} - \mathbf{1})$:

$$\psi^m(\mathbf{C}, \mathbf{A}, \mathbf{W}) = \sum_{i=1}^{13} \alpha_i L_i, \quad L_i \in \mathcal{B}^m.$$

The coefficient scheme of the elasticity tensor derived by the second derivative of ψ^m with respect to \mathbf{C} , i.e.,

$$\begin{aligned} \mathbb{C}^{(V)m} &= 4\partial_{\mathbf{C}\mathbf{C}}\psi(\mathbf{C}, \mathbf{A}, \mathbf{W}) \\ &= \lambda \mathbf{1} \otimes \mathbf{1} + 2\mu \mathbf{1} \boxtimes \mathbf{1} + 2\alpha_3 \mathbf{A} \otimes \mathbf{A} + \alpha_4 [\mathbf{1} \boxtimes \mathbf{A} + \mathbf{A} \boxtimes \mathbf{1}] \\ &\quad + 2\alpha_5 \mathbf{A}^2 \otimes \mathbf{A}^2 + \alpha_6 [\mathbf{1} \boxtimes (\mathbf{AW}) + (\mathbf{AW}) \boxtimes \mathbf{1}] \\ &\quad + 2\alpha_7 \mathbf{AW} \otimes \mathbf{AW} + \alpha_8 (\mathbf{1} \otimes \mathbf{A} + \mathbf{A} \otimes \mathbf{1}) \\ &\quad + \alpha_9 (\mathbf{1} \otimes \mathbf{A}^2 + \mathbf{A}^2 \otimes \mathbf{1}) + \alpha_{10} (\mathbf{1} \otimes \mathbf{AW} + \mathbf{AW} \otimes \mathbf{1}) \\ &\quad + \alpha_{11} (\mathbf{A} \otimes \mathbf{A}^2 + \mathbf{A}^2 \otimes \mathbf{A}) + \alpha_{12} (\mathbf{A} \otimes \mathbf{AW} + \mathbf{AW} \otimes \mathbf{A}) \\ &\quad + \alpha_{13} (\mathbf{A}^2 \otimes \mathbf{AW} + \mathbf{AW} \otimes \mathbf{A}^2) \end{aligned} \quad (\text{G.11})$$

is in Voigt notation equal to the classical one and appears as

$$\mathbb{C}^{(V)m} = \begin{bmatrix} \mathbb{C}_{1111} & \mathbb{C}_{1122} & \mathbb{C}_{1133} & \mathbb{C}_{1112} & 0 & 0 \\ & \mathbb{C}_{2222} & \mathbb{C}_{2233} & \mathbb{C}_{2212} & 0 & 0 \\ & & \mathbb{C}_{3333} & \mathbb{C}_{3312} & 0 & 0 \\ & & & \mathbb{C}_{1212} & 0 & 0 \\ & sym. & & & \mathbb{C}_{2323} & \mathbb{C}_{2313} \\ & & & & & \mathbb{C}_{1313} \end{bmatrix}.$$

In detail, the constant coefficients depending on the material parameters $\alpha_1, \dots, \alpha_{13}$ are

$$\begin{aligned} \mathbb{C}_{1111} &= \lambda + 2\mu + 2\alpha_3 + 2\alpha_4 + 2\alpha_5 + 2\alpha_8 + 2\alpha_9 + 2\alpha_{11}, \\ \mathbb{C}_{1122} &= \lambda - 2\alpha_3 + 2\alpha_5 + 2\alpha_9, \quad \mathbb{C}_{1133} = \lambda + \alpha_8 + \alpha_9, \\ \mathbb{C}_{1112} &= \alpha_6 + \alpha_{10} + \alpha_{12} + \alpha_{13}, \\ \mathbb{C}_{2222} &= \lambda + 2\mu + 2\alpha_3 - 2\alpha_4 + 2\alpha_5 - 2\alpha_8 + 2\alpha_9 - 2\alpha_{11}, \\ \mathbb{C}_{2233} &= \lambda - \alpha_8 + \alpha_9, \quad \mathbb{C}_{2212} = \alpha_6 + \alpha_{10} - \alpha_{12} + \alpha_{13}, \\ \mathbb{C}_{3333} &= \lambda + 2\mu, \quad \mathbb{C}_{3312} = \alpha_{10}, \\ \mathbb{C}_{1212} &= \mu + 2\alpha_7, \quad \mathbb{C}_{2323} = \mu - \frac{1}{2}\alpha_4, \\ \mathbb{C}_{2313} &= \frac{1}{2}\alpha_6, \quad \mathbb{C}_{1313} = \mu + \frac{1}{2}\alpha_4. \end{aligned}$$

Rhombic Anisotropy Group \mathcal{G}_3 :

Set of Bilinear Invariants: To be able to derive a *set of bilinear invariants* for the rhombic important anisotropy group \mathcal{G}_3 we have to consider two symmetric structural tensors, i.e., \mathbf{P}_2 from Table 4.2 and the transversely isotropic structural tensor $\mathbf{e}_3 \otimes \mathbf{e}_3$. For details on the resulting invariants from Table 4.3 see Table G.3. The *set of bilinear invariants* results in

$$\mathcal{F}^o(\mathbf{E}, \mathbf{A}) = \{\text{tr}[\mathbf{E}], \text{tr}[\mathbf{E}^2], \text{tr}[\mathbf{E}\mathbf{A}], \text{tr}[\mathbf{E}^2\mathbf{A}], \text{tr}[\mathbf{E}\mathbf{A}^2], \text{tr}[\mathbf{E}^2\mathbf{A}^2]\} \quad (\text{G.12})$$

and in terms of the components of \mathbf{E}

$$\mathcal{F}^o(\mathbf{E}, \mathbf{A}) = \{E_{11} + E_{22} + E_{33}, E_{11}^2 + E_{22}^2 + E_{33}^2 + 2E_{12}^2 + 2E_{13}^2 + 2E_{23}^2, \\ E_{11} - E_{22}, E_{11}^2 + E_{13}^2 - E_{22}^2 - E_{23}^2, E_{11} + E_{22}, \\ E_{11}^2 + 2E_{12}^2 + E_{13}^2 + E_{22}^2 + E_{23}^2\}, \quad (\text{G.13})$$

where the following relations have been taken into account:

$$\text{tr}[\mathbf{E}\mathbf{M}] = \text{tr}[\mathbf{E}] - \text{tr}[\mathbf{E}\mathbf{A}^2], \quad \text{tr}[\mathbf{E}^2\mathbf{M}] = \text{tr}[\mathbf{E}^2] - \text{tr}[\mathbf{E}^2\mathbf{A}^2], \quad \text{tr}[\mathbf{E}\mathbf{A}\mathbf{M}] = 0. \quad (\text{G.14})$$

A comparison of the scalar invariants (G.12) with the *classical set of bilinear invariants*

$$\bar{\mathcal{F}}^o = \{E_{11}, E_{22}, E_{33}, E_{23}^2, E_{13}^2\} \quad (\text{G.15})$$

Table G.3: Set of Rhombic Bilinear Invariants.

| | |
|---------------------------------|--|
| Structural Tensors: | $\mathbf{A} = \mathbf{P}_2, \mathbf{M} = \mathbf{e}_3 \otimes \mathbf{e}_3, (\text{with } \mathbf{M}^2 = \mathbf{M})$ |
| Invariants for one argument: | $\text{tr}[\mathbf{E}], \text{tr}[\mathbf{E}^2]$ |
| Invariants for two arguments: | $\text{tr}[\mathbf{EA}], \text{tr}[\mathbf{E}^2\mathbf{A}], \text{tr}[\mathbf{EA}^2], \text{tr}[\mathbf{E}^2\mathbf{A}^2],$ $\text{tr}[\mathbf{EM}], \text{tr}[\mathbf{E}^2\mathbf{M}]$ |
| Invariants for three arguments: | $\text{tr}[\mathbf{EAM}]$ |

given in DIMITRIENKO [43], shows that all invariants in the set (G.12) can be uniquely expressed by nontrivial combinations of all terms appearing in (G.15).

Quadratic Energy Function: All possible quadratic combinations of linear invariants and all a priori quadratic isotropic terms appearing in the set $\mathcal{F}^o(\mathbf{E}, \mathbf{A})$ are summarized in the final rhombic set:

$$\mathcal{B}^o := \{\text{tr}[\mathbf{E}]^2, \text{tr}[\mathbf{E}^2], \text{tr}[\mathbf{EA}]^2, \text{tr}[\mathbf{E}^2\mathbf{A}], \text{tr}[\mathbf{EA}^2]^2, \text{tr}[\mathbf{E}^2\mathbf{A}^2], \text{tr}[\mathbf{E}]\text{tr}[\mathbf{EA}], \text{tr}[\mathbf{E}]\text{tr}[\mathbf{EA}^2], \text{tr}[\mathbf{EA}]\text{tr}[\mathbf{EA}^2]\}. \quad (\text{G.16})$$

The quadratic function $\psi^o(\mathbf{C}, \mathbf{A}) = \psi^o(\mathbf{E} = \frac{1}{2}(\mathbf{C} - \mathbf{1}), \mathbf{A})$ that is invariant with respect to the material symmetry group \mathcal{G}_3 can be now formulated in terms of the elements of the final set:

$$\psi^o(\mathbf{C}, \mathbf{A}) = \sum_{i=1}^9 \alpha_i L_i, \quad L_i \in \mathcal{B}^o.$$

The classical fourth-order elasticity tensor results from the second derivative, i.e.,

$$\begin{aligned} \mathbb{C}^o &= 4\partial_{CC}\psi^o(\mathbf{C}, \mathbf{A}) \\ &= \lambda \mathbf{1} \otimes \mathbf{1} + 2\mu \mathbf{1} \boxtimes \mathbf{1} + 2\alpha_3 \mathbf{A} \otimes \mathbf{A} + \alpha_4 [\mathbf{1} \boxtimes \mathbf{A} + \mathbf{A} \boxtimes \mathbf{1}] \\ &\quad + 2\alpha_5 \mathbf{A}^2 \otimes \mathbf{A}^2 + \alpha_6 [\mathbf{1} \boxtimes \mathbf{A}^2 + \mathbf{A}^2 \boxtimes \mathbf{1}] \\ &\quad + \alpha_7 (\mathbf{1} \otimes \mathbf{A} + \mathbf{A} \otimes \mathbf{1}) + \alpha_8 (\mathbf{1} \otimes \mathbf{A}^2 + \mathbf{A}^2 \otimes \mathbf{1}) \\ &\quad + \alpha_9 (\mathbf{A} \otimes \mathbf{A}^2 + \mathbf{A}^2 \otimes \mathbf{A}) \end{aligned} \quad (\text{G.17})$$

and has in Voigt notation the form

$$\mathbb{C}^{(V)o} = \begin{bmatrix} \mathbb{C}_{1111} & \mathbb{C}_{1122} & \mathbb{C}_{1133} & 0 & 0 & 0 \\ & \mathbb{C}_{2222} & \mathbb{C}_{2233} & 0 & 0 & 0 \\ & & \mathbb{C}_{3333} & 0 & 0 & 0 \\ & & & \mathbb{C}_{1212} & 0 & 0 \\ & sym. & & & \mathbb{C}_{2323} & 0 \\ & & & & & \mathbb{C}_{1313} \end{bmatrix},$$

where the constants are explicitly given by

$$\begin{aligned}
\mathbb{C}_{1111} &= \lambda + 2\mu + 2\alpha_3 + 2\alpha_4 + 2\alpha_5 + 2\alpha_6 + 2\alpha_7 + 2\alpha_8 + 2\alpha_9, \\
\mathbb{C}_{1122} &= \lambda - 2\alpha_3 + 2\alpha_5 + 2\alpha_8, \quad \mathbb{C}_{1133} = \lambda + \alpha_7 + \alpha_8, \\
\mathbb{C}_{2222} &= \lambda + 2\mu + 2\alpha_3 - 2\alpha_4 + 2\alpha_5 + 2\alpha_6 - 2\alpha_7 + 2\alpha_8 - 2\alpha_9, \\
\mathbb{C}_{2233} &= \lambda - \alpha_7 + \alpha_8, \quad \mathbb{C}_{3333} = \lambda + 2\mu, \\
\mathbb{C}_{1212} &= \mu + \alpha_6, \quad \mathbb{C}_{2323} = \mu - \frac{1}{2}\alpha_4 + \frac{1}{2}\alpha_6, \\
\mathbb{C}_{1313} &= \mu + \frac{1}{2}\alpha_4 + \frac{1}{2}\alpha_6.
\end{aligned}$$

Tetragonal Anisotropy Group \mathcal{G}_5 :

Set of Bilinear Invariants: For the second important tetragonal material symmetry group \mathcal{G}_5 the appropriate isotropic extension functions are obtained from (4.5) by replacing the skew-symmetric tensor $\mathbf{W} = \epsilon\mathbf{e}_3$ by $\mathbf{M} = \mathbf{e}_3 \otimes \mathbf{e}_3$. Exploiting Table 4.3 gives the fundamental invariants depending on up to three arguments, see Table G.4.

Table G.4: Set of Tetragonal Bilinear Invariants, \mathcal{G}_5 .

| | |
|---------------------------------------|--|
| Structural Tensors: | $\mathbf{A} = \mathbb{P}_4 : \mathbf{E}, \mathbf{B} = \mathbb{P}_4 : \mathbf{E}^2, \mathbf{M} = \mathbf{e}_3 \otimes \mathbf{e}_3, (\text{with } \mathbf{M}^2 = \mathbf{M})$ |
| Invariants depending on one variable: | $\text{tr}[\mathbf{E}], \text{tr}[\mathbf{E}^2], \text{tr}[\mathbf{A}], \text{tr}[\mathbf{A}^2], \text{tr}[\mathbf{B}]$ |
| Invariants for two arguments: | $\text{tr}[\mathbf{EA}], \text{tr}[\mathbf{EM}], \text{tr}[\mathbf{E}^2\mathbf{M}], \text{tr}[\mathbf{AM}], \text{tr}[\mathbf{A}^2\mathbf{M}], \text{tr}[\mathbf{BM}]$ |
| Invariants for three arguments: | $\text{tr}[\mathbf{EAM}]$ |

For the derivation of the *set of bilinear invariants* the dependent elements have to be dropped:

$$\begin{aligned}
\text{tr}[\mathbf{A}] &= 0, \text{tr}[\mathbf{B}] = 0, \text{tr}[\mathbf{AM}] = 0, \text{tr}[\mathbf{A}^2\mathbf{M}] = 0, \text{tr}[\mathbf{BM}] = 0, \text{tr}[\mathbf{EAM}] = 0, \\
\text{tr}[\mathbf{A}^2] &= -2\text{tr}[\mathbf{E}]^2 + 4\text{tr}[\mathbf{E}^2] + 4\text{tr}[\mathbf{E}]\text{tr}[\mathbf{EM}] - 8\text{tr}[\mathbf{E}^2\mathbf{M}] + 2\text{tr}[\mathbf{EM}]^2,
\end{aligned}$$

so that the set is finally given by

$$\mathcal{F}^{t2}(\mathbf{E}, \mathbf{A}, \mathbf{M}) = \{\text{tr}[\mathbf{E}], \text{tr}[\mathbf{E}^2], \text{tr}[\mathbf{EA}], \text{tr}[\mathbf{EM}], \text{tr}[\mathbf{E}^2\mathbf{M}]\} \quad (\text{G.18})$$

and with respect to the components of \mathbf{E} :

$$\boxed{\mathcal{F}^{t2}(\mathbf{E}, \mathbf{A}, \mathbf{M}) = \{E_{11} + E_{22} + E_{33}, E_{11}^2 + E_{22}^2 + E_{33}^2 + 2E_{12}^2 + 2E_{13}^2 + 2E_{23}^2, (E_{11} - E_{22})^2 - 4E_{12}^2, E_{33}, E_{13}^2 + E_{23}^2 + E_{33}^2\}.} \quad (\text{G.19})$$

A comparison with the *classical set of bilinear invariants*, cf. DIMITRIENKO [43],

$$\bar{\mathcal{F}}^{t2} = \{E_{11} + E_{22}, E_{33}, E_{13}^2 + E_{23}^2, E_{11}^2 + E_{22}^2, E_{12}^2\}. \quad (\text{G.20})$$

shows that all invariants of (G.18) can be uniquely derived by the linear and quadratic elements of (G.20).

Quadratic Energy Function: We arrive with all linear, combined quadratic and a priori quadratic elements of $\mathcal{F}^{t2}(\mathbf{E}, \mathbf{A}, \mathbf{M})$ at the tetragonal final set \mathcal{B}^{t2} containing 6 quadratic elements

$$\mathcal{B}^{t2} := \{\text{tr}[\mathbf{E}]^2, \text{tr}[\mathbf{E}^2], \text{tr}[\mathbf{E}\mathbf{A}], \text{tr}[\mathbf{E}\mathbf{M}]^2, \text{tr}[\mathbf{E}]\text{tr}[\mathbf{E}\mathbf{M}], \text{tr}[\mathbf{E}^2\mathbf{M}]\}, \quad (\text{G.21})$$

which leads to the formulation of a quadratic coordinate-free energy function $\psi^{t2}(\mathbf{E}, \mathbf{A}, \mathbf{M})$ in case of \mathcal{G}_5 -type anisotropy while applying $\mathbf{E} = \frac{1}{2}(\mathbf{C} - \mathbf{1})$

$$\psi^{t2}(\mathbf{C}, \mathbf{A}, \mathbf{M}) = \sum_{i=1}^6 \alpha_i L_i, \quad L_i \in \mathcal{B}^{t2}.$$

Finally, the classical matrix representation of the corresponding tetragonal elasticity tensor is here obtained by the Voigt notation of the tangent moduli $\mathbb{C}^{t2} = 4\partial_{CC}\psi^{t2}(\mathbf{C}, \mathbf{A}, \mathbf{M})$, with

$$\begin{aligned} \mathbb{C}^{t2} = & \lambda \mathbf{1} \otimes \mathbf{1} + 2\mu \mathbf{1} \boxtimes \mathbf{1} + 2\alpha_3 \mathbb{P}_4 + 2\alpha_4(\mathbf{M} \otimes \mathbf{M}) \\ & + \alpha_5(\mathbf{1} \otimes \mathbf{M} + \mathbf{M} \otimes \mathbf{1}) + \alpha_6[\mathbf{1} \boxtimes \mathbf{M} + \mathbf{M} \boxtimes \mathbf{1}], \end{aligned} \quad (\text{G.22})$$

which results in

$$\mathbb{C}^{(V) t2} = \begin{bmatrix} \mathbb{C}_{1111} & \mathbb{C}_{1122} & \mathbb{C}_{1133} & 0 & 0 & 0 \\ & \mathbb{C}_{1111} & \mathbb{C}_{1133} & 0 & 0 & 0 \\ & & \mathbb{C}_{3333} & 0 & 0 & 0 \\ & & & \mathbb{C}_{1212} & 0 & 0 \\ & sym. & & & \mathbb{C}_{2323} & 0 \\ & & & & & \mathbb{C}_{2323} \end{bmatrix}.$$

The linear dependencies between the coefficients and the material parameters are

$$\begin{aligned} \mathbb{C}_{1111} &= \lambda + 2\mu + 2\alpha_3, & \mathbb{C}_{1122} &= \lambda - 2\alpha_3, \\ \mathbb{C}_{1133} &= \lambda + \alpha_5, & \mathbb{C}_{3333} &= \lambda + 2\mu + 2\alpha_4 + 2\alpha_5 + 2\alpha_6, \\ \mathbb{C}_{1212} &= \mu - 2\alpha_3, & \mathbb{C}_{2323} &= \mu + \frac{1}{2}\alpha_6. \end{aligned}$$

Trigonal Anisotropy Group \mathcal{G}_8 :

Set of Bilinear Invariants: Zheng and Spencer [146] propose the trigonal \mathcal{G}_8 -invariant structural tensors $\mathbb{P} = \mathbf{e}_3 \otimes \mathbf{P}'_3$ and $\mathbf{W}_2 = \epsilon \mathbf{e}_3$. Since the representation theory is based on symmetric and skew-symmetric second-order tensors we have to check if the resulting isotropic extension functions are of such type. Here, for the trigonal symmetry classes \mathcal{G}_8 (and later for \mathcal{G}_9) we construct the linear and quadratic second-order isotropic extension functions in terms of \mathbf{E}

$$\begin{aligned} D_1(\mathbf{E}) &= (\mathbf{e}_3 \otimes \mathbf{P}'_3) : \mathbf{E}, & D_2(\mathbf{E}) &= \mathbf{E} : (\mathbf{e}_3 \otimes \mathbf{P}'_3), \\ D_3(\mathbf{E}) &= (\mathbf{e}_3 \otimes \mathbf{P}'_3) : \mathbf{E}^2, & D_4(\mathbf{E}) &= \mathbf{E}^2 : (\mathbf{e}_3 \otimes \mathbf{P}'_3). \end{aligned} \quad (\text{G.23})$$

The first and third functions are neither symmetric nor skew-symmetric. Therefore, we use their symmetric and skew-symmetric parts. For instance, the first function appears as

$$\mathbf{D}_1(\mathbf{E}) = \begin{bmatrix} 0 & 0 & 0 \\ 0 & 0 & 0 \\ 2 E_{12} & E_{11} - E_{22} & 0 \end{bmatrix}. \quad (\text{G.24})$$

The split into the symmetric part $\mathbf{A}_1(\mathbf{E})$ and skew-symmetric part $\mathbf{W}_1(\mathbf{E})$, i.e.,

$$\begin{aligned} \mathbf{D}_1(\mathbf{E}) = \mathbf{A}_1(\mathbf{E}) + \mathbf{W}_1(\mathbf{E}) = & \frac{1}{2} (\mathbf{e}_3 \otimes \mathbf{P}'_3 + \mathbf{e}_3 \boxtimes \mathbf{P}'_3) : \mathbf{E} \\ & + \frac{1}{2} (\mathbf{e}_3 \otimes \mathbf{P}'_3 - \mathbf{e}_3 \boxtimes \mathbf{P}'_3) : \mathbf{E}, \end{aligned} \quad (\text{G.25})$$

with

$$\mathbf{A}_1(\mathbf{E}) = \begin{bmatrix} 0 & 0 & E_{12} \\ 0 & 0 & \frac{(E_{11}-E_{22})}{2} \\ E_{12} \frac{(E_{11}-E_{22})}{2} & 0 & 0 \end{bmatrix}, \quad \mathbf{W}_1(\mathbf{E}) = \begin{bmatrix} 0 & 0 & -E_{12} \\ 0 & 0 & -\frac{(E_{11}-E_{22})}{2} \\ E_{12} \frac{(E_{11}-E_{22})}{2} & 0 & 0 \end{bmatrix} \quad (\text{G.26})$$

and the proof of invariance of the auxiliary fourth-order structural tensor

$$(\mathbf{e}_3 \boxtimes \mathbf{P}'_3) = \mathbf{Q} \boxtimes \mathbf{Q} : (\mathbf{e}_3 \boxtimes \mathbf{P}'_3) : \mathbf{Q}^T \boxtimes \mathbf{Q}^T \quad \forall \mathbf{Q} \in \mathcal{G}_9, \quad (\text{G.27})$$

which is here valid, have to be done. The remaining two extension functions $(\text{G.23})_{2,4}$ have the form of a traceless symmetric tensor \mathbf{V} , with

$$\mathbf{V} = \begin{bmatrix} A & B & 0 \\ B & -A & 0 \\ 0 & 0 & 0 \end{bmatrix}. \quad (\text{G.28})$$

Thus, with the symmetric and skew-symmetric parts of \mathbf{D}_1 , \mathbf{D}_3 as well as \mathbf{D}_2 , \mathbf{D}_4 and \mathbf{W}_2 the evaluation of the invariants of Table 4.3 is made possible. In the following, we show the results for the bilinear invariants in terms of the isotropic extension functions \mathbf{A}_1 , \mathbf{W}_1 and the structural tensor $\mathbf{W}_2 = \epsilon \mathbf{e}_3$, see Table G.5. They are already sufficient for the construction of a *complete* quadratic \mathcal{G}_8 -invariant energy function: the *set of bilinear invariants* obtained from Table 4.3 reduces to

$$\mathcal{F}^{ht1}(\mathbf{E}, \mathbf{A}_1, \mathbf{W}_2) := \{\text{tr}[\mathbf{E}], \text{tr}[\mathbf{E}^2], \text{tr}[\mathbf{E}\mathbf{A}_1], \text{tr}[\mathbf{E}\mathbf{W}_2^2], \text{tr}[\mathbf{E}^2\mathbf{W}_2^2], \text{tr}[\mathbf{E}\mathbf{A}_1\mathbf{W}_2]\}, \quad (\text{G.29})$$

which is represented in a component-by-component notation by

$$\boxed{\begin{aligned} \mathcal{F}^{ht1}(\mathbf{E}, \mathbf{A}_1, \mathbf{W}_2) = & \{E_{11} + E_{22} + E_{33}, E_{11}^2 + E_{22}^2 + E_{33}^2 + 2 E_{12}^2 + 2 E_{13}^2 + \\ & 2 E_{23}^2, 2 E_{12}E_{13} + E_{23}(E_{11} - E_{22}), -E_{11} - E_{22}, -E_{11}^2 \\ & - E_{22}^2 - E_{13}^2 - E_{23}^2 - 2 E_{12}^2, E_{12}E_{23} + 1/2 E_{13}(E_{22} - E_{11})\}. \end{aligned}}$$

Here, the functional dependencies between the following invariants of Table G.5 have been considered:

$$\begin{aligned} \text{tr}[\mathbf{W}_1^2] &= \text{tr}[\mathbf{E}^2] - (\text{tr}[\mathbf{E}] + \text{tr}[\mathbf{E}\mathbf{W}_2^2])^2 + 2 \text{tr}[\mathbf{E}^2\mathbf{W}_2^2] + \frac{1}{2} \text{tr}[\mathbf{E}\mathbf{W}_2^2]^2, \quad \text{tr}[\mathbf{A}_1] = 0, \\ \text{tr}[\mathbf{A}_1^2] &= -\text{tr}[\mathbf{W}_1^2], \quad \text{tr}[\mathbf{A}_1\mathbf{W}_2^2] = 0, \quad \text{tr}[\mathbf{A}_1^2\mathbf{W}_2^2] = \frac{1}{2} \text{tr}[\mathbf{W}_1^2], \quad \text{tr}[\mathbf{E}\mathbf{W}_2^2\mathbf{A}\mathbf{W}_2] = 0. \end{aligned} \quad (\text{G.30})$$

Table G.5: Set of Trigonal Bilinear Invariants, \mathcal{G}_9 .

| | |
|---------------------------------|---|
| Structural Tensors: | $\mathbf{A}_1 = 1/2(\mathbf{e}_3 \otimes \mathbf{P}'_3 + \mathbf{e}_3 \boxtimes \mathbf{P}'_3) : \mathbf{E}$, |
| | $\mathbf{W}_1 = 1/2(\mathbf{e}_3 \otimes \mathbf{P}'_3 - \mathbf{e}_3 \boxtimes \mathbf{P}'_3) : \mathbf{E}$, $\mathbf{W}_2 = \epsilon \mathbf{e}_3$ |
| Invariants for one variable: | $\text{tr}[\mathbf{E}]$, $\text{tr}[\mathbf{E}^2]$, $\text{tr}[\mathbf{A}_1]$, $\text{tr}[\mathbf{A}_1^2]$, $\text{tr}[\mathbf{W}_1^2]$ |
| Invariants for two arguments: | $\text{tr}[\mathbf{E}\mathbf{A}_1]$, $\text{tr}[\mathbf{E}\mathbf{W}_2^2]$, $\text{tr}[\mathbf{E}^2\mathbf{W}_2^2]$, $\text{tr}[\mathbf{A}_1\mathbf{W}_2^2]$, $\text{tr}[\mathbf{A}_1^2\mathbf{W}_2^2]$ |
| Invariants for three arguments: | $\text{tr}[\mathbf{E}\mathbf{A}_1\mathbf{W}_2]$, $\text{tr}[\mathbf{E}\mathbf{W}_2^2\mathbf{A}_1\mathbf{W}_2]$ |

The *classical set of bilinear invariants* proposed in DIMITRIENKO [43] in terms of \mathbf{E} also contains six functionally independent linear and quadratic invariants. It has the form

$$\begin{aligned} \bar{\mathcal{F}}^{ht2} = \{ & E_{11} + E_{22}, E_{33}, E_{13}^2 + E_{23}^2, E_{13}(E_{11} - E_{22}) - 2E_{12}E_{23}, \\ & E_{11}^2 + E_{22}^2 + 2E_{12}^2, E_{23}(E_{11} - E_{22}) + 2E_{12}E_{13} \}, \end{aligned} \quad (\text{G.31})$$

where each element represents a unique function of the independent elements of (G.29).

Quadratic Energy Function: Combining all invariants of the set $\mathcal{F}^{ht1}(\mathbf{E}, \mathbf{A}_1, \mathbf{W}_2)$ in such a way that we only obtain quadratic terms in \mathbf{E} leads to the assembled set \mathcal{B}^{ht1} :

$$\begin{aligned} \mathcal{B}^{ht1} := \{ & \text{tr}[\mathbf{E}]^2, \text{tr}[\mathbf{E}^2], \text{tr}[\mathbf{E}^2\mathbf{W}_2^2], \text{tr}[\mathbf{E}\mathbf{A}_1], \\ & \text{tr}[\mathbf{E}\mathbf{W}_2^2]^2, \text{tr}[\mathbf{E}]\text{tr}[\mathbf{E}\mathbf{W}_2^2], \text{tr}[\mathbf{E}\mathbf{A}_1\mathbf{W}_2] \}. \end{aligned} \quad (\text{G.32})$$

Thus, a possible *complete* coordinate-free representation for a quadratic function in terms of elements L_1, \dots, L_7 of \mathcal{B}^{ht1} with $\mathbf{E} = \frac{1}{2}(\mathbf{C} - \mathbf{1})$ reads

$$\psi^{ht1}(\mathbf{C}, \mathbf{A}_1, \mathbf{W}_2) = \sum_{i=1}^7 \alpha_i L_i, \quad L_i \in \mathcal{B}^{ht1}.$$

The twice differentiation of ψ^{ht1} with respect to \mathbf{C} , i.e., $\mathbb{C}^{(V)ht1} = 4\partial_{\mathbf{C}\mathbf{C}}\psi(\mathbf{C}, \mathbf{A}_1, \mathbf{B}, \mathbf{W})$, with

$$\begin{aligned} \mathbb{C}^{ht1} = & \lambda \mathbf{1} \otimes \mathbf{1} + 2\mu \mathbf{1} \boxtimes \mathbf{1} + \alpha_3 [\mathbf{1} \boxtimes \mathbf{W}_2^2 + \mathbf{W}_2^2 \boxtimes \mathbf{1}] \\ & + \alpha_4 \mathbb{D} + 2\alpha_5 \mathbf{W}_2^2 \otimes \mathbf{W}_2^2 + \alpha_6 (\mathbf{1} \otimes \mathbf{W}_2^2 + \mathbf{W}_2^2 \otimes \mathbf{1}) + \alpha_7 \mathbb{L}, \end{aligned} \quad (\text{G.33})$$

where $\mathbb{D}_{opab} = \mathbb{P}_{opab} + \mathbb{P}_{abop}$ and $\mathbb{L}_{opab} = \mathbb{P}_{pkab}W_{2,ko} + \mathbb{P}_{bkop}W_{2,ka}$, with $\mathbb{P} = 1/2(\mathbf{e}_3 \otimes \mathbf{P}'_3 + \mathbf{e}_3 \boxtimes \mathbf{P}'_3)$, exhibits in Voigt notation the same form as the well-known constant classical fourth-order trigonal elasticity tensor of \mathcal{G}_8 -type:

$$\mathbb{C}^{(V)ht1} = \begin{bmatrix} \mathbb{C}_{1111} & \mathbb{C}_{1122} & \mathbb{C}_{1133} & 0 & \mathbb{C}_{1123} & \mathbb{C}_{1113} \\ & \mathbb{C}_{1111} & \mathbb{C}_{1133} & 0 & -\mathbb{C}_{1123} & -\mathbb{C}_{1113} \\ & & \mathbb{C}_{3333} & 0 & 0 & 0 \\ & & & \frac{1}{2}(\mathbb{C}_{1111} - \mathbb{C}_{1122}) & -\mathbb{C}_{1113} & \mathbb{C}_{1123} \\ & sym. & & & \mathbb{C}_{2323} & 0 \\ & & & & & \mathbb{C}_{2323} \end{bmatrix}. \quad (\text{G.34})$$

The coefficients can be uniquely determined by functions of the material parameters $\alpha_i, i = 1, \dots, 7$, i.e.,

$$\begin{aligned} \mathbb{C}_{1111} &= \lambda + 2\mu + 2(\alpha_5 - \alpha_3 - \alpha_6), & \mathbb{C}_{1122} &= \lambda + 2(\alpha_5 - \alpha_6), \\ \mathbb{C}_{1133} &= \lambda - \alpha_6, & \mathbb{C}_{1123} &= \alpha_4/2, \\ \mathbb{C}_{1113} &= -\alpha_7/4, & \mathbb{C}_{3333} &= \lambda + 2\mu, \\ \mathbb{C}_{2323} &= \mu - \alpha_3/2. \end{aligned}$$

Trigonal Anisotropy Group \mathcal{G}_9 .

Set of Bilinear Invariants: For the second trigonal material symmetry group \mathcal{G}_9 Zheng and Spencer [146] propose the same fourth-order structural tensor as for the group \mathcal{G}_8 . Thus, the functions (G.23) act also here as isotropic extension functions. The second-order structural tensor is different. It is here symmetric, cf. Table G.5. We neglect the quadratic isotropic extension functions of (G.23), since they are not necessary for the construction of *complete* quadratic energy functions. Using Table 4.3 gives 14 invariant terms, see Table G.5. Dropping out the obvious dependent invariants

$$\begin{aligned} \text{tr}[\mathbf{W}_1^2] &= -\text{tr}[\mathbf{E}^2] + 2\text{tr}[\mathbf{E}^2\mathbf{M}] - \text{tr}[\mathbf{EM}]^2 + 1/2(\text{tr}[\mathbf{E}] - \text{tr}[\mathbf{EM}])^2, \\ \text{tr}[\mathbf{A}_1] &= 0, \text{tr}[\mathbf{A}_1^2] = -\text{tr}[\mathbf{W}_1^2], \text{tr}[\mathbf{A}_1\mathbf{M}] = 0, \text{tr}[\mathbf{A}_1^2\mathbf{M}] = -1/2\text{tr}[\mathbf{W}_1^2], \\ \text{tr}[\mathbf{MW}_1^2] &= 1/2\text{tr}[\mathbf{W}_1^2], \text{tr}[\mathbf{EA}_1\mathbf{M}] = 1/2\text{tr}[\mathbf{EA}_1], \\ \text{tr}[\mathbf{EMW}_1] &= 1/2\text{tr}[\mathbf{EA}_1], \text{tr}[\mathbf{A}_1\mathbf{MW}_1] = -1/2\text{tr}[\mathbf{W}_1^2], \end{aligned} \quad (\text{G.35})$$

Table G.6: Set of Trigonal Bilinear Invariants, \mathcal{G}_9 .

| | |
|---------------------------------|--|
| Structural Tensors: | $\mathbf{A}_1 = 1/2(\mathbf{e}_3 \otimes \mathbf{P}'_3 + \mathbf{e}_3 \boxtimes \mathbf{P}'_3) : \mathbf{E}, \mathbf{W}_1 = 1/2(\mathbf{e}_3 \otimes \mathbf{P}'_3 - \mathbf{e}_3 \boxtimes \mathbf{P}'_3) : \mathbf{E}, \mathbf{M} = \mathbf{e}_3 \otimes \mathbf{e}_3 \text{ (with } \mathbf{M}^2 = \mathbf{M})$ |
| Invariants for one variable: | $\text{tr}[\mathbf{E}], \text{tr}[\mathbf{E}^2], \text{tr}[\mathbf{A}_1], \text{tr}[\mathbf{A}_1^2], \text{tr}[\mathbf{W}_1^2]$ |
| Invariants for two arguments: | $\text{tr}[\mathbf{EA}_1], \text{tr}[\mathbf{EM}], \text{tr}[\mathbf{E}^2\mathbf{M}], \text{tr}[\mathbf{A}_1\mathbf{M}], \text{tr}[\mathbf{A}_1^2\mathbf{M}], \text{tr}[\mathbf{MW}_1^2]$ |
| Invariants for three arguments: | $\text{tr}[\mathbf{EA}_1\mathbf{M}], \text{tr}[\mathbf{EMW}_1], \text{tr}[\mathbf{A}_1\mathbf{MW}_1]$ |

leads finally to the *set of bilinear invariants*

$$\mathcal{F}^{ht2}(\mathbf{E}, \mathbf{A}_1, \mathbf{M}) = \{\text{tr}[\mathbf{E}], \text{tr}[\mathbf{E}^2], \text{tr}[\mathbf{EA}_1], \text{tr}[\mathbf{EM}], \text{tr}[\mathbf{E}^2\mathbf{M}]\}, \quad (\text{G.36})$$

which is presented in terms of the components of \mathbf{E} by

$$\boxed{\mathcal{F}^{ht2}(\mathbf{E}, \mathbf{A}_1, \mathbf{M}) = \{E_{11} + E_{22} + E_{33}, E_{11}^2 + E_{22}^2 + E_{33}^2 + 2E_{12}^2 + 2E_{13}^2 + 2E_{23}^2, 2E_{12}E_{13} + E_{23}(E_{11} - E_{22}), E_{33}, E_{13}^2 + E_{23}^2 + E_{33}^2\}.$$

Following DIMITRIENKO [43] the underlying trigonal *classical set of bilinear invariants* of a symmetric second-order tensor includes also five functionally independent elements, i.e.,

$$\bar{\mathcal{F}}^{ht2} = \{E_{11} + E_{22}, E_{33}, E_{13}^2 + E_{23}^2, E_{23}(E_{11} - E_{22}) + 2E_{12}E_{13}, E_{11}^2 + E_{22}^2 + 2E_{12}^2\},$$

which can be uniquely expressed by the terms (G.36).

Quadratic Energy Function: Combining the linear invariants of the set $\mathcal{F}^{ht2}(\mathbf{E}, \mathbf{A}_1, \mathbf{M})$ to quadratic terms in \mathbf{E} yields together with the quadratic invariants of $\mathcal{F}^{ht2}(\mathbf{E}, \mathbf{A}_1, \mathbf{M})$ the set \mathcal{B}^{ht2} containing 6 quadratic elements:

$$\mathcal{B}^{ht2} := \{\text{tr}[\mathbf{E}]^2, \text{tr}[\mathbf{E}^2], \text{tr}[\mathbf{E}\mathbf{A}_1], \text{tr}[\mathbf{E}\mathbf{M}]^2, \text{tr}[\mathbf{E}]\text{tr}[\mathbf{E}\mathbf{M}], \text{tr}[\mathbf{E}^2\mathbf{M}]\}. \quad (\text{G.37})$$

The coordinate-invariant material model $\psi^{ht2}(\mathbf{E} = \frac{1}{2}(\mathbf{C} - \mathbf{1}), \mathbf{A}_1, \mathbf{M})$ characterizing the symmetry group \mathcal{G}_9 is expressible in terms of the 6 elements of the set \mathcal{B}^{ht2} :

$$\psi^{ht2}(\mathbf{C}, \mathbf{A}_1, \mathbf{M}) = \sum_{i=1}^6 \alpha_i L_i, \quad L_i \in \mathcal{B}^{ht2}. \quad (\text{G.38})$$

The classical trigonal elasticity tensor is obtained from the Voigt notation of the second derivative $\mathbb{C}^{ht2} = 4\partial_{CC}\psi^{ht2}(\mathbf{C}, \mathbf{A}_1, \mathbf{M})$, with

$$\begin{aligned} \mathbb{C}^{ht2} = & \lambda \mathbf{1} \otimes \mathbf{1} + 2\mu \mathbf{1} \boxtimes \mathbf{1} + \alpha_3 \mathbb{D} \\ & + 2\alpha_4 \mathbf{M} \otimes \mathbf{M} + \alpha_5 (\mathbf{1} \otimes \mathbf{M} + \mathbf{M} \otimes \mathbf{1}) + \alpha_6 (\mathbf{1} \boxtimes \mathbf{M} + \mathbf{M} \boxtimes \mathbf{1}), \end{aligned} \quad (\text{G.39})$$

where $\mathbb{D}_{opab} = \mathbb{P}_{opab} + \mathbb{P}_{abop}$ with $\mathbb{P} = 1/2(\mathbf{e}_3 \otimes \mathbf{P}'_3 + \mathbf{e}_3 \boxtimes \mathbf{P}'_3)$. The coefficient matrix has the well-known arrangement

$$\mathbb{C}^{(V)ht2} = \begin{bmatrix} \mathbb{C}_{1111} & \mathbb{C}_{1122} & \mathbb{C}_{1133} & 0 & \mathbb{C}_{1123} & 0 \\ & \mathbb{C}_{1111} & \mathbb{C}_{1133} & 0 & -\mathbb{C}_{1123} & 0 \\ & & \mathbb{C}_{3333} & 0 & 0 & 0 \\ & & & \frac{1}{2}(\mathbb{C}_{1111} - \mathbb{C}_{1122}) & 0 & \mathbb{C}_{1123} \\ & \text{sym.} & & & \mathbb{C}_{2323} & 0 \\ & & & & & \mathbb{C}_{2323} \end{bmatrix}.$$

The six distinct coefficients are functions in terms of the 6 independent material parameters:

$$\begin{aligned} \mathbb{C}_{1111} &= \lambda + 2\mu, & \mathbb{C}_{1122} &= \lambda, \\ \mathbb{C}_{1133} &= \lambda + \alpha_5, & \mathbb{C}_{1123} &= \frac{1}{2}\alpha_3, \\ \mathbb{C}_{3333} &= \lambda + 2\mu + 2\alpha_4 + 2\alpha_5 + 2\alpha_6, \\ \mathbb{C}_{2323} &= \mu + \frac{1}{2}\alpha_6. \end{aligned}$$

Cubic Anisotropy Group \mathcal{G}_7 :

Set of Bilinear Invariants: The cubic material symmetry group is \mathcal{G}_7 . The set of two isotropic extension functions, Table G.7, can be used to construct isotropic quadratic energy functions for the considered symmetry group. Dropping out the dependent terms

$$\text{tr}[\mathbf{A}] = \text{tr}[\mathbf{E}], \text{tr}[\mathbf{B}] = \text{tr}[\mathbf{E}^2], \text{tr}[\mathbf{E}\mathbf{A}] = \text{tr}[\mathbf{A}^2], \quad (\text{G.40})$$

in the *set of invariants* deduced from Table 4.3 gives the *set of bilinear invariants*

$$\mathcal{F}^c(\mathbf{E}, \mathbf{A}) = \{\text{tr}[\mathbf{E}], \text{tr}[\mathbf{E}^2], \text{tr}[\mathbf{A}^2]\} \quad (\text{G.41})$$

Table G.7: Set of Cubic Bilinear Invariants, \mathcal{G}_7 .

| | |
|---------------------------------------|---|
| Structural Tensors: | $\mathbf{A} = (\boldsymbol{\Theta}) : \mathbf{E}, \mathbf{B} = (\boldsymbol{\Theta}) : \mathbf{E}^2$ |
| Invariants depending on one variable: | $\text{tr}[\mathbf{E}], \text{tr}[\mathbf{E}^2], \text{tr}[\mathbf{A}], \text{tr}[\mathbf{A}^2], \text{tr}[\mathbf{B}]$ |
| Invariants for two arguments: | $\text{tr}[\mathbf{E}\mathbf{A}]$ |

and with respect to the components of \mathbf{E}

$$\mathcal{F}^c(\mathbf{E}, \mathbf{A}) = \{E_{11} + E_{22} + E_{33}, E_{11}^2 + E_{22}^2 + E_{33}^2 + 2E_{12}^2 + 2E_{13}^2 + 2E_{23}^2, E_{11}^2 + E_{22}^2 + E_{33}^2\}. \quad (\text{G.42})$$

In DIMITRIENKO [43] one can find the cubic *classical set of bilinear invariants*:

$$\bar{\mathcal{F}}^c = \{E_{11} + E_{22} + E_{33}, E_{11}^2 + E_{22}^2 + E_{33}^2, E_{12}^2 + E_{13}^2 + E_{23}^2\}. \quad (\text{G.43})$$

All three elements appearing in (G.42) can be obtained explicitly by specific combinations of the three terms of (G.43).

Quadratic Energy Function: The set of all quadratic and multiplicatively combined linear invariants of $\mathcal{F}^c(\mathbf{E}, \mathbf{A})$ consists of 3 linearly independent elements:

$$\mathcal{B}^c := \{\text{tr}[\mathbf{E}]^2, \text{tr}[\mathbf{E}^2], \text{tr}[\mathbf{A}^2]\}. \quad (\text{G.44})$$

These invariant functions finally serve as a possible set for the construction of the isotropic quadratic function $\psi^c(\mathbf{E} = \frac{1}{2}(\mathbf{C} - \mathbf{1}), \mathbf{A})$ for \mathcal{G}_7 -symmetry:

$$\psi^c(\mathbf{C}, \mathbf{A}) = \sum_{i=1}^3 \alpha_i L_i, \quad L_i \in \mathcal{B}^c. \quad (\text{G.45})$$

The second derivative of the quadratic function $\mathbb{C}^c = 4\partial_{CC}\psi(\mathbf{C}, \mathbf{A})$, with

$$\mathbb{C}^c = \lambda \mathbf{1} \otimes \mathbf{1} + 2\mu \mathbf{1} \boxtimes \mathbf{1} + 2\alpha_3 \boldsymbol{\Theta}, \quad (\text{G.46})$$

leads in Voigt notation to the well-known cubic elasticity tensor

$$\mathbb{C}^{(V)c} = \begin{bmatrix} \mathbb{C}_{1111} & \mathbb{C}_{1122} & \mathbb{C}_{1122} & 0 & 0 & 0 \\ & \mathbb{C}_{1111} & \mathbb{C}_{1122} & 0 & 0 & 0 \\ & & \mathbb{C}_{1111} & 0 & 0 & 0 \\ & & & \mathbb{C}_{1212} & 0 & 0 \\ sym. & & & & \mathbb{C}_{1212} & 0 \\ & & & & & \mathbb{C}_{1212} \end{bmatrix}, \quad (\text{G.47})$$

with the coefficients in terms of the three independent material parameters

$$\begin{aligned} \mathbb{C}_{1111} &= \lambda + 2\mu + 2\alpha_3, & \mathbb{C}_{1122} &= \lambda, \\ \mathbb{C}_{1212} &= \mu. \end{aligned}$$

H Further Proofs of Polyconvexity and Ellipticity .

Tetragonal Sets of Bilinear Invariants. Let us investigate further mixed bilinear invariants of the form

$$I_6 = \mathbf{1} : \mathbb{P} : \mathbf{C}, \quad I_7 = \mathbf{1} : \mathbb{P} : \mathbf{C}^2, \quad I_{10} = \mathbf{1} : [\mathbf{C}(\mathbb{P} : \mathbf{C})\mathbf{W}]$$

in terms of Xiao's tetragonal structural tensor $\mathbb{P} = \mathbf{e}_1^{(4)} + \mathbf{e}_2^{(4)}$. I_6, I_7, I_{10} are needed for the construction of quadratic tetragonal \mathcal{G}_4 -invariant energies; I_6, I_7 for \mathcal{G}_5 -invariant energy functions (cf. APEL [3]). The invariant I_6 appears as

$$I_6 = \mathbf{1} : \mathbb{P} : \mathbf{C} = \sum_{i=1}^2 \text{tr}[\mathbf{e}_i \otimes \mathbf{e}_i] \text{tr}[\mathbf{C}(\mathbf{e}_i \otimes \mathbf{e}_i)],$$

which is polyconvex, since the individual functions are convex w.r.t. \mathbf{F} , see (5.51). The mixed invariant I_7 has the form

$$I_7 = \mathbf{1} : \mathbb{P} : \mathbf{C}^2 = \sum_{i=1}^2 \text{tr}[\mathbf{e}_i \otimes \mathbf{e}_i] \text{tr}[\mathbf{C}^2(\mathbf{e}_i \otimes \mathbf{e}_i)].$$

The non-ellipticity of the individual terms of the latter invariant is proven in SCHRÖDER & NEFF [104], see also the part **ii.a** of section 5.7.1. But, instead of I_7 the polyconvex function

$$K_7 = \mathbf{1} : \mathbb{P} : \text{Cof} \mathbf{C} = \sum_{i=1}^2 \text{tr}[\mathbf{e}_i \otimes \mathbf{e}_i] \text{tr}[\text{Cof}[\mathbf{C}](\mathbf{e}_i \otimes \mathbf{e}_i)],$$

can be alternatively used. However, the term I_{10}

$$I_{10} = \mathbf{1} : [\mathbf{C}(\mathbb{P} : \mathbf{C})\mathbf{W}] = \sum_{i=1}^2 \langle \mathbf{F}^T \mathbf{F} \mathbf{W}^T, \mathbf{e}_i \otimes \mathbf{e}_i \rangle \|\mathbf{F} \mathbf{e}_i\|^2,$$

with $\mathbf{W} = \mathbf{W}_3 = \epsilon \mathbf{e}_3$ is not elliptic and hence not polyconvex.

Proof We obtain

$$\begin{aligned} P(\mathbf{F}) &= \sum_{i=1}^2 \langle \mathbf{F}^T \mathbf{F} \mathbf{W}^T, \mathbf{e}_i \otimes \mathbf{e}_i \rangle \|\mathbf{F} \mathbf{e}_i\|^2 \\ \delta \mathbf{F} : \partial_{\mathbf{F} \mathbf{F}}^2 P(\mathbf{F}) : \delta \mathbf{F} &= \sum_{i=1}^2 \left[2 \langle \delta \mathbf{F}^T \delta \mathbf{F} \mathbf{W}^T, \mathbf{e}_i \otimes \mathbf{e}_i \rangle \|\mathbf{F} \mathbf{e}_i\|^2 + 2 \langle \mathbf{F}^T \mathbf{F} \mathbf{W}^T, \mathbf{e}_i \otimes \mathbf{e}_i \rangle \|\delta \mathbf{F} \mathbf{e}_i\|^2 \right. \\ &\quad \left. + 4 (\langle \delta \mathbf{F}^T \mathbf{F} \mathbf{W}^T, \mathbf{e}_i \otimes \mathbf{e}_i \rangle + \langle \mathbf{F}^T \delta \mathbf{F} \mathbf{W}^T, \mathbf{e}_i \otimes \mathbf{e}_i \rangle) \langle \delta \mathbf{F}^T \mathbf{e}_i, \mathbf{F} \mathbf{e}_i \rangle \right]. \end{aligned}$$

Setting

$$\mathbf{F} = \begin{bmatrix} 2 & -1 & 0 \\ 0 & 1 & 0 \\ 0 & 0 & 1 \end{bmatrix}, \quad \boldsymbol{\eta} = \begin{pmatrix} 1 \\ -1 \\ 0 \end{pmatrix}, \quad \boldsymbol{\zeta} = \begin{pmatrix} 1 \\ 0 \\ 0 \end{pmatrix}, \quad \delta \mathbf{F} = \boldsymbol{\eta} \otimes \boldsymbol{\zeta}$$

the second derivative is negative, i.e.,

$$\delta \mathbf{F} : \partial_{\mathbf{F} \mathbf{F}}^2 P(\mathbf{F}) : \delta \mathbf{F} = -24 < 0,$$

which excludes the ellipticity and therefore the polyconvexity of I_{10} .

I Table of Crystallographically Motivated Structural Tensors.

| Triclinic system, group \mathcal{G}_1 : | |
|--|--|
| $\mathbf{a}_1 = (a, 0, 0)^T, \quad \mathbf{a}_2 = (b \cos \gamma, b \sin \gamma, 0)^T, \quad \mathbf{a}_3 = (c \cos \beta, X, Y)^T$ | |
| $\mathbf{G}^a = \begin{bmatrix} \tilde{a} & \tilde{d} & \tilde{e} \\ \tilde{d} & \tilde{b} & \tilde{f} \\ \tilde{e} & \tilde{f} & \tilde{c} \end{bmatrix},$ | |
| with $\tilde{a} = a^2 + b^2 \cos^2 \gamma + c^2 \cos^2 \beta$ | |
| $\tilde{b} = b^2 \sin^2 \gamma + \frac{c^2 (\cos \alpha - \cos \beta \cos \gamma)^2}{\sin^2 \gamma}$ | |
| $\tilde{c} = \frac{c^2 (1 + 2 \cos \alpha \cos \beta \cos \gamma - \cos^2 \alpha - \cos^2 \beta - \cos^2 \gamma)}{\sin^2 \gamma}$ | |
| $\tilde{d} = b^2 \cos \gamma \sin \gamma + \frac{c^2 \cos \beta (\cos \alpha - \cos \beta \cos \gamma)}{\sin \gamma}$ | |
| $\tilde{e} = \frac{c^2 \cos \beta (1 + 2 \cos \alpha \cos \beta \cos \gamma - \cos^2 \alpha - \cos^2 \beta - \cos^2 \gamma)^{1/2}}{\sin \gamma}$ | |
| $\tilde{f} = \frac{c^2 (\cos \alpha - \cos \beta \cos \gamma)}{\sin \gamma}$ | |
| $X = c (\cos \alpha - \cos \beta \cos \gamma) / \sin \gamma$ | |
| $Y = c [1 + 2 \cos \alpha \cos \beta \cos \gamma - (\cos^2 \alpha + \cos^2 \beta + \cos^2 \gamma)]^{1/2} / \sin \gamma$ | |
| Monoclinic system, group \mathcal{G}_2 : | |
| $\mathbf{a}_1 = (a, 0, 0)^T, \quad \mathbf{a}_2 = (b \cos \gamma, b \sin \gamma, 0)^T, \quad \mathbf{a}_3 = (0, 0, c)^T$ | |
| $\mathbf{G}^m = \begin{bmatrix} a^2 + b^2 \cos^2 \gamma & b^2 \cos \gamma \sin \gamma & 0 \\ b^2 \cos \gamma \sin \gamma & b^2 \sin^2 \gamma & 0 \\ 0 & 0 & c^2 \end{bmatrix}$ | |
| Rhombic system, group \mathcal{G}_3 : | |
| $\mathbf{a}_1 = (a, 0, 0)^T, \quad \mathbf{a}_2 = (0, b, 0)^T, \quad \mathbf{a}_3 = (0, 0, c)^T$ | |
| $\mathbf{G}^o = \begin{bmatrix} a^2 & 0 & 0 \\ 0 & b^2 & 0 \\ 0 & 0 & c^2 \end{bmatrix}$ | |

| | |
|---|--|
| Tetragonal system, group \mathcal{G}_4 : | |
| $\mathbf{a}_1 = (\tilde{a}, \tilde{b}, 0)^T, \quad \mathbf{a}_2 = (-\tilde{b}, \tilde{a}, 0)^T, \quad \mathbf{a}_3 = (0, 0, \tilde{c})^T$ | |
| $\mathbb{G}^{t1} =$ | $\begin{bmatrix} \tilde{a}^4 + \tilde{b}^4 & 2\tilde{a}^2\tilde{b}^2 & 0 & \tilde{a}^3\tilde{b} - \tilde{b}^3\tilde{a} & 0 & 0 \\ & \tilde{a}^4 + \tilde{b}^4 & 0 & \tilde{b}^3\tilde{a} - \tilde{a}^3\tilde{b} & 0 & 0 \\ & & \tilde{c}^4 & 0 & 0 & 0 \\ & sym. & & 2\tilde{a}^2\tilde{b}^2 & 0 & 0 \\ & & & & 0 & 0 \\ & & & & & 0 \end{bmatrix}$ |
| Tetragonal system, group \mathcal{G}_5 : | |
| $\mathbf{a}_1 = (a, 0, 0)^T, \quad \mathbf{a}_2 = (0, a, 0)^T, \quad \mathbf{a}_3 = (0, 0, c)^T$ | |
| $\mathbb{G}^{t2} = \text{diag}[a^4, a^4, c^4, 0, 0, 0]$ | |
| Trigonal system, group \mathcal{G}_8 : | |
| $\mathbf{a}_1 = \begin{pmatrix} \frac{\tilde{a}}{\sqrt{3}} \\ -\frac{\tilde{b}}{\sqrt{3}} \\ \frac{\tilde{c}}{3} \end{pmatrix}, \quad \mathbf{a}_2 = \begin{pmatrix} -\frac{\tilde{a}}{2\sqrt{3}} + \frac{\tilde{b}}{2} \\ \frac{\tilde{b}}{2\sqrt{3}} + \frac{\tilde{a}}{2} \\ \frac{\tilde{c}}{3} \end{pmatrix}, \quad \mathbf{a}_3 = \begin{pmatrix} -\frac{\tilde{a}}{2\sqrt{3}} - \frac{\tilde{b}}{2} \\ \frac{\tilde{b}}{2\sqrt{3}} - \frac{\tilde{a}}{2} \\ \frac{\tilde{c}}{3} \end{pmatrix}$ | |
| $\mathbb{G}^{ht1} =$ | $\begin{bmatrix} \frac{1}{8} C^2 & \frac{1}{24} C^2 & \frac{1}{18} C \tilde{c}^2 & 0 & A & B \\ & \frac{1}{8} C^2 & \frac{1}{18} C \tilde{c}^2 & 0 & -A & -B \\ & & \frac{1}{27} \tilde{c}^4 & 0 & 0 & 0 \\ & sym. & & \frac{1}{24} C^2 & -B & A \\ & & & & \frac{1}{18} C \tilde{c}^2 & 0 \\ & & & & & \frac{1}{18} C \tilde{c}^2 \end{bmatrix}$ |
| with $A = -\frac{1}{4\sqrt{3}}\tilde{a}^2\tilde{b}\tilde{c} + \frac{1}{12\sqrt{3}}\tilde{b}^3\tilde{c}, \quad B = -\frac{1}{4\sqrt{3}}\tilde{a}\tilde{b}^2\tilde{c} + \frac{1}{12\sqrt{3}}\tilde{a}^3\tilde{c}, \quad C = \tilde{a}^2 + \tilde{b}^2$ | |
| Trigonal system, group \mathcal{G}_9 : | |
| $\mathbf{a}_1 = (0, -\tilde{b}/\sqrt{3}, \tilde{c}/3)^T, \quad \mathbf{a}_2 = (\tilde{b}/2, \tilde{b}/(2\sqrt{3}), \tilde{c}/3)^T, \quad \mathbf{a}_3 = (-\tilde{b}/2, \tilde{b}/(2\sqrt{3}), \tilde{c}/3)^T$ | |
| $\mathbb{G}^{ht2} =$ | $\begin{bmatrix} \frac{1}{8} \tilde{b}^4 & \frac{1}{24} \tilde{b}^4 & \frac{1}{18} \tilde{b}^2 \tilde{c}^2 & 0 & \frac{1}{12\sqrt{3}} \tilde{b}^3 \tilde{c} & 0 \\ & \frac{1}{8} \tilde{b}^4 & \frac{1}{18} \tilde{b}^2 \tilde{c}^2 & 0 & -\frac{1}{12\sqrt{3}} \tilde{b}^3 \tilde{c} & 0 \\ & & \frac{1}{27} \tilde{c}^4 & 0 & 0 & 0 \\ & sym. & & \frac{1}{24} \tilde{b}^4 & 0 & \frac{1}{12\sqrt{3}} \tilde{b}^3 \tilde{c} \\ & & & & \frac{1}{18} \tilde{b}^2 \tilde{c}^2 & 0 \\ & & & & & \frac{1}{18} \tilde{b}^2 \tilde{c}^2 \end{bmatrix}$ |
| Cubic system, group \mathcal{G}_7 : | |
| $\mathbf{a}_1 = (a, 0, 0)^T, \quad \mathbf{a}_2 = (0, a, 0)^T, \quad \mathbf{a}_3 = (0, 0, a)^T$ | |
| $\mathbb{G}^c = \text{diag}[a^4, a^4, a^4, 0, 0, 0]$ | |

List of Figures

| | | |
|------|---|----|
| 2.1 | Representations of reference and actual configuration and corresponding geometric mappings (transport theorems). | 4 |
| 2.2 | Coaxiality of the traction vectors $\mathbf{t} \in \partial\mathcal{B}_t$ and $\mathbf{T} \in \partial\mathcal{B}_0$ | 9 |
| 2.3 | Heat flux Q_0 and q with respect to the reference and current placement. . . | 10 |
| 2.4 | Rigid body motion of the actual configuration. | 17 |
| 2.5 | Orthogonal Transformations of the reference configuration. | 18 |
| 2.6 | Characterization of isotropic elastic material behavior: a) reference configuration, b) deformed configuration: (left) with principal directions $\mathbf{n}_{C1}, \mathbf{n}_{C2}$ of deformation \mathbf{C} , (right) with principal directions $\mathbf{n}_{S1}, \mathbf{n}_{S2}$ of the stresses \mathbf{S} , which are coaxial to $\mathbf{n}_{C1}, \mathbf{n}_{C2}$ | 19 |
| 2.7 | Characterization of anisotropic elastic material behavior: a) reference configuration, b) deformed configuration: (left) with principal directions $\mathbf{n}_{C1}, \mathbf{n}_{C2}$ of deformation \mathbf{C} , (right) with principal directions $\mathbf{n}_{S1}, \mathbf{n}_{S2}$ of the stresses \mathbf{S} , which are non-coaxial to $\mathbf{n}_{C1}, \mathbf{n}_{C2}$ | 19 |
| 2.8 | Illustration of a ten-noded tetrahedral finite element in the parametrized space Ω^e and reference configuration \mathcal{B}_0^e | 23 |
| 3.1 | Example of crystal structure. | 29 |
| 3.2 | Space lattice: a) Unit cell with base vectors $\mathbf{a}_1, \mathbf{a}_2, \mathbf{a}_3$, axial angles α, β, γ and axes a_1, a_2, a_3 , b) Grid line $[112], [231]$, c) Grid plane $(111), (211)$. . . | 29 |
| 3.3 | 2,3,4,6-fold rotation axes and below the corresponding stereographic projections. | 31 |
| 3.4 | $\bar{2}, \bar{1}, \bar{3}, \bar{4}, \bar{6}$ -fold rotoinversion axes and below the corresponding stereographic projections. | 31 |
| 3.5 | Rotations about the X_1 -, X_2 - and X_3 -axis, see DE BOER & SCHRÖDER [42]. | 32 |
| 3.6 | Triclinic Bravais lattice, (P) Primitive cell: $a \neq b \neq c, \alpha \neq \beta \neq \gamma \neq 90^\circ$. . . | 33 |
| 3.7 | Monoclinic Bravais lattice, (P) Primitive and (C) centered cell: $a \neq b \neq c, \gamma \neq \alpha = \beta = 90^\circ$ | 33 |
| 3.8 | Rhombic Bravais lattice, (P) Primitive cell, (C) centered cell, (I) body-centered cell, (F) face-centered cell: $a \neq b \neq c, \gamma = \alpha = \beta = 90^\circ$ | 34 |
| 3.9 | Tetragonal Bravais lattice, (P) Primitive cell, (I) body-centered cell: $a = b \neq c, \gamma = \alpha = \beta = 90^\circ$ | 34 |
| 3.10 | Cubic Bravais lattice, (P) Primitive, (I) body-centered, (F) face-centered cell: $a = b = c, \gamma = \alpha = \beta = 90^\circ$ | 34 |
| 3.11 | Hexagonal Bravais lattice, (P) Primitive cell: $a = b \neq c, \gamma = 120^\circ, \alpha = \beta = 90^\circ$ | 35 |
| 3.12 | Hexagonal lattice with four base vectors: $\mathbf{a}_h, \mathbf{b}_h, \mathbf{c}_h$ and the redundant base vector $\mathbf{d}_h = -\mathbf{a}_h - \mathbf{b}_h$ | 35 |

| | | |
|------|---|-----|
| 3.13 | Trigonal Bravais lattice, (P) Primitive trigonal cell: $a = b = c, \alpha = \beta = \gamma$. | 35 |
| 3.14 | Point group symmetry elements (left) and corresponding crystal structure (right) for: a) point group $2/m$, b) point group 2. | 36 |
| 3.15 | Orientation of crystals in space I, left: general form with crystallographical axes, center: cross-section perpendicular to a_3 -axis, right: stereographic projection. | 39 |
| 3.16 | Orientation of crystals in space II, left: general form with crystallographical axes, center: cross-section perpendicular to a_3 -axis, right: stereographic projection. | 40 |
| 3.17 | Visualization of the spherical point groups. a) $SO(3)$, b) $O(3)$ | 40 |
| 3.18 | Visualization of the cylindrical point groups. a) \mathcal{C}_∞ , b) $\mathcal{C}_{\infty h}$, c) \mathcal{D}_∞ , d) $\mathcal{C}_{\infty v}$, e) $\mathcal{D}_{\infty h}$ | 41 |
| 4.1 | Principle of Isotropy of Space: a) the eigenvectors $\mathbf{n}_{C1}, \mathbf{n}_{C2}$ of the deformation \mathbf{C} and the eigenvectors $\mathbf{n}_{S1}, \mathbf{n}_{S2}$ of the stresses \mathbf{S} , respectively, w.r.t. the initial basis $\mathbf{a}_1, \mathbf{a}_2$, b) the same eigenvectors of \mathbf{C} and \mathbf{S} , respectively, w.r.t. the transformed basis $\mathbf{Qa}_1, \mathbf{Qa}_2$ | 53 |
| 4.2 | a) Homogeneous biaxial compression/tension test, b) Characteristic surface of transversely isotropic elasticities. | 67 |
| 4.3 | Values of first Piola-Kirchhoff stresses in X_2 -and X_3 -directions in $[\text{N}/\text{mm}^2]$ | 68 |
| 5.1 | Relations between principal stresses and stretches, a) of an isotropic material, b) of an transversely isotropic material with preferred direction \mathbf{a} | 71 |
| 5.2 | Two-dimensional convex and non-convex set. | 73 |
| 5.3 | One-dimensional convex and non-convex function. | 73 |
| 5.4 | a) Convex and b) strictly convex function. | 74 |
| 5.5 | Illustration of strict convexity of $\psi(\mathbf{F})$ | 74 |
| 5.6 | a) Non-convex function ψ ((5.18) with $\alpha = 1$) describing quasi-incompressibility of a typical rubber sheet in a homogeneous deformation, b) projection of ψ to the $\lambda_1 - \lambda_2$ - plane. | 75 |
| 5.8 | Rank-one convex function $\psi(\mathbf{F})$ | 80 |
| 5.9 | Monotonicity of \mathbf{P} with respect to all rank-one deformation tensors $\boldsymbol{\eta} \otimes \boldsymbol{\zeta}$ | 80 |
| 5.10 | Implications of generalized convexity conditions, s.w.l.s. and existence of minimizers. | 82 |
| 5.11 | a) Characteristic surface of isotropic elasticities, b) Values of first Piola-Kirchhoff stresses in x_1 -direction. | 96 |
| 5.12 | Non-convex function $f(n)$ | 99 |
| 6.1 | Push-forward operation \mathbf{G} | 104 |
| 6.2 | Possible orientations of the crystallographical base system $\mathbf{a}_1, \mathbf{a}_2, \mathbf{a}_3$ of the lattice and the base system $\mathbf{c}_1, \mathbf{c}_2, \mathbf{c}_3$ of the morphology (geometry of the outer structure) of the crystal: a) coincidence, b) relative orientation described by the angle φ | 105 |

| | | |
|------|--|-----|
| 6.3 | Triclinic Crystal \mathcal{C}_i . | 106 |
| 6.4 | Monoclinic Crystal \mathcal{C}_{2h} . | 107 |
| 6.5 | Rhombic Crystal \mathcal{D}_{2h} . | 108 |
| 6.6 | Tetragonal Crystals, a) \mathcal{C}_{4h} , b) \mathcal{D}_{4h} . | 109 |
| 6.7 | Trigonal Crystal \mathcal{C}_{3i} . | 110 |
| 6.8 | Trigonal Crystal \mathcal{D}_{3d} . | 111 |
| 6.9 | Cubic Crystal \mathcal{O}_h . | 112 |
| 7.1 | Boundary conditions of the homogeneous biaxial compression/tension test. | 129 |
| 7.2 | First Piola-Kirchhoff stresses in x_1 -direction and x_2 -direction versus stretch λ : a) $\psi_{I,1}^{ti}$, b) $\psi_{I,2}^{ti}$, c) $\psi_{II,1}^{ti}$, d) $\psi_{II,2}^{ti}$. | 131 |
| 7.3 | Tapered cantilever. System and boundary conditions. | 131 |
| 7.4 | Tapered cantilever. Different views on a) the undeformed system, deformed system at b) $\lambda = 0.50$ and c) $\lambda = 1.00$, cf. SCHRÖDER [101]. | 132 |
| 7.5 | Aegirite: a) Characteristic surface of Young's moduli, b) $\mathbb{C}^{(V)e}$ and $\mathbb{C}^{(V)c}$ in [GPa]. | 135 |
| 7.6 | Aragonite: a) Characteristic surface of Young's moduli, b) $\mathbb{C}^{(V)e}$ and $\mathbb{C}^{(V)c}$ in [GPa]. | 136 |
| 7.7 | Rhenium: a) Characteristic surface of Young's moduli, b) $\mathbb{C}^{(V)e}$ and $\mathbb{C}^{(V)c}$ in [GPa]. | 137 |
| 7.8 | Calcium molybdate: a) Characteristic surface of Young's moduli, b) $\mathbb{C}^{(V)e}$ and $\mathbb{C}^{(V)c}$ in [GPa]. | 138 |
| 7.9 | Indium: a) Characteristic surface of Young's moduli, b) $\mathbb{C}^{(V)e}$, $\mathbb{C}^{(V)c}$ in [GPa]. | 139 |
| 7.10 | Lithium niobate: a) Characteristic surface of Young's moduli, b) $\mathbb{C}^{(V)e}$ and $\mathbb{C}^{(V)c}$ in [GPa]. | 141 |
| 7.11 | Aluminium: a) Characteristic surface of Young's moduli, b) $\mathbb{C}^{(V)e}$ and $\mathbb{C}^{(V)c}$ in [GPa]. | 142 |
| 7.12 | a) Cuticle of <i>Homarus americanus</i> , b) Structure of single crystalline α -chitin with crystallographic base vectors $\mathbf{a}_1, \mathbf{a}_2, \mathbf{a}_3$ taken from [86]. | 143 |
| 7.13 | Cuticle of American Lobster: a) Characteristic surface of Young's moduli, b) $\mathbb{C}^{(V)e}$ and $\mathbb{C}^{(V)c}$ in [GPa]. | 144 |
| 7.14 | Lightweight constructions: a) Olympia Stadium, Berlin, b) Nelson Mandela Bay Stadium, Port Elizabeth, South Africa. | 145 |
| 7.15 | a) Machine for biaxial tension tests. b) Load-strain behavior of a PVC-Polyester composite. | 145 |
| 7.16 | Microstructure of a woven fiber composite: a) fibers in fill and warp direction, b) cross-sections perpendicular to the warp direction (left) and to the fill direction right. | 146 |
| 7.17 | Biaxial tension test of microstructure: a) Boundary conditions, b) FE-Discretization. | 147 |

| | | |
|------|--|-----|
| 7.18 | Fitting of macroscopic model: First Piola-Kirchhoff-stresses P_{33} (left curve) and P_{11} (right curve) vs. stretches $\lambda_3 = 1 + u_3/L$ and $\lambda_1 = 1 + u_1/L$, respectively. | 147 |
| 7.19 | Distribution of Cauchy stresses in x_3 -direction (σ_{33}) at different stretch states. | 148 |
| 7.20 | Quadrilateral shell element. | 149 |
| 7.21 | Thin hexagonal plate: a) System with boundary conditions, b) discretization with 800 four-noded shell elements, c) first and d) second type of orientation of the preferred direction \mathbf{a}_1 | 151 |
| 7.22 | Contour plot of the vertical displacements for the isotropic i) and anisotropic ii+iii) plates. | 152 |
| 7.23 | Hyperbolic shell: a) schematic sketch of the system with boundary conditions, b) discretization with 4608 four-node shell elements, c) orientation of fiber direction \mathbf{a}_1 of the transversely isotropic shell and d) orientation of fiber directions \mathbf{a}_1 and \mathbf{a}_2 of the monoclinic shell. | 153 |
| 7.24 | Different deformation states (from the left to the right: from the undeformed to the completely deformed state) for the a) isotropic, b) transversely isotropic and c) monoclinic shell. | 155 |
| 7.25 | Configurational Mechanics: two parametrizations of the same reference configuration \mathcal{B}_0 | 157 |
| 7.26 | Undeformed SET specimen, boundary conditions. | 162 |
| 7.27 | Undeformed SET specimen, discretization with 7886 6-noded triangle elements. | 162 |
| 7.28 | Angle η versus angle φ . Ratios of norms of material forces. | 163 |
| 7.29 | Angle of configurational force η versus angle of preferred direction φ , [°]. | 163 |

List of Tables

| | | |
|------|--|-----|
| 3.1 | The seven crystal systems. | 33 |
| 3.2 | Herrmann-Maugin and Schoenflies Notations | 37 |
| 3.3 | Multiplication Table, $\mathbf{Q} = \mathbf{Q}_{X_3}^{2\pi/3}$ | 38 |
| 3.4 | Point Group Symbols I: 32 Crystal Classes. | 46 |
| 3.5 | Point Group Symbols II: 32 Crystal Classes. | 47 |
| 3.6 | Point Group Symbols III: Non-Crystal Classes. | 47 |
| 4.1 | Invariants Depending on One Tensor-Valued Variable. | 52 |
| 4.2 | Structural Tensors which Characterize Material Symmetry Groups. | 55 |
| 4.3 | Invariants Depending on Two, Three or Four Tensor-Valued Variables ($\mathbf{A} \in \text{Sym}(3)$, $\mathbf{W} \in \text{Skew}(3)$), cf. BOEHLER [30]. | 57 |
| 4.4 | Set of Bilinear Invariants, \mathcal{G}_{12} | 66 |
| 4.5 | Set of Bilinear Invariants, \mathcal{G}_4 | 69 |
| 6.1 | Polyconvex Anisotropic Energy Functions Satisfying the Stress-Free Reference Configuration Condition. | 125 |
| 7.1 | Table of material parameters (MP) and Young's moduli (YM). | 130 |
| 7.2 | Material parameter set of Aegirite | 135 |
| 7.3 | Material parameter set of Aragonite | 136 |
| 7.4 | Material parameter set of Rhenium | 137 |
| 7.5 | Material parameter set of Calcium molybdate | 138 |
| 7.6 | Material parameter set of Indium | 139 |
| 7.7 | Material parameter set 1 of Lithium niobate | 141 |
| 7.8 | Material parameter set 2 of Lithium niobate | 141 |
| 7.9 | Material parameter set 1 of Aluminium | 142 |
| 7.10 | Material parameter set 2 of Aluminium | 143 |
| 7.11 | Material parameter set of American Lobster | 144 |
| 7.12 | Material Parameter Sets. | 147 |
| G.1 | Set of Triclinic Bilinear Invariants. | 175 |
| G.2 | Set of Monoclinic Bilinear Invariants. | 178 |
| G.3 | Set of Rhombic Bilinear Invariants. | 180 |
| G.4 | Set of Tetragonal Bilinear Invariants, \mathcal{G}_5 | 181 |
| G.5 | Set of Trigonal Bilinear Invariants, \mathcal{G}_9 | 184 |
| G.6 | Set of Trigonal Bilinear Invariants, \mathcal{G}_9 | 185 |
| G.7 | Set of Cubic Bilinear Invariants, \mathcal{G}_7 | 187 |

References

- [1] D. Ackermann, F. J. Barth, and P. Steinmann. Theoretical and computational aspects of geometrically nonlinear problems in fracture mechanics. In *Proceedings of the European Conference on Computational Mechanics*, volume 385, Munich, 1999.
- [2] S.S. Antman. The influence of elasticity on analysis: Modern developments. *Bulletin of the American Mathematical Society*, 9:267–291, 1983.
- [3] N. Apel. *Approaches to the description of anisotropic material behaviour at finite elastic and plastic deformations - Theory and numerics*. Bericht I-12 (2004), Institut für Mechanik (Bauwesen), Lehrstuhl I, Prof. Dr.-Ing. C. Miehe, Universität Stuttgart, 2004.
- [4] Y. Başar and Y. Ding. Shear deformation models for large-strain shell analysis. *International Journal of Solids and Structures*, 34:1687–1708, 1997.
- [5] Y. Başar and R. Grytz. Incompressibility at large strains and finite-element implementation. *Acta Mechanica*, 168:75–101, 2004.
- [6] Y. Başar and D. Weichert. *Nonlinear continuum mechanics of solids*. Springer-Verlag, Berlin, 2000.
- [7] M. Baker and J. L. Ericksen. Inequalities restricting the form of the stress-deformation relations for isotropic elastic solids and Reiner-Rivlin fluids. *Journal of the Washington Academy of Sciences*, 44:33–35, 1954.
- [8] J. M. Ball. Convexity conditions and existence theorems in non-linear elasticity. *Archive for Rational Mechanics and Analysis*, 63:337–403, 1976.
- [9] J. M. Ball. Constitutive inequalities and existence theorems in nonlinear elastostatics. In R. J. Knops, editor, *Herriot Watt Symposion: Nonlinear Analysis and Mechanics*, volume 1, pages 187–241. Pitman, London, 1977.
- [10] J.M. Ball. Some open problems in elasticity. In *Geometry, Mechanics and Dynamics*, pages 3–59. Springer, New York, 2002.
- [11] D. Balzani. *Polyconvex anisotropic energies and modeling of damage applied to arterial walls*. PhD thesis, Institut für Mechanik, Abteilung Bauwissenschaften, Fakultät für Ingenieurwissenschaften, Universität Duisburg-Essen, 2006.
- [12] D. Balzani, F. Gruttmann, and J. Schröder. Analysis of thin shells using anisotropic polyconvex energy densities. *Computer Methods in Applied Mechanics and Engineering*, 197:1015–1032, 2008.
- [13] D. Balzani, J. Schröder, and P. Neff. Applications of anisotropic polyconvex energies: thin shells and biomechanics of arterial walls. In J. Schröder and P. Neff, editors, *Poly-, quasi- and rank-one convexity in applied mechanics*, volume 516 of *CISM Courses and Lectures*, pages 131–176. Springer, 2010.
- [14] K. J. Bathe. *Finite Elemente Methoden*. Springer, 1986.

- [15] L. Bergmann and C. Schäfer. *Lehrbuch der Experimentalphysik Band 6*, chapter Kristallstrukturen, pages 109–137. de Gruyter, 1997.
- [16] A. Bertram, T. Böhlke, and M. Silhavy. On the rank 1 convexity of stored energy functions of physically linear stress-strain relations. *Journal of Elasticity*, 86:235–243, 2007.
- [17] P. Betsch, F. Gruttmann, and E. Stein. A 4-node finite shell element for the implementation of general hyperelastic 3D-elasticity at finite strains. *Computer Methods in Applied Mechanics and Engineering*, 130:57–79, 1996.
- [18] J. Betten. Integrity basis for a second-order and a fourth-order tensor. *International Journal of Mathematics and Mathematical Sciences*, 5(1):87–96, 1982.
- [19] J. Betten. Invariants of fourth-order tensors. In J. P. Boehler, editor, *Applications of tensor functions in solid mechanics*, volume 292 of *CISM Courses and Lectures*, pages 203–221. Springer, 1987.
- [20] J. Betten. *Tensorrechnung für Ingenieure*. Teubner-Verlag, Stuttgart, 1987.
- [21] J. Betten. Recent advances in applications of tensor functions in solid mechanics. *Advances in Mechanics*, 14(1):79–109, 1991.
- [22] J. Betten. Anwendungen von Tensorfunktionen in der Kontinuumsmechanik anisotroper Materialien. *Zeitschrift für Angewandte Mathematik und Mechanik*, 78(8):507–521, 1998.
- [23] J. Betten and W. Helisch. Irreduzible Invarianten eines Tensors vierter Stufe. *Zeitschrift für Angewandte Mathematik und Mechanik*, 72(1):45–57, 1992.
- [24] J. Betten and W. Helisch. Simultaninvarianten bei Systemen zwei- und vierstufiger Tensoren. *Zeitschrift für Angewandte Mathematik und Mechanik*, 75:753–759, 1995.
- [25] J. Betten and W. Helisch. Tensorgeneratoren bei Systemen von Tensoren zweiter und vierter Stufe. *Zeitschrift für Angewandte Mathematik und Mechanik*, 76(2):87–92, 1996.
- [26] P. J. Blatz. On the thermodynamic behavior of elastomers. In *Polymer Networks, Structure and Mechanical Properties*, pages 23–45. Plenum Press, New York, 1971.
- [27] J. P. Boehler. On irreducible representations for isotropic scalar functions. *Zeitschrift für Angewandte Mathematik und Mechanik*, 57:323–327, 1977.
- [28] J. P. Boehler. Lois de comportement anisotrope des milieux continus. *Journal de Mécanique*, 17(2):153–190, 1978.
- [29] J. P. Boehler. A simple derivation of representations for non-polynomial constitutive equations in some cases of anisotropy. *Zeitschrift für Angewandte Mathematik und Mechanik*, 59:157–167, 1979.
- [30] J. P. Boehler, editor. *Application of tensor functions in solid mechanics*, volume 292 of *CISM courses and lectures*. Springer-Verlag, Wien, 1987.

- [31] J. P. Boehler. Introduction to the invariant formulation of anisotropic constitutive equations. In J. P. Boehler, editor, *Applications of Tensor Functions in Solid Mechanics*, volume 292 of *CISM Courses and Lectures*, pages 13–30. Springer, 1987.
- [32] T. Böhlke and C. Brüggemann. Graphical representation of the generalized Hooke’s law. *Technische Mechanik (Magdeburg)*, 21(2):145–158, 2001.
- [33] R. Borchardt and S. Turowski. *Symmetrielehre der Kristallographie*. Oldenburg, 1999.
- [34] W. Borchardt-Ott. *Kristallographie*. Springer, 1997.
- [35] M. Braun. Configurational forces induced by finite-element discretization. *Proceedings of the Estonian Academy of Sciences, Physics, Mathematics*, 46:24–31, 1997.
- [36] M. Brünig. Eshelby stress tensor in large strain anisotropic damage mechanics. *International Journal of Mechanical Sciences*, 46:1763–1782, 2004.
- [37] P. Chadwick. *Continuum mechanics. Concise theory and problems*. Dover Publications, Inc., 1999.
- [38] P.G. Ciarlet. *Mathematical elasticity, vol I: Three-dimensional elasticity*. Elsevier Science Ltd, 1988.
- [39] P.G. Ciarlet and G. Geymonat. Sur les lois de comportement en élasticité non-linéaire compressible. *Les Comptes Rendus de l’Académie des Sciences*, 295:423–426, 1982.
- [40] B. D. Coleman and W. Noll. On the thermostatics of continuous media. *Archive for Rational Mechanics and Analysis*, 4:97–128, 1959.
- [41] B. Dacorogna. *Direct methods in the calculus of variations*, volume 78 of *Applied Mathematical Sciences*. Springer, Berlin, first edition, 1989.
- [42] R. de Boer and J. Schröder. *Tensor calculus for engineers with applications to continuum and computational mechanics*. Springer, manuscript, to be published in 2011.
- [43] Y. I. Dimitrienko. *Tensor analysis and nonlinear tensor functions*. Kluwer Academic Publishers, 2002.
- [44] V. Ebbing, D. Balzani, J. Schröder, P. Neff, and F. Gruttmann. Construction of anisotropic polyconvex energies and applications to thin shells. *Computational Materials Science*, 46:639–641, 2009.
- [45] V. Ebbing, J. Schröder, and P. Neff. On the construction of anisotropic polyconvex energy densities. In *Proceedings in Applied Mathematics and Mechanics*, volume 7, pages 4060009–4060010, 2007.
- [46] V. Ebbing, J. Schröder, and P. Neff. Polyconvex models for arbitrary anisotropic materials. In *Proceedings in Applied Mathematics and Mechanics*, volume 8, pages 10415–10416, 2008.

- [47] V. Ebbing, J. Schröder, and P. Neff. Approximation of anisotropic elasticity tensors at the reference state with polyconvex energies. *Archive of Applied Mechanics*, 79:651–657, 2009.
- [48] V. Ebbing, J. Schröder, and P. Neff. Construction of polyconvex energies for non-trivial anisotropy classes. In J. Schröder and P. Neff, editors, *Poly-, quasi- and rank-one convexity in applied mechanics*, volume 516 of *CISM Courses and Lectures*, pages 107–130. Springer, 2010.
- [49] V. Ebbing, J. Schröder, P. Neff, and F. Gruttmann. Micromechanical modeling of woven fiber composites for the construction of effective anisotropic polyconvex energies. *Proceedings in Applied Mathematics and Mechanics*, 9(1):333–334, 2009.
- [50] V. Ebbing, J. Schröder, P. Steinmann, and P. Neff. On the computation of configurational forces in anisotropic hyperelastic solids. In P. Steinmann, editor, *Proceedings of the IUTAM Symposium on Progress in the Theory and Numerics of Configurational Mechanics*, pages 261–270, Erlangen 2008, 2009.
- [51] A. Ehret and M. Itskov. A polyconvex hyperelastic model for fiber-reinforced materials in application to soft tissues. *Journal of Materials Science*, 42:8853–8863, 2007.
- [52] C. Giacovazzo, H.L. Monaco, G. Artioli, D. Viterbo, G. Ferraris, G. Gilli, G. Zanotti, and M. Catti. *Fundamentals of crystallography*. Oxford Science Publications, 2002.
- [53] J.H. Grace and A. Young. *The algebra of invariants*. Cambridge University Press, Cambridge, 1903.
- [54] D. Gross and T. Seelig. *Bruchmechanik: Mit einer Einführung in die Mikromechanik*. Springer, 2001.
- [55] G. B. Gurevich. *Foundations of the theory of algebraic invariants*. Nordhoff, 1964.
- [56] P.R. Halmos. *Finite-dimensional vector spaces*. Van Nostrand, New York, 1958.
- [57] S. Hartmann and P. Neff. Polyconvexity of generalized polynomial type hyperelastic strain energy functions for near incompressibility. *International Journal of Solids and Structures*, 40:2767–2791, 2003.
- [58] P. Haupt. *Continuum Mechanics and theory of materials*. Springer, Berlin, Heidelberg, New York, 2000.
- [59] D. Hilbert. Ueber die Theorie der algebraischen Formen. *Mathematische Annalen*, 36:473–534, 1890.
- [60] D. Hilbert. Ueber die vollen Invariantensysteme. *Mathematische Annalen*, 42:313–373, 1893.
- [61] R. Hill. On uniqueness and stability in the theory of finite elastic strains. *Journal of the Mechanics and Physics of Solids*, 5:229–241, 1957.
- [62] G. A. Holzapfel. *Nonlinear solid mechanics, a continuum approach for engineering*. Wiley, 2000.

- [63] K. Hutter and K. Jöhnk. *Continuum methods of physical modeling*. Springer, 2004.
- [64] M. Itskov and N. Aksel. A class of orthotropic and transversely isotropic hyperelastic constitutive models based on a polyconvex strain energy function. *International Journal of Solids and Structures*, 41:3833–3848, 2004.
- [65] M. Itskov, A.E. Ehret, and D. Mavrillas. A polyconvex anisotropic strain-energy function for soft collagenous tissues. *Biomechanics and Modeling in Mechanobiology*, 5:17–26, 2006.
- [66] N. Kambouchev, J. Fernandez, and R. Radovitzky. A polyconvex model for materials with cubic symmetry. *Modelling and Simulation in Material Science and Engineering*, 15:451–467, 2007.
- [67] R. Kienzler and G. Herrmann. *Mechanics in material space with application to defect and fracture mechanics*. Springer, 2000.
- [68] A. Krawietz. *Materialtheorie - Mathematische Beschreibung des phänomenologischen thermomechanischen Verhaltens*. Springer, 1986.
- [69] I. S. Liu. On representations of anisotropic invariants. *International Journal of Engineering Science*, 20:1099–1109, 1982.
- [70] L. E. Malvern. *Introduction to the mechanics of a continuous medium*. Prentice-Hall Inc., New-York, 1996.
- [71] B. Markert, W. Ehlers, and N. Karajan. A general polyconvex strain-energy function for fiber-reinforced materials. *Proceedings in Applied Mathematics and Mechanics*, 5:245–246, 2005.
- [72] J. E. Marsden and J. R. Hughes. *Mathematical foundations of elasticity*. Prentice-Hall, 1983.
- [73] A. Menzel and P. Steinmann. On the comparison of two strategies to formulate orthotropic hyperelasticity. *Journal of Elasticity*, 62:171–201, 2001.
- [74] J. Merodio and P. Neff. A note on tensile instabilities and loss of ellipticity for a fiber-reinforced nonlinearly elastic solid. *Archives of Mechanics*, 58:293–303, 2006.
- [75] J. Merodio and R.W. Ogden. Instabilities and loss of ellipticity in fiber-reinforced compressible non-linearly elastic solids under plane deformation. *International Journal of Solids and Structures*, 40:4707–4727, 2003.
- [76] A. Mielke. Necessary and sufficient conditions for polyconvexity of isotropic functions. *Journal of Convex Analysis*, 12:291–314, 2005.
- [77] C. B. Morrey. Quasi-convexity and the lower semicontinuity of multiple integrals. *Pacific Journal of Mathematics*, 2:25–53, 1952.
- [78] R. Müller, D. Gross, and G. A. Maugin. Use of material forces in adaptive finite element methods. *Computational Mechanics*, 33:421–434, 2004.

- [79] R. Müller, S. Kolling, and D. Gross. On configurational forces in the context of the finite element method. *International Journal for Numerical Methods in Engineering*, 53:1557–1574, 2002.
- [80] R. Müller and G. A. Maugin. On material forces and finite element discretization. *Computational Mechanics*, 29:52–60, 2002.
- [81] I. Münch. *Ein geometrisch und materiell nichtlineares Cosserat-Modell - Theorie, Numerik und Anwendungsmöglichkeiten*. Dissertation in der Fakultät für Bauingenieur-, Geo- und Umweltwissenschaften, ISBN 978-3-935322-12-6, electronic version available at <http://digbib.ubka.uni-karlsruhe.de/volltexte/1000007371>, Karlsruhe, 2007.
- [82] P. Neff. *Mathematische Analyse multiplikativer Viskoplastizität*. Ph.D. Thesis, Technische Universität Darmstadt, Shaker Verlag, ISBN:3-8265-7560-1, Aachen, 2000.
- [83] P. Neff. A geometrically exact Cosserat shell-model including size effects, avoiding degeneracy in the thin shell limit. Part 1: Formal dimensional reduction for elastic plates and existence of minimizers for positive Cosserat couple modulus. *Continuum Mechanics and Thermodynamics*, 16(6):577–628, 2004.
- [84] P. Neff. A geometrically exact planar Cosserat shell-model with microstructure. Existence of minimizers for zero Cosserat couple modulus. *Mathematical Models and Methods in Applied Sciences (M3AS)*, 17(3):363–392, 2007.
- [85] F. E. Neumann. *Vorlesungen über die Theorie der Elastizität der festen Körper und des Lichtäthers*. Teubner, 1885.
- [86] S. Nikolov, M. Petrov, L. Lymperakis, M. Friák, C. Sachs, H. Fabritius, D. Raabe, and J. Neugebauer. Revealing the design principles of high-performance biological composites using ab initio and multiscale simulations: the example of lobster cuticle,. *Acta Mechanica*, 22(4):519–526, 2010.
- [87] W. Noll. *The foundations of mechanics and thermodynamics*. Springer, 1974.
- [88] R. W. Ogden. Large deformation isotropic elasticity: on the correlation of theory and experiment for compressible rubber-like solids. *Proceedings of the Royal Society of London*, 328(1575):567–583, 1952.
- [89] R. W. Ogden. *Non-linear elastic deformations*. Dover Publications, 1984.
- [90] P. Pedregal. *Variational methods in nonlinear elasticity*. SIAM, Philadelphia, 2000.
- [91] S. Pennisi and M. Trovato. On the irreducibility of Professor G. Smith’s representations for isotropic functions. *International Journal of Engineering Science*, 25(8):1059–1065, 1987.
- [92] A. Raoult. Non-polyconvexity of the stored energy function of a St.-Venant-Kirchhoff material. *Aplikace Matematiky*, 6:417–419, 1986.
- [93] I. Rechenberg. *Evolutionstrategie '94*. Frommann-Holzboog, 1994.

- [94] R. S. Rivlin. Large elastic deformations of isotropic materials II. Some uniqueness theorems for pure homogeneous deformation. *Philosophical Transactions of the Royal Society of London*, 240:491–508, 1948.
- [95] R. S. Rivlin. Stability of pure homogeneous deformations of an elastic cube under dead loading. *Quarterly of Applied Mathematics*, 32:265–272, 1974.
- [96] R.S. Rivlin. Further remarks on the stress–deformation relations for isotropic materials. *Archive for Rational Mechanics and Analysis*, 4:681–702, 1955.
- [97] D. Royer and E. Dieulesaint. *Elastic waves in solids I, Free and guided propagation*. Springer, 2000.
- [98] M. Scherer, R. Denzer, and P. Steinmann. On a solution strategy for energy-based mesh optimization in finite hyperelastostatics. *Computer Methods in Applied Mechanics and Engineering*, 197:609–622, 2008.
- [99] J. Schröder. *Theoretische und algorithmische Konzepte zur phänomenologischen Beschreibung anisotropen Materialverhaltens*. Dissertationsschrift, Universität Hannover, F 96/3, 1996.
- [100] J. Schröder. *Homogenisierungsmethoden der nichtlinearen Kontinuumsmechanik unter Beachtung von Instabilitäten*. Habilitationsschrift, Institut für Mechanik (Bauwesen), Lehrstuhl I, Universität Stuttgart, 2000.
- [101] J. Schröder. Anisotropic polyconvex energies. In J. Schröder and P. Neff, editors, *Poly-, quasi- and rank-one convexity in applied mechanics*, volume 516 of *CISM Courses and Lectures*, pages 53–106. Springer, 2010.
- [102] J. Schröder, V. Ebbing, and P. Steinmann. Configurational forces in anisotropic solids. *Archive of Applied Mechanics*, 2010. In preparation.
- [103] J. Schröder and P. Neff. On the construction of polyconvex anisotropic free energy functions. In C. Miehe, editor, *Proceedings of the IUTAM Symposium on Computational Mechanics of Solid Materials at Large Strains*, pages 171–180. Kluwer Academic Publishers, 2001.
- [104] J. Schröder and P. Neff. Invariant formulation of hyperelastic transverse isotropy based on polyconvex free energy functions. *International Journal of Solids and Structures*, 40:401–445, 2003.
- [105] J. Schröder, P. Neff, and D. Balzani. A variational approach for materially stable anisotropic hyperelasticity. *International Journal of Solids and Structures*, 42(15):4352–4371, 2005.
- [106] J. Schröder, P. Neff, and V. Ebbing. Anisotropic polyconvex energies on the basis of crystallographic motivated structural tensors. *Journal of the Mechanics and Physics of Solids*, 56(12):3486–3506, 2008.
- [107] J. Schröder, P. Neff, and V. Ebbing. Polyconvex energies for trigonal, tetragonal and cubic symmetry groups. In K. Hackl, editor, *Proceedings of the IUTAM Symposium on Variational Concepts with Applications to the Mechanics of Materials*, Bochum 2008, 2009. In print.

- [108] I. Schur. *Vorlesungen über Invariantentheorie*. Springer-Verlag, Berlin, 1968.
- [109] H. P. Schwefel. *Evolution and Optimum Seeking*. Wiley, 1996.
- [110] L. A. Shuvalov. *Modern crystallography IV, Physical properties of crystals*. Springer, 1988.
- [111] G. Simmons and H. Wang. *Single crystal elastic constants and calculated aggregate properties*. The M.I.T. Press, 1971.
- [112] J. C. Simo. Numerical analysis and simulation of plasticity. In P.G. Ciarlet and J.L. Lions, editors, *Handbook of numerical analysis*, volume VI. Elsevier Science, 1998.
- [113] J. C. Simo and F. Armero. Geometrically non-linear enhanced strain mixed methods and the method of incompatible modes. *International Journal for Numerical Methods in Engineering*, 33:1413–1449, 1992.
- [114] G. F. Smith. On a fundamental error in two papers of C.-C. Wang ” On representations for isotropic functions, Parts I and II ”. *Archive for Rational Mechanics and Analysis*, 36:161–165, 1970.
- [115] G. F. Smith. On isotropic functions of symmetric tensors, skew-symmetric tensors and vectors. *International Journal of Engineering Science*, 9:899–916, 1971.
- [116] S. Specht. *Micromechanical FE-Analysis of fiber-reinforced membranes*. Institut für Mechanik, Universität Duisburg Essen, Report No. 55, 2010.
- [117] A. Spencer, editor. *Continuum theory of the mechanics of fibre-reinforced composites*, volume No. 282 of *CISM courses and lectures*. Springer-Verlag, Wien, 1984.
- [118] A. J. M. Spencer. Theory of invariants. In A.C. Eringen, editor, *Continuum Physics*, volume 1, pages 239–353. Academic Press, 1971.
- [119] A. J. M. Spencer and R. S. Rivlin. Further results in the theory of matrix polynomials. *Archive for Rational Mechanics and Analysis*, 4:214–230, 1959.
- [120] D. J. Steigmann. Frame-invariant polyconvex strain-energy functions for some anisotropic solids. *Mathematics and Mechanics of Solids*, 8:497–506, 2003.
- [121] E. Stein and F.-J. Barthold. Elastizitätstheorie. In G. Mehlhorn, editor, *Der Ingenieurbau: Grundwissen: Werkstoffe, Elastizitätstheorie*. Ernst und Sohn, 1996.
- [122] P. Steinmann. Application of material forces to hyperelastostatics fracture mechanics. Part I: Continuum mechanical setting. *International Journal of Solids and Structures*, 37:7371–7391, 2000.
- [123] P. Steinmann, D. Ackermann, and F. J. Barth. Application of material forces to hyperelastostatics fracture mechanics. Part II: computational setting. *International Journal of Solids and Structures*, 38:5509–5526, 2001.
- [124] P. Steinmann and G. A. Maugin, editors. *Mechanics of material forces*. Springer, 2005.

- [125] P. Steinmann, M. Scherer, and R. Denzer. Secret and joy of configurational mechanics: From foundations in continuum mechanics to applications in computational mechanics. *Zeitschrift für Angewandte Mathematik und Mechanik*, 89(8):614–630, 2009.
- [126] P. Thoutireddy and M. Ortiz. A variational r-adaption and shape-optimization method for finite-deformation elasticity. *International Journal for Numerical Methods in Engineering*, 61:1–21, 2004.
- [127] C. Truesdell and W. Noll. *The non-linear field theories of mechanics*. Springer, third edition, 2004.
- [128] W. Voigt. Theoretische Studien über die Elastizitätsverhältnisse der Kristalle. *Abhandlung der Gesellschaft der Wissenschaften zu Göttingen*, 34:3–52, 1887.
- [129] W. Voigt. *Lehrbuch der Kristallphysik*. Teubner, 1966.
- [130] M. Šilhavý. *The mechanics and thermodynamics of continuous media*. Springer, 1997.
- [131] C.-C. Wang. On a general representation theorem for constitutive relations. *Archive for Rational Mechanics and Analysis*, 33:1–25, 1969.
- [132] C.-C. Wang. On representations for isotropic functions. Part I. Isotropic functions of symmetric tensors and vectors. *Archive for Rational Mechanics and Analysis*, 33:249–267, 1969.
- [133] C.-C. Wang. On representations for isotropic functions. Part II. Isotropic functions of skew-symmetric tensors, symmetric tensors, and vectors. *Archive for Rational Mechanics and Analysis*, 33:268–287, 1969.
- [134] C.-C. Wang. A new representation theorem for isotropic functions: An answer to professor G. F. Smith’s Criticism of my papers on representations for isotropic functions. Part 1. Scalar-valued isotropic functions. *Archive for Rational Mechanics and Analysis*, 36:166–197, 1970.
- [135] C.-C. Wang. A new representation theorem for isotropic functions: An answer to professor G. F. Smith’s Criticism of my papers on representations for isotropic functions. Part 2. Vector-valued isotropic functions, symmetric tensor-valued isotropic functions, and skew-symmetric tensor-valued isotropic functions. *Archive for Rational Mechanics and Analysis*, 36:198–223, 1970.
- [136] C.-C. Wang. Corrigendum to my recent papers on ” Representations for isotropic functions ”. *Archive for Rational Mechanics and Analysis*, 43:392–395, 1971.
- [137] H. Weyl. *The classical groups, their invariants and representation*. Princeton Univ. Press, Princeton, New Jersey, 1946.
- [138] P. Wriggers. *Nonlinear finite element methods*. Springer, 2008.
- [139] G. Wulff. Untersuchungen im Gebiete der optischen Eigenschaften isomorpher Kristalle. *Zeitschrift für Kristallographie*, 36:1–28, 1902.

- [140] H. Xiao. On isotropic extension of anisotropic tensor functions. *Zeitschrift für Angewandte Mathematik und Mechanik*, 76(4):205–214, 1996.
- [141] H. Xiao. A unified theory of representations for scalar-, vector- and second order tensor-valued anisotropic functions of vectors and second order tensors. *Archives of Mechanics*, 49:995–1039, 1997.
- [142] J.M. Zhang and J. Rychlewski. Structural tensors for anisotropic solids. *Archives of Mechanics*, 42:267–277, 1990.
- [143] Q.-S. Zheng. A note on representation for isotropic function of 4th-order tensors in 2-dimensional space. *Zeitschrift für Angewandte Mathematik und Mechanik*, 74:357–359, 1994.
- [144] Q.-S. Zheng. Theory of representations for tensor functions – a unified invariant approach to constitutive equations. *Applied Mechanics Reviews*, 47:545–587, 1994.
- [145] Q.-S. Zheng and J. Betten. On the tensor function representations of 2nd-order and 4th-order tensors. Part I. *Zeitschrift für Angewandte Mathematik und Mechanik*, 75:269–281, 1995.
- [146] Q.-S. Zheng and A. J. M. Spencer. Tensors which characterize anisotropies. *International Journal of Engineering Science*, 31(5):679–693, 1993.
- [147] O. C. Zienkiewicz and R. L. Taylor. *The finite element method for solid and structural mechanics*. Elsevier, 2005.

Curriculum Vitae

| | |
|-------------------|--|
| Name | Vera Ebbing |
| Geburtsdatum | 19. März 1982 |
| Geburtsort | Bottrop-Kirchhellen |
| Familienstand | ledig |
| 1988 - 1992 | Marien Grundschule , Bottrop-Feldhausen |
| 1992 - 2001 | Ratsgymnasium, Gladbeck |
| 10/2001 - 04/2006 | Studium der Fachrichtung Bauingenieurwesen, Universität Duisburg–Essen |
| 2005-2006 | Diplomarbeit am Institut für Mechanik, Fakultät Ingenieurwissenschaften, Abteilung Bauwissenschaften, Universität Duisburg-Essen, Thema: <i>A Generalized Time-Integration Scheme for Finite Elasto-Plasticity</i> |
| 04/2006 | Diplom |
| 2006 - 2010 | Wissenschaftliche Mitarbeiterin für Forschung und Lehre am Institut für Mechanik, Fakultät Ingenieurwissenschaften, Abteilung Bauwissenschaften, Universität Duisburg-Essen |
| 05/2010 | Promotion |

